PROTECTIVE RELAYING FOR POWER GENERATION SYSTEMS

© 2006 by Taylor & Francis Group, LLC

PROTECTIVE RELAYING FOR POWER GENERATION SYSTEMS

DONALD REIMERT



Taylor & Francis
Taylor & Francis Group
Boca Raton London New York

A CRC title, part of the Taylor & Francis imprint, a member of the Taylor & Francis Group, the academic division of T&F Informa plc.

© 2006 by Taylor & Francis Group, LLC

Published in 2006 by
CRC Press
Taylor & Francis Group
6000 Broken Sound Parkway NW, Suite 300
Boca Raton, FL 33487-2742

© 2006 by Taylor & Francis Group, LLC
CRC Press is an imprint of Taylor & Francis Group

No claim to original U.S. Government works
Printed in the United States of America on acid-free paper
10 9 8 7 6 5 4 3 2 1

International Standard Book Number-10: 0-8247-0700-1 (Hardcover)
International Standard Book Number-13: 978-0-8247-0700-2 (Hardcover)
Library of Congress Card Number 2005052952

This book contains information obtained from authentic and highly regarded sources. Reprinted material is quoted with permission, and sources are indicated. A wide variety of references are listed. Reasonable efforts have been made to publish reliable data and information, but the author and the publisher cannot assume responsibility for the validity of all materials or for the consequences of their use.

No part of this book may be reprinted, reproduced, transmitted, or utilized in any form by any electronic, mechanical, or other means, now known or hereafter invented, including photocopying, microfilming, and recording, or in any information storage or retrieval system, without written permission from the publishers.

For permission to photocopy or use material electronically from this work, please access www.copyright.com (http://www.copyright.com/) or contact the Copyright Clearance Center, Inc. (CCC) 222 Rosewood Drive, Danvers, MA 01923, 978-750-8400. CCC is a not-for-profit organization that provides licenses and registration for a variety of users. For organizations that have been granted a photocopy license by the CCC, a separate system of payment has been arranged.

Trademark Notice: Product or corporate names may be trademarks or registered trademarks, and are used only for identification and explanation without intent to infringe.

Library of Congress Cataloging-in-Publication Data

Reimert, Donald.
Protective relaying for power generation systems / Donald Reimert.
p. cm.
Includes bibliographical references and index.
ISBN-13: 978-0-8247-0700-2 (alk. paper)
ISBN-10: 0-8247-0700-1 (alk. paper)
1. Protective relays. 2. Electric power systems--Protection. I. Title.

TK2861.R36 2005
621.31'7--dc22 2005052952

informa
Taylor & Francis Group
is the Academic Division of Informa plc.

Visit the Taylor & Francis Web site at
http://www.taylorandfrancis.com

and the CRC Press Web site at
http://www.crcpress.com

© 2006 by Taylor & Francis Group, LLC

Preface

The importance of a generating unit in terms of economics and system reliability cannot be overstated. This is true for units connected to the nations power grid or for units operating at industrial facilities. Although there are many books on protective relaying these tend to focus on transmission and distribution relaying. Many include generator and motor topics. But the coverage provided does not promote a thorough understanding of the hazards to the generator or the limitation of protective elements applied.

Settings applied to any protective device represent a balance between adequate sensitivity to detect a damaging condition and the security required to prevent false tripping during events that do not threaten the protected equipment. The importance of this balance at generation facilities is highlighted by the intense scrutiny given these protection schemes in the wake of large-scale system outages. This scrutiny is not limited to the generator but extends to the auxiliary system as well.

The aim of this book is to provide in-depth discussions of the major electrical protection schemes associated with synchronous generators and induction motors. The principles and criteria presented are applicable to both large and small machines. The discussions include analysis of the damage and damaging mechanisms relating to each protective function. An understanding of these parameters is important not only for the application of protection but also when operability issues arise during or after abnormal operating events.

This book includes detailed derivations of complex system interaction. An understanding of such phenomena is generally not required when applying rule-of-thumb setting criteria. However, such derivations provide insight into the basis for the rule-of-thumb settings and the framework to recognize situations when such settings are not appropriate. These derivations are also often useful for post-incident analysis.

Included in the text are constructions for Mathcad and Excel workbooks for the analysis of CT performance in generator differential applications, generator shaft torque transients following out-of-phase closing, fault-induced impedance swings for two generator systems, steady-state and dynamic stability limits, under manual and automatic voltage control. These files are available for download at taylorandfrancis.com.

In the text analytical techniques are presented to assess motor capability and relay response to transients such as starting and cyclic loading.

I have attempted to present each subject as a stand alone chapter that allows quick reference on detailed analysis. Example settings calculations are provided.

© 2006 by Taylor & Francis Group, LLC

Author

Donald Reimert, a registered professional engineer, graduated from Penn State University more than 35 years ago. His professional career was focused on the design and application of protective relays and relay systems. This has included distribution, transmission, and generation system facilities. In addition to protective relaying, he has design experience in substation and electrical systems associated with fossil, nuclear, and hydro-generation facility. As a system planner, he developed regional projects with financial justifications to meet future load requirements. He has helped to develop and present a series of protective relay courses for the University of Wisconsin-Milwaukee including "Introduction to Protective Relaying," "Protective Relay Principles and Applications," and "Advanced Protective Relaying for Transmission Systems." He has also developed and presented "Advanced Protective Relaying for Generator and Generator Auxiliaries."

© 2006 by Taylor & Francis Group, LLC

Contents

Chapter 1
Generator Normal Operations 1
1.1 The Sample System 1
1.2 Generator Capability 1
1.3 Voltage Limitations 3
1.3.1 Sample System GSU Transformer Limits 3
1.4 System Limitations 4
1.5 Generator Capability Variations with Voltage 7
1.6 Excitation System 9
Reference 13

Chapter 2
Generator Short Circuit Calculations 15
2.1 Introduction 15
2.2 Short-Circuit Current Characteristics 15
2.3 Generator Internal Magnetics 15
2.4 Generator Magnetic Structures 19
2.5 Generator Constants 23
2.6 Fault Current Calculations 25
2.6.1 Initial Load 26
2.6.2 Fault Calculation Overview 28
2.6.3 Determination of X_f and Fault Currents 30
2.6.4 Three-Phase Short Circuit 31
2.6.5 Phase-to-Phase Short Circuit 32
2.6.6 Phase-to-Ground Fault 33
2.6.7 Other Fault Conditions 35
2.6.8 DC Component of Short-Circuit Current 35
2.6.9 RMS Asymmetrical Current 37
2.7 Voltage Regulator 37
2.8 Practical Shortcuts 38
2.9 Short Circuit Calculation Example 40
2.9.1 Establish Prefault Conditions 40
2.9.2 Three-Phase Fault at Generator Terminals 41
2.9.3 Phase-to-Ground Fault on High-Voltage Terminals of GSU 42
2.9.4 Effects of the Automatic Voltage Regulator 45
References 46

Chapter 3
Generator Differential Relay: 87G 47
3.1 Introduction 47
3.2 Ideal Differential Relay 47
3.3 Practical Considerations 47
3.3.1 CT Ratings 49
3.3.2 CT Saturation 50
3.3.3 CTs and Fault Current Replication 53

© 2006 by Taylor & Francis Group, LLC

3.4 Percentage Differential Relay 56
3.5 Relay Characteristics 57
3.5.1 Electromechanical Relays 57
3.5.2 Solid-State and Microprocessor Relays 57
3.6 Minimum Operating Current Setting 59
3.7 Slope Setting 59
3.7.1 Requirements for Slope Setting 59
3.7.2 Advantage of Low Slope 60
3.7.3 Sensitivity and Load Current 60
3.7.4 Relay Response to Saturation 61
3.7.5 Methods of Choosing Slope Settings 63
3.7.5.1 Manufacturer's Recommendations 63
3.7.5.2 Qualitative Determination of Slope 63
3.7.5.3 Error Current Calculations for Unsaturated CT 63
3.7.5.4 Mason's Method 64
3.7.5.5 Example of Mason's Method 65
3.7.5.6 Fundamental Frequency Analysis 66
3.8 Sample System Differential Relay Settings 68
3.8.1 Sample System Differential Circuit 68
3.8.2 Electromechanical Relay 68
3.8.2.1 Specifications for Relay Chosen 68
3.8.3 Choosing Slope Static and Microprocessor Relays 69
3.9 Stabilizing Resistor 70
3.10 Balancing Burden 73
3.11 Time Delay 74
3.12 Frequency Response 74
References 75

Chapter 4

Backup Fault Protection 77
4.1 Purpose and Implementation 77
4.1.1 Standard Overcurrent Relays 77
4.1.2 Voltage-Dependent Relays 78
4.1.3 Electromechanical vs. Electronic Relays 79
4.2 Voltage Supervised Overcurrent Relays 79
4.2.1 Voltage-Controlled and Voltage-Restrained Relays 79
4.2.2 Application Options and Fault Sensitivity 80
4.2.2.1 Scheme Sensitivity vs. Potential Transformer (PT) and Current Transformer (CT) Connection 80
4.2.2.2 Sensitivity Related to Relay Type 82
4.2.2.3 Delta Relay Currents 82
4.2.3 Settings Considerations 83
4.2.3.1 Basic Requirement 83
4.2.3.2 Automatic Voltage Regulator in Service 84
4.2.3.3 51 V Transmission System Backup Limitations 84
4.2.3.4 Effects of Wye-Delta Transformer 86
4.2.3.5 Self-Excitation Generators 87
4.2.3.6 Relay Response to Transient Current 88
4.2.3.7 Equipment Protection 90
4.2.4 Setting Criteria 93

© 2006 by Taylor & Francis Group, LLC

4.2.5 Relay Current and Voltage Calculations 93
4.2.5.1 Relay Current and Voltage Equations 94
4.2.5.2 Sequence Currents and Voltages Calculations 95
4.2.6 Sample System 51 V Relay Settings 98
4.2.6.1 Fault Calculations 99
4.2.6.2 Choosing the Undervoltage Setting 102
4.2.6.3 Choosing Overcurrent Setting 103
4.2.6.4 Choosing Time Delay Setting 103
4.2.6.5 Auxiliary PTs to Correct for Wye-Delta Phase Shift 104
4.3 Distance Relays 105
4.3.1 Distance Relay Characteristics 105
4.3.1.1 *Z* Measured by Phase Distance Relay 105
4.3.1.2 Mho Distance Relay 107
4.3.1.3 System Impedance vs. Relay Characteristic 109
4.3.2 Setting Considerations 111
4.3.2.1 Load Limits 111
4.3.2.2 Apparent Impedance 112
4.3.2.3 Influence of an Interposing Wye-Delta Transformer 113
4.3.2.4 Auxiliary PTs to Correct for Wye-Delta Phase Shift 115
4.3.3 Other Distance Relay Applications 116
References 116

Chapter 5
Generator Ground Fault Protection 117
5.1 Introduction 117
5.2 Generator Grounding Considerations 117
5.2.1 Ground Fault Current Limitation 117
5.2.2 Overvoltage Concerns 118
5.2.3 Core Damage Cause by Ground Fault 120
5.3 Methods of Grounding 121
5.3.1 Ungrounded System 121
5.3.2 Solidly Grounded/Effectively Grounded 125
5.3.3 High-Impedance Grounding 128
5.3.3.1 Distribution Transformer Grounding 128
5.3.3.2 High-Resistance Grounding on Sample System 130
5.3.3.3 Ground Fault Neutralizers 130
5.3.4 Low-Impedance Grounding 141
5.3.4.1 Low-Resistance Grounding 143
5.3.4.2 Low-Reactance Grounding 144
5.3.4.3 Grounding Transformers 144
5.4 Ground Fault Protection 145
5.4.1 Alarm vs. Tripping for High-Impedance Grounded System 146
5.4.2 Electromechanical and Electronic Relays 146
5.4.3 High-Impedance Ground Protection 146
5.4.3.1 Neutral Overvoltage Scheme 146
5.4.3.2 Application of 59GN on Sample System 148
5.4.3.3 Broken Delta Overvoltage Scheme 150
5.4.3.4 Overcurrent Scheme 151
5.4.4 Low-Impedance Ground Protection 154
5.4.4.1 Ground Differential 154

© 2006 by Taylor & Francis Group, LLC

5.4.5 100% Stator Protection Schemes 155
5.4.5.1 Third-Harmonic Schemes 155
5.4.5.2 Third-Harmonic Undervoltage Scheme 157
5.4.5.3 Settings for Sample System 27H Scheme 158
5.4.5.4 Third-Harmonic Overvoltage Scheme 159
5.4.5.5 Third-Harmonic Voltage Ratio Scheme 159
5.4.6 Neutral Injection Scheme 161
References 163

Chapter 6
Unbalanced Current Protection 165
6.1 Introduction 165
6.2 What Is Negative-Sequence Current? 165
6.3 Effects of Negative-Sequence Current 166
6.3.1 Rotor Heating 166
6.3.1.1 Cylindrical Rotor Generators 166
6.3.1.2 Salient Pole Generators 168
6.3.2 Pulsating Torque 169
6.4 Generator Negative-Sequence Capability 169
6.4.1 Continuous Unbalanced Capabilities 170
6.4.2 Short Time Unbalanced Currents 170
6.5 Sources of Negative Sequence Current 171
6.5.1 Unbalanced Faults 171
6.5.2 Open Phases 172
6.6 In-Service I_2^2t Duty vs. Standards 172
6.6.1 Calculation of I_2^2t Duty 174
6.6.1.1 Isolated Generator 174
6.6.1.2 The Interconnected Generator 174
6.6.1.3 The'venin's Equivalent Circuit 175
6.6.2 Unbalanced Duty on Sample System 175
6.7 Unbalanced Current Protection 182
6.8 Negative-Sequence Relay Settings 184
6.8.1 Calculation of Open-Circuit Current 184
6.8.2 Negative Sequence Relay Setting 187
References 189

Chapter 7
Motoring Protection 191
7.1 Introduction 191
7.2 Effects of Motoring 191
7.2.1 Consequences for a Steam Turbine 192
7.2.2 Consequences for Other Prime Movers 192
7.3 Protection 192
7.3.1 Mechanical Protection: Steam Turbines 193
7.3.2 Electrical Protection 193
7.4 Sequential Trip Logic 196
7.5 Backup Protection 196
7.6 Setting Device 32 197
7.7 Applying Reversed Power Relay on the Sample System 197
References 199

© 2006 by Taylor & Francis Group, LLC

Chapter 8

Field Winding Protection 201
8.1 Field Ground Protection 201
8.1.1 Field Ground Hazard 201
8.1.2 Field Ground Protection 201
8.1.3 Field Ground Detection 202
8.1.3.1 Field Ground Relay Selection and Settings 205
8.2 Field Overcurrent Protection 206
8.2.1 Field Overcurrent Transients 206
8.2.2 Overcurrent Protection Schemes 208
8.2.3 Application of AC Relays to Protect the Field Winding 209
8.2.3.1 Basic Rectifier Operation 210
8.2.3.2 Relay Quantities 213
8.3 Settings For Field Overcurrent/Overvoltage Relays 215
8.3.1 Full Load Values 215
8.3.2 Maximum Field Current 215
8.3.3 Maximum Field Current from a Bridge Rectifier 215
8.4 Applying Field OC Protection on the Sample System 216
8.4.1 Rated Field Voltage 216
8.4.2 Maximum Available Field Current 217
8.4.3 Pickup Setting 217
8.4.4 Time Delay 219
References 220

Chapter 9

Overexcitation 221
9.1 Introduction 221
9.2 Causes of Overexcitation 221
9.3 Damage 223
9.4 V/Hz Limits 224
9.5 Protection 225
9.5.1 Field Monitoring Relays 225
9.5.2 V/Hz Limiter 226
9.5.3 V/Hz Relay Applications 227
9.6 Settings 228
9.6.1 Generator V/Hz Settings 229
9.6.2 Transformer Settings 229
9.6.3 Generator/Transformer Settings 230
9.6.4 Setting Limitations 230
9.6.5 Time Delay Settings 231
9.7 Differential Relay Response to Overexcitation 233
9.8 Application of V/Hz Protection on the Sample System 234
References 236

Chapter 10

Abnormal Frequency Protection 237
10.1 Introduction 237
10.2 Effect on Generator 237
10.3 Steam Turbines 237
10.4 Combustion Turbines 241
10.5 Hydro Generators 241
10.6 Excitation System 241

© 2006 by Taylor & Francis Group, LLC

10.7 Protection and Settings 244
10.7.1 Primary Protection 244
10.7.2 Backup Protection 245
10.7.3 Combustion Turbine Generators Protection 248
References 248

Chapter 11
Minimum Excitation Limiter 249
11.1 Overview of the Minimum Excitation Limiter Application 249
11.1.1 Operation in the Leading Mode 249
11.1.2 Limits on Leading Var Operation 250
11.2 Setting Criteria Background 251
11.3 Setting Criteria 252
11.4 Generator Leading Var Capability 253
11.4.1 Stator End-Core Heating in the Round Rotor Generator 254
11.4.2 Leading Var Capability of a Salient Pole Machine 257
11.5 Coordination with the LOF Relay 258
11.6 System Stability Limits 260
11.6.1 Classical View of Steady-State Stability 260
11.6.2 Manual Regulator Steady-State Stability Limit 262
11.6.3 Automatic Regulator Stability Limits 263
11.7 MEL Protective Characteristic 270
11.7.1 Straight Line Characteristic: Type UEL2 Model 272
11.7.2 Multisegment Straight Line Model Type UEL3 274
11.7.3 Circular Characteristic Type UEL1 Model 275
11.8 MEL Dynamic Performance 277
11.8.1 Problems with MEL Stability 277
11.8.2 Interaction with V/Hz 278
11.8.3 Isolated on Capacitive Load 278
11.9 MEL Application on the Sample System 279
References 284

Chapter 12
Loss of Synchronism 287
12.1 Introduction 287
12.2 Turbine Generator Damage 288
12.3 Transient Stability 288
12.4 Out-of-Step Protection 292
12.5 Classical Swing Impedance Characteristic 294
12.6 Dynamic Swing Representation 296
12.7 Setting Consideration 301
12.7.1 Recoverable Swings 302
12.7.2 Current Limitation 303
12.7.3 Out-of-Phase Switching Rating for Breakers 303
12.7.4 Swing Velocity 303
12.8 Out-of-Step Relay: Device 78 304
12.8.1 Simple Mho Scheme 304
12.8.2 Single Blinder Scheme 307
12.8.3 Double Blinder 310
12.8.4 Double Lens and Concentric Circle Schemes 311
12.8.5 Detection Problems 312

© 2006 by Taylor & Francis Group, LLC

12.9 Setting Out-of-Step on Sample System 313
References 319

Chapter 13
Loss of Field Protection 321
13.1 General 321
13.1.1 Other Factors Affecting Loss of Field Severity 323
13.2 System Impact 325
13.3 Generator Damage 325
13.3.1 Stator Winding Overload 326
13.3.2 Rotor Damage 327
13.3.3 Stator End-Core Damage 330
13.3.4 Torque Pulsations 330
13.4 Loss of Field Protection: Device 40 331
13.5 Distance Relay Schemes 331
13.5.1 Distance Scheme 1: Unqualified Trip Scheme 331
13.5.1.1 Coordination for Stable Swings 334
13.5.1.2 Coordination with Minimum Excitation Limiter and Generator Capability Curve 335
13.5.1.3 Modified Scheme: Two Impedance Elements 336
13.5.2 Distance Scheme 2: Qualified Trip Scheme 337
13.5.2.1 Trip Delay Considerations 338
13.5.2.2 Criteria for Setting Mho Characteristic 339
13.5.2.3 Undervoltage Element 341
13.5.2.4 Modified Scheme 341
13.5.2.5 Special Consideration for Bussed Generators 341
13.6 Other Causes for LOF Relay Operations 342
13.6.1 Operator Error on Startup 342
13.6.2 Frequency-Sensitive Excitation Systems 343
13.7 LOF Relays During System Disturbances 344
13.8 Special Considerations for Hydro Units 346
13.9 Application of the LOF on the Sample System 346
13.9.1 Application of Scheme 1 on the Sample System Generator 347
13.9.1.1 Setting Review against Dynamic Data 349
13.9.2 Application of Scheme 2 on the Sample System Generator 350
13.9.2.1 Setting Review against Dynamic Data 351
References 354

Chapter 14
Synchronization Protection 357
14.1 Introduction 357
14.2 Damage 357
14.2.1 Transformer Damage 358
14.2.1.1 Maximum Withstand Current 358
14.2.1.2 Maximum Synchronizing Current 359
14.2.2 Generator Damage 360
14.2.2.1 Shaft Torque 360
14.2.2.2 Fatigue Damage 363
14.2.2.3 Relative Damage Assessment 365
14.2.2.4 Considerations for Gas Turbines and Hydro Units 366
14.2.3 Breaker Considerations 367

© 2006 by Taylor & Francis Group, LLC

14.3 Synchronizing Methods 368
14.3.1 Manual Synchronizing 369
14.3.2 Automatic Synchronizing 371
14.4 Synchronism Check Relays (Device 25) 371
14.4.1 Electromechanical Sync-Check Relays 372
14.4.2 Electronic-Based Sync-Check Relays 374
14.4.2.1 Phase Angle Supervision 375
14.4.2.2 Slip Frequency Limitation 375
14.4.2.3 Anticipatory Close Initiation 375
14.4.2.4 Minimum and Maximum Voltage Limits 375
14.4.2.5 Maximum Voltage Difference 376
14.4.2.6 Generator Voltage Priority 376
14.4.2.7 PT Phase Angle Compensation 376
14.4.2.8 Voltage Magnitude Compensation 376
14.4.2.9 Built-In Dead Bus Logic 377
14.5 Automatic Synchronizer (Device 25A) 377
14.5.1 Speed Control 377
14.5.2 Frequency Modulation Speed Control 378
14.5.3 Pulse Width Modulation Speed Control 379
14.6 Slow Breaker Protection 379
14.7 Settings 380
14.8 Synchronizing Equipment on the Sample System 381
14.8.1 Input Circuit Settings 382
14.8.2 Autosynchronizer Settings 383
14.8.3 Sync-Check Relay 384
14.8.4 Slow Close Protection 385
References 386

Chapter 15
Accidental Energization Protection 389
15.1 Introduction 389
15.2 Generator State at Energization 389
15.3 Inadvertent Energization 391
15.3.1 Initial Current for a Three-Phase Energization from Standstill 392
15.3.2 Single-Phase Energization from Standstill 392
15.3.3 Initial Current for a Single-Phase Energization at Standstill 394
15.4 Breaker Flashover 396
15.4.1 Initial Single-Phase Flashover Current 396
15.4.2 Initial Current for Two-Phase Flashover 397
15.5 Dynamic Analysis of Three-Phase Energization from Standstill 399
15.5.1 System Voltage Impressed on d- and q-Axes 399
15.5.2 Axis Voltages Produced by Generator 400
15.5.3 Derivation of Axis Currents 400
15.5.4 Defining Generator Shaft Torque 402
15.5.5 d- and q-Axes Circuit Impedance 403
15.5.6 Acceleration 405
15.6 Generator Damage 406
15.6.1 Rotor Heating 406
15.6.2 Other Considerations 408
15.7 Turbine Damage 409

© 2006 by Taylor & Francis Group, LLC

15.8 Energization Protection 410
15.9 Protection Provided by Native Schemes 411
15.9.1 Loss-of-Field Relay: Device 40 411
15.9.1.1 LOF Scheme 1 412
15.9.1.2 LOF Scheme 2 412
15.9.2 Backup Distance Protection: Device 21 413
15.9.3 Voltage Restraint/Voltage Control Relays: Device 51V 415
15.9.4 Motoring Protection: Device 32 415
15.9.5 Negative-Sequence Current Protection: Device 46 416
15.9.6 Backup Ground Relay: Device 51N 417
15.10 Dedicated Energization Protection 417
15.10.1 Dedicated Inadvertent Energization Schemes 417
15.10.2 Dedicated Breaker Flashover Protection 419
15.11 Applying Energization Protection on the Sample System 420
15.11.1 Inadvertent Energization Scheme Settings 420
15.11.2 Open Breaker Flashover 423
15.11.2.1 Initial Current for Single-Phase Flashover 423
15.11.2.2 Initial Current for Two-Phase Flashover 424
15.11.2.3 Setting the OBF Fault Detector (50N) 425
References 425

Chapter 16
Motor Protection 427
16.1 Introduction 427
16.2 Motor Characteristics and Representation 427
16.2.1 Classical Motor Equivalent Circuit 427
16.2.1.1 Motor Torque 432
16.3 Motor Ratings 433
16.3.1 Rated Voltage and Frequency 434
16.3.2 Service Factor 435
16.4 Motor Characteristics 435
16.4.1 Motor Current 436
16.4.2 Speed–Torque Curves 436
16.5 Motor Applications 438
16.5.1 Horsepower Rating 438
16.5.2 Matching Motor and Load Torque Characteristics 439
16.5.3 Inertial Capability of NEMA Motors 441
16.6 Motor Starting 441
16.6.1 System Voltage Degradation during Starting 441
16.6.2 Starting Time Calculation 443
16.6.3 Motor Model for Starting Studies 444
16.6.4 Starting Calculation Example 450
16.6.5 Effect of Load Torque Characteristic 452
16.6.5.1 Centrifugal Pumps 453
16.6.6 Rotor Heating during Acceleration 459
16.7 Motor Overload Protection 461
16.7.1 Motor Thermal Limit Curves 461
16.7.2 Overcurrent Coordination 464
16.7.3 Thermal vs. Disk Elements 465
16.7.4 Time Overcurrent Trip Settings 467
16.7.5 Duty Cycle Motor Protection 467

© 2006 by Taylor & Francis Group, LLC

16.7.6 Induction Disk Operating Characteristics 468
16.7.6.1 Dynamic Characteristic of the Disk Element 470
16.7.6.2 Practical Disk Element Model 470
16.7.6.3 Disk Element Response to Starting Current 472
16.7.6.4 Disk Element Response to Cyclic Load 473
16.7.7 Basic Thermal Element 477
16.7.7.1 Dynamic Characteristic of the Thermal Element 481
16.7.7.2 Thermal Element Response to Starting Current 482
16.7.7.3 Thermal Element Response to Cyclic Load 483
16.8 Multifunction Microprocessor Relays 484
16.8.1 Thermal Model Protection Scheme 486
16.8.1.1 Derivation of Model Parameters 487
16.8.1.2 Scheme Application Example 489
16.8.2 Thermal Limit Based Protection Scheme 490
16.8.2.1 Application of Thermal Limit Based Scheme 492
16.8.3 Unbalanced Current Protection 495
16.9 Special Schemes for Difficult Starts 495
16.10 Direct Temperature Measurement 497
16.11 Phase Fault Protection 499
16.11.1 Cable Protection 500
16.11.2 Upstream Coordination 502
16.12 Ground Fault Protection 503
16.13 Phase Unbalanced Protection 505
16.13.1 Current and Voltage Unbalanced Relays 508
16.14 Sample Setting Calculations 509
16.14.1 Set Device 51 Operating Current 510
16.14.2 Set Device 50 Operating Current 510
16.14.3 Checking the Maximum Three-Phase Fault Current at the Motor 511
16.14.4 Device 51 Time Delay 512
16.14.5 Coordination with Upstream Protection 513
References 515

Appendix A
Generator Data Sheet 517

Appendix B
CT Performance in Differential Relay Circuits 519

Appendix C
Dynamic and Steady State Stability Limits 527

Appendix D
Swing Impedance Locus Calculation Using Excel® 533

Appendix E
Generator Shaft Torsional Transients 545

© 2006 by Taylor & Francis Group, LLC

1 Generator Normal Operations

1.1 THE SAMPLE SYSTEM

Before we begin to analyze the various malfunctions that can befall a generator and the connected auxiliary system, we must have an understanding of the parameters that define normal operation. Our review of generator and generator auxiliary protection will be based on the sample system shown in Figure 1.1. During normal operations, the generator supplies power to the grid through the Generator Step Up (GSU) transformer and to auxiliary loads at 4.16 kV buses A and B through auxiliary transformers. When the unit is off line, the auxiliary load is supplied from the auxiliary transformer at Bus B.

The GSU transformer connects to a moderate strength power system. With all lines in service, the power system and GSU transformer appear as a 14.8% impedance at the generator terminals. Line A is the strongest line connected to the 69 kV bus; its outage increases the impedance seen by the generator to 29%.

The system voltage also varies. During light load periods the voltage drop through system components such as lines and transformers is minimal. As load increases, the increased voltage drop caused by the flow of Watts and Vars through these components causes system voltage to fall. Because these power system components are highly inductive, the voltage drop caused by an amp of reactive current is greater than that caused by an amp of real current.

The system voltage regulation between light and peak load is amplified by the reactive characteristic of the long high-voltage (HV) transmission lines. These lines behave as capacitors when lightly loaded. The Vars they produce flow into the system, boosting voltage just as distribution capacitors do. As the HV line loading increases, the line characteristic changes from capacitive to inductive. At peak system load, the Vars consumed by HV lines significantly increases system voltage drop.

During light load periods, generators may be required to operate with reduced field current, consuming excess Vars from the system, to reduce system voltage. At peak system load, generators operate near full field current, supplying Vars to support system voltage.

It is not desirable to operate generators at rated Var output in peak load situations if the system is in a normal configuration. A portion of the generators' reactive capability should be held in reserve to boost voltage in the event of a forced outage of a major tie line or generator.

Maximum system voltages would be anticipated at night in the spring and fall. Minimum system voltages typically occur during the day in the summer and winter when the system load is at peak. These variations in system configuration and voltage have a significant effect on the operation of the generator and associated auxiliary equipment, as will be seen later in this chapter.

1.2 GENERATOR CAPABILITY

The proper application of protective relaying requires knowledge of the operating range of each component and an understanding of the interactions of the generating unit and the power system. First we will look at component ratings.

The nameplate rating of our sample system generator is 104.4 MVA at 0.85 power factor, 13.8 kV. This defines only one limiting point of operation for the machine. It is logical to assume that a reduction in MVAR output would allow some increase in MW output and that a reduction in MW would allow higher MVAR output.

© 2006 by Taylor & Francis Group, LLC

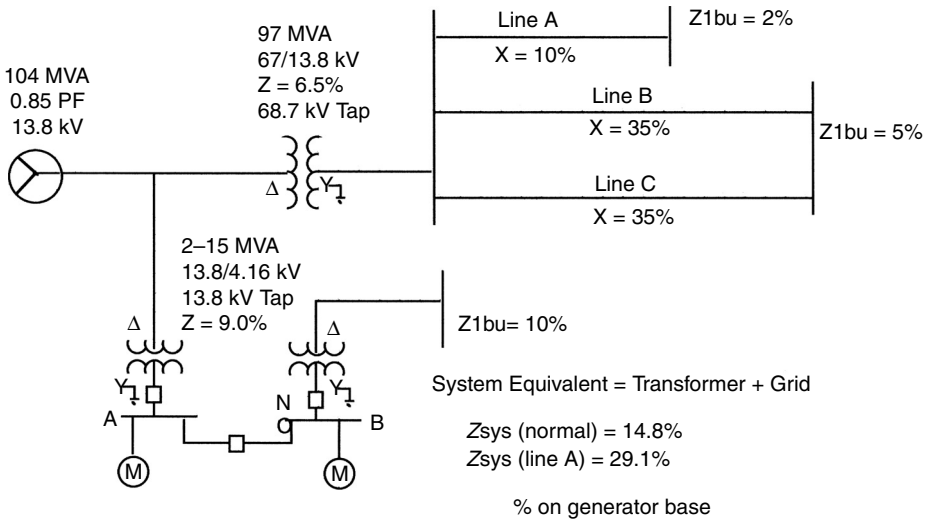


FIGURE 1.1 System online.

These allowable variations are defined by the generator capability curve, which is provided by the manufacturer. Figure 1.2 is such a curve plotted for a hydrogen-cooled generator. It defines the Watt/Var operating limit as a function of coolant pressure. Note that the maximum design coolant pressure for the generator defines the outermost boundaries, 75# H_2. The actual coolant pressure for an operating unit is often less than the design maximum pressure.

The capability curve shown is for a steam-driven generator with a cylindrical rotor. It is a composite of three distinct limits. The right-hand section, between the B and C, represents the limit

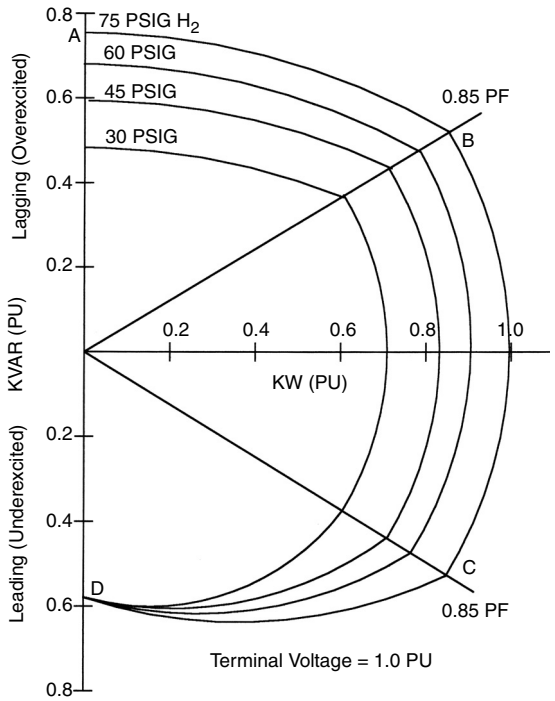


FIGURE 1.2 Generator capability curve.

© 2006 by Taylor & Francis Group, LLC

imposed by the ampere rating of the stator winding. The ampere rating of the field winding imposes the limit between A and B, which limits the output of Vars into the power system. These are termed "lagging Vars." The bottom limit, C to D, defines the maximum Vars the generator can consume from the power system. These are termed "leading Vars." This limit is the result of heating in the end laminations of the stator core. It is caused by flux that flares from the end of the stator when the generator is operating at low field current. The capability curve is normally plotted at the rated terminal voltages for the generator.

The capability curve for a hydro unit will differ from that of a steam unit. Hydro units are of salient pole construction and do not have end core regions. Thus they will only have two distinct limits. The field circuit imposed lagging Var limit from A to B and the stator winding current limit which for a hydro unit extends as a continuous arc from B to D. The leading Var limit is determined by the current rating of the stator winding.

1.3 VOLTAGE LIMITATIONS

The allowable voltage variations at the generator terminals may be bounded by the operating limits of the generator or connected transformers. ANSI/IEEE C50.12 and C50.13 define the permissible operating range of cylindrical rotor or salient pole machines to be $\pm 5\%$ rated voltage.

Standards set two voltage requirements for transformers. The primary winding must be capable of operating continuously at the voltage required to carry rated transformer load at 80% power factor (pf) with 105% rated voltage at the secondary terminals. The transformer shall also be capable of operating at 110% rated voltage with no load. These requirements must be met for any primary or secondary tap position.

To determine the actual voltage limitation at the generator terminals, an evaluation of both these voltage limits is required. Remember that the secondary winding (output winding) of the GSU transformer is the high-voltage winding.

1.3.1 Sample System GSU Transformer Limits

The GSU transformer is rated 67 kV to 13.8 kV, but it is operating on the 68.7 kV tap. Therefore, the generator side winding (the primary winding) must be capable of operating at the voltage necessary to produce 105% of 68.7 kV (72.1 kV) on the high-side winding with rated load at 80% lagging pf.

Calculating the primary voltage for this condition using the transformer impedance of 6.5%:

$$I = \frac{\text{kVA}}{E_{\text{sec}}} = \frac{1.0}{1.05} = 0.952\angle -36.9^\circ = 0.76 - j0.57$$

$$E_P = 1.05 + j0.065\,(0.76 - j0.57) = 1.087 + j0.050$$
$$= 1.088\angle 2.6^\circ$$

Standards therefore require this transformer to be capable of operation with a primary voltage of 108.8% or 15.01 kV. This transformer has low impedance; consequently, the primary voltage at rate load is less than the 110% rating required for no load operation. Therefore, maximum allowable continuous voltage on the primary (low-voltage) winding is 110% as defined by the no load requirement. Transformers with higher impedance will have allowable voltage limits greater than 110%, as determined by the rated load condition.

The above example is academic for the sample system because the generator and transformer windings are both rated at 13.8 kV. Since the generator is limited to $\pm 5\%$ rated voltage, the operating range for the 13.8 kV system is obviously $\pm 5\%$.

It is common practice to rate the transformer low-voltage winding 95% of the generator rating. In these systems the transformer may limit the upper end of the operating range.

© 2006 by Taylor & Francis Group, LLC

1.4 SYSTEM LIMITATIONS

In practice, most units cannot operate at the boundaries of the generator capability curve. The MW output of the generator is limited by the driving torque available for the turbine, not the ampere rating of the stator winding. The turbine is normally sized just large enough to produce rated MW at rated power factor. A vertical line through points B and C of Figure 1.2 would define the practical MW limit for most generators.

The Var output of the generator is a function of the generator terminal voltage, system impedance and system voltage. It is common to encounter transformer or generator voltage limitations before a generator Var limit is reached.

The relationship between real and reactive power, system voltage and impedance is often represented as a circle diagram.[1] A generator connected to a system and operating with a fixed terminal voltage will have a unique Var output for every value of real power output. The circle diagram is the locus of these points and will have the following characteristics:

$$\text{Center} = Et^2/Z\text{sys}$$
$$\text{Radius} = Et * E\text{sys}/Z\text{sys}$$

where
Et = generator terminal voltage
Esys = system voltage
Zsys = impedance between Et and Esys

If resistance is neglected, the center is located on the overexcited (Var out) axis, as shown in Figure 1.3.

A circle diagram for the sample system is plotted over the capability curve for the sample system generator in Figure 1.4. This plot shows the possible operating points at the generator

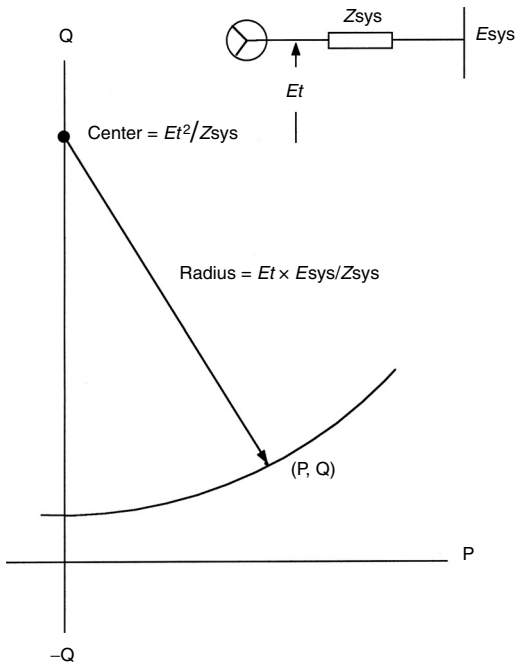


FIGURE 1.3 Power circle diagram.

© 2006 by Taylor & Francis Group, LLC

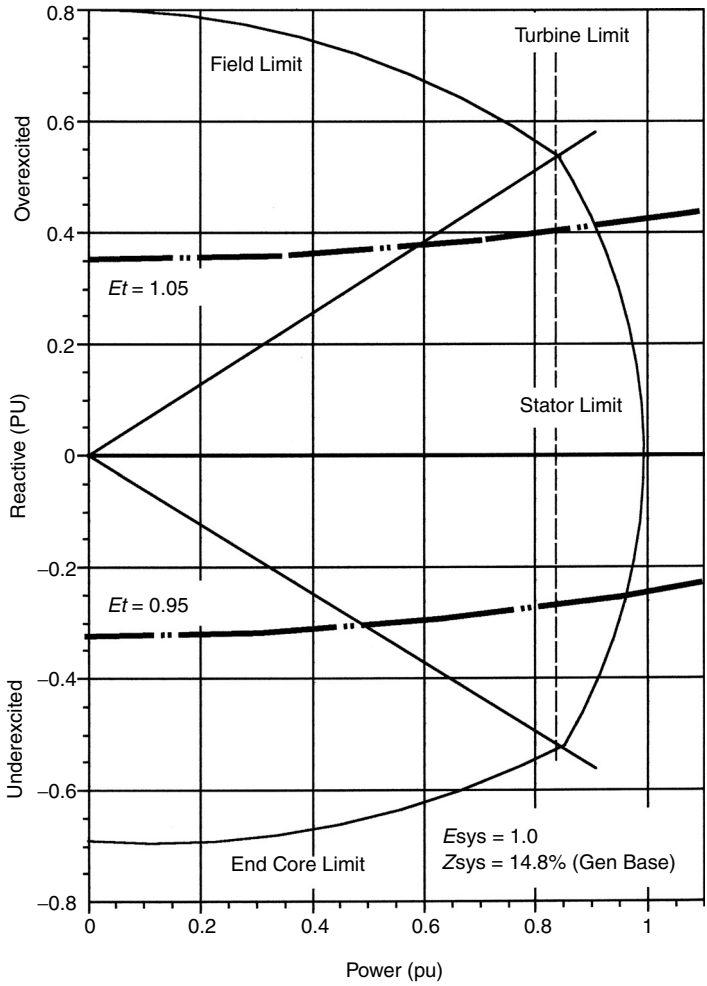


FIGURE 1.4 Practical operating limits: System normal.

voltage limits of 1.05 and 0.95 per unit (pu). The system impedance is normal (no lines out) and system voltage is 1.0 pu. Var output with 1.05 pu terminal voltages is about half the overexcited Var capability of the generator. To utilize the full overexcited Var capability of the generator, the terminal voltage would have to be increased significantly. Likewise, with the terminal voltage at 0.95 pu, the generator is only absorbing about half its leading Var capability. To utilize the full leading Vars capability of the generator, the terminal voltage must be reduced.

Since the terminal voltages plotted, $\pm 5\%$ rated, are the maximum and minimum operating voltages permitted by generator standards, the sample system generator's Var output will be limited by terminal voltage, not generator capability curve.

A voltage limitation would be expected on a relatively weak system like the sample system. The weaker the system, the more severe the limitations. Figure 1.5 shows the effects of switching out the strongest tie line in the sample system, Line A. The equivalent impedance of the system, as seen by the generator terminals, increases from 14 to 29%; as a result, the permissible operating area is sharply reduced.

Variations in system voltage also have a significant effect on the actual operating limits. Figure 1.4 and Figure 1.5 assumed a constant system voltage, but, as previously stated, system

© 2006 by Taylor & Francis Group, LLC

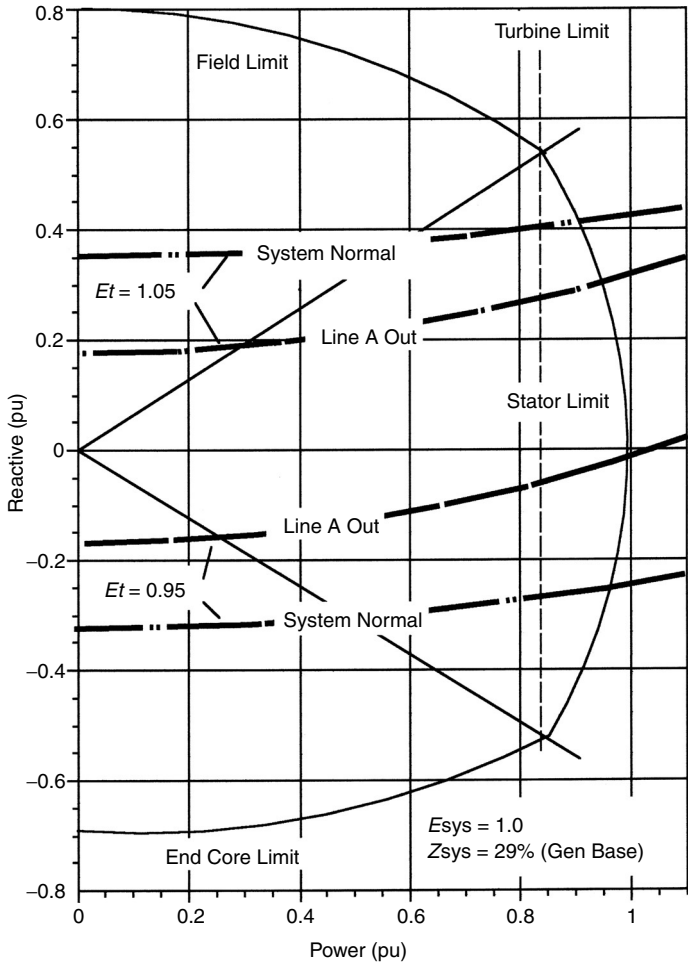


FIGURE 1.5 Practical operating limits: Line A Outaged.

voltage varies significantly between hot summer afternoons with peak system MW and MVAR loads and spring nights with very light loads. The effects of system and terminal voltage variations are shown in Figure 1.6. The three curves in the upper portion of the capability curve are plotted for a generator terminal voltage of 1.05 with the system voltage at 0.96, 1.0, and 1.055 pu. The three curves in the lower portion of the curve represent $Et = 0.95$ pu with the same variations in system voltage.

It is evident that an increased system voltage shifts down the allowable operating area, closer to the underexcited generator limit. This characteristic is desirable. During periods of excess system voltage, the generator would be required to operate in the leading region, taking in Vars from the grid, to reduce system voltage. Conversely, low system voltage shifts the operating area toward the overexcited limit. Again, this shift is beneficial, allowing the unit to maximize Var output to bolster sagging system voltages.

The key point here is that although the sample system generator may appeal severely voltage limited by Figure 1.4 (Esys $= 1.0$) when system conditions require full Var capability this capability is available (Figure 1.6).

© 2006 by Taylor & Francis Group, LLC

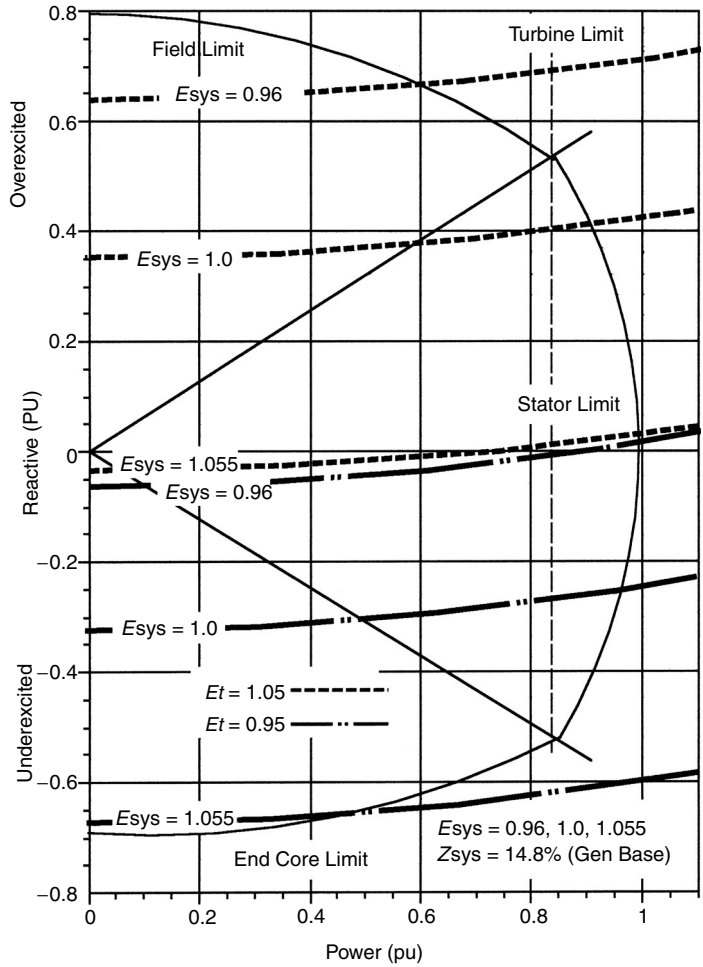


FIGURE 1.6 Practical operating limits: All lines in, vary grid voltage.

1.5 GENERATOR CAPABILITY VARIATIONS WITH VOLTAGE

Load and system conditions require most generators to operate over a wide range of terminal voltages. The operating terminal voltage range allowed by standards is 95–105% of rated voltage, but generator capability curves are only plotted for rated terminal voltage. It is possible to estimate portions of the capability curve for other operating voltages, but knowledge of the construction of the curve is required.

The stator winding limit is an arc centered at the origin of the capability curve ($P = 0$, $Q = 0$). This is shown as radius "Ra" in Figure 1.7. The length of Ra in MVA is equal to the (rated KA amperes of the stator winding at a given coolant pressure) × (generator rated kV) × $\sqrt{3}$. To adjust this section of the curve for other than rated voltage, multiply the Ra by the new operating voltage/rate voltage. Figure 1.7 shows the construction of the stator limit at 0.95 and 1.05 pu terminal voltage.

Adjustment of the upper region of the capability curve, which is limited by the ampere rating of the field winding at a given hydrogen pressure, is more difficult. The field amps do not relate directly to the Var loading on the generator. The overexcited Var limit is a function of the generator

© 2006 by Taylor & Francis Group, LLC

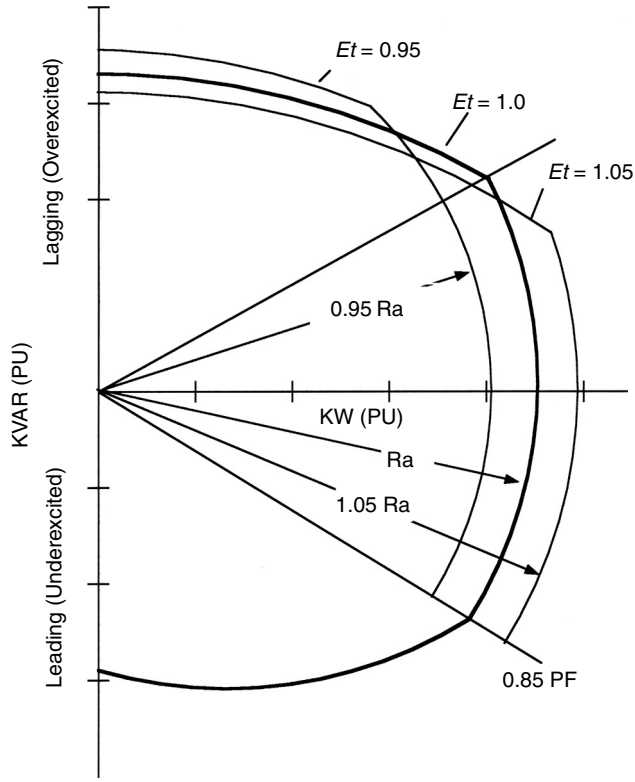


FIGURE 1.7 Stator capability variations with voltage.

terminal voltage produced by rated field current, system voltage, and the generator steady-state impedance. The upper portion of the capability curve is a power circle plot with a center on the −Q axis. The center and radius are:

$$\text{Center} = -Et^2/X_\text{d}$$
$$\text{Radius} = Et * EI/X_\text{d}$$

where EI is the internal generator voltage and X_d is the synchronous impedance (steady-state impedance) of the generator. The location of the center of this circle changes with the square of the terminal voltage, while the radius varies directly with the terminal voltage.

The construction of the field current limit at 0.95 pu terminal voltage is shown on Figure 1.8. First the center of the field current limit at $Et = 1.0$ pu is located by trial and error at point C. This also defines the radius of the limit at rated terminal voltage that is shown as Rf. To establish the limit at $Et = 0.95$, the center of the 0.95 pu limit is found by shifting point C toward the KW axis by a factor 0.95^2. The radius of the 0.95 limit is 0.95 Rf.

The construction described for the field current limit at varied terminal voltage is an estimate. Field current requirements in the overexcited region are influenced by saturation in the magnetic circuits of the stator and rotor. Since saturation is nonlinear, the method described will tend to produce conservative results at reduced voltage and optimistic results at voltages above rated.

No attempt has been made here to estimate variations of the leading Var limit with voltage. This limit is strongly influenced by the thermal characteristics of the end core region of the stator. Any determination of leading Var variation with voltage for use during operations must be determined by the manufacturer. A theoretical derivation of this variation is presented in Chapter 11.

© 2006 by Taylor & Francis Group, LLC

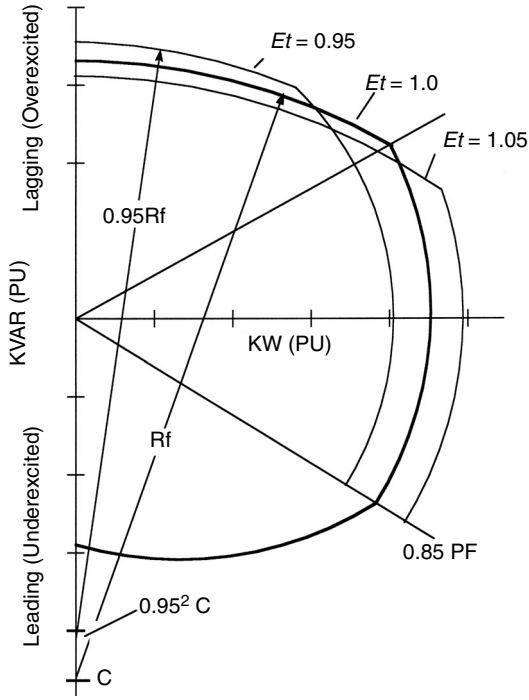


FIGURE 1.8 Field limit variations with voltage.

1.6 EXCITATION SYSTEM

The sample system generator uses a static excitation system as shown in Figure 1.9. This type of system does not include rotating equipment such as an exciter to provide power to the generator field. In the Sample System field, power is derived from an AC auxiliary system bus in

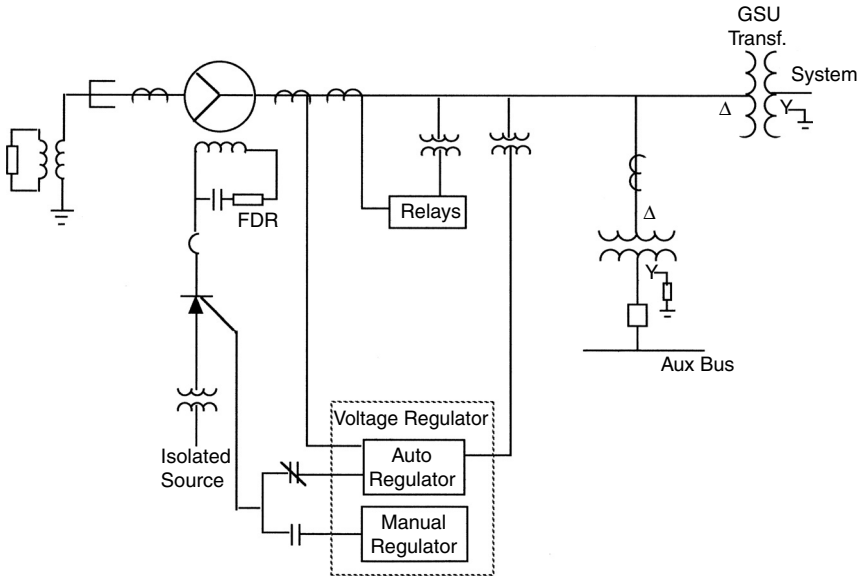


FIGURE 1.9 Generator online.

© 2006 by Taylor & Francis Group, LLC

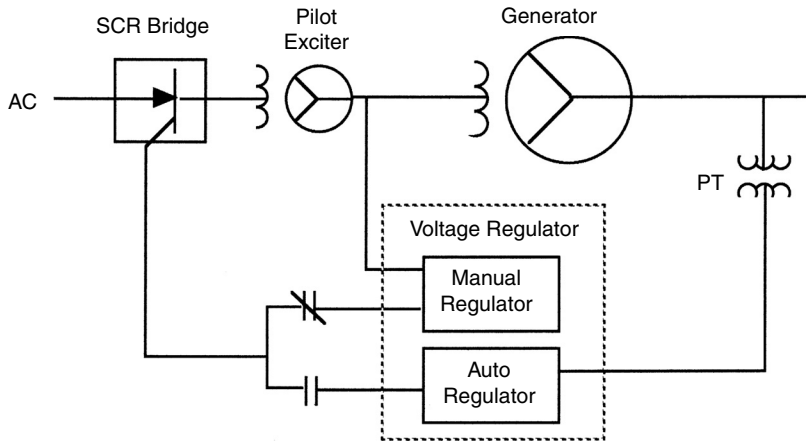


FIGURE 1.10 Pilot exciter.

the plant. The AC voltage is applied to a three-phase bridge rectifier that employs silicon-controlled rectifiers (SCRs). The voltage regulator dictates the firing of the SCRs to control the field current. Static systems have several advantages over rotating systems. They are less expensive to install and maintain. They also have a very fast response. Excitation system speed is a key factor in power system stability. The speed of a rotating system such as that shown in Figure 1.10 is limited by the inherent delays in the exciter's magnetic circuits. The SCRs in a static system can respond almost instantaneously. The only delay in a static system comes from the voltage regulator circuitry.

A disadvantage of this static system is the dependence on the auxiliary bus voltage for generator field power. During system disturbances, the auxiliary bus voltage may decay and reduce the power available to the generator field when that power is most needed. Static excitation system design must provide sufficient margin to assure that generator field current requirements during system disturbances are met with reduced AC system voltage.

There are many other types of excitation systems. Figure 1.11 is a self-excitation system. Power for the generator field is taken from a power potential transformer (PPT) at the generator terminals. A supplementary DC power source may be required to initiate a voltage buildup during startup (field flashing). This system is common with small generators. The main disadvantage is that, because the generator depends on its own voltage for field excitation, this form of

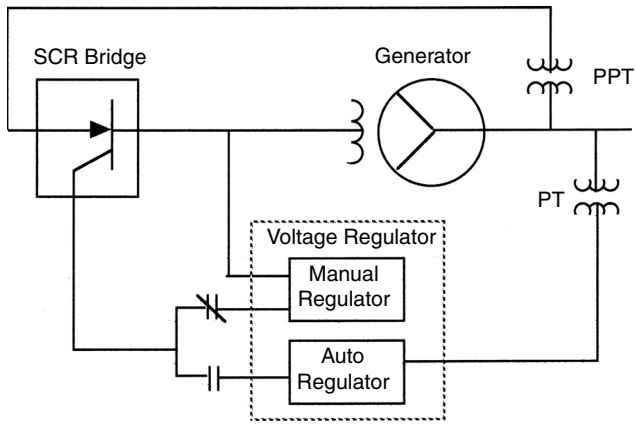


FIGURE 1.11 Self-excited generator.

© 2006 by Taylor & Francis Group, LLC

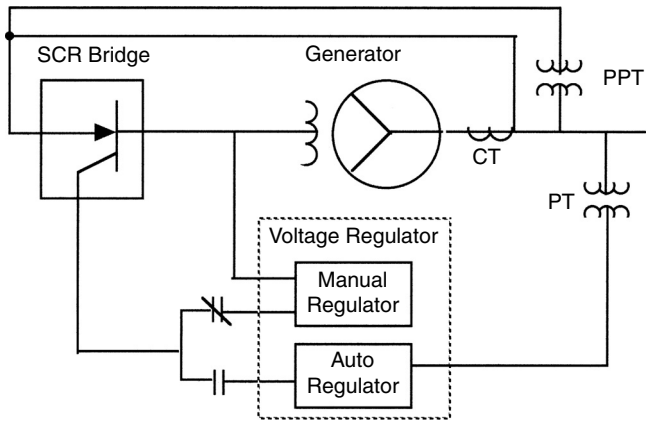


FIGURE 1.12 Self-excited generator with current transformer boost.

excitation can collapse when generator terminal voltage is depressed as would occur during a fault or motor starting. To prevent such a collapse, current transformers (CTs) can be installed to provide additional field current during periods of depressed voltage such as faults and motor starting as shown in Figure 1.12.

A rotating excitation system is shown in Figure 1.10. This type of excitation system is found on large units. It is expensive to apply an SCR-type bridge rectifier directly in the field circuit of large machines because the rate field current often exceeds 5000 A DC. In this system, a moderately rated SCR bridge rectifier in the exciter field circuit can control the large current in the generator field circuit. Of course, the introduction of the rotating exciter does reduce the speed of the excitation system as compared to an all-static system.

The exciter bus system shown in Figure 1.13 has no regulators. It is a fixed field current system where the operators must constantly adjust the rheostats to maintain the required terminal voltage in response to system conditions. This arrangement is common on older hydro stations where a DC bus would provide excitation for a dozen on more small hydro units.

A voltage regulator is a key component of all modern excitation system. The concept that the voltage regulator's function is to maintain output voltage constant as loading varies is an oversimplification. The voltage regulator actually contains two regulating devices: the automatic voltage regulator (AVR) and the manual voltage regulator (MVR), or DC regulator, as it is sometimes called.

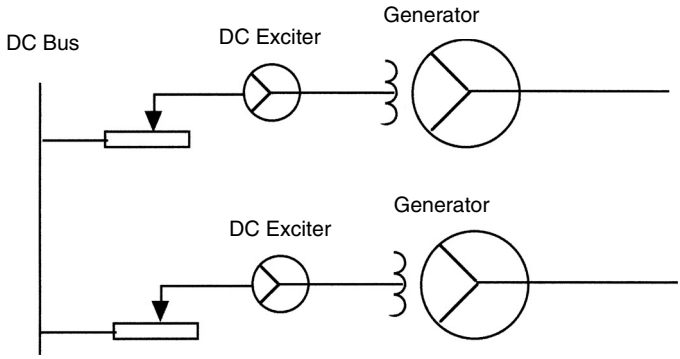


FIGURE 1.13 Exciter bus.

© 2006 by Taylor & Francis Group, LLC

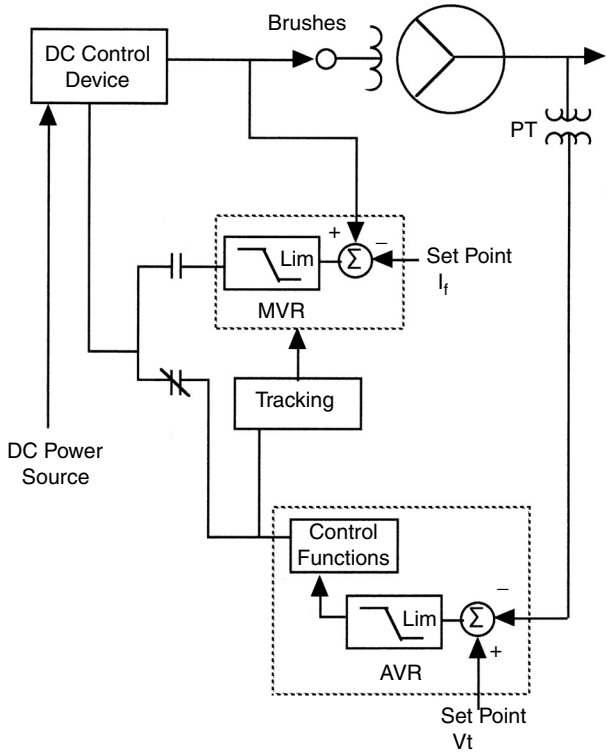


FIGURE 1.14 Automatic and manual regulators.

The automatic regulator has inputs from potential transformers at the generator terminals, as shown in Figure 1.14. It monitors this voltage and compares it to a voltage set point that is under the control of the plant operators. As generator load varies, the AVR adjusts the field current to maintain the generator terminal voltage at the set point value. The manual regulator's control function is to maintain a preset value of generator field current or field voltage depending on the design with no regard to the output voltage or any other power system quantity. A generator should always be under the control of the automatic regulator when it is synchronized to the power grid. The manual regulator would be placed in service in the event of an automatic regulator failure. In older voltage regulators it may also be necessary to place the generator on manual regulator during startup, to prevent damage from overexcitation. This will be discussed in later chapters.

Operation on the automatic regulator is important, and not just from the standpoint of relieving the operator of the responsibility of maintaining system voltage. The automatic regulator's quick response to system conditions is a major factor in maintaining power system stability during and after system disturbances. When a disturbance such as a fault causes a reduction in system voltage, the glue that holds generators throughout the grid in synchronism is weakened. A severe disturbance would result in the loss of synchronism and widespread outages. When generators are operating under AVR control, the voltage regulator will sense the reduced voltage and rapidly increase the field current to bolster system voltage and maintain synchronism.

Another reason generators should always operate under automatic regulator control is that the automatic regulator also performs protective functions. Most automatic regulators include the following protective features:

- Maximum field current limits
- Minimum field current limit

© 2006 by Taylor & Francis Group, LLC

- Volts/Hz limit (flux)
- Leading Var limit

These functions are not in service when the manual regulator is in control of the generator field. Each of these protective limits will be discussed at length in later chapters.

The manual regulator is a backup for the automatic voltage regulator and is not in control of the generator field during normal operations. While the automatic regulator is controlling field current, the manual regulator is on hot standby, tracking the automatic regulator. As the auto regulator varies the field current to maintain voltage, the manual regulator automatically adjusts its set point to match the field current or voltage prescribed by the automatic regulator. Should the automatic regulator fail, the manual regulator would take immediate control of the generator without an abrupt change in field current. This "bumpless" transfer is necessary to avoid generator and power system transients. Without the tracking feature, the manual regulator would take control of the generator and drive the field current to whatever value was last set on the manual regulator. If the manual regulator were last used during startup, the set point would be for a low value of field current. A failure of the automatic regulator at full generator load would result in a drastic reduction in terminal voltage and major system disturbance, which could include a loss of synchronism. Conversely, a high current setting on the manual regulator could result in damaging overvoltage if the automatic regulator failed during a period of moderate generator loading.

REFERENCE

1. Westinghouse Electric Corp., *Electrical Transmission and Distribution Reference Book*, 4th Ed. Westinghouse, East Pittsburgh, PA, 1964.

© 2006 by Taylor & Francis Group, LLC

2 Generator Short Circuit Calculations

2.1 INTRODUCTION

The material covered in this chapter is the most difficult in the book. Less rigorous approaches to the subject exist, but the intent here is to provide more than just a method of calculation. The presentation is intended to provide insight into fault current dynamics and the parameters found on the generator data sheet that define short circuit characteristics of the generator.

2.2 SHORT-CIRCUIT CURRENT CHARACTERISTICS

A short circuit at the terminals of a synchronous generator produces current with decaying AC and decaying DC components. The decaying DC component is a feature of fault currents anywhere in an AC power system. Breaker interrupting ratings and bus bracing are calculated based on the effects of the decaying DC component and the asymmetrical fault current it produces.

The decay of the AC component is a characteristic unique to short circuits near rotating machines. Figure 2.1 shows typical fault current from a synchronous machine. The waveform is initially displaced from the zero axis by a DC component, which disappears in a few cycles. The decay of the AC component is also evident. The AC component may initially have a value as high as 11 times rated current, and typically decays to a steady-state value of 40% to 120% of rated generator current in 2 to 5 seconds, assuming field excitation is not changed. Figure 2.2 separates the AC and DC components so their individual decay can be seen more clearly.

Generator fault current is normally discussed in terms of "subtransient," "transient," and "synchronous" currents and impedances. These terms refer to various time periods during the decay of the *AC component* of current. Figure 2.3 plots the envelope of the AC current for a typical machine. The subtransient current, reactance and related time constant defines the AC current component from the inception of the fault and the following cycle or two. This is the maximum available AC short-circuit current from the generator. Synchronous quantities define the final or steady-state current. The transient parameters define the interim current.

2.3 GENERATOR INTERNAL MAGNETICS

Transmission system fault calculations assume a single voltage source behind and fixed equivalent impedance. The transient response of a synchronous generator to a short circuit is much more complex than the transmission model and cannot be represented by a single voltage source or single impedance. To understand generator fault calculations, some explanation of the machine's internal workings is necessary.

When a generator is operating at no load, that is, with the generator breaker open, the only flux produced in the machine is a result of the DC current in the field windings on the rotor. This rotor flux bridges the air gap between the rotor and the stator and travels around the perimeter of the stator at rotor speed, as shown in Figure 2.4. As it sweeps across the stator, it passes through the A, B, and C phase stator windings, inducing a voltage in each stator coil.

The instantaneous flux in the "A" phase stator winding is a function of the air gap flux magnitude and the angle α between the rotor and the center of the A phase coil. This angle

© 2006 by Taylor & Francis Group, LLC

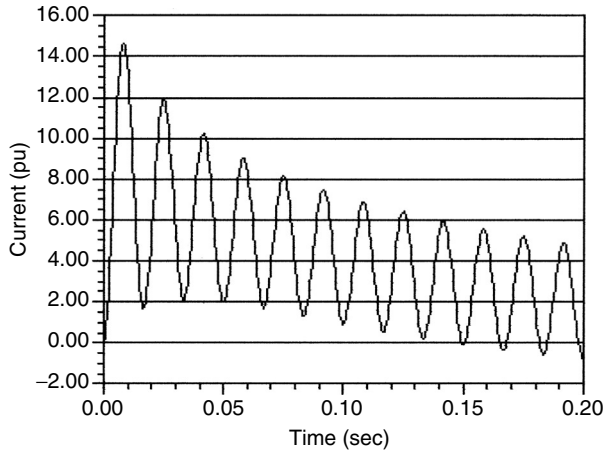


FIGURE 2.1 Generator asymmetric fault current.

varies with time. Assuming a rotor speed of ω, then $\alpha = \omega * t$ and the A phase flux becomes:

$$\Psi_a = \Psi_{rot} \cos \alpha = \Psi_{rot} \cos \omega t$$

From the perspective of a point on the rotor, the field flux appears as a DC flux. When viewed from a point on the stator, the flux appears sinusoidal. Since the phase windings are physically spaced 120 electrical degrees apart around the stator, the flux in each phase is displaced by that same amount

$$\Psi_b = \Psi_{rot} \cos (\omega t + 120^\circ)$$
$$\Psi_c = \Psi_{rot} \cos (\omega t - 120^\circ)$$

The voltage induced in a stator winding is defined by Faraday's law, which states that the voltage induced in a coil is a function of the rate of change of the flux and the number of turns, N. For current out of the generator:

$$e = -N \frac{d\psi}{dt}$$

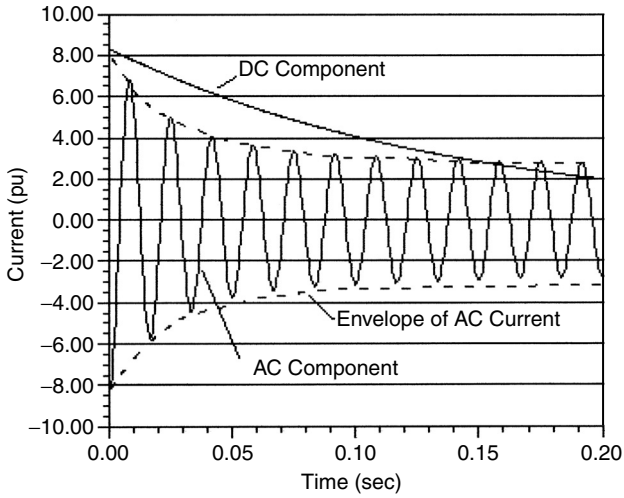


FIGURE 2.2 Fault current components.

© 2006 by Taylor & Francis Group, LLC

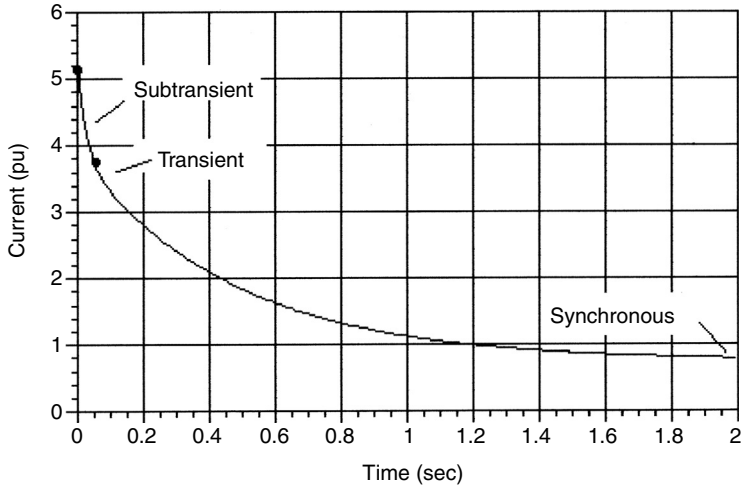


FIGURE 2.3 Subtransient, transient, and synchronous intervals.

Substituting the phase flux expressions into Faraday's equation and taking the derivative, the phase voltages becomes

$$e_a = \omega \Psi_{rot} N \sin(\omega t)$$
$$e_b = \omega \Psi_{rot} N \sin(\omega t + 120^\circ)$$
$$e_c = \omega \Psi_{rot} N \sin(\omega t - 120^\circ)$$

A plot of the cosine dependent phase flux and the sine dependent voltage shows that the voltage lags the rotor flux by 90° in each phase. Just as sinusoidal flux in each phase winding is a projection of

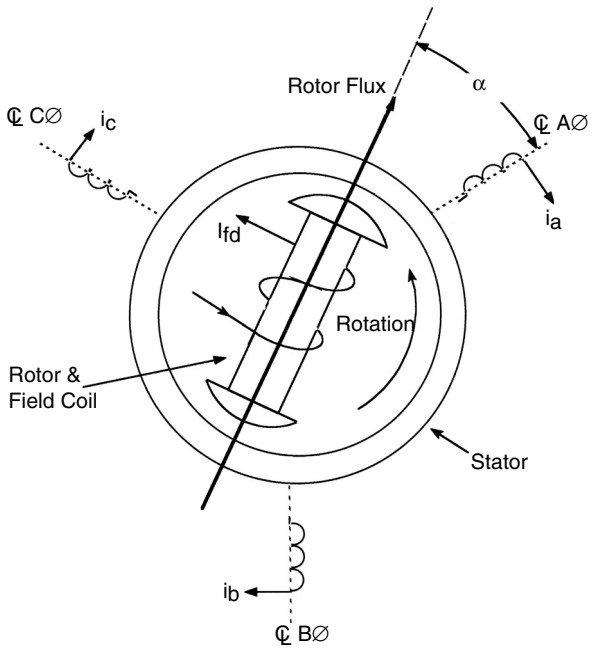


FIGURE 2.4 Rotor flux.

© 2006 by Taylor & Francis Group, LLC

the DC rotor flux, the induced phase voltages can be related to a theoretical DC rotor voltage that lags the rotor flux by 90°. This voltage is referred to as the quadrature voltage, E_q. It is proportional to the rotor flux and DC field current. E_q is substituted for the rotor flux to allow circuit analysis on the basis of current and voltage instead of flux and mmf.

For the no load condition, the phase voltages could be written as

$$e_a = E_q \sin(\omega t)$$
$$e_b = E_q \sin(\omega t + 120^\circ)$$
$$e_c = E_q \sin(\omega t - 120^\circ)$$

The terminal voltage of the generator under load differs from the above stator induced voltage by the *IZ* drop in the stator winding.

When the generator is under load, the stator current will lead or lag E_q by angle B, depending on whether the load is capacitive or inductive, as shown in Figure 2.5. Note that angle B is not the power factor angle. The power factor angle is measured between the current and the generator terminal voltage; under load, E_q is an internal generator voltage.

Load current produces a second flux within the generator. This flux, sometimes referred to as the armature reaction flux, is formed in the air gap by the vector summation of the alternating flux in each stator phase winding. The intuitive conclusion would be that the summation of the phase flux

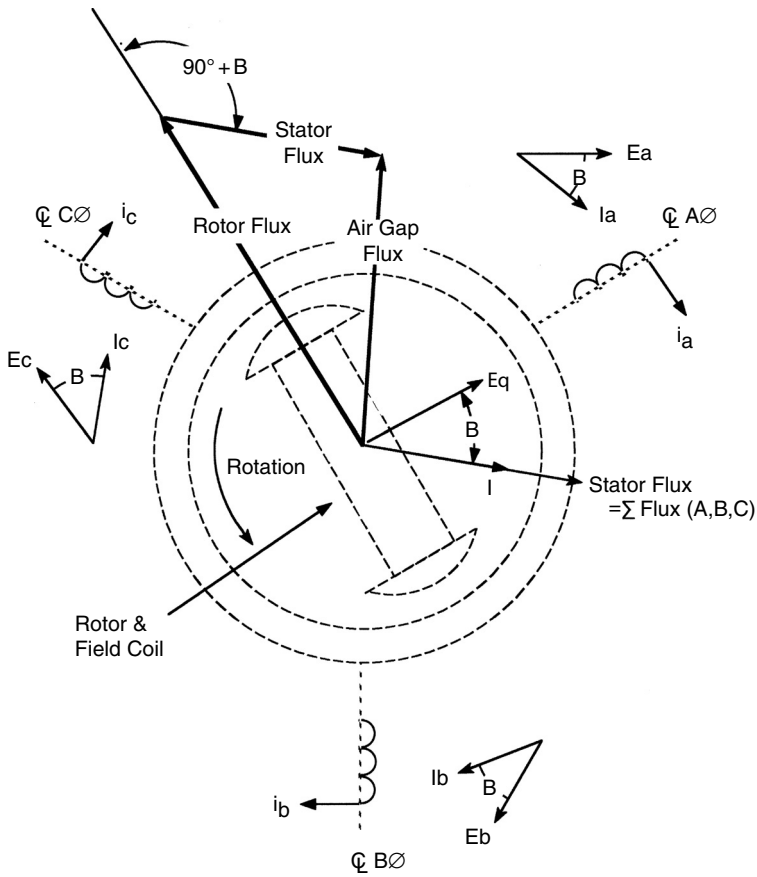


FIGURE 2.5 Rotor and stator flux.

© 2006 by Taylor & Francis Group, LLC

would be zero, because the balanced load currents that produce the individual phase flux sum to zero. This conclusion would be correct if the phase windings were physically aligned with each other. The individual phase flux would then be displaced by 120° and sum to zero just as the currents do. However, since the stator windings are physically displaced by 120° around the stator, the individual phase flux are shifted and produce a resultant flux that is in phase with the "A" phase stator current and lags the rotor flux by $90^\circ \pm$ B, as shown in Figure 2.5.

The air gap flux induces the voltage in the stator windings. In the case of the unloaded generator, this flux is equal to the rotor flux. On a loaded generator, the air gap flux is equal to the vector sum of the rotor and armature reaction flux. When the generator is supplying lagging current, the armature reaction flux detracts from the rotor flux, reducing the voltage induced in the stator windings and hence the terminal voltage. Leading current produces an armature reaction flux that is additive to the rotor flux, boosting the induced stator voltage and the generator terminal voltage. Figure 2.5 depicts a lagging current and a reduction in air gap flux.

2.4 GENERATOR MAGNETIC STRUCTURES

The preceding discussion of generator flux and current is a necessary prerequisite to the discussion of the electrical behavior of the generator under fault conditions. Under load, the vector summation of rotor and stator flux forms the air gap flux. The air gap flux in turn defines the internal voltages used in calculating the generator fault current. The transient behavior of the fault current is governed by the interaction of the air gap flux and the magnetic circuits within the generator.

Figure 2.6 shows the relationship of the air gap flux to the various internal machine structures during normal operation. The generator has two distinct magnetic circuits. The first is aligned with the field pole and is referred to as the "direct" or "d-axis." It contains the rotor field

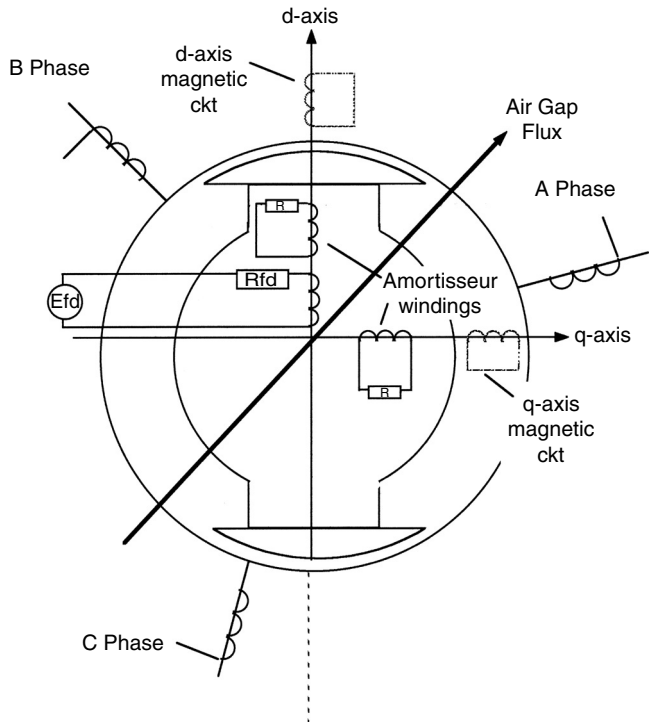


FIGURE 2.6 Air gap flux and internal magnetic circuits.

© 2006 by Taylor & Francis Group, LLC

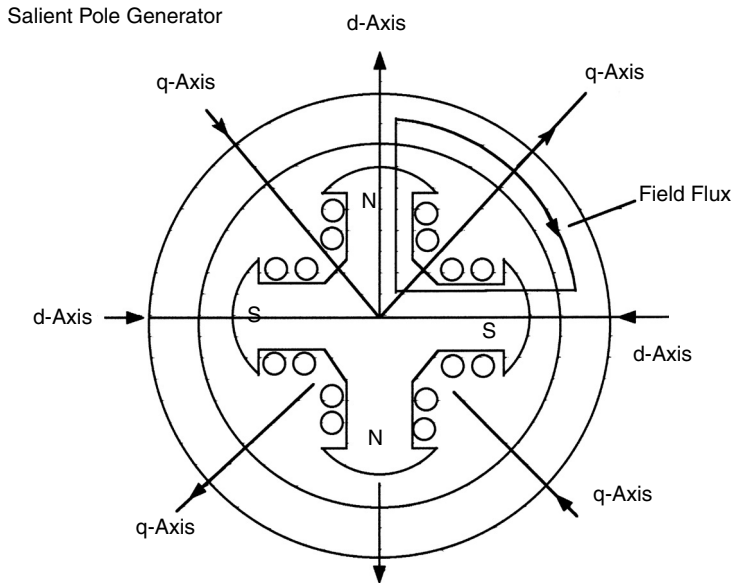


FIGURE 2.7 Salient pole generator.

winding and is characterized by a small air gap. The other magnetic circuit path, known as the "quadrature" or "q-axis," lies between the field poles. This path has a larger air gap and is electrically 90° from the direct axis. Stabilizing windings, called amortisseur windings, or structures that act as stabilizing windings may also be found in one or both axes. Each path, because of the differences in air gap length and because of different windings located in the path, has unique steady-state and transient behavior.

The electrical differences between d- and q-axis paths are more pronounced in the salient pole machine because the pole structures in the salient pole machine creates a much longer air gap in the q-axis than occurs in the d-axis. Figure 2.7 and Figure 2.8 contrast the construction of the salient and round rotor generators. The salient pole design is applicable to low speed generators, primarily hydro unit. These machines require higher pole flux to achieve a given output

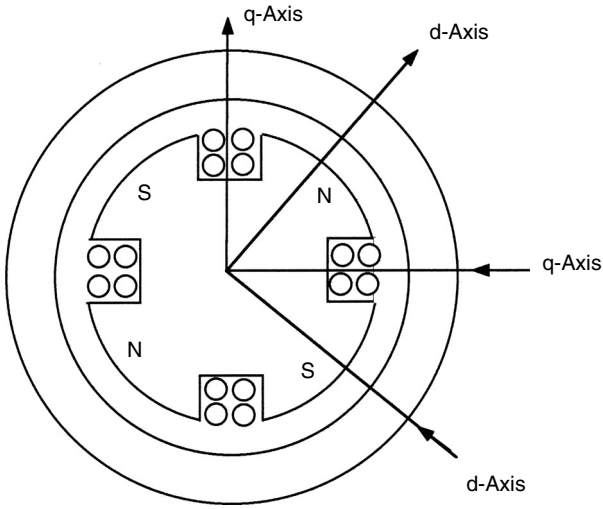


FIGURE 2.8 Round rotor generator.

© 2006 by Taylor & Francis Group, LLC

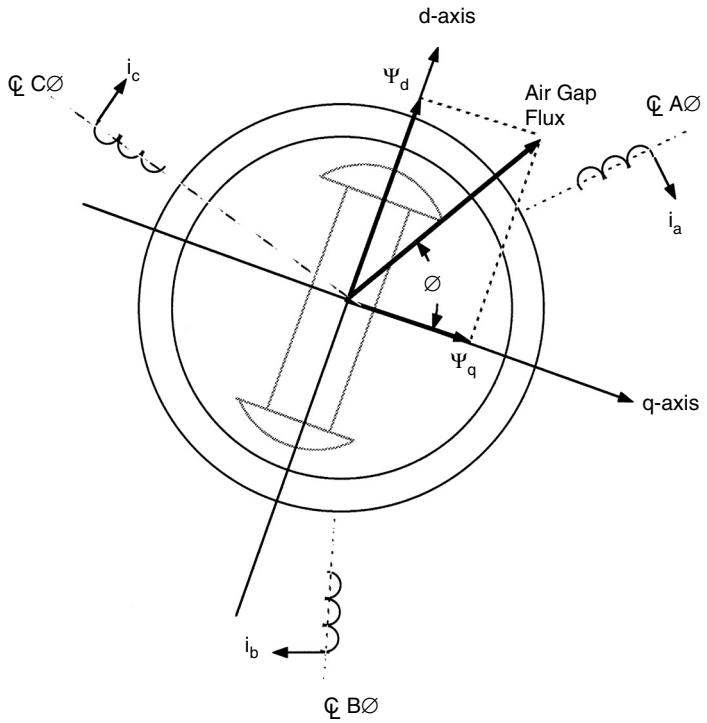


FIGURE 2.9 Air gap flux d- and q-axes components.

voltage. For high speed machines, steam and most other applications a round rotor is used. Because salient rotors will not withstand the mechanical forces of high speed operation. Also note the orientation of the d- and q-axes on the multipole machine. The distance from N–S pole is 180 electrical degrees with two poles one physical revolution of the rotor is 720 electrical degrees. To produce 60 cycle power, a two-pole machine must rotate at a speed 1800 r/min compared to the single pole machine, which must rotate at 3600 r/min.

The air gap flux can be represented by flux components projected on the d- and q-axes, as shown in Figure 2.9. These components are aligned with the machine's two magnetic circuits to facilitate analysis. Because the two axes are at right angles to one another, there is no magnetic interaction between them and the analysis of each axis can be carried out independently of the other.

Generator behavior is predicted by determining the response of each axis individually, then combining the d and q components to define the air gap reresponse. The variations of the air gap flux determine the transient characteristic of the short-circuit current.

Generator loading determines magnitude of the air gap flux and angle ∅ in Figure 2.9; hence, it determines the initial magnitude of the flux component in each axis. Flux linkages between the various windings cannot change instantaneously. When a fault occurs, the initial current is determined by the flux linkages "stamped" into each axis by the prefault load condition.

For fault analysis, the d- and q-axes magnetic paths are represented as equivalent electrical circuits. The d-axis contains the field winding and the q-axis does not; thus, different equivalent circuits apply for each axis. In theory the equivalent circuits shown in Figure 2.10 could be used to represent the two axes.

When a fault occurs at the generator, it has the effect of simultaneously closing the switches in each equivalent circuit. The d- and q-axes circuits have multiple loop current paths; each path has a unique time constant and initial driving voltage. The driving voltages are representative of the

© 2006 by Taylor & Francis Group, LLC

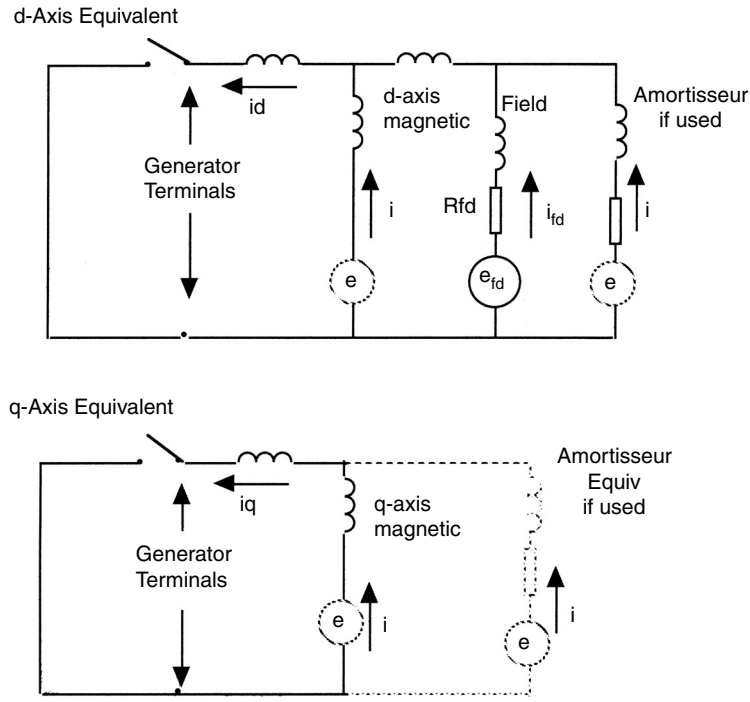


FIGURE 2.10 Equivalent electric circuits: d- and q-axes.

initial flux linkages. This multiloop configuration gives rise to the multi-exponent (subtransient, transient) decay characteristic of the generator fault current shown in Figure 2.3.

The next logical step toward the determination of generator fault current is the derivation and solution of loop equations based on the equivalent circuits. The problem here is that the circuit parameters used in the d- and q-axes circuits shown in Figure 2.10 are internal generator reactances. Values for these elements cannot be determined directly from test. Theoretical values can be obtained, but such calculations are suspect because of the complexities of structure and magnetic paths within the machine. Consequently, an alternative method has been derived as the basis for engineering calculations.

The dual exponential decay is a signature of generator fault current. This decay can be described by the characteristic equations shown below.

d-Axis characteristic equations:

$$i_{\mathrm{d}} = (I''_{\mathrm{d}} - I'_{\mathrm{d}})e^{-t/T''d} + (I'_{\mathrm{d}} - I_{\mathrm{d}})e^{-t/Td'} + I_{\mathrm{d}} \tag{2.1}$$

$$i_{\mathrm{d}} = \left(\frac{e''_{\mathrm{q}}}{X''_{\mathrm{d}}} - \frac{e'_{\mathrm{q}}}{X'_{\mathrm{d}}}\right)e^{-t/T''d} + \left(\frac{e'_{\mathrm{q}}}{X'_{\mathrm{d}}} - \frac{EI}{X_{\mathrm{d}}}\right)e^{-t/T'd} + \frac{EI}{X_{\mathrm{d}}} \tag{2.2}$$

q-Axis characteristic equations:

$$i_{\mathrm{q}} = (I''_{\mathrm{q}} - I'_{\mathrm{q}})e^{-t/T''q} + (I'_{\mathrm{q}} - I_{\mathrm{q}})e^{-t/T'q} \tag{2.3}$$

$$i_{\mathrm{q}} = \left(\frac{e''_{\mathrm{d}}}{X''_{\mathrm{q}}} - \frac{e'_{\mathrm{d}}}{X'_{\mathrm{q}}}\right)e^{-t/T''q} + \left(\frac{e'_{\mathrm{d}}}{X'_{\mathrm{q}}} - \frac{Ed}{X_{\mathrm{q}}}\right)e^{-t/T'_{\mathrm{q}}} \tag{2.4}$$

© 2006 by Taylor & Francis Group, LLC

The equations are shown in two forms, in terms of subtransient, transient, and synchronous currents and in terms of subtransient, transient, and synchronous reactances. Subtransient quantities are I''_d, I''_q, X''_d, X''_q, e''_q, and e''_d. Transient quantities are I'_d, I'_q, X'_d, X'_q, e'_d, and e'_q. Synchronous quantities are I_d, X_d, X_q, Ed, and EI. The voltages included in the reactance form represent initial flux linkages. These voltages are best visualized as voltages behind each associated reactance, as prescribed by the prefault loading condition.

The q-axis equations may appear without the transient terms if the generator does not have amortisseur windings in that axis.

Having adopted this representation equation parameters for an individual generator are determined by test.

2.5 GENERATOR CONSTANTS

Generator testing normally includes short circuit tests to establish the exact transient fault current characteristic of the generator.

The test data obtained are similar to those shown in Figure 2.11. The impedances and time constants published for the d- and q-axes on the generator data sheet (Appendix A) are values, which when substituted into the characteristic equations, produce a time–current trace that matches the test results.

To understand fault calculations we will work backwards, first deriving the generator reactances and time constants from test data, then applying that data to predict fault currents for in-service fault conditions.

Figure 2.11 is a plot of the AC component of three-phase fault current obtained from a short circuit test on the sample system generator. Short circuit tests are performed with the generator initially at no load, terminal voltage at 1.0 pu, and constant generator field current. When there is no initial load on the generator and fault resistance is negligible, no q-axis current will exists for a three-phase fault. The reason for this will be made clear in Section 2.6.1. Therefore, the three-phase short-circuit test current is d-axis current only.

If the d-axis characteristic equation is evaluated at $t = 0$, the exponential terms reduce to 1.0. The d-axis current at $t = 0$ reduces to $i_d = I''_d$ (the subtransient current). Therefore, the value of the AC component at $t = 0$ is equal to the subtransient current. From the test data plotted in Figure 2.11, $I''_d = 7.35$ pu. At $t = \infty$, the exponential terms of the characteristic equation equal zero and $i_d = I_d$ (the synchronous current). The test data shows the sustained fault current, I_d, is 0.68 pu. The transient current I'_d is more difficult to isolate.

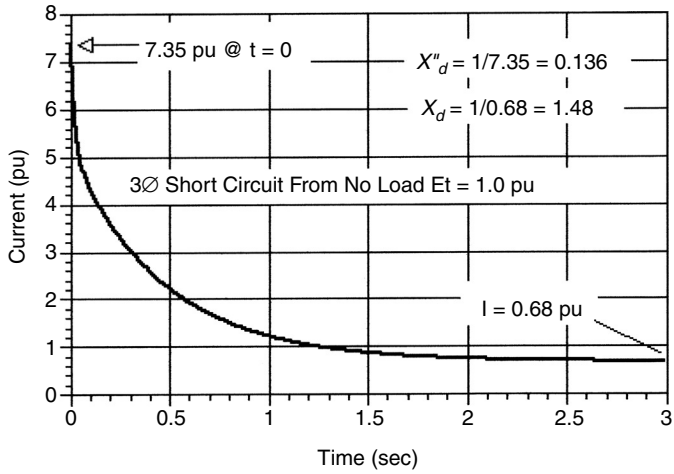


FIGURE 2.11 Short circuit test data.

© 2006 by Taylor & Francis Group, LLC

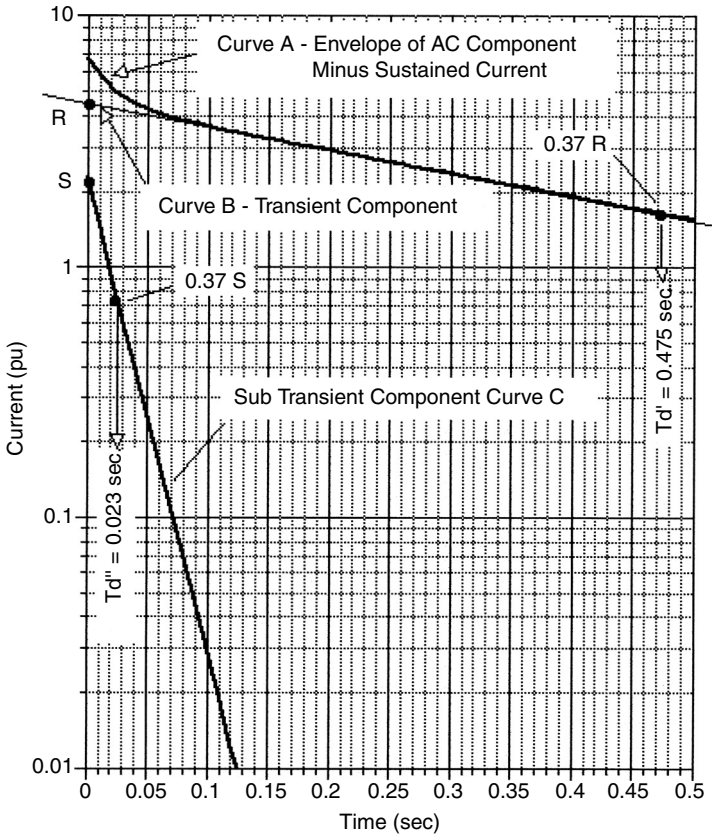


FIGURE 2.12 Transient current and time constants.

To find the transient current, I'_d, it is necessary to isolate the exponential terms of the d-axis equation. Curve A on Figure 2.12 is a semilog plot of the first 30 cycles of the AC component of fault current with the synchronous current $I_d = 0.68$ subtracted out. It is a plot of the sum of the $(I''_d - I'_d)$ and $(I'_d - I_d)$ terms of the d-axis characteristic equation, which has two distinct slopes. The initial slope is a result of the rapid decay of the $(I''_d - I'_d)$ term. The portion to the right is the slower decay of the $(I'_d - I_d)$ term after the $(I''_d - I'_d)$ term has dissipated. The transient current I'_d is found by extending the slope of the $(I'_d - I_d)$ portion back to the y-axis (curve B). The current at which this line extension crosses the y-axis ($t = 0$), shown as point R, equals $(I'_d - I_d)$ at $t = 0$. I'_d equals point R (4.4 pu) plus current I_d (0.68) or $I'_d = 5.1$.

One of the most common misconceptions relating to generator data is that there is a specific time related to the definition of the transient current and the reactance that it defines. It is clear from the above derivation that transient terms have no direct correlation to any point on the fault current decay characteristic. When transient currents or impedances are referenced, they provide only an approximation of generator conditions several cycles after a transient is initiated.

The values for the subtransient, transient, and synchronous reactances can be found from the e/x form of the characteristic equation if the prefault voltage behind each reactance is known (voltages EI, e'_q, e''_q). Since the short circuit test is performed with no initial load on the generator, there are no internal voltage drops in the generator. The voltages in question, EI, e'_{q0}, and e''_{q0} all equal the prefault terminal voltage, which is 1.0 pu. Then, the following equations apply.

Synchronous reactance

$$X_d = \frac{EI}{I_d} = \frac{1.0}{0.68} = 1.48 \text{ pu}$$

© 2006 by Taylor & Francis Group, LLC

Transient reactance

$$X'_{\mathrm{d}} = \frac{e'_{\mathrm{q0}}}{I'_{\mathrm{d}}} = \frac{1.0}{5.1} = 0.196$$

Subtransient reactance

$$X''_{\mathrm{d}} = \frac{e''_{\mathrm{q0}}}{I''_{\mathrm{d}}} = \frac{1.0}{7.35} = 0.136 \text{ pu}$$

The generator time constants are also derived from Figure 2.12. The exponential terms in the characteristic equations equal 0.37 when the elapsed time equals the time constant:

$$e^{-t/Tc} = 0.37 \quad \text{when } t = Tc$$

The time constants T'_{d} for the $(I'_{\mathrm{d}} - I_{\mathrm{d}})$ term can be found directly from curve B. At time $t = 0$, the value of $(I'_{\mathrm{d}} - I_{\mathrm{d}})$ is 4.4 pu. Follow Curve B to the right until curve B $= 0.37 \times 4.4$ or 1.63 pu; the time at this point is equal to the time constant T'_{d}.

The subtransient time constant T''_{d} can be determined in a similar manner, except curve B must be subtracted from curve A to isolate the $I''_{\mathrm{d}} - I'_{\mathrm{d}}$ term. The result of this subtraction is plotted as curve C. The time constant T''_{d} is equal to the point where curve C has decayed to 0.37 of its initial value. Using these techniques, $T'_{\mathrm{d}} = 0.475$ sec and $T''_{\mathrm{d}} = 0.023$ sec.

These values were derived for the d-axis quantities, but q-axis reactances and time constants, although derived by different methods, define the response of the q-axis current in the same manner. Detailed test procedures for both d- and q-axes parameters are described in standards.[1]

2.6 FAULT CURRENT CALCULATIONS

In the preceding section, the d- and q-axes characteristic equations were introduced and used to derive the generator impedances and time constants from generator short-circuit data. Normally the derivation is not necessary, because the generator manufacturer provides them on a generator data sheet similar to the one included in Appendix A.

The next step is to use the generator data and the characteristic equations to calculate generator fault currents. By backstepping through the derivation of the generator reactances and time constants, a three-phase fault at the generator terminals can be calculated. Only d-axis quantities are involved. The calculation is simple and the decaying fault current obtained will be equivalent to the generator short-circuit test current.

Unfortunately, the calculation is only valid for the conditions constraining the short circuit test. It can only represent a three-phase fault at the generator terminals with no initial load on the generator and with field current held constant.

The application of protective schemes requires knowledge of a full range of fault conditions. In the following sections, methods for evaluating these conditions will be presented, including:

- Load on the generator prior the fault
- Reactance between the fault and the generator
- Phase-to-phase and phase-to-ground faults
- Field current variations due to voltage regulator action

The calculations presented in this section are for the AC component of fault current only.

© 2006 by Taylor & Francis Group, LLC

To facilitate these discussions, the characteristic equations are restated here in more general terms.

$$i_{\mathrm{d}} = (I''_{\mathrm{d}} - I'_{\mathrm{d}})e^{-t/T''_{\mathrm{df}}} + (I'_{\mathrm{d}} - I_{\mathrm{d}})e^{-t/T'_{\mathrm{df}}} + I_{\mathrm{d}}$$

$$i_{\mathrm{d}} = \left(\frac{e''_{\mathrm{q0}}}{X''_{\mathrm{df}}} - \frac{e'_{\mathrm{q0}}}{X'_{\mathrm{df}}}\right)e^{-t/T''_{\mathrm{df}}} + \left(\frac{e'_{\mathrm{q0}}}{X'_{\mathrm{df}}} - \frac{EI}{X_{\mathrm{df}}}\right)e^{-t/T'_{\mathrm{df}}} + \frac{EI}{X_{\mathrm{df}}} \tag{2.5}$$

$$i_{\mathrm{q}} = (I''_{\mathrm{q}} - I'_{\mathrm{q}})e^{-t/T''_{\mathrm{qf}}} + (I'_{\mathrm{q}} - I_{\mathrm{q}})e^{-t/T'_{\mathrm{qf}}}$$

$$i_{\mathrm{q}} = \left(\frac{e''_{\mathrm{d0}}}{X''_{\mathrm{qf}}} - \frac{e'_{\mathrm{d0}}}{X'_{\mathrm{qf}}}\right)e^{-t/T''_{\mathrm{qf}}} + \left(\frac{e'_{\mathrm{d0}}}{X'_{\mathrm{qf}}} - \frac{Ed}{X_{\mathrm{qf}}}\right)e^{-t/T'_{\mathrm{qf}}} \tag{2.6}$$

Since excitation does not exist in the q-axis steady state voltage $Ed = 0$ and the q-axis equation becomes

$$i_{\mathrm{q}} = (I''_{\mathrm{q}} - I'_{\mathrm{q}})e^{-t/T''_{\mathrm{qf}}} + I'_{\mathrm{q}}e^{-t/T'_{\mathrm{qf}}}$$

$$i_{\mathrm{q}} = \left(\frac{e''_{\mathrm{d0}}}{X''_{\mathrm{qf}}} - \frac{e'_{\mathrm{d0}}}{X'_{\mathrm{qf}}}\right)e^{-t/T''_{\mathrm{qf}}} + \frac{e'_{\mathrm{d0}}}{X'_{\mathrm{qf}}}e^{-t/T'_{\mathrm{qf}}}$$

Also note that transient and subtransient parameters are not always provided for the q-axis. In such cases the current would reduce to:

$$i^*_{\mathrm{q}} = \frac{e^*_{\mathrm{d0}}}{X^*_{\mathrm{qf}}}e^{-t/T^*_{\mathrm{qf}}}$$

where $*$ represents the transient or subtransient parameter provided.

2.6.1 Initial Load

The inclusion of load on the generator impacts the fault calculation in two ways. The preloaded generator gives rise to a q-axis current component. The short circuit analysis now requires the calculation of current in each axis, individually, using Equation (2.5) and Equation (2.6), then combining these currents to find the positive sequence current using Equation (2.7).

$$I_1 = \sqrt{i_{\mathrm{d}}^2 + i_{\mathrm{q}}^2} \tag{2.7}$$

The fault current is found from the relationship between the positive sequence current and phase current for the fault condition under study. These relationships will be developed for three-phase, phase-to-phase, and phase-to-ground faults.

The inclusion of prefault loading also produces voltage drops in the generator. The voltages behind the subtransient, transient and synchronous reactances (EI, e''_{q}, e'_{q}) are no longer equal to the terminal voltage and e_{d0}, e'_{d0} and e''_{d0} are no longer equal to zero as was the case for the generator short circuit test. The appearance of d-axis voltages gives rise to q-axis current. These internal voltages are calculated from the d- and q-axes components of prefault terminal voltage and load current. Figure 2.13 shows how load current (I) and terminal voltage (et) can be resolved into components i_{d0}, i_{q0} and e_{d0}, and e_{q0}, respectively, using basic trigonometry if the angle between the phase voltage and the q-axis is known. With the axis component currents and voltages defined, the voltage behind each reactance can be calculated.

As an example, the voltage behind X''_{d} would be calculated as

$$e''_{\mathrm{q0}} = e_{\mathrm{q0}} + (-j\, i_{\mathrm{d0}})(jX''_{\mathrm{d}})$$

$$= e_{\mathrm{q0}} + i_{\mathrm{d0}}X''_{\mathrm{d}}$$

© 2006 by Taylor & Francis Group, LLC

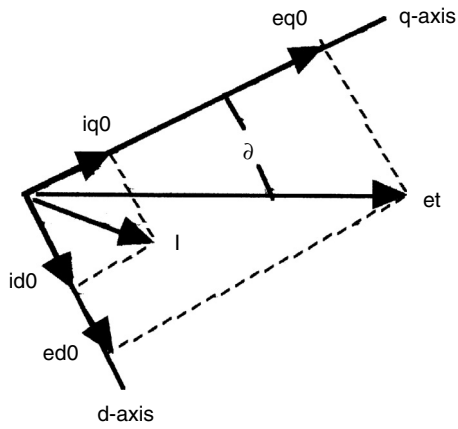


FIGURE 2.13 The d- and q-axes components of load current and voltage.

The voltage e_{q0} is the q-axis component of the prefault terminal voltage *et*. The d-axis component of load current, i_{d0}, lags voltage e_{q0} by 90°. The multiplication of the lagging current i_{d0} and the inductive reactance X''_d produces a voltage rise in phase with e_{q0}.

In the q-axis, current i_{q0} leads voltage e_{d0} by 90°. The result is a voltage drop across impedance X''_q.

$$\begin{aligned} e''_{d0} &= e_{d0} + (j\, i_{q0})(jX''_q) \\ &= e_{d0} - i_{q_0} X''_q \end{aligned}$$

Figure 2.14 shows the component currents and voltages and the internal voltages. As previously stated, the computation of these voltages is predicated on knowing angle between the terminal voltage and the q-axis. The figure shows this angle can be calculated from point M, which is located at the vector sum of $et + jIX_q$. Equation (2.8) determines the angle δ from point M. Once δ is established, Equation (2.9) through Equation (2.18) can be used to determine the internal voltages for any prefault loading condition.

$$\delta = \arctan\left(\frac{IX_q \cos\theta}{et + IX_q \sin\theta}\right) \tag{2.8}$$

$$e_{q0} = et\cos\delta \tag{2.9}$$

$$I_{q0} = I\cos(\theta + \delta) \tag{2.10}$$

$$e_{d0} = et\sin\ \delta \tag{2.11}$$

$$I_{d0} = I\sin(\theta + \delta) \tag{2.12}$$

q-Axis voltages:

$$e''_{q0} = e_{q0} + I_{d0}X''_d \tag{2.13}$$

$$e'_{q0} = e_{q0} + I_{d0}X'_d \tag{2.14}$$

$$EI = e_{q0} + I_{d0}X_d \tag{2.15}$$

d-Axis voltages:

$$e''_{d0} = e_{d0} - I_{q0}X''_q \tag{2.16}$$

$$e'_{d0} = e_{d0} - I_{q0}X'_q \tag{2.17}$$

$$Ed = e_{d0} - I_{q0}X_q = 0 \tag{2.18}$$

© 2006 by Taylor & Francis Group, LLC

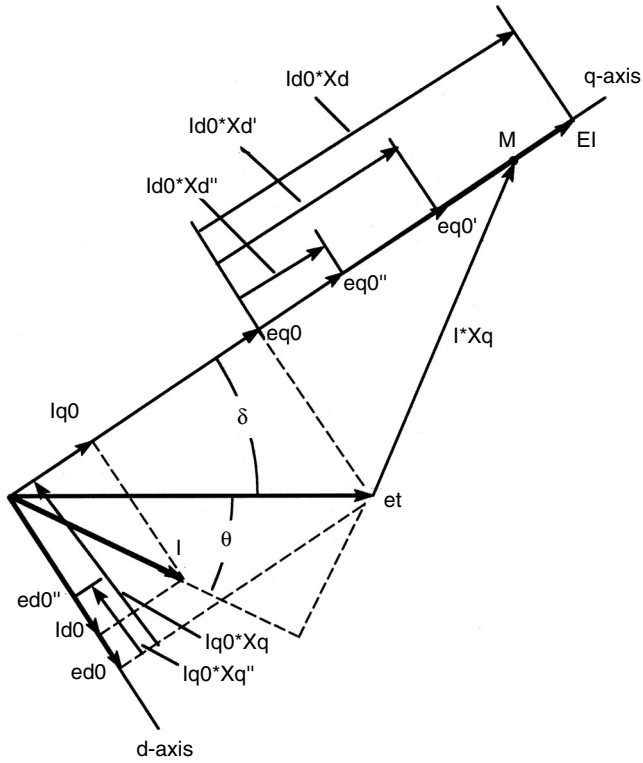


FIGURE 2.14 Initial d- and q-axes quantities. (From F.P. deMello, Course Notes, Electrical Machine Dynamics I. Siemens Power Transmission and Distribution, Inc., Power Technologies International. With permission.)

The internal voltages are fixed by the prefault load conditions. Once these voltages are established, they are applicable to all fault conditions, three-phase, phase-to-phase, or phase-to-ground.

2.6.2 Fault Calculation Overview

The general methodology for calculating three-phase (3P), phase-to-phase (P–P) and phase-to-ground (P–G) fault currents is the same. In each case, the d- and q-axes currents are calculated individually, then combined using Equation (2.7) to yield the positive sequence current. The fault current is derived directly from the positive sequence current.

The calculation of the positive sequence current from the d- and q-axes synchronous, transient and subtransient currents is summarized in Figure 2.15. Each subcomponent current can be calculated from the individual circuits shown at the bottom of the figure. The voltage in each circuit is the prefault internal voltage behind the operative generator reactance, as calculated from Equation (2.8) through Equation (2.18).

Reactance X_f is the fault reactance as seen from terminals x–y of the positive sequence network of Figure 2.15. For a three-phase fault, X_f is the positive sequence reactance between the generator and the fault. For other fault conditions such as P–P and P–G faults, X_f is an equivalent impedance derived from the positive, negative, and zero sequence impedance networks as viewed from terminals x–y. X_f will vary with fault location and with the type of fault. If 3P, P–P, and P–G faults are calculated at the same location in the system, the value of X_f will be different for each type fault. The derivation of this reactance will be explained in detail.

The external reactance, X_f, also increases time constants T''_{df}, T'_{df}, T''_{qf}, and T'_{qf} in characteristic Equation (2.5) and Equation (2.6). Their values must be determined for each value of X_f calculated. Since the value of X_f is different for 3P, P–P and P–G faults at the same location, so the time

© 2006 by Taylor & Francis Group, LLC

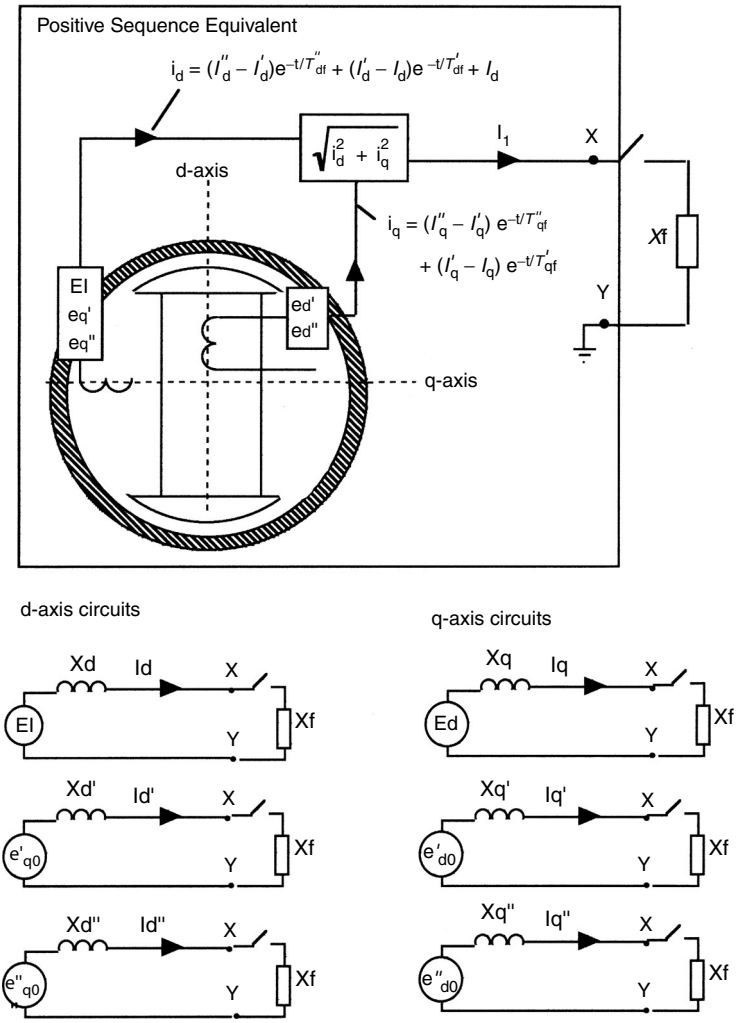


FIGURE 2.15 Generator positive sequence equivalent.

constants will differ for each fault condition at the same location. The modified time constants are calculated from open circuit values T''_{d0}, T'_{d0}, and T''_{q0}, which are found on the generator data sheet.[2]

$$T''_{df} = T''_{d0}\frac{X''_d + X_f}{X'_d + X_f} \tag{2.19}$$

$$T'_{df} = T'_{d0}\frac{X'_d + X_f}{X_d + X_f} \tag{2.20}$$

$$T''_{qf} = T''_{q0}\frac{X''_q + X_f}{X'_q + X_f} \tag{2.21}$$

$$T'_{qf} = T'_{q0}\frac{X'_q + X_f}{X_q + X_f} \tag{2.22}$$

Once subcomponent currents I_d, I'_d, I''_d, I_q, I'_q, I''_q and modified time constants are known, the d- and q-axes currents can be found from Equation (2.5) and Equation (2.6). The positive sequence current I_1 is calculated from i_d and i_q using Equation (2.7).

© 2006 by Taylor & Francis Group, LLC

The fault current is determined from the positive sequence current using relations that will be developed for 3P, P–P, and P–G faults.

Remember that i_d, i_q, and I_1 are all time-varying quantities. A point by point calculation using Equation (2.5) through Equation (2.7) is required to establish the time-varying fault current.

The calculation method described above is used for all fault types. Summarizing the steps:

1. Determine the internal voltages from the prefault loading condition.
2. Determine X_f for the given fault condition.
3. Calculate synchronous, transient and subtransient currents in each axis.
4. Calculate the modified axis time constants as determined by X_f.
5. Calculate time varying axis current i_d and i_q.
6. Calculate time varying positive sequence current I_1 from i_d and i_q using Equation (2.7).
7. Calculate the phase fault current from the positive sequence current.

2.6.3 Determination of X_f and Fault Currents

Fault calculations use symmetrical component techniques. Three-phase, phase-to-phase, and phase-to-ground faults each have a unique symmetrical component representation. This includes the way positive, negative, and zero sequence impedance networks are interconnected and the relationships between positive, negative, and zero sequence currents. The connections and relationships are shown in Figure 2.16 and will be familiar to those aquainted with transmission system fault calculations.

The figure represents the calculation for a fault on the high-voltage side of the GSU transformer. The positive sequence current is determined from the subcomponent circuits using X_f in exactly the same manner as was discussed for Figure 2.15.

Components in the axis circuits are designated with an asterisk to indicate that the circuit is applicable to subtransient, transient or synchronous values. Reactance Xtr_1 is the positive sequence reactance of the GSU transformer.

The calculations of 3P, P–P, and P–G faults are progressively more complex, because each involves additional sequence networks. Three-phase faults involve only positive sequence quantities. Phase-to-phase fault currents are derived from positive and negative sequence parameters and phase-to-ground faults includes the positive, negative, and zero sequences.

When the positive sequence current is known, the negative and zero sequence currents can be determined from symmetrical component theory, which defines the relationship of the sequence currents for each fault type:

For three-phase fault: $I_2 = 0$, $I_0 = 0$
For phase-to-phase fault: $I_2 = -I_1$, $I_0 = 0$
For phase-to-ground fault: $I_1 = I_2 = I_0$

where I_1 = positive sequence current; I_2 = negative sequence current; and I_0 = zero sequence current.

The fault current is determined by calculating the phase current for the faulted phase from the positive sequence current. Symmetrical components define phase currents regardless of the fault condition, as follows for an A–B–C rotation:

$$I_a = I_1 + I_2 + I_0 \tag{2.23}$$

$$I_b = I_1 a^2 + I_2 a + I_0 \tag{2.24}$$

$$I_c = I_1 a + I_2 a^2 + I_0 \tag{2.25}$$

where $a = 1\angle 120^\circ$.

© 2006 by Taylor & Francis Group, LLC

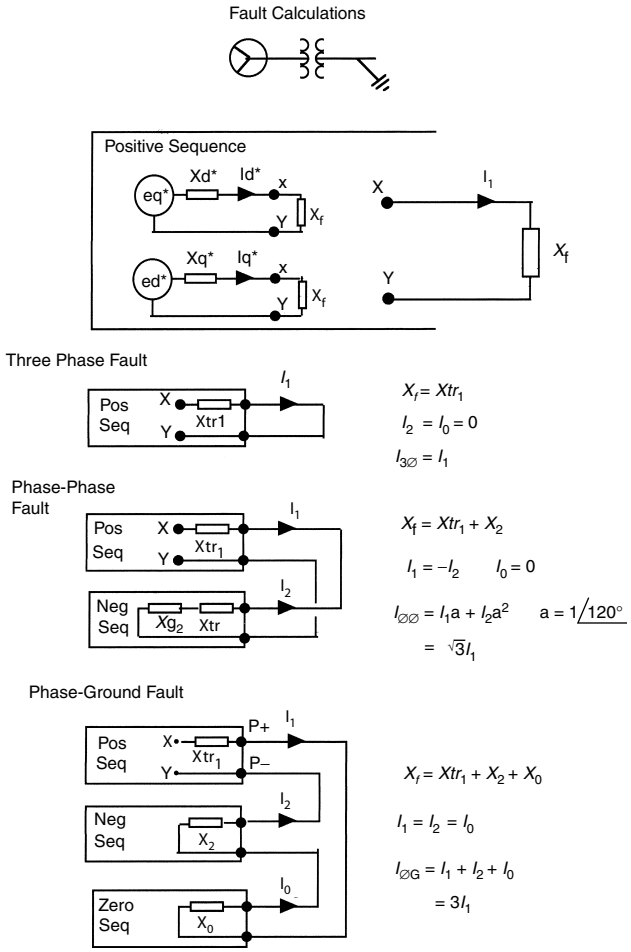


FIGURE 2.16 Fault current calculations.

2.6.4 Three-Phase Short Circuit

The three-phase fault includes only positive sequence impedance. Therefore, the reactance connected to terminals x–y of the generator equivalent circuit, Figure 2.15 and Figure 2.16, is the positive sequence reactance between the generator and the fault. This reactance is designated as Xe_1. $X_f = Xe_1$ as shown in Figure 2.17. The value of $Xe_1 = 0$ for a fault at the generator terminals and $Xe_1 = X\text{tr}_1$ for a short circuit on the GSU or unit auxiliary transformer. Whatever the fault condition or fault type X_f will be used to calculate the subtransient, transient and synchronous circuit currents using Equation (2.26) through Equation (2.31) and to modify the time constants from Equation (2.19) to Equation (2.22).

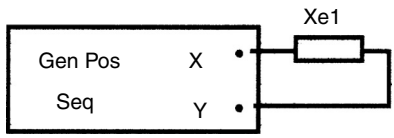


FIGURE 2.17 Sequence diagram, three-phase fault.

© 2006 by Taylor & Francis Group, LLC

d-Axis currents:

$$I_d = \frac{EI}{X_d + X_f} \quad \text{synchronous} \tag{2.26}$$

$$I'_d = \frac{e'_{q0}}{X'_d + X_f} \quad \text{transient} \tag{2.27}$$

$$I''_d = \frac{e''_{q0}}{X''_d + X_f} \quad \text{subtransient} \tag{2.28}$$

q-Axis currents:

$$I_q = \frac{Ed}{X_q + X_f} \quad \text{synchronous} \tag{2.29}$$

$$I'_q = \frac{e'_{q0}}{X'_q + X_f} \quad \text{transient} \tag{2.30}$$

$$I''_q = \frac{e''_{d0}}{X''_q + X_f} \quad \text{subtransient} \tag{2.31}$$

The positive sequence component of short-circuit current is then determined from Equation (2.5) through Equation (2.7).

The fault current for any fault condition is determined by calculating the current in the faulted phase using Equation (2.23) through Equation (2.25) and applying the appropriate constraints to the sequence currents. In the case of a three-phase fault, the current constraints are:

$$I_2 = I_0 = 0$$

Since the three-phase fault involves all phases, the fault current can be determined by calculating current in any phase. For simplicity, the "A" phase current is calculated:

$$I_{3\varnothing} = I_a = I_1 + 0 + 0 = I_1 \tag{2.32}$$

This confirms the statements made earlier in the text that the three-phase fault current is equal to the positive sequence current.

2.6.5 Phase-to-Phase Short Circuit

The calculation of a phase-to-phase fault requires the interconnection of the positive and negative sequence networks as shown in Figure 2.18.

The reactances Xe_1 and Xe_2 are the positive and negative sequence reactance between the generator and the short circuit. Xg_2 is the negative sequence reactance of the generator itself as

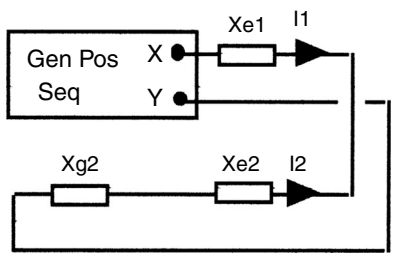
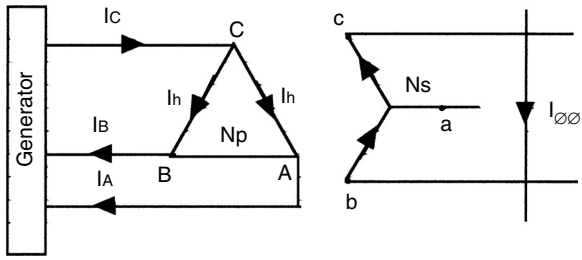


FIGURE 2.18 Sequence diagram, phase-to-phase fault.

© 2006 by Taylor & Francis Group, LLC



$$I_h = I_{\theta\theta}\,\frac{N_s}{N_p} = I_{\theta\theta}\,\frac{Ey_{\theta N}}{E\Delta_{\theta\theta}}$$

$$I_C = 2I_{\theta\theta}\,\frac{Ey_{\theta N}}{E\Delta_{\theta\theta}} \qquad I_A = I_B = \frac{1}{2}\,I_C$$

FIGURE 2.19 Phase-to-phase fault through a Y-delta transformer.

provided on the generator data sheet. For the phase-to-phase fault condition:

$$X_f = Xe_1 + Xe_2 + Xg_2$$

Using the same methods as in the three-phase case, X_f modifies the axis time constants and defines the d- and q-axis steady state, transient and subtransient current components for the fault condition. These components are combined using Equation (2.7) to yield the positive sequence current.

Again, the fault current is determined from the positive sequence current by the use of Equation (2.23) through Equation (2.25) to calculate the current in the faulted phase. Symmetrical component theory assumes a phase-to-phase fault to be a B–C phase fault. Symmetrical component theory also imposes the constraints that $I_1 = -I_2$ and $I_0 = 0$.

Calculating the B phase current from Equation (2.24):

$$\begin{aligned} I_{\varnothing\varnothing} = I_B &= I_1a^2 + I_2a + I_0 \\ &= I_1a^2 - I_1a + 0, \quad a = 1\angle 120^\circ \\ &= I_1(a^2 - a) = \sqrt{3}I_1 \end{aligned} \tag{2.33}$$

The phase-to-phase fault current is then $\sqrt{3}$ times the positive sequence current.

Note that the phase-to-phase short-circuit current calculated by Equation (2.33) is the current at the point of fault. This is an important concept. If the short circuit is located on the high-voltage winding of the GSU or the low side of the auxiliary transformer, and generator currents are needed, the current in the generator leads will be determined by the delta-wye connection of the aforementioned transformers. Figure 2.19 shows how the fault current calculated using Equation (2.33) is reflected to the generator side of the transformer.

2.6.6 Phase-to-Ground Fault

A ground fault includes positive, negative, and zero sequence reactance connected as shown in Figure 2.20. Xe_0 is the zero sequence reactance between the generator and the short circuit. Xg_0 is the zero sequence reactance of the generator. The value of Xg_0 is provided on the generator data sheet. The reactance seen at terminal x–y of Figure 2.20 is

$$X_f = Xe_1 + Xe_2 + Xe_0 + Xg_2 + Xg_0$$

© 2006 by Taylor & Francis Group, LLC

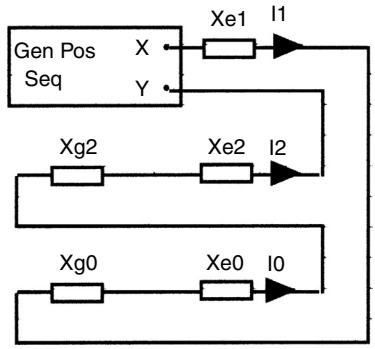


FIGURE 2.20 Sequence diagram, phase-to-ground fault at generator.

Reactance X_f is again used to modified axis time constants as defined by Equation (2.19) through Equation (2.22) and to establish the positive sequence current from Equation (2.5) through Equation (2.7).

Symmetrical components theory assumes a phase-to-ground fault to be an "A" phase-to-ground fault with the constraints that $I_1 = I_2 = I_0$. Substituting the sequence currents into the symmetrical current equation for the "A" phase current:

$$\begin{aligned} I_{\varnothing G} &= I_a = I_1 + I_2 + I_0 \\ &= I_1 + I_1 + I_1 \\ &= 3I_1 \end{aligned} \tag{2.34}$$

The phase-to-ground fault current is three times the positive sequence current.

The preceding derivation describes the calculation of short-circuit current for a ground fault at the generator terminals. In practice, generators are normally grounded through a high impedance, which limits the ground fault current to a few amperes; hence, the calculation of a phase-to-ground fault at the generator terminals is generally unnecessary. Ground fault calculations are often required for faults on the high-voltage winding of the GSU or the low-voltage winding of the auxiliary transformer. These calculations are carried out in the same manner, with two exceptions. First, the generator is connected to the delta winding of the transformer and no ground current will flow at the generator for a phase-to-ground fault on the wye side of the transformer. Therefore, the generator's zero sequence reactance is not included in the calculation. Only the zero sequence reactance of the transformer is included. The connection of the sequence impedances for a phase-to-ground fault on the wye side of a delta-wye transformer is shown in Figure 2.21. Here *Xe* represents the

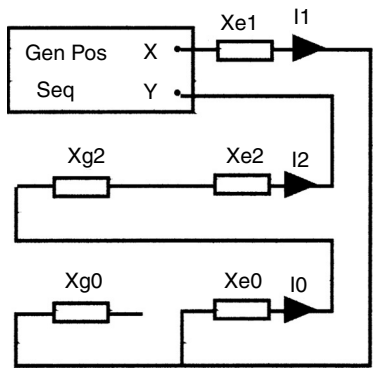
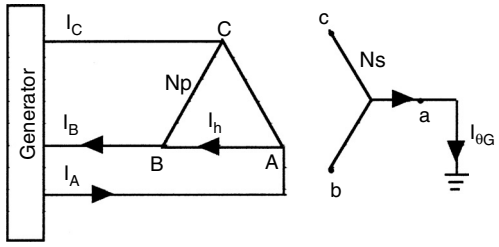


FIGURE 2.21 Sequence diagram, phase-to-ground fault at GSU.

© 2006 by Taylor & Francis Group, LLC



$$I_A = I_B = I_{\theta G} = \frac{Ey_{\theta N}}{E\Delta_{\theta\theta}} \qquad I_C = 0$$

FIGURE 2.22 Phase-to-ground fault through a Y-Delta transformer.

positive, negative and zero sequence impedance of the GSU transformer. The value of X_f for this case is:

$$X_f = Xe_1 + Xe_2 + Xe_0 + Xg_2$$

The second exception is that, like the phase-to-phase fault, the current in the generator leads must be determined by reflecting the short-circuit current determined by Equation (2.34) through the wye-delta transformer as shown in Figure 2.22.

2.6.7 Other Fault Conditions

In the preceding sections, the generator d- and q-axes models have been interconnected with symmetrical component networks to represent three basic fault types. Expanded explanations of symmetrical component theory are available in the various texts. These references provide additional sequence network connections for conditions such as double-line-to-ground faults and open phases. The response of a generator to these faults is evaluated using the same methodology described above.

The value of X_f for any condition is determined from the configuration of the sequence diagram as viewed from terminal x–y in Figure 2.15 and Figure 2.16. The fault current is established using the current constraints unique to the fault under consideration and Equation (2.23) through Equation (2.25).

2.6.8 DC Component of Short-Circuit Current

At first glance, the occurrence of a DC current in an AC power system seems illogical. To understand its existence, let us look at a few electrical rules learned in EE 101. First, in an inductive circuit, the current lags the voltage by 90°. If a fault occurs when the voltage is zero, the current must be at a positive or negative maximum value. Secondly, the generator is a large inductor. The current in an inductor cannot change instantaneously.

Now we assume the generator is carrying no load prior to the fault. We also assume the fault occurs at the instant when the voltage is at zero. The generator current prior to the fault was zero, so the current at the instant after the fault is applied must also be zero for the inductive circuit. But the phasing of the inductive circuit also requires that if the voltage is zero when the fault is applied, the current must be at a maximum. Either one of these electrical rules is wrong or something is missing.

The missing piece is the DC component of the fault current. It is created at the instant that the fault occurs. Its initial magnitude is equal to the instantaneous value of the AC current component, but of opposed polarity, $I_{DC} = -i_{AC}$ at $t = 0$. The result is the total fault current $i_{AC} + I_{DC} = 0$ at $t = 0$. This maintains the current equivalency in the instants before and after the fault, as is required by the circuit inductance.

© 2006 by Taylor & Francis Group, LLC

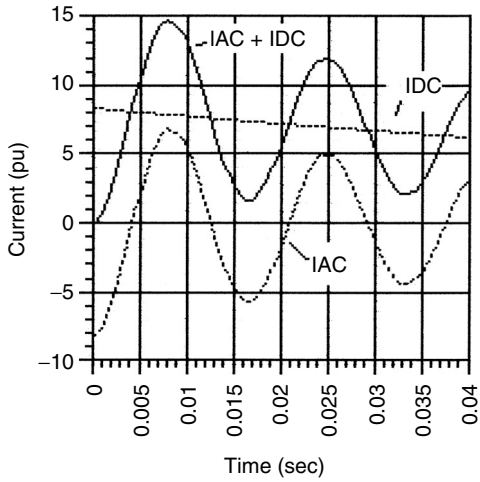


FIGURE 2.23 DC offset and asymmetric current.

The actual magnitude of the DC component current is dependent on the point on the voltage wave where the fault occurs and the circuit angle (X/R). A worst case analysis assumes the fault occurs at a point in time when the AC current component is at an instantaneous peak, thus producing the largest DC component.

The component currents along with the total fault current are plotted in Figure 2.23. The DC component offsets the total current waveform and produces the instantaneous peak current in the first half cycle. This peak is important, because it determines the maximum mechanical force electrical components must withstand.

Although the DC component begins to decay immediately, tens of cycles may be required for it to dissipate because of the high X/R ratio associated with generator faults. Modern circuit breakers operate in two to five cycles, and will be required to interrupt a significantly offset current. The offset or "asymmetrical current" dictates the minimum interrupting rating required for a breaker installation. This may seem inconsistent, because most breaker ratings are quoted on the basis of "symmetrical current," which is the AC component alone. The symmetrical current rating system assumes a specific DC component; thus, the actual rating is an asymmetrical current.

The DC component decays at a rate governed by the armature time constant. Specific time constants are listed on the generator data sheet, Ta3, Ta2, and Ta1 for three-phase, phase-to-phase, and phase-to-ground faults, respectively. Since the DC component is normally of interest for maximum duty a calculation only, adjusting the time constants or external reactance is not required.

The maximum DC component would occur if the fault is coincident with the peak value of the AC component. Assuming the AC component is expressed in terms of RMS current, the maximum DC component of current is then

$$I_{\mathrm{DC}} = \sqrt{2} I_{\mathrm{AC}}(\mathrm{RMS})$$

or, for a three-phase fault, the maximum DC component can be expressed as

$$I_{\mathrm{DC}} = \sqrt{2}\sqrt{I''^{2}_{\mathrm{d}} + I''^{2}_{\mathrm{q}}} \tag{2.35}$$

The instantaneous value of the decaying DC current for a three-phase fault is

$$i_{\mathrm{DC}} = I_{\mathrm{DC}}\, e^{-t/T_{\mathrm{a3}}} \tag{2.36}$$

© 2006 by Taylor & Francis Group, LLC

2.6.9 RMS Asymmetrical Current

Equipment ratings are often based on the maximum RMS short-circuit current. When both AC and DC components of current exist, the RMS current is given by

$$I_{\text{RMS}} = \sqrt{I_{\text{AC}}^2 + I_{\text{DC}}^2} \tag{2.37}$$

2.7 VOLTAGE REGULATOR

The assumption of constant field current was used in the preceding short circuit calculations. This is an accurate assumption when the generator is operating under control of the manual regulator. In this mode, field excitation is set at a value by the operator and remains at that value unresponsive to system conditions.

Short circuit calculations for the manual regulator condition are valid for maximum current calculations, because the maximum current occurs at the inception of the short circuit, before the automatic regulator could react to increase fault current. Manual regulator short circuit calculations are also of interest because they define the minimum sustained fault current. This calculation would be done to check the sensitivity of a backup relaying.

The generator is normally under control of the automatic voltage regulator, which varies the field current, as required, to maintain a preset generator terminal voltage. The manual regulator is normally placed in service only in the event of an automatic regulator failure. The automatic voltage regulator is usually capable of delivering 1.2 to 1.5 times the field voltage required for rated generator load. This upper voltage limit is known as the "ceiling" voltage of the excitation system.

When a short circuit occurs, the generator terminal voltage drops to a level dependent on the amount of impedance between the generator and the short circuit. The automatic voltage regulator will sense the low voltage and boost the field voltage to its ceiling value in an attempt to restore the terminal voltage. The field current will increase at a rate determined by the speed of the voltage regulator, the ceiling voltage and the time constant of the generator field circuit. The internal voltage EI is representative of the field current. The increase in field current increases the internal voltage EI, thus increasing the short-circuit current.

Some excitation system use power potential transformers (PPT) to take power from the generator terminals to supply field current. A solid three-phase fault on generator terminals will remove the source of field current in these systems and the fault current will decay to zero. If there is impedance between the generator and the three-phase short circuit, some voltage will be available at the terminals to provide field current. When the field current available is sufficient to maintain the terminal voltage, a steady-state fault current will be sustained. However, if the available field current cannot support the terminal voltage, the excitation will collapse and the short-circuit current will decay to near zero. Some PPT excitation systems employ current transformers to inject short-circuit current back into the field circuit to prevent excitation system collapse for three-phase faults.

Another area where the excitation system can dramatically alter the short-circuit current is the inclusion of de-excitation circuitry. When a generator, generator step up (GSU), or auxiliary transformer short circuit occurs, relays act within a few cycles to trip the generator and field breakers. However, if there is no breaker between the generator and the fault, this does not interrupt the fault current. The fault current will decay as determined by the modified time constants, exposing the generator and transformers to severe stress for seconds. Excitation systems often include equipment to accelerate the rate of decay of the fault current in an attempt to minimize equipment damage. These "de-excitation" circuits can use field-shorting resistors to accelerate the decay of fault current. Some circuits apply a negative voltage to the field to drive the field current toward zero.

© 2006 by Taylor & Francis Group, LLC

The sample system employs a static exciter powered by a source isolated from the generator terminals. The system includes a de-excitation circuit consisting of a contactor that closes when the field breaker opens to insert a field discharge resistor (FDR) across the field winding (see Figure 1.9). This resistor dramatically increases the resistance in the field circuit, thus reducing the field current decay time constant. The rapid field current decay produces an equally rapid decay in the fault current.

The current boost effect of the exciter and the current quenching effect of the FDR can be included into the short circuit calculation by adding an additional component I_{ex} into Equation (2.5) for d-axis current.

For exciter action add:

$$I_{ex} = \frac{Ec - EI}{X_{df}}[1 - e^{-t/T'_{df}}] \tag{2.38}$$

For de-excitation add:

$$I_{ex} = -\frac{EI}{X_{df}}\left[1 - e^{-t/T'_{df1}}\right] \tag{2.39}$$

$$T'_{df1} = \left[\frac{1}{1 + FDR\Omega/R_f\Omega}\right]T'_{df} \tag{2.40}$$

Equation (2.38) and Equation (2.39) describe the effect changes in field current have on the generator's fault performance. These equations are written in terms of *EI*, because this internal voltage is representative of the field flux. If the saturation is neglected, the per-unit values of field current and *EI* are equivalent.

To determine the value of *Ec*, the ceiling voltage or maximum forcing current for the regulator must be known. Assume that the sample system's voltage regulator is capable of producing a ceiling voltage of 500 V DC. Neglecting saturation, the per unit ceiling voltage is obtained by dividing 500 V by the field voltage that is equal to 1.0 pu.

It is important to remember that 1.0 per unit field current or field voltage is equal to the field quantity required to produce rated terminal voltage ($et = 1.0$) at no load. The field current or field voltage at rated load is not 1.0 pu.

The field current required to produce rated voltage at no load is referred to as "Amps of the Field at No Load" (AFNL). For the sample system generator, AFNL = 410 A DC. The field resistance is 0.427 Ω at normal operation temperature. Then "Volts of the Field at No Load" (VFNL) equals 410 A × 0.427 Ω = 175 V DC.

The per unit ceiling voltage for the sample system generator is 500 V/175 V = 2.86 pu. An alternative calculation is to determine the maximum forcing current 500 V/0.427 Ω = 1170 A. The per unit forcing current is 1170 A/410 A = 2.86 pu.

2.8 PRACTICAL SHORTCUTS

Having gone through the rigorous derivation of the various fault conditions we can now look at some short cuts.

The most common fault conditions calculated are the maximum and minimum current conditions. These can be determined quickly without the evaluation of time constants. The maximum AC component of fault current occurs at the inception of the fault. An examination of Equation (2.5) and Equation (2.6) shows that at $t = 0$ the d- and q-axes currents are equal to I''_d and I''_q, respectively. It follows that the maximum positive sequence currents for a given fault condition are given by:

$$I_1(\max) = \sqrt{I''^2_d + I''^2_q} \tag{2.41}$$

© 2006 by Taylor & Francis Group, LLC

If the generator is operating on the manual voltage regulator, the field current is held constant and fault current will decay with time. The minimum fault current will occur when the fault current reaches its sustained value at $t = \infty$. Since there is no excitation in the q-axis the q-axes current will decay to zero and the minimum positive sequence current for a given condition can be calculated as

$$I_1(\min) = \sqrt{I_d^2 + I_q^2} = \sqrt{I_q^2 + 0} = I_d \tag{2.42}$$

These equations can be used to calculate minimum and maximum three-phase, phase-to-phase, and phase-to-ground faults. The axis currents are calculated from the appropriate value of X_f and the faulted phase current is determined using the relationships developed in Equation (2.32) through Equation (2.34).

If the automatic voltage regulator is in service, Equation (2.42) is not valid. Here, the natural decay of the fault current is offset by the action of the voltage regulator. Typically, the fault current will decay rapidly for several tenths of a second, then begin to increase as the voltage regulator reacts to increase field current. Therefore, it is necessary to plot the fault current as a function of time to determine the minimum current.

The sustained value for fault current ($t = \infty$) for a generator operation on the automatic regulator can be determined by substituting the ceiling voltage of the regulator *Ec* for *EI* in Equation (2.26). The value of I_d obtained is then the sustained fault current.

An excitation system is not designed to operate at ceiling voltage indefinitely. The calculated sustained current will persist until circuitry within the regulator acts to reduce the excitation voltage to its rated full load value or the generator is tripped.

A shortcut is also applicable for estimating the decaying short-circuit currents on a cylindrical rotor machine. Since the d- and q-axes impedances for this type of machine are nearly equal, they are combined. The voltages behind the various reactances are assumed to act as one circuit.

Neglecting external reactance:

$$i_{AC} = (I'' - I')e^{-t/T_d''} + (I' - I)e^{-t/T_d'} + I \tag{2.43}$$

where the subtransient component is

$$I'' = \frac{e''}{X_d''} \tag{2.44}$$

$$e'' = e_t + I_0 X_d''[\sin\phi + j\cos\phi] \tag{2.45}$$

and ϕ = power factor angle which is positive for lagging Var output, I_0 is the initial load current.

The transient component is given by

$$I' = \frac{e'}{X_d'} \tag{2.46}$$

$$e' = e_t + I_0 X_d'(\sin\theta + j\cos\theta) \tag{2.47}$$

The sustained component is given by

$$I = \frac{e_t}{X_d}\left(\frac{I_F}{I_{Fg}}\right) \tag{2.48}$$

where I_F = field current at the given load condition, and I_{Fg} = field current at no load rated voltage.

© 2006 by Taylor & Francis Group, LLC

Three-phase, phase-to-phase, and phase-to-ground fault currents can be estimated from the above equations by using the appropriate value of X_f to determine currents I, I', and I''. The faulted phase current is determined using the relationships developed in Equation (2.32) through Equation (2.34).

These equations provide reasonable accuracy for estimating the decay of fault current. The error increases as the magnitude of d- and q-axes impedances diverge.

2.9 SHORT CIRCUIT CALCULATION EXAMPLE

Having gone through the theory, we can now determine fault currents on the sample system. We will look at two conditions: a three-phase fault at the generator terminals and a phase-to-ground fault on the high-voltage side of the GSU transformer. A generator data sheet is provided in Appendix A. We will assume that the unit is operating at rated load and power factor, with a terminal voltage of 1.05 prior to the short circuit.

2.9.1 Establish Prefault Conditions

First, the internal voltages in each subtransient, transient and synchronous circuit must be determined from the prefault load on the generator. The generator data sheet shows that the sample system generator is rated for 0.85 PF. The prefault generator loading is 104,400 kVA (1.0 pu) at 0.85 PF Lag.

The power factor angle = arccos 0.85 = 31.8°. The generator current is given by

$$et = 1.05$$

$$I = \frac{\text{kVA}}{et} = \frac{1.0}{1.05} = 0.952\angle -31.8^\circ \qquad \theta = 31.8^\circ$$

The generator data sheet provides the following reactances and time constants. The reactance values are in per unit values on the generator base, which is 104.4 MVA at 13.8 kV. Generator data sheets often provide saturated and unsaturated reactance values for each reactance value. The saturated values should be used for short-circuit calculations.

$$X_d = 1.48 \qquad X'_d = 0.196 \qquad X''_d = 0.136$$

$$X_q = 1.42 \qquad X'_q = 0.484 \qquad X''_q = 0.132$$

$$T'_{d0} = 3.59 \text{ sec} \qquad T''_{d0} = 0.033 \text{ sec}$$

$$T'_{q0} = 0.312 \text{ sec} \qquad T''_{q0} = 0.084 \text{ sec}$$

The internal voltages are determined in accordance with Figure 2.14 and Equation (2.8) through Equation (2.18). The first step is to determine the location of the machine axis by finding the power angle from Equation (2.8):

$$\delta = \arctan\left(\frac{IX_q \cos\theta}{et + IX_q \sin\theta}\right) = 33.1^\circ$$

© 2006 by Taylor & Francis Group, LLC

The d- and q-axes voltage and current components for the pre-fault loading condition are now found using Equation (2.9) through Equation (2.18).

$$e_{q0} = et_0 \cos\delta = 0.880 \qquad I_{q0} = I_0 \cos(\theta + \delta) = 0.404$$

$$e_{d0} = et_0 \sin\delta = 0.573 \qquad I_{d0} = I_0 \sin(\theta + \delta) = 0.862$$

$$e''_{q0} = e_{q0} + I_d X''_d = 0.997 \qquad e'_{q0} = e_{q0} + I_{d0} X'_d = 1.049$$

$$e'_{d0} = e_{d0} - I_q X'_q = 0.378 \qquad e''_{d0} = e_{d0} - I_{q0} X''_q = 0.520$$

$$Ed = e_{d0} - I_q X_q = 0.0 \qquad EI = e_{q0} + I_{d0} Xd = 2.16$$

Now that the voltages in the subtransient, transient and synchronous circuits are known, the individual circuit short-circuit currents can be found for each axis using Equation (2.26) through Equation (2.31).

2.9.2 Three-Phase Fault at Generator Terminals

Since we are considering a short circuit at the 13.8 kV terminals of the generator, the reactance between the generator terminals and the short circuit is zero ($X_f = 0$).

$$I_d = \frac{EI}{X_d} = \frac{2.16}{1.48} = 1.46$$

$$I'_d = \frac{e'_q}{X'_d} = \frac{1.049}{0.196} = 5.35$$

$$I''_d = \frac{e''_q}{X''_d} = \frac{0.997}{0.136} = 7.33$$

$$I_q = \frac{E_d}{X_q} = \frac{0.0}{1.42} = 0.0$$

$$I'_q = \frac{e'_{d0}}{X'_q} = \frac{0.378}{0.484} = 0.781$$

$$I''_q = \frac{e''_{d0}}{X''_q} = \frac{0.520}{0.132} = 3.94$$

The time varying d- and q-axes currents are then derived from Equation (2.5) and Equation (2.6). The time constants defined by Equation (2.19) through Equation (2.22) with $X_f = 0$ are given as

$$T'_{df} = \left(\frac{X'_d}{X_d}\right) T'_{d0} = \left(\frac{0.196}{1.48}\right) 3.59 = 0.475 \text{ sec}$$

$$T''_{df} = \left(\frac{X''_d}{X'_d}\right) T''_{d0} = \left(\frac{0.136}{0.196}\right) 0.033 = 0.023 \text{ sec}$$

$$T'_{qf} = \left(\frac{X'_q}{X_q}\right) T'_{q0} = \left(\frac{0.484}{1.42}\right) 0.312 = 0.106 \text{ sec}$$

$$T''_{qf} = \left(\frac{X''_q}{X'_q}\right) T''_{q0} = \left(\frac{0.132}{0.484}\right) 0.084 = 0.023 \text{ sec}$$

© 2006 by Taylor & Francis Group, LLC

Note that the d-axis time constants derived here are equal to those calculated from the three phase short circuit test in Section 2.4, axis currents are then:

$$i_d = (7.33 - 5.35)e^{-t/0.023} + (5.35 - 1.46)e^{-t/0.475} + 1.46$$
$$i_q = (3.94 - 0.781)e^{-t/0.023} + (0.781 - 0)e^{-t/0.106}$$

The d- and q-axes currents are combined in Equation (2.7) to give the positive sequence component of AC current, which, for a three-phase fault, equals the short-circuit current.

$$I_{3\varnothing} = \sqrt{i_d^2 + i_q^2} I_{base}$$
$$I_{base} = \frac{104{,}400\,\text{kVA}}{\sqrt{3}\ 13.8\,\text{kV}} = 4370\,\text{A}$$

The maximum value of the AC component of current is calculated from the subtransient currents:

$$I_{max_{AC}} = \sqrt{I_d''^2 + I_q''^2} = \sqrt{7.33^2 + 3.94^2} = 8.32\,\text{pu}$$
$$= 8.32 \times 4370 = 36{,}360\,\text{A}$$

The maximum DC component of current is determined from Equation (2.35) and the subtransient d- and q-axes currents are given as

$$I_{DC} = \sqrt{2} \times 36{,}360 = 51{,}420\,\text{A}$$

The instantaneous DC current is determined from the armature time constant given on the generator data sheet for a three-phase fault:

$$T_{a3} = 0.239\ \text{sec}$$
$$i_{DC} = 51{,}420\, e^{-t/0.239}$$

The maximum RMS asymmetrical short circuit duty on the 13.8 kV bus is determined from Equation (2.37):

$$I_{RMS} = \sqrt{36{,}360^2 + 51{,}420^2} = 62{,}980\,\text{A}$$

2.9.3 Phase-to-Ground Fault on High-Voltage Terminals of GSU

The prefault operating conditions are the same as those assumed for the three-phase fault. Therefore, the internal voltages used for the three-phase calculation will still apply. The major difference between the two calculations is that for the phase-to-ground fault $X_f \neq 0$.

The applicable sequence connection is shown in Figure 2.21.

$$X_f = Xe_1 + Xe_2 + Xe_0 + Xg_2$$

© 2006 by Taylor & Francis Group, LLC

where Xe = positive, negative and zero sequence transformer reactances, and Xg_2 = generator negative sequence reactance.

The GSU data are as follows:

$$97\,\text{MVA}\ 67\,\text{kV}/13.8\,\text{kV},\quad Z = 6.5\%\ \text{on}\ 97\,\text{MVA}\ \text{base}$$

From the generator data sheet

$$Xg_2 = 0.129\ \text{on}\ 104.4\,\text{MVA}\ \text{base}$$

The generator reactances are given on a 104.4 MVA base, while the transformer is on a 97 MVA base. Before the impedances can be added, they must be on the same voltage and MVA base. The generator base must be used, because the prefault voltage calculations are based on the generator voltage and kVA base.

The base conversion is as follows:

$$Z_{\text{base 1}} = Z_{\text{base 2}} \frac{\text{kVA}_{\text{base 1}}}{\text{kVA}_{\text{base 2}}} \left(\frac{\text{kV}_{\text{base 2}}}{\text{kV}_{\text{base 1}}}\right)^2$$

The transformer impedance is on the transformer base. That makes the transformer kVA and voltage base = base 2. The new kVA and voltage base is the generator = base 1.

Since both impedances are quoted on the same kV base, 13.8 kV, no voltage correction is required. Converting the transformer to a 104.4 MVA base:

$$X_{\text{tr}} = 0.065 \times \frac{104.4}{97} = 0.07\,\text{pu}\ \text{on}\ 104.4\,\text{MVA}\ \text{base}$$

The positive and negative sequence reactances of a transformer are equal. If no specific zero sequence impedance data are available for the transformer, it is assumed to be equal to the positive and negative sequence impedance.

$$X_{\text{f}} = 3(0.07) + 0.129 = 0.339\ \text{pu}\ \text{on}\ 104.4\,\text{MVA}\ \text{base}.$$

The individual circuit currents and circuit time constants are again determined from Equation (2.19) through Equation (2.22) and Equation (2.26) through Equation (2.31).

$$I_{\text{d}} = \frac{E_I}{X_{\text{d}} + X_{\text{f}}} = \frac{2.16}{1.48 + 0.339} = 1.19$$

$$I'_{\text{d}} = \frac{e'_{\text{q}}}{X'_{\text{d}} + X_{\text{f}}} = \frac{1.049}{0.196 + 0.339} = 1.96$$

$$I''_{\text{d}} = \frac{e''_{\text{q}}}{X''_{\text{d}} + X_{\text{f}}} = \frac{0.997}{0.136 + 0.339} = 2.10$$

© 2006 by Taylor & Francis Group, LLC

$$I_q = \frac{E_d}{X_q + X_f} = \frac{0.0}{1.42 + 0.339} = 0.0$$

$$I'_q = \frac{e'_d}{X'_q + X_f} = \frac{0.378}{0.464 + 0.339} = 0.459$$

$$I''_q = \frac{e''_d}{X''_q + X_f} = \frac{0.520}{0.132 + 0.339} = 1.10$$

$$T'_{df} = \left(\frac{X'_d + X_f}{X_d + X_f}\right) T'_{d0} = \left(\frac{0.196 + 0.339}{1.48 + 0.339}\right) 3.59 = 1.06 \text{ sec}$$

$$T''_{df} = \left(\frac{X''_d + X_f}{X'_d + X_f}\right) T''_{d0} = \left(\frac{0.136 + 0.339}{0.196 + 0.339}\right) 0.033 = 0.029 \text{ sec}$$

$$T'_{qf} = \left(\frac{X'_q + X_f}{X_q + X_f}\right) T'_{q0} = \left(\frac{0.484 + 0.339}{1.42 + 0.339}\right) 0.312 = 0.146 \text{ sec}$$

$$T''_{qf} = \left(\frac{X''_q + X_f}{X'_q + X_f}\right) T''_{q0} = \left(\frac{0.132 + 0.339}{0.484 + 0.339}\right) 0.084 = 0.048 \text{ sec}$$

Substituting these values into Equation (2.5) and Equation (2.6) for the d- and q-axes currents:

$$i_d = (2.1 - 1.96)\, e^{-t/0.029} + (1.96 - 1.19)\, e^{-t/1.06} + 1.19$$

$$i_q = (1.10 - 0.459)\, e^{-t/0.048} + (0.459 - 0)\, e^{-t/0.146}$$

These currents are then used in Equation (2.7) to determine the positive sequence current:

$$I_1 = \sqrt{i_d^2 + i_q^2}$$

The phase-to-ground short-circuit current at the 67 kV terminals of the GSU transformer is found using Equation (2.34).

$$I_{\varnothing G} = 3 I_1 I_{base} = 3\sqrt{i_d^2 + i_q^2}\, I_{base}$$

The base current at the fault location (67 kV) is calculated as

$$I_{base} = \frac{\text{kVA}}{\sqrt{3}\,\text{kV}} = \frac{104{,}400}{\sqrt{3}\,67} = 900\,\text{A}$$

The subtransient currents determine the maximum AC component of ground fault current seen at the 67 kV side of the transformer.

$$\text{Max } I_{\varnothing G} = 3\sqrt{I''^2_d + I''^2_q}\, I_{base} = 3\sqrt{2.1^2 + 1.1^2}\; 900 = 6400\,\text{A}$$

The d-axis synchronous current determines the final or sustained value of the phase-to-ground fault current:

$$\text{Sustained } I_{\varnothing G} = 3\, I_d I_{base} = 3 \times 1.19 \times 900 = 3210\,\text{A}$$

© 2006 by Taylor & Francis Group, LLC

These currents are on the 67 kV side of the transformer. To reflect them to the 13.8 kV generator leads, refer to Figure 2.22.

$$\text{Sustained } I_A = I_{\varnothing G}\frac{Ey_{\varnothing N}}{E\Delta_{\varnothing\varnothing}} = 3210\frac{67/\sqrt{3}}{13.8} = 8970\text{ A}$$

2.9.4 Effects of the Automatic Voltage Regulator

Both fault conditions considered above are based on the assumption that the generator is under the control of the manual regulator; thus, field current is held constant. The current boosting effects of the automatic regulator can be included into the calculations by the addition of component I_{ex}, as defined by Equation (2.38) to the d-axis current equation.

$$i_d = (I''_d - I'_d)e^{-t/T''_{df}} + (I'_d - I_d)e^{-t/T'_{df}} + I_d + I_{ex}$$

where

$$I_{ex} = \frac{Ec - EI}{X_{df}}\left(1 - e^{-t/T'_{df}}\right)$$

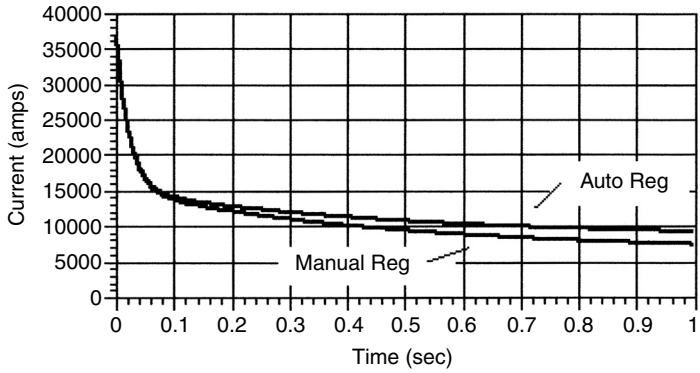


FIGURE 2.24 Three-phase fault at generator terminals.

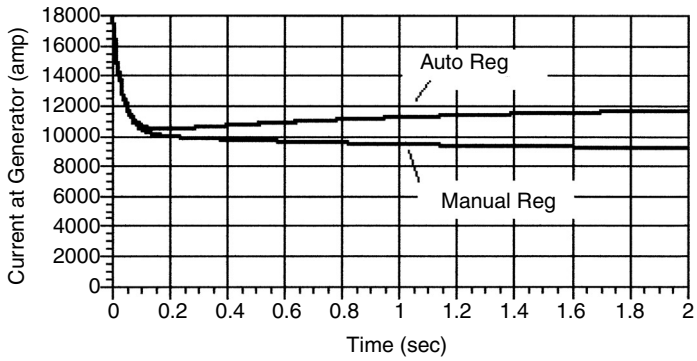


FIGURE 2.25 Phase-to-ground fault on GSU transformer.

© 2006 by Taylor & Francis Group, LLC

The values of *Ec* and *EI* are the same for both fault conditions, while X_{df} and T'_{df} are dependent on reactance X_f and differ for the two fault conditions.

Assuming that the ceiling voltage of the regulator is 500 V or 2.86 pu as previously calculated, then, for the three-phase fault at the generator terminals:

$$I_{ex} = \frac{2.86 - 2.16}{1.48}\left(1 - e^{-t/0.475}\right)$$

Also, for the phase-to-ground fault on the high-voltage side of the GSU transformer:

$$I_{ex} = \frac{2.86 - 2.16}{1.48 + 0.339}\left(1 - e^{-t/1.06}\right)$$

Figure 2.24 plots the current for a three-phase fault at the generator terminals with manual and automatic voltage regulators in service. Figure 2.25 shows a similar plot for the GSU phase-to-ground fault.

REFERENCES

1. IEEE Std 115, *IEEE Guide: Test Procedure for Synchronous Machines*, IEEE.
2. Power Technologies, Inc (PTI) course notes "Electrical Machine Dynamics I," F.P. deMello Schennectady, New York, July 1974.
3. T. Higgins, H. Holler, C. Wall, "Generator Representation and Characteristics for three phase faults", presented at the Pennsylvania Electrical Association, Allentown, Pennsylvania, January 31–February 1, 1990.

© 2006 by Taylor & Francis Group, LLC

3 Generator Differential Relay: 87G

3.1 INTRODUCTION

Short circuits associated with the stator winding or the generator leads produce very large short-circuit currents. These currents can cause extensive thermal damage to insulation. The magnetic forces associated with these currents can deform windings and subject the shaft and couplings to mechanical shock. This chapter is dedicated to the application of current differential relaying to provide rapid clearing of these faults.

The generator differential relay will normally trip the generator or GSU transformer breaker, the field breakers and initiate an immediate shutdown of the prime move.

3.2 IDEAL DIFFERENTIAL RELAY

The simplest form of differential protection is provided by an instantaneous relay connected as shown in Figure 3.1. The direction of current flow shown is for load or for a fault outside of the differential zone of protection. Assuming ideal current transformers (CT), currents I_1 and I_2 will be identical and relay operating current, I_o, will be zero.

When a fault occurs within the differential zone of protection, as shown in Figure 3.2, the current in one CT will reverse and the relay current is the full short-circuit current as reflected by the CT ratio, $I_o = I_1 + I_2$. The only limit to the sensitivity and operating time of this scheme would be the settable range and speed of the instantaneous relay chosen.

It is important to note that this differential scheme will not detect turn-to-turn faults within a stator phase winding. This type of failure may cause dissimilar phase currents, but because the current in each differential CT will be equal, the relay will not detect the fault.

3.3 PRACTICAL CONSIDERATIONS

In practice, nonideal current transformers impose significant sensitivity and operating speed restrictions on this scheme. The ideal scheme is predicated on the assumption that the CTs provide a precise reproduction of the primary current. Unfortunately, this is not the case.

A CT, like any other transformer, must develop a secondary voltage to produce secondary current. This requires establishing a magnetic flux in the CT's core and exciting current to maintain this core flux. Figure 3.3 is an equivalent circuit for a CT. The output of the CT is the ideal secondary current (I_p/N) less the exciting current (I_e). As CT secondary voltage increases, so does the excitation current and with it the CT error.

The impact of the CT error on the differential scheme is shown in Figure 3.4. In the ideal differential scheme, load current or a fault external to the differential zone of protection will not produce current in the relay. When practical CTs are considered, an error current equal to the difference of the two exciting currents will flow in the relay. The main consideration in the design and application of any differential relay is that the error current resulting from a fault external to the differential zone shall not cause the scheme to misoperate.

The relationship between CT secondary voltage and exciting current is described by the CT's excitation curve as shown in Figure 3.5. Note that the variation of excitation current with secondary voltage is not linear.

© 2006 by Taylor & Francis Group, LLC

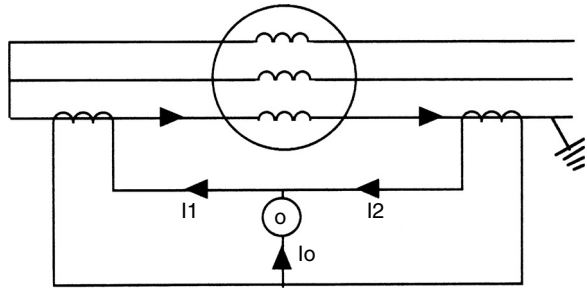


FIGURE 3.1 Differential relay external fault.

The secondary current and the total impedance of the CT's secondary circuit determine the voltage the CT must produce. This impedance is known as the CT's burden and includes the resistance of the CT itself, the resistance of current circuit conductors, and the impedance of the differential relay's input circuit:

$$V_{ct} = Z_b \frac{I_p}{N} \tag{3.1}$$

where V_{ct} = secondary voltage the CT must produce, Z_b = total impedance of the CT secondary circuit including the resistance of the CT, I_p = the primary current, N = CT turns ratio. When the generator is operating at full load (about 5 A in the secondary circuit), the CT voltage is minimal. The resulting excitation current for each CT is in the milliamp (ma) range and the error current is very low. A high current fault outside the differential zone may require hundreds of volts. Under this extreme condition, dissimilarities in the excitation characteristics and burden

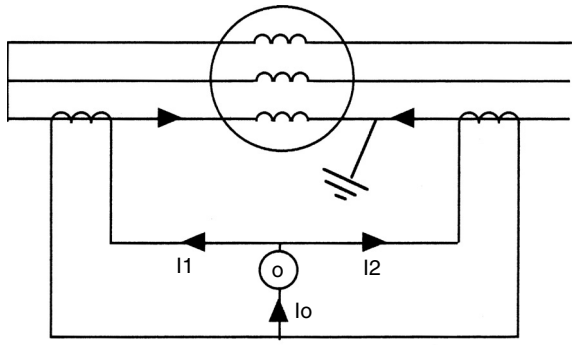


FIGURE 3.2 Differential relay internal fault.

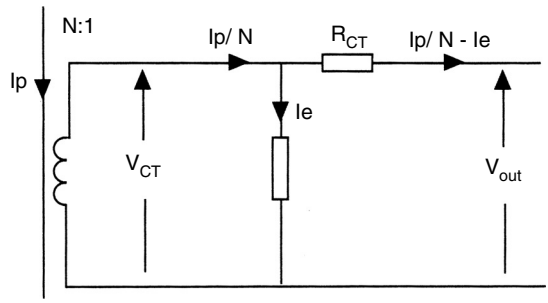


FIGURE 3.3 Current transformer equivalent circuit.

© 2006 by Taylor & Francis Group, LLC

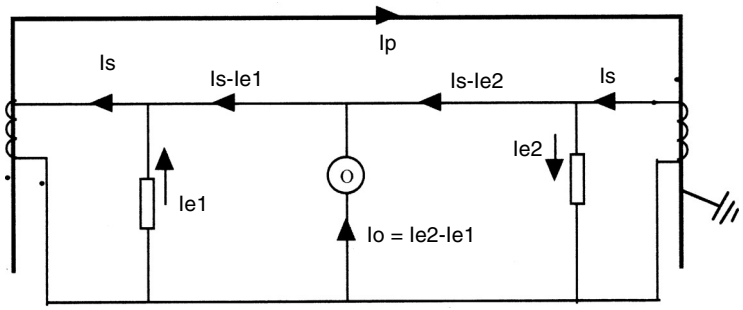


FIGURE 3.4 Error current.

will result in large variations in the exciting current between the two CTs. An instantaneous relay would have to be set above the large error current to prevent misoperation.

Maximum relay sensitivity is obtained by minimizing the difference in excitation currents for external fault conditions. The optimum design would include CTs with identical excitation characteristics and burdens. However, circuit burdens are at the mercy of the physical location of equipment and cable routing. Even when the CTs are of the same type and manufacturer a large error current can result because of manufacturing tolerances.

3.3.1 CT Ratings

CTs used for protective relaying are classified for accuracy by C, K, or T ratings. The rating system is based on a 10% current error at 20 times rated current. A 1000/5, C400 CT is capable of producing a secondary output of 400 V without exceeding an error of 10% up to a secondary current of 100 secondary amps. The C and K designations are used for CTs with negligible secondary leakage reactance. These CTs are constructed such that windings are fully distributed around the core. This construction virtually eliminates secondary leakage reactance and allows direct computation of performance from the excitation curves.

The T rating has the same accuracy parameters, but these CTs have significant leakage reactance and their performance can only be determined from tests. T-rated CTs are not recommended

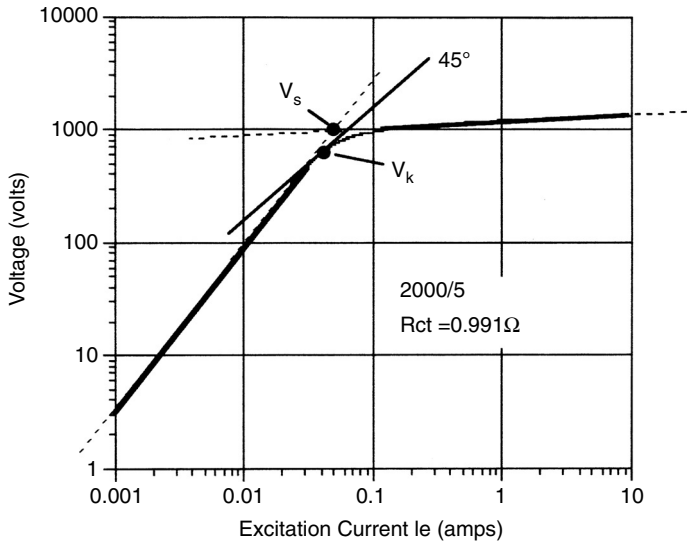


FIGURE 3.5 CT excitation curve.

© 2006 by Taylor & Francis Group, LLC

for use in differential circuits because of the increased burden caused by the leakage reactance and the inability to analyze circuit behavior.

The C, K, or T rating is for the full winding of the CT. If tapped windings are used, the rating is reduced by the ratio of the tapped to the full winding. A C400 1200/5 multiratio CT applied on the 600/5 tap is rated at C400 $*$ 600/1200 = C200 on the reduced tap.

Standards provide only seven voltage ratings for 5 A CTs: 10, 20, 50, 100, 200, 400, and 800 V. The ratings are based on 100 A secondary current and a 10% error; therefore, the voltage rating is determined from the voltage at which the exciting current is 10 A. The CT shown in Figure 3.5 has 10 A exciting current at 1040 V and a secondary resistance of 0.991 Ω. The secondary output at 100 A is 1040 V − 0.991 $*$ 100 = 941 V. Since a C941 V rating does not exist, it would be rated at the closest lower standard rating, which would be C800. Hence, all CTs with errors of 10% or less at 800 V are classified as C800. This demonstrates why CTs with comparable C or K ratings do not necessarily have comparable excitation curves.

Note that actual accuracy classification is based on standard burdens with a specified power factor; the above is a close approximation.

A more effective way to compare excitation curves is by knee-point or saturation voltages. These voltages are determined graphically from the excitation curve plotted on log–log coordinates as shown in Figure 3.5. The knee-point voltage (Vk) is the voltage at the point on the excitation curve tangent to a 45° slope. The saturation voltage (Vs) is the voltage at the intersection of the saturated and unsaturated slopes of the excitation curve.

The knee-point voltage also differentiates the C-rated CTs from K-rated CTs. A K-rating includes the requirement that the knee-point voltage must be at least 70% of the rating voltage. A K200 CT must have a knee-point voltage of 0.7 × 200 = 140 V or more. There is no knee-point requirement for the C rating.

3.3.2 CT Saturation

Another complication in the application of differential relaying caused by the nonlinearity of the CT core is nonsinusoidal relay currents. To appreciate this problem, deeper insight into the operation of a current transformer is required.

The impedance of the secondary circuit and the current being reproduced determine the required CT secondary voltage as defined by Equation (3.1). The CT's ability to produce this voltage is governed by the amount of flux the magnetic core of the CT can generate.

It is important to note that the secondary voltage (e) is not determined by the magnitude of flux in a transformer core but by the rate-of-change of the flux ($\mathrm{d}\varphi/\mathrm{d}t$) linking the secondary winding and the number of secondary turns (N).

$$e = N\frac{\mathrm{d}\varphi}{\mathrm{d}t} \tag{3.2}$$

This does not mean that there is no relation between voltage and core flux magnitude. If the CT secondary voltage is low, a small rate of change is required over a cycle and the total flux built up at the end of each cycle will also be low. A higher voltage requires an increased rate of change, which will result in a higher magnitude of core flux at the end of each cycle. A CT can only produce a given secondary voltage if the core can support the resulting end of cycle flux associated with that voltage.

The flux magnitude can be determined from the above equation. Solving for the change in flux and integrating, the flux required to produce a given voltage is then

$$\varphi = \frac{1}{N}\int e\,\mathrm{d}t \tag{3.3}$$

© 2006 by Taylor & Francis Group, LLC

The integral of the voltage with respect to time is effectively the area under the secondary voltage vs. time plot. The capability of a CT is sometimes evaluated on the basis of volt-second capability.

Assuming the secondary current and voltage are sinusoidal, the expression for core flux becomes

$$\begin{aligned} v &= E\sin(\omega t) \\ \varphi &= \frac{E}{N}\int \sin(\omega t)\,dt \\ \varphi &= -\frac{E}{N\omega}\cos(\omega t) \end{aligned} \tag{3.4}$$

where v = instantaneous CT secondary voltage; E = peak secondary voltage $\omega = 2\pi *$ frequency; N = number of secondary turns; and φ = flux in Webers.

The relationship between the CT voltage, excitation current and core flux for a CT operating within its flux capability is shown in Figure 3.6. Note that the voltage is positive while the flux change is positive and negative when the flux change is negative. Also note that the exciting current is in phase with the flux. The maximum flux level occurs when the voltage is zero.

The maximum and minimum flux peaks occur at $t = 0$ and at $\omega t = \pi$. During this period, the flux variation is from a positive maximum to a negative minimum value. The core flux requirement can then be calculated as

$$\begin{aligned} 2\varphi_{\max} &= \frac{1}{N}\int_0^{\pi} \sqrt{2}E_{\mathrm{RMS}}\sin(\omega t)dt \\ &= \frac{\sqrt{2}E_{\mathrm{RMS}}}{N\omega}\cos(\omega t)_0^{\pi} \\ \varphi_{\max} &= \frac{\sqrt{2}E_{\mathrm{RMS}}}{N\omega} \end{aligned} \tag{3.5}$$

The core material and the core's physical dimensions determine the flux level that a CT can support. The steel used in most CT applications can support a flux of 125,000 lines/in.^{2} or 1.8 Weber/m^2

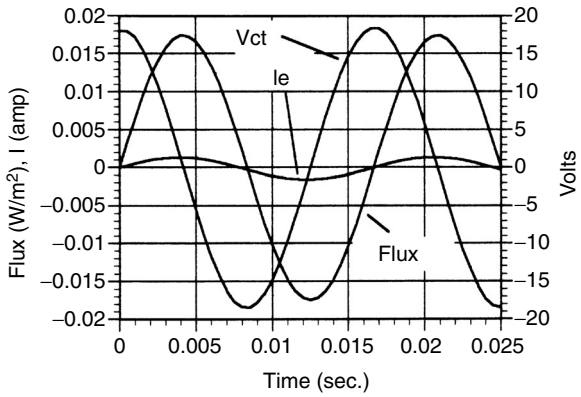


FIGURE 3.6 CT current and flux, unsaturated.

© 2006 by Taylor & Francis Group, LLC

depending on the system of units being used. If a 600/5 CT (120/1 ratio) is required to produce 200 V RMS, the core must be capable of sustaining

$$\varphi_{\max} = \frac{\sqrt{2}E_{\text{RMS}}}{N\omega} = \frac{\sqrt{2} \times 200}{120 \times 377} = 0.0063 \text{ Weber}$$

The core steel can support 1.8 Wb/m^2; hence, the CT must have a core area of $0.0063/1.8 = 0.0069$ m^2 or 5.4 in^2.

If this CT were applied at a location that had an 11,000 A fault current and CT circuit burden impedance of 3.2 Ω, the CT would be required to produce 11,000 A/120 ∗ 3.2 Ω = 293 V. This would require a flux density in excess of the core's capability of 1.8 Weber/m^2. The core is said to saturate.

There is no hard definition when saturation actually occurs. As voltage and core flux increase, excitation current increases. When the core flux density approaches the core's capability (the saturation flux density), the excitation current begins to increase at a disproportionate rate. This rapid increase is apparent in Figure 3.5. IEEE standards[1] define a "saturation voltage" at the intersection of tangents to the saturated and nonsaturated portions of the excitation curve. Other texts use the knee-point voltage as a benchmark for saturation.

A flux density vs. field intensity or B–H plot for a material defines its magnetic properties. Figure 3.7 is representative of the B–H characteristic of typical CT core material. The y-axis B represents the flux density (flux/area), while the x-axis is magnetizing force H in amp-turns provided by the exciting current per unit of core length (amp-turn/L). The curve has two notable characteristics, hysteresis and nonlinearity.

Hysteresis is the property that causes the material to remain magnetized after the magnetizing force is removed ($H = 0$). We are primarily concerned with the nonlinearity and the maximum flux density the core material can produce. Therefore, we will neglect hysteresis and use the simplified representation of the core as shown in Figure 3.8.

The slope of the B–H plot is steep and fairly linear up to the region where the core saturates, $B = 1.8$ Wb/m^2. Below saturation, a small increase in excitation current produces a large change in flux. Remember that voltage is proportional to the rate of flux change, not the magnitude of the flux, so little exciting current is required to produce secondary voltage. After saturation, the core's magnetic characteristic degrades to approximately that of free space. In this area the core will draw a huge AC exciting current, but the large change in excitation current produces

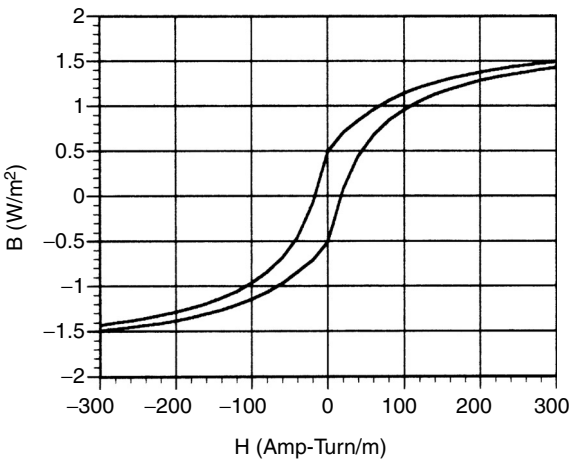


FIGURE 3.7 Typical B–H plot with hysteresis.

© 2006 by Taylor & Francis Group, LLC

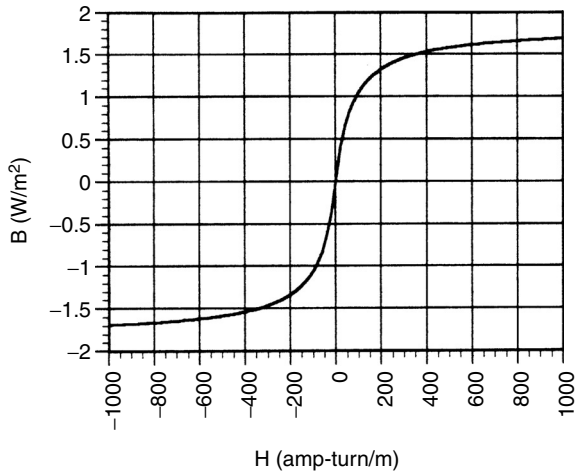


FIGURE 3.8 $B-H$ plot neglecting hysteresis.

little change in flux. With a negligible flux change, the CT output voltage and with it the current output fall to near zero.

The CT output current and core flux shown in Figure 3.9 are typical for a CT attempting to reproduce sinusoidal primary current but operating just beyond saturation. The flux plot becomes flat topped when the saturation flux density is reached. With no change in flux, the CT voltage and output current collapse and the excitation current becomes very large. If a higher secondary voltage is required, the saturation flux limit will be reached earlier in the cycle, as shown in Figure 3.10.

3.3.3 CTs and Fault Current Replication

Figure 3.9 and Figure 3.10 are representative of saturation resulting from a sinusoidal primary current. They provide insight into the theory of CT operation, but they do not reflect the actual fault environment in which the CT and differential relay must perform. The differential relay is intended to provide high-speed tripping. Like all high-speed current relays, it must contend with both the AC and DC components of fault current. The origin of the DC component was discussed

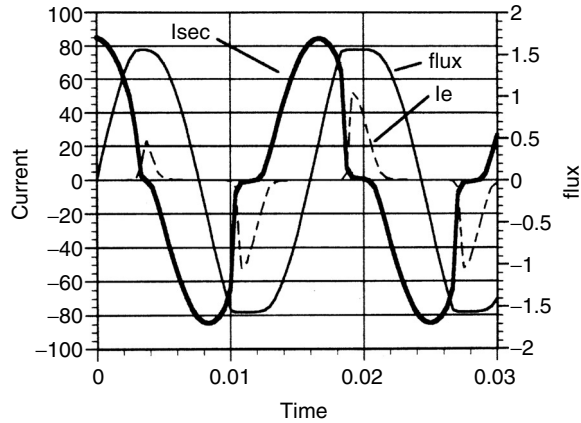


FIGURE 3.9 CT current and flux, slight AC saturation.

© 2006 by Taylor & Francis Group, LLC

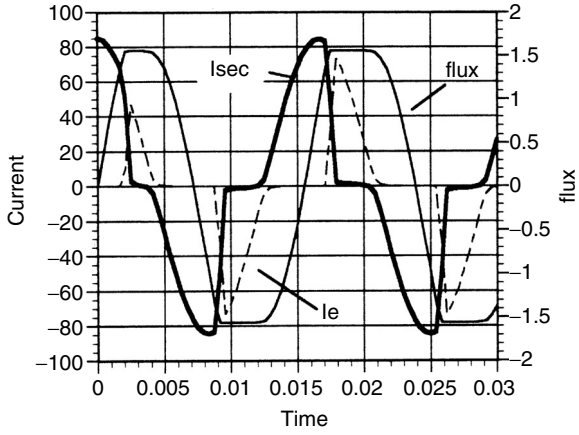


FIGURE 3.10 CT current and flux, moderate AC saturation.

in Chapter 2. Of particular interest for the generator differential function is the rather nasty effect the DC component has on current transformers.

The expression below describes fault current in terms of both the AC and DC components. It represents a worst case condition by assuming fault inception at a point where the AC component is at a maximum value. This constraint produces the maximum DC component and an AC waveform fully displaced from the zero axis.

$$i = I_{\mathrm{m}}\left[e^{-t/\tau} - \cos(\omega t)\right] \tag{3.6}$$

The i and I_{m} terms can represent CT primary or secondary quantities. The time constant τ is L/R of the primary circuit.

Replication of the AC current component in the secondary circuit requires the creation of a sinusoidal secondary voltage and sinusoidal core flux. Alternating positive and negative rates of flux change generates this AC voltage. The direction reversal limits the flux magnitude for each cycle. Replication of the DC current component requires a DC voltage and a unidirectional rate of flux change until the DC component dissipates.

Figure 3.11 shows the core flux transient resulting from both AC and DC components. The rapid increase in core flux due to the DC component is apparent for the first two cycles. During

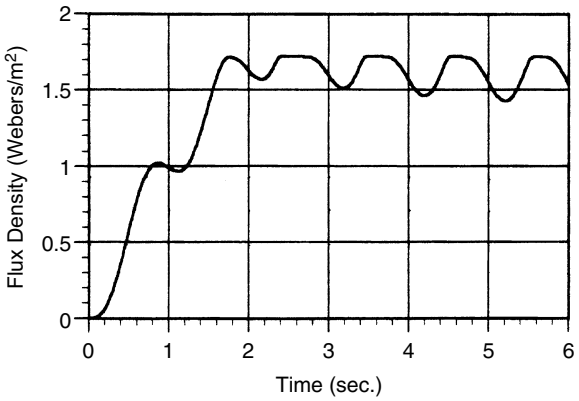


FIGURE 3.11 Core flux with AC and DC component.

© 2006 by Taylor & Francis Group, LLC

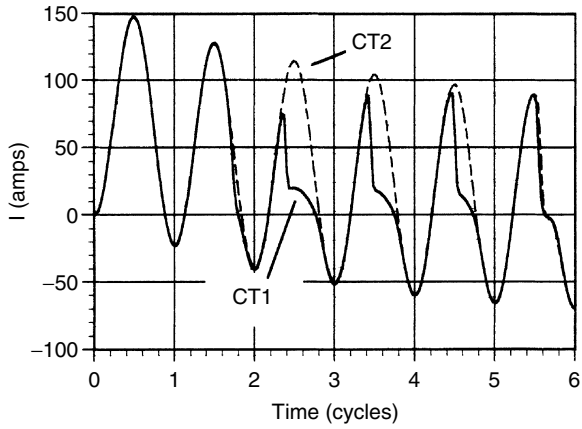


FIGURE 3.12 CT output with DC saturation.

this period, the positive and negative variations necessary to reproduce the AC component are also visible. However, after two cycles, the DC component drives the core to its saturation flux density. Since the core is not capable of producing flux in excess of this amount, the positive rate of change necessary to reproduce the positive half cycle of the AC component cannot be obtained.

The result of DC saturation on the CT outputs is shown in Figure 3.12. The effect of DC saturation is not immediate. Both CTs accurately reproduce secondary current for two cycles then distortion occurs in CT1. Distortion is not seen in CT2 until the sixth cycle. Also note that the CT1 waveform recovers as the DC component dissipates. The examples presented assumed the initial DC component was of positive polarity. Had the initial fault occurred a half cycle earlier or later, the polarity would have been negative and the negative half cycle of output current would have been distorted instead of the positive half cycle.

The severity of DC induced saturation can be seen in the following comparison. A CT must be capable of producing a voltage greater than $Z_b * I_p/N$ to avoid saturation caused by the AC component of current. To avoid saturation when the DC current component is included, the CT must be capable of producing a secondary voltage of

$$V_{ct} > \frac{I_p}{N} * Z_b(1 + X/R) \quad \text{[Ref. 1]} \tag{3.7}$$

where $X/R =$ ratio of primary circuit.

Avoiding DC induced saturation is nearly impossible for generator differential applications. The typical X/R ratio for transmission circuits is between 8 and 15. The X/R ratio at the terminals of a generator is much higher than the transmission case. The generator data sheet for the sample system generator lists a DC time constant for a three-phase fault $\text{Ta3} = 0.239$ sec ($\text{Ta3} = L/R$). This represents an X/R ratio for the generator of $X/R = 0.239 * 2\pi f = 90$. The sample system's CTs would have to be capable of producing 91 times the voltage required by the AC component to avoid DC saturation.

The error current for a fault external to the differential zone is the instantaneous difference between the output currents of the two CTs. When saturation causes dissimilar current distortion in the two CTs, large error current results. The error current resulting from the distortions in Figure 3.12 is plotted in Figure 3.13. Note that when CT1 saturates, the error current nearly equals the full output of the unsaturated CT. The high error current persists until both CTs reach the same degree of saturation or saturation abates.

© 2006 by Taylor & Francis Group, LLC

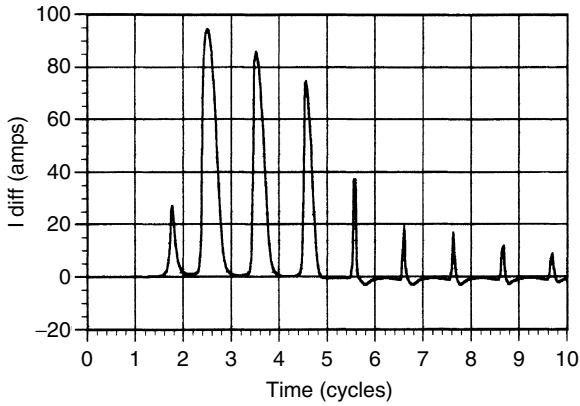


FIGURE 3.13 False differential current from DC saturation.

It is not practical to set the pickup of the instantaneous relay above the error current caused by DC saturation to prevent misoperation. The resulting settings would provide poor sensitivity for faults within the differential zone.

One way to avoid a false tripping and maintain a reasonable level of sensitivity is to delay operation of the relay to override the false current. To accomplish this the delay should be set about 3× the DC time constant. In the case of the sample system, this criterion would require delaying tripping for 0.7 seconds. This is clearly undesirable.

3.4 PERCENTAGE DIFFERENTIAL RELAY

The percentage differential relay has been developed to overcome the shortcomings of the idealized scheme. Electromechanical units have restraint as well as operate windings as shown in Figure 3.14. Current in the restraint coils produces contact opening torque; current in the operating coil produces contact closing torque. Relay contacts will close when the operating current exceeds the restraining value by a given percentage. The percentage is referred to as the slope of the relay. This design provides an automatic increase in the operating coil current necessary to tripping as fault current and the resulting CT error increase.

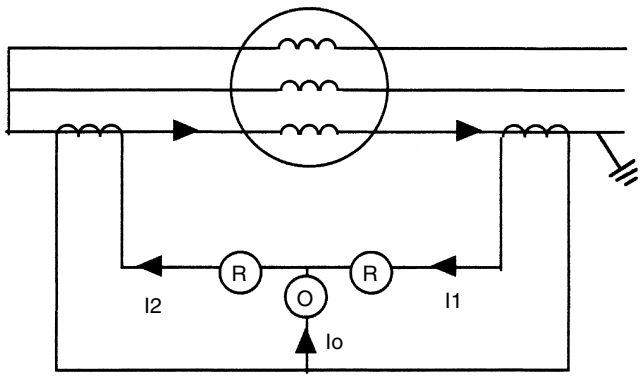


FIGURE 3.14 Percentage differential relay.

© 2006 by Taylor & Francis Group, LLC

Referring to Figure 3.2, assume a high magnitude fault external to the differential zone causes the CT at the generator terminals to saturate. The RMS currents in the differential circuit are $I_1 = 60$ A and $I_2 = 50$ A. The resulting current in the operating coil is $I_1 - I_2 = 10$ A. By design, the effective restraint for the relay is $(I_1 + I_2)/2 = 55$ A. The operating current is $10/55 = 0.18$ (18%) of the restraint current. If the relay has a slope of greater than 18%, it will not operate. If the slope of the relay is less than 18%, it will misoperate for the external fault.

When a fault occurs within the differential zone of protection, Figure 3.2, current I_2 will reverse and the restraint becomes $(I_1 - I_2)/2$ and the operating current becomes $I_1 + I_2$. If the same current magnitudes are assumed to exist for the internal fault, the restraint would be $(60 - 50)/2 = 5$ A, and the operate current would be $(60 + 50) = 110$ A.

The practicality of the design is apparent. The scheme has minimal sensitivity for faults external to the zone of protection when CT error can cause misoperation, and maximum sensitivity for faults within the zone of protection. The percentage differential principle originated from electromechanical technology, but its success has led to emulation in static and microprocessor relays.

Note that relay quantities are not standardized. The operating quantity is usually defined as $(I_1 - I_2)$, but the restraint quantity definition varies among manufacture's. The quantity $(I_1 + I_2)/2$ is often used for restraint, but the following restraint quantities are also employed by various manufacture's: $(I_1 + I_2)$, $(|I_1| + |I_2|)$, the larger of I_1 and I_2, and the smaller of I_1 and I_2. The instruction book for the specific relay in question must be consulted to determine the actual restraint definition used.

3.5 RELAY CHARACTERISTICS

Although all percentage differential elements use the same operating principle, the implementation varies between electromechanical, static and microprocessor functions. The variations affect the number of setpoints required and the method of calculations.

3.5.1 Electromechanical Relays

The slope of most electromechanical relays is not adjustable; it is determined when the relay is purchased. Typically, slopes of 10, 25, 40, 50%, and variable slope relays are available. The variable slope characteristic increases from around 10% to over 50% as restraint current increases. Typical electromechanical percentage differential relay characteristics are plotted in Figure 3.15.

The relay characteristic includes a minimum operating current. This is the minimum current passing through one restraint winding and the operate coil required to actuate the relay. It is indicative of the maximum sensitivity for a generator fault with the generator disconnected from the power system. The minimum operating current of an electromechanical relay is usually not adjustable, but is determined by the slope setting. It may vary from about 0.2 A for the 10% slope relay to about 1.0 A for the 50% slope relay.

Some relays have a time delay adjustment. This delay is often factory set to override the effects of DC saturation. The setting is based on the manufacturer's experience with his relay design. The factory setting is normally retained.

3.5.2 Solid-State and Microprocessor Relays

These relays are not subject to the magnetic and physical constraints that limit the flexibility of their electromechanical counterparts. Solid-state relays often have adjustable slopes. Some have fixed steps similar to those available with electromechanical relays, namely 10, 25, 40, 50% slopes; others have continuously adjustable slopes. The minimum operating current may or may not be independently adjustable.

The microprocessor differential function is usually included as part of a complete generator protection relay. The differential function will normally have a continuously adjustable slope

© 2006 by Taylor & Francis Group, LLC

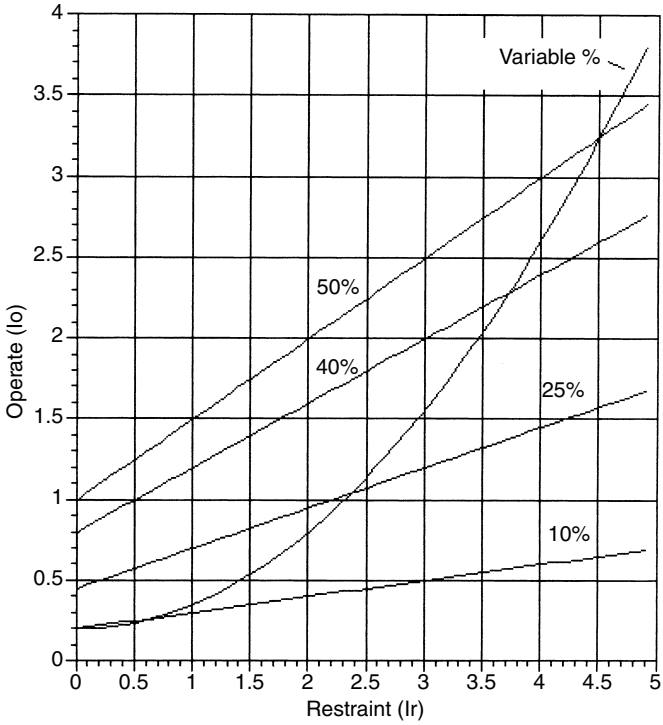


FIGURE 3.15 Electromechanical relay slope characteristics.

setting, from 1 to 100% in some cases. Minimum pickup setting is also continuously adjustable, usually in a range from 0.1 to 2 or 3 A.

A typical slope characteristic for solid-state and microprocessor elements is shown in Figure 3.16. This relay has no slope for operating current in excess of its minimum operating current setting up to an operating current of about 5.0 A. This provides maximum sensitivity for low current faults. Above 5.0 A, an increased CT error is anticipated and a minimal slope characteristic is implemented from 5 to about 10 A restraint. Above 10 A restraint, a second and steeper slope provides security from misoperation for maximum fault and resulting maximum CT error

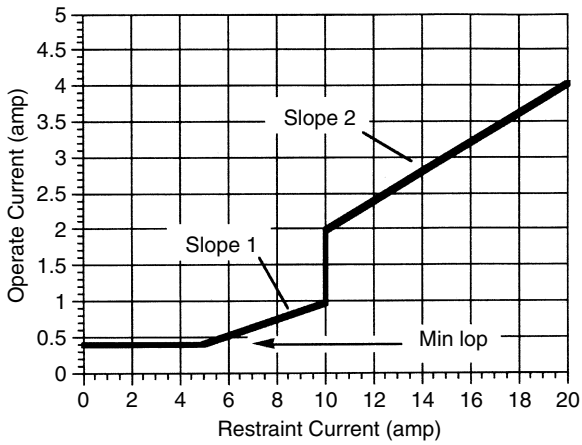


FIGURE 3.16 Solid-state and microprocessor relay slope characteristics.

© 2006 by Taylor & Francis Group, LLC

condition. Not all solid-state or microprocessor relays have multiple slopes. Of those that do, some allow each slope to be chosen independently, while others automatically set the second slope at two to four times the first.

The microprocessor-based differential function normally includes an adjustable time delay that can be set to near zero. Solid-state relays may or may not have adjustable delays.

3.6 MINIMUM OPERATING CURRENT SETTING

This setting is not required for most electromechanical relays because the slope usually determines the minimum operating current. A setting is required for solid-state and microprocessors relays.

Given the slope characteristic of Figure 3.16, the relay will actuate for an error current equal to the minimum operating current up to a restraint of 5 A. The minimum operating current must be set above the maximum differential error current present at this restraint.

At 5 A secondary current, a CT error of $<2\%$ would be expected. If one CT is assumed to be $+2\%$ and the other -2%, a net error of 4% would produce an operating current of $5.0 * 0.04 = 0.2$ A. A setting equal to or greater than this value should be satisfactory for most applications. Actual error current can be estimated from excitation curves, but a setting below 0.1 A is not recommended.

Some characteristics extend the unsloped characteristic to restraint currents greater than 5.0 A. In these cases, the minimum operating current must be set above the error at the maximum restraint current applicable.

The 0.2 A setting will not be adequate if additional errors are introduced by the proximity effect.[2] Generator differential CTs can be high ratio installed in locations with tight spacing. Under these circumstances, stray flux from adjacent phase conductors can enter the CT core and add vectorally to the normal core flux. When this occurs, the flux around the core will not be uniform. The increased flux levels in portions of the core will necessitate higher exciting current. The resulting error will be greater than that derived from the CT's excitation curve. If any section of the CT is driven to saturation by the external flux, the resulting errors can cause differential relay misoperation under fault and load conditions.

A common practice with high ratio CTs is to employ compensation winding, which minimizes the proximity effect. Proximity error for noncompensated CTs can be estimated using the methods outlined in ref. (2). At existing installations error current measurement is an option. When microprocessor relays are applied, the metering functions provided with these relays can be used to confirm maximum error currents during full load operations.

3.7 SLOPE SETTING

3.7.1 Requirements for Slope Setting

The slope setting must be high enough to ensure that the differential element does not operate for a fault external to the differential relay zone of protection. The minimum setting would be calculated from the maximum error current generated by an external fault and the associated restraint current as shown below.

$$\%\text{Min slope} > K * 100 * (\text{max error current})/(\text{restraint current})$$

where $K =$ safety factor (a value of 2 is often used). Although this criterion is simple, a specific slope setting recommendations is not.

First the error current is difficult to define. Each differential circuit contains at least two nonlinear elements, the CT cores, and the operating current circuit of an electromechanical

© 2006 by Taylor & Francis Group, LLC

relay would introduce a third nonlinear element. A direct algebraic solution of the circuit is not possible; iterative or graphical solutions are required. Secondly, in worst case conditions, namely saturation, relay operating and restraint currents are nonsinusoidal and relay response is unclear.

The simplest approach to the analytical ambiguities described above would be to use the highest available slope setting. This would maximize security for external faults, but the reduction in sensitivity could unnecessarily sacrifice generator protection.

3.7.2 Advantage of Low Slope

Insulation failure is an evolving process. A small leakage current causes local heating; with time, the heating deteriorates the insulation and increases the leakage current. The process continues until the deterioration cascades into a complete failure, with current reaching the maximum short circuit magnitude. A relay with low slope will have greater sensitivity and can detect the evolving faults sooner, thus minimizing damage. The choice of slope must be a balance between sensitivity and security. One of the advantages of solid-state or microprocessor relaying is the operating characteristic, as shown in Figure 3.16. The flat response up to rated current provides maximum sensitivity when the CTs are most accurate. The electromechanical relay characteristic (Figure 3.15) only approaches this level of sensitivity at minimum slope.

3.7.3 Sensitivity and Load Current

The sensitivity of a percentage differential relay will vary with load. Load current flows in one restraint coil and out the other and is therefore a restraint quantity. By design, restraint current will increases the operating current necessary to actuate the relay. This desensitizing action is not of interest when evaluating maximum faults internal to the differential zone. High-magnitude, short-circuit current overwhelms the minimal restraint from load. However, when scheme sensitivity to restricted internal faults, such as insulation deterioration, is evaluated, the effect of load can be significant.

The interaction of load and fault current is shown in Figure 3.17. Load current adds to the generator's contribution of fault current in one restraint winding and subtracts from the system's contribution in the other restraint winding:

$$I_1 = I_L + KI_F \tag{3.8}$$

$$I_2 = I_L - (1 - K)I_F \tag{3.9}$$

where K is the ratio of fault current from the generator to the total fault current. Referring to Figure 3.17:

$$K = \frac{X_{\text{tr}} + X_{\text{syst}}}{X''_{\text{d}} + X_{\text{tr}} + X_{\text{syst}}} \tag{3.10}$$

If the relay restraint quantity is assumed to be $(I_1 + I_2)/2$, then the restraint with load included becomes

$$I_{\text{R}} = \frac{I_1 + I_2}{2} = I_{\text{L}} + \frac{(2K - 1)}{2} I_{\text{F}} \tag{3.11}$$

Because low current is being considered, the CTs are assumed to be ideal, and the relay operating current will equal the fault current as reflected by the CT ratio. Equating fault and operating current and rearranging terms:

© 2006 by Taylor & Francis Group, LLC

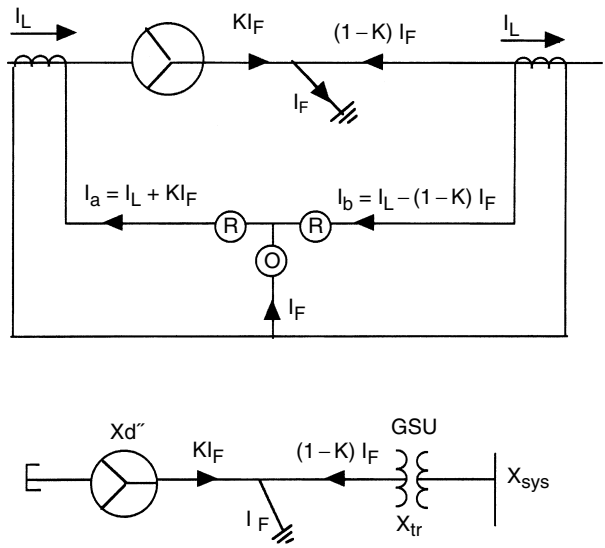


FIGURE 3.17 Generator loading and fault current.

$$I_{op} = \left(\frac{2}{2K-1}\right)(I_R - I_L) \tag{3.12}$$

This expression describes the variations of operating current with restraining current and load as dictated by the power system.

Equation (3.12) is plotted, using sample system parameters, against the various electromechanical differential characteristics in Figure 3.18. Load current induced restraint will prevent relay operation for faults in the area to the left of this plot. The sensitivity advantages of a low slope relay are clearly shown on this plot. Load limits the minimum operating current for the 10% relay to about 0.6 A in the relay. With 6000/5 CT this relates to a minimum detectable fault of 720 A at the generator terminals. The minimum operating current for the 50% relay with load is about 3.0 A in the relay or 3600 A at the generator terminals.

3.7.4 Relay Response to Saturation

Most installations experience some degree of CT saturation. Slope settings are based on the maximum error current for a fault external to the differential zone of protection. This error current is caused by unequal saturation of the CTs on either side of the generator. The resulting restraining and operating currents are nonsinusoidal, as shown in Figure 3.12 and Figure 3.13.

Unfortunately, because of the large diversity of magnetic and electrical circuit designs found in electromechanical relays, the varied input and detector circuit used in static relays, and the different sampling and filtering techniques found in microprocessor relays, no general conclusions about relay response to these distorted waveforms is possible.[3]

The intent here is to set forth some specific assumptions that will be used as a basis for discussion of slope settings in this text. These assumptions are not applicable to all relays. When determining settings for any relay, the guidelines provided in the manufacturer's literature must be followed.

Electromechanical differential relays use the induction disk principle. Two or more coils produce flux that is applied to a nonmagnetic but electrically conducting disk. When sinusoidal

© 2006 by Taylor & Francis Group, LLC

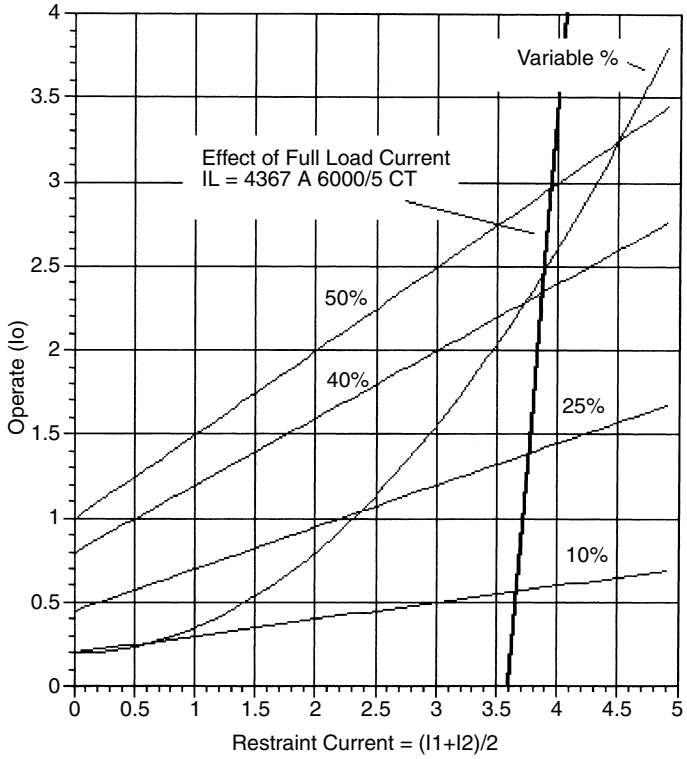


FIGURE 3.18 Relay sensitivity with loading.

current is applied to the coils, a current is induced in the disk. Coil flux interacts with flux produced by the disk current. If currents of the same frequency are applied to the coils, a constant torque is exerted on the disk that is proportional to the phase angle between the coil currents. The torque is contact closing or contact opening depending upon the phase relation of the currents. If different frequency currents are applied to the two coils, the phase angle will vary sinusoidally with time producing contact closing torque over half the cycle and contact opening torque over the other half the average torque produced is zero.

Assuming one CT saturates and the other does not, the unsaturated CT would apply a 60-cycle sinusoidal current to one coil. The saturated CT's output would include some amount of fundamental (60 cycle) current mixed with other harmonics. In theory, because one input to the relay is pure 60 cycle, net torque will only be produced by the fundamental (60 cycle) component of current from the saturated CT. In practice, nonideal magnetic materials may allow dissimilar harmonics to produce torque. This torque can be operating or restraining and will vary widely with individual relay designs.

Most electromechanical relays do, however, include circuitry designed to minimize the effect of the DC component and maximize the influence of the fundamental component. Over the years electromechanical relays have been applied successfully, with analysis based on the fundamental RMS value of operating and restraint currents.

Static relay response to the distorted waveform is affected by the design of sensing and detector circuits. The microprocessor relay response to these harmonics is determined by the filtering techniques used at the input circuits. The tendency has been toward relay designs that are responsive to the fundamental frequency component.

© 2006 by Taylor & Francis Group, LLC

The analysis presented in this text will be based on traditional fundamental frequency RMS calculations for electromechanical relays and on the fundamental component for the solid-state and microprocessor relays. Again, these techniques are not universally applicable, and when specific relay models are being set, the relay manufacturer recommendations must be followed.

3.7.5 Methods of Choosing Slope Settings

3.7.5.1 Manufacturer's Recommendations

As a result of the analytical problems, choosing the slope of a differential relay has been more art than science. Manufacturer's guidelines tend to be qualitative or empirical in nature. They are based on the manufacturer's experience and knowledge of his design. This is unavoidable in the case of electromechanical relays, where the designer is at the mercy of the physical constraints related to iron and wire. He has little control over or methods to analyze the relay response to distorted waveforms. The mathematical nature of sampling and filtering techniques used in static and microprocessor relays makes their response to a given waveform more predictable. However, because of the analytical difficulty in predicting the waveform, electronic-based relay literature usually offers little guidance in slope selection.

As an example, one manufacturer offers a generator differential relay with 10% or 25% slope characteristics. The literature for the relay provides a rule-of-thumb for slope selection. If the error in neither CT exceeds 1% for a maximum external fault, the 10% slope is recommended. Above 1%, a 25% slope relay is recommended. Another manufacturer of a variable slope relay requires that the CT error at twice rated current (10 A) shall not exceed 1% to assure proper operation of the relay.

3.7.5.2 Qualitative Determination of Slope

The error current seen by the differential relay is a function of the differences between the two CT circuits that supply the relay. A traditional method for choosing the slope of electromechanical relays is based on a qualitative assessment of similarity. At installations where the differential CTs on either side of the generator are of the same type with similar knee-point voltages and have similar burdens, a 10% slope relay could be applied. This would be the case if the differential scheme is applied using bushing CTs on each end of the generator.

If the differential scheme uses one set of bushing CTs at the neutral end of the generator and one set of CTs at a remote generator breaker located in switchgear, the CT characteristics and burdens will differ. In this instance, a higher slope would be required. If the CT characteristics differ significantly or there are large variations in burden, a variable slope relay may be required.

3.7.5.3 Error Current Calculations for Unsaturated CT

This error calculation is valid for a differential circuit under load or if fault currents and burdens are such that the relay is not driven into saturation by the AC component of fault current.

Using Figure 3.19, the secondary voltage of each CT is calculated assuming I_o is small such that $I_o\, Z_o \approx 0$:

$$V_a = Z_a * I_s$$
$$V_b = Z_b * I_s$$
$$I_s = I_{prim}/N$$

Impedance Z_a and Z_b include the resistance of the CT itself, the impedance of the conductor, and the impedance of the restraint coil to which the CT is connected.

© 2006 by Taylor & Francis Group, LLC

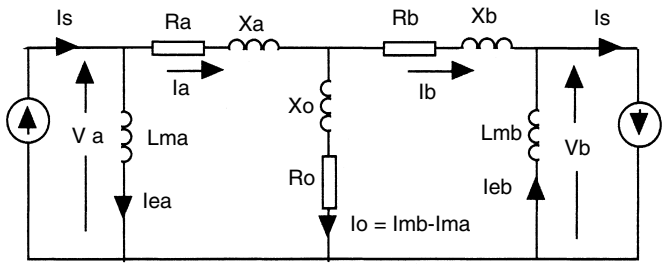


FIGURE 3.19 Differential circuit impedance.

The excitation currents I_{ea} and I_{eb} are determined from the excitation curve of each CT. The error and restraint current can then be calculated as follows:

$$I_a = I_s - I_{ea}$$
$$I_b = I_s - I_{eb}$$
$$I_{diff} = I_{eb} - I_{ea}$$
$$I_{rest} = (I_a + I_b)/2$$

3.7.5.4 Mason's Method

If AC saturation is present, which would be the case if either of the CT voltages calculated above is significantly above the saturation voltage, or the voltage across the differential relay operating coil cannot be neglected a method proposed by Mason[5] can be used to determine the RMS relay currents. It employs a graphical solution using CT saturation curves and secondary circuit impedance data. The method has been employed for electromechanical relays. Once the error and restraint currents are known, the relay slope requirement can be determined.

Figure 3.19 shows the differential CT circuits with associated burdens. The following equations can be written for this circuit:

For CT_a:

$$0 = V_a - I_a Z_a - Z_o(I_a - I_b)$$
$$Z_o(I_a - I_b) = V_a - I_a Z_a \tag{3.13}$$

For CT_b

$$0 = V_b - I_b Z_b + Z_o(I_a - I_b)$$
$$Z_o(I_a - I_b) = -V_b + I_b Z_b \tag{3.14}$$

Voltage and corresponding excitation current points can be taken from the excitation curves of each CT. For each voltage point set, I_a and I_b can be determined by subtracting the excitation current from the ideal secondary current: $I_a = I_s - I_{ea}$ and $I_b = I_s - I_{eb}$. With V_a, I_a, V_b and I_b now known, the term $(I_a - I_b)$ can be found as a function of I_a and I_b from Equation (3.13) and Equation (3.14). If I_a vs. $(I_a - I_b)$ from Equation (3.13) and I_b vs. $(I_a - I_b)$ from Equation (3.14) are plotted on the same graph, the actual error current is found at the point where the difference between I_a and I_b equals the same value on the $(I_a - I_b)$ axis.

The error current found by this method and the corresponding restraining current is plotted against differential relay characteristics to evaluate the required slope. This method is a benchmark of the error current. CT excitation curves often have a 25% tolerance associated with the region beyond the knee. Also, this graphical method does not include allowances for DC saturation that

© 2006 by Taylor & Francis Group, LLC

may occur. Consequently a safety factor of at least 2 should be used in conjunction with error currents determined by this procedure.

3.7.5.5 Example of Mason's Method

Assume a differential zone is to extend from the bushing CTs on the neutral end of the generator to CTs at a breaker at remote switchgear. The CTs are 1000/5, C200 relay accuracy classification and the generator's contribution to a three-phase fault current at the switchgear is 15,000 A.

The current circuit from the switchgear to the relay is single conductor #10 Cu per phase with a one-way length of 4700 ft. The current circuit from the generator to the relay is also #10 Cu with a one-way length of 1300 ft. The generator is grounded through high impedance, limiting the ground fault current to a few amps; therefore, the generator differential relay will not need to detect phase-to-ground faults.

The instruction book for the differential relay being considered lists the following impedances.

Restraining coils = 0.2 Ω
Operation coil = 0.5 Ω

The resistance of #10 Cu control cable is normally assumed to be 1.0 Ω/1000 ft. With this data the circuit burdens are established as:

CTA	CTB
CT resistance = 0.49 Ω	CT resistance = 0.49 Ω
1300 ft #10 CU = 1.3 Ω	4700 ft #10 CU = 4.7 Ω
Restraint coil = 0.2 Ω	Restraint coil = 0.2 Ω
$R_a = 2.0\ \Omega$	$R_b = 5.4\ \Omega$

Note that since ground fault conditions are not being considered, one-way cable resistance is used. If the differential relay were required to operate for a phase-to-ground fault, the return path in the CT circuits would have to be considered. This would double the impedance of each circuit.

This is not an ideal installation. In theory, the CT excitation characteristic and burdens should be matched to minimize the relay error current for an external fault. Here the burdens differ by almost 3:1. The CTs have the same accuracy class, C200, but this does not equate to matching the excitation characteristics. CTA has a knee-point voltage of 147 V, CTB 127 V. Also note that the circuit routing will resulted in a higher burden on the poorer quality CT at the switchgear.

Substituting resistance values into Equation (3.13) and Equation (3.14):

For CT1:

$$Z_o(I_a - I_b) = V_a - I_a R_a \qquad (3.15)$$
$$0.5(I_a - I_b) = V_a - 2.0 I_a$$

For CT2:

$$Z_o(I_a - I_b) = -V_b + I_b R_b \qquad (3.16)$$
$$0.5(I_a - I_b) = -V_b + 5.4 I_b$$

Excitation data and the calculation of $(I_a - I_b)$ for each voltage value are tabulated in Table 3.1 and Table 3.2. The excitation current I_e is subtracted from the ideal secondary current of 15,000 × 5/1000 = 75 A. The operating coil current is then found using Equation (3.15) and Equation (3.16).

© 2006 by Taylor & Francis Group, LLC

TABLE 3.1
CT1 I_1 vs. $I_1 - I_2$

CT1 Excitation Curve		CT Output	Operate Coil
V_{CT}	I_e	$I_1 = I_s - I_e$	$(I_1 - I_2)$
146.74	0.05	74.95	−6.30
149.18	0.06	74.94	−1.41
151.63	0.06	74.94	3.49
154.08	0.06	74.94	8.38
156.52	0.06	74.94	13.28
158.97	0.06	74.94	18.17
161.41	0.06	74.94	23.07
163.86	0.06	74.94	27.97
166.30	0.06	74.94	32.86
168.75	0.06	74.94	37.76

Figure 3.20 plots I_a and I_b vs. the quantity $(I_a - I_b)$. The operating point is found where the vertical difference between I_a and I_b equals the same value on the $(I_a - I_b)$ axis. This point occurs where $I_a = 75$ A and $I_b = 55$ A, and $(I_a - I_b) = 20$. From Tables 3.1 and 3.2, the voltages at CTA and CTB are approximately 160 V and 266 V respectively.

The operating quantity $(I_a - I_b)$ is 20 A and the restraining quantity is $(75 + 55)/2 = 65$ A. The resulting slope minimum is $100 * 20/65 = 31\%$. If a safety factor of 2 is applied, a slope of 62% is required to prevent misoperation. These values are plotted against various differential relay characteristics (Figure 3.21). It is apparent that the variable slope relay would be required to maintain the recommended safety margin.

3.7.5.6 Fundamental Frequency Analysis

Microprocessor relays are assumed to use filtering techniques that limit relay response to the fundamental frequency component of current. Although these relays will not respond to the DC

TABLE 3.2
CT2 I_2 vs. $I_1 - I_2$

CT2 Excitation Curve		CT Output	Operate Coil
V_{CT}	I_e	$(I_2 = I_s - I_e)$	$(I_1 - I_2)$
254.35	8.08	66.92	214.07
256.30	9.75	65.25	192.11
258.26	11.84	63.16	165.63
260.22	13.93	61.07	139.16
262.17	16.71	58.29	105.17
264.13	20.19	54.81	63.65
266.09	23.67	51.33	22.14
268.04	29.25	45.75	−41.94
270.00	34.82	40.18	−106.01
271.96	41.78	33.22	−185.13

© 2006 by Taylor & Francis Group, LLC

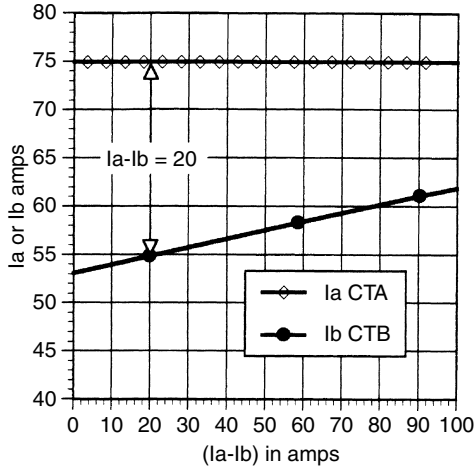


FIGURE 3.20 Plot I_1 and I_2 vs. $(I_1 - I_2)$.

component directly, DC saturation dramatically affects the fundamental component provided to the relay by the CTs. These relay also respond in approximately a cycle. The trip no-trip decision is made while the CTs are under the effects of the DC component of fault current. A setting determination for these relays cannot be made with confidence without knowledge of the input waveforms and their harmonic content.

A Mathcad® worksheet included as Appendix B was developed for this analysis. The model assumes a fully offset primary fault current, thus maximizing the combined effects of AC and DC components.

The worksheet uses Mathcad "solve blocks" to perform a point-by-point iterative circuit solution of the differential equations describing the circuit in Figure 3.19. The solution is similar to that described by Zocholl and Smaha.[6] The nonhysteresis Frolich equation was used to model the nonlinearity of the CT cores. Solutions for faults external and internal to the differential zone can be simulated by toggling specified equations "On" and "Off."

A simulated Fourier filter is also included in the worksheet to extract the fundamental frequency component of relay current. Restraint and operating currents derived from the fundamental

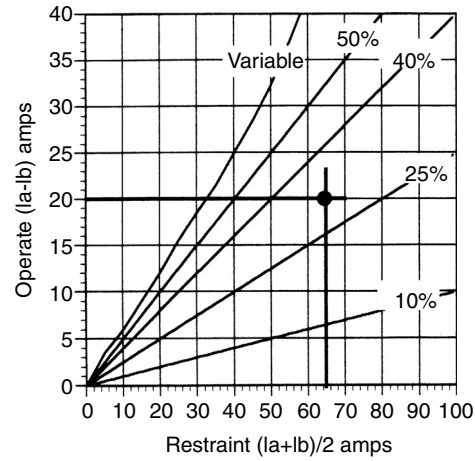


FIGURE 3.21 Choosing relay slope.

© 2006 by Taylor & Francis Group, LLC

components will be used to assess the performance and determine settings for a microprocessor relay later in the chapter.

3.8 SAMPLE SYSTEM DIFFERENTIAL RELAY SETTINGS

3.8.1 Sample System Differential Circuit

An electromechanical and a microprocessor relay will be evaluated for protection of the sample system generator. At each end of the differential zone, 6000/5 CTs with an accuracy class of C800 are used. CTA has a knee-point voltage of 550 V and CTB has a knee-point voltage of 650 V. The circuit from CTA to the relay is 2700 ft of #10 CU and from CTB 200 ft of #10.

The maximum three-phase fault current from the generator is 36,000 A and the associated DC time constant (L/R) from the generator data sheet is Ta3 = 0.239 sec. This is equivalent to an X/R ratio of $2\pi f * 0.239 = 90$.

3.8.2 Electromechanical Relay

3.8.2.1 Specifications for Relay Chosen

One option for the sample system is the installation of an electromechanical differential relay. The model being considered is available with 10% or 25% slope. The minimum operating current for the 10% relay is 0.18 A, and 0.45 A for the 25% relay. The burdens imposed on the current circuit by the relay are:

Each restraint coil = $0.04 + j\,06 = 0.072\ \Omega$
Operate circuit = $5.4\ \Omega$ at 5 A

The resulting burdens are:

CTA	CTB
$R_{ct} = 3.1\ \Omega$	$R_{ct} = 2.8\ \Omega$
$R_{cond} = 2.7\ \Omega$	$R_{cond} = 0.2\ \Omega$
Relay = $0.07\ \Omega$	Relay = $0.07\ \Omega$
$R_a = 5.87\ \Omega$	$R_b = 3.07\ \Omega$

The relay manufacturer recommends that the CT knee-point voltages and burdens be matched to reduce the error during external faults, but provides no guidance on slope selection. Electromechanical relays have a high immunity and are generally set without regard to the effects of DC saturation. Since the manufacturer's publication for the relay has no specific requirements in this area, the slope will be determined by an assessment of the CT error resulting from the maximum AC component of external fault current.

The maximum secondary fault current for an external fault is 36,000 A × 5/6000 = 30 A. The resulting CT voltages, assuming no voltage across the operating circuit, are

$$V\,\text{CTA} = 30\,\text{A} \times 5.87\,\Omega = 176\,\text{V}, \quad I_e\,(\text{CTA}) = 0.0035\,\text{A}$$
$$V\,\text{CTB} = 30\,\text{A} \times 3.07\,\Omega = 92\,\text{V}, \quad I_e\,(\text{CTB}) = 0.0017\,\text{A}$$

These voltages are well below the knee-point voltage of each CT; hence, no AC saturation is evident. The excitation currents were obtained from the excitation curves and are listed above. The voltage across the relay operating coil can now be estimated as $5.4\,\Omega$ (0.0035 A–0.0017 A) = 0.01 V justifying the initial assumption.

© 2006 by Taylor & Francis Group, LLC

The minimum slope assuming a safety factor of 2 is:

$$I_{\mathrm{d}} = 0.0035 - 0.0017 = 0.0018\,\mathrm{A}$$
$$I\mathrm{CTA} = 30.0 - 0.0035\,\mathrm{A} = 29.9\,\mathrm{A}$$
$$I\mathrm{CTB} = 30.0 - 0.0017\,\mathrm{A} = 29.9\,\mathrm{A}$$
$$I_{\mathrm{restraint}} = (29.9 + 29.9)/2 = 29.9\,\mathrm{A}$$
$$\text{Min Slope}\% = 2 * I_{\mathrm{d}}/I_R = 2 * 100 * 0.0018/29.9 = 0.012\%$$

The maximum external fault would not operate a relay with a 0.012% slope. The 10% relay will be more than sufficient for this application. The minimum operating current for the 10% slope relay is 0.18 A; because the error current is only 0.0018 under fault conditions the error at full load will be well below the minimum operating current.

3.8.3 Choosing Slope Static and Microprocessor Relays

The microprocessor relay being considered uses operate and restraint quantities calculated from the fundamental component of the input currents. The relay restraint current is the average of the two input currents $(I_{\mathrm{a}} + I_{\mathrm{b}})/2$. As was pointed out previously, this is not a universal definition for restraint. Many relays use the minimum or the maximum input current, alone as restraint. Others use the average input current, but use a scalar calculation.

The relay burden is 0.01 Ω at each input. There is no operating circuit burden because there is no operating current circuit. The relay has independent input circuits for each CT and calculates the operating current internally.

The minimum operating current is adjustable from 0.05 to 2.0 A. The relay's slope characteristic (Figure 3.16) shows that the minimum operating current must be set above the maximum error current up to a restraint of 5 A. The circuit error current will be less than the error calculated for the electromechanical relay, 0.0018 A. A minimum setting of 0.2 A will be well above the error current and provide good-sensitivity. The minimum operating current for the relay in terms of primary circuit amps is:

$$I_{\mathrm{op}} = 0.2\,\mathrm{A} \times 6000/5 = 240\,\mathrm{A} \quad \text{at } 13.8\,\mathrm{kV}$$

Burden and CT data for the sample system were input to the Mathcad worksheet. The CT data include the core cross-section area and length of the core's magnetic circuit. The calculated results for an external fault are plotted in Figure 3.22. The CTA saturates at about 1/2 cycle CTB at 1.4 cycle. The result is nearly one cycle with the operating current (or differential current as it is often called) equal to the output of CTB. The peak differential current of nearly 80 A as shown on the plot.

The relay views the fault through its sampling and filtering algorithm. We have assumed that the relay under consideration calculates restraining and operating quantities from the fundamental frequency component of the input currents. Restraint current is $(I_{\mathrm{a}} + I_{\mathrm{b}})/2$ and the operate current is $(I_{\mathrm{a}} - I_{\mathrm{b}})$. These quantities are plotted in Figure 3.23.

The plot shows that for nearly one cycle, 1.5–2.4 cycles on the time axis, the differential current (I_{d}) actually exceeds the restraint (I_{r}). Because the relay has an operating time of one cycle, the relay will misoperate for this condition, regardless of the slope setting. Also note that during most of the 0.5 to 1.5 cycle time period the restraint current is approximately 40 A and the differential current is 25 to 30 A. A slope setting of greater than $100 * 30/40 = 75\%$ would be required to prevent operation during this period.

© 2006 by Taylor & Francis Group, LLC

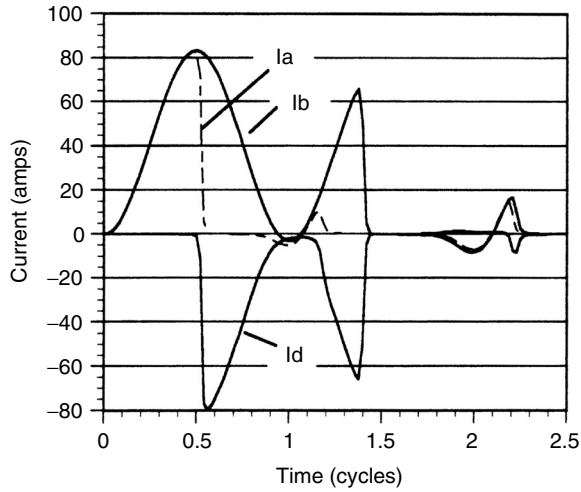


FIGURE 3.22 Microprocessor relay currents with DC saturation.

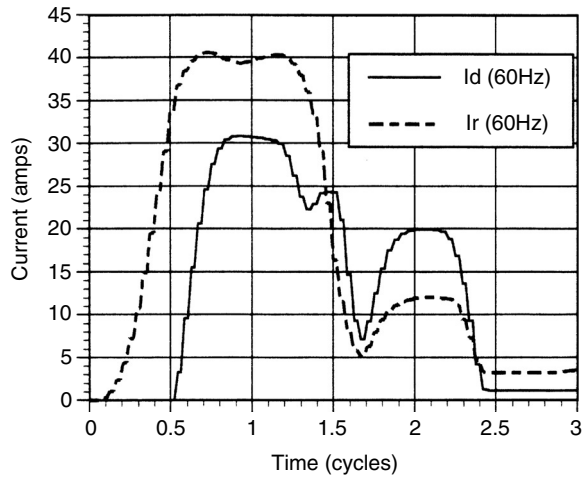


FIGURE 3.23 Fundamental frequency, operate and restraint.

This result would lead one to wonder how electromechanical percentage differential relays have been applied successfully for so many years without considering the effects of DC saturation. The key is the operating circuit impedance or the lack of one, in microprocessor designs.

3.9 STABILIZING RESISTOR

Electromechanical relay designers added impedance to the operating circuit. Note that the electromechanical relay proposed for the sample system 3.8.2.1 had an operating coil impedance of 5.4 ohm. This would seem counterproductive, because increased circuit burden will increase saturation. In reality, the large differential error current is not a result of saturation, but unequal saturation of the two CTs. Figure 3.4 showed that, for external faults, the current through the operating circuit is equal to the difference in the excitation currents. As one CT saturates and its excitation current increases, the voltage across the operating circuit impedance will increase. This will increase the voltage at the unsaturated CT, forcing it closer to saturation. The effect of the operating

© 2006 by Taylor & Francis Group, LLC

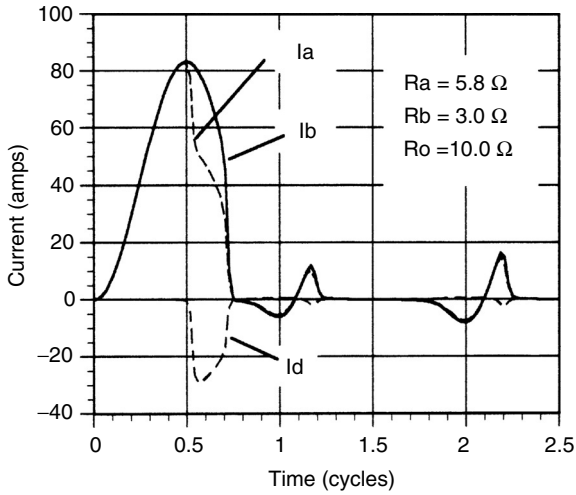


FIGURE 3.24 Relay currents with stabilizing resistor.

circuit impedance is then to equalize saturation of the two CTs and to stabilize the differential relay. If sufficient resistance is added to the operating circuit, the two CTs will saturate nearly simultaneously, virtually eliminating the error current.

The microprocessor relay has no operating current circuit to equalize saturation between the two CTs. An operating circuit can be simulated by forming a common return from the individual microprocessor inputs together through a resistor. The effect of adding a 10 Ω "stabilizing" resistance into a common return circuit is shown in Figure 3.24. The difference in saturation times is reduced to about a quarter of a cycle. The operating and restraining currents with the stabilizing resistor are plotted in Figure 3.25. The restraining current now exceeds the operating current at all points. This will allow the slope setting to prevent misoperation.

During the maximum current period, one cycle on the time axis, the operating and restraint currents are approximately 10 and 43 A respectively. A slope greater than $100 * 10/43 = 23\%$ is required. At 1.7 cycles, the restrain and operate quantities are at their closest postsaturation values of 2.0 and 0.4 A. The required slope here is $100 * 0.4/2.0 = 20\%$. Allowing a 10% margin, the relay slope could be set at 33% if the 10 Ω resistor is incorporated.

The effects of adding the stabilizing resistor are not all positive. The currents from the two CTs sum for a fault within the differential zone. This total current must be forced through the stabilizing

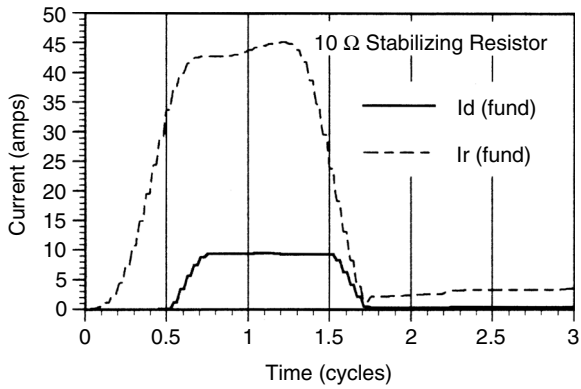


FIGURE 3.25 Operate and restraint currents with stabilizing resistor.

© 2006 by Taylor & Francis Group, LLC

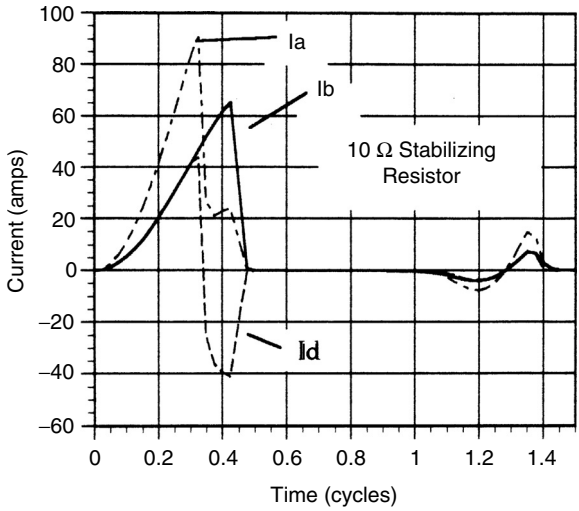


FIGURE 3.26 Relay currents for internal fault with stabilizing resistor.

resistance, causing very rapid saturation. The CT output is reduced to current spikes that may have insufficient fundamental frequency component to operate the relay.

In the electromechanical design, a saturating reactance was used in the operating circuit. At a low error current, the reactor had high impedance, perhaps 30 Ω, to equalize the CT exciting currents. For internal faults, the reactor would saturate, reducing its impedance to a few ohms. The lower impedance reduced the burden on the CTs for the internal fault to maximize the energy available to the operating circuit.

An internal fault was simulated with the 10 Ω stabilizing resistor, assuming infeeds from both CTs summed to equal the generator fault current. The results are plotted in Figure 3.26 and Figure 3.27 and show over 20 A of operating current for one cycle and about 2 A after saturation. In both cases the operating current exceeds the restraint current and is of sufficient magnitude to operate the relay.

In summary, the addition of a 10 Ω stabilizing resistor will allow the microprocessor relay to be set with a 33% slope. Whenever a stabilizing resistor is added, a check must be made to assure CT output during an internal fault is sufficient to actuate the relay.

The resistor must have a continuous wattage rating based on the maximum error current during normal operations. This could be calculated assuming a current equal to the operating current

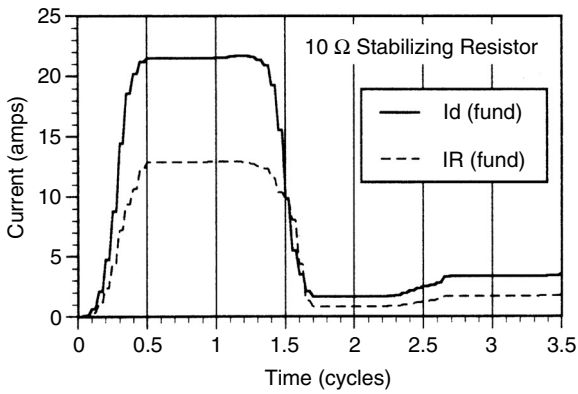


FIGURE 3.27 Operate and restraint current for internal fault.

© 2006 by Taylor & Francis Group, LLC

necessary to trip at full load restraint. The resistor must also have a short time capability sufficient to withstand an internal fault.

3.10 BALANCING BURDEN

Another way to equalize saturation and reduce the differential error current is to adjust the individual CT burdens so they are proportional to the knee-point voltages of the two CTs. The simple system differential circuit, Figure 3.19 has the following parameters:

$R_a = 5.8$
$R_b = 3.0$
$R_o = 0.0$
CTA knee-point voltage = 550 V
CTB knee-point voltage = 650 V

The knee-point voltage ratio is:

$$V_{kb}/V_{ka} = 650\,\text{V}/550\,\text{V} = 1.18$$

Adjusting R_b to 6.84 Ω equalizes the ratios:

$$R_b/R_a = 6.84\,\Omega/5.8\,\Omega = 1.18$$

Figure 3.28 and Figure 3.29 show the relay quantities for a fault external to the differential zone with no stabilizing resistor ($R_o = 0$), $R_a = 5.8\ \Omega$ and $R_b = 6.84\ \Omega$. Saturation is nearly simultaneous with virtually no operating current. At minimum restraint of 2 A, the operating current is 0.02 A. The operate and restraint quantities at maximum current are approximately 2 and 35 A, respectively, requiring a minimum slope of $(100 * 2/35)$ 6% to prevent a misoperation. Adding a conservative margin of 10%, the relay should be set at a 16% slope.

The addition of a 3.84 Ω resistor in series with CTB would virtually eliminate the error current. However, at full load, the current in the CT secondary circuit would by about 5 A and the resistor

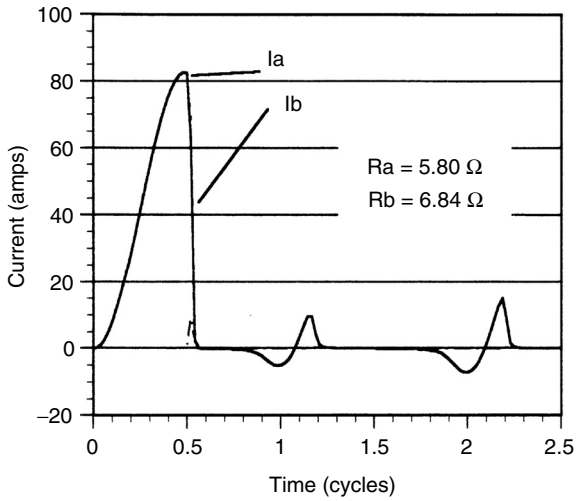


FIGURE 3.28 Relay currents with burden adjusted.

© 2006 by Taylor & Francis Group, LLC

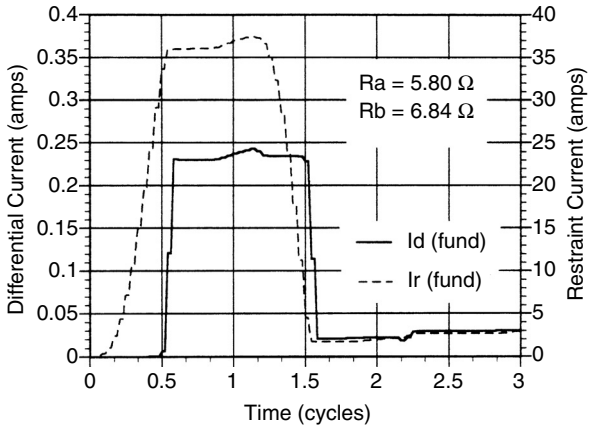


FIGURE 3.29 Operate and restraint currents with burdens adjusted.

would dissipate $3.84 \times 5^2 = 96$ watts, a significant heat load to put inside a switchgear cubical or a control cabinet. Burden balancing is normally accomplished by rerouting cable or paralleling conductors to reduce the impedance of the high-impedance circuit. This method seldom results in ideal balancing, but can significantly reduce error currents and the relay slope setting.

3.11 TIME DELAY

The third option to avoid a misoperation is to set a time delay on the differential relay. The idea of delaying a differential trip seems to defeat the purpose of using this type of relaying in the first place. However, as seen in Chapter 2, when the differential relay operates to trip the generator and field breaker, it does not interrupt the fault. High-magnitude current will persist for seconds as the generator's stored magnetic energy dissipates into the fault. A small delay in tripping may not substantially increase the damage caused by the generator's infeed to the fault. If there is a substantial system infeed, the delay has a more significant effect on the total fault energy. The relative effect of the delayed clearing can be evaluated based on the total fault I^2t, with and without the time delay.

A delay of a few cycles can be set to override the period when only one CT is saturated. In the case for the sample system, the delay would be about 2.5 cycles, as shown on Figure 3.23. This approach assumes high-speed clearing of the fault by some other protective relay before the DC component dissipates and differential CTs come out of saturation. If this is not the case, a misoperation can occur on error current caused by unequal desaturation.

The most secure delay setting would be one that overrides the entire DC transient. As previously stated, this requires a delay of about three times the DC time constant. Because the time constant for a generator is very large, this will usually result in unacceptable delays, 0.7 sec for the sample system generator.

3.12 FREQUENCY RESPONSE

The final consideration is the frequency response of the relay. Plant procedures normally specify the generator speed at which field is to be applied during startup. In many cases, this is done below rated speed. The relay must be capable of detecting a short circuit at the minimum speed at which the field is applied. If the field is applied to an 1800 r/min machine, at 900 r/min this corresponds to 30 cycles.

© 2006 by Taylor & Francis Group, LLC

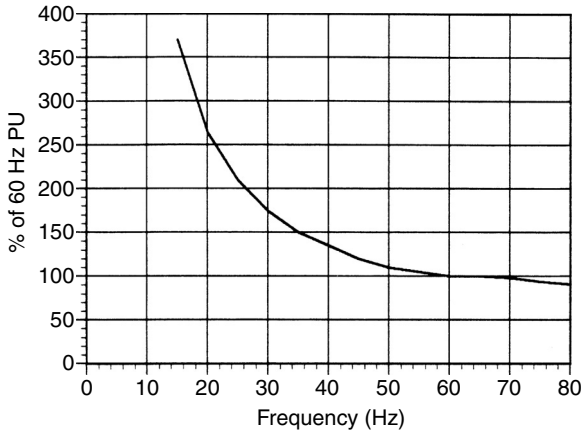


FIGURE 3.30 Typical frequency response, electromechanical relay.

Electromechanical percentage differential relays tend to become less sensitive at lower frequency. Figure 3.30 describes the response of one manufacturer's relay. During startup, generator voltage is normally reduced in proportion to the frequency, but since generator reactance is reduced by the same proportion, fault currents will remain near the full voltage 60 cycle values. If the percentage differential relay maintains moderate sensitivity at the field application frequency, fault clearing should not be a problem.

The frequency response of a microprocessor-based percentage differential function can vary widely. If the function is of an older design or designed for transmission or distribution applications, the sampling rate may be fixed. These units respond accurately only to 60 cycle input. Relays designed for generator application usually employ frequency tracking techniques, which provide a wide band of frequency response. Operating ranges of 40–70 Hz would be typical.

REFERENCE

1. IEEE Std C37.110-1996, *IEEE Guide for the Application of Current Transformers Used for Protective Relaying Purposes*, IEEE, 1996.
2. Pfuntner, R. A., The accuracy of current transformers adjacent to high-current buses, *AIEE Transactions*, 50, 1656–1662, 1951.
3. IEEE Power System Relay Committee Report, *Sine-Wave Distortions in Power Systems and the Impact on Protective Relaying*, 84 TH 0115–6 PWR, IEEE, New York, May 1984.
4. Jost, F. A., Menzies, D. F., and Sachdev, M. S., *Effects of System Harmonics on Power System Relays*, Canadian Electric Association System Planning and Operations Section Power Protection Committee Spring Meeting, March 1974.
5. Mason, C. Russel, *The Art and Science of Protective Relaying*,. 6th ed., John Wiley & Sons, Inc., New York, 1967.
6. Zocholl, S. E. and Smaha, D. W., *Current Transformer Concepts*, 19th Annual Western Protective Relay Conference, Spokane Washington, October 20–22, 1992.

© 2006 by Taylor & Francis Group, LLC

4 Backup Fault Protection

4.1 PURPOSE AND IMPLEMENTATION

The differential relay provides primary fault protection for the generator. Backup fault protection is also recommended to protect the generator from the effects of faults that are not cleared because of failures within the normal protection scheme. The backup relaying can be applied to provide protection in the event of a failure at the generation station, on the transmission system, or both.

Specific generating station failures would include the failure of the generator or GSU transformer differential scheme. On the transmission system, failures would include the line protection relay scheme or the failure of a line breaker to interrupt.

Figure 4.1 shows the sample system generator. Backup protection is provided by distance relays (Device 21) or voltage supervised overcurrent relays (Device 51V). These relays can be connected to CTs at the neutral end of the generator or they can be connected to CTs at the generator terminals. The neutral end configuration is preferred because this connection will allow the relaying to provide protection when the unit is off line. Terminal connected relays will not see internal generator faults for this condition, because there is no relay current.

If the scheme is intended to provide backup protection for both generating station and system faults, the backup relays should initiate a unit shutdown. This entails tripping the breaker on the high-voltage side of the GSU, the generator field breaker, the auxiliary transformer breakers and initiating a prime mover shutdown. If the station configuration included a generator breaker it would be tripped instead of the high-voltage breaker.

When relays are applied solely to backup transmission line relaying, only the GSU transformer or generator breaker need be tripped. This would allow a faster resynchronizing after the failure has been isolated. This assumes the unit can withstand the effects of the full load rejection that will occur when the outlet breaker opens. If the unit cannot withstand this transient, a unit shutdown must be initiated.

4.1.1 Standard Overcurrent Relays

Standard overcurrent relays are not recommended for backup protection of a generator. The backup relay must be capable of detecting the minimum generator fault current. This minimum current is the sustained current following a three-phase fault assuming no initial load on the generator and assuming the manual voltage regulator in service.

If the automatic voltage regulator where service, it would respond to the fault-induced low terminal voltage and boost the field current, thus increasing the fault current. The assumption of no initial load on the generator defines the minimum field current to drive the fault.

Typically, a generator's synchronous reactance, which controls the value of the sustained fault current, is greater than unity. If the generator is unloaded and at rated terminal voltage ($E_t = 1.0$) prior to the fault, the sustained short-circuit current will be $1/X_d$ which will be less than full load current. In the case of the sample system generator $X_d = 1.48$ and the resulting sustained three-phase fault current would be 0.67 pu or 67% of full load current.

A standard overcurrent relay must be set above load and could not detect the minimum sustained fault current. Tripping would be dependent on rapid relay operation before the fault current decays below the relay's pickup setting. Figure 4.2 plots the decaying current for the minimum fault condition on the sample system generator vs. an overcurrent relay set to carry full load. The figure shows that the relay must be set with a very short time delay

© 2006 by Taylor & Francis Group, LLC

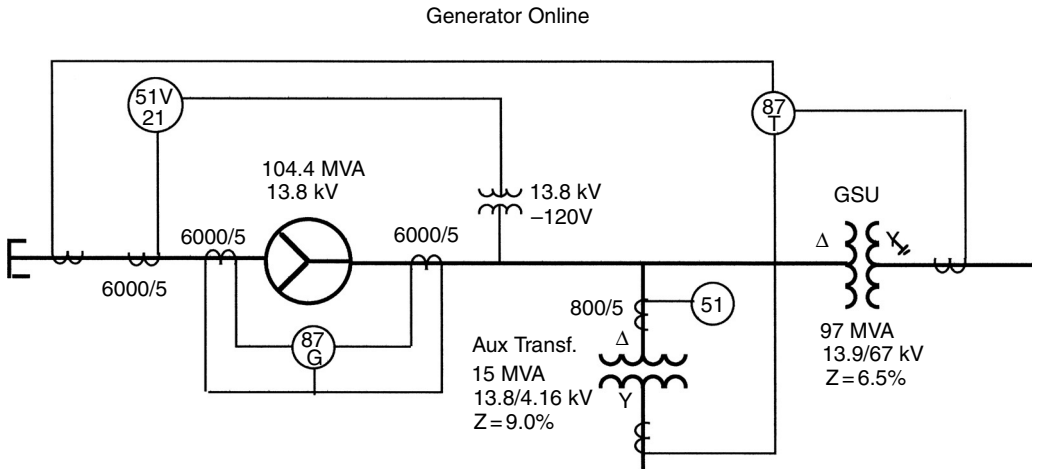


FIGURE 4.1 Generator online.

(Time Dial = 1/4) to intersect the current plot to assure tripping. This fast tripping is undesirable, because it would preclude coordination with system relays and could cause misoperation during system disturbances that do not require protective action.

4.1.2 Voltage-Dependent Relays

The problems associated with standard overcurrent protection can be overcome if fault detection is based on current and voltage. At full load, the generator terminal voltage will be near rated voltage. Under sustained three-phase fault conditions, the internal generator impedance will increase to the synchronous value and the terminal voltage will decrease sharply.

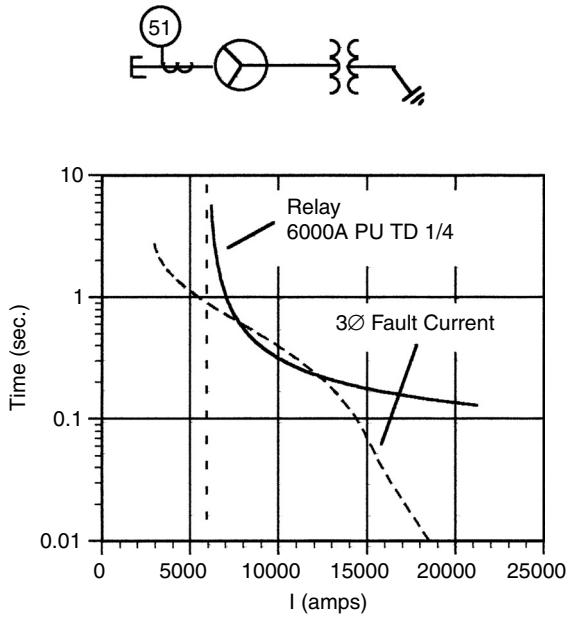


FIGURE 4.2 Fault clearing with overcurrent relay.

© 2006 by Taylor & Francis Group, LLC

Both distance relays and voltage supervised overcurrent relays use the voltage degradation to differentiate between load current and a sustained fault current condition.

Because of this design, these backup relays are supervised by a potential failure detection element, device 60. This element blocks tripping in the event of an open phase or blown fuse in the potential circuit. Without this blocking feature, these instrument circuit malfunctions would trip the fully loaded unit.

The decision to use a 21 or a 51 V function as backup protection is normally dependent on the type of phase protection applied on the transmission or distribution system to which the generator is connected. Distance backup protection is chosen if phase distance relaying is applied on the transmission system. A 51 V function is chosen if overcurrent relays are used for phase protection on the connected system. These choices are made to facilitate relay coordination.

4.1.3 Electromechanical vs. Electronic Relays

Unlike the differential function discussed in the previous chapter, there are few application differences between the 21 and 51 V functions when packaged as electromechanical, solid-state relays, or in microprocessor generator protection relays.

Electromechanical distance relays do have minimum current requirements for accurate measurement that can influence settings. Minimum measurement currents are not a practical consideration with solid-state or microprocessor distance elements themselves, but these relays often have overcurrent fault detectors associated with the distance function that must operate to allow tripping by the distance function.

The major difference in these functions is that the microprocessor units provide many setting options that are purchase options with discrete relays. These options may include:

- Selectable time current characteristics for the 51 V function
- Selectable 51 V as voltage controlled or voltage restrained
- Selectable current and voltage inputs to 51 V
- Multiple 21 functions with optional offset
- Internal compensation for delta-wye GSU transformer connection

The options listed may not be available in any single microprocessor relay. The list is a compilation of options provided by several manufacturers.

4.2 VOLTAGE SUPERVISED OVERCURRENT RELAYS

4.2.1 Voltage-Controlled and Voltage-Restrained Relays

There are two kinds of voltage-supervised overcurrent relays used in generator backup applications. The voltage-restrained overcurrent relay is normally set 125–175% of full load current. The relay uses voltage input from the generator terminals to bias the overcurrent setpoint. At rated voltage, a current equal to the setpoint is required to actuate the relay. As input voltage decreases, presumably due to a short circuit, the overcurrent setpoint also decreases. Typically a current equal to 25% of the setpoint is require to operate the relay at zero volts input. Figure 4.3 is a typical pickup characteristic for a voltage-restrained relay.

The voltage-controlled relay is set below full load with sufficient margin to detect the minimum fault current. The relay includes an undervoltage element that senses generator terminal voltage. If the voltage is above the undervoltage element setting, the overcurrent unit is not functional. When voltage is depressed by a fault, the undervoltage element drops out, allowing the relay to operate as a standard overcurrent relay in accordance with its pickup and time delay settings.

The voltage-restrained relay is more difficult to apply because operating time is a function of both current and voltage.

© 2006 by Taylor & Francis Group, LLC

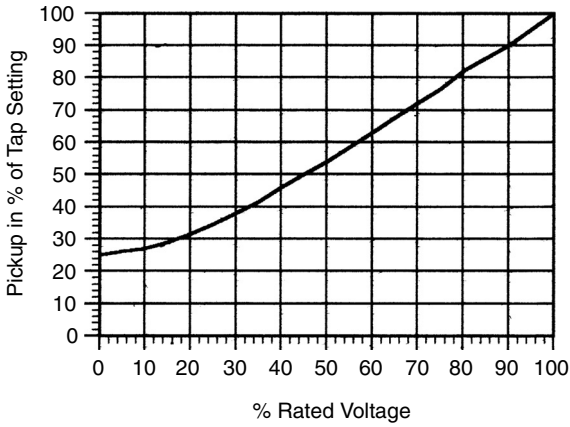


FIGURE 4.3 Voltage-restrained OC relay characteristic.

The voltage-restrained relay has two adjustable setpoints, a voltage-dependent minimum pickup current, and a time delay setting. The voltage-controlled relay has a voltage-independent current pickup setting, a time delay setting, and an undervoltage drop out setting.

4.2.2 Application Options and Fault Sensitivity

Voltage-supervised overcurrent relays allow many input options. The 51 V function comprises three single-phase units. The current and voltage connections are not standardized. Phase-to-neutral or phase-to-phase voltages can be applied in conjunction with line or delta currents. There is also the option of voltage-controlled or voltage-restrained relays.

4.2.2.1 Scheme Sensitivity vs. Potential Transformer (PT) and Current Transformer (CT) Connection

Phase-to-neutral voltage and line current are chosen as relay input quantities when maximum ground fault sensitivity is required. Phase-to-phase voltages would be chosen for maximum phase-to-phase fault sensitivity. All connection schemes have the same sensitivity to three-phase faults.

Ground faults sensitivity would be desired for a generator connected to a solidly grounded distribution system directly or through a wye-wye transformer. Most generators, however, are grounded through impedance, reducing the ground fault current to a few amps. Specialized schemes are incorporated for ground fault detection; consequently the 51 V function is more often required to provide backup phase fault protection and use a phase-to-phase voltage connection.

These sensitivity characteristics are applicable to the initial fault condition when the generator's positive sequence reactance approximates the magnitude of its negative or zero sequence reactance. As the machine positive sequence reactance increases to X_d with time, the fault current diminishes and so too does the sensitivity distinction between the schemes.

Figure 4.4 plots relay voltage vs. line current when generator positive sequence reactance is equal to X'_d. This would represent an initial fault condition a few cycles after fault inception. These plots are for the sample system generator, neglecting fault resistance. The relay voltages are plotted as percent of nominal voltage to allow a comparison of phase-to-ground and phase-to-phase voltages.

Because the 51 V function requires reduced voltage along with current, relative sensitivity is assessed on the basis of voltage drop per amp of fault current. The connection scheme with

© 2006 by Taylor & Francis Group, LLC

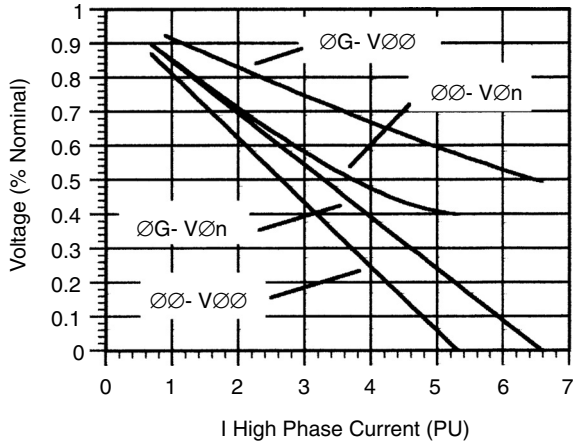


FIGURE 4.4 Initial fault sensitivity.

the larger voltage drop for a given fault current is the most sensitive. The advantage of the phase-to-ground potential connection for ground faults and the phase-to-phase potential for phase faults is evident.

Relay voltage vs. fault current is also plotted with the sample system generator reactance equal to X_d (Figure 4.5). This is the minimum current condition. It will dictate the pickup setting and is the condition where maximum sensitivity is desired. The phase-to-ground connection shows some advantage for ground faults, but the phase-to-phase response of the two schemes is virtually the same.

The conclusion here is that there are definite advantages for using one PT connection scheme over another for transmission line applications. In this application the positive, negative and zero sequence impedance of the source are approximately equivalent and the sensitivity distinctions shown in Figure 4.4 can be realized. However, in generator backup applications the relay must have a significant delay to coordinate with normal relaying. The delay allows a substantial increase in the generator's positive sequence impedance. At the minimum fault condition, the generator's positive sequence impedance, X_d, is approximately ten times that of the negative or zero sequence. With this impedance mix the sensitivity distinction between PT input configurations is minimal.

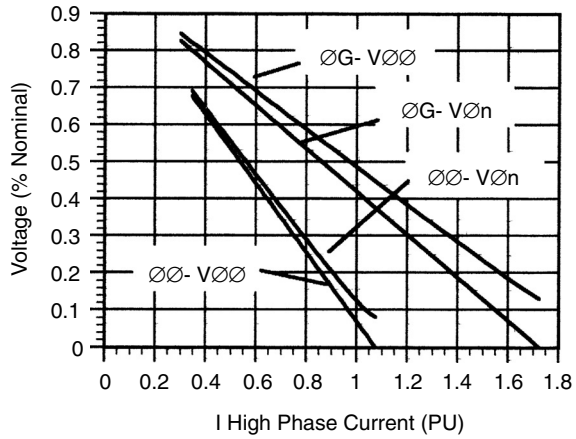


FIGURE 4.5 Sensitivity with steady-state current: LL and ground fault.

© 2006 by Taylor & Francis Group, LLC

4.2.2.2 Sensitivity Related to Relay Type

Sensitivity to the minimum fault conditions is influenced more by the type 51 V function applied than the relay input connection used. The current pickup of the voltage-controlled relay can be set more sensitively than the voltage-restrained relay because the voltage-controlled relay is set without regard to load current. In theory, the voltage-controlled relay pickup could be set as low as necessary to detect the minimum fault condition. In practice a minimum pickup setting may be dictated by coordination with other protective devices.

Assuming that overcurrent pickup is not constrained, operation of the voltage-controlled relay would be dependent on voltage. Figure 4.5 and Figure 4.6 plot relay voltage vs. fault current with the sample system generator reactance equal to X_d. If a typical undervoltage dropout setting of 80% is assumed, the figures show that a voltage-controlled relay applied on the sample system generator could detect fault currents as low as 0.12 pu for a three-phase fault and 0.4 pu current for a phase-to-ground fault.

The sample system generator is rated at 104 MVA 13.8 kV, therefore the scheme could detect a three-phase 13.8 kV fault of

$$I3\theta_{\min} = \frac{104,400}{\sqrt{3} * 13.8} * 0.12 = 525\,\text{A}$$

The voltage-restrained relay must be set at least 125% of maximum load current. The actual operating current during a fault is dependent on the voltage applied to the relay. Figure 4.7 plots the relay pickup characteristic and fault voltage for various fault conditions. A voltage-restrained relay will respond to fault conditions below its characteristic. The plot shows the minimum operating currents for three-phase and ground faults are 0.5 and 0.8 pu, respectively, clearly less sensitive than the voltage-controlled relay. This is not always a disadvantage. The desensitizing of the relay with increased voltage will aid in coordination with remote devices.

4.2.2.3 Delta Relay Currents

The relay inputs that result from delta-connected CTs are shown in Figure 4.8. The effect on scheme sensitivity is again a function of the type 51 V relay installed.

Since a voltage-controlled relay can be set without regard to load, the sensitivity improvement is relative to the current increase in the relay. There will be no improvement for phase-to-ground faults, but there is a 200% increase in relay current for a phase-to-phase fault.

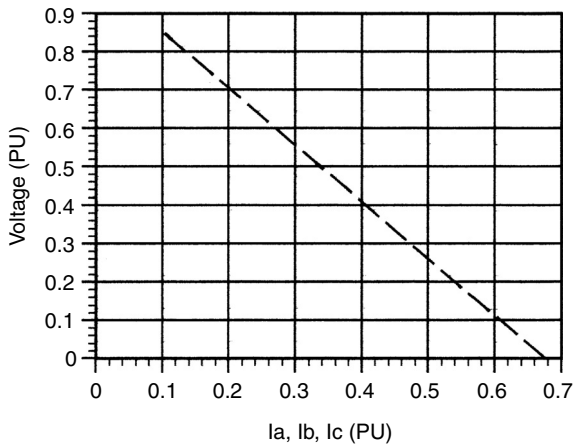


FIGURE 4.6 Sensitivity with steady-state current: three-phase fault.

© 2006 by Taylor & Francis Group, LLC

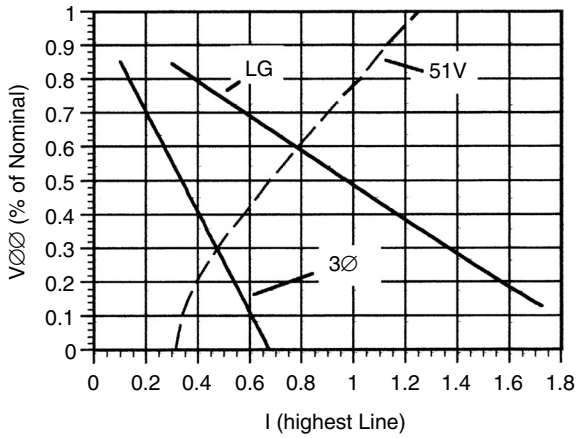


FIGURE 4.7 Fault response of voltage-restrained relay.

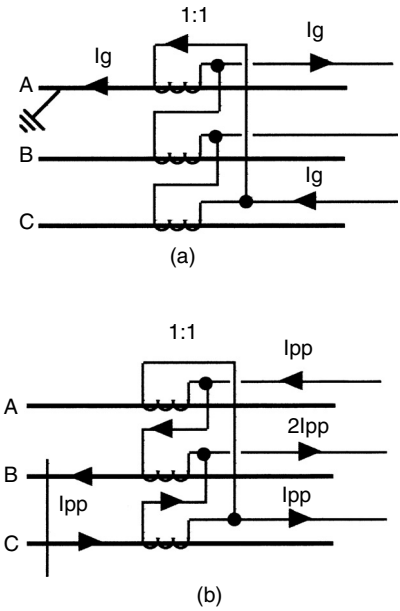


FIGURE 4.8 Delta relay currents.

The voltage-restrained relay must be set above load. The delta current input will increase the relay current at full load by $\sqrt{3}$, necessitating an equivalent increase in the pickup setting. Consequently the relative sensitivity improvement would be equivalent to relay current increase for a given fault condition divided by $\sqrt{3}$. As a result of the setting increase, ground fault sensitivity will be reduced by $1/\sqrt{3} = 0.58$ and phase-to-phase fault sensitivity would be increased by $2/\sqrt{3} = 1.15$.

4.2.3 Settings Considerations

4.2.3.1 Basic Requirement

There are several current and voltage input configurations that can be used for the 51 V function. Each will present the relay with a unique set of phase voltages and currents for a given fault

© 2006 by Taylor & Francis Group, LLC

condition. Regardless of the input configuration, the successful application of this function requires that at least one of the three relays receives current high enough and voltage low enough to operate for every fault condition within the relay's zone of responsibility.

4.2.3.2 Automatic Voltage Regulator in Service

The 51 V function must be set to detect the minimum anticipated fault current within its zone of responsibility which is a sustained three-phase fault with the manual regulator in service. However, fault detection for a voltage-controlled or voltage-restrained relay is a function of both voltage and current. The generator is normally operated with the automatic voltage regulator in service. Therefore it is likely that the automatic regulator will be in service to boost field current and fault current.

Typically, a generator's excitation system is capable of delivering 1.3 to 1.5 times the field current required for full load operation. The excitation boost is a benefit for the overcurrent element of either type of 51 V function, but if there is impedance between the generator and the fault, the increased field current will also significantly increase the generator terminal voltage. The effect will be to desensitize the voltage-restrained relay, or possibly prevent the dropout of the undervoltage element of the voltage-controlled relay. Consequently, setting calculations are not only required to establish the minimum fault current conditions, but also maximum fault voltage conditions.

Voltage supervised relays are applied because of their unique characteristics to facilitate clearing of sustained three-phase faults. However, once installed the 51 V function must also clear phase-to-phase faults, and if no dedicated ground protection is provided, the 51 V function must also clear ground faults. The maximum voltage condition will be one of the latter two fault conditions.

4.2.3.3 51 V Transmission System Backup Limitations

The amount of backup protection these relays can provide for faults external to the generation station is sharply limited by network lines connected at the generating station's transmission bus. Figure 4.9 shows the current distribution for a three-phase fault at the end of a line connected to the sample system 69 kV bus. The breaker at the remote station has cleared, but breaker "A" at the generating station bus has failed to open. The currents shown are calculated using X''_d for the generator impedance to represent the initial fault condition.

To clear this condition, relaying at each remote breaker, including the 51 V function at the generator, must detect the fault. This is known as "remote backup" protection and is very difficult to apply at locations where multiple network lines are terminated. Network lines produce two adverse effects. The more network lines that terminate at a bus, the more paths to divide the fault current and the less current available to each remote relay, including the 51 V.

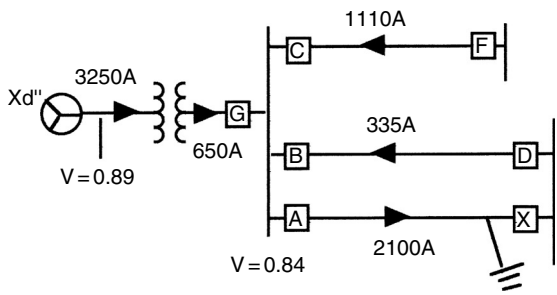


FIGURE 4.9 System fault: initial currents.

© 2006 by Taylor & Francis Group, LLC

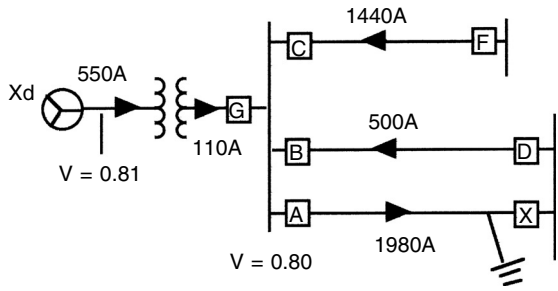


FIGURE 4.10 System fault: sustained currents.

The maximum infeed current for the fault shown is approximately equal to rated line current (about 1100 A). Transmission line relaying set to carry the line rating will not detect this fault condition. The current at the generator terminals is 3250 A, about 75% of rated load.

Also, because of the infeeds to the fault from other network lines, the voltage rise on the faulted line is greater than would be produced by the generator current alone. In Figure 4.9, the faulted voltage at the generator is 89% of rated. The near-normal generator terminal voltage defeats the advantage of the voltage-controlled and voltage-restrained relays. Under these circumstances, backup clearing of this fault is not obtainable.

As time progresses, the generator impedance increases to X_d and the generator current is reduced, while network infeed currents increase as shown in Figure 4.10. If the increased current causes relaying at one remote terminal to actuate, the number of infeeds will reduce by one. The currents in the remaining circuits will increase, thus improving the chance that a second line will trip and then a third to clear the fault. This sequential clearing, if obtainable, can take many seconds to isolate the fault.

If all transmission paths supplying the fault are tripped, the voltage at the generator terminals will drop to allow operation of the 51 V relay as shown in Figure 4.11.

Remote backup protection is even more difficult to apply for line-to-ground faults. The fault current magnitude for a ground fault is significantly less than for phase faults. Also, ground fault current will divide, not only among network lines, but also wye-delta transformers at the generating station bus, further reducing the current available to remote relays.

Because of the fault detection problem inherent with a remote backup scheme, most generating stations with multiple network lines are designed with "local backup" protection in the form of breaker failure relaying. This scheme consists of a precision timing relay at each breaker that is actuated when any relay trip signal is applied to the breaker. The timer runs as long as current through the breaker energizes a low set instantaneous fault detector relay. The time delay is sufficient to allow the breaker to trip, plus time for the fault detector relay to drop out. If the fault detector does not drop out in the allotted time, indicating the breaker has failed to open or has failed to

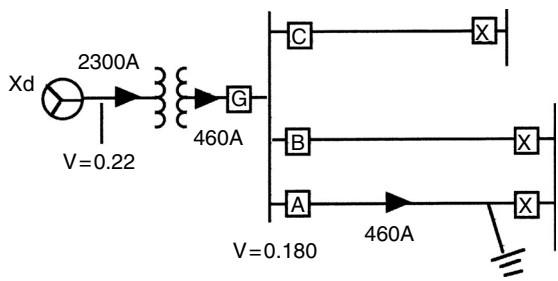


FIGURE 4.11 System fault: no infeeds.

© 2006 by Taylor & Francis Group, LLC

interrupt the fault current, the timer actuates a lockout relay that trips all the breakers on the associated bus section to clear the fault.

If the failed breaker terminates a network line a communication channel may be activated to trip the associated line breaker at the remote substation.

When local breaker failure is applied at a generating station's transmission bus, the generator backup relay need only provide backup for faults within the generating station.

4.2.3.4 Effects of Wye-Delta Transformer

When either 51 V function is required to detect faults through a delta-wye transformer, the currents and voltages at the relay will differ from those at the point of fault. This was discussed in Chapter 2. This distortion is caused by a phase shift in the transformer. Figure 4.12 shows the results of this shift on generator currents for various fault conditions.

Ground faults are more difficult to detect from the delta side of this transformer because the relative relay current is reduced by $1/\sqrt{3} = 0.58$. This may not be of significance for the 51 V function, because a ground relay is often provided in the transformer neutral to detect these faults.

On the other hand, a phase-to-phase fault will result in a relay current 1.15 times greater in one relay. Since a phase-to-phase fault is $1/1.15$ times the magnitude of a three-phase fault, this relay is actually seeing current equivalent to a three-phase fault current.

If current inputs are derived from delta-connected CTs, wye side transformer faults will produce the relay currents shown in Figure 4.13. This connection will result in a 115% increase in relay current for a phase-to-ground fault and 173% increase in relay current for a phase-to-phase fault. Remember that delta CTs will also increase the full load current in the relay by $\sqrt{3}$.

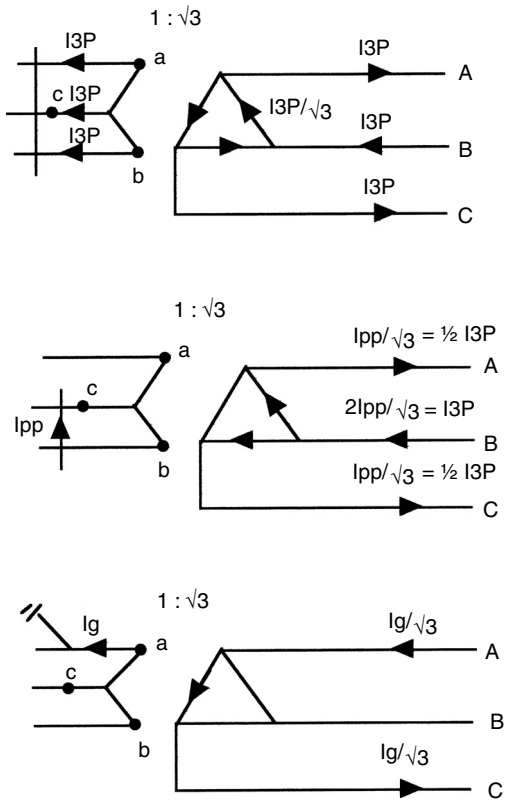


FIGURE 4.12 Current distribution in wye-delta transformer.

© 2006 by Taylor & Francis Group, LLC

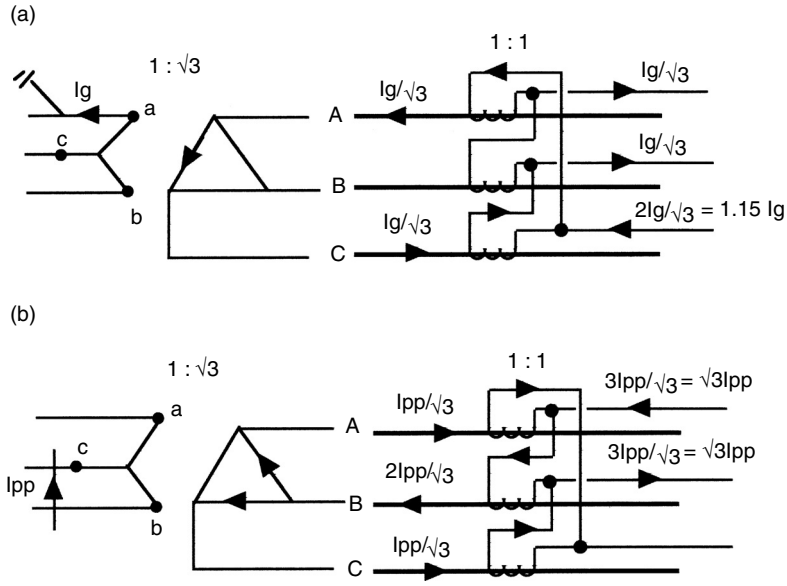


FIGURE 4.13 Wye-delta transformer with delta CTs.

If voltage-restrained relays are applied, the pickup setting must also be increased by $\sqrt{3}$. As a result, there is a net reduction in sensitivity of $1.15/\sqrt{3} = 0.66$ for a phase to ground fault and no change in relative sensitivity for a phase-to-phase fault.

The effects of the transformer's phase shift on relay voltages must also be considered. The voltage shift can be corrected if properly phased wye-delta auxiliary PTs are installed. Without the auxiliary PT correction voltage setting calculations must include the effects of the phase shift. The calculation of delta side currents and voltages will be presented in Section 4.2.5.

The insertion of a wye-delta transformer between the relay and the fault does not have an impact on the choice of relay input voltage. Initially, the phase-to-phase voltage connection has a definite sensitivity advantage for both phase-to-phase and ground faults on the wye side of the transformer. But again, as the generator's positive sequence impedance increases with time to X_d, the advantages of the phase-to-phase scheme disappear.

4.2.3.5 Self-Excitation Generators

Application problems associated with self-excited units were discussed in Chapter 1. These systems take excitation power from the generator terminals using power potential transformers (PPTs). Faults cause a reduction in terminal voltage that in turn reduces the available excitation voltage. If the resulting excitation is insufficient to support the fault current, the excitation will collapse and fault current will decay to near zero. The greater the impedance between the fault and the generator terminals, the higher the terminal voltage and the more likely the system is to sustain fault current.

A complete collapse would certainly occur for a three-phase fault at the generator terminals. Phase-to-phase faults and phase-to-ground faults would retain some voltage on the unfaulted phases, but this voltage is generally not sufficient to maintain fault current at a level suitable for overcurrent tripping. Fast-operating differential relays can initiate tripping for these faults as current delays. Under voltage elements will also provide protection for this fault condition.

If 51 V functions are to apply to a self-excited system, current transformers should be included to boost excitation during fault conditions as shown in Figure 1.21. The supplemental excitation provided by the CT should be sufficient to maintain fault current at a level that will facilitate

© 2006 by Taylor & Francis Group, LLC

overcurrent tripping. Without such CTs, fault clearing for a primary protection failure becomes a race between the collapsing fault current and the backup relay's time–current characteristic.

The fault current decay for a three-phase fault at the terminals of a self-excited generator can be calculated from the d- and q-axes equations presented in Chapter 2.

The d-axis current is calculated as

$$i_{\mathrm{d}} = (I''_{\mathrm{d}} - I'_{\mathrm{d}})e^{-t/T''_{\mathrm{df}}} + (I'_{\mathrm{d}} - I_{\mathrm{d}})e^{-t/T'_{\mathrm{df}}} + I_{\mathrm{d}} + I_{\mathrm{ex}}$$

The q-axis current equation is

$$i_{\mathrm{q}} = (I''_{\mathrm{q}} - I'_{\mathrm{q}})e^{-t/T''_{\mathrm{qf}}} + (I'_{\mathrm{q}} - I_{\mathrm{q}})e^{-t/T'_{\mathrm{qf}}}$$

The change in excitation component is

$$I_{\mathrm{ex}} = \frac{E_{\mathrm{c}} - EI}{X_{\mathrm{df}}}\left[1 - e^{-t/T'_{\mathrm{df}}}\right] \tag{2.38}$$

In Chapter 2, the I_{ex} term was used to represented the effect of the automatic voltage regulator forcing the field voltage to a final ceiling value of E_{c}. Here the excitation collapses and the final field voltage $E_{\mathrm{c}} = 0$.

A three-phase fault at the generator terminals of the sample system generator was calculated in Chapter 2. The calculation assumed that the generator was initially at full load and on the manual regulator. The addition of the I_{ex} term with $E_{\mathrm{c}} = 0$ defines the same fault for a self-excited system. The fault current characteristic obtained from the full load calculation will be somewhat optimistic, but a fault under load is more probable and is presented here to demonstrate the technique.

The d- and q-axes current equations, from Chapter 2, assuming full load prior to the fault, are

$$i_{\mathrm{d}} = (7.33 - 5.35)e^{-t/0.023} + (5.35 - 1.46)e^{-t/0.475} + 1.46 + I_{\mathrm{ex}} \tag{4.1}$$

$$i_{\mathrm{q}} = (3.94 - 0.781)e^{-t/0.023} + (0.781 - 0)e^{-t/0.106} \tag{4.2}$$

The I_{ex} term has been added to the Chapter 2 equation:

$$I_{\mathrm{ex}} = \frac{0 - 2.16}{1.48}\left[1 - e^{-t/0.475}\right] \tag{4.3}$$

The phase current is determined from the axis currents:

$$I_{\mathrm{a}} = \sqrt{I_{\mathrm{d}}^2 + I_{\mathrm{q}}^2} \tag{4.4}$$

The resulting fault current decay is plotted in Figure 4.14. Also plotted is a moderately inverse time overcurrent relay set to carry rated load, with pickup of 6000 A, and time dial of 0.6 for fast operation. The plot appears to show that the relay will not operate for this fault in that the decaying fault current never crosses the relay's time current characteristic (TCC).

In fact, the relay setting plotted will operate in 0.41 sec for the fault condition shown. This leads to a discussion of the transient characteristic of overcurrent relays.

4.2.3.6 Relay Response to Transient Current

A relay Time Current Characteristic (TCC) is a static characteristic plotted by applying a constant value of current to the relay and recording the operation time. Figure 4.14 compares this static characteristic to a plot that describes the instantaneous changes of generator fault current with time. The two plots have no connection to one another. To assess an overcurrent relay's response

© 2006 by Taylor & Francis Group, LLC

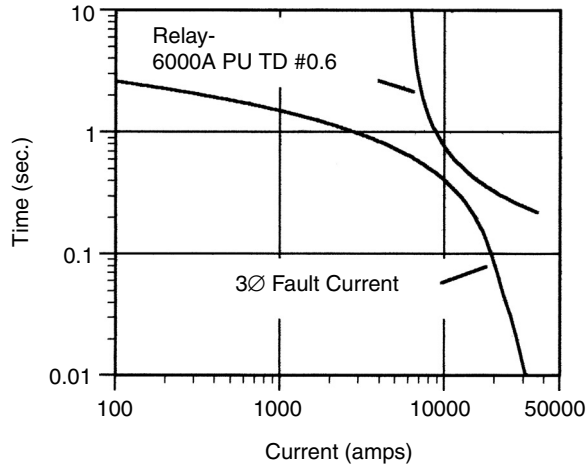


FIGURE 4.14 Fault on self-excited generator.

to time-varying currents such as a generator fault or a motor starting, the relay's dynamic characteristic must be used.

Standards[1] provide mathematical definitions for both the steady-state (TCC) and dynamic relay characteristics. The steady-state characteristic for an overcurrent relay is defined by

$$t(I) = \left[B + \frac{A}{M^p - 1}\right] * TD \tag{4.5}$$

where A, B, and p are constants. These values are fixed by relay design. M is the operating current in multiples of the pickup setting; fault current divided by the relay pickup setting. TD is the time dial setting and $t(I)$ is the relay operating time in seconds at relay current I. The relay characteristic plotted in Figure 4.14 was generated using a relay pickup of 6000 A, $TD = 0.6$ with $A = 0.0226$, $B = 0.014$, and $p = 0.022$.

The dynamic characteristic is defined by

$$\int_0^{t_o} \frac{1}{t(I)}\,\mathrm{d}t = 1 \tag{4.6}$$

where t_o is the operating time of the relay.

The above equations state that if the reciprocal of the operating time of the relay is plotted vs. time, relay operation will occur when the area under this curve accumulates to equal unity.

The incremental form of the equations can be written as

$$\mathrm{Trip}_n = \frac{\Delta t}{t(I)_{\mathrm{AVE}}} + \mathrm{Trip}_{n-1} \tag{4.7}$$

The derivation of Equation (4.7) is provided in Section 16.7.6.1. The denominator is the average of the relay operating times calculated from Equation (4.5) for the currents at the beginning and end of each time interval.

The dynamic evaluation of the relay response to the fault plotted on Figure 4.14 is easily accomplished using a spreadsheet as shown in Table 4.1. Column B represent decaying fault current plotted from the d- and q-axes Equation (4.1)–Equation (4.4). Column C is the operation time for the relay calculated for each value of fault current in Column B using the relay static characteristic

© 2006 by Taylor & Francis Group, LLC

TABLE 4.1
Relay Dynamic Response to Varying Current

A t	B Ia (amps)	C t(I) sec.	D 1/t(I)	E 1/t(I)av	F Δt/t(I)av	G Σ
0	36349	0.2213	4.518	0.000	0.000	0.000
0.01	31001	0.2419	4.134	4.326	0.04326	0.043
0.02	27505	0.2601	3.844	3.989	0.03989	0.083
0.03	25165	0.2757	3.627	3.736	0.03736	0.121
0.04	23542	0.2887	3.464	3.546	0.03546	0.156
0.05	22363	0.2996	3.338	3.401	0.03401	0.190

Equation (4.5). Column D is the reciprocal of Column C. Column E is the average value of the reciprocal over the last 0.01 sec interval. Column F is the average value for $1/t(I)$ for the interval times Δt. Entries in this column are equivalent to the area under the $1/t(I)$ curve for that time interval. Column G is the summation of Column F, and represents the accumulated relay trip.

A continuation of the spreadsheet would show that Column G reaches the trip value of 1.0 at 0.41 sec. This establishes the relay operating time for the fault condition.

4.2.3.7 Equipment Protection

The 51 V time delay setting must be chosen to clear a fault before generator or transformer damage occurs. This is accomplished by coordinating the relay operating time with the Generator Short Time Thermal Capability "curve as defined by ANSI C50.13-1989 and with the transformer" "Through Fault" Protection Curve from IEEE C37.91-2000. These curves are shown in Figure 4.15 and Figure 4.16.

Generator rotor damage can also occur as a result of unbalanced currents (negative sequence current) generated by uncleared phase-to-phase and phase-to-ground faults. Unbalanced current protection and negative sequence relaying will be discussed in Chapter 6.

Generator Stator Protection

Relay coordination with the generator thermal limit curve is straightforward. The x-axis of this curve is multiples of rated stator current. Rated current is calculated from the generator rating at 100% hydrogen pressure and rated terminal voltages.

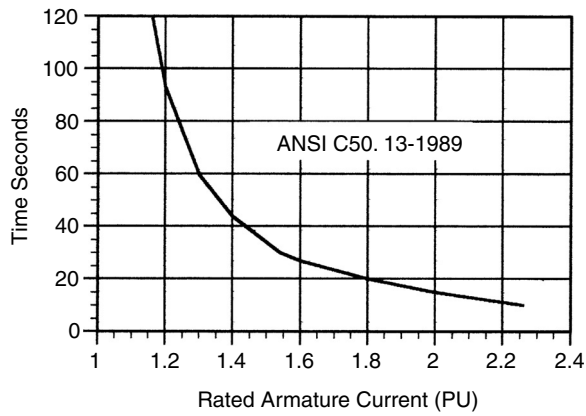


FIGURE 4.15 Generator stator short time overload capability.

© 2006 by Taylor & Francis Group, LLC

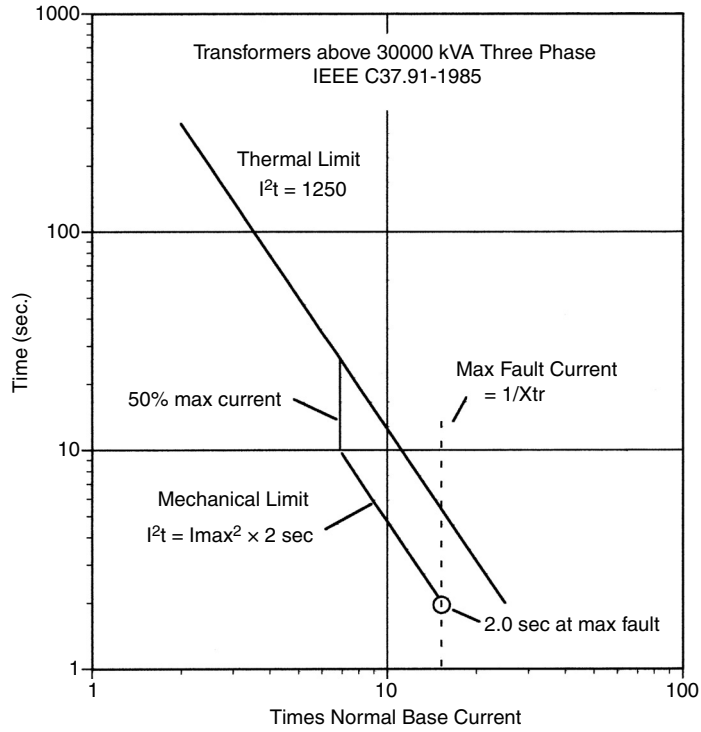


FIGURE 4.16 Transformer through fault capability.

Transformer Protection

Coordination with the transformer through fault capability curve is more complex. There are two protection curves for a transformer, thermal limit and a mechanical damage curves. The thermal curve is applicable to all transformers and is defined by the expression $I^2t = 1250$. Here, current is expressed in multiples of rated current and time is in seconds. In the case of a multirated transformer, "rated current" is defined by the lowest kVA rating of the transformer.

The mechanical limit is also an $I^2t = k$ function but the constant "k" is dependent on transformer impedance. A transformer must be capable of withstanding mechanical forces associated with a maximum fault condition for two seconds. From this requirement the mechanical I^2t limit for a transformer is define as $k = I^2_{\max} \times 2.0$ sec.

The sample system GSU transformer is a 97 MVA unit with an impedance of 6.5%. The maximum through fault current for this transformer is

$$I_{\max} = \frac{1}{Z_{\text{pu}}} = \frac{1}{0.065} = 15.38 \text{ pu current}$$

$$k = I^2_{\max} * 2.0 = 15.38^2 * 2 = 473.4$$

The thermal and mechanical limits for this transformer are plotted in Figure 4.16.

Transformer size and application determine the applicability and range of the mechanical limit curve. Standard IEEE C37.91 defines Category I, II, III, and IV transformers and the application of fault withstand curves associated with them as follows:

- Category I (5 to 500 kVA 1Ø, 15 to 500 kVA 3Ø)
  - Through fault capabilities are defined by the thermal capability curve alone

© 2006 by Taylor & Francis Group, LLC

- Category II (501 to 1667 kVA 1Ø, 501 to 5000 kVA 3Ø)
  - A thermal capability curve and optional mechanical limit curve define through fault capabilities
  - When applied, the mechanical limit's range extends from 70% to 100% of maximum current
- Category III (1668 to 10,000 kVA 1Ø, 5001 to 30,000 kVA 3Ø)
  - A thermal capability curve and optional mechanical limit curve define through fault capabilities
  - When applied, the mechanical limit's range extends from 50% to 100% of maximum current
- Category IV (above 10,000 kVA 1Ø, above 30,00 kVA 3Ø)
  - A thermal capability curve and required mechanical limit curve define through fault capabilities for all applications
  - The mechanical limit extends from 50% to 100% of maximum current.

The mechanical limit is optional for Category II and III transformers. It is applicable when transformers are subjected to frequent through faults. This is the case when the transformer's secondary is connected to a bus serving overhead distribution lines. These circuits are prone to conductor contacts and lightning strikes, each constituting a through fault for the transformer. In addition, circuit breakers on overhead lines normally employ automatic reclosing which increases the through fault frequency.

At installations where the transformer's secondary feeders are protected by conduit or some other method, as would be the case inside an industrial complex or powerplant, through faults are infrequent and an optional mechanical limit is not applied.

When the mechanical limit is imposed by overhead distribution lines, coordination between the 51 V function and the mechanical limit is not required. The 51 V function provides protection for the very infrequent occurrence of a primary relay failure and, as such, is coordinated with the thermal limit curve. The protective devices on the individual feeders must protect the transformer from frequent fault damage originating on the feeders.

The mechanical limit is not optional for Category IV. It is an integral part of the through fault capability curve. No distinction is made between frequent and infrequent faults. The 51 V must be coordinated with both the thermal and mechanical limits to protect a Category IV transformers.

Protection of Wye-Delta Transformer

When the transformer being protected is connected wye-wye or delta-delta, the current axis of the through fault curve can be plotted directly against the time–current characteristic of the 51 V function. This is not the case if the transformer being protected is connected delta-wye.

A delta-wye connected transformer produces different current distributions in the wye and delta windings for phase-to-phase and phase-to-ground faults. These distributions were shown in Figure 4.12.

A wye side phase-to-ground fault produces a higher fault current magnitude than does a three-phase or phase-to-phase fault. A wye side ground fault produces the maximum current with maximum stress on the faulted winding and at the same time, the ground fault provides the minimum relay operating current and the longest clearing time for the delta side protective relay. These characteristics make a ground fault the worst case for overcurrent protection of a delta-wye-connected transformer.

To account for the adverse ground fault current distribution, the current axis of the transformer through fault curve must be shifted to the left by 58% when plotted against the delta-side overcurrent relay. This is shown in Figure 4.17.

© 2006 by Taylor & Francis Group, LLC

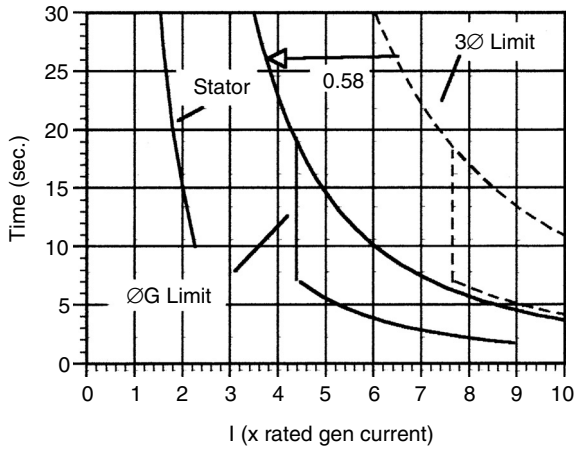


FIGURE 4.17 Generator and wye-delta transformer limits.

Backup Protection for Auxiliary Transformer Faults

The sensitivity of the 51 V relay is limited by the ratio of the generator CTs to which it is connected. These CTs are normally sized for about 125% rated generator load. The resulting high CT ratio and relative low kVA rating of the auxiliary transformer precludes the 51 V from providing backup protection to that transformer. Consequently, the auxiliary transformer is provide with its own backup overcurrent relay.

4.2.4 Setting Criteria

It is recommended that the relay's current pickup setting should not exceed 80% of the minimum fault current (calculated with the manual regulator in service). The pickup of the voltage-restrained relay would be a function of the relay input voltage.

The undervoltage element, if present, should be set no lower than 125% of the maximum fault voltage (calculated with the automatic voltage regulator at full boost).

After the overcurrent tap setting is chosen, a time delay can be chosen. The 51 V is a backup function and should not operate unless a primary relay fails. As such, the time delay chosen should provide ample margin to assure coordination with normal relaying. The delay must not exceed the generator short time thermal capability or the transformer through fault protection curve.

4.2.5 Relay Current and Voltage Calculations

Symmetrical component meteorology will be used to calculate the relay quantities. Symmetrical components resolve a three-phase power system into three single-phase systems, namely, positive, negative and zero sequences. The positive, negative, and zero sequence currents (I_1, I_2, and I_0, respectively) and positive, negative, and zero sequence voltages (V_1, V_2, and V_0, respectively) are calculated from single-phase positive, negative and zero sequence impedance networks. These networks are interconnected in specific configurations to represent each fault conditions. Once sequence currents and voltages are known for given fault conditions, they are combined to provide phase currents and voltages.

The following sections will develop equations that are used to calculate the relay currents and voltages for three-phase, phase-to-phase, and phase-to-ground faults. The first section derives general equations for current and voltage at the relay in terms of sequence quantities. These equations are valid for any fault condition.

© 2006 by Taylor & Francis Group, LLC

The second section describes how positive, negative and zero sequence quantities specific to each fault condition are calculated. These sequence values are substituted into the general relay input equations to yield actual relay operating currents and voltages for each fault condition.

4.2.5.1 Relay Current and Voltage Equations

The equations governing the conversion of sequence quantities to phase quantities are as follows, where $a = 1\angle 120^\circ$:

$$\begin{aligned} V_A &= V_1 + V_2 + V_0 & I_A &= I_1 + I_2 + I_0 \\ V_B &= V_1 a^2 + V_2 a + V_0 & I_B &= I_1 a^2 + I_2 a + I_0 \\ V_C &= V_1 a + V_2 a^2 + V_0 & I_C &= I_1 a + I_2 a^2 + I_0 \end{aligned}$$

The current and voltage equations are identical in form and can be written in as

$$Q_A = Q_1 + Q_2 + Q_0 \tag{4.8}$$

$$Q_B = Q_1 a^2 + Q_2 a + Q_0 \tag{4.9}$$

$$Q_C = Q_1 a + Q_2 a^2 + Q_0 \tag{4.10}$$

where Q represents current or voltage as required.

These equations are defined for a system with A–B–C rotation. To accommodate a system with a C–B–A rotation, the "a" operator in the B and C phase terms would be switched:

$$Q_B = Q_1 a + Q_2 a^2 + Q_0$$

$$Q_C = Q_1 a^2 + Q_2 a + Q_0$$

An A–B–C rotation will be assumed for all the derivations that follow.

The 51 V at the generator can be connected to respond to phase-to-ground or phase-to-phase voltage, line currents or delta currents. If the 51 V function responds to phase-to-ground voltages and line currents, Equation (4.8) to Equation (4.10) are used directly to calculate relay input quantities. When line-to-line potential or delta currents are required, they are found by subtracting the phase quantities.

Phase-to-phase voltages or delta currents:

$$Q_A - Q_B = \sqrt{3}(Q_1\angle 30^\circ + Q_2\angle -30^\circ) \tag{4.11}$$

$$Q_B - Q_C = \sqrt{3}(Q_1\angle 270^\circ + Q_2\angle 90^\circ) \tag{4.12}$$

$$Q_C - Q_A = \sqrt{3}(Q_1\angle 150^\circ + Q_2\angle -150^\circ) \tag{4.13}$$

Note that the subtraction removes all zero sequence quantities from the above equations.

If the 51 V function is to provide backup protection for faults on a bus or distribution system directly connected to the generator or to a system connected through a wye-wye or delta-delta transformer, Equation (4.8) to Equation (4.13) would be used depending upon the input quantity used. Of course, all zero sequence terms would be ignored in the case of the delta-delta transformer.

If the system interconnection is through a wye-delta transformer, the equations must be modified to account for the transformer's phase shift. Figure 4.18 depicts the standard connection in which the primary phase-to-neutral voltage (generator side) leads the secondary phase-to-neutral voltage. For this connection, the positive sequence is shifted $+30^\circ$ and the negative sequence is

© 2006 by Taylor & Francis Group, LLC

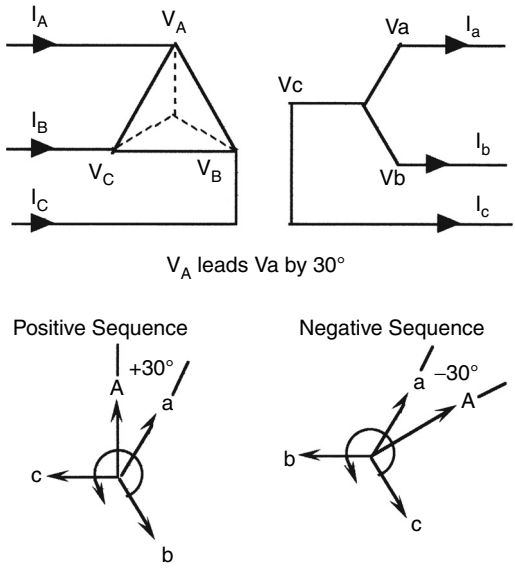


FIGURE 4.18 Phase shift wye-delta transformer.

shifted -30°. The zero sequence terms are dropped because they are associated with a neutral conductor and cannot pass through the delta winding.

The following equations define the delta-side generator phase-to-ground voltages and line currents for a fault on the wye side of the transformer. They are derived by applying the applicable phase shift to Equation (4.8) through Equation (4.10).

$$Q_A = Q_1 \angle 30^\circ + Q_2 \angle -30^\circ \tag{4.14}$$

$$Q_B = Q_1 a^2 \angle 30^\circ + Q_2 a \angle -30^\circ \tag{4.15}$$

$$Q_C = Q_1 a \angle 30^\circ + Q_2 a^2 \angle -30^\circ \tag{4.16}$$

The phase-to-phase voltages and delta currents seen at the generator are again then found by subtraction as follows:

$$Q_{AB} = Q_A - Q_B = \sqrt{3}(Q_1 \angle 60^\circ + Q_2 \angle -60^\circ) \tag{4.17}$$

$$Q_{BC} = Q_B - Q_C = \sqrt{3}(Q_1 \angle -60^\circ + Q_2 \angle 60^\circ) \tag{4.18}$$

$$Q_{CA} = Q_C - Q_A = -\sqrt{3}(Q_1 + Q_2) \tag{4.19}$$

Relay currents and voltages can now be determined for any fault condition by substituting sequence quantities derived for the fault condition of interest into the appropriate equations above.

4.2.5.2 Sequence Currents and Voltages Calculations

In Chapter 2, sequence currents were calculated from time-dependent d- and q-axes equations. The following derivations pertain to the sustained or $t = \infty$ current only. The equations are approximations, because line impedance is use instead of reactance. Theoretically, the inclusion of resistance into the generator fault calculation gives rise to interaction between the d- and q-axis current

© 2006 by Taylor & Francis Group, LLC

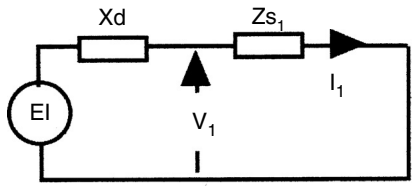


FIGURE 4.19 Sequence connection for three-phase fault.

and removes the independence between axes circuits models. Since the resistive portion of most transmission and distribution circuit impedance is small, the axis interaction is ignored.

Three-Phase Fault

Only positive sequence components are present for a three-phase fault. The symmetrical component network connection for this condition is shown in Figure 4.19. Z_{s1} represents the positive sequence reactance from the generator terminals to the point of fault.

To calculate the minimum sustained current, the generator is assumed to be at no load and on the manual voltage regulator prior to the fault. These constraints dictate that $EI = 1.0$ pu. The positive sequence current and positive sequence voltage at the terminals of the generator are given by

$$I_1 = \frac{EI}{X_d + Z_{s1}} \tag{4.20}$$

$$V_1 = EI - I_1 * X_d \tag{4.21}$$

Because no negative or zero sequence quantities exists in a three-phase fault, currents and voltages at the generator would be calculated by substituting these positive sequence values into Equation (4.8) to Equation (4.13) depending on the relay connection used.

If the 51 V function is to provide backup protection in the event of a protection scheme failure on lines connected to the generating station bus, the backup relay must be set to detect faults at the end of the longest line extending from the station. If the distribution system is connected to the generator through a GSU transformer $Z_{s1} = X_{tr1} + Z_{L1}$ where X_{tr1} and Z_{L1} are the positive sequence impedances of the GSU transformer and line, respectively.

The three-phase fault does not include negative or zero sequence components; therefore, the connection of the stepup transformer does not affect the magnitude of the current or voltage presented to the relay. A delta-wye transformer would only shift both the currents and voltages at the generator by 30°.

All the phase currents and voltages are of equal magnitude for a three-phase fault. Therefore, it is only necessary to calculate values for one relay. From Equation (4.8) and Equation (4.17):

$$I_{\varnothing} = I_1 \tag{4.22}$$

$$E_{\varnothing n} = V_1 \tag{4.23}$$

$$E_{\varnothing\varnothing} = \sqrt{3}V_1 \tag{4.24}$$

Phase-to-Phase Fault

A phase-to-phase fault includes positive and negative sequence components. The interconnection of the sequence impedances is shown in Figure 4.20.

© 2006 by Taylor & Francis Group, LLC

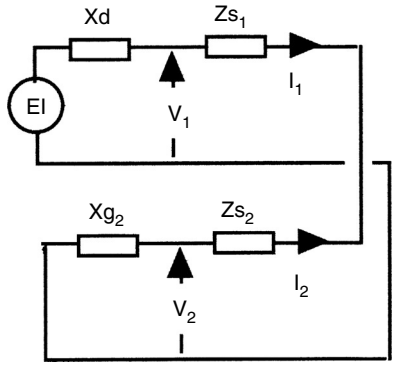


FIGURE 4.20 Sequence connections for phase-to-phase fault.

The following relationships are derived from symmetrical component theory and are evident from the sequence diagram.

$$I_1 = -I_2 \tag{4.25}$$

$$V_1 = EI - I_1 X_d \tag{4.26}$$

$$V_2 = -I_2 X_{g2} \tag{4.27}$$

$$I_1 = \frac{EI}{X_d + X_{g2} + Z_{s1} + Z_{s2}} \tag{4.28}$$

Line and transformer positive and negative sequence impedance are equivalent and Equation (4.28) can be rewritten as

$$I_1 = \frac{EI}{X_d + X_{g2} + 2Z_{s1}} \tag{4.29}$$

The expressions for relay currents and voltages for faults that do not involving an interposing delta-wye transformer are found by substituting Equation (4.25) through Equation (4.29) into Equation (4.8) through Equation (4.13).

Likewise, relay input quantities for faults through a delta-wye are found by substituting Equation (4.25) through Equation (4.29) into Equation (4.14) through Equation (4.19).

Phase-to-Ground Fault

A phase-to-ground fault includes positive, negative and zero sequence components. The sequence connection diagram is shown in Figure 4.21. The ground fault calculation is dependent on system configuration. If the fault is at the generator terminals or through a wye-wye transformer, zero sequence current will flow in the generator and connection "a" to "b" is used with that from "b" to ground removed.

The following relationships are developed for this connection diagram.

$$I_1 = \frac{EI}{X_d + 2Z_{s1} + Z_{s0} + X_{g2} + X_{g0}} \tag{4.30}$$

$$I_1 = I_2 = I_0 \tag{4.31}$$

$$V_1 = EI - I_1 X_d \tag{4.32}$$

© 2006 by Taylor & Francis Group, LLC

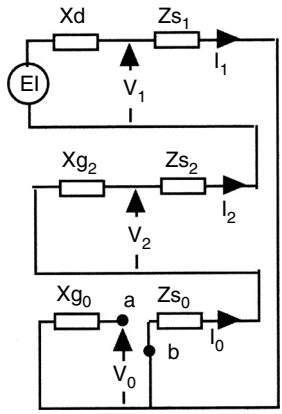


FIGURE 4.21 Sequence connections for phase-to-ground fault.

$$V_2 = -I_2 X_{g2} \tag{4.33}$$

$$V_0 = -I_0 X_{g0} = 0 \tag{4.34}$$

In the above equation $Z_{s0} = X_{tr0} + Z_{L0}$ (transformer plus line zero sequence impedance).

Unlike the positive and negative sequence $Z_{s0} \neq Z_{s1}$ or Z_{s2}. The transformer's positive and negative sequence impedance may or may not equal its zero sequence impedance. In the absence of data to the contrary all may be assumed equal, but this is not true of the line. If the circuit has a ground wire, circuit zero sequence impedance will be about three times higher than its positive or negative sequence impedance. This ratio will increase significantly if no ground wire is present.

If the fault is through a delta-wye transformer, with the generator on the delta side, transformer connection "b" to ground as shown is used and generator zero sequence quantities are not included in the calculation, $I_0 = 0$ and $V_0 = 0$. This is because the delta winding prevents zero sequence current from flowing in the generator.

As with the phase-to-phase fault, the sequence currents and voltages calculated above for the phase-to-ground fault are substituted into Equation (4.8) to Equation (4.19) as appropriate to determine the relay input quantities.

4.2.6 Sample System 51 V Relay Settings

The following example demonstrates the fault current calculation and the generator and transformer protection principles discussed previously.

An electromechanical voltage-controlled 51 V relay will be applied on the sample system connected as shown in Figure 4.22. The relay has a settable range of 1.5 to 6 A. The available taps are (1.5, 2.0, 2.5, 3.0, 4.0, 5.0, and 6 A). The dropout of the undervoltage unit is continuously adjustable from 40 to 100 V and has a pickup to dropout ratio of 104%.

The 51 V function is being applied to provide backup protection for the generator and GSU transformer. Backup protection is not required for the 69 kV lines extending from the high-voltage bus, because breaker failure relaying is provided for each 69 kV breaker. No ground overcurrent relay is provided at the GSU transformer high-side neutral, so the 51 V must detect ground faults on the 69 kV transformer leads.

The overcurrent setting must be low enough to detect the minimum current at the generator terminals for a sustained three-phase fault on the wye-side of the GSU transformer. Likewise, the undervoltage unit must be set high enough to assure dropout for all fault condition associated with the 69 kV transformer leads.

© 2006 by Taylor & Francis Group, LLC

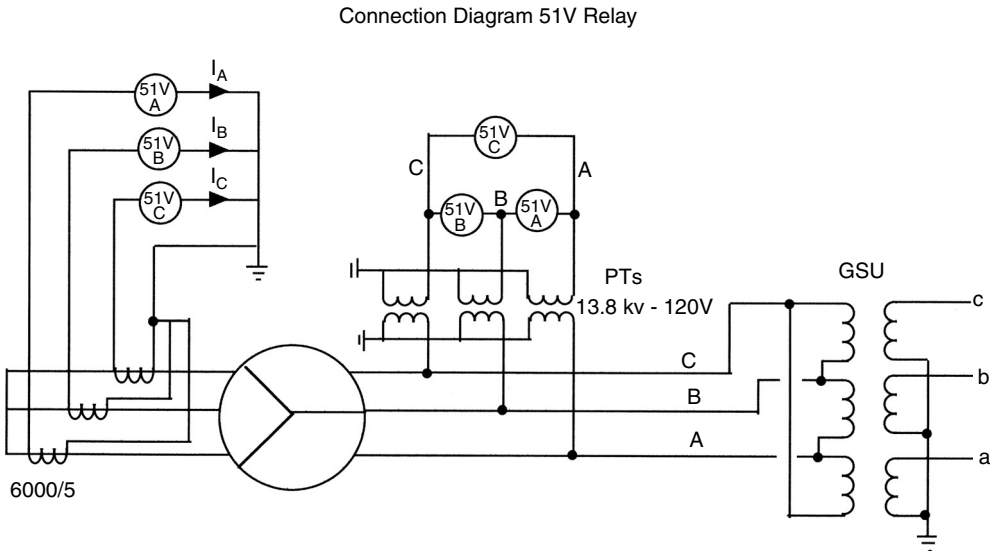


FIGURE 4.22 Sample system 51 V relay connection.

First, the overcurrent pickup and undervoltage dropout settings will be determined. Then the time delay can be chosen. Relay currents and voltages will be calculated for three-phase, phase-to-phase and phase-to-ground faults, assuming the manual voltage regulator is in service and the generator is carrying no load prior to the fault. This will establish the minimum current condition.

As previously stated, voltages calculated with the manual regulator in service are not used to set the undervoltage unit because these are minimum voltages and maximum fault voltage values are required. The manual regulator calculation will, however, identify which fault condition is the most adverse from the undervoltage unit standpoint. The undervoltage unit is then set above the maximum fault voltage for that condition with automatic voltage regulator in service.

4.2.6.1 Fault Calculations

The voltage-controlled relays applied here use phase-to-phase voltage and line currents as input quantities. Since the sample system GSU transformer is connected delta-wye, relay current and voltage calculations must include the effects of the transformer phase shift.

These constraints dictate the use of Equation (4.14) through Equation (4.16) to calculate the line current and Equation (4.17) through Equation (4.19) to calculate phase-to-phase input voltage for the relay. Below, the positive, negative, and zero sequence currents and voltages applicable to each specific fault conditions are calculated and substituted into the phase equations to determine the relay currents and voltages.

The assumption that the generator is on manual regulator, at rated voltage, with no initial load, dictates that the equivalent voltage behind the synchronous reactance, $EI = 1.0$.

The sample system data are as follows:

Generator data: $X_d = 1.48$ pu, $X_{g2} = 0.129$ pu on 104.4 MVA, 13.8 kV base
Transformer impedance: $X_{tr} = 0.065$ pu on 97 MVA, 13.8 kV base

Before the generator and transformer impedances can be used in the same equation they must be converted to a common base. The generator base will be used here. The base conversion was discussed in Chapter 2. Since both the generator and transformer impedances are on the same kV base (13.8 kV), only an MVA base conversion is required.

© 2006 by Taylor & Francis Group, LLC

Converting the transformer to the 104.4 MVA generator base:

$$X_{\text{tr}} = 0.065 * \frac{104.4}{97} = 0.70 \text{ pu on } 104.4 \text{ MVA base}$$

Three-Phase Fault

A three-phase fault contains only positive sequence quantities. Equation (4.20) and Equation (4.21) are used to calculate the sequence current and voltage.

$$I_1 = \frac{EI}{X_{\text{d}} + X_{\text{tr}}} = \frac{1.0}{j\,(1.48 + 0.07)} = -j\,0.645 \text{ pu}$$

$$V_1 = EI - I_1 * X_{\text{d}} = 1.0 - j\,1.48 * (-j\,0.645) = 0.045 \text{ pu}$$

The phase-to-phase voltage and line current magnitudes for a fault on the high-voltage side of the GSU transformer are found using Equation (4.14) and Equation (4.19). Only one voltage and current need be calculated, because all three phases have the same magnitude.

$$\begin{aligned} I_{\text{A}} &= I_1 \angle 30^\circ + I_2 \angle -30^\circ \\ &= -j\,0.654 \angle 30^\circ + 0 = 0.645 \angle -60^\circ \\ V_{\text{AB}} &= \sqrt{3}(V_1 \angle 60^\circ + V_2 \angle -60^\circ) \\ &= \sqrt{3}(0.045 \angle 60^\circ + 0 \angle -60^\circ) = 0.08 \end{aligned}$$

The base quantities at the generator terminals are

$$I_{\text{base}} = \frac{104,400\,\text{kVA}}{\sqrt{3}\ 13.8\,\text{kV}} = 4370\,\text{A}$$

$$V_{\text{base}} = \frac{13,800}{\sqrt{3}} = 7970\,\text{V}$$

Then, for the three-phase fault, the quantities available to the relay are

$$I_{\text{A}} = 0.645 \times 4370\,\text{A} = 2818\,\text{A}$$

$$V_{\text{AB}} = 0.08 \times 7970\,\text{V} = 637\,\text{V}$$

Phase-to-Phase Fault

Equation (4.25) to Equation (4.29) describe the sequence currents and voltages for a phase-to-phase fault.

$$I_1 = \frac{EI}{X_{\text{d}} + X_{\text{g}_2} + 2X_{\text{tr}}} = \frac{1.0}{j\,(1.48 + 0.129 + 2(0.07))} = -j\,0.571$$

$$I_2 = -I_1 = j0.571 \text{ pu}$$

$$V_1 = EI - I_1 X_{\text{d}} = 1.0 - j0.571 * j1.48 = 0.155$$

$$V_2 = -I_2\, X_{\text{g}_2} = -j0.571 * j0.129 = 0.074$$

© 2006 by Taylor & Francis Group, LLC

Substituting the sequence currents into phase currents from Equation (4.14) to Equation (4.16)

$$\begin{aligned} I_A &= (I_1\angle 30^\circ + I_2\angle -30^\circ)I_{base} \\ &= (-j0.571\angle 30^\circ + j0.571\angle -30^\circ) * 4370\,A \\ &= 0.571 * 4370 = 2495\,A \end{aligned}$$

$$\begin{aligned} I_B &= (I_1 a^2\angle 30^\circ + I_2 a\angle -30^\circ) * I_{base} \\ &= (-j0.571 * \angle 270^\circ + j0.571\angle 90^\circ) * 4370\,A \\ &= -1.142 * 4370\,A = -4990\,A \end{aligned}$$

$$\begin{aligned} I_C &= (I_1 a\angle 30^\circ + I_2 a^2\angle -30^\circ) * I_{base} \\ &= (-j0.571\angle 150^\circ + j0.571\angle 210^\circ) * 4370\,A \\ &= -0.571 * 4370\,A = 2495\,A \end{aligned}$$

Substituting sequence voltages into the phase-to-phase voltages Equation (4.17) to Equation (4.19):

$$\begin{aligned} V_{AB} &= \sqrt{3}(V_1\angle 60^\circ + V_2\angle -60^\circ) * V_{base} \\ &= \sqrt{3}(0.155\angle 60^\circ + 0.074\angle -60^\circ) * 7970\,A \\ &= 0.232\angle 31.5^\circ * 7970\,V = 1854\,V \end{aligned}$$

$$\begin{aligned} V_{BC} &= \sqrt{3}(V_1\angle -60^\circ + V_2\angle 60^\circ) * V_{base} \\ &= \sqrt{3}(0.155\angle -60^\circ + 0.074\angle 60^\circ) * 7970\,V \\ &= 0.232\angle -31.5^\circ * 7970\,V = 1853\,V \end{aligned}$$

$$\begin{aligned} V_{CA} &= -\sqrt{3}(V_1 + V_2) * V_{base} \\ &= -\sqrt{3}(0.155 + 0.074) * 7970\,V \\ &= -0.397 * 7970\,V = 3161\,V \end{aligned}$$

Phase-to-Ground Fault

Equation (4.30) to Equation (4.34) describe the sequence currents and voltages at the generator for a ground fault. Since the sample system GSU transformer is delta-wye the "b" to ground connection of Figure 4.20 is used and X_{g0}, I_0, and V_0 all equal zero.

$$I_1 = \frac{EI}{X_d + 3X_{tr} + X_{g2}} = \frac{1}{j\,(1.48 + 3(0.07) + 0.129)} = -j\,0.55\ \text{pu}$$

$$I_2 = I_1 = -j0.55\ \text{pu}$$

$$V_1 = EI - I_1 X_d = 1.0 - (-j0.55) * j1.48 = 0.186\ \text{pu}$$

$$V_2 = -I_2 X_{g2} = -(-j0.55) * j0.129 = -0.071\ \text{pu}$$

© 2006 by Taylor & Francis Group, LLC

Substituting the sequence currents into phase currents from Equation (4.14) to Equation (4.16):

$$\begin{aligned} I_A &= (I_1\angle 30^\circ + I_2\angle -30^\circ) * I_{base} \\ &= \{-j0.55\angle 30^\circ + (-j0.55)\angle -30^\circ)\} * 4370\,A \\ &= -j0.953 * 4370 = 4160\,A\angle -90^\circ \end{aligned}$$

$$\begin{aligned} I_B &= (I_1 a^2\angle 30^\circ + I_2 a\angle -30^\circ) * I_{base} \\ &= (-j0.55\angle 270^\circ - j0.55\angle 90^\circ) * 4370\,A = 0 \end{aligned}$$

$$\begin{aligned} I_C &= (I_1 a\angle 30^\circ + I_2 a^2\angle -30^\circ) * I_{base} \\ &= (-j0.55\angle 150^\circ - j0.55\angle 210^\circ) * 4370\,A \\ &= j0.953 * 4370\,A = 4162\,A\angle 90^\circ \end{aligned}$$

Substituting sequence voltages into the phase-to-phase voltages Equation (4.17) to Equation (4.19):

$$\begin{aligned} V_{AB} &= \sqrt{3}(V_1\angle 60^\circ + V_2\angle -60^\circ) * V_{base} \\ &= \sqrt{3}(0.186\angle 60^\circ - 0.071\angle -60^\circ) * 7970\,V \\ &= 0.398\angle 75.5^\circ * 7970\,V = 3173\,V\angle 75.5^\circ \end{aligned}$$

$$\begin{aligned} V_{BC} &= \sqrt{3}(V_1\angle -60^\circ + V_2\angle 60^\circ) * V_{base} \\ &= \sqrt{3}(0.186\angle -60^\circ - 0.071\angle 60^\circ) * 7970\,V \\ &= 0.398\angle -75.5^\circ * 7970\,V = 3173V\angle -75.5^\circ \end{aligned}$$

$$\begin{aligned} V_{CA} &= -\sqrt{3}(V_1 + V_2) * V_{base} \\ &= -\sqrt{3}(0.186 - 0.071) * 7970\,V \\ &= -0.199 * 7970\,V = 1587\,V\angle 180^\circ \end{aligned}$$

Table 4.2 summarizes the fault conditions by grouping the three 51 V relays with their input quantities for the connection shown in Figure 4.22.

4.2.6.2 Choosing the Undervoltage Setting

The undervoltage unit must be set high enough to drop out for the most adverse fault condition. From Table 4.2, the maximum fault voltage presented to the relays with the manual regulator in service is $V_{ab} = 3173$ V at the AØ relay for a phase-to-ground fault. Note that the CØ relay will see the same fault current and a much lower voltage $V_{ca} = 1587$ V for the same fault condition.

TABLE 4.2
Voltage and Currents at 51 V

	Relay AØ		Relay BØ		Relay CØ	
Fault	I_a	V_{ab}	I_b	V_{bc}	I_c	V_{ca}
3Ø	2818	637	2818	637	2818	637
Ø-Ø	2495	1854	4990	1853	2495	3161
Ø-G	4160	3173	0	3173	4162	1587

Note: 3Ø, three-phase; Ø-Ø, phase-to-phase; Ø-G, phase-to-ground.

© 2006 by Taylor & Francis Group, LLC

It would be advantageous for two relays to actuate for the fault. This would require the AØ undervoltage element to be set above the ground fault voltage with the automatic voltage regulator in service.

The assumption is that the automatic regulator and exciter are capable of forcing the field current to 1.4 times the field current necessary for full load operations. In Chapter 2, the voltage behind synchronous reactance at full load was calculated to be $EI = 2.16$ pu. The voltage behind synchronous reactance with full forcing would then be $EI = 2.16 \times 1.4 = 3.02$ pu.

If V_{ab} for the phase-to-ground fault is recalculated using $EI = 3.02$, the voltage will be $3.02 \times 3173 = 9595$ V.

The recommended setting for the undervoltage unit is 125% of the maximum fault voltage. Applying this margin, the minimum undervoltge dropout setting is: 1.25×9595 V $= 11{,}994$ V. This setting is 87% of generator rated voltage.

The generator terminal voltage could drop below this value during severe, yet recoverable system disturbances. If this occurred, the overcurrent unit of the 51 V relay would actuate, and because it is set below load, 1800 A, a unit trip will result. If the 51 V time delay is insufficient to override the disturbance.

Also note that the pickup to dropout ratio for the undervoltage unit is 104%. Once the undervoltage unit drops out, voltage must recover to $1.04 \times 11{,}780$ V $= 12{,}250$ V (89% of rated generator voltage) to reset the UV unit and avert a trip.

The desire for redundant relay coverage must be weighed against the probability and consequences of a misoperation. In this application, redundant 51 V elements are not required. The 51 V relay is itself a backup function that must operate only when the primary protection fails. A lower, more secure undervoltage setting with single relay fault response is preferred.

With the acceptance of a single relay criterion, the phase-to-ground fault is no longer the basis for the undervoltage unit setting. Voltage V_{bc} applied to the BØ relay for a phase-to-phase fault becomes the determining voltage.

Recalculating V_{bc} for the sustained phase-to-phase fault current with the automatic voltage regulator in service ($EI = 3.02$) yields $V_{ab} = 3.02 \times 1853$ V $= 5603$ V.

Applying the 125% margin, a setting as low as 1.25×5603 V $= 7004$ V or 51% rated generator voltage could be used. A setting of 75% rated generator voltage is chosen to provide increased margin. This setting is judged to be low enough to avoid misoperation during recoverable system disturbances. Although some system disturbances may cause voltages to drop more than 75% if they persist for the time necessary to cause a 51 V operation, such transients are considered nonrecoverable.

A 75% rating setting is $0.75 \times 13{,}800 = 10{,}350$ V. The relay PTs are $13{,}800/120$ V. The resulting undervoltage unit dropout setting is $10{,}350$ V $\times\ 120/13{,}800 = 90$ V.

4.2.6.3 Choosing Overcurrent Setting

The relay must be set to detect the minimum sustained three-phase fault current, 2818 A. It is recommended that the overcurrent element should not be set higher than 80% of the minimum current. Therefore, the maximum overcurrent setting is: 0.8×2818 A $= 2254$ A.

The relay is supplied from 6000/5 CTs (ratio = 1200:1). Then a 2254 primary amps setting will equal $2254/1200 = 1.88$ A in the CT secondary circuit supplied to the relay.

The relay does not have a 1.88 A tap. The closest taps are 2.0 and 1.5 A. The 1.5 A tap is chosen to maintain 80% margin. The relay pickup is then set at 1.5 secondary amps or $1.5 \times 1200 = 1800$ A on the primary circuit.

4.2.6.4 Choosing Time Delay Setting

The time dial setting is chosen graphically. The relay characteristic, stator overload, and transformer through-fault curves are plotted on the same graph. For this plot to be meaningful, all curves

© 2006 by Taylor & Francis Group, LLC

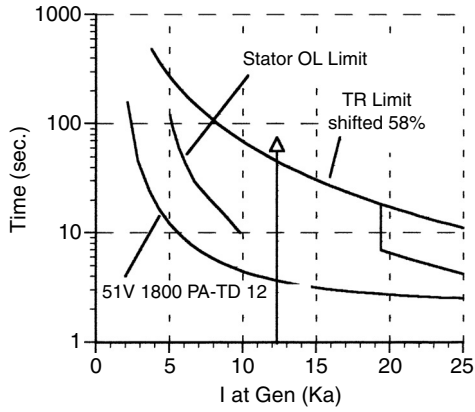


FIGURE 4.23 51 V time dial setting.

must be related to the same transformer winding. It is customary to plot the generator side winding because this allows the relay and stator limit to be plotted without compensation.

The transformer curve is also plotted on the basis of 13.8 kV winding full load current. However, this plot must be shifted to the left by 58% along the current axis to account for the adverse effects of the delta-wye transformer connection on ground fault protection. The resulting plot is shown in Figure 4.23.

The relay time delay setting is chosen such that the relay characteristic is below the stator limit and transformer thermal and mechanical damage curves at the maximum sustained ground fault current.

The sustained ground fault at the generator terminals was calculated to be 4160 A, with the manual regulator in service ($EI = 1.0$). The maximum sustained current would result from operation with the automatic regulator in service ($EI = 3.02$) and is equal to 3.02×4160 A $= 12{,}563$ A at the generator.

A low time dial (TD) setting is not recommended. 51 V is a backup function and as such must have a sufficient delay to override fault clearing by primary relaying. A # 12 TD setting is chosen here because it provides adequate protection for the stator winding and the transformer and allows sufficient time for primary relaying to clear faults.

4.2.6.5 Auxiliary PTs to Correct for Wye-Delta Phase Shift

Standards[2] recommend that an auxiliary delta-wye PT should be installed in the relay's potential circuit to correct for the 30° phase shift caused by the delta-wye power transformer. If such an auxiliary PT were installed at the sample system generator, the phase-to-phase relay voltages would be calculated from Equation (4.11) to Equation (4.13). Table 4.3 tabulates the resulting relay currents and voltages.

TABLE 4.3
Voltage and Currents at 51 V with Phase Correcting Auxiliary PTs

	Relay AØ		Relay BØ		Relay CØ	
Fault	I_a	V_{ab}	I_b	V_{bc}	I_c	V_{ca}
3Ø	2818	637	2818	637	2818	637
Ø-Ø	2495	2797	4990	1116	2495	2797
Ø-G	4160	2216	0	3520	4162	2218

Note: 3Ø, three-phase; Ø-Ø, phase-to-phase; Ø-G, phase-to-ground.

© 2006 by Taylor & Francis Group, LLC

A comparison of Table 4.2 and Table 4.3 shows that the shift-correcting auxiliary PTs provide a better alignment of maximum current and minimum voltage. Also, note that in the shift corrected case, the phase-to-ground fault becomes the high fault voltage condition against which the voltage regulator action must be checked. The resulting minimum setting would be 8372 V (2218 V × 3.02 × 1.25) or 60% of rated voltage. Overall, the additions of the PTs will not have a substantial effect on the final setting for this installation.

4.3 DISTANCE RELAYS

The term *distance relays* refers to a general class of relays that measure circuit impedance. The relay distinguishes between fault current and load current in a manner similar to the 51 V functions. The voltage applied to the distance relay tends to restrain operation, while current promotes operation.

Both phase and ground distance relays are applied on the transmission system. Unique relay designs are required for phase and ground fault protection. There are many different algorithms used in these relays, but in all cases the common goal is to measure the positive sequence impedance from the relay to the fault. When full fault protection is provided by distance relaying, six elements are required, phase elements A–B, B–C, C–A and ground elements A–G, B–G, and C–G.

Phase distance relays are applied at generators for system backup protection; ground distance relays are not applied. Most generators are grounded through impedance to limit the ground fault current. Specialized ground fault protection schemes are required. These schemes will be discussed in Chapter 5.

When a generator is solidly grounded and connected to a distribution system directly or through a wye-wye transformer, overcurrent ground relays provide superior fault sensitivity and economy when compared to ground distance relays. Overcurrent ground relaying is applicable because generator ground faults do not decay to values less than full load current and ground overcurrent relays are not subject to setting limitations due to load current.

Likewise, when a generator is connected to a system through a delta-wye grounded transformer, backup ground protection is usually provided by a time overcurrent ground relay connected in the transformer neutral.

4.3.1 Distance Relay Characteristics

4.3.1.1 *Z* Measured by Phase Distance Relay

There are many different techniques for phase distance measurement. The analysis presented here is for so-called self-polarized distance elements, because the polarizing voltage is taken from the same phases as the current.

Each phase distance element measures the impedance defined by phase-to-phase voltage and delta currents as shown below:

$$Z_{AB} = \frac{E_A - E_B}{I_A - I_B} \tag{4.35}$$

$$Z_{BC} = \frac{E_B - E_C}{I_B - I_C} \tag{4.36}$$

$$Z_{CA} = \frac{E_C - E_A}{I_C - I_A} \tag{4.37}$$

The circuit impedance measured by each relay for the various fault conditions can be found in the same way relay quantities were found for the 51 V function. Sequence currents and voltages are substituted for phase quantities in each impedance equation. The applicable sequence quantities are then determined for the fault conditions of interest and substituted into the impedance equations.

© 2006 by Taylor & Francis Group, LLC

Assuming the fault is not through a delta-wye transformer but using phase to phase voltages and delta currents, sequence Equation (4.11) through Equation (4.13) would be substituted into impedance Equation (4.35) to Equation (4.37), with the following results:

$$Z_{AB} = \frac{V_1 \angle 30^\circ + V_2 \angle -30^\circ}{I_1 \angle 30^\circ + I_2 \angle -30^\circ} \tag{4.38}$$

$$Z_{BC} = \frac{V_1 \angle 270^\circ + V_2 \angle 90^\circ}{I_1 \angle 270^\circ + I_2 \angle 90^\circ} \tag{4.39}$$

$$Z_{CA} = \frac{V_1 \angle 150^\circ + V_2 \angle -150^\circ}{I_1 \angle 150^\circ + I_2 \angle -150^\circ} \tag{4.40}$$

Three-Phase Fault

Only positive sequence current and voltage exists for a three-phase fault. Substituting $V_2 = 0$, $I_2 = 0$ into the above equations:

$$Z_{AB} = Z_{BC} = Z_{CA} = \frac{V_1}{I_1}$$

From Figure 4.19, it can be seen that the voltage at the generator terminals where the relay PTs are located is $V_1 = Z_{s1} * I_1$. Substituting this value into the above equation:

$$Z_{AB} = Z_{BC} = Z_{CA} = Z_{s1}$$

For a three-phase fault, each element will see the impedance of the circuit from the relay to the fault.

Phase-to-Phase Fault

The sequence currents and voltages for a C–B phase fault are defined by Equation (4.25) to Equation (4.29). Substituting these equations into the relay impedance Equation (4.38) to Equation (4.40) yields the following:

$$Z_{AB} = 2Z_{s1} \angle -60^\circ + \sqrt{3} X_{g2} \angle -90^\circ \tag{4.41}$$

$$Z_{BC} = Z_{s1} \tag{4.42}$$

$$Z_{CA} = 2X_{s1} \angle 60^\circ + \sqrt{3} X_{g2} \angle 90^\circ \tag{4.43}$$

One element, the C–B phase element, will see the correct circuit impedance from the relay to the point of fault. The other elements will see impedances with significantly higher value and angular displacement.

Phase-to-Ground Fault

Phase distance relays are not designed to measure circuit impedance for ground faults. Ground distance relays are designed for this purpose and use a different impedance equation. For academic interest, the response of the phase-distance relays to a phase-to-ground fault can be found by the

© 2006 by Taylor & Francis Group, LLC

same procedure used above. Substituting sequence Equation (4.30) to Equation (4.34) into the relay impedance equations, the resulting equations are

$$Z_{AB} = \frac{\sqrt{3}}{3}\left[(2Z_{s1} + Z_{s0} + X_{g0})\angle 30^\circ + X_{g2}\angle 90^\circ\right] \tag{4.44}$$

$$Z_{BC} = \infty \tag{4.45}$$

$$Z_{CA} = \frac{\sqrt{3}}{3}\left[(2Z_{s1} + Z_{s0} + X_{g0})\angle -30^\circ - X_{g2}\angle 90^\circ\right] \tag{4.46}$$

None of the measured impedances is representative of the positive sequence line impedance to the fault.

The most important point of the above derivations is that the impedance measured by the distance relays is not a function of the generator's positive sequence impedance. The measured impedance does not change with time as the generator impedance changes from subtransient to synchronous. This makes application of these relays much simpler than the 51 V function.

4.3.1.2 Mho Distance Relay

Distance relays operate when the impedance measured by the relay falls within its operating characteristic. There are many different characteristics available. Figure 4.24 shows a "mho" characteristic, which is the most common. The origin of the plot is defined by the location of the relay's PTs. The angle between the R axis and a line drawn through the center of the characteristic circle and the origin is the *maximum torque angle* (MTA) of the relay. The *Reach* of the relay is the distance from the origin to the point where the MTA crosses the circumference. The reach and MTA are settable parameters.

The relay is set on the basis of the impedance seen at the secondary of the PTs and CTs supplying the relay. This "Secondary ohm" reach must be converted to an equivalent primary circuit reach if the setting is to be compared with the impedances of power system components such as a line or transformer. The conversion from secondary ohms to primary ohms is a function of the PT and CT ratios:

$$Z_{Prim} = Z_{Sec}\frac{R_{PT}}{R_{CT}} \tag{4.47}$$

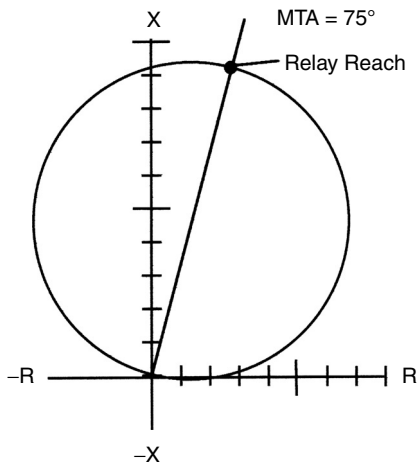


FIGURE 4.24 Mho distance characteristic.

© 2006 by Taylor & Francis Group, LLC

The relay can be connected to CTs at the neutral end of the generator or to CTs at the output terminals. In either case, the PTs are located at the generator terminals. When the neutral CT connection is used, faults on the power system or in the generator stator winding are detected in the first quadrant of the $R-X$ plot. This is because the direction of the relay current and the polarity of the relay voltage are the same for both conditions.

When the relay is connected to CTs at the generator terminals, a fault in the stator winding, with the generator connected to the power system, will produce relay current in the opposite direction of a system fault. The stator fault impedance will appear in the third quadrant of the R-X plot and will not operate the relay. The impedance for a system fault will remain in the first quadrant and is detected.

An application consideration for the mho characteristic is a solid three-phase fault at the generator terminals. Because this is the location of the relay PTs, the voltage input to the relay would be zero and the impedance seen by the relay would also be zero. Although the mho characteristic includes the origin, both electromechanical and solid-state mho relays require voltage to operate. Electromechanical relays require both current and voltage to produce torque; without a voltage input there is no relay operation. Static and microprocessor relays require voltage to determine directionality; with no voltage reference, again no relay operation.

One method used by relay manufacturers to overcoming this problem is inclusion of a memory circuit in the mho relay design. The prefault voltage is remembered for a few cycles after the fault and is used to produce torque or determine directionality.

A memory circuit is a standard feature in relays designed for Zone 1 applications on transmission lines. The Zone 1 distance relays are set to see approximately 90% of the distance from the relay location to the remote substation. Because they do not respond to faults at the remote station, they require no time delay for coordination with remote relays. The fast operating Zone 1 relay can make the trip decision for a zero voltage fault before the memory circuit voltage dissipates.

Distance relays applied for generator backup protection must have significant time delay, 0.5 sec or more, to coordinate with normal system relaying. This delay negates the use of a memory circuit to accommodate zero voltage fault conditions.

A solution more compatible with the generator backup application is the use of an offset mho characteristic (Figure 4.25). Here the relay's voltage circuit is biased with current. The relay will operate for faults at the origin and for faults in the reverse direction as limited by the amount of offset, which is settable.

Note that the relay shown in the figure is offset along the MTA line. Some mho relays have characteristics that are offset along the $-X$ axis.

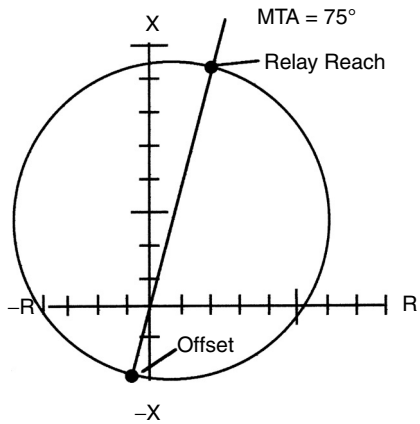


FIGURE 4.25 Offset mho characteristic.

© 2006 by Taylor & Francis Group, LLC

When relay current is taken from the generator terminals. The offset characteristic must be used if the relay is to provide backup protection for the system and stator winding because the stator fault impedance appears in the third quadrant. There are no hard rules for the amount of offset required for this application, but if the relay is intended to provide backup fault protection for the generator, the offset should include X_d''. This application will not provide stator protection when the generator is off line since the terminal CTs would see no current for this condition.

The probability of the 21 function being required to operate for a zero voltage three-phase fault is very low. A three-phase fault is itself a very improbable event. Equally improbable is the occurrence of this fault without arcing in any phase; arcing would result in fault voltage. The final requirement is that these sets of circumstances occur in conjunction with the failure of the primary relaying. In the end, a decision to use a mho relay and not cover the zero voltage condition could be justified. However, when an option exists between using a mho or offset mho characteristic, the latter would be the right choice.

4.3.1.3 System Impedance vs. Relay Characteristic

For the purpose of discussion, assume that the sample system generator supplies a radial system as shown in Figure 4.26. The transformer is connected delta-delta and has impedance of 6.5% on the transformer's MVA base. Phase distance relays are connected to 6000/5 CTs at the neutral end of the generator. The relays receive potential from 13,800–120 V PTs at the generator terminals. The 21 function is intended to provide backup tripping for faults on the radial lines extending from the station's 69 kV bus. The longest line has a positive sequence of 35% $\angle 70^\circ$. The line impedance is given on the generator base, 104.4 MVA. The reach, offset and maximum torque angle of the relay must be chosen.

The relay reach must be set such that the impedance seen by the relay for a fault at the end of the longest line will be within the relay's characteristic circle. The relay PTs are located at the 13.8 kV terminals of the generator; therefore, the impedance measured by the relay will include the stepup transformer and the line.

The per unit impedances of the line and transformer must be converted to ohms as viewed from the 13.8 kV system, where the relay PTs and CTs are located. Ohms are found by multiplying the per unit impedance by the base ohms:

$$I_{\text{base}} = \frac{\text{kVA}_{\text{base}}}{\sqrt{3} * \text{kV}_{\text{base}}}$$

$$Z_{\text{base}} = \frac{\text{kV}_{\text{base}} * 1000}{\sqrt{3} I_{\text{base}}}\ \Omega \text{ or } Z_{\text{base}} = \frac{\text{kV}_{\text{base}}{}^2}{\text{MVA}_{\text{base}}} \tag{4.48}$$

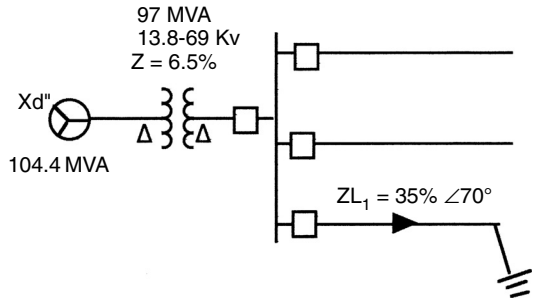


FIGURE 4.26 Distribution system.

© 2006 by Taylor & Francis Group, LLC

The transformer impedance is 6.5% or 0.065 pu on a 97 MVA base and is assumed to be a pure reactance. The transformer's ohmic impedance as seen from the 13.8 kV system is

$$Z_{\text{tr}} = \frac{13.8^2}{97} * j0.065 = j0.128\,\Omega$$

The line impedance is 35% at 70° on a 104.4 MVA base, or

$$\begin{aligned} Z_{\text{L}} &= \frac{13.8^2}{104.4} 0.35\angle 70^\circ \\ &= 0.638\angle 70^\circ\,\Omega \\ &= 0.218 + j\,0.600\,\Omega \end{aligned}$$

The transformer reactance and line impedance are plotted on Figure 4.27. The total impedance for the line and transformer is $0.218 + j\,0.728\,\Omega = 0.76\,\Omega\,\angle 73.3^\circ$. The maximum torque angle is set close to, but less than the total impedance angle. A MTA of 70° is chosen here. The reduced angle allows the relay to see some additional resistance, which can result from arcing at the point of fault.

The minimum relay reach is chosen to be 125% of the impedance of the line and transformer or $1.25 \times 0.76 = 0.95$ primary ohms at 73.3°.

The relay reach at 70° MTA to include the required reach at the line angle (θ_{L}) is given by

$$\text{Reach(MTA)} = \frac{\text{Reach}(\theta_{\text{L}})}{\cos(\text{MTA} - \theta_{\text{L}})}$$

for a line angle of 73.3° the conversion has little effect

$$\text{Reach}(70^\circ) = \frac{0.95\Omega}{\cos(\text{MTA} - \theta_{\text{L}})} = 0.951\ \text{ohm@}70^\circ$$

Because neutral end CTs are used, an offset is not necessary to detect faults in the stator winding. A small offset will be incorporated to ensure relay operation for a three-phase bolted fault at the generator terminals. An offset of about 10% of the reach or 0.1 primary ohm will be used.

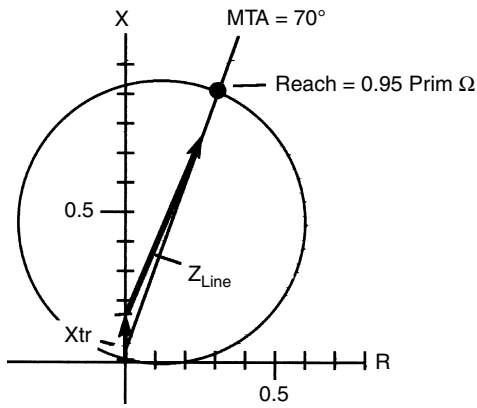


FIGURE 4.27 Circuit impedance and mho setting.

© 2006 by Taylor & Francis Group, LLC

The PT and CT ratios are 115:1 and 1200:1, respectively; therefore, the actual reach setting applied to the relay in secondary ohms is

$$Z_{\text{sec}} = Z_{\text{prim}} \frac{R_{\text{CT}}}{R_{\text{PT}}} = 0.95 \frac{1200}{115} = 9.91 \text{ sec } \Omega \angle 70^\circ$$

The offset in secondary ohms would be

$$Z_{\text{sec}} = 0.10 \frac{1200}{115} = 1.04 \text{ sec } \Omega \angle -70^\circ$$

4.3.2 Setting Considerations

4.3.2.1 Load Limits

The load at the generator terminals can be represented as an equivalent impedance. If this load impedance falls within the phase distance relay's characteristic, the relay will operate. The sample system generator is rated at 104.4 MVA, 13.8 kV, 0.85 PF. Full load current is 4368 A. At rated load and voltage the distance relay will measure system impedance as

$$Z_{\text{full_load}} = \frac{13,800}{\sqrt{3} * 4368} = 1.82 \text{ prim } \Omega \angle \theta^\circ$$

where

$$\theta = \arccos(0.85) = 31.8^\circ$$

This point is well outside the 0.95 ohm reach chosen for the relay but this does not imply that a setting that excludes the load point will be immune from misoperation under load. Network transients such as faults and line switching require generators connected to the power system to adjust to the new system configuration. In a stable system, each machine will settle to a new operating point after a damped oscillation. During these transients, generator Watt/Var output can substantially exceed the generator rating.

These power system swings will appear as a point on the R–X diagram with a circular or spiral trajectory. If the impedance swing enters and remains within the relay characteristic for a period of time exceeding the relay's trip delay, the relay will operate. This is a worst-case scenario for a misoperation of a generator protective relay. The resulting loss of generation will tend to amplify the system transient, with the potential to initiate tie line trips and cascading loss of generation and system collapse.

To avoid misoperation on power system swings, the distance relay reach should not be less then two times the generator rating. Primary ohmic reach and load are related as follows:

$$Z_{\text{prim}} = \frac{\text{kV}^2}{\text{MVA}} \Omega \tag{4.49}$$

Limiting the phase distance relay to 2 × 104.4MVA, the maximum reach would be

$$Z_{\text{prim}} = \frac{(13.8 \text{ kV})^2}{2 * (104.4 \text{ MVA})} = 0.91 \text{ prim } \Omega$$

© 2006 by Taylor & Francis Group, LLC

The previously calculated relay reach was 0.95 prim Ω. This exceeds the suggested maximum setting, but the 0.95 Ω setting was applicable to a radial system, which would not be exposed to swings.

4.3.2.2 Apparent Impedance

When a distance relay is required to provide backup protection for network line faults, the effect of infeed currents must be considered. The infeeds increase the impedance of the faulted line seen by the distance relay. This increase occurs because relay current and the faulted line current are not the same. Referring to Figure 4.28, with infeeds, the voltage at the relay is

$$V = X_{tr}I_r + Z_L I_f$$

The impedance seen by the relay is

$$Z = \frac{V}{I_r} = \frac{X_{tr}I_r + Z_L I_f}{I_r} = X_{tr} + Z_L \frac{I_f}{I_r} \tag{4.50}$$

The "apparent impedance" of the line is determined by the ratio of fault current to relay current.

The sample system generator is connected to a network bus. This configuration apparent impedance would necessitate a much larger reach to detect a line end fault than that calculated for the radial system of Figure 4.26. An additional complication arises because the apparent impedance increases with time as the generator current decays. The initial impedance seen by the 21 function is determined by the current distribution with the generator impedance equal to X_d'' as shown in Figure 4.9. The current angles are not shown in the figure but are included in the calculation. The resulting impedance seen initially by the relay is

$$\begin{aligned} Z &= Z_{tr} + Z_L \frac{I_f}{I_r} \\ &= j0.128 + 0.638\angle 70^\circ \frac{2100\angle -71^\circ}{650\angle -81^\circ}\ \Omega \\ &= 2.19\angle 80^\circ\ \Omega \end{aligned}$$

The 21 function must have a time delay and will not clear the fault immediately. If the fault persists until the generator impedance reaches X_d, the generator current will decay from its

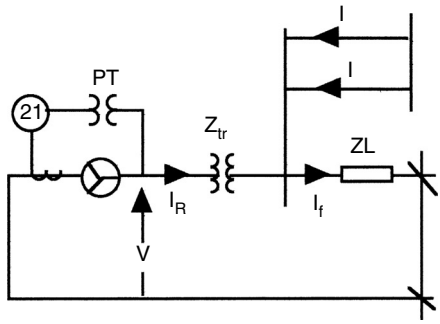


FIGURE 4.28 Apparent impedance.

© 2006 by Taylor & Francis Group, LLC

initial value of 650 A to a sustained value of 110 A, as shown in Figure 4.10. The apparent impedance increases to

$$Z = j0.128 + 0.638\angle 70^\circ \frac{1980\angle -71^\circ}{110\angle -84^\circ}$$
$$= 11.6\angle 83^\circ\ \Omega$$

Neither of the settings required to see line end faults under network conditions can be applied, because either would limit load significantly. Equation (4.49) can be used to relate relay reach to load. The 2.19 primary ohm setting is equivalent to 86 MVA and the 11.6 Ω setting equals a 16.4 MVA limit. These load limits do not include the 200% setting margin recommended to prevent misoperation for system transients.

This example demonstrates why remote backup relaying cannot be applied effectively in the majority of cases. It also shows why local breaker failure schemes are required to clear network line faults when the primary protect system failures.

4.3.2.3 Influence of an Interposing Wye-Delta Transformer

When the 21 function is required to detect faults through a wye-delta transformer the phase shift may alter the impedance measured by the relay elements. This is dependent on the relay design. Distance relays whose response is defined by Equation (4.35) to Equation (4.37) will not measure the true positive sequence impedance for phase-to-phase or phase-to-ground faults.

There are distance relays that measure circuit impedance using sequence quantities generated within the relay. A phase-to-phase and a three-phase sensing unit instead of A–B, B–C, and C–A units distinguish this type of relay. These relays are not affected by the transformer phase shift and accurately measure three-phase and phase-to-phase fault impedance through the delta-wye transformer.

The impedance measured by distance elements that sense V/I as defined by Equation (4.35) to Equation (4.37) can be determined from the input equations that include the 30° shift imposed by the wye-delta transformer. General equations are derived by substituting the shifted phase-to-phase voltages and delta currents, Equation (4.17) to Equation (4.19), into impedance Equation (4.35) to Equation (4.37).

$$Z_{AB} = \frac{V_1\angle 60^\circ + V_2\angle -60^\circ}{I_1\angle 60^\circ + I_2\angle -60^\circ} \tag{4.51}$$

$$Z_{BC} = \frac{V_1\angle -60^\circ + V_2\angle 60^\circ}{I_1\angle -60^\circ + I_2\angle 60^\circ} \tag{4.52}$$

$$Z_{CA} = \frac{V_1 + V_2}{I_1 + I_2} \tag{4.53}$$

Again, the specific impedances measured for a given fault condition are found by substituting the sequence quantities for that fault conditions into the general equations.

Three-Phase Fault

For a three-phase fault there is no effect. Only positive sequence quantities are generated by the fault. Since both positive sequence current and voltage are shifted by +30°, the impedance seen is Z_{s1}.

$$Z_{AB} = Z_{BC} = Z_{CA} = Z_{s_1}$$

© 2006 by Taylor & Francis Group, LLC

Phase-to-Phase

The impedances seen by the delta-side relays for a wye-side B–C phase fault are found by substituting Equation (4.25) to Equation (4.29) into Equation (4.51) to Equation (4.53). The resulting impedances are

$$Z_{AB} = 1.15Z_{s1}\angle -30^\circ + \frac{\sqrt{3}}{3}X_{g2}\angle -90^\circ \tag{4.54}$$

$$Z_{BC} = 1.15Z_{s1}\angle 30^\circ + \frac{\sqrt{3}}{3}X_{g2}\angle 90^\circ \tag{4.55}$$

$$Z_{CA} = \infty \tag{4.56}$$

If the transformer for the radial distribution system shown in Figure 4.26 were delta-wye, the impedances measured for a phase-to-phase fault at the end of the longest line would have been

$$\begin{aligned} Z_{AB} &= 1.15(0.76\angle 73^\circ)\angle -30^\circ + \frac{\sqrt{3}}{3}(0.129\angle 90^\circ)\angle -90^\circ \\ &= 0.93\angle 40^\circ\ \Omega \\ Z_{BC} &= 1.15(0.76\angle 73^\circ)\angle 30^\circ + \frac{\sqrt{3}}{3}(0.129\angle 90^\circ)\angle 90^\circ \\ &= 0.89\angle 107^\circ\ \Omega \end{aligned}$$

Not only is the magnitude of the measured impedance increased, but the angle is shifted. A much larger reach setting will be required. The setting must encompass the impedance seen for a three-phase fault and at least one of the phase-to-phase fault impedances as shown in Figure 4.29.

Phase-to-Ground Fault

Generally the 21 function would not be required to detect ground faults on the wye side of the stepup transformer. A ground relay in the transformer neutral is usually provided for this purpose.

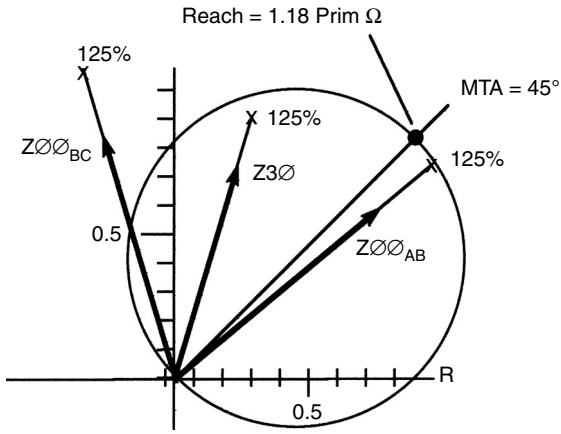


FIGURE 4.29 Distance relay setting with delta-wye transformer.

© 2006 by Taylor & Francis Group, LLC

The impedance measured by the delta-side relay for an A-phase-to-ground on the wye winding is found by substituting Equation (4.30) through Equation (4.34) into Equation (4.51) through Equation (4.53); the resulting equations are

$$Z_{AB} = (2Z_{s1} + Z_{s0})\angle 60^\circ + \sqrt{3}X_{g2}\angle 90^\circ \tag{4.57}$$

$$Z_{BC} = (2Z_{s1} + Z_{s0})\angle -60^\circ - \sqrt{3}X_{g2}\angle 90^\circ \tag{4.58}$$

$$Z_{CA} = Z_{s1} + \frac{Z_{s0}}{2} \tag{4.59}$$

Substituting values for the radial system in Figure 4.26 into these equations and assuming $Z_{s0}/Z_{s1} = 3.8$, the resulting impedances are $Z_{AB} = 4.55\ \Omega$ at 135°, $Z_{BC} = 4.61\ \Omega$ at 12°, and $Z_{CA} = 2.20\ \Omega$ at 73°.

A setting to detect the 69 kV ground fault could not be applied because it would be load limiting. This emphasizes the reason an overcurrent ground relay is applied at the transformer neutral.

The above analysis is applicable to a radial system without infeeds. If infeeds are involved, the measured impedances will be increased. To evaluate this condition the sequence currents at the relay and the sequence voltages at the generator must be derived from a reduction of the individual sequence networks. An example of this calculation is found in the literature.[3]

4.3.2.4 Auxiliary PTs to Correct for Wye-Delta Phase Shift

The installation of wye-delta auxiliary PTs is advocated by many texts including standards.[3] These PTs, when phased properly, will negate the voltage phase shift caused by the power transformer. The resulting voltages seen by the distance relays are equivalent to those seen for a fault through a wye-wye or delta-delta transformer. The impedance measured by distance relaying connected in this fashion is proportional to the line impedance. An exact replica of the line impedance would only be achieved if the auxiliary CTs were added to eliminate the phase shift in the relay current.

With auxiliary PTs installed, the impedance measured by the distance relays would be derived from Equation (4.11) to Equation (4.13) and Equation (4.17) to Equation (4.19) as follows:

$$Z_{AB} = \frac{V_1\angle 30^\circ + V_2\angle -30^\circ}{I_1\angle 60^\circ + I_2\angle -60^\circ} \tag{4.60}$$

$$Z_{BC} = \frac{V_1\angle 270^\circ + V_2\angle 90^\circ}{I_1\angle -60^\circ + I_2\angle 60^\circ} \tag{4.61}$$

$$Z_{CA} = \frac{V_1\angle 150^\circ + V_2\angle -150^\circ}{-(I_1 + I_2)} \tag{4.62}$$

Three-Phase Fault

The magnitude of the measured impedance for a three-phase fault is again unaffected. But the resulting -30° would affect the reach setting necessary to encompass the measured impedance within the relay characteristic.

$$Z_{AB} = Z_{BC} = Z_{CA} = \frac{V_1}{I_1\angle 30^\circ} = Z_{s_1}\angle -30^\circ \tag{4.63}$$

© 2006 by Taylor & Francis Group, LLC

Phase-to-Phase Fault

Substituting phase-to-phase constraints into Equation (4.60) to Equation (4.62) above results in:

$$Z_{AB} = \left(\frac{\sqrt{3}}{3} - j\right)Z_{s1} - jX_{g2} \tag{4.64}$$

$$Z_{BC} = \frac{2}{3}\sqrt{3}Z_{s1} \tag{4.65}$$

$$Z_{CA} = \infty \tag{4.66}$$

Although the voltage phase correction does not result in an ideal measurement of the B–C impedance, it is a vast improvement over the uncorrected value. The resultant impedance is solely dependent on X_{s1} and easily related to the relay characteristic.

Phase-to-Ground Fault

Substituting ground fault constraints from Equation (4.30) to Equation (4.34) as modified for the "b" zero sequence connection in Figure 4.21 into relay Equation (4.60) through Equation (4.62) above yields

$$Z_{AB} = (2Z_{s1} + Z_{s0})\angle 30^\circ + X_{g2}\angle 90^\circ \tag{4.67}$$

$$Z_{BC} = -(2Z_{s1} + Z_{s0} + 2X_{g2})\angle 90^\circ \tag{4.68}$$

$$Z_{CA} = \frac{1}{2}\left[(2Z_{s1} + Z_{s0})\angle -30^\circ - X_{g2}\angle 90^\circ\right] \tag{4.69}$$

The phase correcting PTs do not improve the response for ground faults.

4.3.3 Other Distance Relay Applications

Other applications of the 21 function are also possible. Phase distance relaying can be connected to CTs at the generator terminals with the 21 function connected to look into the generator instead of the system. This relay can be applied without a time delay to provide fast backup clearing for generator faults when connected to the system.

Many generator protection microprocessor packages include two phase distance relay functions. One zone can be implemented with a short reach and a short time delay sufficient to coordinate with high-speed bus and line relaying plus breaker failure time if applicable. The second zone is then set to see into the transmission system with a delay sufficient to coordinate with zone 2 line relaying and applicable breaker failure time. This scheme can provides 0.3 sec clearing for high current faults in the vicinity of the generator as opposed to the single zone scheme that would require a delay of about a second to coordinate with zone 2 and breaker failure relaying.

REFERENCES

1. IEEE Std C37.112-1996, *IEEE Standard Inverse-Time Characteristic Equations for Overcurrent Relays*, IEEE, New York, 1997.
2. IEEE Std C37.102-1995, *IEEE Guide for AC Generator Protection*, IEEE, New York, 1996.
3. ABB Power T&D Company Inc, *Protective Relaying Theory and Applications*, Marcel Dekker, New York, 1994, pp. 28–33.

© 2006 by Taylor & Francis Group, LLC

5 Generator Ground Fault Protection

5.1 INTRODUCTION

There are many methods for generator grounding and even more methods of ground fault protection. The subject is vast enough to warrant a sizeable IEEE standard[1] dedicated to the subject. Our intent here is to examine the more prevalent schemes with sufficient detail to allow the reader to successfully apply and set these schemes.

Grounding systems are generally classified as ungrounded, effectively grounded, low-impedance, or high-impedance grounded. Ungrounded systems have no physical connection between the generator neutral and ground. But a small ground fault current will flow as a result of shunt system capacitance. Effectively grounded systems have a direct connection from the generator neutral to system ground. The phase-to-ground fault current on an effectively grounded system is very high, in many cases higher than that of a three-phase fault. A low-impedance grounded system has minimal impedance connected between the generator neutral and ground. This impedance limits the ground fault current to a value typically between 100 A and the magnitude of a three-phase fault. In a high-impedance grounded system, the ground-to-neutral impedance is large enough to limit the ground fault current to a value between 2 and 15 A.

Over the years, all of these methods have been used to ground generators. Current practice excludes ungrounded operation, but the other methods are still employed. This is in contrast to the fairly standard transmission and distribution practice of a solid connection between neutral and ground. Although ungrounded systems remain popular in some areas this standardized grounding has led to fairly standardized ground fault protection at T&D installations. The variations in generator grounding and the resulting variety of protection schemes are a result of grounding considerations that are unique to generator installations.

5.2 GENERATOR GROUNDING CONSIDERATIONS

5.2.1 Ground Fault Current Limitation

At the heart of the differences between generator and transmission grounding is the difficulty in designing a generator to withstand the thermal and mechanical forces associated with a fault. Although the same constraints are placed on T&D system components, they are more difficult to satisfy for generator. Generator fault current does not cease immediately following the operation of a protective relay. The generator fault current will require anywhere from 1 to 10 sec to decay to zero as the magnetic energy stored in the generator dissipates onto the fault.

Also, the X/R ratio for a fault at the generator terminals is much higher than at substations. The higher ratio prolongs the mechanical and electrical stress produced by the DC component of the fault current.

Another factor is the low zero-sequence impedance of a generator. Typically, a generator's zero-sequence impedance is much less than its subtransient or negative-sequence reactance. As a result, the magnitude of an unrestricted phase-to-ground fault at the generator terminals is significantly higher than that of a three-phase fault.

Both heating and mechanical force vary as the square of the fault current. Therefore, a small reduction in fault current significantly reduces thermal and bracing requirements for the generator.

© 2006 by Taylor & Francis Group, LLC

To facilitate the most economical design, standards require that generators withstand only the effects of fault current up the magnitude of a three-phase fault at the generator terminals. Thus, indirectly, standards require that impedance be included in the grounding system to limit the ground fault current magnitude to that of a three-phase fault or less.

5.2.2 Overvoltage Concerns

Ungrounded operation would eliminate concerns relating to excessive ground fault current, because the only current flow would be the minimal current sustained by the system shunt capacitance. Unfortunately, this solution is unacceptable because this capacitance can cause damaging overvoltages.

A primary requirement of any grounding scheme is that it limits overvoltages to nondamaging levels. Overvoltages can be steady state, caused by ground faults, or transient, caused by switching or arcing ground faults. The magnitude of these overvoltages is a function of the ground path impedance. When a generator neutral is connected solidly to system ground, the low ground path impedance will permit very high fault currents, but it will also prevent significant overvoltages. The addition of impedance into the neutral to limit fault current increases the overvoltages imposed on the system. The neutral impedance must be chosen using specific criteria to eliminate the possibility of damaging overvoltages.

Steady-state overvoltages will appear on the unfaulted phases during a ground fault. The unfaulted phase voltage during a ground fault is composed of the phase voltage plus the neutral displacement. Figure 5.1(a) shows the normal relation between phase voltages and ground. On high-impedance grounded and ungrounded systems, the neutral displacement is approximately equal to the faulted phase voltage. The unfaulted phase-to-ground voltage rises to full phase-to-phase voltage as shown in Figure 5.1(b). This is an overvoltage of 173%. A ground fault on an effectively grounded system is shown in Figure 5.1(c). This system has very low ground path impedance and little neutral displacement; consequently the voltage rise on the unfaulted phases is minimal.

Transient overvoltages resulting from restriking currents are the most dangerous. Current restrikes occur when the voltage across breaker contacts or other gaps increases faster than the gap dielectric, causing a previously interrupted arc to restrike. An ungrounded system or improperly designed grounding scheme will allow cumulative voltage increases with each restrike. Theoretically, crest voltages in excess of five times that of the normal peak phase-to-ground voltage are possible for arcing grounds.

Voltage transients occur whenever system conditions change abruptly. Currents and voltages must then change from the initial steady-state value to a new steady-state value. During this transition, currents and voltages are composed of two components: a steady-state component and a transient component. In a circuit with resistive and inductive components or a circuit with resistive and capacitive components, the transient is a DC component with an exponential rate of change. The DC component of fault current discussed in Chapter 2 is an example of this phenomenon.

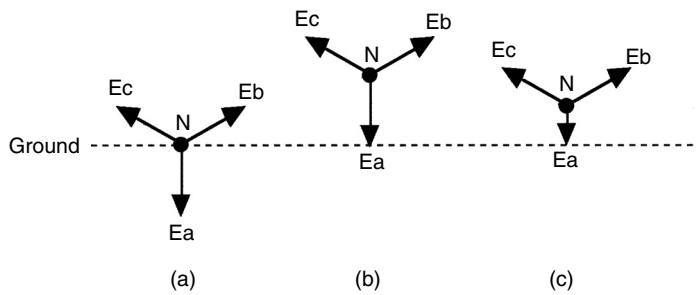


FIGURE 5.1 Unfaulted phase voltage.

© 2006 by Taylor & Francis Group, LLC

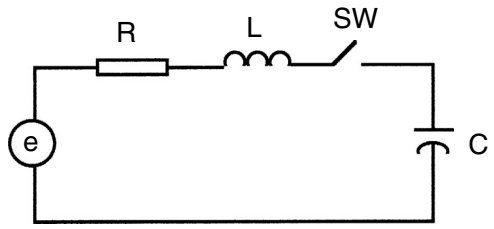


FIGURE 5.2 Capacitor switching circuit.

A generator and its connected system have a significant amount of shunt capacitance to ground. When inductive and capacitive components interact, the resulting transient component is an exponentially decaying AC component. The frequency of the transient components is the system's natural frequency, usually in the 1–20 kHz range.

Each type of voltage transient has a unique mechanism. The following is a simplified description of the transient that results when capacitive current is interrupted on an ungrounded system and the arc across the opening breaker-contact restrikes.

Figure 5.2 is a simple R–L–C circuit that will represent one phase of a three-phase ungrounded system. Initially, the current leads the voltage across the system shunt capacitance by 90°. The current is not interrupted when the breaker contacts part. Arcing occurs across the contacts until current interruption at the first current zero. The circuit phase angle is 90° hence, the current zero coincides with a voltage maximum of 1.0 pu. Because the system is not grounded, there is no path to discharge the shunt capacitance. The trapped charge will maintain the capacitor voltage at 1.0 pu after current interruption.

The phase voltage on the other side of the open switch continues toward a minimum of −1.0 pu and the voltages across the switch approach 2.0 pu as shown in Figure 5.3. If the voltage buildup across the switch is faster than the buildup of the switch dielectric, an arc will reestablish across the breaker contacts. The capacitor voltage was +1.0 prior to the flashover; after the flashover the capacitor is reconnected to the phase with a voltage of −1.0 pu, but capacitor voltage cannot change instantaneously.

To maintain the capacitor voltage equality before and after flashover, a transitory AC component of voltage with an initial value of +2.0 pu is generated. This voltage adds to the −1.0 pu

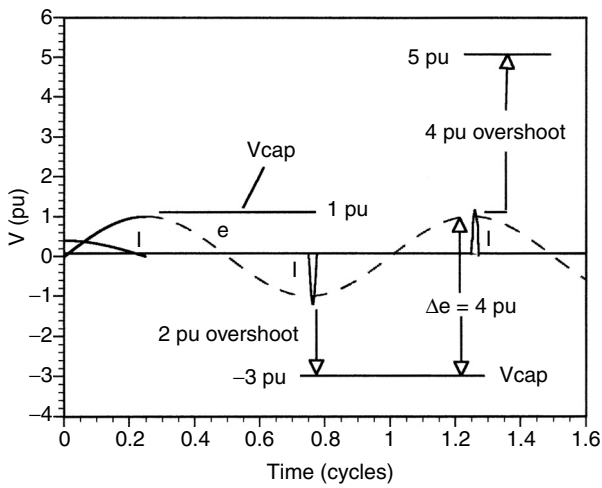


FIGURE 5.3 Voltage escalation with restrike.

© 2006 by Taylor & Francis Group, LLC

phase voltage to maintain the post flashover capacitor voltage at +1.0 pu. The frequency of the transitory AC voltage is in the 1 to 20 kHz range. The transient AC voltage changes polarity very rapidly now, adding to the −1.0 pu 60 cycle phase voltage. The result is a voltage at the capacitor of −3.0 pu within a fraction of a cycle after the flashover. This is illustrated in Figure 5.3.

When the associated high-frequency current zero occurs, the current is again interrupted, leaving a −3 pu voltage on the capacitor as the phase voltage moves toward a +1.0 pu maximum. Another flashover at the phase voltage maximum would produce another AC transient voltage. This time the initial value of the transient must be −4.0 pu to maintain the capacitor voltage at −3 pu after flashover. When this AC transient reverses polarity the capacitor voltage will become +5.0 pu and so on.

The overvoltage scenario described is for an ungrounded system, but an improperly grounding system would produce the same effect if the ground path impedance did not quickly discharge the capacitor. The breaker flashover described is similar to the mechanism that generates overvoltages during arcing ground faults. Both these transients can cause insulation failure on ungrounded and grounded systems with improperly chosen neutral impedance.

The earlier description is an oversimplification, with assumptions weighted to maximize overvoltage. More realistic quantitative definitions of transient voltages have been published.[2,3] These studies find a correlation between the overvoltage severity and the X_0/X_1 ratio of the system. X_1 and X_0 are the positive-sequence and zero-sequence reactance of the system as viewed from the point of fault.

As a result of this work, it is apparent that the effective reduction of overvoltages is not automatic when impedance is inserted between ground and the generator neutral. The value of the neutral impedance chosen must be within limits defined by the system reactance and capacitance if overvoltages are to be effectively limited. Improper neutral impedance can actually amplify overvoltages. These impedance constraints limit the range of ground fault current permitted from some grounding scheme.

5.2.3 Core Damage Cause by Ground Fault

An important protective concern is a ground in the stator winding. This fault would result from insulation failure caused by deterioration due to aging or mechanical damage caused by vibration.

Stator phase windings are formed from coils laid in slots along the parameter of the stator. The coils may be constructed as loops of wire with a slot for each side of the coil. Coils can also be constructed using insulated bars laid in two slots and interconnected at the ends to form a coil. Each coil is individually insulated. Each slot may have one side of one or more coils. Because the insulation between coils of different phases is twice as thick as the insulation between a coil and ground (the stator core being ground), the vast majority of internal generator faults begin in the slots as ground faults.

Two types of ground fault are recognized: (1) fault current is conducted from the faulted coil to the core through direct contact or the carbonized remains of insulation; (2) conduction through an arc. The latter is the more destructive because the arc concentrates the fault energy at one point on the core. A stator winding ground will require the replacement of the damaged coils, which is an expensive repair. However, if arcing at the point of failure causes significant burning of the stator core laminations, the cost and duration of the outage will increase dramatically.

The stator core is constructed by stacking thin sheets of high-permeable steel. Each sheet is insulated from the next. This insulation is necessary to prevent eddy currents within the core. The arcing grounds can cause welding of adjacent laminations at the point of fault and destruction of the insulation between laminations. This damage must be corrected. The loss of insulation will short-circuit the potential gradient between laminations. The resulting current flow will produce local overheating at the point of failure during normal operation. More insulation deterioration will occur, with an end result of stator insulation failure.

© 2006 by Taylor & Francis Group, LLC

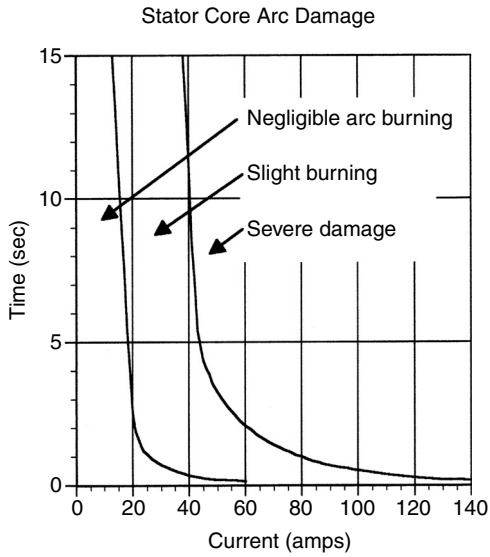


FIGURE 5.4 Stator core damage from arcing fault.

Minimum core damage would be characterized by a slight burning of the laminations, without a loss of insulation integrity. This may not require any repair. If more severe welding occurs with the loss of insulation in a small area, repairs entail grinding the affected area and reinsulating the laminations in that area. If damage is deep into the core, it will be necessary to replace laminations. This is accomplished by removing all the stator windings, and dismantling and restacking the core. This is a very expensive repair.

Core damage is a function of current magnitude and duration. Figure 5.4 is one manufacturer's[4] assessment of arc damage with time. This and other data suggest that there is a threshold value of current necessary to produce lamination damage requiring repairs.

Tests carried out in 1930 by Dr. Pohl[5] demonstrated faults of 5 A and probably higher through a conducting medium do not produce sufficient heat to damage laminations. These tests also indicated that an arcing fault of 5 A for one minute will cause some welding of laminations. Note that Pohl did not consider the lamination damage from the 5 A arc serious enough to warrant major repair. Other research[6] indicated 10 A current could be permitted without incurring major damage, but a current of 20 A would cause major damage. There is no consensus on a value for the repair threshold current, but values from 5 and 15 A are commonly used. One reason for the variance in data is that damage is strongly influenced by the type of lamination insulation.

The popularity of high-impedance grounding schemes for generator applications is directly related to the fact that these schemes limit ground fault current to values below 15 A.

5.3 METHODS OF GROUNDING

The grounding method chosen for a generator determines the type of ground fault protection that will be applied. A key factor is the ground fault current available from the grounding scheme. The schemes listed subsequently provide a range from a few tenths of an amp up to the magnitude of a three-phase fault.

5.3.1 UNGROUNDED SYSTEM

The generator in Figure 5.5 would be termed ungrounded because the generator neutral is not connected to ground. A ground is, however, established by the phase-to-ground capacitance of

© 2006 by Taylor & Francis Group, LLC

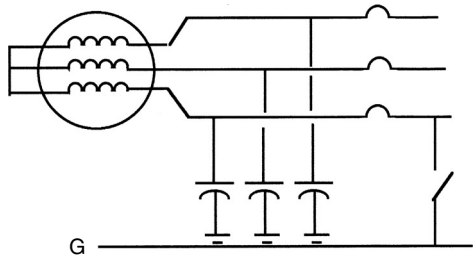


FIGURE 5.5 Ungrounded generator.

the system components. A large portion of this capacitance is from the generator's stator winding. Other sources of shunt capacitance include bus, cable, the GSU and auxiliary transformers.

If each phase capacitance to ground is equal and no unbalancing influences are present in the system, normal phase-to-neutral voltage will exist between each phase and ground as shown in Figure 5.1(a). A phase-to-ground fault will cause a full displacement of the neutral as shown in Figure 5.1(b). The phase-to-ground voltages on the unfaulted phases will then rise to the full phase-to-phase potential. The ungrounded system must therefore be insulated for full phase-to-phase voltage. Current practice is not to operate generators ungrounded. Ungrounded systems are prone to damaging overvoltages caused by arcing ground faults as described in Section 5.2.2.

The phase-to-ground fault current on an ungrounded system is a function of the system shunt capacitance and is normally less than 10 A. The generator shown in Figure 5.6 has equal phase-to-ground capacitance in each phase. Under normal operating conditions, the shunt capacitance charging currents are

$$I_a = \frac{E_{\theta n} \angle 90^\circ}{-jX_c}$$

$$I_b = \frac{E_{\theta n} \angle -30^\circ}{-jX_c}$$

$$I_c = \frac{E_{\theta n} \angle 210^\circ}{-jX_c}$$

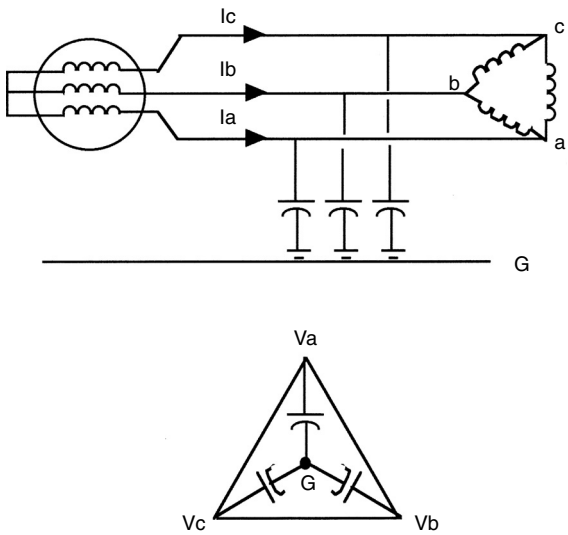


FIGURE 5.6 Ungrounded system with shunt capacitance.

© 2006 by Taylor & Francis Group, LLC

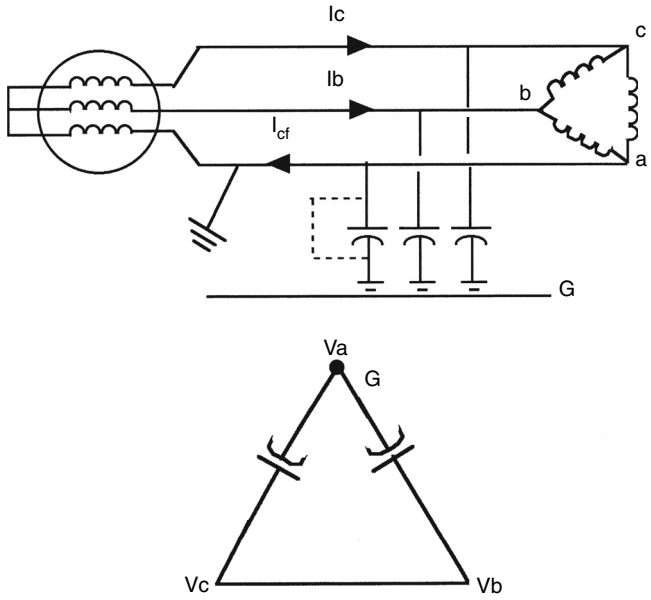


FIGURE 5.7 Ungrounded system with ground fault.

When a phase-to-ground fault occurs, the system voltage triangle shifts and the voltage between the unfaulted phases and ground increases to phase-to-phase potential. This increases the charging current in each unfaulted phase by $\sqrt{3}$. Also, the angle between the unfaulted phase voltages changes from 120° to 60° as shown in Figure 5.7. The resulting ground fault current (I_{cf}) is the summation of the charging currents in the unfaulted phases ($I_b + I_c$). The currents in the unfaulted phases become

$$I_b = \frac{V_{BA}}{-jX_c} = \frac{\sqrt{3}E_{\theta n} \angle -60^\circ}{-jX_c}$$

$$I_c = \frac{V_{CA}}{-jX_c} = \frac{\sqrt{3}E_{\theta n} \angle 240^\circ}{-jX_c}$$

The ground fault current is then three times the normal charging current as is shown below.

$$I_{cf} = I_b + I_c = \frac{\sqrt{3}E_{\theta n}(1\angle -60^\circ + 1\angle 240^\circ)}{-jX_c} = \frac{3E_{\theta n}}{X_c} \tag{5.1}$$

The same conclusions can be reached using symmetrical component methodology. Figure 5.8 is the sequence connection diagram representing a phase-to-ground fault. Because the system is ungrounded, the zero-sequence path is established through the single-phase reactance of the shunt capacitance (X_c).

For a phase-to-ground fault:

$$I_1 = I_2 = I_0 = \frac{E_1}{Z_1 + Z_2 + Z_0} \tag{5.2}$$

© 2006 by Taylor & Francis Group, LLC

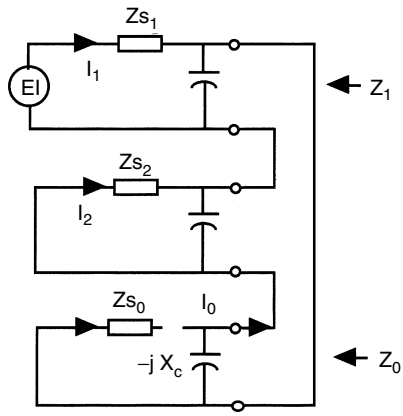


FIGURE 5.8 Sequence diagram for phase-to-ground fault.

where

$$E_1 = E_{\theta n}$$
$$Z_0 = X_c$$

and the fault current I_T is

$$I_T = I_1 + I_2 + I_0 = 3I_1 \tag{5.3}$$

The value of X_c is very large in comparison to the value of Z_{s1}, Z_{s2}, or Z_{s0}, hence these can be neglected $Z_{s1} = Z_{s2} = Z_{s0} = 0$ with little error. The expression for the total ground fault current becomes:

$$I_1 = \frac{E_1}{X_c}$$
$$I_T = \frac{3E_1}{Z_0} = \frac{3E_{\theta n}}{X_c} \tag{5.4}$$

If the sample system were ungrounded, the system ground fault current would be calculated as follows. The per phase shunt system capacitance is composed of the following:

Generator stator winding per phase:	0.315 μF
GSU transformer 13.8 kV winding:	0.09 μF
Auxiliary transformer 13.8 kV winding:	0.03 μF
13.8 kV leads:	0.05 μF
Generator potential transformer:	0.005 μF
Total per phase:	0.49 μF

Capacitive reactance per phase equals

$$X_c = \frac{1}{2\pi fC}\ \Omega \tag{5.5}$$

where f = frequency in Hz and C = capacitance in Farads.

© 2006 by Taylor & Francis Group, LLC

The single-phase-to-ground impedance of the sample system shunt capacitance would be

$$X_c = \frac{1}{2\pi 60 * 0.49 \times 10^{-6}} = 5413\ \Omega \tag{5.6}$$

The resulting phase-to-ground fault current would be

$$I_T = \frac{3E_{\theta n}}{X_c} = \frac{3 * 13{,}800\,\text{V}/\sqrt{3}}{5413\,\Omega} = 4.42\,\text{A} \tag{5.7}$$

5.3.2 Solidly Grounded/Effectively Grounded

The terms "solidly grounded" and "effectively grounded" are often used interchangeably, but this is incorrect. The term "solidly grounded" only signifies that a hardwired connection with negligible impedance has been made between the neutral and ground. The term does not address the stiffness of the ground source. For example a wye-wye transformer can be solidly grounded if a conductor connects the low-side neutral to ground, but if there is no ground connection to the primary side to establish a continuous ground path, a system ground is not established.

An "effectively grounded" system has sufficient grounding capacity to limit the voltage rise on the unfaulted phases during a ground fault such that 80% rated arresters can be applied. (These 80% rated arresters are those rated at 80% of the phase-to-phase voltage.) A system will meet this criterion if:

$$\frac{X_0}{X_1} < 3 \quad \text{and} \quad \frac{R_0}{X_1} < 1 \tag{5.8}$$

X_1, X_0, and R_0 are components of the positive- and zero-sequence impedances values as seen from the fault as shown in Figure 5.8. The zero sequence diagram for the solidly grounded generator is shown in Figure 5.9. Note that system shunt capacitance is present, but its value is very high in comparison to the system zero-sequence impedance and is ignored.

Generators are normally not "solidly grounded," because the generator's zero-sequence reactance is less than the positive sequence (X''_d) or negative sequence (X_{g2}). The low zero-sequence reactance makes solidly and effective grounding synonymous. The resulting phase-to-ground fault current is in excess of the three-phase fault current. Because standards do not require generator designs to withstand fault current greater than a three-phase fault, a ground fault of this magnitude may cause damage.

Solid grounding of a generator is applicable only if the zero-sequence reactance is large enough to limit the ground fault current below that of the three-phase fault or when the generator is specifically designed to withstand the effects of the higher current. Generators can be effectively grounded by adding impedance in the neutral to limit the fault current. The impedance added must be small to maintain the relations defined in Equation (5.8).

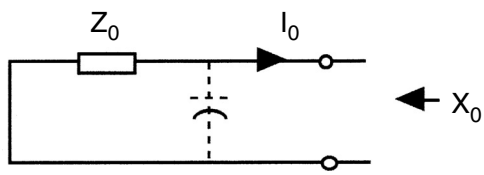


FIGURE 5.9 Zero sequence network for solid grounding.

© 2006 by Taylor & Francis Group, LLC

To benchmark current magnitudes, assume the sample system generator is solidly grounded. A rough comparison of the ground and three-phase fault currents can be established by neglecting the DC component and assuming no initial load on the generator. The sample system three-phase fault is then

$$I_{3\theta} = \frac{E''_q}{X''_d} I_{base} = \frac{1.0}{0.136} 4370\,\text{A} = 32{,}100\,\text{A} \tag{5.9}$$

With the sample system generator solidly grounded, the phase-to-ground fault current at the generator terminals for the same condition would be

$$\begin{aligned} I_{\theta g} &= \frac{3E''_q}{X''_d + X_2 + X_0} I_{base} \\ &= \frac{3.0}{0.136 + 0.129 + 0.06} 4370\,\text{A} = 40{,}338\,\text{A} \end{aligned} \tag{5.10}$$

The phase-to-ground fault current is 26% higher than the three-phase fault. Because thermal and mechanical stress is a function of the current squared, the ground fault would produce stress 59% greater than the three-phase fault.

At older installations, generators are sometimes bussed with provisions to individually ground each generator as shown in Figure 5.10. These systems may operate with only one generator grounded to limit the ground fault current. This mode of operation will significantly amplify the severity of the ground fault stress on the grounded generator.

The sequence diagram for this installation is shown in Figure 5.11. The transformer and system impedances must be converted to the 10 MVA generator base for inclusion in the diagram.

$$Z_{s1} = Z_{s2} = (0.04 + 0.12)\frac{10\,\text{MVA}}{30\,\text{MVA}} = 0.053\ @\ 10\,\text{MVA} \tag{5.11}$$

The zero-sequence system impedance is infinite, because the delta low-side winding of the transformer blocks zero-sequence current from flowing through the transformer and system impedance.

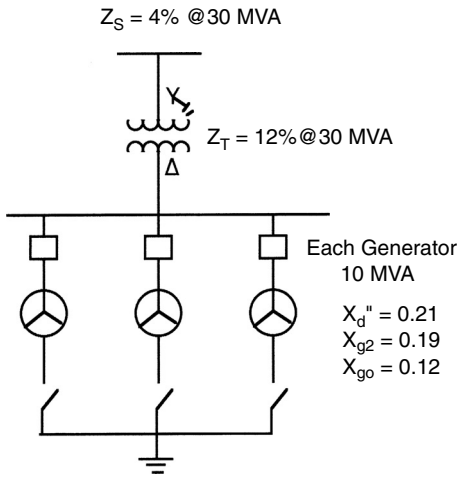


FIGURE 5.10 Bussed generators.

© 2006 by Taylor & Francis Group, LLC

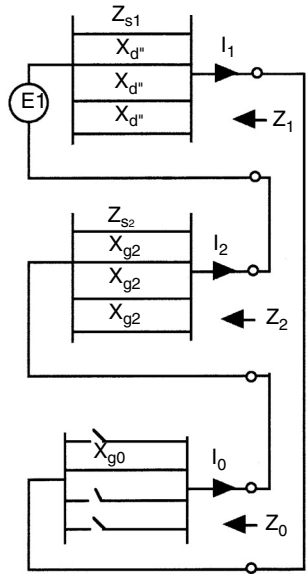


FIGURE 5.11 Sequence diagram for bussed generators.

The positive sequence network impedance is equal to the parallel combination of X''_d for the three generators and the positive sequence system impedance:

$$Z_1 = \frac{X''_d}{3} // Z_{s1} = 0.030 \tag{5.12}$$

Likewise, the negative sequence

$$Z_2 = \frac{X_{g2}}{3} // Z_{s2} = 0.029 \tag{5.13}$$

In the zero sequence, only one generator is grounded

$$Z_0 = X_{g0} = 0.12 \tag{5.14}$$

The sequence currents for a ground fault are then:

$$I_1 = I_2 = I_0 = E/(Z_1 + Z_2 + Z_0) = 5.59 \text{ pu} \tag{5.15}$$

The fault current in the grounded generator is found from the summation of the sequence currents in that generator. The positive- and negative-sequence currents divide between the three generators and the system. The positive- and negative-sequence currents from one generator are:

$$I_{g1} = \frac{1}{3}\left(I_1 \frac{Z_{s1}}{Z_{s1} + X''_d/3}\right) = 0.80 \text{ pu} \tag{5.16}$$

$$I_{g2} = \frac{1}{3}\left(I_2 \frac{Z_{s2}}{Z_{s2} + X_{g2}/3}\right) = 0.85 \text{ pu} \tag{5.17}$$

© 2006 by Taylor & Francis Group, LLC

All the zero-sequence current passes through the only grounded generator:

$$I_{g0} = I_0 = 5.59 \text{ pu} \tag{5.18}$$

The current in "a" phase of the grounded generator is

$$I_a = (I_{g1} + I_{g2} + I_{g0}) = 7.24 \text{ pu} \tag{5.19}$$

The three-phase fault current for any one of these generators is $1/X''_d = 4.76$ pu. The bussed installation with single ground results in a ground fault $7.24/4.76 = 1.52$ times the three-phase short circuit.

For a single generator installation, the ground fault would be

$$\begin{aligned} I_g &= \frac{3E}{(X''_d + X_{g2} + X_0)} \\ &= \frac{3}{(0.21 + 0.19 + 0.12)} = 5.77 \text{ pu} \end{aligned} \tag{5.20}$$

The ground fault on an individual generator is only $5.77/4.76 = 1.2 \times$ the three-phase fault. The increased ground fault stress in the bussed application is caused by the reduction of the impedance in the positive- and negative-sequence networks.

5.3.3 High-Impedance Grounding

High-impedance grounding is generally applicable when one generator is connected to the delta winding of an output transformer. The value of the impedance inserted between the generator neutral and ground is chosen to limit overvoltages to a safe value. The resulting ground fault currents are low and will not result in significant damage to the stator core.

5.3.3.1 Distribution Transformer Grounding

Distribution transformer grounding is the most common form of high-impedance grounding and has become the standard for unit connected generators. This scheme is shown in Figure 5.12. The resistance seen at the generator neutral is equal to the ohmic value of the secondary resistor times the square of the transformer turns ratio. An equivalent grounding scheme could also be accomplished by inserting a resistor directly between neutral and ground. The distribution transformer arrangement allows the use of an inexpensive low-voltage resistor.

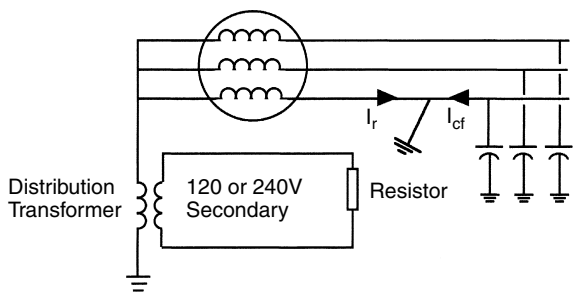


FIGURE 5.12 Distribution transformer grounding.

© 2006 by Taylor & Francis Group, LLC

The primary winding of the transformer must have a rating equal to or greater than the generator phase-to-neutral voltage. The secondary winding is normally 120 or 240 V. The 240 V secondary is preferred because it improves increased ground relay sensitivity. The grounding transformer must have sufficient overvoltage capability to avoid saturation if a ground fault occur with the generator operating at 105% rated voltage.

The resistor connected across the secondary winding is chosen such that the ground fault current supplied from the distribution transformer (I_r) in Figure 5.12 equals or exceeds the ground fault current supplied by the shunt capacitance (I_{cf}). If this criterion is met, the overvoltages will be limited to 2.6 times the normal line-to-neutral peak voltage,[3] which is within the capability of the generator's insulation.

Increasing the resistive current from the distribution transformer above the capacitive current produces little reduction in overvoltage, while damage will increase as a result of increased fault current. Consequently, the resistive current is generally chosen to equal the capacitive current.

The ground fault current resulting from shunt capacitance (I_{cf}) was derived as Equation (5.1):

$$I_{cf} = \frac{3E_{\text{Øn}}}{X_c} \tag{5.1}$$

The resistive component from the distribution transformer will be

$$I_r = \frac{E_{\text{Øn}}}{R_{sec}N^2}$$

where

$$N^2 = \left(\frac{V_{prim}}{V_{sec}}\right)^2 \tag{5.21}$$

The ohmic value of the secondary resistor such that $I_{cf} = I_r$ is given by

$$R_{sec} = \frac{X_c}{3N^2} \tag{5.22}$$

The total ground fault current equals

$$I_f = I_r + jI_{cf} \tag{5.23}$$

If the resistor is chosen to these specifications, fault current is usually limited to between 5 and 15 A.

The zero-sequence circuit for the high-resistance scheme is shown in Figure 5.13. Sequence networks are drawn on a per phase basis. Each phase has a zero sequence current equal to I_0.

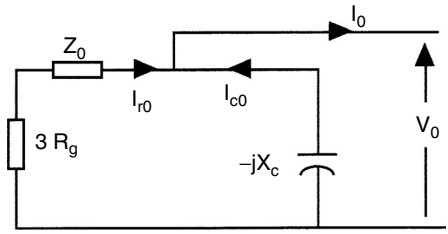


FIGURE 5.13 Zero sequence for distribution transformer grounding.

© 2006 by Taylor & Francis Group, LLC

Any impedance placed in the neutral will have the sum of the phase zero sequence currents or $3I_0$ flowing through it. The neutral circuit impedance must appear in the sequence diagram at three times its actual value to maintain the proper voltage drop. Therefore, the neutral resistance is shown as 3 R_g and as described earlier $R_g = X_c/3$ for proper high-resistive grounding.

5.3.3.2 High-Resistance Grounding on Sample System

If this method of grounding is used for the sample system generator, the resistive current supplied from the grounding transformer must equal the 4.42 A capacitive fault current calculated in Section 5.3.1 for the ungrounded system.

The total fault current (I_f) will become

$$I_f = I_r + I_{cT} = 4.42 + j\,4.42 = 6.25\,\text{A}\angle 45^\circ \tag{5.24}$$

The resistance required between the neutral and ground would be

$$R_{prim} = \frac{E_{\text{ØN}}}{I_c} = \frac{7970\,\text{V}}{4.42\,\text{A}} = 1803\,\Omega \tag{5.25}$$

The resistance at the secondary winding of the distribution transformer necessary to provide the required resistance in the primary circuit is found using the square of the transformer turns ratio:

$$R = R_{prim}\left(\frac{E_{sec}}{E_{prim}}\right)^2 = 1803\left(\frac{120}{7970}\right)^2 = 0.409\,\Omega \tag{5.26}$$

The resulting secondary current in the distribution transformer for a ground fault is

$$I_{sec} = I_{prim}\frac{E_{prim}}{E_{sec}} = 4.42\,\text{A}\frac{7970}{120} = 293.6\,\text{A} \tag{5.27}$$

The required wattage for a continuously rated secondary resistor and distribution transformer is

$$P = I^2R = 293.6\,\text{A}^2 \times 0.409\,\Omega = 35.2\,\text{kW} \tag{5.28}$$

Assuming that the protective scheme applied on the sample system will trip the unit upon the occurrence of a ground fault, a 294 A resistor with a 10 sec rating can be used. The transformer rating could also be reduced, but with little economic advantage; consequently a 37.5 kVA unit will be used.

5.3.3.3 Ground Fault Neutralizers

The ground fault neutralizer (GFN), also known as a Petersen Coil or resonant grounding, is physically identical to the high-resistance scheme described earlier, with the exception that an adjustable reactor is connected across the secondary winding of the distribution transformer. The distribution transformer in the GFN scheme uses windings rated similar to those of the high-resistance scheme.

The zero-sequence representation of the GFN circuit is identical to Figure 5.13 with the grounding resistor $3R_g$ replaced by a reactance equal to $3X_g$. The secondary reactor is set such that reactance seen in the primary circuit equals one-third the total system per phase capacitive reactance, $X_g = X_c/3$. This choice of neutral reactance forms a parallel resonant circuit in the zero sequence. I_{r0} and I_{c0} are equal in magnitude, with opposite phasing. Theoretically, the two currents cancel each other and the resulting zero-sequence network impedance is infinite and $I_0 = 0$. In theory,

© 2006 by Taylor & Francis Group, LLC

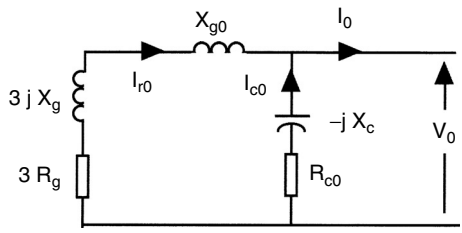


FIGURE 5.14 Zero sequence for ground fault neutralizer.

no current will flow at the point of fault, yet current is available at the distribution transformer for fault detection. In practice, circuit losses result in a very large but finite zero-sequence impedance that allows a small fault current to flow.

Zero-Sequence Impedance of GFN

Figure 5.14 is a more detailed depiction of the zero sequence circuit for the GFN scheme. Losses in the grounding reactor circuit R_n and dielectric losses in the system R_{c_0} determine the equivalent 60 Hz zero-sequence network impedance and hence the ground fault current.

The value of R_g is determined by the GFN designer to meet constants that will be discussed later. The designer specifies the reactance and the "coil constant" for the inductor in the distribution transformer's secondary circuit. The coil constant is the X/R ratio of the inductor.

The equivalent zero-sequence impedance for the GFN system is the impedance of the grounding reactor as seen from the primary of the distribution transformer paralleled with the shunt capacitive branch as shown in Figure 5.14. The zero-sequence impedance of the generator is small in comparison to X_g and X_c and is ignored in the calculation. The zero-sequence equivalent impedance is then the parallel equivalent of the two branches.

$$R_0 = \frac{(3R_g + j3Xg)(R_{c0} - jX_c)}{3R_g + j3X_g + R_{c0} - jX_c} \tag{5.29}$$

At 60 Hz the circuit is tuned such that $3X_g = X_c$. Substituting these and expanding the equation:

$$R_0 = \frac{3R_gR_{c0} + j3X_g(R_{c0} - 3R_g) + 9X_g^2}{3R_g + R_{c0}}$$

A determination of R_0 will require a value for R_{c0}. Because actual values for dielectric loss are not normally available, an assumption is required. If these losses are assumed to be zero, the required coil constant will be lower, unnecessarily increasing the ground fault current. If exaggerated losses are assumed, the coil constant will be too high and damaging overvoltages could occur. A middle-of-the-road design assumption that has been applied succesfully is that $R_{c0} = 3R_g$.[7]

Making this substitution and neglecting the small resistive terms, Equation (5.29) becomes:

$$R_0 = \frac{3X_g^2}{2R_g} = k\frac{3X_g}{2} \tag{5.30}$$

The resulting zero-sequence impedance is shown to be resistive.

A high coil constant ($k = X_g/R_g$) is desired, because this will result in maximum zero-sequence network impedance, minimum ground fault current, and minimum fault damage. However, there exists a maximum allowable R_0, which in turn defines the maximum allowable coil constant. The R_0 limit is determined by the displacement of the generator's neutral and the resulting

© 2006 by Taylor & Francis Group, LLC

phase-to-ground overvoltage at the generator for a ground fault on the high-voltage side of the GSU transformer.

Neutral Displacement for High Voltage Faults

A GFN grounded generator is normally connected to the delta winding of a GSU transformer. This effectively isolates the generator from zero-sequence currents associated with high-voltage ground faults. However a portion of the zero sequence voltage produced by these faults is impressed on the generator via the interwinding coupling capacitance in the GSU transformer. The impressed voltage appears as a neutral displacement of the generator phase voltages.

The generator phase-to-ground voltage is equal to the vector sum of the impressed displacement voltage (V_{nd}), the normal 60 cycle zero-sequence voltage produced by the generator, and the individual phase voltage. Since the normal 60 Hz zero-sequence voltage is negligible for most installations, the maximum generator phase voltage occurs when the displacement voltage is in phase with one of the phase voltages.

The displacement voltage is not transient and it will remain until the ground fault is cleared. The maximum allowable coil constant is that which limits the phase-to-ground voltage plus the displacement voltage to a value equal to the voltage at which the system is insulated.[7] On a high-impedance grounded system, insulation is rated for phase-to-phase voltage.

The displacement voltage is not affected by the GSU transformer's turn ratio. The magnitude of the displacement voltage at the generator is determined by the magnitude of the zero-sequence voltage generated at the high-voltage bushings of the transformer and the voltage divider formed by the R_0 and the interwinding capacitance as shown in Figure 5.15. The displacement voltage is then given by

$$V_{nd} = e_{x0} * \frac{R_0}{R_0 - jX_{cw}}$$

where e_{x0} = zero-sequence fault voltage at the high side of the GSU transformer and $X_{cw} = 60$ Hz reactance of interwinding capacitance.

The neutral displacement is of concern for the GFN scheme because of the very high zero-sequence impedance that characterizes this grounding scheme. In other grounding schemes, the displacement voltage is usually not an issue, because the impedance of the generator's zero-sequence network is small compared to that of the interwinding capacitance. In these schemes, most of the displacement voltage is impressed across the GSU capacitance. This would also be true for ungrounded generators, because the large shunt capacitance at the generator terminals provides a zero-sequence impedance significantly less than the interwinding capacitance.

Application of a GFN on the Sample System

The reactance of the GFN is chosen using the same criteria used to choose the resistance of the high-resistance scheme. The reactance as seen from the primary of the distribution transformer

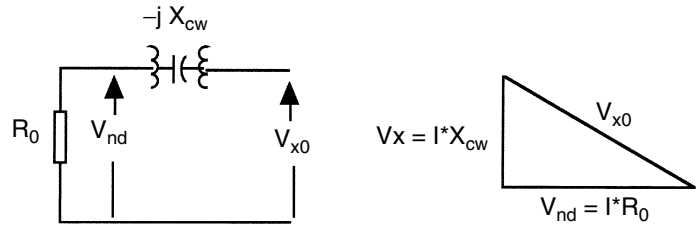


FIGURE 5.15 Winding capacitance voltage divider.

© 2006 by Taylor & Francis Group, LLC

should equal one-third of the per phase capacitive reactance to ground. The shunt capacitive reactance for the sample system was determined to be 5413 Ω/phase in Section 5.3.1. The required reactance as seen from the primary of the grounding transformer is then

$$X_g = \frac{X_c}{3} = \frac{5413\,\Omega}{3} = 1803\,\Omega \tag{5.31}$$

Because the two schemes have equivalent impedances, the current from the distribution transformer and the distribution transformer rating will also be equivalent, 4.42 A and 37.5 kVA, respectively.

High-Side Zero-Sequence Voltage

The most challenging aspect of GFN design is establishing the maximum coil constant. This requires a calculation to determine the maximum zero sequence voltage at the high-voltage bushings of the GSU transformer for a high-voltage ground fault. If this voltage is calculated with the generator isolated and with the generator online, the maximum ground fault voltage is usually found for the online condition. Figure 5.16 illustrates the sequence network connections of the online case with system impedance taken from Figure 1.1.

The equivalent positive-sequence network impedance is derived from the parallel combination of the generator-side and system-side impedances:

$$Z_1 = \frac{(X_d'' + X_{tr1})Z_{s1}}{X_d'' + X_{tr1} + Z_{s1}} = \frac{(0.136 + 0.07)0.078}{0.136 + 0.07 + 0.078} = 0.057 \tag{5.32}$$

The equivalent negative-sequence network impedance is

$$Z_2 = \frac{(X_{g2} + X_{tr2})Z_{s2}}{X_{g2} + X_{tr2} + Z_{s2}} = \frac{(0.129 + 0.07)0.078}{0.129 + 0.07 + 0.078} = 0.056 \tag{5.33}$$

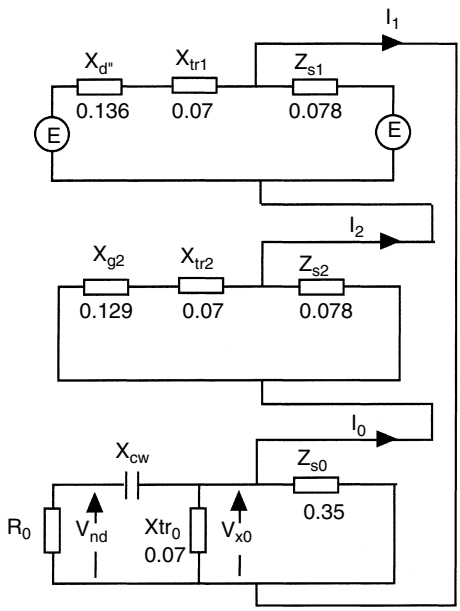


FIGURE 5.16 Sequence connection for high-voltage ground fault.

© 2006 by Taylor & Francis Group, LLC

The equivalent zero-sequence network impedance neglecting the high impedance interwinding branch is

$$Z_0 = \frac{X_{tr0} Z_{s0}}{X_{tr0} + Z_{s0}} = \frac{0.07 * 0.35}{0.07 + 0.35} = 0.058 \tag{5.34}$$

The impedances of the interwinding capacitance and R_0 of the ground fault neutralizer are very large in comparison to the transformer reactance and are neglected in this calculation.

The sequence currents for the ground fault are then

$$\begin{aligned} I_1 = I_2 = I_0 &= \frac{E}{Z_1 + Z_2 + Z_0} \\ &= \frac{1.0}{0.057 + 0.056 + 0.058} = 5.84 \text{ pu} \end{aligned} \tag{5.35}$$

The high-side, zero-sequence voltage is then

$$V_{0h} = I_0 * Z_0 * V_{base} = 5.84 * 0.058 * \frac{69{,}000}{\sqrt{3}} = 13{,}494 \text{ V} \tag{5.36}$$

It may be apparent from the calculation why the online case produces the maximum zero-sequence voltage. The system's zero-sequence impedance is high and does not significantly reduce the zero-sequence network impedance for the online case. The positive and negative sequence network impedances are sharply reduced for the online case, resulting in higher zero-sequence current and, with it, a larger zero-sequence voltage.

Maximum Displacement Voltage

The sample system, like any other system with high-impedance grounding, is insulated for full phase-to-phase voltage. The phase-to-ground voltage at the generator during a high-voltage, phase-to-ground fault must not exceed this value. The generator phase-to-ground voltage equals the phase voltage ($V_{\theta n}$) plus the displacement voltage (V_{nd}):

$$E_{\theta n}(\max) = V_{\theta\theta} = V_{\theta n} + V_{nd} \tag{5.37}$$

Then for the sample system, the maximum allowable displacement voltage is

$$\begin{aligned} V_{nd}(\max) &= E_{\theta\theta} - E_{\theta n} \\ &= 13{,}800 - \frac{13{,}800}{\sqrt{3}} = 5830 \text{ V} \end{aligned} \tag{5.38}$$

The reactor coil constant must be chosen such that the resultant zero-sequence impedance of the GFN circuit (R_0) is such that V_{nd} does not exceed 5830 V.

Knowing the maximum neural displacement voltage, the limiting value of R_0 can be derived from Figure 5.15.

$$I = \frac{\sqrt{V_{h0}^2 - V_{nd}^2}}{X_{cw}} \tag{5.39}$$

Then, the displacement voltage is given by

$$V_{nd} = \frac{R_0 \sqrt{V_{x0}^2 - V_{nd}^2}}{X_{cw}} \tag{5.40}$$

© 2006 by Taylor & Francis Group, LLC

Solving for R_0,

$$R_0 = \frac{V_{nd} X_{cw}}{\sqrt{V_{x0}^2 - V_{nd}^2}} \tag{5.41}$$

The interwinding capacitance of the GSU transformer is 0.025 μF/phase. The reactance is

$$X_{cw} = \frac{1}{2\pi f C} = \frac{1}{377 * 0.025 \times 10^{-6}} = 106{,}100\,\Omega \tag{5.42}$$

Substituting values into Equation (5.41), the maximum allowable value of R_0 is

$$R_0 = \frac{V_{nd} X_{cw}}{\sqrt{V_{x0}^2 - V_{nd}^2}} = \frac{5830 * 106{,}100}{\sqrt{13{,}494^2 - 5830^2}} = 50{,}829\,\Omega \tag{5.43}$$

The coil constant (X_g/R_g) for the neutral reactance is derived from Equation (5.30):

$$k = \frac{X_g}{R_g} = \frac{2R_0}{3X_g} \tag{5.44}$$

Again, substituting known values into Equation (5.44),

$$k = \frac{2R_0}{3X_g} = \frac{2 * 50{,}829\,\Omega}{3 * 1803\,\Omega} = 18.8 \tag{5.45}$$

The coil constant calculated above is based on resistance and reactance as viewed from the primary side of the grounding transformer. The values applicable to the reactor connected at the grounding transformer secondary must include considerations for the resistance and reactance of the grounding transformer itself.

The distribution transformer used on the sample system has the following characteristics:

37.5 kVA $Z = 6\%$
7970 – 120 V
Losses = 450 W

The total primary reactance required for resonant grounding was determined from Equation (5.31) to be 1803 Ω. Relating this reactance to an equivalent at the secondary of the distribution transformer:

$$X_T = X_g\left(\frac{V_{sec}}{V_{prim}}\right)^2 = 1803\,\Omega\left(\frac{120}{7970}\right)^2 = 0.4087\,\Omega \tag{5.46}$$

The resistance and reactance of the transformer as seen from the 120 V terminals are calculated as follows:

$$I_{fullload} = \frac{37.5\,\text{kVA}}{0.120\,\text{kV}} = 312.5\,\text{A} \tag{5.47}$$

© 2006 by Taylor & Francis Group, LLC

Base ohms for the transformer is is given by

$$Z_{\text{base}} = \frac{E_{\text{rated}}}{I_{\text{fullload}}} = \frac{120}{312.5\,\text{A}} = 0.384\,\Omega \tag{5.48}$$

Grounding transformer resistance and impedance in ohms are

$$\begin{aligned} Z_{\text{tr}} &= Z_{\text{base}} Z_{\text{tr}}(\text{pu}) = 0.384 * 0.06 = 0.0230\,\Omega \\ R_{\text{tr}} &= \frac{\text{Losses}}{I^2} = \frac{450\,\text{W}}{312.6\,\text{A}^2} = 0.0046\,\Omega \end{aligned} \tag{5.49}$$

Transformer reactance is

$$\begin{aligned} X_{\text{tr}} &= \sqrt{Z^2 - R^2} \\ &= \sqrt{0.0230^2 - 0.0046^2} = 0.0225\,\Omega \end{aligned} \tag{5.50}$$

If X_{L} and R_{L} are the reactance and resistance of the inductor installed in the distribution transformer secondary circuit, then

$$X_{\text{L}} = X_{\text{T}} - X_{\text{tr}} = 0.4087 - 0.0225 = 0.3862\,\Omega \tag{5.51}$$

Relating the coil constant that was calculated from primary quantities to the secondary quantities:

$$k = 18.8 = \frac{X_{\text{g}}}{R_{\text{g}}} = \frac{X_{\text{tr}} + X_{\text{L}}}{R_{\text{tr}} + R_{\text{L}}} \tag{5.52}$$

X_{L} and R_{L} are the reactance and resistance of the inductor installed in the distribution transformer secondary circuit. Substituting values:

$$18.8 = \frac{0.3862 + 0.0225}{R_{\text{L}} + 0.0046} \tag{5.53}$$

From the above, $R_{\text{L}} = 0.0171\ \Omega$, and the actual coil constant for the secondary reactor (k_{a}) is

$$k_{\text{a}} = \frac{X_{\text{L}}}{R_{\text{L}}} = \frac{0.3862\,\Omega}{0.0171\,\Omega} = 25.6 \tag{5.54}$$

A resonant grounding scheme applied in the sample system would require a secondary reactor of $0.386\ \Omega$ with a coil constant of 25.6.

The resulting zero-sequence impedance for the scheme, calculated from Equation (5.30), would be $R_0 = 50{,}829\ \Omega$, and the ground fault current will be

$$I_{\text{g}} = \frac{3 * E_1}{R_0} = \frac{3 * 7970\,\text{V}}{50{,}829\,\Omega} = 0.470\,\text{A} \tag{5.55}$$

This is significantly less than the 6.25 A fault current produced by the high-resistance scheme.

Advantages and Disadvantages of the GFN Scheme

The high impedance of the zero-sequence network is the defining characteristic of the ground fault neutralizer scheme and is directly responsible for the scheme's major advantages and disadvantages.

© 2006 by Taylor & Francis Group, LLC

Advantages of the GFN Scheme

1. The resonant grounding scheme results in ground fault currents well below that possible with a high-resistance scheme. The lower fault current reduces damage.
2. Resonant grounding eliminates arcing ground faults and the associated transient overvoltages. The resistive characteristic of the tuned neutralizer keeps the fault current in phase with the voltage, thus virtually eliminating an interruption transient at zero current. The GFN also eliminates the restrikes necessary to support arcing by slowing the buildup of the recovery voltage after fault interruption. This ensures dielectric recovery of the arc path, eliminating the restrike mechanism necessary to sustain an arc.
3. Relaying applied on a GNF system can detect ground faults with significantly higher resistance that on any other type of grounding scheme. This is important, because stator-winding faults generally do not occur as a result of a sudden flashover; they evolve as insulation deteriorates over time. A small leakage current develops at a point of weakness. The leakage current produces local heating that further damages the insulation and increases the current. The cycle continues until a complete failure occurs.

   The failure process will appear as a continuous decrease in the impedance to ground. The extremely sensitive protection obtainable from a GFN system will detect insulation deterioration at a very early stage. Damage is therefore limited by early detection when the current at the point of failure is minimal.

   The impedance of deteriorating insulation (R_f) will appear in the positive-, negative-, and zero-sequence networks. The sequence currents for the restricted ground fault are:

$$I_1 = I_2 = I_0 = \frac{E}{(Z_1 + R_f) + (Z_2 + R_f) + (Z_0 + R_f)} \tag{5.56}$$

For a high-resistance or resonant grounded scheme, the positive- and negative-sequence impedance of the generator will be small when compared to Z_0 and R_f; as a result, the sequence current can be approximated as

$$I_0 = \frac{E}{R_0 + 3R_f} \tag{5.57}$$

A relay connected to measure voltage across the grounding impedance is a common form of fault detection on high-impedance grounded systems. The voltage impressed on such a relay would is V_0:

$$V_0 = I_0 Z_0 = \frac{EZ_0}{Z_0 + 3R_f} \tag{5.58}$$

If, for a basis of comparison, the detection relay is assumed to operate at 5% voltage and the system voltage (E) is assumed to be 1.0 pu, then

$$V_0 = 0.05 = \frac{Z_0}{Z_0 + 3R_f} \tag{5.59}$$

and the maximum detectable fault impedance becomes

$$R_f(\max) = 6.3\, Z_0 \tag{5.60}$$

Neglecting the impedance of the generator, the zero-sequence impedance of the high-resistance and resonant grounding schemes applied on the sample system were $Z_0 = 3R_g = 3 * 1803\ \Omega = 5413\ \Omega$ and $Z_0 = R_0 = 50{,}829\ \Omega$, respectively.

© 2006 by Taylor & Francis Group, LLC

From Equation (5.60), the resonant ground scheme would be capable of detecting a fault resistance of 320 kΩ, vs. 34 kΩ for the high-resistance scheme. The resonant grounding scheme is 9.4 times more sensitive. This comparative sensitivity between the two schemes is typical.

Disadvantages

1. Resonant grounding amplifies the fundamental zero-sequence voltages normally produced by the generator. The ambient 60 Hz zero sequence voltage is small, normally less than 0.1%, but because the GFN is tuned to 60 Hz, the gain is very high for this voltage. The result may be unacceptably high voltage appearing across the grounding transformer.

   Other harmonic voltage may also be amplified, but to a much lesser extent. The third harmonic may also be of interest. Although the amplification for this frequency is far less than for the fundamental, the third harmonic voltage is the largest harmonic voltage produced by the generator. Even with much lower amplification, the third harmonic voltage, by nature of its large initial value, may add significantly to the neutral voltage. The third harmonic voltage produced by a generator normally ranges from 1 to 10% of the phase-to-neutral voltage.

   The circuit shown in Figure 5.17 can be used to estimate amplification of zero-sequence harmonic voltages impressed on the grounding scheme by the generator.

   The current in the circuit is equal to

$$I = \frac{e_{h0}}{\left(3R_g + j3hX_g + R_{c0} - j\dfrac{X_c}{h}\right)} \tag{5.61}$$

   where e_{h0} = harmonic voltage produced by the generator, $R_g = X_g k$ = ground circuit resistance, $R_{c0} = 3R_g$ = dielectric losses, k = coil constant of primary circuit, X_g = ground circuit reactance at 60 Hz, X_c = shunt capacitive reactance/phase at 60 Hz, and h = harmonic order.

   Assuming, as was done in Section 5.3.3.3 (Zero-Sequence Impedance of GFN), that the per-phase dielectric losses equal three times the losses in the resonant grounding device and that the 60 Hz reactance of $3X_g = X_c$, the equation becomes

$$I = \frac{e_{h0}}{3R_g\left[2 + jk\left(h - \frac{1}{h}\right)\right]} \tag{5.62}$$

   The voltage across the grounding transformer is then

$$\begin{aligned} V_{0n} &= I(3R_g + j3X_g h) \\ &= I(3R_g + j3kR_g h) = 3IR_{gh}(1 + jkh) \end{aligned} \tag{5.63}$$

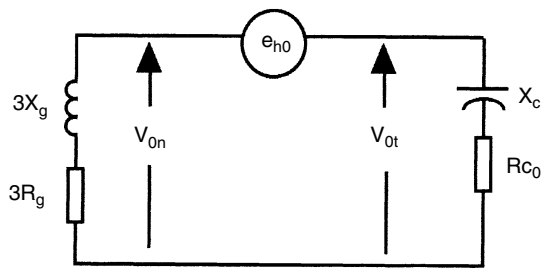


FIGURE 5.17 Zero-sequence lumped capacitance.

© 2006 by Taylor & Francis Group, LLC

Substituting

$$V_{0n} = \frac{e_{h0}\,(1 + jkh)}{\left[2 + jk\left(h - \frac{1}{h}\right)\right]} \tag{5.64}$$

The amplification factor for the harmonic voltage across the grounding transformer is then:

$$A_{Vn0} = \frac{(1 + jkh)}{\left[2 + jk\left(h - \frac{1}{h}\right)\right]} \tag{5.65}$$

At the fundamental frequency $h = 1$ and, assuming k is large, the amplification factor becomes

$$\begin{aligned} A_{Vn0}(60\,\text{Hz}) &= \frac{(1 + jk)}{2} \\ &\approx k/2 \end{aligned} \tag{5.66}$$

For the third harmonic voltage, again assuming k is large,

$$\begin{aligned} A_{Vn0}(180\,\text{Hz}) &= \frac{(1 + j3k)}{[2 + jk(2.66)]} \\ &\approx 1.13 \end{aligned} \tag{5.67}$$

The manufacturer of the sample system generator reports the expected fundamental and third harmonic zero-sequence voltages as 3.5 V and 410 V, respectively. If the sample system were resonant grounded with a primary circuit coil constant of 18.8 (as calculated from Equation 5.45) the fundamental and third harmonic voltages across the grounding transformer would be

$$\begin{aligned} V_{0n}(60\,\text{Hz}) &= \frac{k * eh\,(60\,\text{Hz})}{2} \\ &= \frac{18.8 * 3.5\,\text{V}}{2} = 32.9\,\text{V} \end{aligned} \tag{5.68}$$

$$V_{0n}(3\text{rd}) = 1.13 * 410\,\text{V} = 463\,\text{V} \tag{5.69}$$

Neither of these voltages is significant. If excessive voltage is found, reductions can be accomplished by reducing the coil constant or detuning the GNF. Detuning of up to $\pm 30\%$ (a mismatch of $3X_g$ to X_c) will not negate the GFN's ability to inhibit arcing grounds or result in unacceptable overvoltages. The detuning will increase the ground fault current.

The preceding calculation is an approximation of harmonic voltage at the neutral. An exact representation is not practical because the stator winding capacitance, which is the largest component of circuit capacitance, is distributed throughout the stator winding. Equation (5.66) and Equation (5.67) approximate system response by lumping all the shunt capacitance at the generator terminals. This representation results in a conservative estimate of the neutral voltage.

A more accurate determination of the third harmonic voltage across the grounding device and/or at the generator terminals is required for the relay applications. The representation provided in Figure 5.18, along with the accompanying zero-sequence connection shown in Figure 5.19, provide improved accuracy over the lumping representation of

© 2006 by Taylor & Francis Group, LLC

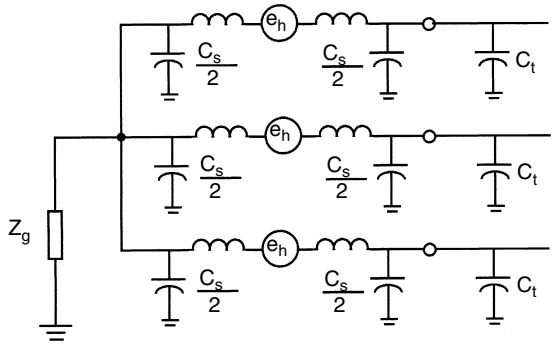


FIGURE 5.18 Split capacitance representation of system.

Figure 5.17. These figures account for the distributed capacitance by splitting the stator capacitance between the terminals and neutral end of the generator. All remaining system capacitance (C_t) is connected at the terminal end of the generator.

The split capacitance model is not preferred for fundamental frequency analysis. The GFN is resonant at 60 Hz and calculations using either the lumped or the split capacitance model are dominated by the loss assumptions. Although the split capacitance model is the better system representation, results are no better than the loss assumption. The lumped capacitance model is preferred for the fundamental frequency analysis because of its simplicity.

The split capacitance model should be used for higher order harmonics. These calculations are dominated by the circuit reactance allowing losses to be neglected completely.

2. The GFN scheme must be tuned, therefore it cannot be applied if the connected capacitance in the system varies significantly with operating configurations. This would be the case when multiple generators are bussed together or where various bus configurations are possible.
3. Resonant grounding is not recommended for a system that will experience periods of operation with frequency deviations greater than $\pm 15\%$ of normal. Application of the field at reduced speed would be one example.

When the frequency of the generator voltage does not match the tuned frequency of the grounding circuit, the phase voltage recovery following a current interruption includes not only the normal high-frequency transient component, but also a low-frequency beat oscillation. Theoretical studies[8] have shown that the beat frequency can result in increased phase-to-ground crest voltages with successive restrikes. The referenced study analyzed GFN tuned for 60 Hz operating between 50 and 70 Hz and found that transient restrike voltages approached those of an ungrounded system at the extreme frequencies.

Historically, field tests do not confirm the high transient voltages predicted by theoretical analysis. Experience and testing also show that resonant grounding can effectively limit

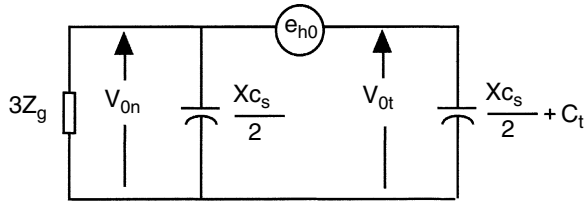


FIGURE 5.19 Zero-sequence circuit for split capacitance model.

© 2006 by Taylor & Francis Group, LLC

overvoltage and retain its self-extinguishing characteristic for arcing ground faults when detuned to $\pm 30\%$. To relate the tuning tolerance to a frequency deviation, the variations of inductive and capacitive reactance with frequency must be considered. At 60 Hz, $3X_g = X_c$ for the perfectly tuned circuit:

$$0 = 3X_{g60} - X_{c60} \tag{5.70}$$

At frequencies other than 60 Hz, inductive reactance will change by $f/60$ and capacitive reactance will change by $60/f$. A frequency reduction of 15% will result in detuning of about 30%.

$$0.85 * X_{L60} - \frac{1}{0.85} X_{c60} = 0.32 \tag{5.71}$$

Hence, the 30% detuning tolerance equates to a frequency band of ~50–70 Hz. Operation outside this band is not recommended.

5.3.4 Low-Impedance Grounding

This method of grounding employs a resistor or reactor directly connected between the generator neutral and ground or the installation of a grounding transformer. The range of fault current available from low-impedance grounding varies from 100 A up to the three-phase fault magnitude depending on whether low-resistance or low-reactance grounding is implemented.

Low-impedance grounding is used when two or more units are bussed together without interposing transformers or when generation is directly connected to a low-impedance grounded distribution system. This method is chosen to provide adequate fault current for selective fault clearing. The system in Figure 5.20 illustrates the relay coordination problems associated with

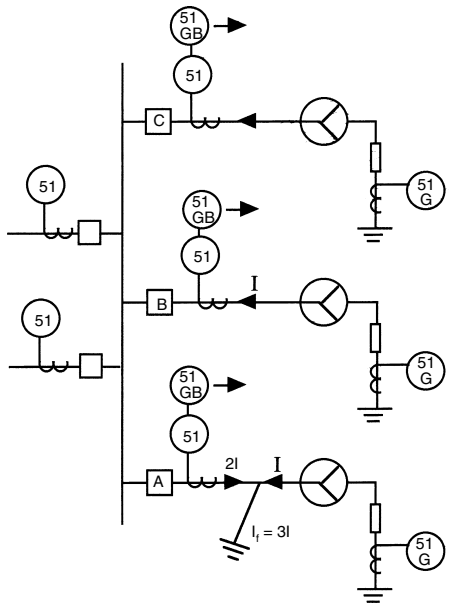


FIGURE 5.20 Generator bus coordination.

© 2006 by Taylor & Francis Group, LLC

high-impedance grounding. Assume each generator in this system is grounded through high impedance and that the ground fault current from each unit is limited to 15 A. All 51G relays at the generator neutral and all 51GB relays at the generator breakers would be set the same.

For the fault condition shown, 51G could operate to trip generator breaker "A" but since the fault currrent in each machine is the same all generators would trip by their respective 51G relays. To prevent this 51GB elements must be added at each generator breaker. These relays must be directionally controlled to respond only to faults between the breaker and generator. By setting 51GB faster than 51G only the faulted generator is tripped. Unfortunately high impedance grounding schemes do not provide sufficient fault current to reliably operate the directional element hence low impedance grounding is required. Selective tripping between 51G and 51GB is most easily obtainable when all generators are in service. For the example shown current through breaker "A" will be greater than the current in breakers "B" and "C." Breaker "A" will have the summation of all in service generators less generator "A." Higher current will facilitate faster operation of the breaker "A" 51GB relay. As generators are taken out of service fault current in breaker "A" approaches that of generator "A." The lower the relative current in 51GB the higher the time delay required on 51B to maintain coordination. This degrades protection because 51G provides off-line ground fault protection for the generator and either primary or backup ground fault protection for the main bus.

The application of a high-speed differential relaying as shown in Figure 5.21 is an alternate method of obtaining coordination with the benefit of faster cleaning. However, the high-impedance grounding scheme does not provide sufficient fault current to operate a differential scheme. Implementation of low-impedance grounding allows the ground fault current to be chosen to facilitate operation of the differential and any directional relaying necessary for full coordination.

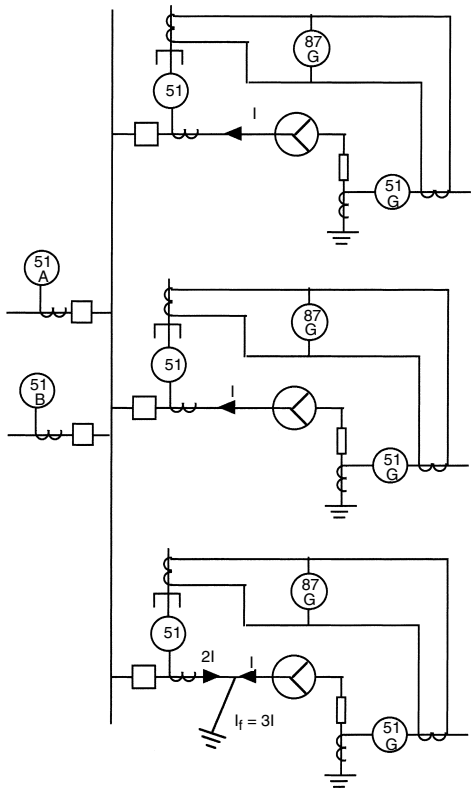


FIGURE 5.21 Generator bus with differential relaying.

© 2006 by Taylor & Francis Group, LLC

The low-impedance scheme is also applicable on systems where the shunt capacitance is large and a high-resistance scheme cannot limit the ground fault current to a value below the core damage threshold. This can be the case when surge capacitors are applied or if several generators are connected to a common bus.

In the latter case, the grounding resistance for each unit must be sized on the basis of full system capacitance. This typically results in a total fault current of less than 15 A when one unit is operating. When multiple unit are placed online, the ground fault current is the sum of all the individual unit ground currents plus the capacitive current. The summed current can be far in excess of 15 A.

One design philosophy is that if the total ground fault current cannot be held below the damage threshold, the advantage of the high-impedance grounding system is lost and a high-current scheme more conducive to fault detection and rapid clearing should be implemented. Supplemental protection, usually in the form of differential relaying, is then added to detect and rapidly clear low-magnitude ground faults.

An important consideration in the implementation of low-impedance grounding is the damage caused by delayed fault clearing. High-speed relaying and rapid tripping of the generator and field breakers does not equal rapid fault clearing. Like all generator faults, ground fault current will continue to flow until the energy stored in the generator's magnetic circuits dissipates. The amount of additional damage caused by the posttrip current is a function of the generator time constants, the method of field deexcitation used, and the magnitude of the initial ground fault current.

At installations where low-impedance grounding schemes are designed to provide high ground fault currents, the installation of a neutral breaker may be justified. The neutral breaker would be tripped when the generator and field breaker are tripped. This instantaneously reduces the fault current to the level of a few amps supplied by the system shunt capacitance.

5.3.4.1 Low-Resistance Grounding

Resistance grounding is also used when two or more generators are bussed together directly, without interposing transformers, and when generators are connected to distribution systems that are low-impedance grounded.

Low-resistance grounding provides a range of ground fault current from about 100 A up to about 1.5 times rated generator current. These limits are loosely established by the economics of resistor design. The upper limit is also based on limiting the power dissipation in the resistor. At 1.5 times rated current, the resistor dissipation is approximately 50% of the generator rating.[3]

Increasing the current above 1.5 times the limit rapidly increases the power loss in the resistor. This power loss is a concern from a turbine-generator standpoint. Other generator faults, both phase and ground, are dominated by system reactance. The resistance associated with these faults is very low; consequently, negligible real power is delivered to the fault from the generator. A high-current ground fault on a resistance-grounded system is unique in that real power approaching the rating of the turbine-generator is required.

The sudden application of this type of fault not only produces the current-related stress in the stator and field windings common to all faults, but will also produce significant mechanical stress.

The instantaneous application of the watt load represented by the grounding resistor is transmitted from the turbine by way of the shaft and couplings. The ground fault current limit of 1.5 times rating is intended to minimize the impact of the fault on the mechanical system.

Another constraint on a low-resistance grounded system is $R_0/X_0 > 2.0$. This is to limit overvoltages to 2.5 times the normal line-to-ground crest value. The zero sequence circuit for the low-resistance grounded system is similar to Figure 5.14. In the figure, R_g is the grounding resistance, X_g represents any inductance associated with the resistor. The shunt capacitive branch is neglected because the value of R_g is much smaller than that of X_c. Note that $3R_g$ and $3X_g$ are used in the calculation of the R_0/X_0 ratio. The inductance of the grounding resistor should be included in the calculations. Cast iron resistors have a power factor (PF) of about 0.98, but stainless steel resistors,

© 2006 by Taylor & Francis Group, LLC

approximately 0.92. At some installations R_0/X_0 may be less than 2. If this is the case, the additional constraint that $X_0/X_1 < 10$ must be met to avoid excess overvoltages. From a practical standpoint, these ratios are usually not a problem. Ground resistors are usually chosen to significantly reduce ground fault current; generally, this results in an R_0/X_0 ratio that meets the above criterion.

5.3.4.2 Low-Reactance Grounding

Low-reactance grounding is applied when generators are directly connected to a solidly grounded distribution system. This grounding method allows a range of ground fault current from 25 to 100% of the three-phase fault value. The zero-sequence representation of this grounding scheme is again similar to Figure 5.14, with the capacitive branch ignored because of its large value compared to $3R_g$ and $3X_g$.

The grounding reactance must limit the ground fault current below that of a three-phase fault as discussed in Section 5.2.1. The inductance chosen must also result in an X_0/X_1 ratio at the generator terminals of 10 or less to avoid damaging overvoltages. In most applications, the X_0/X_1 ratio is less than three to provide "effective grounding" and allow the application of 80% rated arresters.

If the maximum $X_0/X_1 = 10$ is assumed and $X_1 = X_2$, the minimum allowable ground fault with this form of grounding is

$$I_g = \frac{3E_1}{X_1 + X_2 + X_0} = \frac{3E_1}{X_1 + X_1 + 10X_1} = \frac{3E_1}{12\,X_1} \quad \text{or} \quad 0.25\,I_{3\theta} \tag{5.72}$$

Hence, the minimum allowable ground fault current is determined by overvoltage considerations and is significantly higher than other forms of grounding. If the X_0/X_1 ratio is limited to three, the minimum allowable ground fault current increases to 60% of the three-phase fault current.

5.3.4.3 Grounding Transformers

Grounding transformers are wye-delta or zig-zag transformers, connected to the generator, bus or delta winding of the main transformer. These transformer connections establish a ground on an otherwise ungrounded system, Figures 5.22(a), (b) and can include a neutral resistor or reactor to provide low-impedance grounding. They can also be applied without neutral impedance to provide "effective grounding."

The wye-broken delta connection with a resistor in the delta can provide an alternative method of high-impedance grounding. This connection is illustrated in Figure 5.22(c). In such applications, the criteria for choosing the secondary resistor differs from that used to select the resistor in the secondary winding of the distribution transformer scheme. Resistor selection for this scheme is discussed in Section 5.4.3.3.

The winding configuration of these transformers provides a low-impedance path for ground fault current. The fault current distribution for a wye-delta grounding transformer is shown in Figure 5.23.

A grounding transformer can also be used to provide a ground for a group of generators. Grounding the configuration shown in Figure 5.10 is difficult. If each generator is grounded individually the system has no ground when all generators are off. Alternatively, when all generators are in service, the ground fault current may be excessive. A ground independent of generator operation could be established by connecting a grounding transformer at the bus and operating individual machines ungrounded.

Figure 5.24 is the zero-sequence network for a grounding bank installation. Note that the grounding transformer impedance X_{t0} is not entered at three times its value, as is the optional neutral impedance $3R_g$ and $3X_g$. This is because the grounding transformer is a three-phase

© 2006 by Taylor & Francis Group, LLC

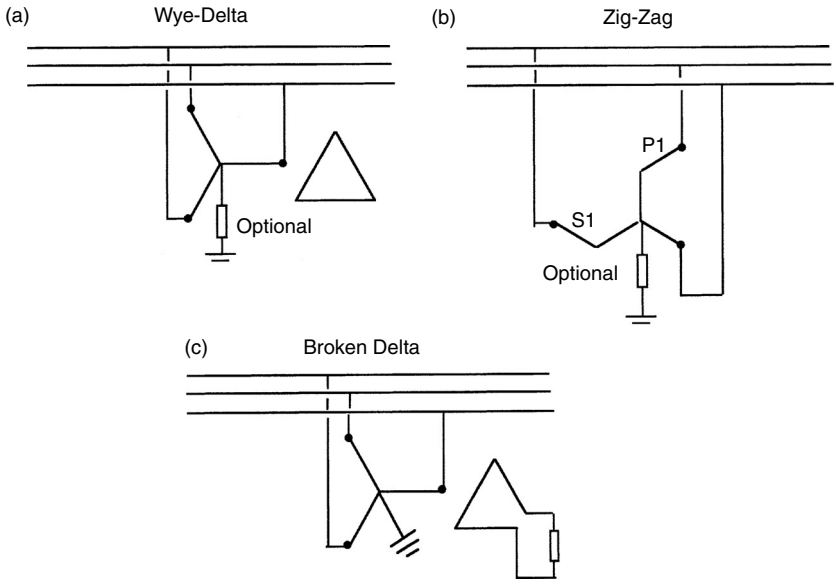


FIGURE 5.22 Grounding transformers.

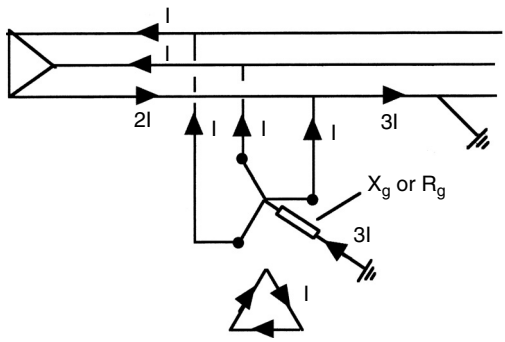


FIGURE 5.23 Wye-delta grounding transformer.

device with I_0 in each phase, whereas the neutral impedance has I_0 from each phase; $3I_0$ total flowing through it, as explained in Section 5.3.3.1.

The grounding transformer impedance and the impedance of a neutral resistor or reactor must be within the X_0/X_1 and/or R_0/X_0 constraints for the type scheme under design to avoid damaging overvoltages. The zero-sequence resistance and reactance used to calculate these ratios are derived from Figure 5.24.

5.4 GROUND FAULT PROTECTION

The type of grounding employed and the system configuration determine the choice of protective scheme. If a high-impedance scheme is chosen, the ground fault current is limited to a value that will not cause mechanical or thermal stress on the generator. Protective schemes applied on high-impedance grounded systems are focused on sensitivity and not on speed of operation. On the other hand, protection for grounding schemes that do not limit the ground fault current below damaging levels are less sensitive, but must operate quickly.

© 2006 by Taylor & Francis Group, LLC

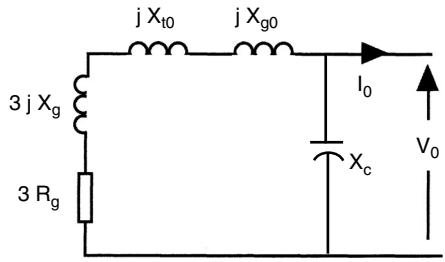


FIGURE 5.24 Grounding transformer zero-sequence network.

For systems with damaging ground fault current rapid tripping of the generator, field breaker and, shutdown of the prime mover are recommended. On high impedance grounded systems tripping is an option.

5.4.1 Alarm vs. Tripping for High-Impedance Grounded System

The decision to use high-impedance grounding is based on the desire to minimize core damage by limiting the ground fault current below a damage threshold value. In theory, if the fault current is not damaging, then the protective relaying need not trip but can be applied to alarm only. This would allow generation to be manually shut down in an orderly manner, thus avoiding mechanical and thermal stresses that would accompany a trip and load rejection.

This practice is fairly common, but is not recommended. If the system ground fault current is below 10 A, significant core damage is unlikely. The major risk of continued operation is that a second ground will occur. This creates a two-phase-to-ground fault, a very high-current and damaging condition.

The initial reaction might be that the occurrence of the second ground is a very improbable event. This is not necessarily true. The insulation system for a high-impedance grounded system must be rated for phase-to-phase voltage, but it normally operates at phase-to-neutral voltage. When the first ground fault occurs, the voltage triangle is shifted such that the unfaulted phases are subjected to full phase-to-phase voltage as shown in Figure 5.1(b). If weakness is present in the insulation, the first ground may initiate the second ground.

The worst-case scenario would have both grounds occurring in the same winding, one near the neutral and one near the high-voltage terminal. The resulting fault would be an unrestricted ground fault with a current magnitude likely in excess of a three-phase fault. Because the current, although huge, is equal at the neutral and high-voltage bushings, the faults would not be detected by the generator differential relay. The fault would remain undetected until a second phase was involved. At that point, the differential relay would actuate to trip the generator and field breaker.

Another reason for immediate tripping on the occurrence of the first ground is that the fault may not be a result of simple insulation deterioration and could be a symptom of some other stator problem.

5.4.2 Electromechanical and Electronic Relays

Not all the protective schemes to be discussed here are applicable to electromechanical relays. Some schemes that operate on harmonic voltages are generally available only in solid-state or microprocessor relays.

5.4.3 High-Impedance Ground Protection

5.4.3.1 Neutral Overvoltage Scheme

This scheme is commonly employed on high-impedance grounded systems and has become standard protection for unit connected generators. As shown in Figure 5.25, protection is provided

© 2006 by Taylor & Francis Group, LLC

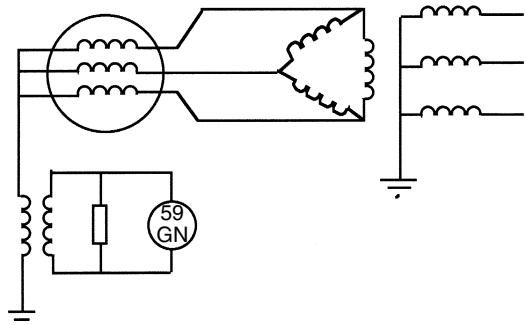


FIGURE 5.25 Neutral overvoltage scheme.

by connecting a sensitive inverse-time overvoltage relay across the grounding resistor or reactor at the secondary winding of the grounding transformer. This relay sees a voltage equivalent to V_0.

When a ground fault occurs, generator phase-to-neutral voltage is impressed across the primary of the distribution transformer. The voltage at the relay is a function of the transformer turns ratio. The maximum voltage will appear across the relay for a fault at the generator terminals. For grounds in the stator winding, the relay voltage decreases as the fault moves toward the generator neutral. When applied in a high-resistance scheme, a typical setting for 59GN is 6 V for a 120 V secondary (12 V for a 240 volt secondary). Assuming that the distribution transformer's primary winding is rated equal to the generator phase-to-ground voltage and has a 120 V secondary voltage, the relay will see 120 V for a fault at the generator terminals. The voltage distribution along the stator winding being linear, the relay set at 6 V will not see 6 V/120 V or 5% of the generator winding at the neutral end.

When the 59GN is applied in a GFN scheme amplification of the 60 Hz zero-sequence voltage as discussed in Section 5.3.3.3 (Advantages and Disadvantages of the GFN Scheme), may require a much higher setting on the 59GN relay.

Relay 59GN is typically an inverse-time relay to allow coordination with fusing associated with the generator PT circuits. It is common practice to use wye-wye PTs at the generator terminals. The 59GN relay should be coordinated with the PT fuses to prevent generator tripping for grounds on the PTs or secondary PT circuits.

This coordination can result in unacceptable tripping delays. A design employed to minimize miscoordination of ground faults in the PT secondary is shown in Figure 5.26. A secondary phase

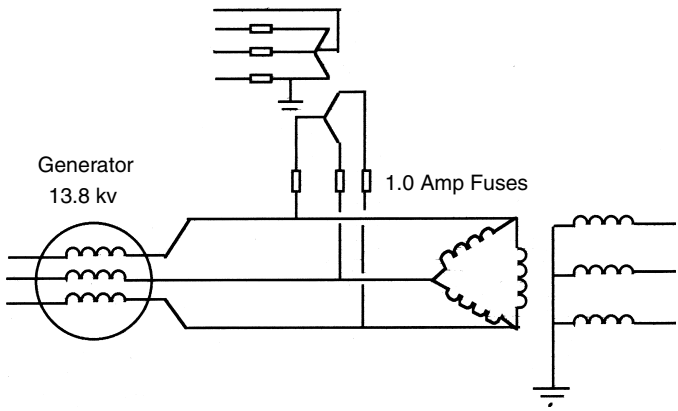


FIGURE 5.26 PT grounding.

© 2006 by Taylor & Francis Group, LLC

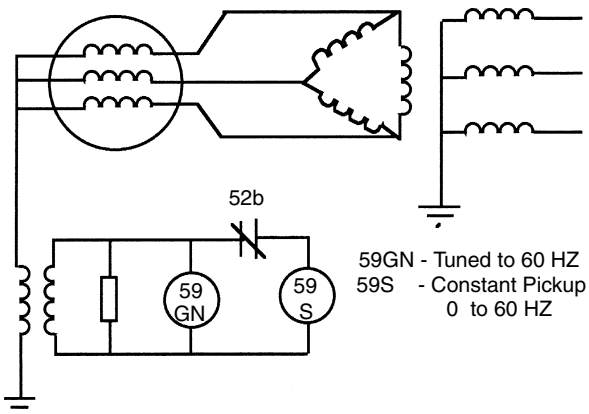


FIGURE 5.27 Presynchronizing ground relay.

conductor is grounded instead of the PT neutral. With this connection, a secondary phase contacting ground will produce a phase-to-phase fault as viewed from the PT primary. This fault will not be detected by the 59GN relay. With this design, only grounding of one conductor, the secondary neutral, will trip the unit if fuse coordination does not exist.

Generators can produce significant zero-sequence harmonic voltages during normal operations. These harmonic voltages will appear across the secondary resistor and voltage relay. The most significant is the third harmonic, which can be from 1 to 10% of the generator terminal voltage.[9] If the 59GN relay is to be set near 6 V to achieve 95% coverage of the stator winding, the relay used must be tuned to fundamental frequency (60 Hz) rendering it insensitive to third and other zero-sequence harmonic voltages.

Obviously, if the 59GN relay is tuned to 60 Hz, it will provide poor protection if startup procedures include closing the field breaker when the generator is below rated speed, or if other procedures included off-normal frequency operation. To cover this condition it is common to supplement the 59GN relay with a 59S "presynchronizing relay" as shown in Figure 5.27. This relay is in service only when the generator breaker is open. The relay used for this application must have a near constant pickup from 60 Hz down to DC. Because it is not in service during normal operation, the relay need not coordinate with PT transformer fusing and therefore can be an instantaneous relay.

Although the GSU transformer is delta connected, the 59GN relay is not immune to miscoordination with ground relaying on the power grid. Zero-sequence voltage can be impressed on the 59GN relay for power system ground faults through the interwinding coupling capacitance of the GSU transformer as was discussed in Section 5.3.3.3 (Neutral Displacement for High Voltage). The impressed voltage is usually small with a high-resistance grounded scheme owing to the relatively low impedance of this type of grounding circuit in relation to the impedance of the interwinding capacitance. The impressed voltage can become significant on resonant grounded generators because of the extremely high ground circuit impedance of these installations. Normally this is not a problem in either scheme. Although voltages impressed on the 59GN relay may be above the relay set point, the time delay setting required for coordination with PT fuses normally provides sufficient time delay to override fault clearing by the transmission system relaying.

5.4.3.2 Application of 59GN on Sample System

The grounding resistor and transformer for the sample system were chosen in Section 5.3.3.2. The grounding transformer is a 37.5 kVA, 7970 V/120 V transformer with 0.409 Ω secondary resistor. The ground fault current supplied by the transformer is 4.42 A at 13.8 kV and the total fault current for the system is 6.25 A. The system is shown in Figure 5.28.

© 2006 by Taylor & Francis Group, LLC

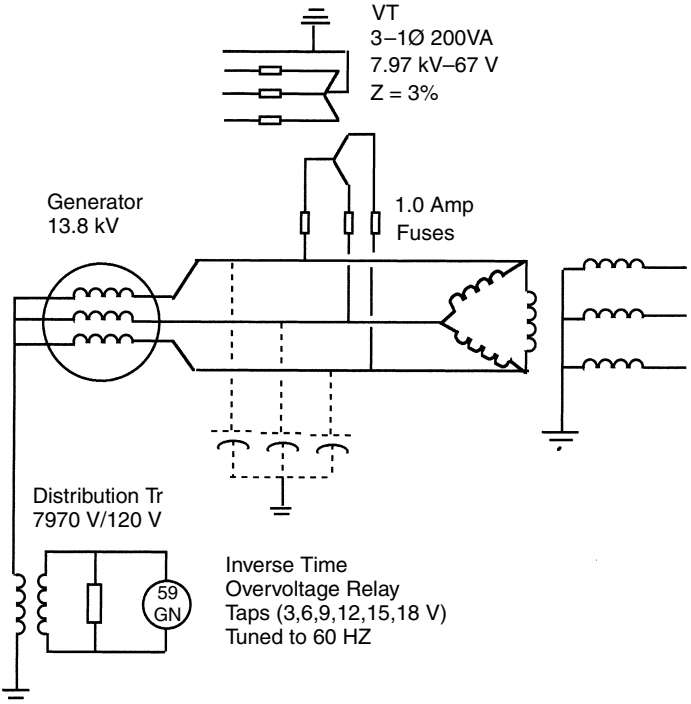


FIGURE 5.28 Sample system 59GN.

The voltage applied to the relay for a phase-to-ground fault at the generator terminals will be

$$V_r = E_{\text{ØN}} \frac{E_{\text{sec}}}{E_{\text{prim}}} = \frac{13{,}800}{\sqrt{3}} \frac{120}{7970} = 120\,\text{V} \tag{5.73}$$

A pickup setting of about 6 V is typical for this application. The coverage provided for the stator winding is:

$$\text{Coverage} = \left(1 - \frac{6\,\text{V}}{120\,\text{V}}\right) 100 = 95.0\% \tag{5.74}$$

The time dial setting for the relay will be chosen to provide the minimum delay necessary for reasonable coordination with the 1.0 A PT fuses.

To plot the 59GN relay characteristic on the same curve with the PT fuse, the relay pickup must be converted from volts in the secondary circuit to amps in the primary circuit. A maximum ground fault at the generator terminals has a magnitude of 6.25 A and impresses 120 V on the relay. Assuming a 6 V setting, this is $120\,\text{V}/6\,\text{V} = 20 \times$ pickup. One times pickup equals $6.25/20 = 0.313$ A. The equivalent pickup current for the 59GN relay set at 6.0 V is 0.313 A.

The 59GN relay with 6.0 V setting is plotted against the fuse in Figure 5.29. Coordination between the relay and fuse is desired for faults on both the PT primary and secondary circuits. The primary fault current was previously calculated at 6.25 A. The approximate 13.8 kV current for a secondary single-phase PT fault can be calculated from the following PT data:

3–1Ø PTs	200 VA each
7970–67 V	$Z = 3\%$

© 2006 by Taylor & Francis Group, LLC

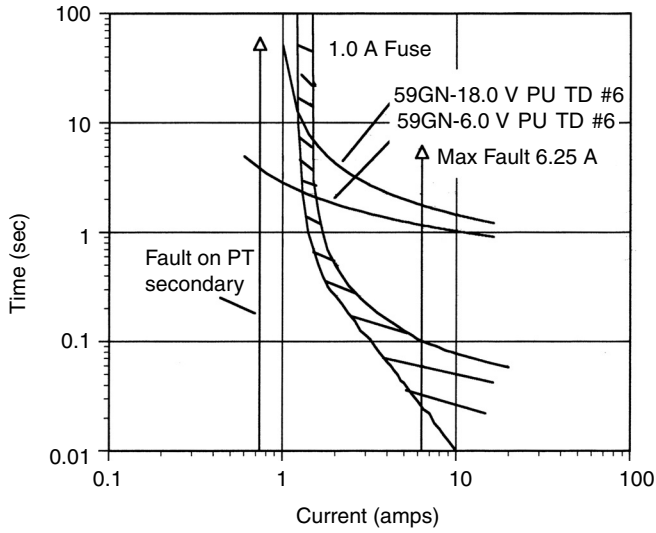


FIGURE 5.29 Plot 59GN vs. PT fuse.

A fault on the secondary side of the PT would have a maximum value of

$$I_{sc} = \frac{1}{Z}\frac{\text{kVA}_{1\text{Ø}}}{\text{kV}_{1\text{Ø}}} = \frac{1}{0.03}\frac{200}{7970} = 0.84\,\text{A} \tag{5.75}$$

The plot shows that coordination for secondary faults is unobtainable with a 6 V setting. Coordination would require a pickup setting greater than 0.84 A or 6.0 V 0.84/0.313 = 16.1 V. The closest available relay tap is 18 V. The resulting coverage of the stator winding is

$$\text{Coverage} = \left(1 - \frac{18\,\text{V}}{120\,\text{V}}\right)100 = 85\% \tag{5.76}$$

The setting is a matter of judgment, but we would consider 15% exposure on the stator winding an unacceptable risk to get fuse coordination for a fault on the PT secondary. An alternative solution would be to retain the 6 V setting with 95% coverage and reconnect the PT ground, as shown in Figure 5.26, to minimize the chance of having a secondary phase-to-ground fault.

5.4.3.3 Broken Delta Overvoltage Scheme

This scheme is formed by connecting a 59GN relay across the grounding resistor inside the broken-delta as illustrated in Figure 5.30. The voltage across the relay in this scheme is $3V_0$. This scheme is functionally equivalent to the distribution transformer 59GN scheme discussed previously. It can be used as an alternate to, or as an independent backup for, the distribution transformer scheme. Comments made for the distribution transformer scheme relating to fundamental frequency tuning, PT fuse coordination, supplemental presynchronizing protection, and coordination with power system ground relaying are valid for the broken-delta connection.

The broken-delta connection imposes the vector sum of the phase voltages on the 59GN relay. This is equivalent to $3V_0$.

$$V_r = (V_a + V_b + V_c) = 3V_0 \tag{5.77}$$

© 2006 by Taylor & Francis Group, LLC

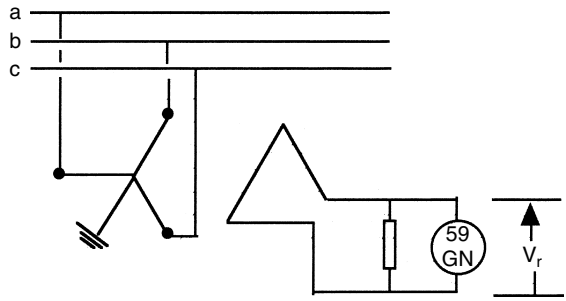


FIGURE 5.30 Broken delta with overvoltage scheme.

Under normal operation, the voltages are equal and displaced by 120°, as shown in Figure 5.31.

$$V_r = (E_{\theta g}\angle 0^\circ + E_{\theta g}\angle 120^\circ + E_{\theta g}\angle 240^\circ) = 0 \tag{5.78}$$

For an "A" phase-to-ground fault on a high-impedance system (Figure 5.31), $E_{an} = 0$ and the unfaulted phase voltages increase to phase-to-phase voltage with a 60° displacement. The relay voltage becomes

$$V_r = 3V_0 = (0 + \sqrt{3}E_{\theta g}\angle 150^\circ + \sqrt{3}E_{\theta g}\angle 210^\circ) = -3E_{\theta g} \tag{5.79}$$

The voltage appearing across the delta-side resistor and relay for a fault at the generator terminals is three times the normal phase-to-ground voltage. If the broken delta transformer is rated 13.8 kV–120 V, the normal secondary phase-to-ground voltage would be $120/\sqrt{3} = 69.3$ V and the voltage impressed across the resistor and relay for an unrestricted ground fault is $3 \times 69.3 = 208$ V.

Because the resistor within the broken delta is subject to I_0 and $3V_0$ as opposed to the $3I_0$ and V_0 seen by the resistor in a distribution transformer grounding scheme the resistor required for the broken delta scheme has an ohmic value nine times that given by Equation (5.2.2) for the distribution transformer scheme.

5.4.3.4 Overcurrent Scheme

An overcurrent protection scheme can be applied to a high-resistance grounded system if adequate sensitivity is maintained. This precludes the use of residually connected CTs. Figure 5.32 illustrates the consequences of a residually connected overcurrent relay.

Phase CT ratios are chosen on the basis of generator full load current and are large when compared to the ground fault current. A ground fault on a high-impedance grounded system would

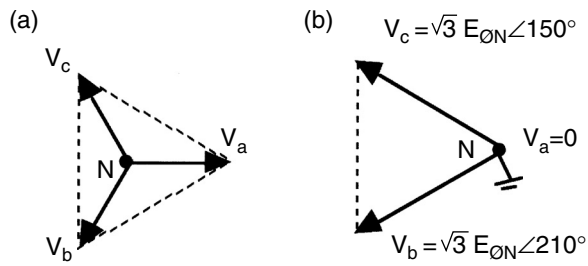


FIGURE 5.31 Phase-to-ground fault voltages.

© 2006 by Taylor & Francis Group, LLC

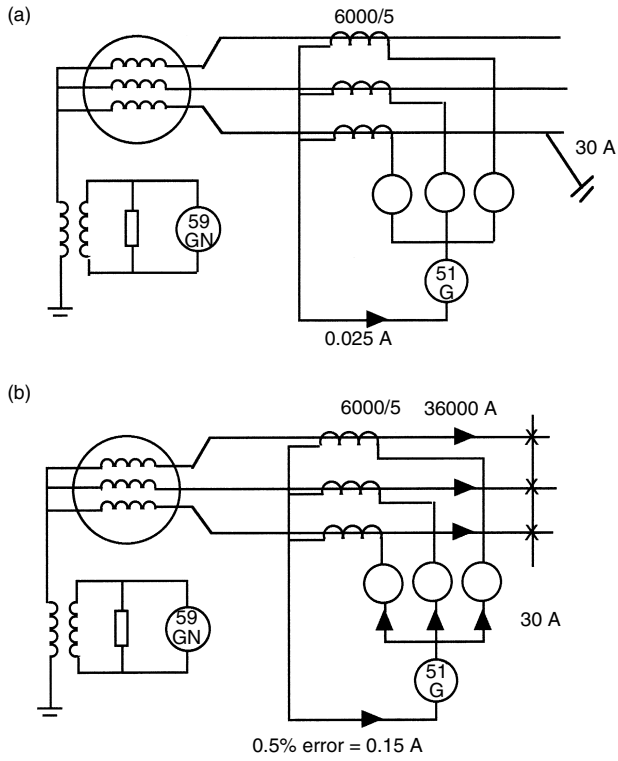


FIGURE 5.32 Residual connected overcurrent relay.

typically range from 2 to 30 A. The resulting secondary CT current presented to the ground relay would be in the milliamp range. A ground relay connected in the CT residual circuit would have to be set below this value to detect the fault.

At higher currents, such as full load and phase faults, differences in the individual CTs will produce a false residual current. A residual connected relay would have to be set above the error current to avoid false tripping. As shown in Figure 5.32, even if the phase fault error is less than 0.5%, the residually connected relay must be set above the ground fault current to avoid a false trip.

Figure 5.33 shows three applications of overcurrent relaying where 2–30 A sensitivity can be achieved. Figure 5.33(a) uses a window CT to supply the ground relay. In this application, all three-phase conductors pass through a single CT, and the flux produced by the current in each conductor is summed in the CT core, thus eliminating errors. The secondary CT current is representative of $3I_0$. Because the window CT does not pass balanced current, the CT ratio can be chosen without regard to load. A 50/5 ratio is commonly used.

This scheme would be an ideal method of protection for all grounding systems, but for two limitations. First, the available space in switchgear limits the size of the CT. With core area constrained the CT can saturate and render the relay inoperative if applied on systems with large ground fault currents. Also, window CT applications are limited to small generating units because the CT window is limited to about 14 inches and cannot be used with large multiphase cable.

The scheme in Figure 5.33(b) can be applied as a backup to the 59GN relay or on its one. The CT ratio is chosen to provide adequate current to the relay. On a high impedance system the relay current can be chosen to approximate the fault current. If we use this scheme on the sample system with the distribution transformer ratio of $7970/120 = 66.4$, then the CT ratio should be

© 2006 by Taylor & Francis Group, LLC

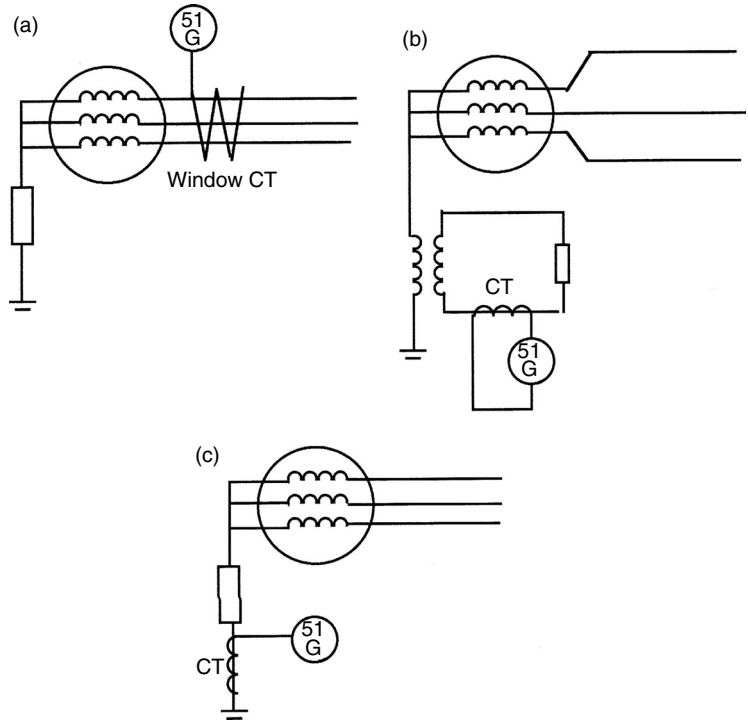


FIGURE 5.33 Ground overcurrent schemes.

approximatly 66/1 or 300/5. The sample system's ground fault is limited to 6.25 A, of which $6.25/\sqrt{2} = 4.42$ A is from the distribution transformer. The 51G relay would see

$$I_r = 4.42\,\text{A} \times \frac{7970}{120} \times \frac{5}{300} = 4.9\,\text{A} \tag{5.80}$$

Applying the same criteria to scheme Figure 5.33(c) would require a 5/5 CT.

During normal operations, current will flow in the neutral driven by zero-sequence harmonic voltages produced by the generator. The dominant current will be third harmonic. Electromechanical and electronic overcurrent relays not tuned for 60 Hz operation must be set above the harmonic current. If the CTs are chosen to the aforementioned criterion, the total residual current is generally less than 0.5 A at the relay. It is recommended that a minimum setting of 0.7 A should be used for initial installation. The relay current should then be monitored to determine if a reduced setting is applicable. Maximum neutral current usually occurs at maximum load.

If the scheme (b) overcurrent relay were applied in the neutral circuit of the sample system with a trip setting of 0.7 A, the relay would not protect the last 14.2% (0.7 A/4.9 A × 100) of the generator winding at the neutral end of the generator. Solid-state or microprocessor current functions with filtering to exclude non-60 Hz currents should be considered for this application. The tuned relay would permit a lower setting with improved stator coverage.

Each of the overcurrent schemes should incorporate time overcurrent relays to allow coordination with fusing associated with the generator PTs. Like overvoltage 59GN, the time delay necessary for PT fuse coordination will also provide the trip delay necessary to prevent misoperation for ground faults on the transmission system, which could occur as a result of the coupling effect of the interwinding capacitance of the GSU transformer.

© 2006 by Taylor & Francis Group, LLC

5.4.4 Low-Impedance Ground Protection

When low-impedance grounding is used, ground fault currents can range from 100 A up to the magnitude of a three-phase fault. These higher currents facilitate overcurrent protection. The configuration of this protection is determined by the magnitude of the ground current chosen.

At the low end of the range current, both Figure 5.33(a) and (c) are applicable. The applicable current range for the window CT scheme would be limited by CT saturation. The Figure 5.33(c) scheme is applicable over the full range of currents. The CT ratio for this configuration is chosen to provide 10 to 20 secondary amps at the maximum ground fault current. For all applications, the CT must be capable of producing sufficient secondary voltage to drive the connected relay without excessive saturation.

Overcurrent relay pickup and time delay settings chosen to provide selective tripping may provide unacceptable generator protection, and supplemental protection may be required.

5.4.4.1 Ground Differential

The ground differential schemes shown in Figure 5.34 are two methods used to provide supplemental ground fault protection on a low-impedance grounded system. Ground differential relaying may be applied to provide increased sensitivity or to provide selective tripping when multiple units are directly connected to a common bus. The schemes should use percentage differential relays.

The ratio of the phase CTs is chosen on the basis of load current and the neutral CT ratio is chosen to provide about 10 to 20 secondary amps for a maximum ground fault current. An auxiliary CT is usually required to match the two currents at the relay in either scheme. These differential

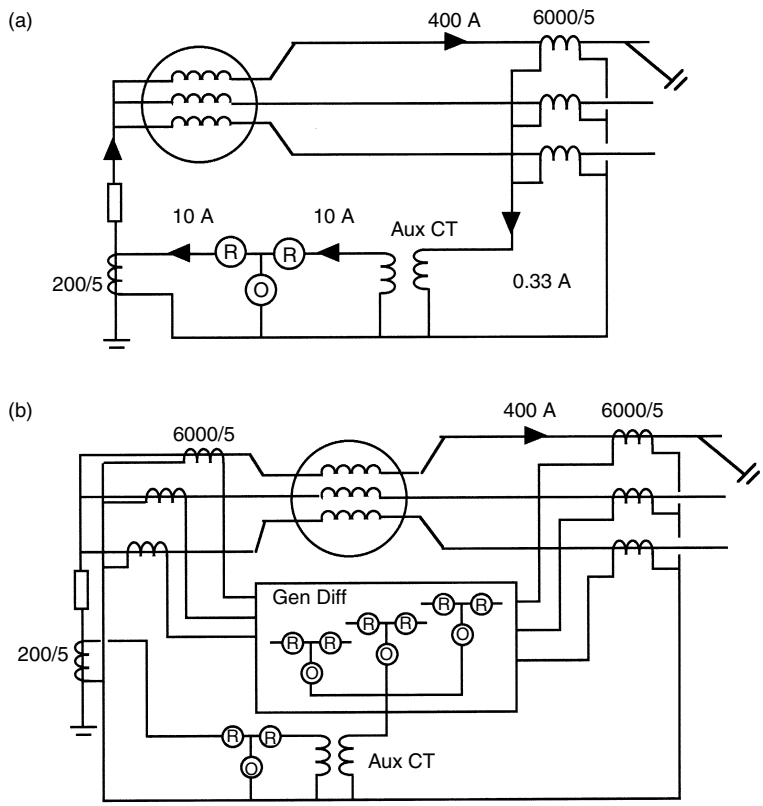


FIGURE 5.34 Ground differential relays.

© 2006 by Taylor & Francis Group, LLC

schemes are less prone to misoperate on external fault currents than the generator differential relay scheme discussed in Chapter 4, because the magnitude of the ground fault current is usually limited sharply by the grounding system. The use of a residual CT connection to obtain ground current will result in false residual current for phase faults. The ground differential relay must have a sufficient slope setting to prevent operation for these error currents.

5.4.5 100% Stator Protection Schemes

A shortcoming of each of the aforementioned high-impedance schemes is that none provides 100% protection for the stator winding. The neutral overvoltage and broken-delta schemes can detect faults over 95% of the winding, but the 5% near the neutral is unprotected. The lack of protection in this area had not been considered a problem. Insulation stress is a function of voltage; hence, maximum stress and consequently most insulation failures occur in the upper portions of the stator winding near the generator terminals. Also, it was thought that a fault in the unprotected portion of the winding would not produce significant damage.

Experience has shown that damaging faults can occur near the neutral end of the winding. Another serious consideration is that an undetected fault near the neutral end of the generator will bypass the grounding transformer and the ground-fault relaying. If a second ground occurs in the same phase near the generator terminal it will be undetectable and unrestricted by the grounding impedance. The generator differential relay would not operate for this fault, because current at each end of the winding would be the same. This extremely high magnitude fault would persist until it evolved into a phase-to-phase fault that is detectable by the differential relay.

As a result of these considerations and the development of electronic relay technology, several 100% winding protection schemes are now available. They fall into two categories: third-harmonic voltage schemes and neutral injection schemes.

5.4.5.1 Third-Harmonic Schemes

These schemes take advantage of the harmonic voltages produced by all generators. Generator output voltage is not a perfect sine wave. All machines produce harmonic voltages. Of these harmonics, the so-called triplen harmonics 3rd, 9th, 15th, 21st, and so on, appear in each phase, equal in magnitude and phase angle. Because these harmonic are in phase, they do not sum to zero and appear in the neutral circuit as zero-sequence quantities. The third-harmonic voltage is the largest of these harmonic voltages.

The harmonic voltage is divided between the neutral end and the terminal end shunt impedances as dictated by the zero-sequence network (Figure 5.19). The distribution of the third-harmonic voltages through the stator during normal operations is shown in Figure 5.35. The figure also shows the variation of third-harmonic voltage with load. At some point within the stator winding, the third-harmonic voltage is zero.

Refering to Figure 5.19 when a ground fault occurs near the generator neutral, the capacitive shunt impedance at that end of the generator is bypassed. The third-harmonic voltage at the neutral decreases to zero ($V_{0n} = 0$), while the third harmonic voltage at the generator terminals increases to equal the total third-harmonic voltage produced by the generator ($V_{0t} = eh$). The opposite occurs for a ground fault at the generator terminals. Here the terminal shunt impedance is bypassed. The terminal third-harmonic voltage decreases to zero ($V_{0t} = 0$), while the neutral quantity increases to equal the value produced by the generator ($V_{0n} = eh$). The profiles of the harmonic voltages for both conditions are shown in Figure 5.36.

These characteristics can be used to detect ground faults through 100% of the stator winding. Harmonic voltage schemes use the 59GN neutral overvoltage relay tuned to 60 Hz previously discussed to detect faults from the terminals to within about 5% of the neutral. A third-harmonic undervoltge or overvoltage relay is added to detect faults in the last 5% of the winding. The 59GN relay provides fault detection at the third harmonic null point within the stator.

© 2006 by Taylor & Francis Group, LLC

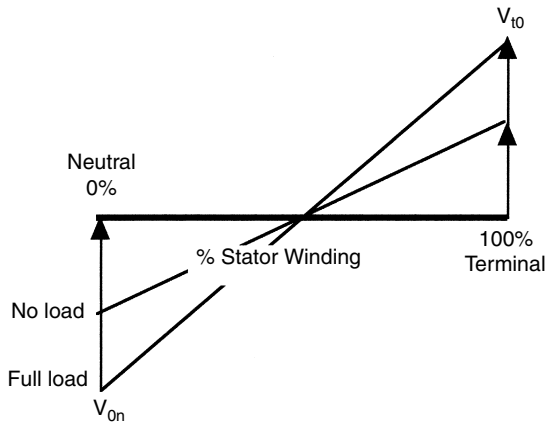


FIGURE 5.35 Third-harmonic voltage under normal operations.

The amount of third-harmonic voltage produced by the generator is critical to the successful application of these schemes. The minimum third-harmonic voltage produced by the protected machine should be about 1% through all load levels and operation modes. This is necessary if the relaying is to differentiate between normal and fault conditions. The third-harmonic voltage produced is a function of generator design and loading with values varying dramatically from machine to machine. Most machines will produce a third-harmonic voltage between 1 and 10% of the phase-to-neutral voltage. Typically, the light load value is about half that of the full load value. However, full load values as low as 0.2% are reported in the literature.[10]

Before attempting to apply a third harmonic schemes, the range of third-harmonic voltage should be confirmed over the full range of generator output conditions. Harmonic voltage levels should be measured with the unit open circuited and synchronized to the power system and at light and full load to confirm that sufficient harmonic voltage levels exist to operate the scheme.

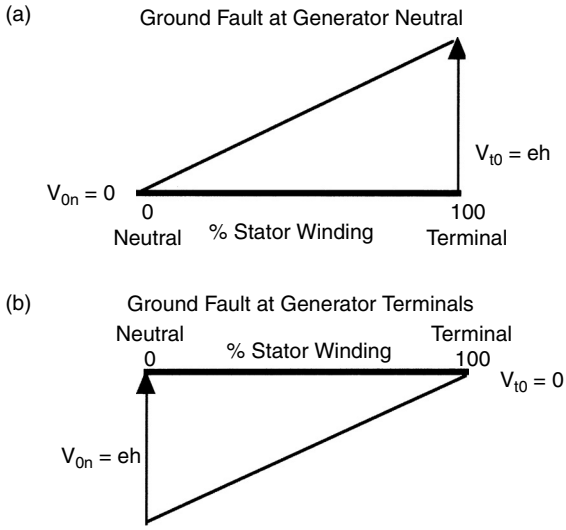


FIGURE 5.36 Third-harmonic fault voltages.

© 2006 by Taylor & Francis Group, LLC

5.4.5.2 Third-Harmonic Undervoltage Scheme

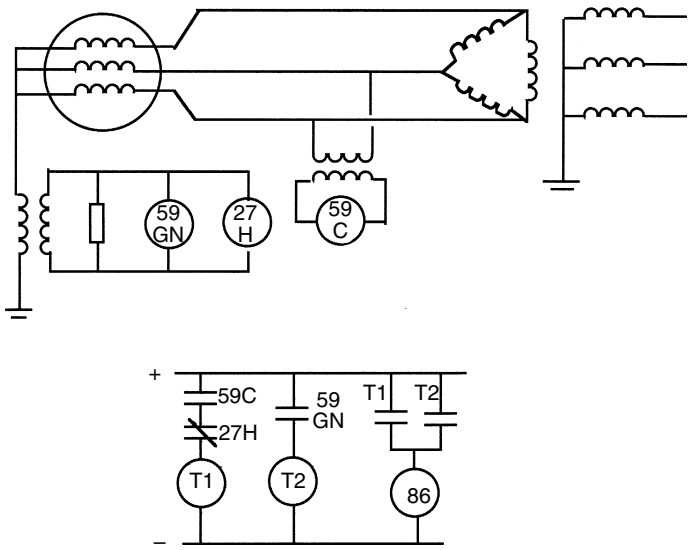
This scheme, shown in Figure 5.37, includes a 27H undervoltage relay tuned to detect third-harmonic voltage (180 Hz) and a 59GN overvoltage relay tuned to the fundamental frequency (60 Hz). Both relays are connected across the resistor on the secondary of the grounding transformer. Ground faults that occur in the stator winding from the generator terminals to within about 5% of the neutral generally produce sufficient fundamental zero-sequence voltage to operate the 59GN relay. A ground fault at the neutral point will cause the third-harmonic voltage there to fall to zero, actuating the 27H undervoltage relay.

As the ground fault is moved from the neutral toward the generator terminals, the third-harmonic voltage reduction at the relay becomes less. A fault at the null point will produce no change in the harmonic voltage at the neutral. To achieve 100% stator protection, the zones of protection provided by 27H and 59GN must overlap.

Achieving an acceptable setting can be difficult. The 27H relay must be set sufficiently low to avoid dropout during periods of normal operation when third-harmonic voltage is at a minimum. At the same time, the setting must be high enough to detect all faults not seen by the 59GN relay with the generated third-harmonic voltage at a maximum.

It may not be possible to meet both the above constraints if the third-harmonic voltage produced by the generator is minimal under certain operating conditions. Overvoltage relays may be required to supervise the 27H relay during startup and shutdown. Or overcurrent supervision may be required if the machine provides insufficient third-harmonic voltage at light load. A blocking relay may also be desired to prevent operation of the 27H relay when excitation is removed from the generator.

The third-harmonic undervoltage scheme is generally preferred over the overvoltage scheme because it will also detect shorted and open circuits on the primary and secondary winding of the grounding transformer. The scheme will not detect an open grounding resistor, but the 59GN relay will operate if a ground fault develops with the resistor open.



27H	UV Relay Tuned to Respond to Third Harmonic Voltage (180 HZ)
59C	Voltage Supervision relay, blocks tripping by 27H during startup
59GN	Time Delay OV Relay Tuned to Fundamental Voltage (60 HZ)
T1, T2	Timers

FIGURE 5.37 100% stator protection: undervoltage scheme.

© 2006 by Taylor & Francis Group, LLC

5.4.5.3 Settings for Sample System 27H Scheme

The settings chosen for the 59GN and 27H relay must be such that their respective areas of stator winding protection overlap through the full range of third-harmonic voltage. To illustrate the application, assume a 27H function is added to the 59GN scheme developed for the sample system in Section 5.4.3.2.

The third-harmonic voltage produced by the sample system generator varies from a maximum of 410 V to a minimum of 190 V. The dropout of the 27H relay must be set below 190 V to ensure it will not operate during normal operations. The 59GN relay was set at 6.0 V pickup. The relay will not detect faults in the last 5% of the stator winding. The undervoltage relay 27H must be set to provide positive fault detection in this area of the winding with the generator producing maximum (410 V) third-harmonic voltage.

The harmonic voltage produced by the generator is divided between the terminal and neutral shunt impedances as governed by the zero-sequence circuit shown in Figure 5.19. In this application Z_g is equivalent to the grounding resistance (R_g), calculated to be 1803 Ω in Section 5.3.3.2. The neutral end capacitance (C_{0n}) is equal to half the stator winding capacitance. The terminal shunt capacitance (C_{0t}) includes half the stator winding capacitance plus the shunt capacitance of all equipment connected to the generator terminals:

Using the capacitance listed in Section 5.3.1

$$C_{0n} = 0.5 \text{ stator capacitance} = 0.158\ \mu\text{F}$$
$$C_{0t} = 0.5 \text{ stator capacitance} + \text{other} = 0.333\ \mu\text{F}$$

The resulting capacitive reactances at 180 Hz are:

$$X_{n0} = -j5600\ \Omega$$
$$X_{t0} = -j2655\ \Omega$$

The neutral end impedance is then the parallel combination of X_{n0} and $3R_g$:

$$\begin{aligned} Z_{n0} &= \frac{-jX_{n0}3R_g}{3R_g - jX_{n0}} = \frac{-j5600 * 3 * 1803}{3 * 1803 - j5600} \\ &= 3890\ \Omega\angle -46.0^\circ \end{aligned} \tag{5.81}$$

When the zero-sequence, third-harmonic voltage produced by the generator is at a maximum of 410 V, the third-harmonic voltage across the neutral will be

$$\begin{aligned} V_{0n} &= V_0 \frac{Z_{0n}}{Z_{0n} - jX_{0t}} = 410\text{ V}\frac{3890\angle -46^\circ}{3890\angle -46^\circ - j2655} \\ &= 410\text{ V}\frac{3890\angle -46.0^\circ}{6043\angle -62.4} = 264\text{ V}\angle 18.4^\circ \end{aligned} \tag{5.82}$$

and at the terminal end the third-harmonic voltage will be

$$\begin{aligned} V_{0t} &= V_0 \frac{X_{0t}}{Z_{0n} - jX_{0t}} = 410\text{ V}\frac{2655\angle -90^\circ}{3890\angle -44^\circ - j2655} \\ &= 410\text{ V}\frac{2655\angle -90^\circ}{6086\angle -63.6^\circ} = 179\text{ V}\angle -26.4^\circ \end{aligned} \tag{5.83}$$

Because the total third-harmonic voltage change across the stator is 410 V, the neutral end voltage is $(264/410) \times 100 = 64\%$ of the total. Therefore the null point is 64% from the neutral.

© 2006 by Taylor & Francis Group, LLC

A fault at the limit of the 59GN relay's coverage, 5% from the neutral, is 5%/64% or 7.8% to the null point. The neutral end voltage for this fault is 7.8% of 264 V or 20.6 V at the primary of the grounding transformer. The third-harmonic voltage at the 27H relay will be $20.6 \times 120/7970 = 0.31$ V. The 27H relay must be set above this voltage with sufficient margin to assure operation within the blind spot of the 59GN relay.

To avoid false tripping the 27H must not be set higher than the minimum third-harmonic voltage at the neutral during normal operations. The minimum total third harmonic voltage produced by the generator is 190 V. The neutral end and terminal end voltages for this condition are

$$V_{0n} = 190\,\text{V}\frac{264\,\text{V}}{410\,\text{V}} = 122\,\text{V} \tag{5.84}$$

$$V_{0t} = 190\,\text{V}\frac{179\,\text{V}}{410\,\text{V}} = 83V \tag{5.85}$$

During normal operations, the minimum third-harmonic voltage at the 27H relay is $122\,\text{V} \times 120/7970 = 1.83$ V. Adopting a 75% margin, the maximum dropout setting would be $0.75 \times 1.83\,\text{V} = 1.37$ V. This provides a 440% margin (1.37 V/0.31 V) for detection of a fault at the beginning of the 59GN's blind spot.

The 1.37 V setting is equal to a primary voltage of 91 V. With no fault on the system, the third-harmonic neutral voltage is 264 V and the null point is 64% from the neutral. The 1.37 V setting will detect a voltage of 91 V/264 V = 0.34 of the normal voltage and is therefore capable of detecting a fault within $0.34 \times 64\% = 22\%$ from the neutral. The 27H function will overlap the 59G protection zone by 17%.

5.4.5.4 Third-Harmonic Overvoltage Scheme

A third-harmonic overvoltage scheme incorporates the same principles used in the 27H scheme. In this application, a broken-delta PT connection is used to detect zero-sequence voltage, including the third-harmonic voltage at the generator terminals; see Figure 5.38. The voltage impressed on the relay by the broken-delta connection is equal to $3V_0$. This is in contrast to V_0 imposed on 27H.

The 59T overvoltage relay is tuned to the third-harmonic voltage and operates on the third-harmonic voltage rise at the generator terminals associated with a ground near the generator neutral. The criteria for setting the 59T relay are reversed from those described for the 27H relay. The 59T must be set above the maximum third-harmonic voltage during normal operations and below the minimum voltage for a fault in the 59GN blind spot.

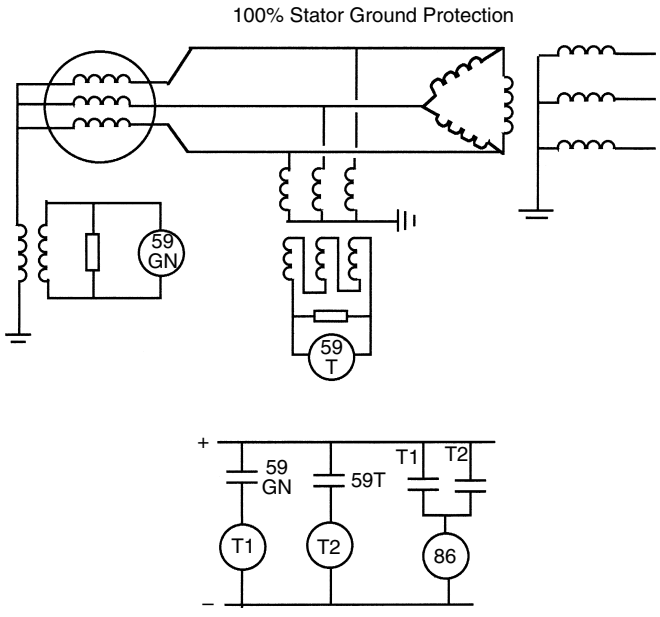
The calculation of voltage is the same as described earlier, except that the normal voltage and fault voltages are calculated with the generator third-harmonic voltages at maximum and minimum, respectively. These voltage conditions are also reversed from those used for the 27H scheme.

5.4.5.5 Third-Harmonic Voltage Ratio Scheme

The applications of third-harmonic undervoltage and overvoltage schemes are often complicated by wide variations of third-harmonic voltage at different modes of operation or by the insufficient third-harmonic voltage at light load. The voltage ratio scheme is an attempt to overcome these problems. A functional sketch of the scheme is provided in Figure 5.39.

During normal operation, the third-harmonic voltage produced by the generator is divided between the terminals and neutral of the generator as a function of the zero-sequence circuit impedances shown in Figure 5.19. The impedances of the zero-sequence circuit theoretically fixes the ratio of third-harmonic terminal voltage to that at the neutral end during normal operation. When a ground fault occurs in the stator winding, except near the null point, this ratio is altered. The voltage ratio scheme uses this change in ratio to detect ground faults at the neutral and at

© 2006 by Taylor & Francis Group, LLC



59GN	Time Delay OV Relay Tuned to 60 Hz
59T	OV Relay Tuned to Third Harmonic Voltage (180 Hz)
T1, T2	Timers

FIGURE 5.38 100% stator protection: overvoltage scheme. (From IEEE, Std C37.101-1993 IEEE Guide for Generator Ground Protection. With permission.)

the terminal end of the stator winding. The balance scheme again requires inclusion of a 60 Hz 59GN overvoltage relay to provide fault detection near the null point in the winding.

Because the relay responds to the harmonic voltage ratio, the scheme is not sensitive to the variations in third-harmonic voltage produced by the generator. Varying relay designs are provided by different manufacturers. In general, these relays have taps to allow the voltages received from the neutral and terminal PTs to be matched at the relay inputs.

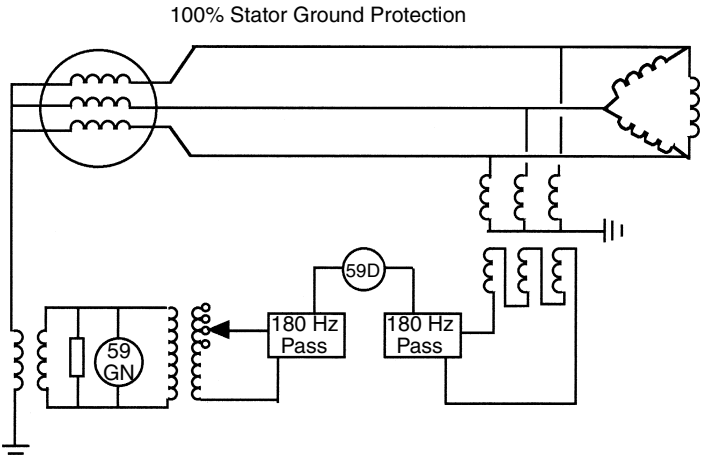


FIGURE 5.39 Third-harmonic ratio scheme.

© 2006 by Taylor & Francis Group, LLC

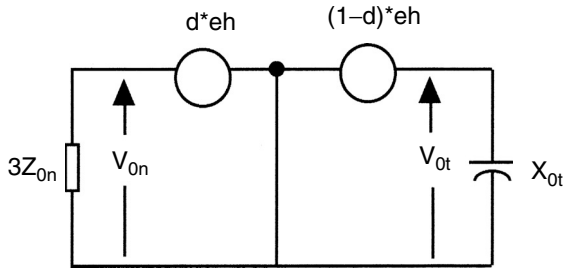


FIGURE 5.40 Voltage variations with stator winding fault.

If the relay is assumed to use the ratio of terminal/neutral voltage, the operation quantities provided at the relay would be

$$Ratio = \frac{3V_{0t}}{V_{0n}} \tag{5.86}$$

The $3V_{0t}$ term is a result of the broken delta PT connection.
The ratio variation with fault location from the neutral (d) can be derived from Figure 5.40.

$$\begin{aligned} Ratio &= \frac{3V_{0t}}{V_{0n}} = \frac{3 * (1-d)e_h}{d * e_h} \\ &= \frac{3 * (1-d)}{d} \end{aligned} \tag{5.87}$$

Ideally, the relay is set at the voltage ratio apparent under normal operations. This is equivalent to the ratio for a fault at the null point. In Section 5.4.5.3, the sample system null point was determined to be 64% from the neutral. The resulting ratio setting would be

$$Ratio = \frac{3(1-0.64)}{0.64} = 1.69 \tag{5.88}$$

The relay would operate when the ratio deviated from the set ratio by a specified amount. The bandwidth of the allowable deviation must be based on field measurements over a full range of generator loading conditions. In theory, the voltage ratio is fixed by the neutral and terminal end shunt impedances, but, in practice, ratio variations do occur. The ratio variations are a function of generator design and loading. These variations can be significant. Variations of 50% have been reported.

The application of the voltage ratio scheme, like in all third-harmonic ground fault detection schemes, requires a survey of third-harmonic voltages at all anticipated load levels and operating conditions to ensure the applicability of the scheme.

5.4.6 Neutral Injection Scheme

The design of some generators makes application of any third-harmonic voltage schemes difficult. The neutral injection scheme is an alternative method of providing 100% ground fault protection.

The designs vary between manufacturers, but Figure 5.41 gives a general overview. An AC voltage signal is applied at the neutral using an injection transformer in series with the grounding transformer. This signal is at a subharmonic of normal operating frequency for a 60 Hz system 15 Hz is often used. The signal is encoded for increased security. The resulting 15 Hz current is

© 2006 by Taylor & Francis Group, LLC

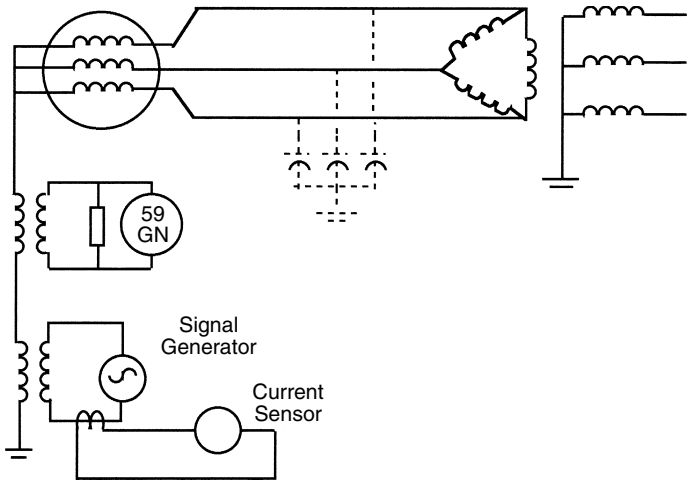


FIGURE 5.41 Neutral injection scheme.

determined by the impedance of the injection and grounding transformers and the shunt capacitance of the stator circuit as shown in Figure 5.42. An overcurrent element at the secondary of the injection transformer monitors the encoded 15 Hz current. A stator ground fault will bypass winding capacitance and increase the current initiating a trip.

Scheme sensitivity is constant over the entire stator winding. It can provide complete ground fault protection during startup, shutdown and even on turning gear. The scheme is normally taken out of service when the machine is offline for personnel safety, because the injected voltage is typically over 100 V. The major disadvantage to the scheme is cost. Also, the scheme will not detect open circuits in the grounding transformer or its secondary circuit.

The scheme uses a subharmonic signal for two reasons. First, the lower frequency increases the impedance of the stator capacitive reactance. This improves scheme sensitivity. Secondly, by measuring the current as an integrated value over full 15 Hz cycles, all other harmonics of 60 Hz are eliminated, allowing more sensitive determination of the injected current.

From Figure 5.42, the injected current is

$$I(15\,\text{Hz}) = \frac{E_{15\,\text{Hz}}}{Z_{\text{inj}} + Z_{\text{gnd}} + X_{\text{c}}} \tag{5.89}$$

where $E_{15\ \text{Hz}}$ = injected 15 Hz voltage, $Z_{\text{inj}} = R$ and 15 Hz X of injection transformer, $Z_{\text{gnd}} = R$ and 15 Hz X of grounding transformer, X_{c} = one-third the single-phase stator capacitive reactance to ground. Note that one-third the single-phase X_{c} to ground is used because the phases will appear as three parallel paths to the 15 Hz current.

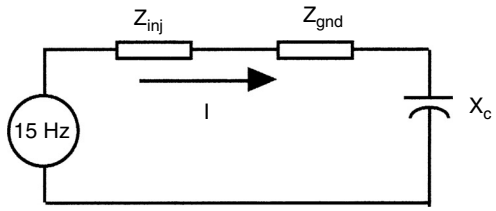


FIGURE 5.42 Neutral injection Ckt.

© 2006 by Taylor & Francis Group, LLC

REFERENCES

1. IEEE Std C37.101-1993, *IEEE Guide for Generator Ground Protection*, IEEE. New York, 1994.
2. Peterson, H. A. *Transients in Power Systems*, John Wiley & Sons, Inc, New York, 1951.
3. *Application Guide for the Grounding of Synchronous Generator System AIEE Committee Report*, AIEE. Transactions on power apparatus & systems, 72(III), New York, 1953, 517–530.
4. ASEA. *Pamphlet RK 64-200E*, Edition 1, Combiflex® Generator Protective Relaying.
5. Pohl, R., *Iron Burns by Electric Arcs of Low Current Value*, AEG Mitteilungen, Berlin-Grunewald, Germany, 1930.
6. Rajk, M. N., Ground-fault protection of unit-connected generators, *AIEE Trans Power Apparatus and System*, 77(III), 1082–1094, 1958.
7. Khunkhum, K. J. S., Koepfinger, J. L., and Haddad, M. V., resonant grounding (ground fault neutralizer) of a unit connected generator, *IEEE Trans Power Apparatus and System*, PAS-96(2), 550–559, 1977.
8. Brown, P. G., Josnson, I. B., and Stevenson, J. R., Generator neutral grounding some aspects of application for distribution transformer with secondary resistor and reactor types, *IEEE Trans Power Apparatus and System*, PAS-97(3), 683–694, 1978.
9. Griffin, C. H. and Pope, J. W., Generator ground fault protection using overcurrent, overvoltage, and undervoltage relays, *IEEE Trans Power Apparatus and Systems*, PAS-101(12), 4490–4501, 1982.
10. Marttial, R. J., Design principles of a new generator stator ground relay for 100% coverage of the stator winding, *IEEE Trans Power Delivery*, PWRD-1(4), 41–51, 1986.

© 2006 by Taylor & Francis Group, LLC

6 Unbalanced Current Protection

6.1 INTRODUCTION

Generators are intended to operate with balanced three-phase loading, but exposure to unbalanced currents is inescapable. Unbalances arise from many sources: untransposed transmission line construction, unbalanced loads, faults and open phases. These unbalances appear as negative sequence current in the generator leads. By definition, negative-sequence quantities have a rotation opposite that of the power system. This reversed rotating stator current induces double frequency currents in rotor structures. The resulting heating can damage the rotor very quickly.

For decades, electromechanical negative sequence overcurrent relays have been provided as standard unbalanced current protection for moderate and large generators. The electromechanical technology severely limited the sensitivity of these relays; as a result, they could provide only backup protection for uncleared phase-to-phase and ground faults. Potentially damaging low-current conditions such as an open phase or restricted fault were undetectable. With the advent of solid-state and microprocessor technology, relaying is now available to provide generator protection over a full range of unbalance conditions.

6.2 WHAT IS NEGATIVE-SEQUENCE CURRENT?

The concept of negative-sequence current is rooted in symmetrical component methodology. The basic theory of symmetrical components is that phase currents and voltages in a three-phase power system can be represented by three single-phase components. These are positive-, negative- and zero-sequence components. The positive sequence component of current or voltage has the same rotation as the power system. This component represents balanced load. If the generator phase currents are equal and displaced by exactly 120°, only positive-sequence current will exist. A current or voltage unbalance between phases in magnitude or phase angle gives rise to negative and zero-sequence components. The negative sequence component has a rotation opposite that of the power system. The zero-sequence component represents an unbalance that causes current flow in the neutral.

To illustrate the derivation of these components refer to the loading on the sample system generator shown in Figure 6.1. The generator loading is unbalanced; therefore, negative- and/or zero-sequence current is present in addition to the positive-sequence current. The sequence currents can be resolved from the phase currents when magnitude and phase angle are known.

Mathematically, positive (I_1), negative (I_2) and zero (I_0) sequence currents in a system with ABC rotation are defined as

$$I_1 = \frac{I_a + aI_b + a^2 I_c}{3} \qquad a = 1\angle 120^\circ$$

$$I_2 = \frac{I_a + a^2 I_b + a\, I_c}{3} \tag{6.1}$$

$$I_0 = \frac{I_a + I_b + I_c}{3}$$

© 2006 by Taylor & Francis Group, LLC

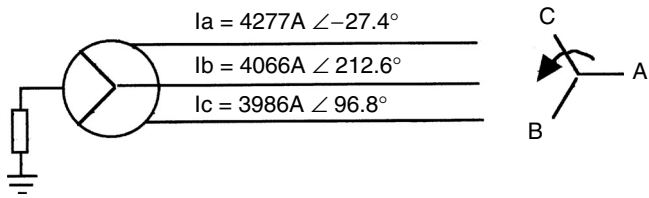


FIGURE 6.1 Generator unbalanced currents.

Substituting phase currents and angles from Figure 6.1 into Equation (6.1), the sequence currents are found to be

$$
\begin{aligned}
I_1 &= \frac{4277\angle -24.4^\circ + a\ 4066\angle 212.6^\circ + a^2\, 3986\angle 96.8^\circ}{3} \\
&= 4108\ \text{A}\angle -25^\circ \\
I_2 &= \frac{4277\angle -24.4^\circ + a^2\ 4066\angle 212.6^\circ + a\ 3986\angle 96.8^\circ}{3} \\
&= 175.7\,\text{A}\angle -10.1^\circ \\
I_0 &= \frac{4277\angle -24.4^\circ + \ 4066\angle 212.6^\circ + \ 3986\angle 96.8^\circ}{3} \\
&= 0.80\angle 168.8^\circ
\end{aligned}
\tag{6.2}
$$

The rated current for the sample system is 4370 A. The positive-sequence current is then 4108 A/4370 A = 0.94 pu and the negative-sequence current is 175 A/4370 A = 0.04 pu. Zero-sequence current is the vector sum of the phase currents and must flow in the neutral or ground. The sample system generator is connected to the delta winding of a GSU transformer. With no neutral return path, zero-sequence current can not exist. The calculated zero-sequence current is a result of measurement errors and should be considered zero.

6.3 EFFECTS OF NEGATIVE-SEQUENCE CURRENT

6.3.1 Rotor Heating

Balanced load current is positive-sequence current. As discussed in Chapter 2, this current produces a magnetic field in the air gap that rotates at synchronous (rotor) speed in the same direction as the rotor. Because the rotor and the positive sequence induced rotor magnetic field move at the same velocity and direction, the field maintains a fixed position with respect to the rotor and no current is induced into the rotor.

Unbalanced current produces negative sequence current, which in turn produces a reverse rotating field in the air gap. This magnetic field rotates at synchronous speed, but in a reverse direction to the rotor. From the perspective of a point on the rotor surface, this field appears to rotate at twice synchronous speed. As this field sweeps across the rotor, it induces double frequency currents into the rotor body of a cylindrical rotor machine and in the pole face of a salient pole machine. Portions of the resulting induced current path present high electrical resistance to the induced current. The result is rapid heating. Damage due to loss of mechanical integrity or insulation failure can occur in seconds.

6.3.1.1 Cylindrical Rotor Generators

A cylindrical rotor is constructed from a solid-steel forging with slots cut along its length. Each field coil requires two slots, one for each side of the coil winding. A slot may contain one or more coil windings. The ridges between the slots are called teeth. Figure 6.2 illustrates the rotor configuration.

© 2006 by Taylor & Francis Group, LLC

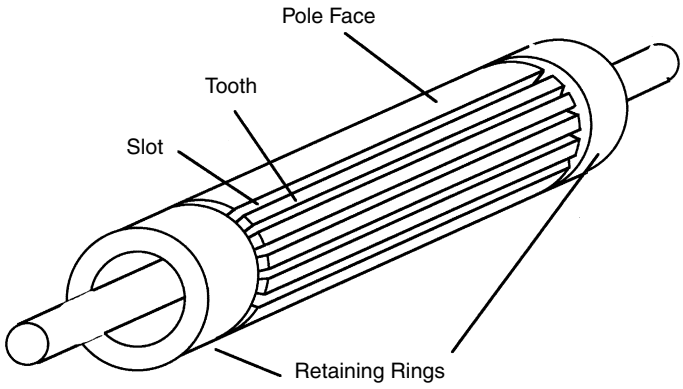


FIGURE 6.2 Salient-pole rotor.

Groves are machined into the sides of each tooth to allow wedges to be forced in along the full length of the slot. The wedges hold the field windings in the slots. In some machines, conducting strips are installed in the slots between the wedge and the field coil. These strips are connected at the retaining rings to provide a low-resistance path for the induced currents. The loops formed by these strips are known as amortisseur windings. The slot configurations of the wedge, field coil and the optional amortisseur winding are shown in Figure 6.3.

At the ends of the rotor body, the retaining rings hold the ends of the field windings in place against centrifugal force. The retaining rings are usually shrink fit to the rotor body, but in older machines they can be free floating with random contact with the rotor body. The rings and

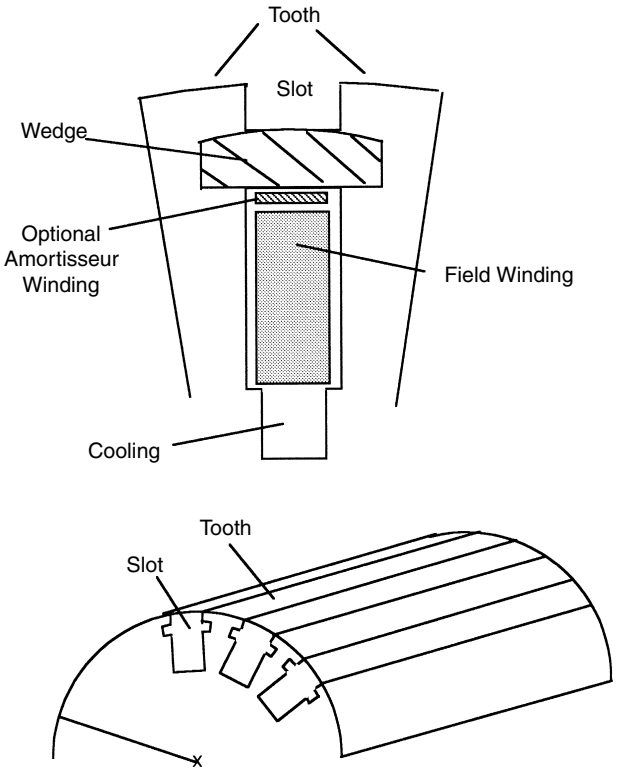


FIGURE 6.3 Slots and wedges.

© 2006 by Taylor & Francis Group, LLC

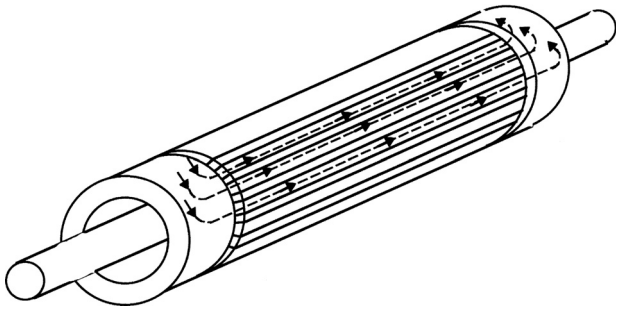


FIGURE 6.4 Rotor currents. (From M.D. Ross, E.I. King, Turbine-Generator Rotor Heating During Single Phase Short Circuits. AIEE Transactions, pt III PAS, Vol 72, February 1953, pp. 40–45. With permission.)

wedges are designed for mechanical strength, because they must restrain the large field windings at rate generator speed. The retaining rings are the highest stress component of the rotor.

The induced 120 Hz currents flow in loops along the body of a cylindrical rotor, as shown in Figure 6.4. There are as many current loops in the rotor as there are stator poles. When alternating current passes through a conductor, in this case the rotor body, current densities are not uniform. The "skin effect" causes alternating current to migrate to the outer surface of the conductor. This tendency increases with frequency. In a cylindrical rotor, the 120 Hz induced current occupies a cross-section extending from the surface to a depth no greater than 0.1 to 0.4 inches. This forces the induced current into the teeth and wedges at the rotor surface. The resulting high current density significantly increases rotor resistance for 120 Hz current over that for DC or 60 Hz current. Higher resistance produces higher losses and more heat per amp for the 120 Hz current than for lower frequency current.

The induced currents produce maximum heating at the ends of the rotor body. Significant heat is generated by contact resistance as the currents transfer from wedges to teeth in order to enter the retaining ring and from the ring to the teeth then to the wedges on the return loop. Increased heating is also caused by high current densities at these locations as current crowds into the teeth to enter and exit the retaining rings at the end of the rotor.

The negative sequence tolerance of a generator is dependent on good electrical contact being maintained between rotor structures. Low resistance minimizes heating and prevents arcing at contact points. Designers include many features to improve conductivity. These include the addition of amortisseur windings in the rotor slots to form low-resistance paths across the rotor surface. The ends of the amortisseur windings are connected to the retaining rings to provide a low-resistance bridge from the slot to the ring. Aluminum slot wedges can also be used to reduce resistance in this current path. Silver-plated aluminum fingers can provide a low-resistance current path from the wedges to the retaining rings. The rotor surface at the location of the retaining ring's shrink fit is often silver-coated to minimize resistance and heating at the junction.

Two types of rotor failures are associated with unbalanced current. Overheating of the slot wedges will cause annealing and a shear failure against the force of material in the slots. The second failure would be the retaining ring. Excessive heating can cause a shrink fit retaining ring to lift free of the rotor body. This would pose two problems. The retaining ring may not realign after it cools, reseating in a cocked position on the rotor body. Vibration would result. Also, the loss of good electrical contact while floating would result in pitting and burning at points of intermittent or poor contact.

Retaining rings that are designed to float will also experience arc damage at points of intermittent contact or poor conductivity. The resulting localized high temperatures can enbrittle areas of the ring and lead to cracking under the varied stress of repeated unit startup and shutdown.

6.3.1.2 Salient Pole Generators

Salient pole generators normally have amortisseur winding in the form of conductive bars spaced across the face of each rotor pole. The ends are brazed to form a low-resistance path on the pole

© 2006 by Taylor & Francis Group, LLC

face. There are two basic types of amortisseurs. Nonconnected amortisseur windings are isolated on each pole face. Connected amortisseurs have conducting bars that bridge between poles to interconnect the ends of all the amortisseurs groups at each pole.

Much of the current induced in the rotor of a salient pole machine flows in the pole face amortisseurs. Because the connections are brazed, this path does not have the contact resistance hot spots inherent with the cylindrical rotor machine. However, amortisseurs' current tends to flow in the outer bars and the induced current can cause stress damaging due to unequal expansion of the bars.

If the amortisseurs are not connected between poles, a large portion of the current induced in these windings flows down the pole body into the dovetail that holds the pole to the rotor then back into the adjacent pole. The junction at the dovetail will afford resistance, thus producing heat that can damage insulation and the rotor structure. If the amortisseurs are connected between poles, the dovetail current is sharply reduced, but high current will flow in the connection between poles. Connecting the amortisseurs also has a current balancing effect on the pole face bars.

Salient-pole machines with connected amortisseurs will have a higher negative sequence current capability than those without. The limiting components on the connected machines are often the bars that bridge the poles. The large induced current flowing in these bars can cause sufficient heat to anneal the bar, resulting in mechanical failure under centrifugal force.

6.3.2 Pulsating Torque

The negative-sequence current produces a reverse rotating magnetic field in the air gap. This field produces a shaft torque pulsation at twice line frequency. The magnitude of the torque is proportional to the per unit negative-sequence current in the stator. The pulsations are transmitted to the stator. If the stator is spring mounted, the pulsation will be absorbed. Without spring mountings, the pulsation will be transmitted to the stator foundation, where they can be a design factor.[1] In general, problems associated with torque pulsation are secondary to rotor heating concerns.

6.4 GENERATOR NEGATIVE-SEQUENCE CAPABILITY

A generator's negative-sequence tolerance is expressed in two forms: the ability to withstand a high level of I_2 for a short time and the maximum I_2 the generator can tolerate continuously. The adverse effects of unbalanced current on the rotor are temperature-dependent. Short time and continuous unbalanced current limits are based on maximum and long-term temperature limitations for the rotor body, wedges, retaining rings and amortisseur windings.

The heat input to the rotor is a result of I^2R losses in the induced current path. The short time limit for unbalanced current is established in the same manner these limits are established for other electrical equipment. Temperature rise calculations assume that no heat is conducted away from the affected material. This is a good assumption for events lasting a minute or two, because the thermal time constant for a mass as large as a rotor is much longer. This assumption also allows the limiting temperature in the rotor circuit to be expressed in terms of a limiting I_2^2t input at the generator terminals. When the duration of unbalanced current events approaches the thermal time constant of the material, heat transfer becomes an important factor and the I_2^2t representation becomes overly conservative.

The minimum short time and continuous negative sequence capabilities for a salient-pole generator are prescribed in ANSI standards C50.12-1982, and for round rotor generators in C50.13-1989. The capabilities are a function of generator size and construction.

Continuous negative-sequence current limits vary between 5 and 10% of the rated armature current. The short time limit, expressed in terms of K, where $K = I_2^2t$, varies from 5 to 40. Salient-pole machines show the greatest tolerance to negative-sequence current. The lowest continuous and short time capabilities are for very large direct cooled cylindrical rotor machines.

© 2006 by Taylor & Francis Group, LLC

TABLE 6.1
Continuous Negative-Sequences Capabilities[7]

Generator Type	Permissible I_2 (percent)
Salient pole	
With connected amortisseur windings	10
Without connected amortisseur windings	5
Cylindrical rotor	
Indirectly cooled	10
Directly cooled:	8
to 960 MVA	
961–1200 MVA	6
1201–1500 MVA	5

Source: IEEE Std C37.102-1995, IEEE Guide for AC Generator Protection. With permission.

6.4.1 Continuous Unbalanced Capabilities

The continuous negative-sequence capabilities for both salient-pole and round rotor machines are listed in C37.102-1995 and are provided in Table 6.1. The aforementioned standards require a generator to withstand the effects of the listed negative-sequence current, provided that loading does not exceed the rated kVA and that current in any phase does not exceed 105% rated current. It should be noted that the 105% phase current restriction is often more limiting than the negative-sequence current.

6.4.2 Short Time Unbalanced Currents

Standards[2,3] require that a generator withstand an unbalanced fault condition that result in the I_2^2t duties listed in Table 6.2. These limits assume no heat dissipation in critical rotor structures and are considered valid for conditions lasting up to 120 seconds.

The standards note that machines subject to I_2^2t duties up to 200% of the prescribed limit will experience varying degrees of damage. Generators exposed to duties above 200% of the listed limits will experience severe damage.

These standards also require that generators withstand unbalanced faults at their terminals, including effects of the DC component of fault current and posttrip decay current. The DC component adds significant heat to the rotor for a phase-to-phase fault at the generator terminals.

TABLE 6.2
Short Time Unbalanced Current Limits[7]

Generator Type	Permissible I_2^2t
Salient pole	40
Synchronous condensers	30
Cylindrical rotor	
Indirectly cooled	30
Directly cooled 0–800 MVA	10
Directly cooled 801–1600 MVA	10–0.00625 (MVA–800)

Source: IEEE Std C37.102-1995, IEEE Guide for AC Generator Protection. With permission.

© 2006 by Taylor & Francis Group, LLC

This component is short lived, but can have a peak magnitude equal to that of the AC component peak. The magnetic field created in the air gap by the DC component is stationary with respect to the stator and appears to move at synchronous speed when viewed from the rotor surface. The DC component of stator current induces a decaying 60 Hz current in the rotor that produces a rapid temperature rise. The inclusion of the DC component for a phase-to-phase fault at the generator terminals has been shown to increase wedge temperatures by 130%.[4] The significance of the DC induced temperature rise diminishes rapidly as the fault moves away from the generator terminals.

A good perspective on the potential damage relating to the combined effects of the 120 Hz and 60 Hz induced current is provided in Ref. (5). This paper reports that the total induced current in one rotor pole of a two-pole 125 MW generator at the inception of a phase-to-phase terminal fault is 500,000 A. In a four-pole machine, this current will be halved.

Both the continuous and short time capabilities of directly cooled machines are sharply reduced from those of an indirectly cooled machine. In an indirectly cooled machine, heat generated in the windings must travel through the winding insulation to reach the cooling medium in the air gap. In a directly cooled generator, channels are provided in the stator and/or rotor slots to allow direct contact between the heat-producing winding conductor and the cooling medium.

Because of the improved cooling, a direct-cooled machine will have a significantly higher kVA rating than an indirectly cooled machine of similar physical size. Unfortunately, methods employed to improve cooling of the field windings do not proportionately improve the heat transfer capability at locations affected by induced current, such as the rotor surface, wedges and retaining rings. Consequently, the unbalanced current capability of a direct-cooled machine will approximate that of a physically equivalent, but lower rated, indirectly cooled machine. When the negative-sequence current capability is expressed on the direct-cooled machine's higher kVA base, the per-unit negative-sequence capability is much lower.

6.5 SOURCES OF NEGATIVE SEQUENCE CURRENT

6.5.1 Unbalanced Faults

Unbalanced faults, which include phase-to-phase, phase-to-ground, or double-line-to-ground faults, produce large negative-sequence currents. Of these, the phase-to-phase fault is the most severe from a negative-sequence current standpoint. The reason for this can be seen from an examination of the sequence diagrams for the three fault conditions (Figure 6.5). The negative-sequence current resulting from a ground fault is limited by the positive-, negative- and zero-sequence impedance. For a phase-to-phase fault, the negative-sequence current is determined by only the positive- and negative-sequence impedance and is therefore higher. The sequence connection of a two-phase-to-ground fault shows that the zero and negative sequences are connected in parallel. This will

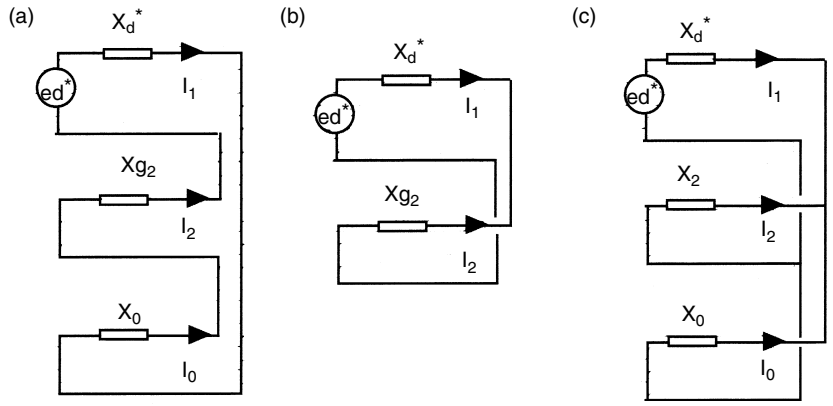


FIGURE 6.5 Sequence connections for unbalanced faults.

© 2006 by Taylor & Francis Group, LLC

result in higher positive-sequence current than for the other two unbalanced fault conditions. However, because the current splits between the zero- and negative-sequence networks, the resulting generator negative-sequence current is normally less than for the phase-to-phase fault. The relative severity of the two-phase-to-ground fault vs. the phase-to-ground fault is dependent on the negative- and zero-sequence impedances.

In practice, a large grounding impedance sharply limits the negative-sequence current during a ground fault. The ground impedance also causes the negative sequence current in the generator for a double phase-to-ground fault to approach that of a phase-to-phase fault.

6.5.2 Open Phases

An open phase can result from a fallen conductor or a failure of a breaker pole. In the former case, the condition is often accompanied by a fault detectable with normal relaying. In the latter case, the condition may be undetected by standard line relaying. The effect on the generator is dependent on the location of the open phase and the load level.

If the open phase occurs in the generator's outlet path, that is, between the generator terminals and the termination of the high-voltage leads of the GSU transformer in the switchyard, and the generator is at full load, damaging negative-sequence current will result. For the same load condition, an open conductor on one of several networked transmission lines that terminate at a generating station's high-voltage bus would result in minimal negative-sequence current at the generator. The more network lines terminated at the station, the lower the unbalanced current at the generator. At a location with many terminated network lines, an open phase on a line can result in negative-sequence current within the generator's continuous capability.

The analysis of the open phase condition will be based once again on symmetrical component methodology. The interconnection of positive-, negative- and zero-sequence networks to represent various fault conditions should be familiar territory at this point. The interconnection provided in Figure 6.14 represents "A" phase open at the high side of the GSU transformer.

The synchronous impedance and *EI* are used in this representation because the magnitude of negative-sequence current associated with an open phase is small. Relay operation times in excess of 10 sec are anticipated. With this delay, the generator is assumed to be in steady state; hence, X_d and *EI* are used in the calculation.

The grounding configuration of the system has a strong effect on the generator negative-sequence current. In the figure, the local and remote busses have wye-grounded delta transformers. This connection will act as a grounding point at both locations. Without the ground connections X_{tr0} and X_{e0} the zero sequence impedance would be infinite and the zero-sequence network open. The positive-sequence current would not split between the negative- and zero-sequence networks and a larger negative-sequence current would appear in the generator.

Also note that the load is assumed to be connected to the delta winding; as such, no zero-sequence current can flow in the load. Therefore, the load impedance is not included in the zero-sequence network. These connections must be considered when constructing the sequence diagram for other system configurations.

6.6 IN-SERVICE I_2^2t DUTY VS. STANDARDS

Standards prescribe minimum continuous and short time negative-sequence conditions a generator must withstand. These where listed in Tables 6.1 and 6.2. The minimum capabilities are intended to assure that generators can withstand the effects of continuous and fault-induced, negative-sequence currents imposed at a typical installation.

The short time unbalanced current limits are expressed in terms of I_2^2t, which is representative of the heat input to the rotor circuit from an unbalanced fault condition. The quantity relates the safe withstand time at a given value of negative-sequence current. Unfortunately, the decaying nature

© 2006 by Taylor & Francis Group, LLC

of generator fault current prevents a direct correlation between the negative sequence component of fault current and the I_2^2t capability. The relative heating during a fault (the I_2^2t duty) must be calculated as the integral of the delaying negative sequence current over the duration of the fault.

$$H = \int_0^t I_2^2 \, dt \tag{6.3}$$

where i_2 is the instantaneous value of RMS negative sequence current and t is the fault duration. A practical method of determining the effective I_2^2t duty is to calculate the negative-sequence current for small increments of time during the fault. The duty then becomes the sum of the incremental $I_2^2 * \Delta t$.

An evaluation of the fault I_2^2t duty actually imposed on a generator at a given installation is not required to set unbalanced protection, but may be required to assess damage following an unusual event. It may also be prudent if clearing times in excess of 1.0 sec are anticipated.

The I_2^2t duty imposed on a generator is not only a function of generator impedance and the initial operation conditions, but also the excitation system and connected power system. A generator connected to a power system can have substantially higher I_2^2t duty than an isolated generator. The reason for this can be seen in Figure 6.6. For a phase-to-phase fault, the isolated generator's negative-sequence current is limited by the generator's positive- and negative-sequence impedance. The positive-sequence impedance increases from X_d'' to X_d with time; thus, negative-sequence current diminishes sharply with time.

When the generator is connected to the power system, both the generator and system contribute to the negative-sequence current. Initially, the generator reactance X_d'' and the system reactance are similar in magnitude, as are the generator and system negative-sequence reactance. Although the total negative-sequence current is approximately double that of the isolated generator case, the negative sequence current is divided between the system and the generator and the generator negative-sequence current is not significantly increased from the isolated case for short-lived faults.

When a fault on an isolated generator is sustained the generator's positive-sequence impedance increases from X_d'' toward X_d, sharply reducing the negative-sequence current. However, when connected to the system the increase in machine reactance does not limit the negative-sequence current because the system positive sequence impedance remains low. The resulting I_2^2t duty for the interconnected generator for a sustained fault is significantly higher then that of an isolated generator.

The boosting action of the excitation system can also become a major factor in the I_2^2t evaluation if the fault is sustained for a protracted period as may result if clearing is accomplished by backup protection schemes. Faults cleared within a few tenths of a second are not affected, because the boosting action is delayed by the effective field time constant, T_{df}'.

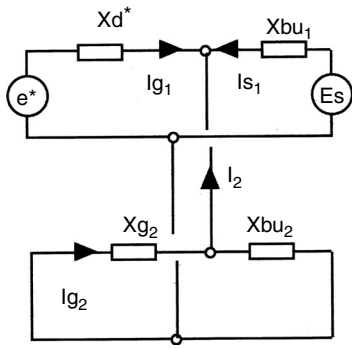


FIGURE 6.6 Sequence connection for interconnected generator.

© 2006 by Taylor & Francis Group, LLC

If the fault occurs between the generator terminals and the generator isolation breaker tripping this breaker and the field breaker will not isolate the fault. Fault current will continue to flow until the generator magnetic field dissipates. In this case the accumulation of posttrip I_2^2t is a function of the excitation system. If the energy stored in the generator's field is dissipated by simply short-circuiting the field after the field breaker is tripped, the rate of current decay will be moderate as determined by T'_{df}. However, if the excitation system includes provisions for accelerated deexcitation, such as a field discharge resistor or the imposition of a reversed polarity deexcitation voltage, the rate of fault current decay can be greatly increased, there by reducing the posttrip I_2^2t significantly.

6.6.1 Calculation of I_2^2T Duty

Calculation of the I_2^2t duty requires a determination of the time-varying generator negative-sequence current, including the effects of excitation boost and deexcitation.

6.6.1.1 Isolated Generator

In the case of an isolated generator, the fault and posttrip decay calculation is as described in Chapter 2. The subtransient, transient, and synchronous currents as applicable in each axis are determined from the prefault voltages behind each reactance and the fault reactance seen at the generator terminals. The rates of decay of the component currents are determined by the d- and q-axes time constants. These time constants are also a function of fault reactance.

The current boost effect of the voltage regulator during the fault and any regulator deexciting action during the posttrip period can be accounted for by adding the appropriate I_{ex} component to the d-axis current, as described in Chapter 2.

Note that when the voltage regulation is in service the value of *EI* used in the posttrip calculation of I_d and the deexcitation equation is the total excitation at the moment when the field breaker trips. If the generator is on manual regulator during the fault, no change in excitation will occur and the posttrip value of *EI* will equal the initial value of *EI*. If the automatic voltage regulator is in service during the fault, excitation will have increased by the the value of boost component I_{ex} as defined by Equation (2.38). *EI* at the time of the trip will be

$$EI_{Trip} = EI_0 + I_{ex\ (at\ trip)} * X_d \tag{6.4}$$

where $EI_{Trip} = EI$ when the field breaker trips, I_{ex} = boost component of d-axis current at the time of trip.

6.6.1.2 The Interconnected Generator

The calculation for the interconnected generator requires additional consideration. The d- and q-axes representation of a phase-to-phase fault at the terminals of an interconnected generator is shown in Figure 6.7. This connection is similar to Figure 2.16, which represented phase-to-phase fault on an isolated generator. In both cases, the equivalent fault impedance seen at X-Y terminals of the d- and q-axes circuits defines the fault impedance X_f. The asterisk denotes quantities applicable to subtransient, transient, or synchronous circuits.

The interconnected case includes the system and transformer positive- and negative-sequence reactances along with the system voltage source. The system voltage source must be resolved into d- and q-axes voltage components for inclusion in the subtransient, transient and synchronous circuits for each axis. The calculation is based on the prefault loading and the assumption that the rotor position remains fixed with respect to the system during the fault.

Another complication of the interconnected machine calculation is the tripping of the generator breaker and field breaker. This circuit change imposes a second transient into the fault calculation, the first being the initial fault. The opening of the generator breaker appears as an abrupt change in

© 2006 by Taylor & Francis Group, LLC

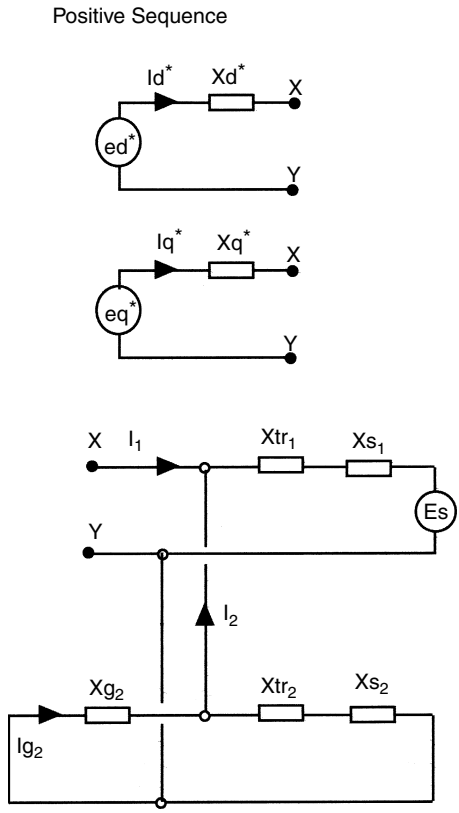


FIGURE 6.7 d- and q-axes diagrams for interconnected generator.

fault reactance and is evaluated in the same manner as the initial fault. New values for I_d, I_d', I_d'', I_q' and I_q'' are found using the post trip fault reactance X_f and Equations (2.26) and Equation (2.31). This calculation assumes that flux linkages as represented by e'_{q0}, e''_{q0}, e'_{d0} and e''_d have not changed from their initial values.

Again as with the isolated generator case current boost and de-excitation effects many also be included.

6.6.1.3 The'venin's Equivalent Circuit

The calculations for the interconnected generator are simplified by reducing the circuit external to the generator to a The'venin's equivalent impedance and voltage source. This is accomplished by resolving the negative-sequence network to an equivalent impedance. Thus forming the "T" circuits shown in Figure 6.8.

The "T" is then replaced by the The'venin's equivalent shown in Figure 6.9. The The'venins voltage (E_{th}) is equal to the open circuit voltage of the "T" network with the generator detached. The The'venins impedance (X_{th}) is the impedance seen from terminals X-Y looking into the "T" equivalent with the voltage source short-circuited.

6.6.2 Unbalanced Duty on Sample System

A phase-to-phase fault at the terminals of the sample system generator was evaluated using the techniques described above. The generator was connected to the power system with the automatic voltage regulator in service. The fault was assumed to persist for six cycles, after which the generator

© 2006 by Taylor & Francis Group, LLC

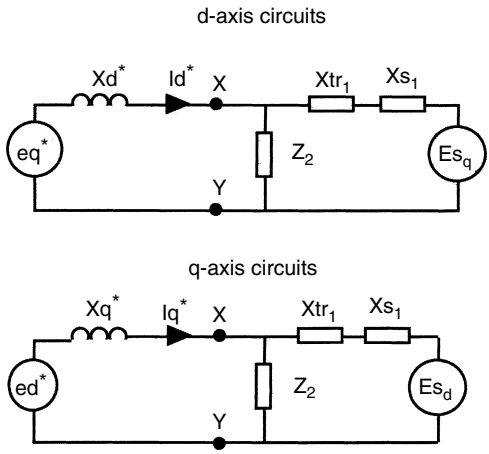


FIGURE 6.8 Equivalent "T" circuit for phase-to-phase fault.

and field breakers were tripped, isolating the generator from the power system and removing field excitation. Two cases are included. The first assumes that no accelerated deexcitation is provided. Here the field is short-circuited after the field breaker opens. Fault current then decays at the rate determined by the inherent inductance and resistance of the field winding. In the second case, a 1.0 Ω field discharge resistor is inserted into the field circuit after the field breaker trips. This reduces the field decay time constant from 0.57 sec to 0.217 sec per Equation (2.39).

As with any generator fault calculation, the initial d- and q-axes internal voltages must be calculated from the prefault load conditions. If the sample system generator initially has a terminal voltage of 1.05 pu with rated load at rated power factor, the voltages behind d- and q-axes subtransient, transient and synchronous reactances are as calculated in Section 2.9.1.

$$
\begin{array}{llll}
e_{q0} = 0.880 & e_{d0} = 0.573 & I_{q0} = 0.404 & I_{d0} = 0.862 \\
e''_{q0} = 0.997 & e'_{q0} = 1.049 & EI = 2.16 & e''_{d0} = 0.520 \\
 & e'_{d0} = 0.378 & E_d = 0 &
\end{array}
$$

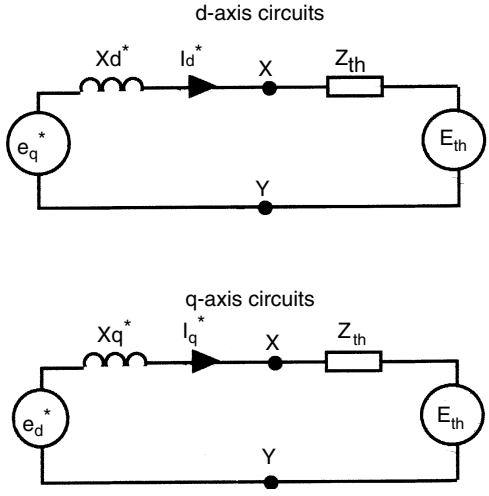


FIGURE 6.9 The'venin's equivalent circuits.

© 2006 by Taylor & Francis Group, LLC

Next, the sequence connection for a phase-to-phase fault, (Figure 6.7) is reduced to a The'venin's equivalent circuit. The first step is forming the "T" equivalent circuit as shown in Figure 6.8 by reducing the negative-sequence network to a single reactance.

$$\begin{aligned} X_2 &= \frac{(X_{s2} + X_{tr2})X_{g2}}{X_{s2} + X_{tr2} + X_{g2}} \\ &= \frac{(0.078 + 0.07) * 0.129}{0.078 + 0.07 + 0.129} = 0.069 \end{aligned} \tag{6.5}$$

The The'venin's equivalent impedance of the circuit is the impedance seen looking from the X-Y terminals into the "T" network with the voltage source short-circuited:

$$\begin{aligned} X_{th} &= \frac{X_2(X_{tr1} + X_{s1})}{X_2 + X_{tr1} + X_{s1}} \\ &= \frac{0.069(0.07 + 0.078)}{0.069 + 0.07 + 0.078} = 0.047 \end{aligned} \tag{6.6}$$

The prefault system voltage is calculated from the prefault load condition as

$$E_{sys} = E_t - IX_{e1} \tag{6.7}$$

The equivalent positive sequence impedance, X_{e1}, seen at the sample system generator terminals, is equal to the GSU transformer impedance plus the 69 kV transmission system impedance or $0.07 + 0.078 = 0.148$ pu. Generator full load current at 1.05 pu terminal voltage is 0.952 (1/1.05). E_{sys} is then:

$$\begin{aligned} E_{sys} &= 1.05 - .952\angle -31.8^\circ * 0.148\angle 90^\circ \\ &= 0.952 \text{ pu} \end{aligned}$$

The d- and q-axes components of system voltage can be determined from Figure 2.14 as

$$\begin{aligned} E_{sq} &= e_{q0} - I_{d0}X_{e1} \\ &= 0.880 - 0.862 * 0.148 = 0.752 \end{aligned} \tag{6.8}$$

$$\begin{aligned} E_{sd} &= e_{d0} + I_{q0}X_{e1} \\ &= 0.573 + 0.404 * 0.148 = 0.633 \end{aligned} \tag{6.9}$$

which again yields to:

$$E_{sys} = \sqrt{0.752^2 + 0.633^2} = 0.952 \text{ pu}$$

The The'venin's voltage is the open circuit voltage of the "T" network as seen at the X-Y terminals with the generator disconnected:

$$\begin{aligned} E_{thq} &= E_{sq}\frac{x_2}{x_2 + xe_1} \\ &= 0.752\frac{0.069}{0.069 + 0.148} = 0.239 \text{ pu} \end{aligned} \tag{6.10}$$

$$\begin{aligned} E_{thd} &= E_{sd}\frac{X_2}{X_2 + X_{e1}} \\ &= 0.633\frac{0.069}{0.069 + 0.148} = 0.201 \end{aligned} \tag{6.11}$$

The resulting d- and q-axes equivalent circuits for the faulted interconnected generator are shown in Figure 6.10.

© 2006 by Taylor & Francis Group, LLC

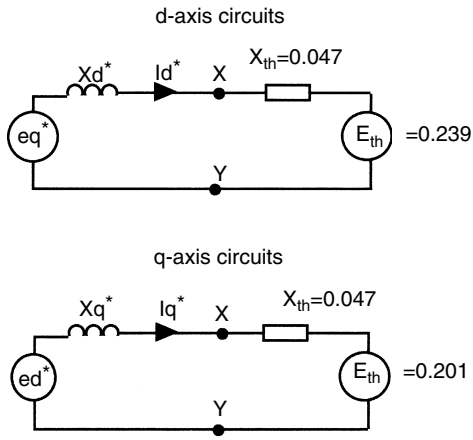


FIGURE 6.10 The'venin's equivalent circuit for the sample system.

The subtransient, transient and synchronous current calculations are similar to those described in Chapter 2. The exception is the inclusion of system d and q-axis component voltages and substituting the The'venin's reactance for X_f. The resulting component current equations are:

$$I''_d = \frac{e''_{q0} - E_{thq}}{X''_d + X_{th}} = \frac{0.997 - 0.239}{0.136 + 0.047} = 4.14 \tag{6.12}$$

$$I'_d = \frac{e'_{q0} - E_{thq}}{X'_d + X_{th}} = \frac{1.049 - 0.239}{0.196 + 0.047} = 3.33 \tag{6.13}$$

$$I_d = \frac{EI - E_{thq}}{X_d + X_{th}} = \frac{2.16 - 0.239}{1.48 + 0.047} = 1.26 \tag{6.14}$$

$$I''_q = \frac{e''_{d0} - E_{thd}}{X''_q + X_{th}} = \frac{0.52 - 0.201}{0.132 + 0.047} = 1.78 \tag{6.15}$$

$$I'_q = \frac{e'_{d0} - E_{thd}}{X'_q + X_{th}} = \frac{0.378 - 0.201}{0.484 + 0.047} = 0.33 \tag{6.16}$$

$$I_q = \frac{E_{d0} - E_{thd}}{X_q + X_{th}} = \frac{0 - 0.201}{1.42 + 0.047} = -0.137 \tag{6.17}$$

Note that the system d-axis voltage gives rise to a sustained component of q-axis current. The time constants are adjusted using the The'venin's equivalent impedance.

$$T''_{df} = T''_{d0}\frac{X''_d + X_{th}}{X'_d + X_{th}} = 0.033\frac{0.136 + 0.047}{0.196 + 0.047} = 0.024\,\text{sec} \tag{6.18}$$

$$T'_{df} = T'_{d0}\frac{X'_d + X_{th}}{X_d + X_{th}} = 3.59\frac{0.196 + 0.047}{1.48 + 0.047} = 0.571\,\text{sec} \tag{6.19}$$

$$T''_{qf} = T''_{q0}\frac{X''_q + X_{th}}{X'_q + X_{th}} = 0.084\frac{0.132 + 0.047}{0.484 + 0.047} = 0.028\,\text{sec} \tag{6.20}$$

$$T'_{qf} = T'_{q0}\frac{X'_q + X_{th}}{X_q + X_{th}} = 0.312\frac{0.484 + 0.047}{1.42 + 0.047} = 0.112\,\text{sec} \tag{6.21}$$

© 2006 by Taylor & Francis Group, LLC

The boosting effect of the automatic voltage regulator is defined by Equation (2.38) with ceiling voltage of 2.86 as calculated in Section 2.8.3.

$$I_{ex} = \frac{E_c - EI}{X_{df}}[1 - e^{-t/T'_{df}}]$$
$$I_{ex} = \frac{2.86 - 2.16}{1.48 + 0.047}[1 - e^{-t/0.571}] \tag{6.22}$$
$$= 0.458[1 - e^{-t/0.571}]$$

It may appear that I_{ex} should be calculated as a function of $E_c - (E_I - E_{thd})$ but this is not the case. Equation (6.22) as written will result in a sustained d-axis current of $(Ec - E_{thd})/(X_d + X_{th})$ which is proper.

Generator axis currents prior to the generator trip are then from Equation (2.5) and Equation (2.6) are:

$$i_d = (4.14 - 3.33)e^{-t/0.024} + (3.33 - 1.26)e^{-t/0.571} + 1.26 + 0.458(1 - e^{-t/0.571}) \tag{6.23}$$

$$i_d = (1.78 - 0.33)e^{-t/0.028} + (0.33 + 0.137)e^{-t/0.122} - 0.137 \tag{6.24}$$

The generator negative sequence current for the initial fault condition is derived from *V*xy in Figure 6.7 and Figure 6.10. Voltage *V*xy is calculated from its d and q axis components:

$$V_{xy} = \sqrt{(E_{thq} + i_d X_{th})^2 + (E_{thd} + i_q X_{th})^2} \tag{6.25}$$

$$V_{xy} = \sqrt{(0.239 + 0.047 i_d)^2 + (0.201 + 0.047 i_q)^2}$$

Note that id and iq in the above equations are the total axis currents as calculated from Equation (6.23) and Equation (6.24)

From Figure 6.8 the generator negative sequence current is then:

$$Ig_2 = \frac{Vxy}{Xg_2} = \frac{Vxy}{0.129} \tag{6.26}$$

The generator's fault current can be calculated from the positive sequence current using Equation (2.33).

$$I_1 = \sqrt{i_d^2 + i_q^2} \tag{2.7}$$

$$I_{\theta\theta} = \sqrt{3} I_1 \tag{2.33}$$

The above parameters apply for the period from the inception of the phase-to-phase fault until the generator and field breakers trip isolating the generator from the system and removing the field excitation. After the trip fault reactance X_f equals X_{g2}. Calculation of the post-trip current and the time constants are now identical to that described in Chapter 2.

New values for I_d, i'_d, i''_d, I_q, i'_q and, i''_q are calculated for Equation (2.26)–Equation (2.31) holding component voltage at their pre fault values. In reality field flux linkages and the transient and subtransient voltages which represent these linkages will decay to some extent but the fixed voltage assumption provides a conservative estimate of accumulated I_2^2t duty.

© 2006 by Taylor & Francis Group, LLC

Since the voltage regulator is in service during the fault and trip time is 0.10 sec. excitation is increase by:

$$\Delta I_{ex} = \frac{E_c - EI}{X_{df}}[1 - e^{-t_{trip}/T'_{df}}]$$
$$= 0.458[1 - e^{-0.10/0.571}] = 0.074\,\text{pu}$$

Therefore the post trip value of EI from Equation (6.4) is:

$$EI(trip) = EI_o + \Delta I_{ex} X_d$$
$$= 2.16 + 0.074 * 1.48$$
$$= 2.27\,\text{pu}$$

Sub component currents for the post trip condition are then:

$$i''_d = \frac{e_{q0}}{X''_d + Xg_2} = \frac{0.997}{0.136 + 0.129} = 3.76$$

$$i'_d = \frac{e'_{q0}}{X'_d + Xg_2} = \frac{1.049}{0.196 + 0.129} = 3.22$$

$$I_d = \frac{EI(trip)}{X_d + Xg_2} = \frac{2.27}{1.48 + 0.129} = 1.41$$

$$i''_q = \frac{e''_{d0}}{X''_q + Xg_2} = \frac{0.52}{0.132 + 0.129} = 1.99$$

$$i'_q = \frac{e'_{d0}}{X'_q + Xg_2} = \frac{0.378}{0.484 + 0.129} = 0.62$$

Post trip time constants are calculated as:

$$T''_{df} = T''_{do}\frac{X''_d + X_f}{X'_d + X_f} = 0.033\frac{0.136 + 0.129}{0.196 + 0.129} = 0.0269$$

$$T'_{df} = T''_{do}\frac{X'_d + X_f}{X_d + X_f} = 3.59\frac{0.196 + 0.129}{1.48 + 0.129} = 0.725$$

$$T''_{qf} = T''_{qo}\frac{X''_q + X_f}{X'_q + X_f} = 0.084\frac{0.132 + 0.129}{0.484 + 0.129} = 0.0357$$

$$T'_{qf} = T''_{qo}\frac{X'_q + X_f}{X_q + X_f} = 0.312\frac{0.484 + 0.129}{1.42 + 0.129} = 0.123$$

With a 1.0 ohm resistor added to the field for de-excitation the field time constant from Equation (2.40) becomes:

$$T'_{df1} = \left(\frac{1}{1 + FDR\Omega/R_{fd}\Omega}\right)T'_{df}$$
$$= \left(\frac{1}{1 + 1.0/0.427}\right)0.725 = 0.217\,\text{sec} \qquad (2.40)$$

© 2006 by Taylor & Francis Group, LLC

The de-excitation component is:

$$I_{ex} = \frac{E_c - EI}{X_{df}}[1 - e^{-t/T'_{df1}}]$$
$$= \frac{0 - 2.27}{1.48 + 0.129}[1 - e^{-t/0.217}]$$
$$= -1.41[1 - e^{-t/0.217}] \quad (6.27)$$

The d- and q-axis currents for the post trip period are:

$$i_d = (3.76 - 3.22)e^{-t/0.0269} + (3.22 - 1.41)e^{-t/0.725} + 1.41 - 1.41(1 - e^{-t/0.217})$$
$$i_d = (1.99 - 0.62)e^{-t/0.0351} + 0.62e^{-t/0.123}$$

If the field circuit where short-circuited after the generator trip without the insertion of the field discharge resistor the decay component would be equivalent to Equation (6.27) except the time constant would remain equal to T′df = 0.571 sec.

The generator's negative-sequence current was calculated at time intervals of $\Delta t = 0.01$ sec for each case. The average current during each interval was used to determine $I_2^2\Delta t$ for each interval. The I_2^2t duty for the fault condition was then found by summing $I_2^2\Delta$t for all intervals.

The results of these cases are plotted in Figure 6.11. Because of the short duration of the fault, the boost action of the excitation system had no noticeable effect. The negative-sequence current requires about 2.5 sec to decay to a minimal value in both cases, but the discharge resistor increases the rate of decay, thus reducing the I_2^2t duty from 5.3 to 3.75. Greater reductions can be obtained when the excitation system forces current reductions by the application of a negative voltage to the field during deexcitation.

As expected, the duty for this generator, which has a typical clearing time, is well below the generator's I_2^2t limit of 30. Various papers[4,6] caution that I_2^2t duties calculated for terminal faults that exclude the heating effects of the DC component of stator current provide optimistic results. Reference [4] demonstrates a 30% increase in heating when this component is included.

The calculation of the I_2^2t duty for a fault at the high-voltage terminals of the GSU transformer is identical to that described for the generator terminal fault. The sequence diagrams of Figure 6.7 must, of course, be modified such that the transformer reactance is now on the generator side of the interconnection with the negative-sequence network in both the positive- and negative-sequence

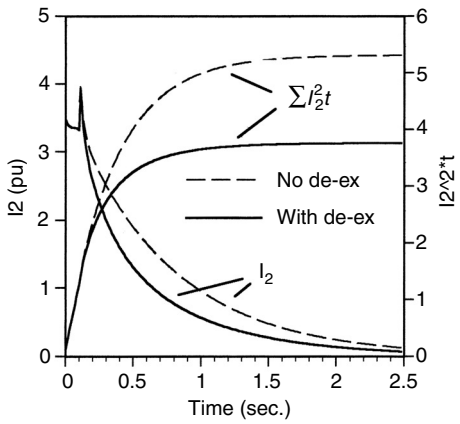


FIGURE 6.11 Terminal fault on the sample system generator.

© 2006 by Taylor & Francis Group, LLC

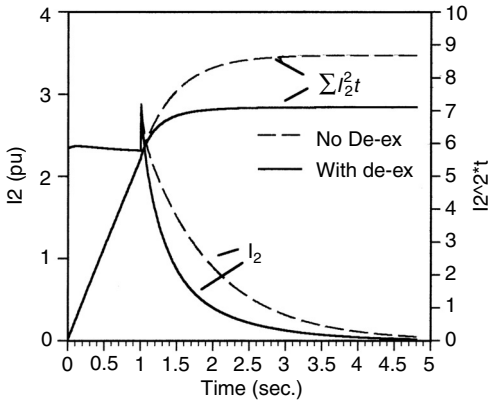


FIGURE 6.12 High-voltage fault at sample system GSU transformer.

networks. This change will affect the calculation of the negative-sequence equivalent impedance and the The'venin's equivalent impedance and voltages.

The significance of the DC component is sharply reduced when the phase-to-phase fault is on the high-voltage terminals of the GSU transformer. This condition is plotted in Figure 6.12. The magnitude of negative-sequence current in the generator is reduced from the previous case by the insertion of the GSU transformer impedance between the generator and the fault. This impedance has also increased the d- and q-axes time constants, thus reducing the rate of current decay. A clearing time of 1.0 sec was assumed for this case. This was considered the maximum clearing time for backup relaying.

The effect of the excitation system boost is noticeable in this case. The fault current remains fairly constant during the first second. Without the boost, the current would decay significantly during this period. The I_2^2t duties for the high-voltage fault are 7.1 and 8.7 with and without a field discharge resistor, respectively.

6.7 UNBALANCED CURRENT PROTECTION

The first line of generator unbalanced fault protection is provided by generator, transformer and bus differential relays at the generating station and transmission line relays at the switchyard. As demonstrated in Section 6.6.2, fault clearing by these schemes or their associated backup schemes normally result in I_2^2t exposure well below the generator limit. Damage from an unbalanced fault would require protection system failures outside normal protective criteria.

Generator damage is more likely from low-magnitude, negative-sequence current caused by an open phase. Standard transmission line relaying will not detect this condition. At higher voltages, above 375 kV, where independent pole tripping is employed to improve system stability, "pole disagreement" schemes are often included. These schemes will detect an open phase in the outlet path of the breaker to which they are associated; they will not detect an open phase on an adjacent line.

It is common practice to provide negative-sequence overcurrent relays, designated as device 46, on all but very small generators. The intent of this protection is to provide protection tailored to the generator's negative- sequence capabilities. The preferred implementation of this relay is to trip the generator breaker only. This will allow for a rapid resynchronization of the unit once the unbalanced condition is cleared. Of course, this trip mode assumes that the plant configuration will provide for the operation of auxiliary systems after the generator breaker opens and that the mechanical system will ride through the resulting full load rejection. If the system can not support the hot standby status after the trip or the load rejection, a complete shutdown must be initiated by tripping the generator and field breakers and tripping the prime mover.

© 2006 by Taylor & Francis Group, LLC

Negative-sequence relays are available in electromechanical and electronic models with adjustable time–current characteristics intended to match the generator I_2^2t capability. The electromechanical relays are rather insensitive, with a minimum I_2 pickup current in the order of 60% of the rated generator current. Because of the poor sensitivity, these relays provide only backup protection for unbalanced faults. They lack the sensitivity to detect negative-sequence currents marginally in excess of the generator's continuous I_2 capability or to detect open phase conditions.

The time–current characteristics of these relays are derived from magnetic circuits and induction-disk motion. They generally do not match the I_2^2t characteristic of a generator and compromise settings are often required. Electromechanical relays normally have two set points, an I_2 pickup current and a time dial setting.

Electronic relays are far more sensitive and more sophisticated. They are capable of detecting open phases and negative sequence current down to the continuous I_2 limits of the generator. Time–current curves are derived electronically and match the machine I_2^2t characteristic exactly. The time dial calibrations on most electronic relays are in terms of K, where $K = I_2^2t$. Many of the electronic relays have an alarm feature that can be set to alert the operator of unbalanced conditions approaching the trip setting. Some relays also have I_2 meters built into the relay.

Electronic relays are also designed with a delayed reset characteristic. When the negative-sequence current exceeds the relay's minimum actuation setting the relay begins to accumulate I_2^2t in memory. If the negative sequence drops below the actuating level before a trip occurs, the memory is not reset, but is allowed to forget at a rate intended to mimic the cooling of the rotor. This feature reduces the trip time should the unbalanced current reoccur before the rotor can cool.

Figure 6.13 is a characteristic curve for one manufacturer's static negative-sequence relay. The features included in this relay are typical of those found in other static relays and in multifunction generator microprocessor relays.

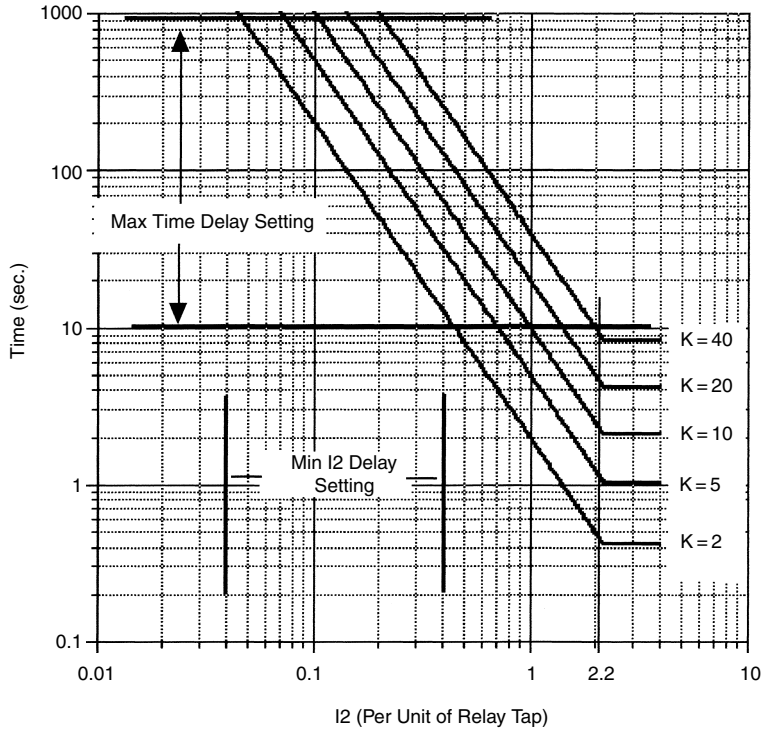


FIGURE 6.13 Solid-state negative-sequence relay.

© 2006 by Taylor & Francis Group, LLC

The relay has taps that are set to match the generator base current. The taps are 3.1, 3.3, 3.5, 3.7, 3.9, 4.1, 4.3, 4.5, 4.7 and 4.9 A. These are necessary if the K calibration on the time dial is to relate to the protected machine. The K setting is adjustable from 5 to 40. The minimum I_2 trip threshold setting is adjustable from 0.04 to 0.4 pu based on the relay tap current. If the relay is set on the 4.5 Å tap with the minimum I_2 trip set at 0.09 pu, the relay will actuate at $4.5 \times 0.09 = 0.405$ A negative-sequence current.

The relay also has a maximum trip delay adjustable from 10 to 990 sec in 10 sec steps. When the I_2 current exceeds the trip threshold setting, the relay begins to accumulate I_2^2t and initiates the maximum delay timer. A trip output occurs when the accumulator reaches the K setting or when the maximum time delay timer times out, whichever occurs first.

The relay characteristic flattens above 2.4 pu current. This delay is necessary to allow the primary fault detection relays in the plant or at the switchyard to clear the unbalanced fault without tripping the generator.

The relay has an alarm threshold adjustable between 0.02 and 0.2 pu referred to as the relay tap. The alarm time delay is adjustable between 0.2 and 3.0 sec.

The memory feature of this relay allows 250 sec to empty the accumulated I_2^2t from a value just below the K setting of the relay.

6.8 NEGATIVE-SEQUENCE RELAY SETTINGS

To illustrate the application of a negative-sequence relay, the relay described above will be use to protect the sample system generator. The settings are based on the generator rating and the rotor's negative-sequence heating limits as defined by the I_2^2t and the continuous I_2 current limits.

The data sheet for the sample system generator can be found in Appendix "A". This sheet lists an I_2^2t limit of 30, but no continuous negative-sequence capability is listed. When specific data are not available, the minimum capabilities listed in IEEE Standard C37.102-1995 and Table 6.1 should be used. The sample system generator is an indirectly cooled machine for which the standard lists a minimum continuous negative-sequence current capability of 10%. Note that the standard also lists an I_2^2t limit of 30 for this machine.

The generator normally runs at rated output, but on occasion may remain online at 70% rated load. It is therefore desirable that the unbalanced protection detects an open phase in the generator's outlet path with load reduced to that level. The power factor at the reduced load is assumed to be 90%.

6.8.1 Calculation of Open-Circuit Current

The negative-sequence current resulting from this open-phase condition is calculated from Figure 6.14. First the voltage behind the synchronous reactance (EI) and the value of Z_L must be found for the 70% loading condition. Figure 6.15 will be used as a simplified single-axis representation of the positive-sequence network for the generator under normal operations.

Generator and system data are derived from the generator data sheet and Figure 1.1:

$$X_d = 1.48$$
$$X_{g2} = 0.129$$
$$X_{tr} = 0.07$$
$$X_{e1} = X_{e2} = 0.078$$
$$X_{e0} = 0.23$$

© 2006 by Taylor & Francis Group, LLC

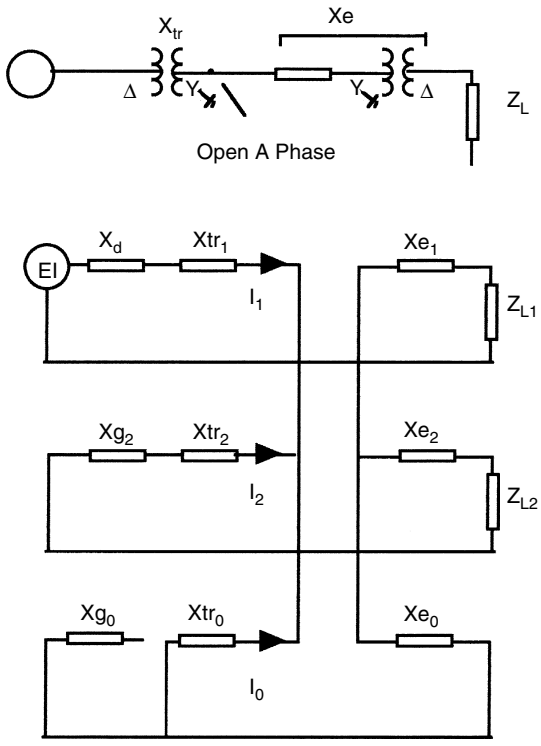


FIGURE 6.14 Open-phase representation by symmetrical components.

At 70% load, 90% power factor, and rated terminal voltage, the current will be

$$\begin{aligned} I_1 &= 0.7\angle -25.8^\circ \\ &= 0.63 - j0.30\,\text{pu} \end{aligned} \tag{6.28}$$

The voltage behind the synchronous reactance is

$$\begin{aligned} EI &= e_\text{t} + I * X_\text{d} \\ &= 1.0 + (0.63 - j0.3) * j1.48 \\ &= 1.73\angle 32.7^\circ \end{aligned} \tag{6.29}$$

From Figure 6.15,

$$\begin{aligned} \frac{e_\text{t}}{I} &= X_\text{tr} + X_\text{e1} + Z_\text{L1} = \frac{1.0}{0.7\angle -25.8^\circ} \\ &= 1.43\angle 25.8^\circ = 1.28 + j0.622 \end{aligned} \tag{6.30}$$

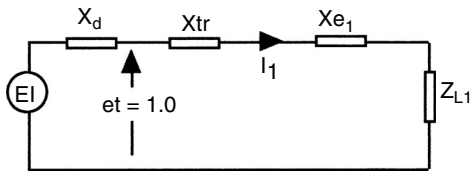


FIGURE 6.15 Initial load condition.

© 2006 by Taylor & Francis Group, LLC

The load impedance is then

$$\begin{aligned} Z_{L1} = Z_{L2} &= 1.28 + j\,0.622 - X_{tr} - X_{e1} \\ &= 1.28 + j0.622 - j0.07 - j0.078 \\ &= 1.37\angle 20.2^\circ \end{aligned} \tag{6.31}$$

These values are applied to the open-phase network connection in Figure 6.14. Resolving the network:

$$X_0 = X_{tr0} + X_{e0} = j(0.07 + 0.23) = j0.30 \tag{6.32}$$

Assuming $Z_{L1} = Z_{L2}$

$$\begin{aligned} X_2 &= X_{g2} + X_{tr2} + X_{e2} + Z_{L2} \\ &= j(0.129 + 0.07 + 0.078) + 1.37\angle 20.2^\circ \\ &= 1.49\angle 30.27 \end{aligned} \tag{6.33}$$

Paralleling the zero- and negative-sequence networks:

$$\begin{aligned} Z_{2/0} &= \frac{X_0 Z_2}{X_0 + Z_2} = \frac{j0.30 * 1.49\angle 30.27^\circ}{j0.30 + 1.49\angle 30.27^\circ} \\ &= 0.269\angle 81^\circ \end{aligned} \tag{6.34}$$

The total circuit impedance is then

$$\begin{aligned} Z_T &= X_d + X_{tr} + X_{e1} + Z_{L1} + Z_{2/0} \\ &= j(1.48 + 0.07 + 0.078) + 1.37\angle 20.2^\circ + 0.269\angle 81^\circ \\ &= 2.71\angle 60.7^\circ \end{aligned} \tag{6.35}$$

The negative-sequence current is determined from the positive-sequence current and the current split between the zero- and negative-sequence current.

$$I_1 = \frac{EI}{Z_T} = \frac{1.72\angle 32.7^\circ}{2.71\angle 60.7^\circ} = 0.635\angle -28^\circ \tag{6.36}$$

This current divides between the negative and zero sequence networks.

$$\begin{aligned} I_2 &= -I_1 \frac{X_0}{Z_2 + X_0} \\ &= -0.635\angle -28^\circ \frac{j0.30}{1.49\angle 30.27^\circ + j0.30} \\ &= -0.12\angle 22.7^\circ \end{aligned}$$

The calculated value of negative-sequence current in the generator is 12%. The data are now available to set the relay.

© 2006 by Taylor & Francis Group, LLC

6.8.2 Negative Sequence Relay Setting

The first step in setting the relay is to choose a tap setting as close to the generator full load current as possible. The relay's I_2^2t time dial calibrations are based on rated tap current being equal to 1.0 pu current.

The generator is rated 104 MVA 13.8 kV at 85% PF. The generator CTs are 6000/5. The generator's full load current is

$$I_{\text{FL}} = \frac{kVA}{\sqrt{3}\,kV} = \frac{104,400}{\sqrt{3}13.8} = 4370\,\text{A} \tag{6.37}$$

The CT secondary current at full load is then

$$I_{\text{sec}} = 4370 \times 5/6000 = 3.64\,\text{A} \tag{6.38}$$

The relay has the following taps available: 3.1, 3.3, 3.5, 3.7, 3.9, 4.1, 4.3, 4.5, 4.7, and 4.9. The closest available tap, 3.7 A, is chosen. With this choice, relay base current is $3.7/3.64 = 1.02\times$ greater than the generator base current. The relay's K setting will be $(1.02)^2 = 1.04\times$ the generator's K. Adjusting the continuous limits to the relay base:

$$K \text{ limit} = 30/1.04 = 28.8$$
$$I_2 \text{ limit} = 10\%/1.02 = 9.8\%$$

The negative-sequence current resulting from an open phase on the relay base is

$$12\%/1.02 = 11.7\%$$

The relay's time dial setting must be below the generator limit. The margin must allow for the accumulation of additional I_2^2t as a result of the current decay after the generator and field breakers have been tripped. The posttrip I_2^2t for terminal and high-voltage faults can be determined from Figure 6.11 and Figure 6.12. The maximum posttrip I_2^2t accumulation is 5.0 for a fault at the generator terminals with no deexcitation circuit. This is 7.1/30 or 24% of the I_2^2t limit of 30 with the de-excitation circuit active. Applying a margin of 10% the maximum "K" setting is:

$$28.8 \times (1 - 0.34) = 19$$
$$\text{Set } K = 19$$

Set the I_2 trip threshold below the negative sequence current seen for an open phase, assume a 10% margin:

$$0.12/1.1 = 0.109$$
$$I_2 \text{ trip threshold} = 0.10$$

Set I_2 alarm threshold slightly below the generator continuous limit of 9.8%. Using 10% margin:

$$9.8/1.10 = 8.92\%$$
$$\text{Set } I_2 \text{ alarm threshold} = 8.0\%$$

© 2006 by Taylor & Francis Group, LLC

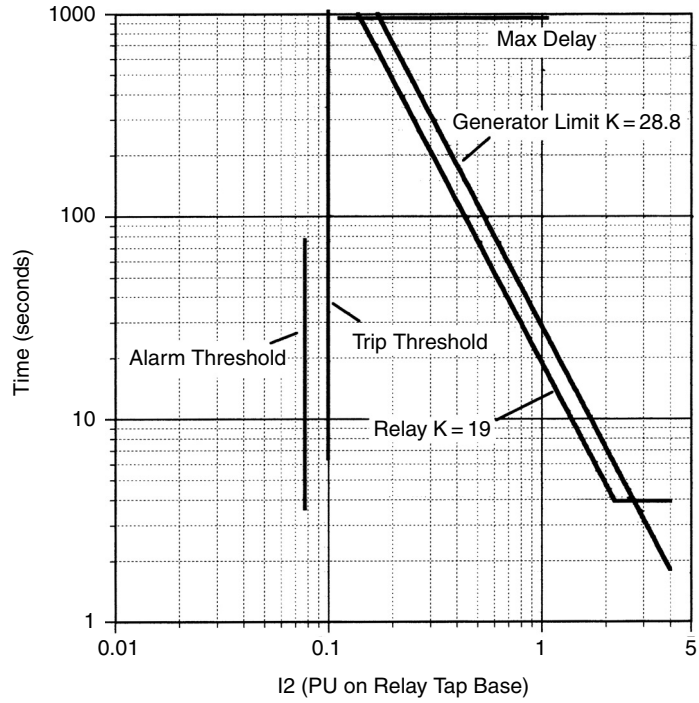


FIGURE 6.16 Relay vs. generator limit.

The only settings remaining are the maximum time delay setting and the alarm timer setting. The maximum trip time delay can be set at maximum, which is 990 sec. This setting will allow the operator maximum time to correct the problem before a trip occurs. Note that the 990 sec setting will overprotect the generator for negative-sequence currents less than $\sqrt{(19/990)} = 0.14$ pu. The maximum available alarm timer setting of 3.0 sec is also suggested to avoid nuisance alarms for system faults.

Figure 6.16 is a plot of the relay characteristic and the generator limit. This plot is on the relay tap base. It shows the relay characteristic crosses the generator I_2^2t limit ($K = 28.8$) at $I_2 = 2.4$ and therefore will not protect the generator above this point. This would be $2.4 \times 1.02 = 2.45$ pu on the generator base current. The maximum negative-sequence current would occur for a phase-to-phase fault at the generator terminals. Assuming the generator was at no load and on the manual regulator prior to the fault, the negative-sequence current would be

$$\begin{aligned} I_2 = -I_1 &= \frac{EI}{X_d + X_{g2}} \\ &= -\frac{1.0}{1.48 + 0.129} = -0.62\,\text{pu} \end{aligned} \tag{6.39}$$

If the generator where on automatic regulator, field forcing could increase EI to a value of 2.86 pu; this would produce maximum sustained value of I_2 equal to $2.86 \times 0.62 = 1.77$ pu, not enough current to cause miscoordination.

© 2006 by Taylor & Francis Group, LLC

REFERENCES

1. Jones, N. H., Temoshok, M., and Winchester, R. L. Design of conductor-cooled steam turbine generators and application to modern power systems, *IEEE Trans*, PAS-84, 131–146, 1965.
2. ANSI C50.12-1982, *American National Standards Requirement for Salient-Pole Synchrouous Generators and Generator/Motor for Hydraulic Turbine Applications.* IEEE, New York, 1977.
3. ANSI C50.13-1989, *American National Standards Requirement for Rotating Electric Machinery—Cylindrical Rotor Synchronous Generators.* IEEE, New York, 1977.
4. Linkinhoker, C. L., Schmitt, N., and Winchester, R. L. Influence of unbalanced currents on the design and operation of large turbine generators, *IEEE Winter Power Meeting*, January 1973, T 73 012–2.
5. Alger, P. L., Franklin, R. F., Kilbourne, C. E., and McClure, J. B. Short-circuit capabilities of synchronous machines for unbalanced faults, *AIEE Trans, vol 72 pt. III Power Apparatus and Systems*, 394–404, 1953.
6. Brown, P. G. Generator I_2^2t requirements for system Faults, *IEEE Trans PSA*, PAS-92, 1247–1251, 1973.
7. IEEE STD C37.102–1995, *IEEE Guide for AC Generator Protection*. 1996.

© 2006 by Taylor & Francis Group, LLC

7 Motoring Protection

7.1 INTRODUCTION

A generator motors when the mechanical input power to its shaft is lost while connected to the power system. Assuming that the generator field is unaffected, the generator becomes a synchronous motor driving the prime mover at synchronous speed. If field excitation is also lost, the generator may lose synchronism and become an induction motor. This chapter will consider only motoring conditions with the field intact and the turbine generator at synchronous speed. Loss-of-field is the subject of a subsequent chapter.

Assuming that excitation is maintained, the generator can operate as a synchronous motor indefinitely. Motoring is damaging to the prime mover, not the generator. Motoring can result from operator error, a failure of the generator breaker to open during shutdown, or because of a mechanical failure.

Both mechanical and electrical antimotoring protection schemes are incorporated at most installations. Electrical motoring protection is in the form of reverse power relays designated device 32. This relay detects power flow into the generator terminals from the power system. Friction and windage losses of the turbine and the electrical losses of the generator determine the power input to the generator while motoring. The reverse power relay trips the generator and field breakers and prime mover.

7.2 EFFECTS OF MOTORING

Motoring a generator that is under the control of the automatic voltage regulator does not threaten the power system. Of course, this assumes that the system can withstand the loss of the failed unit's generating capacity. Because the field circuit is unaffected by the loss of the prime mover, generator Var loading and terminal voltage remains unchanged immediately following the power reversal. Var loading will then adjust to the level necessary to maintain the regulator voltage set point without kW output. If the generator were initially operating at a lagging power factor (Vars out of the generator) an increase in Var output would be expected to accompany motoring. If the generator was operating at a leading power factor prior to the loss of input power, Vars into the generator would decrease.

The rate of Var adjustment will vary. Loss of a steam turbine will result in a slow decline in output power and a slow change in reactive power as steam pressure at the turbine decays. An engine-driven generator has little stored energy and power output would cease immediately upon loss of the engine. The resulting Var adjustment would be rapid, determined by exciter response and generator time constants.

If the generator were operating on the manual voltage regulator near rated load prior to motoring, damaging conditions will arise. The manual regulator will hold field current at the value required for rated load. This current will substantially exceed requirements without kW output. The results may include Var output, terminal voltage, and, possibly, system voltages far above safe limits. These adverse consequences underscore the need to operate on automatic voltage regulator control when synchronized to the power system.

When the generator field excitation remains in service, the generator will act as a synchronous motor without damage. Generator damage may occur if excitation is lost coincident with the loss of the prime mover. Under this condition, the generator can lose synchronism and act as an induction motor driving the prime mover at less than synchronous speed.[1] The speed difference between the

© 2006 by Taylor & Francis Group, LLC

rotor and the stator magnetic field will induce currents in the rotor. These induced currents are low frequency (slip frequency), but can cause the same rotor damage associated with the higher frequency induced currents described in Chapter 6.

7.2.1 Consequences for a Steam Turbine

Motoring is in general a hazard to the prime mover not the generator. In steam turbines, windage losses cause significant heating of the turbine blades. Normally, steam flow removes this heat from the blades and other affected turbine parts. During motoring, there is insufficient steam flow for cooling and the temperature buildup will cause blade distortion and softening. Large-diameter blades have higher tip velocities and greater heating; hence, critical temperatures usually occur first in the low-pressure stage at the exhaust end of the turbine.

Windage losses are also a function of steam density. Condensing turbines operate under vacuum and can withstand motoring much longer than a turbine that operates with high back pressure. It follows that the time a condensing turbine can withstand motoring will be sharply reduced if it loses vacuum.

Damage is not confined to the blades. The loss of steam flow not only removes the turbine's ability to dissipate heat, but also the ability to equalize heating. Localized hot spots can cause stress and distortion within the turbine. The distortion can produce rubbing between components, generating more heat and causing wear.[2]

The minimum steam flow required for cooling varies with turbine design; in some cases flow at very low power output is insufficient to prevent damage. Protection is then required for operation below this minimum power output. In this situation a forward looking power relay would be required set for the allowable minimum power output of the generator. Tripping by such a relay would have to be delayed sufficiently to allow the unit to synchronize and loaded above the relay setting to avoid nuisance trips during startup.

7.2.2 Consequences for Other Prime Movers

Motoring will cause other problems with different prime movers. When the water supply to a hydro turbine is interrupted, the runner may remain under water. Motoring in such a state can lead to runner damage due to cavitation. This phenomenon occurs when the hydro turbine acts as a pump with low head. The low pressure at the back of the blades causes an explosive production of tiny low-temperature steam bubbles at the blade surface. The force of these miniature eruptions chips metal particles from the blade surface. Blade erosion and pitting are the result.

Engine-driven generators have mechanical protection systems that shut down the drive in the event of mechanical failures such as bearing overheating. On these units, motoring may be the result of a mechanical protective trip. In this situation, motoring can cause severe damage, because the initiating mechanical fault has not been cleared. Motoring these units also poses a danger of explosion and fire because of unburned fuel.

Gas turbines and other gear-driven generator units are subject to damage under motoring conditions when gearing is designed to be unidirectional. In such designs, only one side of a gear tooth is machined to act as a drive surface. Motoring reverses the input to the drive and the wrong tooth face acts as the drive face-resulting in excess wear and heating.

7.3 PROTECTION

Mechanical methods, along with reverse power relays, are used to detect the motoring condition. Mechanical motoring protection for a steam turbine can take the form of differential pressure switches, exhaust hood temperature detectors, control oil system monitors, and steam valve limit switch interlocks. Flow indicators and reverse power relays are used on hydro turbines.

© 2006 by Taylor & Francis Group, LLC

Reverse power relaying is not applicable on units that operate as synchronous condensers. This is generally limited to hydro machines. In the condensing mode, these units are motored under controlled conditions to prevent damage.

7.3.1 Mechanical Protection: Steam Turbines

Because maximum heating usually occur in the exhaust end of the steam turbine, temperature detectors in the exhaust hood can detect motoring. These detectors normally alarm and are not used as primary motoring protection because of reliability problems with the detectors and the variations in temperature within the exhaust hood.

Pressure monitors in the turbine trip oil system and governing oil systems can be used to determine steam valve position. The turbine trip oil system is a fail-safe system. Loss of pressure closes all valves. The governing oil pressure varies the position of the governor and intercept valves to control loading during normal operations. Pressures in these systems provide an accurate representation of unit loading and can be used to detect a motoring condition.

Limit switches on the steam valves are set to indicate valve position. These switches are used to indicate valve closure and the resulting loss of steam flow. This scheme has had problems. The number of valves has increased on large units and the series connection of many limit switches is required to provide the "all closed" indication necessary for a motoring trip. Adjustment problems with the switches have resulted in misoperations of this scheme.

The differential pressure drop across the high-pressure turbine is a direct measure of steam flow. A pressure switch set to operate at the no-load-rated speed steam flow is a good method to detect a motoring condition.

Properly designed mechanical schemes use redundant series/parallel logic such that a single contact failure will not compromise the scheme, but these schemes assume steam flow stops when valve closure is indicated. This is not always the case. Steam valves can leak due to warping, mechanical binding or backflow. Malfunctions in these schemes can be disastrous. A false motoring indication will initiate a trip of the generator breaker. The energy from the leaking steam is then be dissipated by accelerating the turbine-generator set. With valve function compromised by the leak, the speed governor cannot limit overspeed and severe damage may result. For this reason, mechanical motoring schemes are usually supervised by a reverse power relay to verify loss of steam flow before the generator breaker is opened.

7.3.2 Electrical Protection

When the prime mover energy input to a generator is removed, the losses must be supplied from the power system. A power relay at the generator terminals looking into the generator can detect this condition. The type of prime mover determines the sensitivity requirement for the relay.

Gas turbines represent a large compressor load when motoring. The power consumed by the unit in kW during motoring can be up to 100% of the name plate kVA rating for a single-shaft machine or as low as 10 to 15% for a double shaft installation. On the other hand, hydro turbines with their blades above the tail-race water level require only 0.2 to 2% of their nameplate rating expressed in kW. When the impeller is fully submerged, motoring power can reach 100% nameplate. Hydro turbines with Kaplan adjustable blades can require less than 0.2% kW when the blades are in the flat position.

Diesel generators, with no cylinders firing, require about 15% or 25% kW for four- and two-cycle engines, respectively. Steam turbines under full vacuum require 0.5 to 3.0% kW. Steam turbines without condensers or condensing turbines that lose vacuum will require more that 3% motoring power. Manufacturers should be consulted for exact motoring power requirement and the maximum permissible motoring time for their units.

© 2006 by Taylor & Francis Group, LLC

The above discussion shows that the sensitivity of the reversed power relay can become the key application issue on large steam turbines and hydro turbines. Electromechanical and electronic reverse power relays are available with a large diversity of designs. These relays may be calibrated in amps or in secondary watts. They may measure single-phase or three-phase power.

The application of single-phase relays is predicated on the assumption that motoring losses are supplied equally by all phases. This is not always the case. On very large units, authors have reported variations of 0.2 to 0.3% of rated output between phases.[3] This is very significant, because the total three-phase motoring power for such units can be as low as 0.5%. When microprocessor relays are applied, unbalance is not a problem, because these relays usually measure three-phase power.

Current calibrated relays are actually watt sensing relays with setting calibrations based on the in-phase component of current, I_r in Figure 7.1. A single-phase relay rated for an input voltage of 120 V and calibrated to operate at 10 mA will operate at that value of current only if the current and voltage are in phase and the input voltage is 120 V. The pickup of this relay is actually $0.010\ \text{A} \times 120\ \text{V} = 1.2\ \text{W}$. Because this relay actually responds to power, the current pickup is a function of input voltage. This same relay with the same setting would require 0.11 A to operate if the input voltage was reduced to 110 V ($1.2\ \text{W}/110\ \text{V} = 0.11\ \text{A}$).

The multifunction generator-protection microprocessor relays usually include two reversed power functions calibrated in per unit watts based on the relay rated voltage and current. One function is applied as motoring protection and the second can be incorporated in the sequential trip logic to be described later. Some microprocessor reverse power functions are settable for power flow in or out of the generator. One such relay has a settable range of $+3.000$ to -3.000 pu power in increments of 0.001 pu. Electromechanical relays are available with sensitivities as low as 4 mA at rated voltage.

All reverse power relays applied on steam turbines and hydro turbines are susceptible to a failure to operate if Var loading is high during motoring. This is a result of the low motoring power required by these units and errors in the measurement of the high power factor angle. Ideally, reverse power relays, whether calibrated for current or secondary watts, measure power as

$$\begin{aligned} P &= IE * \cos\theta \\ &= I_r E \end{aligned} \tag{7.1}$$

where E and I_r are line quantities and θ is the power factor angle.

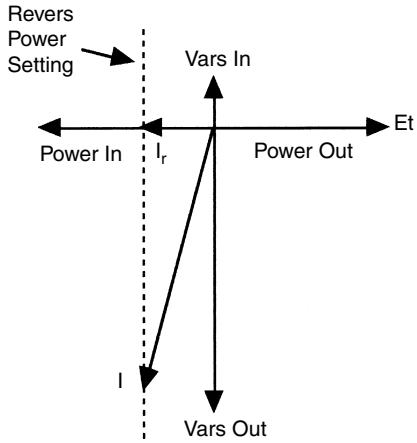


FIGURE 7.1 Power measurement.

© 2006 by Taylor & Francis Group, LLC

The PT and CT error can cause shifts in the current and voltage presented to the relay. Also, slight error in the relay characteristic can cause the relay to measure with an angular error β:

$$P = EI * \cos(\theta \pm \beta) \tag{7.2}$$

In either case, the error appears as a deviation from the true power factor at the relay (Figure 7.2). If the generator motors at a low power factor because of high Var loading and the angular error adds to the true power factor angle, the measured motoring power may be below the relay set point. For example, assume a generator rated at 0.9 PF is operating at rated load prior to motoring and that the motoring power is 2%. At full load, the output will be 0.9 pu power and 0.44 pu Vars. If the Var output remains constant after the prime mover is lost, the output will be

$$\begin{aligned} P, Q &= 0.02 + j0.44 \\ &= 0.44\angle 87.4^\circ \end{aligned} \tag{7.3}$$

If an error of $+1.0^\circ$ is assumed, the measured motoring power will be 1.2%. This is a -40% error, which could result in a failure to operate.

$$\begin{aligned} P, Q &= 0.44\angle 88.40^\circ \\ &= 0.012 + j0.44 \end{aligned} \tag{7.4}$$

The sensitivity to angle error diminishes rapidly below 85°. To avert this problem, control schemes may include logic to reduce Var loading. When manual trips include reverse power supervision, operators should reduce Var output before initiating the manual trip.

When maximum sensitivity is required, metering accuracy CTs may be required instead of relay accuracy CTs. It is important to note that even with the most sensitive relaying, motoring events will be undetectable if steam valves do not seat properly. The leakage can easily reduce the motoring power below the relay set point, rendering the condition undetectable electrically.

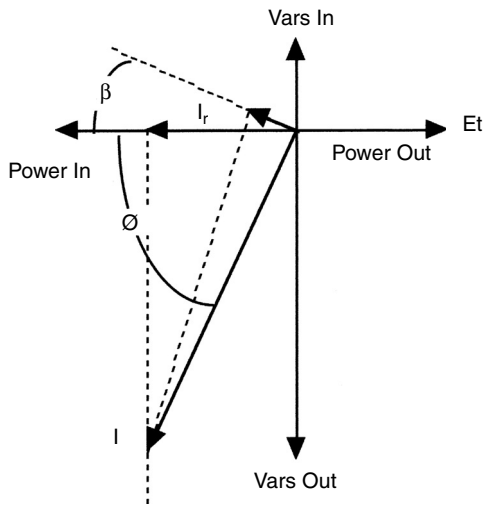


FIGURE 7.2 Phase angle error.

© 2006 by Taylor & Francis Group, LLC

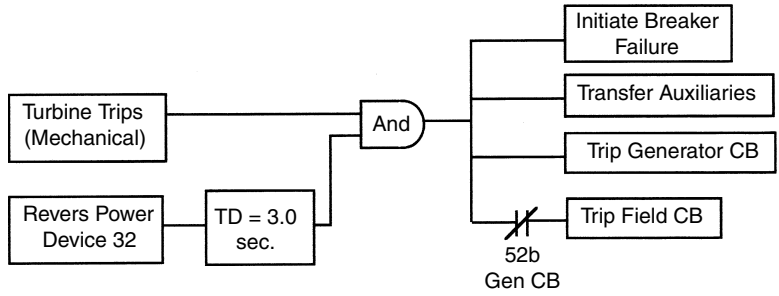


FIGURE 7.3 Sequential trip logic.

7.4 SEQUENTIAL TRIP LOGIC

The application of reverse power relaying is closely linked to the "sequential" trip logic provided as part of the control scheme for various prime movers. The same reverse power relay that provides motoring protection is incorporated into the sequential trip schemes. This trip mode was originally developed for steam turbines, but is now applied with a variety of prime movers. Sequential trip logic first initiates a prime mover trip that includes a shutdown of the steam or fuel supply. Opening of the generator and field breakers is delayed until power flow into the generator is confirmed by the reverse power relay.

Sequential tripping is not part of the motoring protection. This logic assures that energy input to the prime mover has decreased to a value that will not result in overspeed when the generator breaker is opened. At a steam turbine installation, this could be caused by leakage at one of the many steam inlet valves. Typical sequential trip logic is shown in Figure 7.3. A delay of 2 or 3 sec is provided to avoid nuisance tripping during grip events. Note that the field breaker is not tripped until the generator breaker opens. This interlock prevents removal of the field if the generator breaker fails to open. The resulting loss-of-field condition would cause the generator to motor as an induction generator, a potentially damaging condition.

This logic is used when delayed tripping will not jeopardize the generator. It is recommended to supervise for most mechanical oriented trips from the turbine or other prime mover protection logic. It is also used to supervise manual tripping of the unit. Sequential trip logic is not be used in conjunction with electrical trips from the generator of GSU protection logic, because high speed tripping is required. The time delay for the sequential logic includes the steam dissipation time plus the timer setting.

When the same reverse power relay is used for motoring protection and supervision of the sequential trip logic, the motoring function time delay is set at about 3.0 sec to accommodate the requirements of the sequential trip logic.

7.5 BACKUP PROTECTION

The sequential trip logic provides protection against overspeed, but a failure of the sequential trip scheme will result in motoring. Backup protection in the form of an independent reverse power relay and independent trip circuitry is normally provided in conjunction with sequential tripping. The backup relay is set the same as the motoring/sequential trip relay. The only supervision provided for the backup relay is a breaker-closed indication (52a contact) from the generator breaker. The time delay for the backup scheme is set with sufficient delay to override power system transients, but less than the maximum allowable motoring time. A setting of 30 sec is typical.

© 2006 by Taylor & Francis Group, LLC

7.6 SETTING DEVICE 32

When the reverse power functions is calibrated in watts, the motoring power consumed by the generator, expressed in terms of primary watts, must be converted to secondary watts at the relay. The conversion is a function of the relay PT and CT ratio and whether the relay is calibrated in terms of single-phase or three phase-watts:

Secondary Watts 3Ø = Primary watts 3Ø/(PT ratio × CT ratio)
Secondary Watts 1Ø = Primary watts 3Ø/(3 × PT ratio × CT ratio)

When applying an electromechanical reverse power relay be certain that the relay's continuous current rating is above the CT secondary current at full load. To achieve higher sensitivity, some relays are rated at less than 5 A.

Whatever the calibration, the reverse power relay should be set at 20 to 50% of the power drawn by the motoring generator. This may not always be possible when motoring losses are very low.

All reverse power applications include a time delay. The delay is necessary to prevent operations on momentary power swings into the generator caused by power transients following a fault or switching operation. The delay is also required to override momentary power intake to the generator upon synchronization. Standards do not specify an allowable motoring time, but this data is available from the turbine manufacturers. Turbine withstand times can vary from 30 sec to 30 min but a 90 sec maximum is more the norm. Relay trip delays of 10 to 30 sec are common.[4]

7.7 APPLYING REVERSED POWER RELAY ON THE SAMPLE SYSTEM

Two relays will be considered for the sample system generator motoring protection. An electromechanical relay with the following specifications will be considered:

Power measurement = three-phase
Pickup (0.01 − 0.04 A) unity PF amps
Rated 120 V, 5 A

This relay is applied with a time delay relay with a settable range of 0.5 to 300 sec.

Also, settings will be derived for a multifunction microprocessor relay. This relay has the following settable parameters:

Power measurement = three-phase
Rated voltage: settable LL (40–140 V); increments = 1.0 V
Rated current: settable (0.50–5.0 A); increments = 0.01 A
Power: setting range (2.000 to −2.000 pu); increments = 0.001 pu
Time delay:adjustable (1–7200 cycles); Increments = 1 cycle

The reverse power relay will also provide supervision of the sequential trip logic. A second relay will provide backup protection should the primary reverse power relay or the sequential trip scheme fail. The backup relay will be the same type as the primary, but will trip independent of the primary scheme.

The motoring power for the sample system turbine-generator is not listed on the generator data sheet. This is typical because the generator manufacturer would not know the turbine losses. Inquiries to the turbine manufacturer revealed the motoring power is 2% kW based on the generator's kVA rating. The manufacturer also stated that the turbine could withstand motoring for 58 sec.

© 2006 by Taylor & Francis Group, LLC

The generator CTs are 6000/5 and PTs are 13,800–120 V:

CT = 6000/5 = 1200/1
PT = 13,800/120 = 115/1

The motoring power is:

$$\text{Primary watts } 3\text{Ø} = 0.02 \times 104,400\,\text{kVA} = 2088\,\text{kW} \tag{7.5}$$

$$\text{Primary amps} = \frac{2088\,\text{kW}}{\sqrt{3}313.8\,\text{kV}} = 87\,\text{A} \tag{7.6}$$

$$\text{Secondary watts } 3\text{Ø} = \frac{2088\,\text{kW}}{1200 * 115} = 15.13 \text{ secondary watts} \tag{7.7}$$

The electromechanical relay pickup is calibrated in secondary amps and would see

$$\text{Secondary amps } = \frac{87\,\text{A}}{1200} = 0.073\,\text{A} \tag{7.8}$$

$$\text{Secondary volts} = \frac{13,800\,\text{V}}{115} = 120\,\text{V} \tag{7.9}$$

Because the relay is rated 120 V and the PTs provide 120 V at rated output voltage, no relay pickup adjustment is required.

$$I_{\text{pickup}} = I_{\text{setting}} \frac{V_{\text{actual}}}{V_{\text{rated}}} \tag{7.10}$$

The settings should be 20–50% of the motoring power. Choosing 50%,

$$\text{Set pickup} = 0.5 \times 0.073\,\text{A} = 0.036\,\text{A} \tag{7.11}$$

The microprocessor relay is calibrated in per-unit power based on the nominal current and voltage setting. If the power calibration is to match the generator rating, the relay nominal current and nominal voltage must be set to match that of the generator.

The nominal generator current at the microprocessor relay is

$$\begin{aligned} I_{\text{rated}} &= \frac{104,400\,\text{kVA}}{\sqrt{3}313.8\,\text{kV}} = 4370\,\text{A} \\ &= \frac{4370}{1200} = 3.64 \text{ secondary amps} \end{aligned} \tag{7.12}$$

with the relay set for nominal values of 120 V and 3.64 A the base kW for the relay will equal the generator kVA rating. The relay pickup should be set at about 50% motoring power or 1% of the generator rating. The microprocessor settings are then

Rated voltage = 120 V
Rated current = 3.64 A
Power = 0.01 pu

The above settings are applicable to both the primary and backup relays. The time delay for motoring protection could by set at any value less than 58 sec. However, since the primary relay

© 2006 by Taylor & Francis Group, LLC

supervises the sequential trip logic and the turbine manufacturer recommends a three second delay for this logic, the manufacturer recommendation will be used.

The time delay for the backup reverse power relay will be set at 40 sec. This setting will provide a liberal margin against the maximum allowable motoring time of 58 sec and allow sufficient time to establish power output from the generator immediately after synchronizing to avoid a motoring trip.

REFERENCES

1. *IEEE Guide for Operation and Maintenance of Turbine Generators*, IEEE Std 67-1990, IEEE, New York, 1990.
2. *IEEE Guide for AC Generator Protection*, IEEE Std C37.102-1995, IEEE, New York, 1996.
3. Pencinger, C. J. Modern Generator Protection System. *Pacific Coast Electrical Association, Engineering and Operating Conference*, San Francisco, CA, March 18–19, 1982.
4. Mason, C. R. *The Art & Science of Protective Relaying*, John Wiley & Sons Inc., New York, 1967.

© 2006 by Taylor & Francis Group, LLC

8 Field Winding Protection

Field winding protection will be discussed in two parts: field ground protection and field overcurrent protection.

8.1 FIELD GROUND PROTECTION

8.1.1 Field Ground Hazard

When a ground occurs within the field winding, the rotor body will be energized to a potential dependent on the location of the winding failure. Because the field circuit is normally ungrounded, this condition is not damaging. The concern is that a second ground will occur. The second ground will bypass a portion of the field winding and unbalance the air-gap flux. The unbalanced flux will produce vibration. The degree of unbalance and the resulting vibration depends on the location and extent of the winding bypassed. The vibration can be severe enough to cause massive damage. Mason[1] reports a bent rotor, broken bearing pedestals, and rotor–stator contact. On the other hand, the resulting vibration may be undetectable.

A double ground that does not significantly unbalance the air gap can still result in damaging vibration. The second failure can cause a substantial current in the rotor forging and unbalance winding currents. The local heating that results can cause rotor distortion that produces damaging vibration. This mode of failure would be characterized by a slowly increasing vibration, beginning 30 minutes to 2 hours after the second ground.[1]

The first ground will provide a reference voltage on the rotor body. As operation continues, the field insulation will be stressed against this reference. System switching and faults induce transient voltages in the rotor can add to the reference voltage to produce additional voltage stress on the insulation. In short, the first ground increases the probability of the second ground.

8.1.2 Field Ground Protection

Field ground protection is provided by device 64F. The perception of the initial field ground as harmless has led to both trip and alarm applications of this relay. Proponents of the alarm application cite the ungrounded operation of the field and a desire to avoid the unscheduled loss of generation capacity as justification. Advocates of tripping argue that the initial ground may be a result of a mechanical failure such as a broken conductor. Continued operation carries the threat of additional mechanical failure. Also, burning of the rotor forging or at the retaining ring may result from arcing at the break. Such arcing would spray copper or aluminum along the rotor and on the stator winding as the rotor conductor is eroded. Another argument for tripping is that the second ground could be triggered immediately after the first.

Although immediate tripping is recommended for the initial ground, most installations alarm. When the alarm option is chosen, vibration monitoring equipment should be included in the design to trip the prime mover, field and generator breakers immediately. The vibration trip should be calibrated for maximum sensitivity. The unit should be tripped when the vibration level exceeds that normally experienced at synchronizing or for a system fault.

Tripping the unit will not immediately eliminate the vibration. If excess vibration were caused by unbalanced air-gap flux, it would decay at the same rate as the rotor current decays. This could take more than 10 sec. Vibration caused by thermal distortion of the rotor would not be significantly

© 2006 by Taylor & Francis Group, LLC

reduced by a unit trip. If critical speeds exist below nominal speed, this form of vibration can actually increase to damaging levels as the generator winds down after the trip.

Mason has suggested two levels of vibration protection. The first is the high-level trip, described above, to trip the prime mover, generator and field breaker with no time delay. The second trip would become active after the initial ground and respond to a lower level of vibration. This protection would trip the field and generator breakers after a time delay. The second level is designed for thermal-distortion-induced vibration. By tripping the field and generator breakers, the source of unbalanced rotor heating is removed. The prime mover is not tripped to maintain the generator at synchronous speed, thus avoiding vibratory peaks at reduced speed. The scheme also allows the rotor to cool while rotating, thus straightening itself.

8.1.3 Field Ground Detection

Several methods of detecting field grounds have been developed for use on generators with brushes. Brushes or slip rings are necessary to access the field windings. The simplest scheme is shown in Figure 8.1. Two lamps are connected across the field winding with the center point grounded. Normally, the lights will glow with equal brightness. If a ground occurs near one terminal, the light connected to that terminal will extinguish and the other light will show increased brilliance. As the fault is moved from the terminal toward the center of the winding, the difference in brightness between the two lamps will diminish. For a ground at the center of the winding, there will be no change in the lamps from the ungrounded conditions. Thus, a ground at the winding midpoint is not detectable.

The scheme in Figure 8.2 is similar, except the lamps are replaced by resistors and a meter or DC current relay is add in the ground connection. The relay scheme will indicate the presence of a ground, but will give no indication of location. A DC meter will give a positive- or negative-scale deflection depending on which half of the winding is grounded. Again, neither scheme will detect a ground at mid-winding.

The detection of a mid-winding ground requires an external voltage source. Such a scheme is shown in Figure 8.3. An AC voltage is applied to the field through a sensitive current relay. The small AC current that results has two components. The primary component is due to the field winding capacitance to ground, which can be between 0.3 and 0.7 μF on a large machine. A much smaller component is determined by the resistance of the field insulation. The field ground relay must be set above this leakage current. A capacitor is provided in series with the relay to limit the AC current in the event of a ground and to prevent a discharge of DC voltage through the AC circuit.

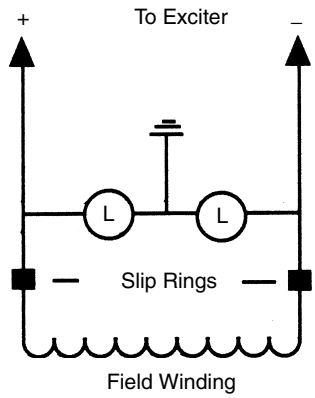


FIGURE 8.1 Indicating lamps.

© 2006 by Taylor & Francis Group, LLC

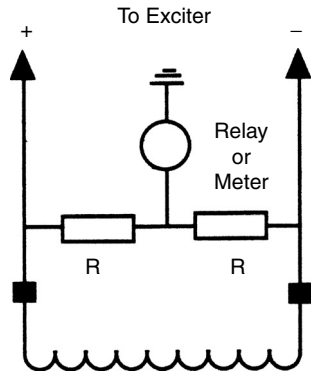


FIGURE 8.2 Relay or meter detection scheme.

A field ground anywhere in the winding will bypass the winding capacitance, increasing the current to actuate the relay. Similarly, deterioration of the insulation will increase the relay current. The impedance of the relay coil must be sufficient to limit the current in the event of a field ground to a safe value. Also, the reactance of the relay coil used in the AC scheme must be chosen to avoid resonance with the rotor capacitance.

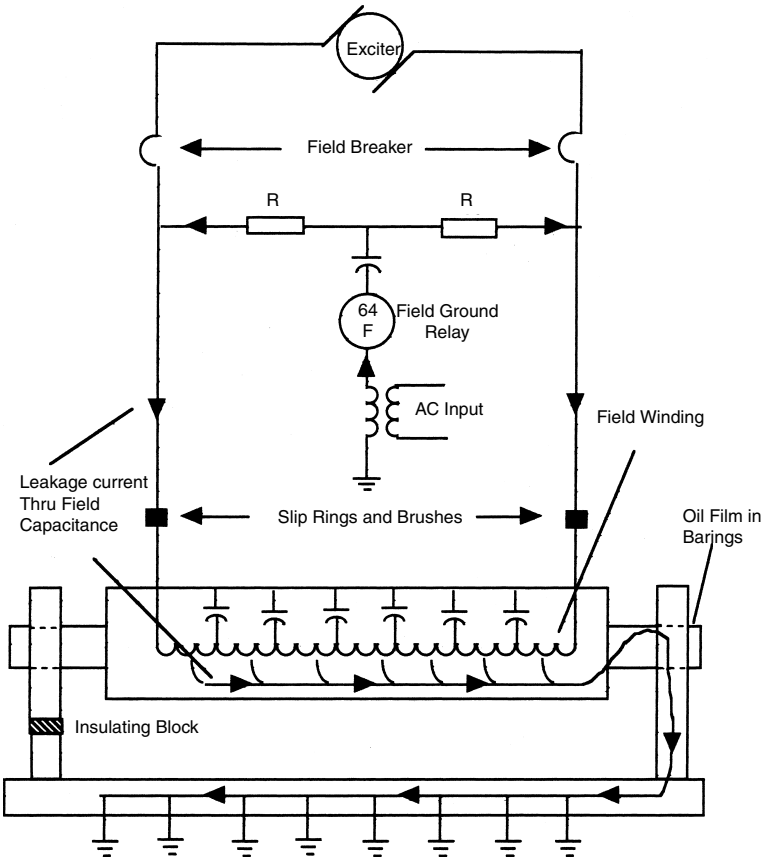


FIGURE 8.3 AC field ground detector. (From ABB Power T & D Company, *Protective Relaying Theory and Applications*, New York: Marcel Dekker. With permission.)

© 2006 by Taylor & Francis Group, LLC

This scheme has two potential problems. First, operation of the relay is completely dependent on the effectiveness of rotor grounding. If no other provisions are made, the only ground current path will be through the oil film of bearings with noninsulated pedestals. The oil film is not a reliable conduction path. For effective ground detection, the voltage impressed on the oil film must be sufficient to cause the oil film to break down and form a conduction medium. The variation of breakdown voltage is largely dependent on many parameters including oil quality and purity, film thickness, and bearing surface area.[2] The oil film can present sufficient impedance to prevent detection of high-impedance grounds. This problem would also affect the lamp and meter schemes described previously. The solution to this problem would appear simple. The AC driving voltage must be sufficiently high to ensure a breakdown of the oil film.

This brings us to the second problem with an AC scheme. If the bearing oil is conductive, a continuous current is established through the bearings. This current can cause bearing deterioration. Generator designers take great pains to insulate one or both generator bearing pedestals to prevent voltages developed along the generator shaft from inducing a circulation current through the bearings. The AC driven detection scheme negates this design.

The solution to the problems of ground path reliability and bearing current are complementary. If effective grounding is established by other means, bearing current is virtually eliminated. Although means of alternative grounding are a continuing subject of debate among equipment suppliers, alternative methods do exist. Many manufacturers provide grounding brushes that ride on slip rings attached to the generator shaft. The intent is to provide positive grounding and bypass current away from the bearings. This method is not universally accepted. Brushes that carry little or no current normally have a strong tendency to develop an insulating surface film. When a film develops, the brushes become no more reliable than the oil film for grounding. Bad brush conductivity also exposes bearings to current-induced wear.

Manufacturers have developed other means of grounding. One manufacturer provides grounding through water-seal glands or carbon-packing glands. Rotor grounding is generally not a problem with hydro turbines, because an effective ground path is usually established through the water in the turbine. When applying field ground protection, the turbine-generator manufacturers should be consulted regarding the effectiveness of rotor grounding.

Whatever the grounding method, it is good practice periodically to allow a ground jumper to ride the shaft and bypass the bearing oil and other grounding method to confirm that undetected grounds do not exist.

The continuous bearing current can also be eliminated if a DC driving voltage is chosen for the scheme. With a DC voltage source, current would flow only as a transient when the circuit is energized. Current flow will cease when the rotor to ground capacitance charges to the driving DC voltage. The elimination of the capacitive current drastically reduces the leakage current, allowing a more sensitive field ground relay setting. The DC source voltage will not improve ground detection through poor conductive bearing oil.

The scheme shown in Figure 8.4 employs both a DC driving voltage and a grounding brush. The source voltage must be connected to the field winding in additive polarity: DC source plus to field minus or vice versa. If this is not done, a blind spot will be created at the point in the winding where the field voltage is equal to, but opposite of, the DC source voltage. The sensitivity of the DC driven scheme in terms of the detectable resistance to ground is highly variable. The relay current is dependent on the fault resistance, location and the field voltage, which varies with generator load. The voltage applied to the fault increases as the fault moves from the negative terminal toward the positive terminal.

The relay current is given by

$$I_r = \frac{V_{dc} + d * V_{fd}}{R_g + R_c} \tag{8.1}$$

© 2006 by Taylor & Francis Group, LLC

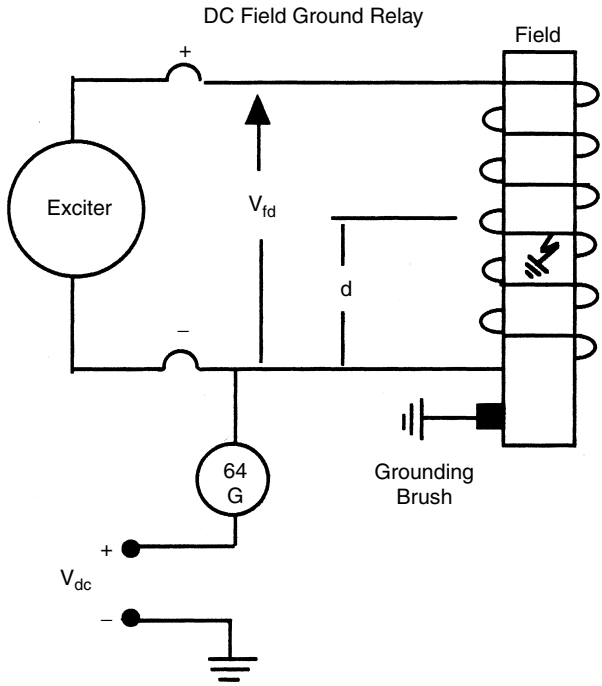


FIGURE 8.4 DC scheme with grounding brush.

where R_c = resistance of the relay circuit, and R_g = resistance of the ground fault. Then, the detectable fault resistance becomes

$$R_g = \frac{V_{dc} + d * V_{fd}}{I_r} - R_c \tag{8.2}$$

Equation (8.2) shows that the fault resistance sensitively increases as the fault moves toward the positive terminal and with increased field voltage.

The scheme in Figure 8.5 takes an alternative approach to full winding detection. A voltage divider is formed using two standard resistors and one nonlinear resistor. The nonlinear resistor's value is a function of voltage. A field ground will impose a voltage on the relay. The maximum voltage will be imposed for grounds at either the positive or negative terminal. As with the other divider schemes, a null point will exist in the winding where no voltages will be impressed on the relay. Such a ground would be undetectable if it where not for the nonlinear resistor. As the exciter voltage varies with the daily load cycle, the value of the nonlinear resistor also changes, varying the location of the null point. This scheme provides 100% field winding coverage provided the generator does not have a fixed load. If this is the case, the push button is provided to shift manually the null point.

8.1.3.1 Field Ground Relay Selection and Settings

Field ground relays are electromechanical or solid-state. This function is not included in multifunction microprocessor relays. Field ground relays are chosen on the basis of voltage rating. The rating must exceed that of the operating field voltage. The relay must also withstand the maximum forcing voltage capability of the excitation system.

© 2006 by Taylor & Francis Group, LLC

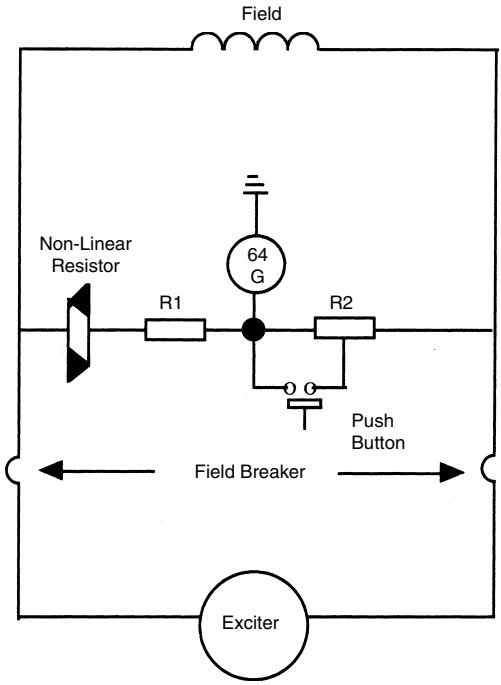


FIGURE 8.5 Nonlinear voltage divider scheme. (From ABB Power T & D Company, Protective Relaying Theory and Applications, New York: Marcel Dekker. With permission.)

A majority of these have fixed settings intended to provide an optimal balance between sensitivity and security. The relays are always applied with a time delay that will range from 2 to 30 sec. The delay is necessary to field override transients.

8.2 FIELD OVERCURRENT PROTECTION

The field circuit is designed for continuous operation at a current equal to that required for full generator load at rated power factor and voltage. This current is abbreviated as AFFL (amps of the field at full load). This current rating also defines the lagging reactive output capability of the generator by forming the top portion of the generator capability curve as shown in Figure 1.4.

Field current in excess of rated field amps (AFFL) can result from power system disturbances, shorted field turns, or excitation equipment malfunctions. The field winding does have short time overload capabilities. Overcurrent protection is required to assure that this capability is not exceeded. Overcurrent protection of the field is not straightforward. The protection scheme must not only prevent thermal damage from excess field currents, but must also permit field forcing to the full capability of the winding. The protection scheme must also include consideration for operation on both the automatic and manual voltage regulator.

The field winding short time overload capabilities as define by ANSI C50.13-1989 are shown in Figure 8.6. Note that the field short time overload curve is defined as a function of rated field voltage. Rated voltage or volts of the field at full load (VFFL) is equal to AFFL × field resistance.

8.2.1 Field Overcurrent Transients

Faults and switching operation on the power system will reduce voltage at the generator terminals. The automatic voltage regulator will sense voltage less that the setpoint voltage and initiate field forcing. With the high-gain excitation systems used today, a small voltage dip will result in

© 2006 by Taylor & Francis Group, LLC

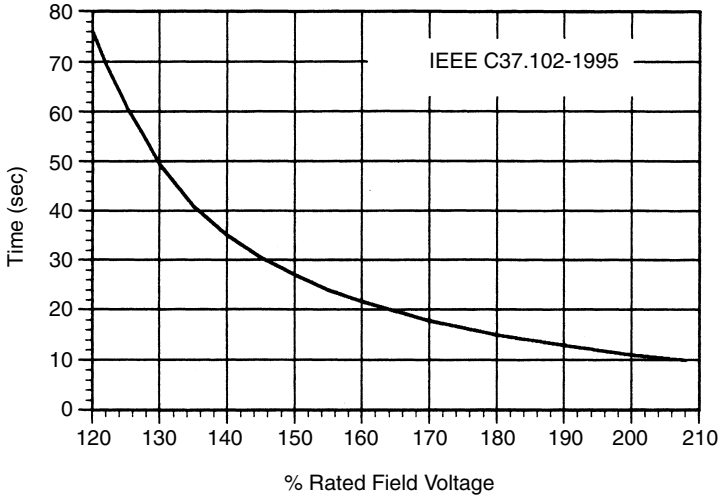


FIGURE 8.6 Field short time overload capability. (From IEEE Std C37.102-1995, IEEE Guide for AC Generator Protection. With permission.)

almost instant application of the maximum excitation voltage to the field winding. The field current that actually determines the air-gap flux and with it the output voltage will increase at a rate set by the effective field time constant. Several seconds will be required for the field current to reach its maximum sustained value of 1.25 to 1.8 times AFFL for most units.

Most disturbances are short-lived, allowing the terminal voltage and field current to return to normal in less than a second. However, disturbances can last much longer. A large-scale power system disturbance can cause a voltage depression that is sustained for minutes. This type of disturbance is a symptom of an acute system Var shortage. If the power system is to remain viable through such a transient, maximum Var support is required from every operating generator on the system. Therefore, field overcurrent protection should be designed to utilize the full field forcing capability of the field winding.

Shorted turns may result from a mechanical failure or a deterioration of the field insulation. Often, multiple turns short-circuit over a period of time and do not initially cause high-magnitude current or vibration that disrupts operations. Nor do they always result in field grounds. Severe consequences are of course possible, but are generally not realized. As turns are lost, field current must be increased to maintain the amp-turns necessary to hold the generator output voltage and Var output at a desired value.

If the generator is under the control of the manual regulator, the field current increase will be determined by the reduced winding resistance and the fixed field voltage applied by the regulator. If the resulting amp-turns are insufficient to maintain the desired output, the operator will need to increase the field current to compensate. When the automatic voltage regulator is in service, the field current is automatically increased to hold the generator output voltage equal to the regulator set point voltage.

Because the increase in field current is often subtle, the only indication of a turn failure can be a small increase in the field current necessary to maintain a given voltage or Var output. Obviously, shorted turns will require field current to exceed the field circuit rating for long periods of time. However, overcurrent protection must be set above rated current with sufficient margin to allow for measurement and setting tolerances and the pickup to dropout ratio of the relay. As a result, overcurrent protection is usually unable to detect the condition until a significant portion of the field winding is involved. A more effective method of early detection is an operator's log of loading vs. field current or a periodic log of field resistance calculated from online data. Increases in field current or a reduction in field resistance will indicate shorted rotor turns.

© 2006 by Taylor & Francis Group, LLC

Excitation system failure can pose the most serious threat to the field winding and associated equipment. A loss of the generator voltage signal to the automatic voltage regulator would be a simple example. This failure would appear to the voltage regulator as a zero voltage condition at the generator terminals. The excitation system would respond by applying maximum ceiling voltage to the field in an attempt to restore the terminal voltage. If no protective action were taken, ceiling voltage would remain on the field until a winding or excitation system failure occurred. It is also worth noting that the maximum ceiling voltage is usually a settable parameter within the voltage regulator. A regulator control failure could result in sustained field voltage in excess of the ceiling value. Also, many voltage regulators include field overcurrent protection and control modules integrated into the regulator circuitry. These circuits cannot be relayed on to provide field protection in the event of a regulator malfunction. Backup protection independent of the regulator is required at such an installation.

8.2.2 Overcurrent Protection Schemes

Field overcurrent detection is accomplished by a direct measurement of field current or field voltages as shown in Figure 8.7. Device 76 can be a contact-making milliammeter or DC current relay connected across a shunt to read current directly. The shunt would be chosen to provide proper scaling for the meter or relay applied. For example, if a relay had a range of 0–50 mV and full load field current was 900 A, a 1500 A–50 mV shunt could be chosen to give the relay an operating range of 0–1500 A DC. An alternative method of detection is a DC voltage relay connected across the field winding, device 59F. The DC voltage is related directly to the field current by the field resistance. In both cases, the relay used must have a high pickup to dropout ratio and tripping would be accomplished through a timer.

On small units, either device 59F or 76 can be applied to trip the generator and field breaker and the prime mover directly after a time delay. On a larger installation, both devices may be applied for redundancy. The trip logic is also more complex on larger units. The intent is to maintain the unit online as long as possible, tripping only when field winding damage is imminent. This is vital during a severe system disturbance, because the premature loss of a large unit and its Var output can lead to a system collapse.

There are many different schemes used to meet this objective. The scheme logic shown in Figure 8.8 is typical for field overcurrent protection. Field current is allowed to exceed rated current (AFFL) up to a preset value, 110% in this example. Above that threshold, protective circuits

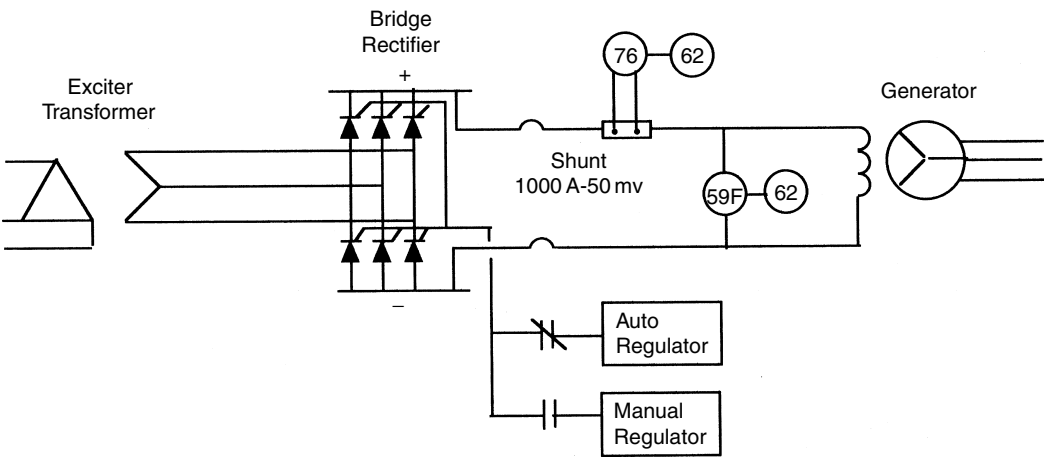


FIGURE 8.7 Field protection with DC relays.

© 2006 by Taylor & Francis Group, LLC

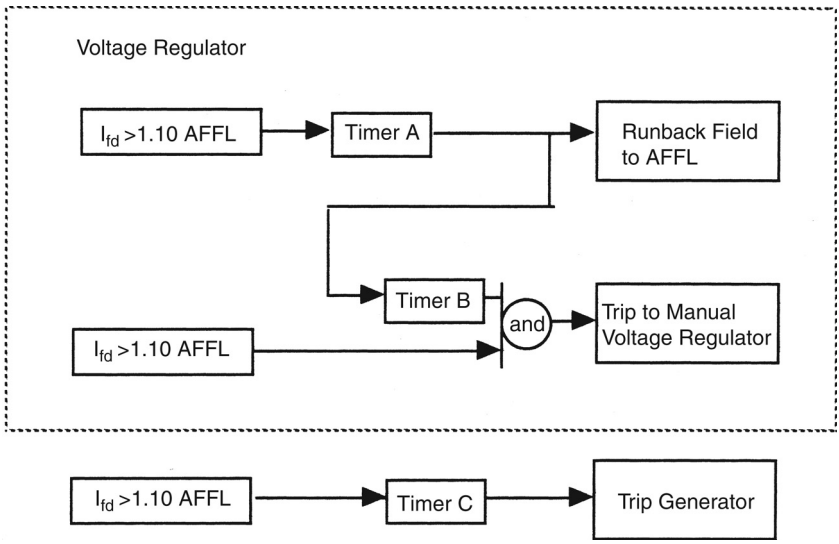


FIGURE 8.8 Field protection logic.

are activated. Timer A would be actuated by device 59F and/or 76. When it times out, the automatic voltage regulator takes action to "runback" field current to a value below the actuation current. If the automatic regulator fails to reduce the current when timer B operates, an automatic regulator failure is assumed and the generator is switched from automatic to the manual regulator. The manual regulator output is limited to a current slightly above AFFL. If the current has not reduced to a value below the actuation current after switching to the manual regulator when timer C actuates, a complete regulator failure is assumed and the generator is tripped. All these actions must be accomplished within the permissible overload capability of the field as defined by ANSI C50.13 (Figure 8.6). If the overcurrent detection and control for the runback and automatic regulator trip are integral to the automatic regulator circuitry, independent generator trip logic must be provided.

The major disadvantage of this scheme is the fixed time delay. The timer must be set to coordinate with the field permissible overload curve at the maximum field current. This fixed delay will severely limit field-forcing time at lower currents. Figure 8.9 shows that replacing the fixed delay "A Timer" with an inverse overcurrent function would provide much better coordination with the permissible overload curve and allow longer periods of field forcing at the lower field current. The major problem with this solution is that DC relays applicable as Device 59F or 76 relays are generally not available with inverse time characteristics. Electronic voltage regulators often have circuitry that provides protection logic similar to Figure 8.8 with inverse time characteristics. These schemes provide an optimal balance between utilization of the field winding overload capability and field winding protection. But again, if the trip circuitry is integrated into the regulator logic, it can be rendered inoperative by the same regulator malfunction that causes the field overcurrent. External backup trip logic is required for this type of installation. A problem arises because the backup protection is provided by a fixed-time DC relay that will not coordinate with the inverse-time characteristics provided with the regulator protection circuitry.

8.2.3 Application of AC Relays to Protect the Field Winding

The majority of excitation systems installed today derive DC power from three-phase rectifiers. At these installations, an inverse-time protection characteristic can be obtained by utilizing AC relays at the input side of the rectifier, as shown in Figure 8.10. The current and voltage at the relay

© 2006 by Taylor & Francis Group, LLC

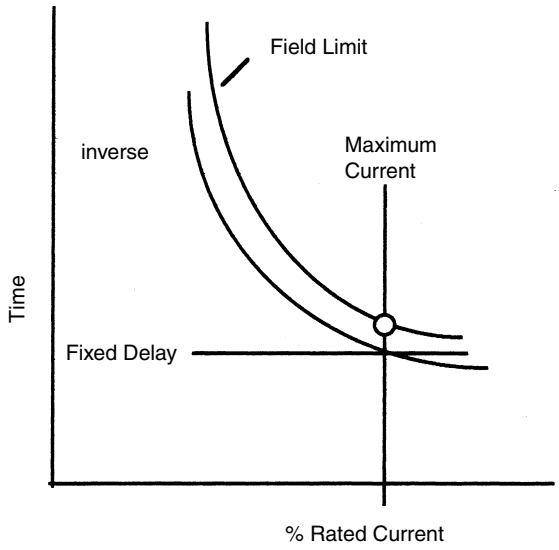


FIGURE 8.9 Fixed time vs. inverse time protection.

location are not sinusoidal; therefore, the key to successful application is an understanding of the relay response to the input waveforms.

8.2.3.1 Basic Rectifier Operation

A brief discussion of rectifier basics is in order. There are many configurations for three-phase power rectifiers. The most common used in excitation circuits is the six-phase double-way rectifier shown in Figure 8.11. The DC load current is continually transferred from one phase to the next as the phase voltage varies to forward-bias each diode in succession. If the rectifier supplied a purely resistive load, the DC voltage and current would have significant ripple corresponding to the peaks of each AC phase voltage. The generator field circuit is highly inductive and acts as a filter, smoothing the DC voltage and DC current to a flat nearly ripple-free waveform.

The idealized rectifier circuit has no reactance in the AC supply circuit. When the DC current is switched from phase to phase the AC line current appears as a square wave. This is illustrated in

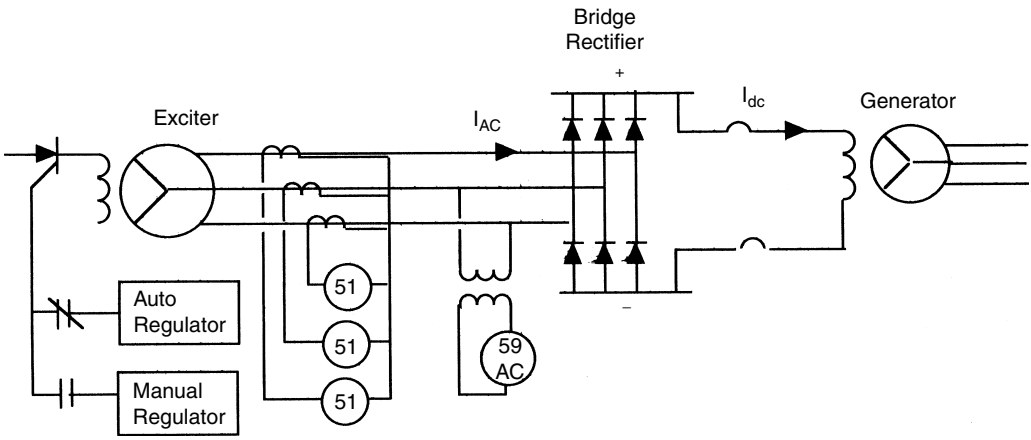


FIGURE 8.10 Field protection with AC relays.

© 2006 by Taylor & Francis Group, LLC

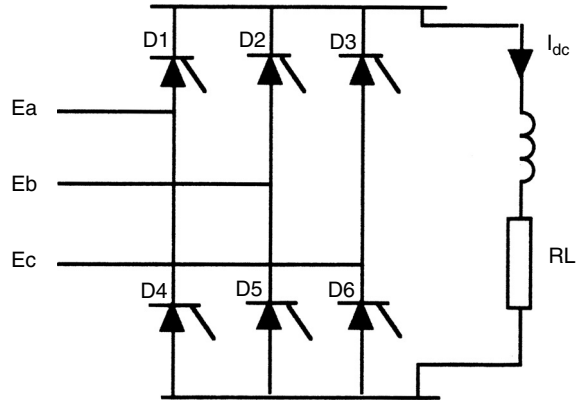


FIGURE 8.11 Six-phase wye, double-way rectifier.

Figure 8.12. During the period when phase A voltage is more positive than phases B and C, diode 1 will conduct. When B phase voltage becomes more positive than phase A, diode 1 turns off and diode 2 begins conduction; with this, phase A current ceases and B phase current begins. Under the idealized condition, the current in each phase current will be a square wave with a magnitude equal to I_{dc}. Each diode would conduct for 120° and each phase would carry alternate positive and negative square-wave current pulses for a total of 240°.

The introduction of reactance into the AC supply circuit causes distortion of the voltage at the input to the rectifier and to the square-wave current. Current in an inductive circuit cannot change instantaneously; therefore, the switching of load current from one diode to the next cannot occur instantaneously. Instead, a transient circulating current is generated between the two switching phases during each switching period, as shown in Figure 8.13. The transient current acts to transfer load current to the newly conducting phase. The transfer current also causes a voltage drop across each phase reactance, resulting in phase voltage notches (Figure 8.14). The voltage

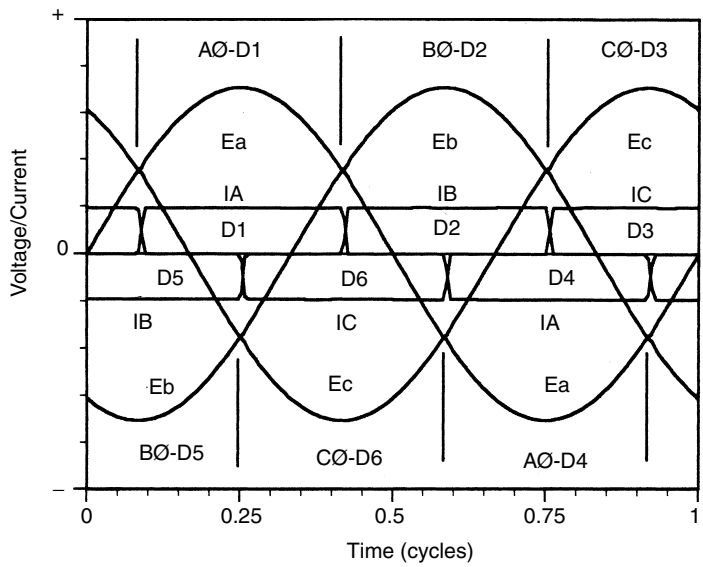


FIGURE 8.12 Rectifier phase conduction.

© 2006 by Taylor & Francis Group, LLC

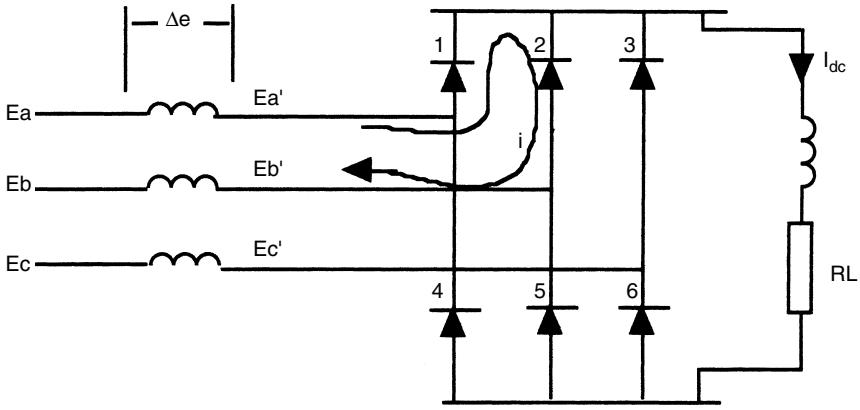


FIGURE 8.13 Commutating current.

drop, known as the commutating voltage drop, reduces the DC output voltage of the rectifier. In effect, the AC circuit reactance appears as a resistance from the DC side of the rectifier.

The commutation voltage drop increases with increased DC load current and/or increased AC system reactance. The equivalent DC voltage drop resulting from AC system reactance is given by

$$\Delta E_{dc} = \frac{sp}{2\pi} X_{com} I_{dc} \text{ V (volts)} \tag{8.3}$$

where $X_{com} = 60$ Hz reactance/Ø in Ω, $I_{dc} =$ DC load current on bridge in amps, and s, $p =$ constants determined by the rectifier configuration.

The commutating reactance is the per-phase reactance of the AC supply circuit. The DC output voltage under load is found by subtracting the commutation drop and resistance drop from the open-circuit DC voltage.

The open-circuit DC output voltage for a phase-controlled rectifier is given by

$$E_{do} = \frac{s\sqrt{2}\pi}{p} E_s \sin\left(\frac{\pi}{p}\right) \cos\alpha \text{ (volts)} \tag{8.4}$$

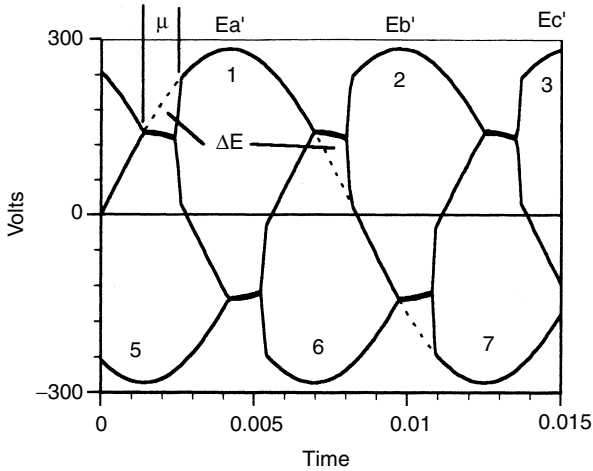


FIGURE 8.14 Effect of commutation on phase voltage.

© 2006 by Taylor & Francis Group, LLC

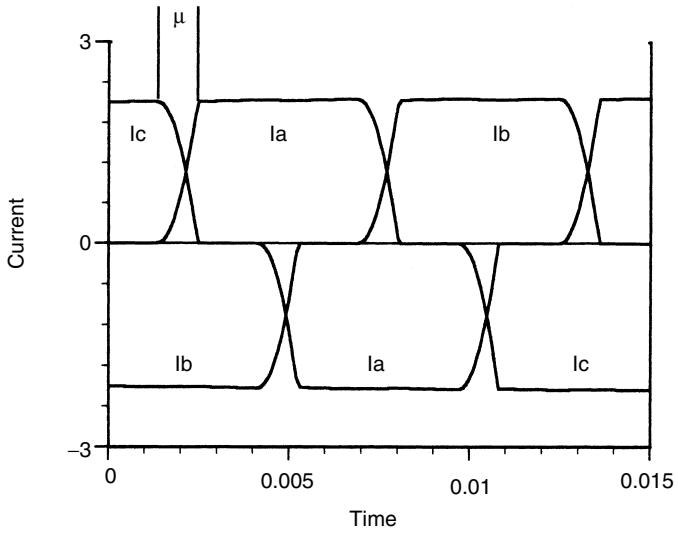


FIGURE 8.15 Effect of commutation on phase current.

where E_s = AC system phase-to-ground voltage RMS, and α = firing angle for phase-controlled bridge.

The rectifier constants for various configurations can be found in Ref. [5]. The constants for the six-phase double-way rectifier shown in Figure 8.11 are $s = 2$ and $p = 3$. The resulting DC commutation voltage drop and output voltage are then

$$\Delta E_{dc} = 0.955 X_{com} I_{dc} \text{ V} \tag{8.5}$$

$$E_{dc} = 2.34 E_s \cos\alpha - 0.955 X_{com} I_{dc} \tag{8.6}$$

During the commutation, both switching diodes are conducting and the sum of the instantaneous current in the two commutating phases is equal to the load current. The resulting current waveform is shown in Figure 8.15. The period of overlapping conduction is defined by the commutation angle μ. The commutating angle in radians is calculated from the following:[3]

$$\mu = \cos^{-1}\left(1 - \frac{2\Delta E_{dc}}{E_{do}}\right) \text{ (radians)} \tag{8.7}$$

8.2.3.2 Relay Quantities

The commutating angle can relate the DC load current and AC system reactance to the RMS and fundamental frequency component of phase current and voltage at the input side of the rectifier. These relationships are necessary when AC relaying is applied to protect DC system components. Electromechanical overcurrent relays tend to response to RMS quantities. Front-end filtering and sampling circuits determine the relay response of solid-state and microprocessor relays. Many microprocessor relays measure the fundamental frequency component, while some solid-state relays use peak detecting circuitry. Whatever the case, the quantity measured by the relay and the relation between that quantity and the DC field quantity must be known.

Because phase current is an approximate square wave with amplitude equal to the DC load current, peak detecting relays will in effect respond to a current equal to the DC current.

The following equations relate the RMS and fundamental frequency components of the current and voltage appearing on the AC side of the rectifier to DC quantities at the rectifier output

© 2006 by Taylor & Francis Group, LLC

terminals. These equations are derived assuming the flat DC waveform characteristic of a highly inductive load such as the generator field circuit.

The fundamental frequency component from Ref. 3:

$$I_{\text{fund}} = \frac{\sqrt{3}I_{\text{dc}}}{\sqrt{2}\pi}\sqrt{a_{\text{fund}}^2 + b_{\text{fund}}^2} \tag{8.8}$$

$$a_{\text{fund}} = \cos\ \alpha + \cos(\alpha + \mu) \tag{8.9}$$

$$b_{\text{fund}} = \frac{\sin(2\mu + 2\alpha) - \sin\ 2\alpha - 2\mu}{2[\cos\alpha - \cos(\mu + \alpha)]} \tag{8.10}$$

The RMS current, again from Ref. 3, is given by

$$I_{\text{RMS}} = \frac{\sqrt{2}I_{\text{dc}}}{\sqrt{3}}\sqrt{1 - 3f(\mu, \alpha)} \tag{8.11}$$

$$f(\mu, \alpha) = \left\{\frac{\sin\mu[2 + \cos(\mu + 2\alpha)] - \mu[1 + 2\cos\alpha\cos(\mu + \alpha)]}{2\pi[\cos\alpha - \cos(\mu + \alpha)]^2}\right\} \tag{8.12}$$

The relationship between the RMS voltage at the input to the bridge and the DC output voltage from Ref. 4, is given by

$$E_{\text{s}}(\text{RMS}) = \frac{4\pi - 3(2\mu - \sin\ 2\mu)}{6\sqrt{6}(1 + \cos\ \mu)}E_{\text{dc}} \tag{8.13}$$

The fundamental voltage component at the input to the rectifier would be found by subtracting the voltage drop caused by the fundamental current component from the source voltage.

The relationships between the commutating angle and the AC side components are plotted in Figure 8.16, assuming the bridge is full-on ($\alpha = 0$).

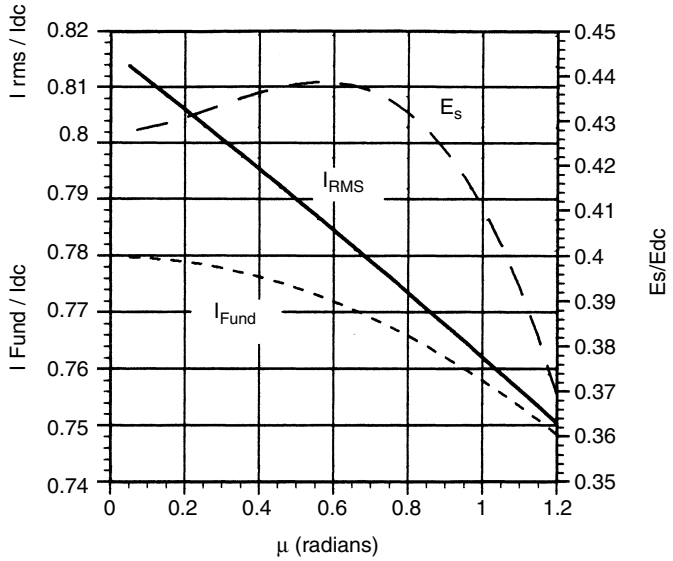


FIGURE 8.16 Fundamental and RMS components of AC current.

© 2006 by Taylor & Francis Group, LLC

8.3 SETTINGS FOR FIELD OVERCURRENT/OVERVOLTAGE RELAYS

The field overcurrent logic is normally set to actuate at 105 to 115% of AFFL or VFFL. Generator manufacturers often have recommended settings. When this is the case, the recommended setting should be used.

The pickup settings for DC relays 59F or 76 as applied in Figure 8.7 are straightforward. The setting must be above AFFL or VFFL with sufficient margin to permit operation at rated kVA output at 105% rated terminal voltage. An allowance for relay and measurement error must be included.

Another important consideration is the dropout to pickup ratio of the relay. Assume the 76 relay has a dropout to pickup ratio of 92%. Then the relay cannot be set less than $1/0.92$ or $1.09\times$ rated current. If this relay were set at 105% rated field current and the generator was operating at rated load, a system transient could occur, causing a momentary field current excursion above the relay set point. Although the field current quickly returns to its rated value, the relay will not drop out because rated current is above the minimum dropout current of 97% (105% × 0.92). A trip will be initiated with the generator at rated field current when the scheme timers time out. The same considerations apply to the 59F relay.

8.3.1 Full Load Values

Whatever scheme is used for field overcurrent protection, a value for AFFL or VFFL must be known. AFFL is given on the generator data sheet; VFFL is not, but can be calculated.

VFFL is the voltage across the field winding at rated output and with the field winding at normal operating field temperature:

$$VFFL = R_{\mathrm{fd}_{T0}} \times \mathrm{AFFL} \tag{8.14}$$

where $R_{\mathrm{fd}_{T0}}$ = field R at operating temperature.

The field resistance provided on the generator data sheet is given at 25°C and must be adjusted to the operating temperature of the field at full load. The operating temperature (T_0) may be available from the generator test report or from the manufacturer. The variation of resistance with temperature for a copper conductor is

$$R_{\mathrm{fd}_{T0}} = R_{\mathrm{fd}_{25^\circ\mathrm{C}}} \frac{T_0{}^\circ\mathrm{C} + 234.5}{25^\circ\mathrm{C} + 234.5} \tag{8.15}$$

8.3.2. Maximum Field Current

The margin between the short time overload capability curve for the field winding and a protective device characteristic declines as current increases. The maximum attainable field current determines the time-delay setting for the field overcurrent protection. This is shown in Figure 8.9. The maximum coordinating current is the DC current available from the excitation system with maximum input voltage and limited only by circuit impedance. A value for this current can be obtained from the manufacturer or it can be calculated if sufficient exciter data are available. When the manufacturer is contacted for this information, he should provide the maximum current available in the event of a regulator failure. The data the manufacturers often provided are the maximum forcing current or ceiling voltage as set by control circuitry within the regulator and may not be the maximum values that could occur if regulator control fails.

8.3.3 Maximum Field Current from a Bridge Rectifier

The maximum field current can be estimated for a six-diode double-way rectifier if the commutating reactance and maximum bridge input voltage are known. The commutating reactance has a

© 2006 by Taylor & Francis Group, LLC

strong influence on the maximum DC current a rectifier can deliver to the field winding and must be considered in the maximum current calculation. The commutating reactance can be the reactance of the excitation supply transformer or for a bridge supplied from a rotating exciter it would be X''_d of the exciter.

The maximum DC field current from a bridge rectifier is calculated as follows. The output of a six-diode bridge was given in Equation (8.6) as

$$E_{dc} = 2.34E_s \cos \alpha - 0.955X_{com}I_{dc} \quad \text{(volts)} \tag{8.16}$$

The DC output voltage of the bridge is also equal to the field voltage, $E_{dc} = I_{dc} R_{fd}$. Neglecting other circuit resistance, the DC output voltage becomes

$$E_{dc} = I_{dc}R_{fd} = 2.34\,E_s - 0.955X_{com}I_{dc} \quad \text{(volts)} \tag{8.17}$$

The DC current is then

$$I_{dc} = \frac{2.34\,E_s \cos \alpha}{R_{fd} + 0.955X_{com}} \quad \text{(amps)} \tag{8.18}$$

The maximum DC current available to the field circuit will occur if the bridge is turned full on ($\alpha = 0$). Note that voltage regulator control circuitry usually limits the minimum firing angle to about 15° but with a regulator failure this limit is also assumed to fail.

8.4 APPLYING FIELD OC PROTECTION ON THE SAMPLE SYSTEM

Field overcurrent protection for the sample system generator will consist of AC current and voltage relays connected as shown in Figure 8.10. Relay 59AC has a pickup range of (55–125 V) in 10 V steps. The time overcurrent relay has a range of (3.6–5.0 A) in 0.2 A steps. Both relays are electromechanical with inverse-time characteristic and dropout to pickup ratios of 95%. Also, both relays are responsive to the RMS value of voltage/current in the AC supply circuit. The inverse-time characteristic of each relay will be substituted into the logic from Figure 8.8 as timer A.

8.4.1 Rated Field Voltage

First, the rated field current and voltage must be determined. The rated field current (AFFL) and the field resistance are found on the generator data sheet in Appendix A.

AFFL = 849 A
$R_{fd} = 0.308\ \Omega$ at 25°C

Rated field voltage is calculated from the field resistance at the operating field temperature. The data sheet quotes the generator time constants at a field temperature of 125°C. We will assume that this is the operating temperature of the field winding. The field resistance at 125°C

© 2006 by Taylor & Francis Group, LLC

is found using Equation (8.15):

$$\begin{aligned} R_{\mathrm{fd}_{T0}} &= R_{\mathrm{fd}_{25^\circ\mathrm{C}}} \frac{T_0{}^\circ\mathrm{C} + 234.5}{25^\circ\mathrm{C} + 234.5} \\ &= 0.308 \frac{125^\circ\mathrm{C} + 234.5}{25^\circ\mathrm{C} + 234.5} \\ &= 0.427\,\Omega \,@\, 125^\circ\mathrm{C} \end{aligned} \tag{8.19}$$

Rated field voltage is calculated as

$$\begin{aligned} VFFL &= AFFL \times R_{\mathrm{fd}_{125^\circ\mathrm{C}}} = 849\,\mathrm{A} \times 0.427\,\Omega \\ &= 363\,\mathrm{V\ DC} \,@\, 125^\circ\mathrm{C} \end{aligned} \tag{8.20}$$

8.4.2 Maximum Available Field Current

The commutating reactance in this example is determined by the exciter and will be equal to X''_{d}. The exciter is a 450 kVA machine rated 480 V and $X''_{\mathrm{d}} = 24\%$.

$$I_{\mathrm{FL}} = \frac{450\,\mathrm{kVA}}{\sqrt{3}\,480\,\mathrm{V}} = 541\,\mathrm{A} \tag{8.21}$$

$$Z_{\mathrm{base}} = \frac{E_{\varnothing \mathrm{n}}}{I_{\mathrm{FL}}} = \frac{277\,\mathrm{V}}{541\,\mathrm{A}} = 0.512\,\Omega \tag{8.22}$$

$$X_{\mathrm{com}} = 0.24 \times 0.512 = 0.123\,\Omega \tag{8.23}$$

The maximum field current available is determined from Equation (8.18); with the bridge "full on" ($\alpha = 0$) we will neglect other circuit resistance:

$$I_{\mathrm{dc}} = \frac{2.34 E_{\mathrm{s}} \cos\alpha}{R_{\mathrm{fd}} + 0.955 X_{\mathrm{com}}} \tag{8.24}$$

$$I_{\mathrm{dc}} = \frac{2.34 \times 277}{0.427 + 0.955 \times 0.123} = 1190\,\mathrm{A} \tag{8.25}$$

The maximum available current is $1190/849 = 1.40 \times$ AFFL.

8.4.3 Pickup Setting

Field over current protection is normally set to actuate between 1.05–1.10 times the full load field current or voltage. A setting of 1.05 will be used here to optimize field overcurrent protection.

A combined error of 3% is assumed for the relay setting and measurements. Both relays have dropout to pickup ratios of 98%.

The minimum DC pickup settings are then

$$I_{\mathrm{pu}} = \mathrm{AFFL} \times 1.03 \times 1.05/0.98 = 1.1 \times \mathrm{AFFL} = 1.1 \times 849\,\mathrm{A} = 934\,\mathrm{A\ DC}$$
$$V_{\mathrm{pu}} = \mathrm{VFFL} \times 1.03 \times 1.05/0.98 = 1.1 \times \mathrm{VFFL} = 1.1 \times 363\,\mathrm{V} = 399\,\mathrm{V\ DC}$$

The above DC set points must be related to the RMS quantities sensed by the AC relay. This relationship is defined by the commutating angle μ and firing angle α.

© 2006 by Taylor & Francis Group, LLC

The firing angle of the bridge when operating at the pickup current and voltage can be calculated from Equation (8.6) as

$$\alpha = \cos^{-1}\left[\frac{399 + 0.955 \times 934 \times 0.123}{2.34 * 277}\right] = 0.668 \quad \text{(radians)}$$

Neglecting diode drop (approximately 0.5 V/diode) and brush drop (approximately 2.0 V total for two brushes), $X = X''_{\mathrm{d}} = 0.123\ \Omega$ and $R = R_{\mathrm{fd}} = 0.427\ \Omega$. The commutation voltage drop is calculated from Equation (8.5) as

$$\begin{aligned}\Delta E_{\mathrm{dc}} &= 0.955 I_{\mathrm{dc}} X_{\mathrm{comm}} \\ &= 0.955 * 934\,\mathrm{A} * 0.123\,\Omega = 109.7\,\mathrm{V}\end{aligned} \tag{8.26}$$

The commutation angle is then determined from Equation (8.7):

$$\begin{aligned}\mu &= \cos^{-1}\left(1 - \frac{2\Delta E_{\mathrm{dc}}}{E_{\mathrm{d0}}}\right) \\ &= \cos^{-1}\left(1 - \frac{2 * 109.7}{2.34 * 277}\right) = 0.848\,\text{radians}\end{aligned} \tag{8.27}$$

The ratio of RMS to DC at pickup can now be determined from Equation (8.11) through Equation (8.13) or from Figure 8.16.

Using the equations with firing angle $\alpha = 0.668$ radians (38.3°):

$$f(\mu,\alpha) = \left\{\frac{\sin(0.848)[2+\cos(0.848+2\times0.668)] - 0.848(1+2\cos(0.668)\cos(0.848+0.668)]}{2\pi[\cos(0.668) - \cos(0.848+0.662)]^2}\right\}$$

$$= 0.044 \tag{8.28}$$

$$I_{\mathrm{RMS}} = \frac{\sqrt{2} I_{\mathrm{dc}}}{\sqrt{3}}\sqrt{1 - 3 * 0.044} = 0.761_{\mathrm{dc}} \tag{8.29}$$

$$E_{\mathrm{s}} = \frac{4\pi - 3[2 * 0.848 - \sin(2 * 0.848)]}{6\sqrt{6}(1+\cos 0.848)} E_{\mathrm{dc}} = 0.428 E_{\mathrm{dc}} \tag{8.30}$$

The required relay pickup values in terms of AC quantities are found to be

$$\begin{aligned}I_{\mathrm{RMS}} &= 934\,\mathrm{A\,DC} \times 0.761 = 711\,\mathrm{A\,RMS} \\ E_{\mathrm{RMS}} &= 399\,\mathrm{V\,DC} \times 0.428 = 171\,\mathrm{V\,PHASE\text{-}NEUTRAL\,RMS} \\ &\quad 171\,\mathrm{V} \times \sqrt{3} = 296\,\mathrm{V\,PHASE\text{-}TO\text{-}PHASE\,RMS}\end{aligned}$$

The voltage relay is supplied from a 480/120 V transformer. The secondary voltage seen by the relay at the desired pickup is:

$$\mathrm{AC\,pickup} = 296\,\mathrm{V} \times 120/480 = 74\,\mathrm{V\,RMS}$$

Choosing the closest available tap 59AC is set on the 75 V tap, then the pickup becomes:

$$75\,\mathrm{V} \times 480/120 = 300\,\mathrm{V}\ \text{at the}\ 480\,\mathrm{V}\ \text{circuit}$$

© 2006 by Taylor & Francis Group, LLC

The current relays are supplied from 1000/5 CTs. The relay current at the desired pickup is

$$\text{AC pickup} = 711\,\text{A} \times 5/1000 = 3.55\,\text{A RMS}$$

Set relay 51 on the 3.6 A tap, then pickup is

$$3.6 \times 1000/5 = 720\,\text{A in the } 480\,\text{V circuit}$$

8.4.4 Time Delay

The time–current characteristic of each relay must be plotted against the field permissible overload curve (Figure 8.6). Then the distance between the relay characteristic and the limit curve will be the time allowed for timers B and C in Figure 8.8 to operate. Five seconds will be allowed for each timer. Therefore, the withstand curve and the relay curve must be separated by at least 10 sec at the maximum field current of 1.4× rated.

To plot the relay characteristics against the field current limit, the relay setting must be expressed in terms of rated field amps or volts. The relay settings are referenced to the DC circuit by Equation (8.29) and Equation (8.30):

$$I_{dc} = I_{pu}\,(\text{RMS})/0.761 \tag{8.31}$$

$$V_{dc} = E_{pu}\,(\text{RMS})/0.428 \tag{8.32}$$

The equivalent DC settings are

$$\begin{aligned} I_{dc}\,(\text{trip}) &= 3.6\,\text{A} * (1000/5)/0.761 = 946\,\text{A} \\ &= 946\,\text{A}/849\,\text{A} = 1.11\,\text{AFFL} \end{aligned} \tag{8.33}$$

$$\begin{aligned} V_{dc}\,(\text{trip}) &= 75\,\text{V} * (480/120)/(\sqrt{3} * 0.428) = 404.7\,\text{V} \\ &= 404.7\,\text{V}/363\,\text{V} = 1.12\,\text{VFFL} \end{aligned} \tag{8.34}$$

Remember that the above equivalent DC trip settings are based on the RMS to DC ratio defined at the pickup current and voltage. This ratio changes with DC current. At the maximum exciter current (1.4 × rated) these ratios become

$$I_{RMS}/I_{dc} = 0.765 \quad V_{RMS}/V_{dc} = 0.415$$

in this instance the ratio change has little effect on the current setting put at the higher current the voltage relay's DC trip setting increases to

$$V_{dc}\,(\text{trip}) = 300\,\text{V AC}/(\sqrt{3} * 0.415) = 417\,\text{V DC}$$

or

$$417\,\text{V}/363\,\text{V} = 1.15\,\text{V FFL}$$

Both relay characteristics are plotted against the field short time capability limit on Figure 8.17. Relay characteristics plotted as solid lines are plotted using the RMS/dc ratio at the pickup current or voltage. The dotted characteristic represents the equivalent 59AC characteristic at maximum current (1.4 × rated). A time delay TD # 7 was chosen to maintain 10 sec between the relay curves and the field limit at the maximum field current of 1.4 × rated. Note that neither

© 2006 by Taylor & Francis Group, LLC

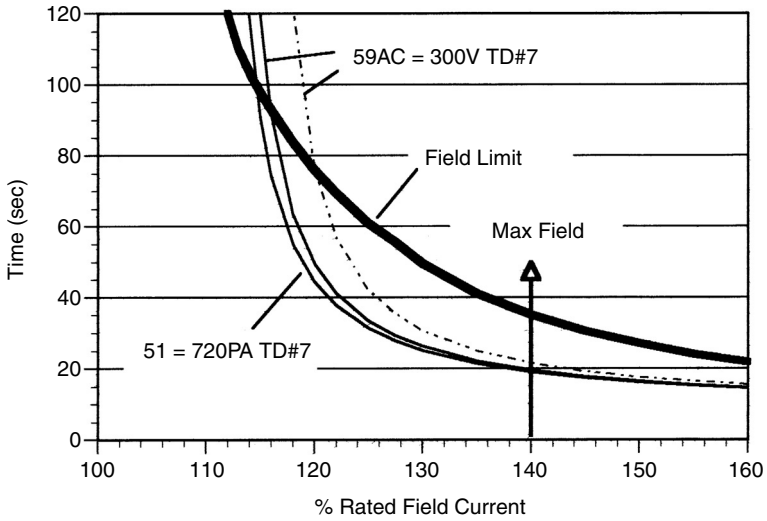


FIGURE 8.17 AC overcurrent relay vs. field short time limit.

relay provides complete protection of the field winding. Relay operating times exceed the field limit at the lower overload currents because the shape of the relay time current characteristic does not match that of the limit and because the relay pickup settings are greater than 1.0× rated current. To improve protection relay trip characteristics more closely matched to the limit curve would be required.

REFERENCES

1. Mason, C. R. *The Art and Science of Protective Relaying*, John Wiley & Sons, Inc., New York, London, Sydney, 1967.
2. Barkle, J. E., Sterrett, C. C., and Fountain, L. L. Detection of grounds in generator field windings, *AIEE Trans*, Part III, 467–472, 1955.
3. Christensen, E. F., Willis, C. H., and Herskind, C. C. Analysis of rectifier circuits, *AIEE Trans*, 61, 496–499, 1942.
4. General Electric Instruction GEK-15014B, *Inverse Time Maximum Excitation Limit 3S7932JA117 & 3S7932JA114*, General Electric Company, Virginia, 1973.
5. Fink, D. G. and Carroll, V. M. *Standard Handbook for Electrical Engineers*, Tenth Addition, McGraw-Hill Inc., 1968.

© 2006 by Taylor & Francis Group, LLC

9 Overexcitation

9.1 INTRODUCTION

Transformers and generators require an internal magnetic field to operate. The core of a transformer and the stator of a generator are designed to provide the magnetic flux necessary for rated load. An overexcitation condition occurs when this equipment is operated such that flux levels exceed design values.

The voltage output of a generator or transformer is a function of the rate of change of the flux and the number of turns in the output winding.

$$e = N\frac{\mathrm{d}\varphi}{\mathrm{d}t} \tag{9.1}$$

During normal power system operation, the voltage is sinusoidal and the rate of change is determined by the frequency, which is in turn determined by generator speed.

The relationship between core flux and output voltage for a current transformer was discussed in detail in Chapter 3. Equation (3.5) was derived to relate the CT core flux requirements to output voltage. The same relationship holds for a power transformer or generator.

$$\varphi_{\max} = \frac{\sqrt{2}\,E_{\mathrm{RMS}}}{N * 2\pi f} \tag{3.5}$$

where $\varphi_{\max}$ = maximum value of core flux required to produce E_{RMS}, E_{RMS} = RMS output voltage, N = number of turns in the output winding, and f = frequency in Hz. The equation shows core flux to be directly proportional to voltage and inversely proportional to frequency:

$$\varphi \propto \frac{V}{f}$$

The actual magnitude of flux in a stator or transformer core is difficult to measure, but can be quantified in terms of per-unit V/f or volts/Hertz. A generator or transformer operating at no load with rated voltage and frequency would have one per unit flux and is said to be operating at one per unit excitation. The same equipment operating at rated voltage and 95% frequency would have $1.0/0.95 = 1.05$ pu flux or 1.05 pu excitation.

Overexcitation will result from high voltage at rated frequency and from rated voltage with low frequency. Note that an overexcitation condition is not the same as an overvoltage voltage condition, where a dielectric breakdown of the insulation is the concern.

Because overexcitation is a function of voltage and frequency, it can occur without notice. Transformers and generators can be subject to repeated overexcitation by inappropriate operating practices or operator error without a disruption to operations. The resulting thermal degradation of insulating material is cumulative. A transformer or generator that survives a serious overexcitation event or many small events may fail as a result of a moderate event or during normal service.

9.2 CAUSES OF OVEREXCITATION

Overexcitation damage usually occurs during periods of off-frequency operation such as startup or shutdown. Classic examples are unit startup or shutdown under automatic voltage regulator control.

© 2006 by Taylor & Francis Group, LLC

Generator output voltage is a function of flux times speed. If startup procedures include the application of the field at reduced speed and the automatic voltage regulator is inadvertently placed in service, overexcitation damage can result. The automatic regulator will increase field current and with it field flux as necessary to maintain rated output voltage. At reduced speed, flux levels in excess of design levels will be required to meet the regulator's voltage setpoint. As an example, if field is applied at 80% speed and the regulator setpoint is 1.0 pu voltage, the resulting V/Hz will be $1.0/0.8 = 1.25$ pu.

A similar scenario could occur during shutdown. Units are often allowed to coast down under manual regulator control after being taken offline. The manual regulator is set to maintain field current at a value that would produce rated voltage at no load and rated frequency (V/Hz = 1.0). This mode of operation uses generator and transformer losses to aid in braking during the coast down period. If the automatic regulator is mistakenly placed in service during this coast down period, overexcitation will again occur as the regulator increases excitation to maintain the voltage setpoint.

These modes of damage would not occur with a modern automatic regulator. Most new regulators are equipped with V/Hz limiting circuitry that will adjust the field current to limit the V/Hz below a preset value regardless of the regulator voltage setpoint.

Another classic V/Hz damage scenario is the failure of the field breaker to open for unit shutdown. When a unit is operating near full load, the field current on most units is high enough to produce a no-load voltage of 1.3 pu or greater. If the loaded generator trips while under the manual regulator and the field breaker fails to open, the pretrip field current will be maintained by the manual regulator with a resulting V/Hz in excess of 1.3 pu throughout coast down. If the field breaker fails to open when the generator trips under control of an automatic voltage regulator without V/Hz limiting circuitry, the resulting overexcitation will be more severe. Again, the automatic regulator will apply full forcing current to the field during coast down in an attempt to maintain the setpoint voltage at reduced frequency.

Some consider overexcitation as an offline phenomenon, but overexcitation damage can occur when the generator is synchronized to the power system. Typically, the connected power system will prevent excessive V/Hz conditions resulting from operator error, but failures within the voltage regulator and associated circuits can cause damaging overexcitation to the synchronized generator and connected transformer.

The loss of the generator voltage signal to the regulator is an example. This failure would appear to the voltage regulator as zero voltage at the generator terminals. The regulator would respond by driving the field current to full boost in an attempt to correct the condition. The regulator would maintain maximum field forcing current until the automatic regulator was tripped by the operator or by action of the field overcurrent protection. In either case, the resulting terminal voltages will far exceed rated and the generator and connected equipment can suffer overexcitation damage.

Tripping the generator by field overcurrent protection does not avert overexcitation damage. This scheme is set to protect the field winding from thermal damage due to excess field current. The resulting operating time may or may not be fast enough to prevent overexcitation damage.

Load rejection with the automatic voltage regulator in service and a capacitive load can cause overexcitation. The capacitive load could be a shunt capacitor used for voltage control or Var support or it could be the charging current for a high-voltage transmission line. In either case, overexcitation could occur in two ways.

The first involves the leading Var limit function found in most automatic regulators. This function will be discussed in detail in a later chapter, but for now it will suffice to say that it is set to limit the Var flow into the generator. If the capacitive load is large enough to activate this limit, the automatic regulator will increase field current, thus increasing the generator voltage. Under normal operation conditions with the generator connected to the power system, this action is proper to reduce the Var flow into the generator. However, when the generator is isolated on a

© 2006 by Taylor & Francis Group, LLC

capacitive load, increasing the generator voltage increases Var output of the capacitive load. This action results in an uncontrolled rise to maximum excitation output and overexcitation of the generator and GSU transformer.

The second mechanism for overexcitation following load rejection is self-excitation. This occurs when the q-axis synchronous reactance of the generator plus the GSU transformer reactance is greater than the capacitive reactance of the connected system ($X_q > X_c$). Self-excitation results in an uncontrolled build up of q-axis voltage, regardless of which voltage regulator is in control. The voltage regulator acts on the d-axis, not the q-axis, and therefore cannot control the runaway voltage rise and resulting overexcitation.

Self-excitation is normally associated with hydro generators because these units typically experience overspeed of 120 to 140% during load rejections. The resulting increase in frequency reduces the value of the connected X_c, thus requiring less capacitance to self-excite during the load rejection.

9.3 DAMAGE

Magnetic materials have a maximum magnetic flux per unit area that they can support. This is known as the material's maximum flux density or saturation flux density. The magnetic core structure of a transformer and the stator of a generator must have sufficient area to produce the flux necessary to meet nameplate voltage requirements and industry standards. Because core area translates to cost, designers provide little margin beyond these requirements.

The core design not only involves providing sufficient area to support flux requirements, but core heating is also an important concern. Heating in magnetic materials is caused by eddy current and hysteresis losses. The eddy current losses vary directly with flux density and the square of frequency. Hysteresis losses vary with the 1.5 to 2.5 power of flux density depending on the material, and directly with frequency.[1] Magnetic structures designed for AC applications like a transformer core and the stator of an AC generator are laminated to minimize eddy current losses and the resulting heat.

When a transformer or generator is operating within rated parameters, flux in the core will be below the saturation flux density and core permeability will be much higher than that of adjacent structures. Consequently, the flux produced in the windings will confine itself to the core. Core heating will also be within design limits. If operating errors or equipment failures producing flux levels in excess of the maximum flux density, the core will saturate. Flux in excess of core capability will spill into the surrounding air space and into nonlaminated metallic structures around the core. Damage to a laminated core due to increased losses requires extreme overexcitation for a significant time. However, eddy currents induced in nonlaminated structures can quickly produce thermal runaway and component damage.

In a generator, the most damaging spill flux will appear at the ends of the stator core. Excess alternating flux will induce high currents in the nonlaminated end core assembly and in the end core laminations. Severe heating will result in this region. Also, the excessive induced currents within the stator laminations can create voltage gradients between core laminations sufficient to break down the interlaminar insulation. If this occurs, the core will be permanently damaged, rendering it incapable of carrying even normal flux without arcing, increased heating and further deterioration. Repairs can include disassembling the core to remove and replace the damaged laminations. Obviously, stator core restacking is a very expensive procedure.

Overexcitation of transformers had not been a problem until advances in core design and magnetic materials allowed sharp reductions in core area. The more economical designs produced normal operating flux densities much closer to the saturation flux density.

Transformers subjected to overexcitation experience saturation in the core legs. The excess flux spills out of the core into the insulating space around the core. This spill flux causes induced currents and excessive heating in windings, connectors, leads, and structural members. The major concern when a

© 2006 by Taylor & Francis Group, LLC

transformer is exposed to overexcitation is insulation damage, but other damage can result. Heating caused by induced currents can cause loss of mechanical strength in structural members and blister paint on the tank. Insulation oil contamination will also result from the deterioration of insulation and paint.

An important factor in the thermal damage caused by overexcitation in transformers is the nonsinusoidal nature of the spill flux. Normally, the core flux varies sinusoidally between positive and negative peaks each cycle. As voltage increases, the peak flux magnitudes increase. If the voltage is significantly above rated, the core will not have sufficient area to support the flux peaks required. Saturation will occur twice a cycle during the portions of each half cycle when the maximum flux density is exceeded. During each period of saturation, spill flux will appear outside the core in a nonsinusoidal burst. This flux and the induced current it produces are rich in harmonics. Because eddy current and hysteresis losses increase with frequency, the harmonics amplify the heating effect within the core and in nonlaminated structures.

As voltage (excitation) increases above rated, the transformer excitation current increases very rapidly. Reference 2 provided the following data for a specific core type transformer. Excitation currents of 10, 50, and 100% rated RMS load current occurred at rated frequency voltages of 125, 133, and 143%, respectively.

Overexcitation causes nonsinusoidal core flux; therefore, the excitation current necessary to produce this flux must also be nonsinusoidal. The harmonic-rich excitation current produces greater heating in the windings than a sinusoidal current of equivalent RMS magnitude. Hence, at high levels of overexcitation, thermal damage to windings can also result.

9.4 V/Hz LIMITS

The core area and the magnetic properties of the core material define the excitation capability of a generator or transformer. The core is designed to support a flux density necessary for full load operation and to dissipate the heat associated with that excitation level.

Standards do not specify V/Hz limits for transformers or generators directly, but the voltage limits specified for this equipment at rated frequency imply continuous, V/Hz limits. For instance, IEEE standards requires a generator to be capable of operation at rated kVA, frequency and power factor with terminal voltage variations of $\pm 5\%$. This implies a continuous, V/Hz limit of 1.05 pu.

Transformer standards are more complex. Under no load conditions, a transformer must withstand 110% rated voltage. At full load and 80% lagging power factor, a transformer must be capable of operating with 105% voltages at the secondary terminals. The required continuous withstand voltage at the primary winding would then depend on the transformer impedance. The primary winding of any transformer with impedance greater than 8.5% impedance would have to withstand more than 110% rated voltage to meet the 105% secondary voltage requirement.

As an example, consider a transformer with impedance of 16%. The primary voltage under the load conditions specified by standards, 1.05 voltage and 0.8 PF, would be calculated as follows.

Full load current at 105% secondary voltage and 80% power factor is:

$$I = \text{kVA}/E = 1.0/1.05 = 0.95 \text{ pu}$$
$$0.8 \text{ PF lag} = -36.9^\circ$$

The resulting primary voltage is

$$E_\text{p} = 1.05 + 0.95\angle -36.9^\circ * 0.16\angle 90^\circ = 1.15 \text{ pu}$$

The primary winding V/Hz capability for a 16% impedance transformer is then 1.15 pu.

© 2006 by Taylor & Francis Group, LLC

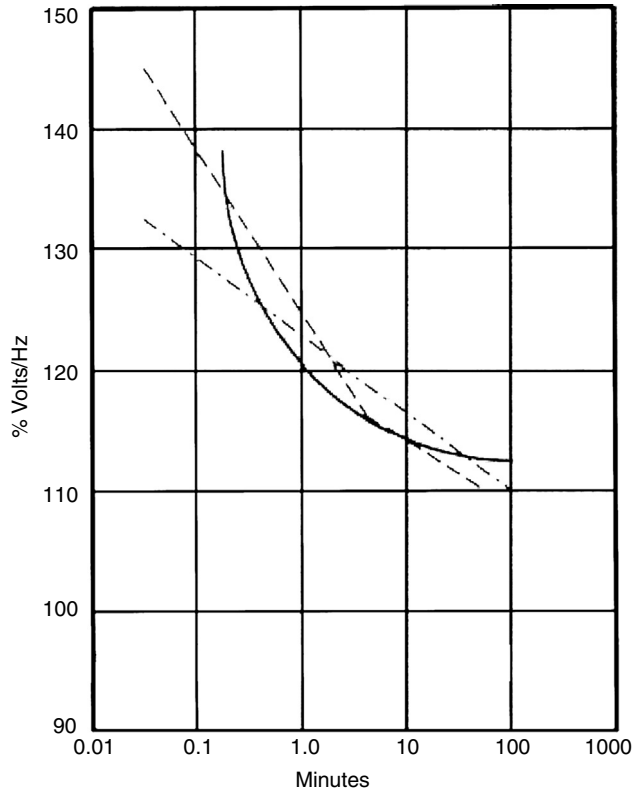


FIGURE 9.1 Transformer V/Hz limits. Individual manufacturers should be consulted for limits of a specific transformer. (From IEEE Std C37.91-2000, Guide for Protective Relay Applications to Power Transformers. With permission.)

Transformers and generators can withstand overexcitation for a short time. Maximum allowable component temperatures and the rate of temperature rise in those components determine the limits. Unfortunately, the limiting components vary for different designs. These variations have prevented the standardization of an overexcitation withstand characteristic. Percent overexcitation vs. allowable time data must be obtained from individual manufacturers. Typical limits are shown in Figure 9.1 and Figure 9.2.

9.5 PROTECTION

V/Hz relaying at the primary or secondary terminals can provide overexcitation protection of a transformer. Protection for a generator or generator and connected transformer can be provided in several forms, by V/Hz relaying at the generator terminals, by V/Hz limiting circuitry within the automatic voltage regulator, or by relaying sensing machine field current or voltage.

9.5.1 Field Monitoring Relays

Relays within the excitation system can provide limited overexcitation protection by monitoring field current or voltage. This relaying would be set slightly above the field current or field voltage necessary to produce rated generator output voltage at no load. No load, rated voltage, rated frequency is equivalent to 1.0 pu excitation. Tripping would be through a timer with a few

© 2006 by Taylor & Francis Group, LLC

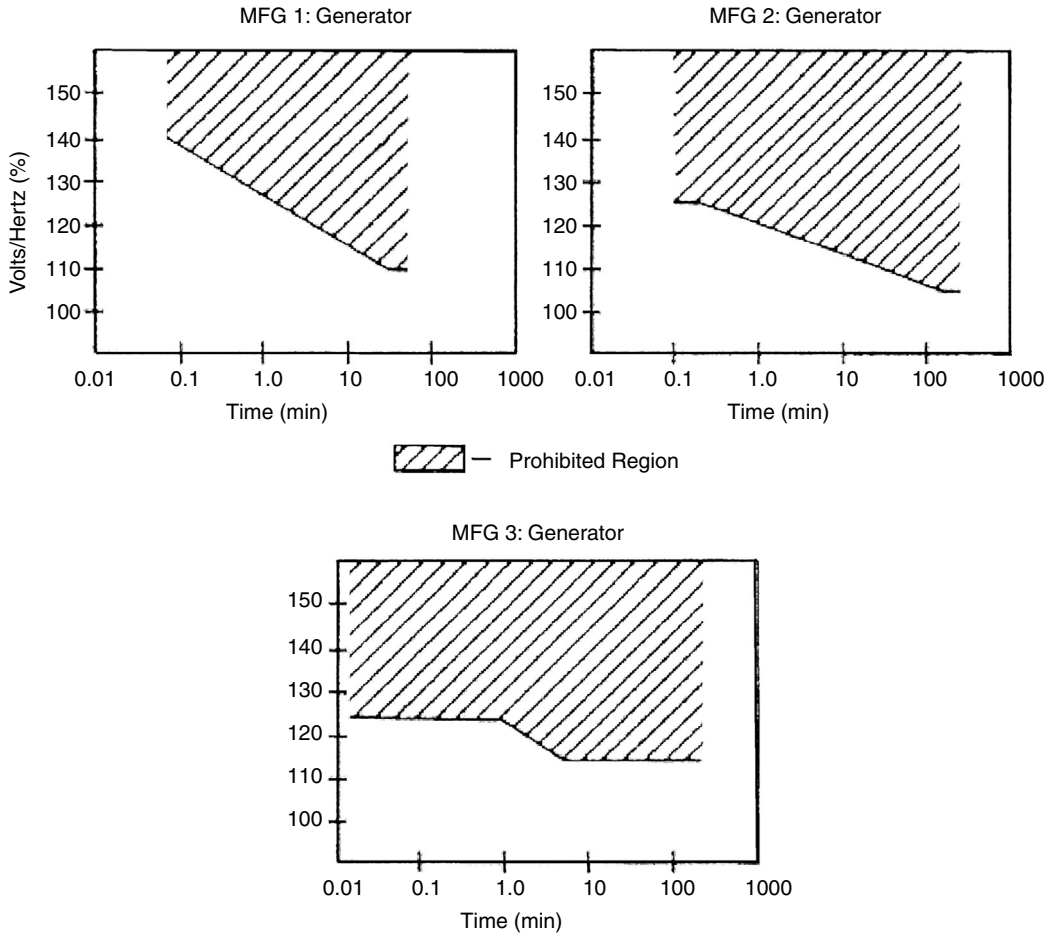


FIGURE 9.2 Generator V/Hz limits. (From IEEE C37.106-1987, IEEE Guide for Abnormal Frequency Protection of Power Generating Plants. With permission.)

second delay. This relaying would be in service only when the generator is offline to provide overexcitation protection during startup and shutdown.

9.5.2 V/Hz Limiter

V/Hz limiters are provided with most modern excitation systems supplied for medium and large units. This circuitry is within the automatic voltage regulator. It senses voltage and frequency at the generator terminals and adjusts the generator field as required to prevent operation above a preset V/Hz value.

Many limiter designs exist. A basic limiter would immediately clamp the generator output V/Hz to the preset value. More sophisticated limiters will allow overexcitation for a specific time as defined by an inverse time characteristic. Immediate actuation is undesirable, because this can prevent optimal generator response during system emergencies. Time delay limiters should be set to operate faster than V/Hz relaying to avoid tripping of the generator.

The V/Hz limiter may be designed for activation below a set frequency such as 95% rated, it may be in service at all times, or it may be in service only when the generator is offline. When the V/Hz limiter is in service only at reduced frequencies, overexcitation protection at higher frequencies can be provided by a maximum voltage limit that is independent of the frequency. This

© 2006 by Taylor & Francis Group, LLC

is an inferior method of V/Hz protection because a fixed-voltage limit produces a V/Hz trip characteristic that is inversely proportional to frequency. This overvoltage trip will not utilize the short time overexcitation capability of the generator during system disturbances.

At installations where the limiter is placed in service only when the generator is offline, overexcitation is assumed not to occur when the generator is connected to the power system. This is not a valid assumption. Although most overexcitation events do occur offline, instances of overexcitation are possible when the generator is synchronized to the power system as previously described. This form of protection is not recommended.

When the V/Hz limiter is in service at all times the output of the limiter is "auctioned" against the output of other regulator control functions. Field current is determined by the most limiting function. During normal operations, the dominant control function is the voltage setpoint for the regulator. When an overexcitation condition occurs, the V/Hz limit will become more restrictive than the voltage setpoint and will take control of the field current. The limiter will reduce the output voltage regardless of the voltage setpoint. Care must be used when setting this type of limit. An overly restrictive setting could limit the generator's ability to respond to system transients by restricting the generator output voltage.

9.5.3 V/Hz Relay Applications

V/Hz relaying is designated as Device 24. If the prime mover and associated mechanical systems are capable of withstanding a load rejection, the V/Hz relaying should trip the field and generator breakers. The prime mover would not be tripped. This will facilitate a rapid restart of the unit after the cause of the overexcitation is cleared. If mechanical systems cannot withstand the load rejection associated with the generator trip, a prime mover trip must also be initiated. When the generator is offline, the V/Hz relay should only trip the field breaker.

Sequential tripping of the turbine then the generator is not recommended for overexcitation. This tripping mode is supervised by reverse power relaying which delays tripping of the generator until the input energy to the prime mover has dissipated. The delay introduced by this logic is sufficient to cause damage for severe overexcitation conditions.

The V/Hz limiter is an excellent method of protection, but because it is part of the automatic voltage regulator, it cannot be applied as a standalone device. It is not available when the manual voltage regulator is in control of the generator. Also, the limiter may be rendered inoperative by the same regulator failure that initiates an overexcitation condition. The limiter requires independent backup in the form of a V/Hz relay.

V/Hz relaying for the protection of the generator, stepup, and auxiliary transformer is applied at the generator terminals as shown in Figure 9.3. V/Hz relays have either a definite time or inverse-time characteristic, as shown in Figure 9.4. Either characteristic must be set to initiate tripping

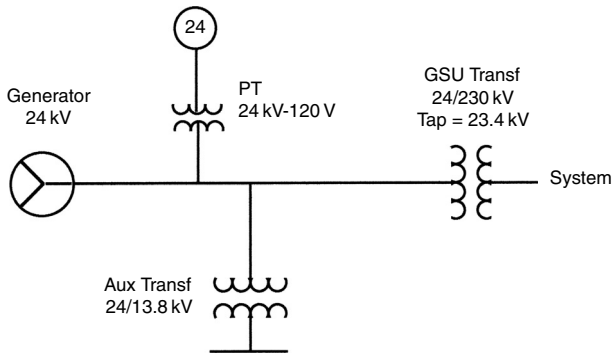


FIGURE 9.3 V/Hz protection.

© 2006 by Taylor & Francis Group, LLC

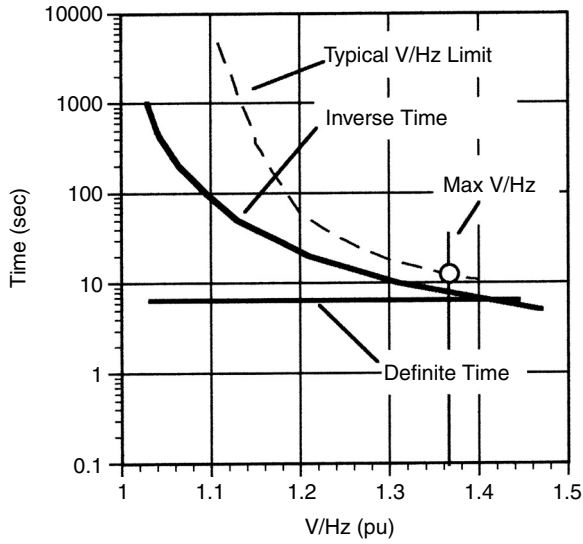


FIGURE 9.4 V/Hz relay characteristic.

before damage occurs at the maximum level of overexcitation anticipated. The inverse-time characteristic is preferred. As is shown in the figure, the inverse characteristic allows maximum utilization of the short time capability of the equipment. The definite time characteristic overprotects at low levels of overexcitation, thus jeopardizing unit availability during system disturbances.

Only the definite time characteristic was available on early V/Hz relays. Some applications used multiple definite time elements set to form stepped protection that roughly emulates an inverse-time characteristic. With the advent of solid-state and microprocessor technology, inverse-time V/Hz relays became available. Microprocessor V/Hz relays are also available with alarm, data recording, and thermal memory.

The latter provides a slow reset of the relay following a nontrip overexcitation event. The reset is intended to mimic the thermal characteristic of the protected transformer and generator. Assume a given overexcitation condition will cause the V/Hz relay to operate in 25 sec. Also assume the same condition will damage equipment in 30 sec. If this condition occurs for 20 sec, abates, then reappears a few seconds later, a V/Hz relay without memory will reset immediately after the initial overexcitation condition. The heat generated in the protected equipment will not dissipate in the short time between events. When the second overexcitation event occurs, the relay will time for the full 25 sec before initiating a trip. The protected equipment would be exposed to the condition for 45 sec. This is 15 sec greater than the permissible withstand time. If the memory feature were provided, the relay would slowly reset at a rate comparable to the cooling time of the protected equipment. In the example given, a memory relay would remember the initial event and operate 5 sec into the second event, limiting the equipment's overexcitation exposure to 25 sec.

9.6 SETTINGS

Ideally, protection should operate for any condition that exceeds equipment capabilities. This is not possible for overexcitation. The system operating voltage range extends to the continuous V/Hz capability of generators and transformers. This being the case, the setting philosophy must be to guarantee that overexcitation protection will not actuate when the system is operating at the maximum continuous V/Hz capability of the equipment. To accomplish this, the settings must

© 2006 by Taylor & Francis Group, LLC

be above the applicable limit with sufficient margin to allow for relay and potential transformer errors. The setting should also include an appropriate safety margin. The resulting V/Hz settings can be substantially above the continuous V/Hz capability. Alarm relays can be added to bridge the protection gap between the continuous capability and V/Hz trip actuation. At this low level of overexcitation, an alarm is an option because the operation would have sufficient time to assess and correct the condition.

The V/Hz relay pickup and V/Hz limiter's minimum initiation settings are based on the lowest V/Hz capability for the connected equipment. As an example, refer to Figure 9.3. V/Hz protection is provided at the generator terminals. The generator is rated at 24 kV and the GSU primary tap is rated 23.4 kV; the auxiliary transformer is on the 24 kV tap.

As a first cut, individual voltage limits are estimated on the basis of low-impedance transformers as:

Generator: 24 kV × 1.05 = 25.2 kV
GSU transformer: 23.4 kV × 1.10 = 25.7 kV
Auxiliary transformer: 24 kV × 1.10 = 26.4 kV

The generator sets the minimum continuous V/Hz limit at 25.2 kV.

Time delay settings associated with the V/Hz relay and limiter must coordinate with the short time withstand capability of the protected equipment. The limiter delay and relay delays should also be coordinated such that the limiter will act to reduce overexcitation before a generator trip is initiated by the relay.

The delays for overexcitation protection, like those for field overcurrent protection, should allow maximum utilization of the short time capability of the protected equipment. Overexcitation can occur during a system disturbance because of field forcing, reduced system frequency, or both. In these situations, the output of every generator on the system is critical to system recovery. Protective functions should be designed and set to allow operation up to the short time limits of the equipment. Protective relays and limiters that do not optimize equipment capability reduce the reliability of the entire power system.

9.6.1 Generator V/Hz Settings

The setting for a generator is straightforward. The V/Hz limit at the generator terminals is 105%, regardless of the load condition. The initiation setting for a limiter or the pickup of a V/Hz relay should be set above 105% + margin (device error + PT error + safety margin).

9.6.2 Transformer Settings

The actuation settings are derived using the same errors as listed above, but the application of V/Hz protection on a transformer involves several options. First the location of the protective devices could be at the primary or secondary winding. The transformer also has different no load and full load V/Hz limits. Protection located at the secondary terminals would provide maximum protection when settings are based on the full load limit of 105% rated voltage. However, this setting may not be applicable if light load system voltage exceeds this value. Setting must allow sufficient margin for the maximum anticipated system voltage to avoid nuisance trips.

When a protective device is applied at the primary terminals, the transformer impedance determines the setting. Protection on a transformer with less than 8.5% impedance can be set based on the 110% no load limit because the primary voltage under load is less than or equal to this value. For higher impedance transformers, the primary voltage under load will exceed the 110% and settings must be based on "full load" primary voltage. The resulting setting will provide reduced protection at light load.

© 2006 by Taylor & Francis Group, LLC

In either case, the minimum setting secure from operation at the maximum anticipated normal system voltage should be used.

9.6.3 Generator/Transformer Settings

When V/Hz protection is applied at the generator terminals to protect the generator, connected GSU, and/or auxiliary transformers, the setting must be based on the most restrictive equipment. The GSU transformer limit would be 110% of the primary tap voltage or the primary voltage associated with full load depending on the transformer impedance. (The primary voltage limit for the 16% impedance transformer discussed previously was 1.15 pu.) When the GSU transformer primary taps are rated equivalent to that of the generator, the V/Hz protection setting would be based on the 105% generator limit. Limiting the transformer primary voltage from 110%, or from 115% for the 16% impedance transformer, to 105% will reduce the permissible full load voltage at the secondary winding from 105% to approximately 100% for a low-impedance transformer and to 95% for the 16% impedance transformer. The latter limit would be unacceptable and demonstrates why transformer primary winding are often rated for 95% of the generator rating.

When a transformer with primary windings rated 95% of the generator is applied the 105% limit based on the generator voltage equals a 110% voltage limit based on the transformer rated voltage. As a result, a low-impedance transformer can operate with 105% output voltage at the secondary terminals. The maximum primary input voltage for 16% impedance transformer at rated load and 80% power factor will be reduced from 115 to 110% of the transformer rating. With the input voltage limited by the generator the maximum allowable output voltage for the transformer at full load and 80% power factor will be reduced from 105 to 100%. In practice, a secondary voltage greater than 100% may be obtainable. The input to the primary winding cannot exceed the generator rating, which is often less than 80% PF.

9.6.4 Setting Limitations

The setting criterion described above is derived from voltage limits and applied to protective devices at the terminals of the generator and transformer. The problem with this approach is that terminal conditions do not specifically reflect limiting V/Hz conditions at the transformer or stator core where damage would occur. The differences between terminal and core conditions reduces the effectiveness of the protection provided.

It would appear that transformers have two excitation limits, a no load limit, and a limit at full load. In reality, this is not the case. Consider the 16% impedance transformer discussed previously. Standards dictate a no load limit of 110% and full load limits of 105% at the secondary winding and 115% on primary winding. The equivalent circuit for a transformer is shown in Figure 9.5. The magnetizing branch of the equivalent circuit represents the core. At no load there is no voltage drop within the transformer. The 110% limit is the actual limit at the core as viewed from either

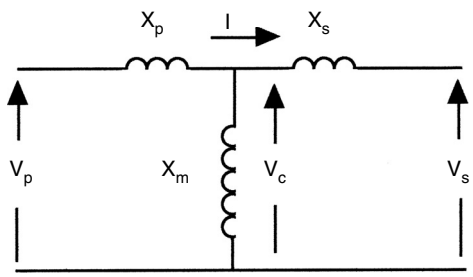


FIGURE 9.5 Transformer equivalent circuit.

© 2006 by Taylor & Francis Group, LLC

the primary or the secondary terminal. At full load, neither the primary nor secondary voltage quantities define conditions at the core. Core voltage differs from the terminal voltage by the primary or secondary voltage drop. A common assumption is that the primary and secondary per unit impedances are equal. Using this assumption, the equivalent core voltage at the designated full load conditions is

$$V_{\text{core}} = 1.05 + 0.95\angle -36.8 * j\ 0.16/2 = 1.097$$

This calculation shows that a core limit of 110% is applicable to both the no load and full load conditions.

Likewise, the generator limit is stated as 105%. This limit is not associated with a loading condition, but the core voltage would be maximized at full load. The difference between the equivalent stator core voltage and the terminal voltage will be the drop across the stator leakage reactance. The sample system generator is rated at 85% power factor and has a leakage reactance of 14%. The implied stator core limiting voltage for the sample system generator is then

$$I = \frac{MVA}{E_{\text{t}}} = \frac{1.0}{1.05} = 0.95 \quad \text{at } 0.85\,\text{PF lag}(-31.8^{\circ})$$

$$V_{\text{core}} = 1.05 + 0.95\angle -31.8^{\circ} * 0.14\angle 90^{\circ} = 1.12\,\text{pu}$$

This explains why a V/Hz limit of 105% forms the basis for protective settings, while generator manufacturers allow voltages in excess of 110% for open-circuit testing.

Short time overexcitation withstand curves provided by manufacturers are often based on actual core limits. When such curves are applied at the equipment terminals, they represent a no load condition. The application of such curves under load may be optimistic. When using short time curves, the applicable conditions for the curve must be known.

9.6.5 Time Delay Settings

The time delay settings for the V/Hz relay and limiter must assure operation before the allowable short time V/Hz capability of the generator and/or GSU transformer is exceeded.

Figure 9.6 compares selected generator and transformer short time withstand characteristics from Figure 9.1 and Figure 9.2. For the specific equipment shown, withstand characteristics of the generator and transformer are similar over much of the range when the transformer and generator have the same voltage rating. However, often the GSU and auxiliary transformers have primary windings rated 95% that of the generator. As shown in the figure, the 95% rated transformer becomes the more vulnerable equipment.

To make this comparison, both the generator and transformer limit curves must be plotted at a common voltage. It is customary to use the generator rated voltage for this comparison. Following this convention, the 95% rated transformer capability curve was plotted over that of the generator by aligning 95% rated generator voltage on the generator curve with 100% rated voltage on the transformer curve. This effectively shifts the transformer curve to the left. Note that there is a wide variety of limit curves and different results can occur with different manufacturers' limits.

The V/Hz relay must be set with sufficient time delay to override system fault voltage transients and to allow the voltage regulator to restore normal voltage following load rejection. These minimum delay conditions are normally met when the delay is set to maximize utilization of the short time overexcitation capability of the equipment.

Coordination between the short time withstand capability of the transformer and generator and the V/Hz relay should exist at the maximum excitation level anticipated. Unfortunately, the determination of this maximum value would require a dynamic study involving the generator,

© 2006 by Taylor & Francis Group, LLC

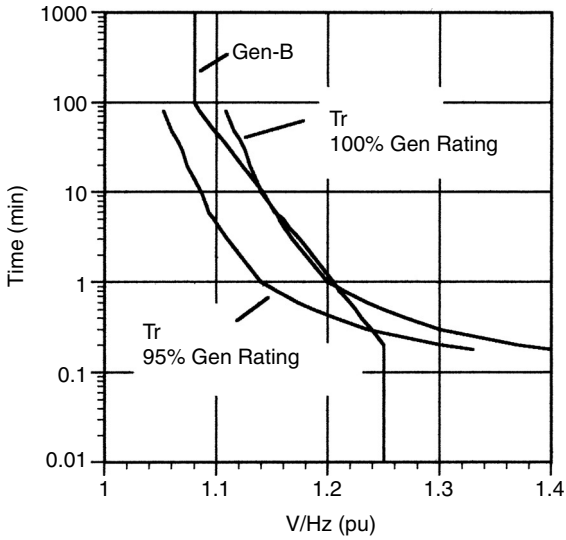


FIGURE 9.6 Comparison of transformer and generator V/Hz limits.

voltage regulator, and governor, saturation characteristics of the generator and transformers, and transmission parameters. In practice, the maximum V/Hz condition at the generator terminals can be estimated from the generator's open-circuit saturation curve. Figure 9.7 is such a curve for the sample system generator. This plot shows the relationship between the generator field current and terminal voltage with no load on the generator. The shape of the curve indicates that saturation of the stator will limit the terminal voltage to less than about 1.25 pu. Therefore at 1.25 pu V/Hz, the V/Hz limiter should act to reduce excitation before relaying initiates a generator trip. If the limiter fails to reduce excitation from 1.25 pu to nominal, the V/Hz relay must initiate a trip before the short time withstand of the generator or connected transformer is exceeded.

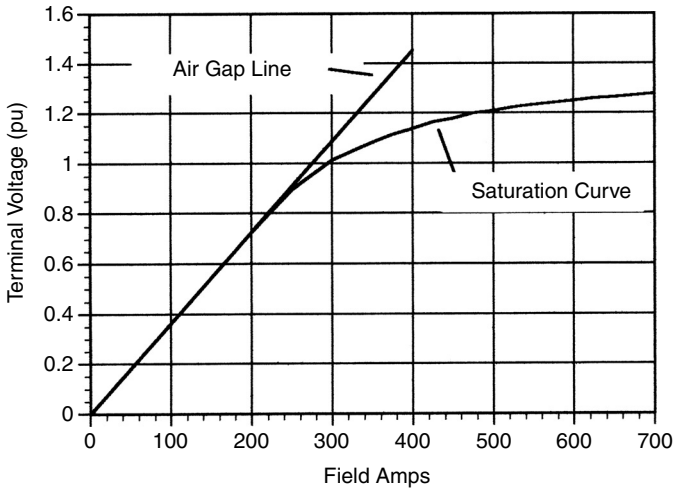


FIGURE 9.7 Generator open-circuit saturation curve.

© 2006 by Taylor & Francis Group, LLC

9.7 DIFFERENTIAL RELAY RESPONSE TO OVEREXCITATION

The large transformer excitation current associated with an overexcitation event will appear as a transformer fault to a transformer differential relay. A differential relay operation during such an event is undesirable because it gives a false indication of a transformer failure, thus complicating the restoration process.

Actuation of the differential relay is dependent on the severity of the overexcitation (magnitude of the exciting current) and the design of the relay's inrush restraint circuit. When a transformer is energized, the transient magnetizing current also appears as a transformer fault to the differential relay. The inrush restraint circuit's function is to differentiate energizing current from a legitimate fault and inhibit tripping for the former. Inrush circuit design varies among manufacturers, but most use harmonic currents. Fault current is sinusoidal. Inrush current is nonsinusoidal and is not symmetrical about the x-axis. The asymmetry produces even harmonics that are used in some circuits to identify an inrush condition. An alternative and more common design uses a mixture of even and odd harmonics. Another design uses the shape of the inrush current waveform as an indicator of inrush.

These circuits are a restraining, not a blocking circuit. Activation of the circuit does not prevent relay operation, but biases the relay toward nontrip. The greater the restraining quantity, the greater the exciting current necessary to actuate the relay. Without an inhibit circuit, the exciting currents previously listed for 125% rated voltage and above are sufficient to cause a differential relay operation.

The waveforms for the transformer excitation current at 125%, 133%, and 145% voltage are plotted in Figure 9.8. The wave shapes are similar to those of inrush current in that the current is near zero for a period at the beginning and end of each half cycle. Relay restraint circuits based shape would tend to prevent a differential relay operation during overexcitation.

The harmonic content of the excitation current at each level of overexcitation are provided in the literature[2] and are shown in Table 9.1.

The excitation current is symmetrical about the x-axis and therefore it contains only odd harmonics. If the transformer differential relay uses only even harmonics for restraint, the differential relay will operate when excitation current exceeds the trip setting.

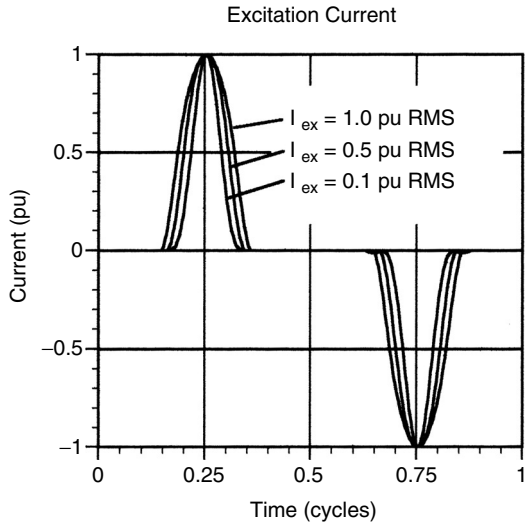


FIGURE 9.8 Excitation current waveform.[2]

© 2006 by Taylor & Francis Group, LLC

TABLE 9.1
Harmonic Content of Excitation Currents[2]

	I_{ex}(RMS) = 100%		I_{ex}(RMS) = 50%		I_{ex}(RMS) = 10%	
Harmonic	**Magnitude**	**Phase Angle**	**Magnitude**	**Phase Angle**	**Magnitude**	**Phase Angle**
1	0.771	0	0.703	0	0.627	0
3	0.567	180	0.575	180	0.552	180
5	0.279	0	0.371	0	0.457	0
7	0.039	180	0.169	180	0.289	180
9	0.062	180	0.025	0	0.169	0
11	0.049	0	0.043	0	0.079	180
13	0.002	0	0.050	180	0.020	0
15	0.028	180	0.027	0	0.011	0

Source: Alexander, G.W., Corbin, S.L., McNutt, W.J. Influence of Design and Operating Practive on Excitation of Generator Step-Up Transformers, IEEE Transactions, Vol. PAS-85, No 8, August 1966. With permission.

A relay that includes odd harmonics in the restraint circuit is not immune to operation. The tabulation shows that the third and fifth are the only excitation current harmonics with sufficient magnitude for use as a restraining quantity. Delta-connected CTs are often required to compensate the differential circuit for the transformer winding configuration. The dominant third-harmonic current is a zero-sequence current and will be blocked by the delta-connected CT. The effectiveness of the remaining fifth-harmonic current as a restrain current will depend on the relay setting, the restraint circuit design and on the severity of the overexcitation.

9.8 APPLICATION OF V/Hz PROTECTION ON THE SAMPLE SYSTEM

The sample system is shown in Figure 9.9. Overexcitation protection is to be provided by a V/Hz limiter within the automatic voltage regulator and a V/Hz relay. The relay will provide backup protection should the limiter or automatic regulator fail. It will also provide primary protection when the manual generator is controlling the generator and the limiter is unavailable.

Before a setting can be chosen for either device, the maximum rated frequency voltage must be determined for the connected equipment. The maximum voltage for the generator is 105% rated

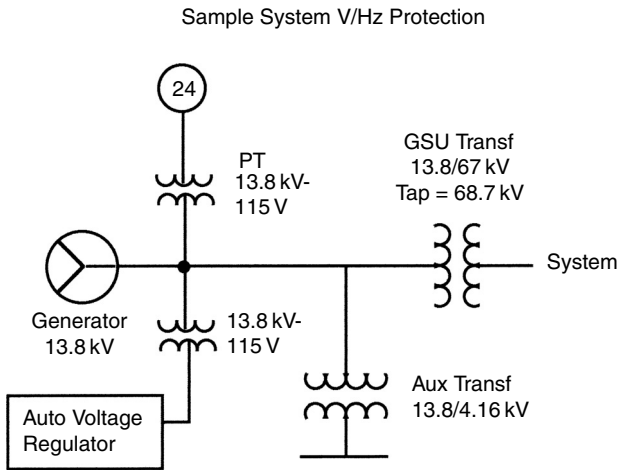


FIGURE 9.9 V/Hz protection on the sample system.

© 2006 by Taylor & Francis Group, LLC

voltage. For simplicity, the transformer's limit is assumed to be 110%. This limit is correct for the GSU transformer with 6.5% impedance, but is low for the 9.0% impedance unit auxiliary transformer. Since the generator and both transformers are rated 13.8 kV continuous voltage, limits are as follows:

Generator = 1.05 × 13.8 kV = 14.49 kV
Auxiliary and GSU transformer = 1.1 × 13.8 kV = 15.18 kV

Because the generator defines the maximum continuous excitation condition as 14.49 kV at 60 Hz, it is not necessary to determine the exact limit for the auxiliary transformer.

The automatic voltage regulator and the V/Hz relay are connected to different sets of PTs at the generator terminals. Both sets are 13,800/115 V. The equivalent limiting voltage at the regulator and relay will be:

$$\text{Limiting voltage} = 14{,}490 \times 115/13{,}800 = 120.75\,\text{V}$$

The maximum allowable continuous V/Hz seen by the limiter and relay is then:

$$\text{Limiting V/Hz} = 120.75\,\text{V}/60\,\text{Hz} = 2.01$$

The V/Hz limiter has an inverse-time characteristic following the following equation and a ±2% accuracy.

$$t(\text{lim}) = K\left[0.02 + \frac{0.5}{M^2 - 1}\right] \tag{9.2}$$

where K = time delay setting and M = overexcitation in multiples of pickup.

The PT error is ±2%. The V/Hz limiter should be set to actuate at 2.01 × 1.04 = 2.09 V/Hz. The pickup setting of the V/Hz relay should be set above that of the limiter to ensure any event that actuates the relay will actuate the limiter. If this is done, limiter action will prevent actuation of the V/Hz relay and the resultant unit trip.

The V/Hz relay will have the following specifications (Device 24):

Setting range = 1.5 to 3.0 V/Hz
Frequency range = 2 to 75 Hz
Reset ratio = 98%
Trip time in seconds:

$$t(\text{relay}) = 0.8 + \frac{0.18 * K}{M^2 - 1} \tag{9.3}$$

Accuracy = ± 3% for 5–75 Hz
± 10% for 2–5 HZ
PT accuracy = ±3%

The setting must allow operation at the maximum permissible voltage; a safety margin of 5.0% will be applied to the trip setting.

The overall setting margin required will be:

Relay errors = 3%
PT errors = 3%
Setting margin = 5%
Total = 11%

© 2006 by Taylor & Francis Group, LLC

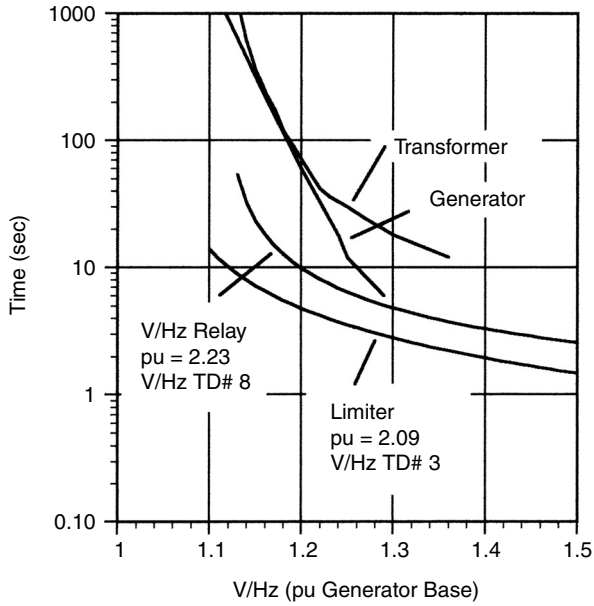


FIGURE 9.10 Sample system V/Hz relay vs. limits.

The setting must allow for 11% error.

$$\text{Set relay pickup at } 2.01 \times 1.11 = 2.23\,\text{V/Hz}$$

The time delay is determined by plotting the short time V/Hz withstand time for the transformer and generator against the relay and limiter characteristic. Because the transformer low-side tap voltage equals the generator rating, the curves need not be shifted. This plot is shown on Figure 9.10. The relay time delay (K) is set for 8.0 and the limiter's delay (K) is set at 3. Note that coordination between the three curves is maintained at the maximum anticipated excitation of 1.25 pu.

REFERENCES

1. Del Toro, V. *Electromechanical Devices for Energy Conversion and Control Systems*, Prentice-Hall, Inc., Englewood Cliffs, New Jersey, 1968.
2. Alexander, G. W., Corbin, S. L., and McNutt, W. J. Influence of design and operating practice on excitation of generator step-up transformers. *IEEE Trans.*, PAS-85(8), 1966.
3. IEEE Std 637.91-2000, *IEEE Guide for Protective Relay Applications to Power Transformers*, New York, 2000.
4. IEEE C37.106–1987, *IEEE Guide for Abnormal Frequency Protection of Power Generation Plants*, New York, 1987.

© 2006 by Taylor & Francis Group, LLC

10 Abnormal Frequency Protection

10.1 INTRODUCTION

Operation at other them 60 Hz is normally a result of occurrences on the connected power system. Overfrequency operation results when generation excess exists. This condition would occur following loss of major load or a major tie line that exports power. Conversely, underfrequency operation occurs as a result of a generation deficiency caused by the loss of a large generator or loss of a major importing tie line.

10.2 EFFECT ON GENERATOR

The effects of off-nominal frequency on the generator are less of a concern for overfrequency operation than underfrequency operation. Because an overfrequency condition results from excess generation, it can be corrected quickly by a reduction in power output via the governor or manual controls. Increased shaft speed during an overfrequency event will improve cooling, thus increasing generator load-carrying capabilities. One concern is that the 105% limit on terminal voltages could be exceeded. The terminal voltage of a generator operating under control of the manual regulator would rise proportional to frequency.

Underfrequency is caused by excess load and cannot be corrected locally. The speed reduction reduces generator ventilation and with it load-carrying capability. Typically, generators can operate down to 95% rated speed for hours if the output is reduced proportional to speed and terminal voltage is limited to rated to avoid overexcitation. From 95% to 90% rated speed, both output voltage and current should be reduced in proportion to speed, thus reducing output capability by the square of the speed reduction.[1]

A system operating below rated frequency is an overloaded system. Connected generators would be expected to exceed their MVA ratings. Field forcing would also be anticipated in an attempt to maintain system voltage. Therefore, the short time overload capabilities of the stator and field circuits become a concern. These short time overload capabilities at rated frequency are specified in ANSI C50.13-1989. The short time overload capability of the field is shown in Figure 8.6. The stator short time capability is shown in Figure 4.15. Generator standards do not specify limits for off-nominal frequency operation. These data must be obtained from the generator manufacturer.

10.3 STEAM TURBINES

Steam turbines are more adversely effected by off-frequency operation than are the generators they drive. A key feature of turbine blade design is assuring that the blades are not damaged by mechanical resonance. Mechanical resonance produces high vibratory stress that can cause fatigue cracking and eventual blade failure. Resonance occurs when a natural frequency of a blade coincides with vibratory stimuli. The steam flow path is not homogeneous. Physical irregularities in the flow path produce turbulence that appears as a cyclic force to the blades. As an example, a single strut would produce excitation once per revolution, whereas a joint would excite twice per revolution. The strut would represent fundamental frequency excitation while the joint would produce second-harmonic excitation.

© 2006 by Taylor & Francis Group, LLC

Each turbine blade has several natural vibration modes, namely tangential, axial, and torsional. Each mode has a natural frequency that varies with the physical dimensions of the blade. Short blades in the high-pressure and intermediate-pressure stages of the turbine can be designed to withstand a resonant condition. This is not practical for the long slender blades in the last few rows of the low-pressure turbine. Instead, these blades are protected from resonant damage by tuning their natural frequencies away from stimuli present at normal operating frequency or any harmonic thereof. These tuned low-pressure stage blades determine the turbine's vulnerability to off-frequency operation.

Figure 10.1 is a Campbell diagram, which plots the natural frequencies for critical modes of tuned blades. Only those modes that could result in damage with operation near rated speed are included. Each band on the diagram represents resonance for a specific mode in a specific set of blades. The figure includes three such bands, but this number will vary with turbine design. The resonant frequency bands roll upward as speed increases due to centrifugal force stiffening of the blades at higher speed. The thickness of a band indicates the possible variation in natural frequency due to manufacturing tolerances and design uncertainties.

The lines flaring out from the origin represent the stimulus frequencies inherent in the steam flow. These lines are harmonics of rated speed. An intersection of the harmonic and resonance band represents a resonant condition with vibratory stress 10 to 30 times normal.[2] Prolonged operation at an intersection will cause fatigue damage to tuned blades. Operation for lesser periods of time will cause fatigue cracking in the wire ties and blade covers. While cracking in these areas does not represent a major failure, this damage can alter blade tuning such that resonance could occur near rated speed. Excess vibration and failure would then result during normal operation.

Blades are designed with sufficient separation between natural frequencies and harmonic stimuli at rated speed to avoid vibratory stress during normal operations. However, the margins

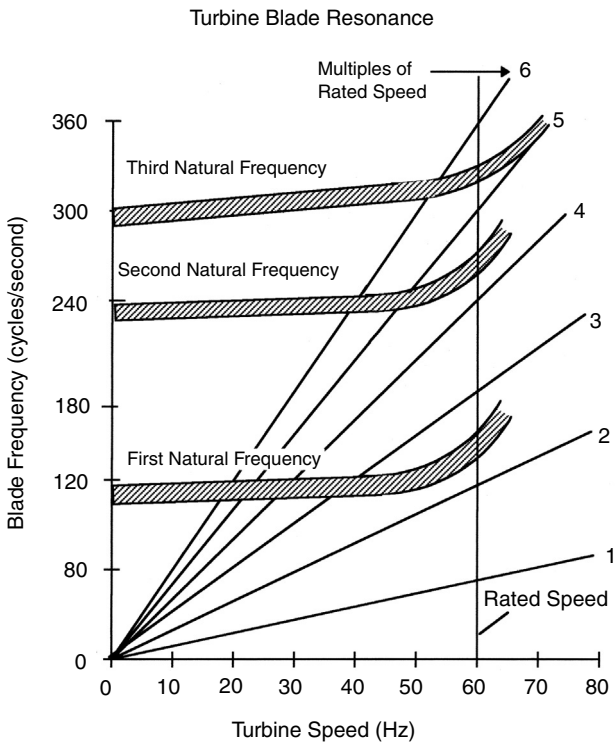


FIGURE 10.1 Campbell diagram. (From IEEE C37.106-1987, IEEE Guide for Abnormal Frequency Protection of Power Generating Plants. With permission.)

© 2006 by Taylor & Francis Group, LLC

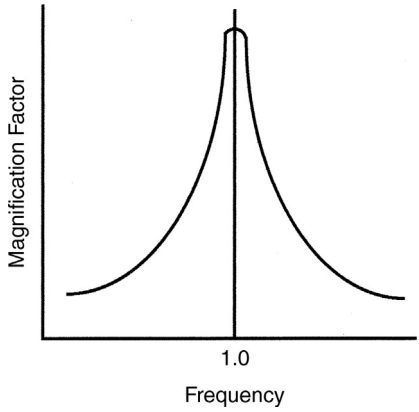


FIGURE 10.2 Amplification factor. (From IEEE C37.106-1987, IEEE Guide for Abnormal Frequency Protection of Power Generating Plants. With permission.)

between resonant points and rated speed harmonics are not large. Although slight speed deviations normally will not cause full resonance, operation near resonance will cause increased blade vibration and can also result in damage. Figure 10.2 shows the typical response of a structure such as a turbine blade to a force applied at frequencies near resonance. The y-axis is the amplification of the force. One per unit on the x-axis represents the natural frequency. The figure shows that operation in close proximity to the resonance bands on the Campbell diagram can also produce damaging stress.

Materials subject to cyclic stress develop fatigue cracks; these cracks propagate through the material, eventually causing mechanical failure. Turbine capability for any off-frequency operating condition must be based on the most fragile blade elements, usually the tie wires and the blade covers. Theoretically, the withstand time for these elements can be determined if the applied force, the number of application cycles of the force, and the material's resistance to fatigue failure are known.

In reality, the prediction of the time to failure is difficult. The number of stress cycles is directly related to the frequency of the excitation, but determination of the force is dependent on the accuracy of the resonant-response curve (Figure 10.2). The natural frequency of the blades is also a variable because similar blades will have different resonant frequencies due to manufacturing tolerances. Another variable is a material's response to fatigue and the material's past history, because fatigue is cumulative. The limits must also consider the decline in the material's fatigue strength during normal operation because of pitting corrosion and erosion of the blade edges. Fatigue strength is also reduced by abnormal operations not related to off-frequency operation.[3] These and other factors make the practical determination of off-frequency limits very difficult. As a result, such limits are usually quoted on the basis of the most pessimistic assumptions.

Standards do not specify short time limits for over-or underfrequency operation. The manufacturer of the specific turbine must provide this data. Reference 4 listed the following limitations for one manufacture's turbines as:

1% change (59.4–60.6 Hz), no adverse effect on blade life
2% change (58.8–61.2 Hz), potential damage in about 90 minutes
3% change (58.2–61.8 Hz), potential damage in about 10–15 minutes
4% change (57.6–62.4 Hz), potential damage in about 1 minute

Reference 5 states that with a 5% frequency deviation, damage could occur within a few seconds. These withstand times are not typical. Limits vary dramatically among manufacturers, as can be seen in Figure 10.3, which includes limitation curves from four manufacturers.

© 2006 by Taylor & Francis Group, LLC

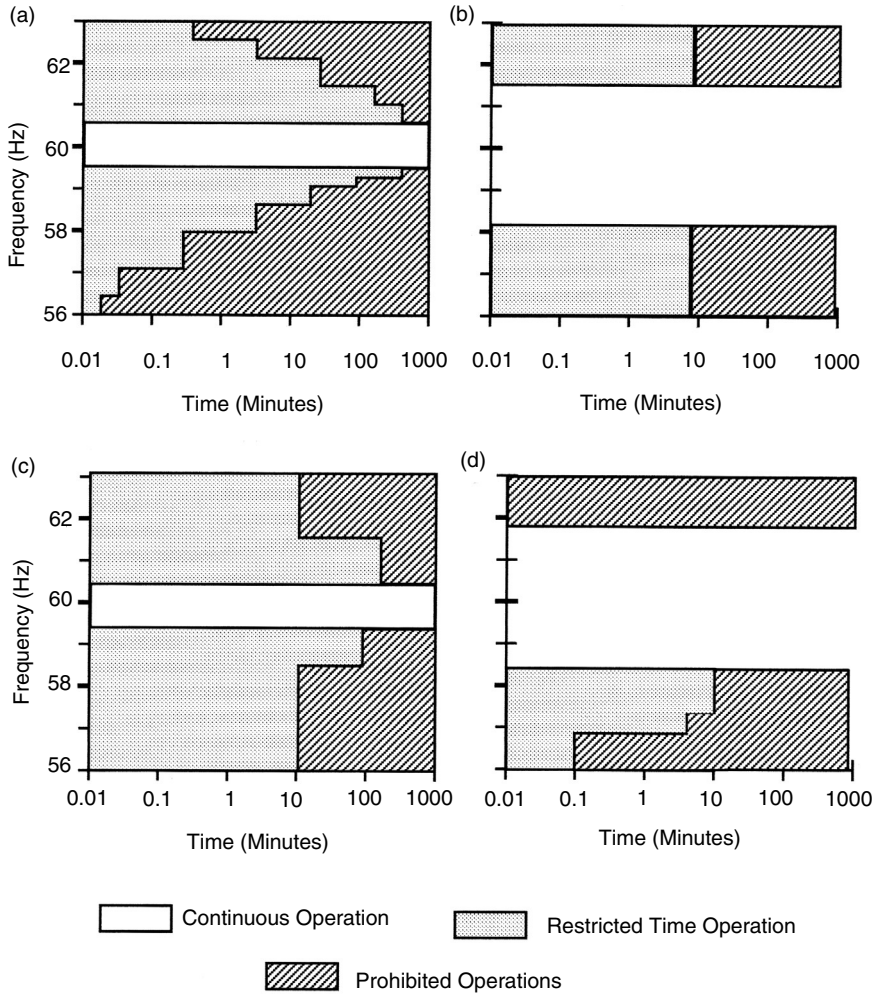


FIGURE 10.3 Abnormal frequency allowable withstand times. (From IEEE C37.106-1987, IEEE Guide for Abnormal Frequency Protection of Power Generating Plants. With permission.)

Fatigue damage is cumulative. Each band of the manufacturer's short time limit relates to a specific vibration mode for a specific blade set. Hence, the withstand times shown are cumulative within the given frequency band. As an example, using the withstand times listed above, if a turbine operates within the 2% band for 40 minutes, future operation in that band must be limited to 50 minutes. The turbine would retain 100% allowable time in all other bands.

Blade vibration is a concern when the turbine is under load not during startup and shutdown. The minimum load at which steam flow is sufficient to cause damage is usually around 5%. Of course, the turbine manufacturer must determine the exact value. A potential for turbine damage exists when the generator is isolated from the power system carrying auxiliary load in excess of the threshold value.

As an aside, blade damage can also occur as a result of excessive unbalanced generator current. As discussed in Chapter 6, the unbalanced current gives rise to negative-sequence stator current, which appears to the generator rotor as a second-harmonic current. This can significantly increase the second-harmonic stimulus at the turbine. Long time operation with unbalanced currents can produce blade damage.

© 2006 by Taylor & Francis Group, LLC

10.4 COMBUSTION TURBINES

Blade resonance is also a primary design consideration for combustion turbine generators (CTGs). Combustion gases produce vibratory stimulation similar to that of steam flow. Combustion turbine generator blades, in general, have a greater tolerance for underfrequency operation than do steam turbine blades. They can usually operate down to 57 or 58 Hz for extended periods of time. Again, the turbine manufacturer must be consulted for exact limitations.

A major consideration in reduced-frequency operation of CTGs is the dramatic loss of output capacity due to reduced airflow through the turbine. One manufacturer estimated a 17% loss in output at 55 Hz. The reduced airflow also decreases blade cooling, causing overtemperature trips.

The combustion turbines are subject to "compressor surge." If a combustion turbine is operated at rated load with reduced frequency, it can experience a collapse of airflow through the turbine. The unit will eventually trip on high blade temperature. Many gas turbines are equipped with a surge protection system that reduces fuel flow with reduced frequency to unload the turbine. This control function, when provided, compounds the loss of output capability with reduced frequency. It also protects the blades from overheating.[2]

10.5 HYDRO GENERATORS

There are no specific concerns related to underfrequency operation of a hydro turbine. Overfrequency, or more precisely overspeed operation, is a concern. A sudden loss of load on a hydro unit will typically result in 130–150% overspeed because of the mass and high kinetic energy of the water in the penstock. On any generator a loss of load will trigger a speed increase. Without load, all energy input to the turbine is expended on acceleration of the turbine-generator mass. On a steam turbine, the speed increase is sensed and control valves close extremely rapidly to shut off input energy, thus removing the accelerating force. The severity of the overspeed is directly proportional to the valve closure time and the inertia of the unit. The rapid valve response limits overspeed on a steam turbine to a few percent.

On a hydro turbine, the input energy is a large mass of water traveling at significant speed. A rapid closure of the gate would result in waterhammer with a pressure spike that would damage the penstock. Consequently, the minimum and maximum design pressures for the penstock limit the rate of gate movement. The delayed gate response allows some hydro units to accelerate to 150% rated speed. These units are designed to withstand this speed for a short time, relying on governor action to return the unit to near rated speed within a few seconds. However, if a failure occurs within the gate or governor system, the hydro unit could attain a speed of 200% rated, incurring major damage.

A time delay overfrequency trip is often provided as backup to the overspeed trip. The delay is set to exceed the time required by the governor to restore the unit to rated speed. If speed does not return to near normal in the allotted time, a gate or governor control failure is assumed and the underfrequency protection initiates closure of an emergency gate upstream of the normal gate.

10.6 EXCITATION SYSTEM

The effect of abnormal frequency operation on excitation is dependent on the type of excitation system and whether the automatic or manual regulator is in service. A generator operating under the control of the automatic regulator with a static exciter powered from an isolated source, as shown in Figure 10.4, would not be noticeably affected by reduced frequency operation. On the other hand, excitation would probably collapse when the frequency dropped below 95% rated if the same generator had a self-excited rotary exciter similar to that in Figure 10.6 or was self-excited (Figure 10.7), and was operating under the control of the manual regulator.

© 2006 by Taylor & Francis Group, LLC

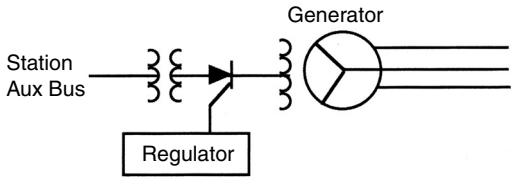


FIGURE 10.4 Separately excited static exciter.

The operation of the manual or automatic regulator themselves is generally unaffected by off-frequency operation. The output of a generator or shaft-driven exciter is a function of the field current and speed (frequency). If the field current is held constant, output voltage decreases directly with frequency. When the field of a shaft driven exciter is supplied from a shaft-driven pilot exciter (Figure 10.5), the effect of a frequency reduction will compound such that the main exciter output decreases with the square of the frequency reduction. Any reduction in excitation will reduce the forcing capability and with it generator short-term Var output capacity. Since Vars provide system voltage support, excitation system performance during an underfrequency event can be crucial to system recovery.

The worst underfrequency response is found in self-excited systems similar to Figure 10.6 or Figure 10.7. The field current is derived from the exciter or generator terminal voltage. In this configuration, the operation of the automatic or manual regulator is analogous to a variable resistance between the output terminal and the field circuit. The resistance value would be that necessary to produce the field current required for the existing terminal voltage. The automatic regulator has the capability of changing its resistance in response to system conditions. The manual regulator is a fixed resistance.

Operation at reduced frequency lowers the exciter and generator output voltage for a given value of field current. The automatic regulator will compensate for reduction in terminal voltage by reducing its equivalent resistance, thus increasing field current and restoring the terminal voltage.

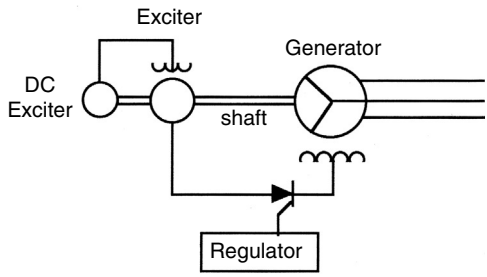


FIGURE 10.5 Separately excited rotating exciter.

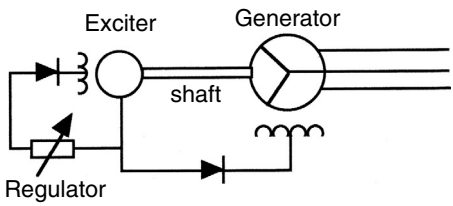


FIGURE 10.6 Self-excited rotating exciter.

© 2006 by Taylor & Francis Group, LLC

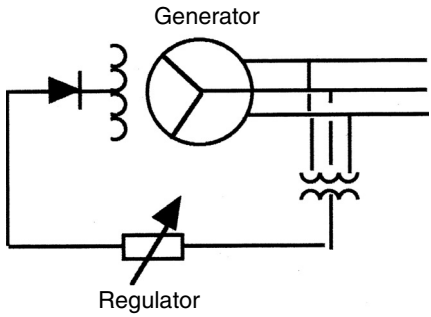


FIGURE 10.7 Self-excited generator.

The manual regulator resistance is fixed and the shape of the terminal voltage vs. field current curve determines the operating point at reduced frequency. Figure 10.8 is a plot of output voltage vs. field current for the rated loaded condition. Superimposed over this plot is the field load line, which is a plot of the equivalent regulator resistance plus the generator field circuit resistance. The point of intersection of the two curves defines the operation point. The figure shows that at rated speed the manual regulator is set such that the load line intersects the output voltage curve at 1.0 pu. With a speed reduction to 95%, the output voltage plot is reduced by 5% and the operating point shifts to 90% voltage as determined by the intersection of the reduced curve with the manual regulator load line. If the frequency were reduced to 90% rated, the load line would parallel the generator voltage curve and no stable operating point would exists. The output voltage would collapse. Although a similar collapse is possible under automatic regulator control it is unlikely because a much larger frequency reduction is required.

This example provides another reason why generators should operate under the control of the automatic voltage regulator. However, operation with the automatic regulator does not ensure the security of the excitation system. During a system underfrequency event, load exceeds generation and machines would be expected to operate in the field-forcing mode in an attempt to maintain system voltage. Reflecting back to Chapter 8, when forcing approaches the thermal limit of the field winding, protective circuits acted to reduce excitation to that required for full load operation.

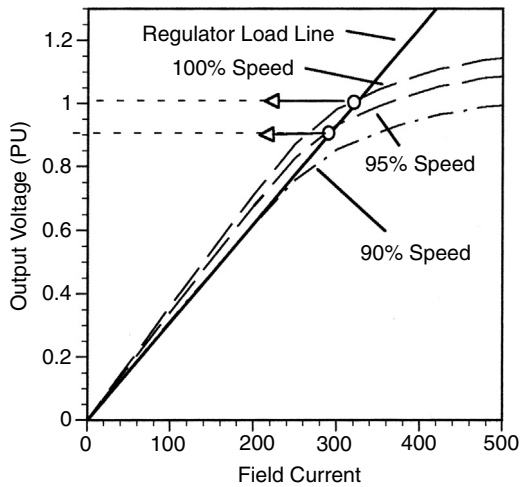


FIGURE 10.8 Self-excitation with frequency variations.

© 2006 by Taylor & Francis Group, LLC

Such a reduction can precipitate an excitation collapse on both self and pilot excitation systems during an under-frequency event.

10.7 PROTECTION AND SETTINGS

Protection of turbine blades from the effects of off-frequency operation is a very difficult problem. The protective scheme must operate with sufficient speed to provide protection for each band of the manufacturer's withstand characteristic. The protection must also have sufficient delay to allow coordination with automatic load shedding schemes on the power grid. Also, since vibratory stress is cumulative, the allowable time at a given abnormal frequency should be a function of the past history of the turbine.

Overfrequency protection is not applied because this condition can be corrected locally by governor action or manual control. Underfrequency protection is provided because this condition cannot be corrected locally.

10.7.1 Primary Protection

The primary protection against underfrequency operation is the automatic load shedding system employed on the power system. Systemwide underfrequency is caused by load in excess of generation. Load shedding is designed to trip enough load to restore the load/generation balance and thus correct the underfrequency condition.

During severe system disturbances, tie lines trip, dividing the power system into isolated islands. The load/generation mixture in each island will vary. Some islands will have excess generation and operate above rated frequency. In these islands, governor or manual intervention will reduce generation to restore the balance, thus reestablishing system frequency. In other islands, load will exceed generation, causing system frequency to decay. A reduction in frequency will reduce load and increase generator torque. Frequency in such an island would decrease until a balance between load and output is reached. If the load/generation mismatch is large enough to cause the frequency to drop below approximately 55 Hz, the operation of auxiliary plant equipment is impaired to the point where generator output falls. Without rapid intervention in the form of load shedding, an island with this level of overload can collapse in minutes.

Because frequency decay is a measure of the severity of a system overload, automatic load-shedding schemes are design to monitor the decay of system frequency. These schemes drop load in steps as the frequency decays. Typically, a load shedding will drop 20 to 50% of the system load in four to six frequency steps. Load shedding is accomplished by tripping designated distribution substation feeders. Each chosen feeder is assigned to one of the load-shedding levels. Typical shedding steps are:

First level, 59.4 Hz for 15 cycles
Second level, 58.8 Hz for 15 cycles
Third level, 58.2 Hz for 20 cycles
Fourth level, 57.8 Hz for 20 cycles

Load shedding schemes are designed to accommodate the maximum credible overload condition.

The final operating frequency for either the overloaded or underloaded condition is determined by the effective droop characteristic on the turbine governors and the variation of load with frequency. Steam turbine governors are drooped about 4%. This means that a 50% load change will produce a 2% speed change or 1.2 Hz.

Ideally, automatic load shedding is designed to shed just enough load to restore the balance between connected load and generation. However the complexity of the power system makes

© 2006 by Taylor & Francis Group, LLC

this goal difficult to attain. Load levels and the mix of available generation change hourly along with system configuration due to equipment outages. These factors may cause the system to form different islands than those used in the design of the load-shedding scheme. Another complication is that the frequency decay itself is oscillatory and nonhomogeneous across the power system. As a result, over or undershedding of load is unavoidable.

10.7.2 Backup Protection

Recognizing the potential for undershedding, it is prudent to install backup underfrequency protection at the generator. It is recognized that the operation of such protection would cause the loss of generation in an already deficient system, thus precipitating a system collapse. This outcome is preferred to turbine damage. With the proper application of underfrequency protection, damage will be avoided and the machine will be available for load restoration following the disturbance.

The backup protection is in the form of multilevel underfrequency tripping. A separate time-delayed underfrequency function is recommended for each band on the manufacturer's limit curve.

Two basic protective schemes are applied. The type of timers applied differentiates these schemes. One scheme uses cumulative timers to store a history of the operating time in each protective band in nonvolatile memory. This scheme is only available in microprocessor relays and would be used to take advantage of the full underfrequency capability of the prime mover. Each timer would be set near the maximum allowable time for the band it protects. This philosophy is intended to maximize the availability of large units during system disturbances, thus improving the power system's ability to survive such disturbances.

A six-level accumulated time scheme is show in Figure 10.9. Underfrequency trip settings are slightly above the start of each band, and timers are set slightly below the total allowable time for each band. When the cumulative operating time in a band for all previous

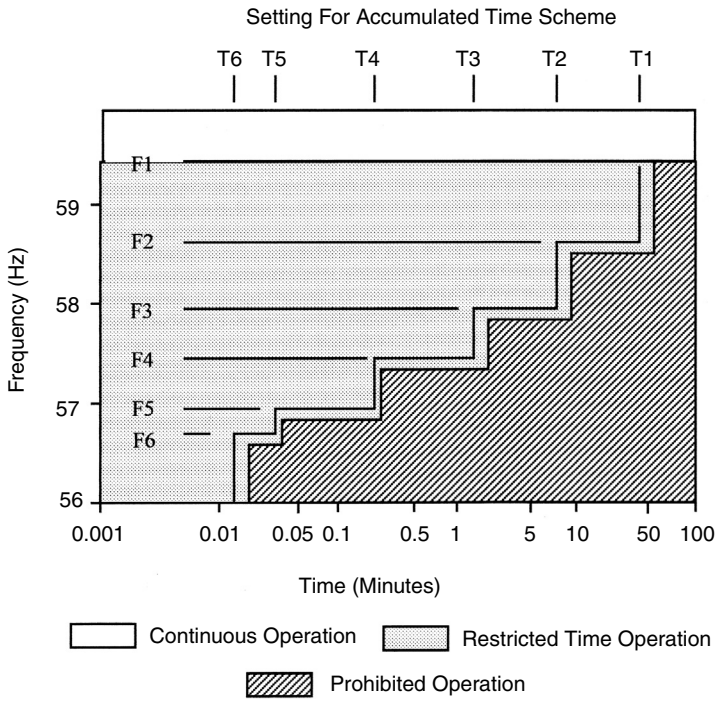


FIGURE 10.9 Accumulating timer scheme.

© 2006 by Taylor & Francis Group, LLC

underfrequency events plus the current event equals that band timer setting, the scheme will operate to trip the generator.

The operation of this scheme indicates that the blades associated with the actuated band are at the end of their useful life. At a minimum, a complete inspection of the blades is indicated.

Once a setting for each level of protection is determined, the composite protection characteristic should be plotted against the system frequency response for the most severe credible system disturbance to assure coordination exists with the system load-shedding scheme. Underfrequency protection at the generator must not operate for disturbances successfully managed by the load-shedding scheme. The system condition considered should be that which requires the maximum load shedding to prevent a system collapse, because this condition will produce the maximum frequency decay and the slowest recovery.

The system frequency response is determined from system dynamic studies that include detailed representations of the mechanical and electrical systems at all generators in the affected area. These studies require a huge amount of data and must be performed by the entity that controls the bulk power transmission in the service area where the generator is located. Frequency vs. time data for the worst case disturbance may be available from that organization. In many areas, the controlling entity will provide specifications for the generator underfrequency trip settings instead of frequency response data. Adherence to these specifications is intended to assure coordination with system load shedding.

Figure 10.10 is an overlay of the turbine underfrequency protection previously shown and a plot of system response to successful and unsuccessful load shedding. For the unsuccessful case, system frequency does not recover and the generator is tripped in about 3 sec (0.05 min) before damage can occur. When system restoration is successful, the timer for the 58.5 to 59.5 Hz band will accumulate times $t_a - t_b$ and $t_e - t_f$, the 58.5 to 57.9 Hz band accumulates times $t_b - t_c$ and $t_d - t_e$, and the 57.9 to 57.4 Hz band accumulates time $t_c - t_d$. By inspection, times $t_a - t_b$ plus $t_e - t_f$ will not sum to the

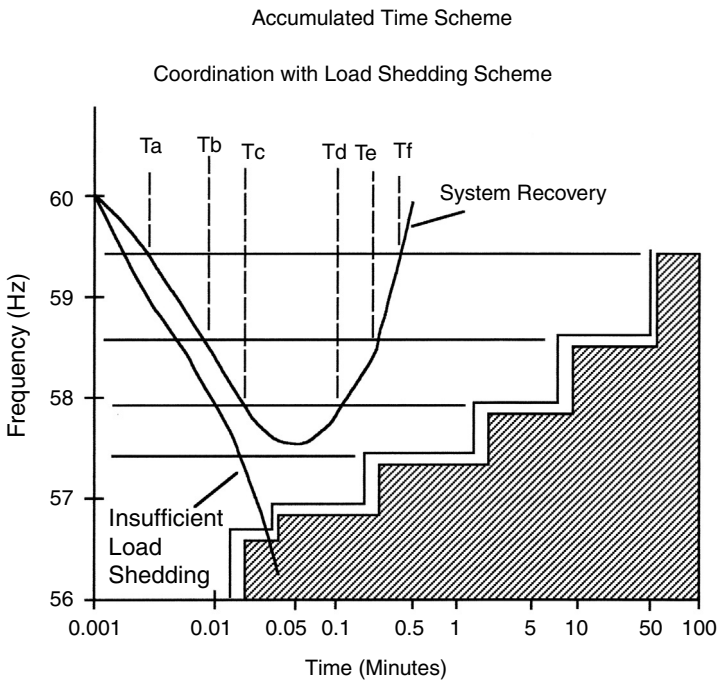


FIGURE 10.10 Coordination with system load shedding. (From IEEE C37.106-1987, IEEE Guide for Abnormal Frequency Protection of Power Generating Plants. With permission.)

© 2006 by Taylor & Francis Group, LLC

50 min timer setting in that band. Likewise, the time in the other bands will not reach the respective timer settings; hence, no tripping will occur and coordination with the power system load-shedding scheme will exist.

The more common scheme uses standard timers that measure the duration of the current underfrequency event then reset to zero. Because the timers in this scheme are without memory, each timer remains actuated as long as the frequency is below its initiating frequency. This is unlike the scheme with cumulative timers where time is not accumulated when the frequency enters a lower frequency band. Timers in this scheme are set to permit only a specific loss of life for each underfrequency event. As an example, each level of underfrequency protection could be set for 10% loss of life by setting the timer at 10% of the allowable delay of the band it protects. The lower the allowed loss -of- life, the better the protection and the higher the probability the generator will be lost during a system disturbance.

To compensate for the lack of memory in the scheme, a method of monitoring and recording the off-frequency operating history of the turbine should be considered for these installations. Although administrative controls could be use to monitor the number of trips from each band, this would not give an indication of available blade life. Most events will be of shorter duration than the trip timer setting and would result in significant undocumented loss of blade life.

Often only one or two levels of underfrequency protection are provided, usually with standard timers. When the number of limiting bands exceeds the number of underfrequency protective functions, compromise settings are required. A scheme of this type is shown in Figure 10.11. Complete turbine protection is not provided in the 56.5 to 57.3 Hz band. Protection is sacrificed here to provide coordination with system load shedding. It is apparent that if the setting of the second underfrequency relay were changed from 57.0 to 57.5 to provide full protection the scheme would operate for a recoverable system disturbance. Abbreviated one- or two-step protection should only be applied when the probability of underfrequency operation is very low and the confidence in the system load-shedding scheme is high.

With any underfrequency scheme, an alarm must be provided to alert operators of the underfrequency condition.

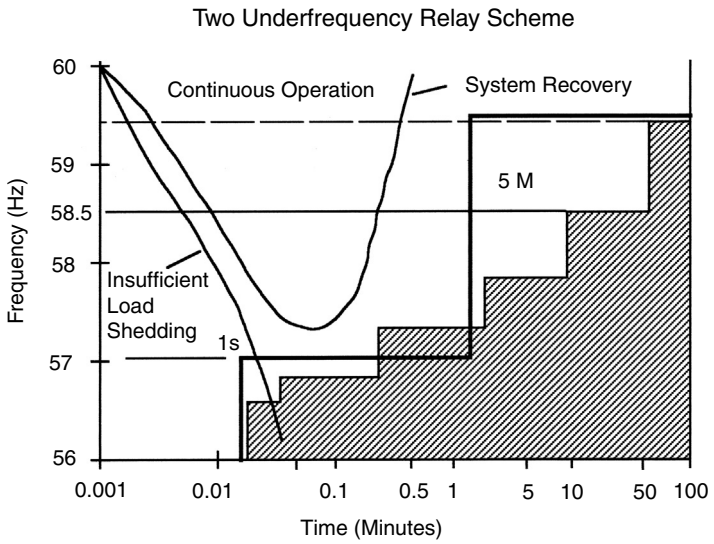


FIGURE 10.11 Compromise scheme.

© 2006 by Taylor & Francis Group, LLC

10.7.3 Combustion Turbine Generators Protection

Combustion turbine generators blades, in general, tolerate a wider frequency range than steam turbine blades. Some CTG turbines can operate continuously at frequencies as low as 57 Hz. This approximates the minimum stable frequency for the power system. A further reduction in frequency will cause a reduction in steam generator output throughout the system due to impaired performance of turbine auxiliary equipment. Above this frequency, steam generator power output increases with reduced frequency; below this frequency, output falls with frequency and the system collapses. The proximity of the CTG minimum operating frequency and minimum system stable frequency sharply reduces the number of underfrequency protection levels needed. CTGs are often provided with only a single time-delayed underfrequency trip.

Because GTGs can be started and load quickly, they are often used as peaking units or for restoration following a disturbance. In either case, such units are placed in service during periods of system stress. Their operation can be critical to system recovery or restoration and consideration should be given to maximizing their availability, even if protection is sacrificed. One approach is for underfrequency protection on these units to alarm instead of trip. Another approach is to keep CTGs on line as long as steam units by setting CTG underfrequency trips below the lowest underfrequency trip level for area steam units. This is practical, because GTGs are more tolerant of underfrequency than steam units.

Underfrequency settings of CTGs and scheme logic may also require coordination with "compressor surge" protection provided in the CTG fuel system.

REFERENCES

1. Crenshaw, M. L. and Temoshok, M., Protection of large steam turbine generators during abnormal operations, *Pennsylvania Electric Association Relay Committee Meeting*, October 21–22, 1971, Reading, PA.
2. Westinghouse Power Generation Systems Publication, GEN 74-009, *Underfrequency Operation of Westinghouse Power Generation Equipment*, Westinghouse, August 1974, East Pittsburg, PA.
3. *IEEE Guide for Abnormal Frequency Protection for Power Generating Plants*, C37.106–1987, IEEE, New York, 1987.
4. Baily, F. G., Bardwick, H. A., and Fenton, R. E. Operating and maintaining steam turbine generators–Operating at off-normal conditions, Power, August 1976, The McGraw-Hill Companies.
5. Berdy, J., Brown, P. G., and Goff, L. E., *Protection of Steam Turbine Generators During Abnormal Frequency Conditions*, General Electric Company, Schenectady, New York.

© 2006 by Taylor & Francis Group, LLC

11 Minimum Excitation Limiter

11.1 OVERVIEW OF THE MINIMUM EXCITATION LIMITER APPLICATION

The minimum excitation limiter (MEL) is unique in that it is not a protective relay, but rather a control function integral to the automatic voltage regulator (AVR) circuitry. It acts to limit Var flow into the generator. During normal operation, the AVR maintains generator voltage at a preset value. When system conditions attempt to produce Var flow into the generator in excess of the MEL setpoint, the MEL activates, overriding the AVR setpoint to increase terminal voltage which reduces the Var in-flow. The voltage increase continues until Var flow is reduced below the MEL setting.

11.1.1 Operation in the Leading Mode

Operation in the leading mode (drawing Vars into the generator from the power system) can be required during periods of light load. High-voltage transmission lines are highly capacitive when lightly loaded. The Vars produced by these lines can raise system voltage to unexceptable levels. Under such conditions, generators are operated in the leading mode to absorb excess reactive power, thus controlling system voltage.

When a relatively large generator is connected to a weak system, the unit may be required to operate in the leading mode to prevent overvoltage caused by the transmission of real power across the system. Neglecting the variation of current with voltage and assuming lagging Vars are positive. Voltage rise can be approximated as

$$\Delta\overline{V} = \overline{RP} + \overline{XQ} + j(\overline{XP} - \overline{RQ}) \tag{11.1}$$

where R and X are system resistance and reactance and P and Q are real and reactive power, respectively. The bars indicate per unit quantities.

In the case of the sample system (Figure 1.1), with line "A" outaged the impedance of the power system is 22.5% on the generator KVA base. If the power system impedance angle is assumed to be 70° and the GSU transformer is 7.0% pure reactance on the generator base the impedance seen at the generator terminals would be $Z = 7.7 + j28.1\%$. The generator is rated at 85% power factor, which translates to a maximum power output of $P = 0.85$ pu. If system voltage is assumed to be 1.0 pu the voltage rise resulting solely from the transmission of real power across the weakened system would be 9% as calculated below.

$$\begin{aligned} e_t &= e_s + \overline{RP} + j\overline{XP} \\ &= 1.00 + 0.077 \times 0.85 + j0.28 \times 0.85 = 1.092\angle 12.5^\circ \end{aligned} \tag{11.2}$$

The maximum permissable operating voltage for a generator is 105%. If the sample system generator is to operate at rated output and below the voltage limit the generator must operate in the leading mode. At full load and 20MVAR leading ($Q = -0.19$) generator voltage becomes $e_t = 1.0 + (0.077 \times 0.85 - 0.28 \times 0.19) + j(0.28 \times 0.85 + 0.077 \times 0.19) = 1.04\angle 14.0$

Generators can be driven far into the leading region by system voltage variations. Any rise in system voltage will cause the AVR to reduce field current and with it Var output in an attempt to restore the voltage defined by the AVR setpoint. A small machine cannot absorb sufficient Vars to

© 2006 by Taylor & Francis Group, LLC

effect a change in voltage on a strong system. If no MEL is provided, the excitation could be driven to zero as the generator attempts to absorb reactive beyond its capability.

A generator may also be driven far into the leading mode by equipment failures. The failure of the excitation system on a nearby generator could cause that unit's excitation system to go to full boost. The resulting Var flow into the system from a medium or large unit could drive area voltages dangerously high. Other area units on AVR control would respond rapidly to reduce field current, absorbing Vars to lower system voltage.

11.1.2 Limits on Leading Var Operation

The most obvious limit to leading Var operation is the bottom portion of the generator's capability curve, but several other limits exist. Var flow is dependent on the difference between the system and generator voltage and the impedance between the two. Leading Var operation requires generator voltage to be less than the system voltage. The minimum allowable continuous generator terminal voltage, which is 95% rated, can therefore limit the leading Vars a generator can absorb during normal operation.

The circle diagram described in Chapter 1 defines the permissible watt/Var operating points associated with a given set of system conditions. Figure 11.1 is such a plot for the sample system under normal conditions and with line "A" out of service. This diagram shows that the leading Var capability is severely reduced when the system is weakened by the line outage.

Another limit is system stability. A power grid and interconnected generator can lose steady-state, dynamic or transient stability. Steady-state stability is the ability of the system and connected generators to remain synchronized during normal operation. Dynamic stability is the absence of undamped oscillation. Transient stability is the system's ability to recover from abrupt changes such as line switching or a fault. Steady-state and dynamic stability are pertinent to the discussion of MEL settings and will be discussed here. Transient stability does not influence MEL settings and will be discussed in a later chapter.

Power is delivered to the generator shaft by a turbine or other prime mover. This power is transmitted across the generator airgap to the electrical system. Under normal operation, the flux produced by the stator and rotor currents is magnetically interlocked by forces within the airgap. This interlock holds the two flux at a fixed angle to one another as they circle the stator at synchronous speed. When a system change occurs; such as switching or a fault there is a transient period when rotor and stator speeds differ and the angle between them varies as the system adjusts to the new operating condition. In a stable system, a damped speed oscillation persists until the rotor and stator return to synchronous operation at a new fixed angular displacement as dictated by the new system condition.

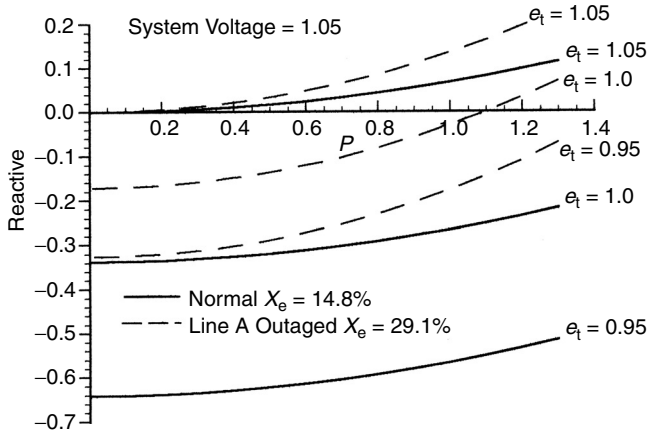


FIGURE 11.1 Leading Var operation.

© 2006 by Taylor & Francis Group, LLC

Using the analysis presented in Ref. [1], stability following a disturbance is dependent on two factors. The interaction of the generator and system must produce sufficient "synchronizing torque" to maintain the interlock between the stator and rotor flux. Secondly, the interaction of the generator and system must produce sufficient "damping torque" to force the decay of oscillations resulting from the disturbance.

A lack of sufficient synchronizing torque would result in an uncoupling of the rotor and stator flux and acceleration of the generator or system. This is a loss of "steady-state stability." A lack of damping torque would be characterized by a growing oscillation of terminal voltage, current, power and speed with time. This is a loss of "dynamic stability."

These modes of instability will be discussed in more detail later. For now it is sufficient to understand that if the generator's operating point is allowed to move deep enough into the leading Var region, the generator will lose both steady-state and dynamic stability. A second point is that the limits of steady-state and dynamic stability can be defined for a specific generator in terms of the generator's minimum allowable Vars output for a given power output.

11.2 SETTING CRITERIA BACKGROUND

Minimum excitation limiters were introduced in the late 1940s when stability was a major concern. The MEL was intended to prevent operation beyond the limits of stability and beyond the leading Var capability of the generator. Later, as the application of distance-type loss of field (LOF) became accepted practice, the MEL was also applied to prevent false LOF relay operation during severe disturbances.

The MEL characteristic represents the boundary of underexcited operation when the generator is under AVR control. Figure 11.2 shows the desired relationship between the MEL, generator capability, manual regulator steady-state stability limit, and LOF relay.

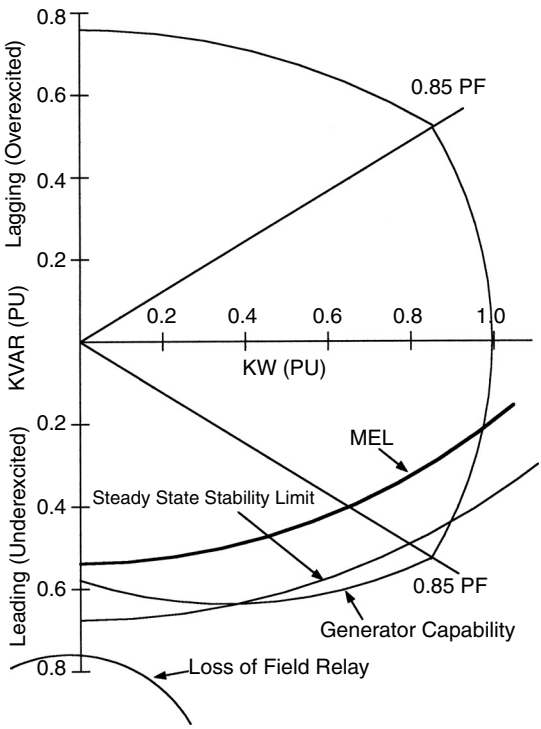


FIGURE 11.2 MEL setting.

© 2006 by Taylor & Francis Group, LLC

At the time when the MEL was introduced, systems were weak and many generators were equipped with manual regulators or with slow-acting automatic regulators having dead bands. Because dead-band regulators provide fixed excitation within each band, they are equivalent to manual regulators in stability analysis. For both regulator types, steady-state stability is usually more limiting than dynamic stability.

From this beginning, the MEL setting has been based on the most limiting of two conditions, the manual regulator steady-state limit or the generator leading Var capability. The MEL was typically set with a 15 to 20% margin above these limits.

The development and application of the continuously acting voltage regulator dramatically increased the steady-state stability limit. This type of regulator allows excitation to respond to and counteract small system changes. In effect, the continuously acting AVR adds synchronizing torque to the system proportional to the regulator gain. The steady-state stability limit under AVR control is far less limiting than the steady-state limit under manual control. Unfortunately, as increased AVR gain adds synchronizing torque it reduces damping torque. As a result, under AVR control the dynamic limit is normally more limiting than the steady-state limit. Note that normally neither AVR limit is as restrictive as the manual regulator steady state limit.

Even after the advent of continuously acting regulators, the more restrictive manual regulator steady-state limit remained part of the MEL setting criteria. This criterion may appear misapplied, because the MEL is only active when the AVR is in control of the generator and with the AVR in control the dynamic limit is usually the actual stability limit. However, the manual regulator limit is a valid setting criterion for the majority of excitation systems. Most excitation systems automatically fast-transfer to the manual regulator in the event of an automatic regulator failure. A MEL setting based on the manual regulator steady-state limit prevents operation in areas that would be unstable in the event of an AVR failure. Another reason the manual regulator steady-state limit has been retained is the difficulty in computing the higher AVR dynamic limit.

In the early 1960s, power system stabilizers (PSS) became available on most excitation systems. A PSS is another auxiliary control function within the AVR. It provides a control action to oppose system oscillation. In effect, it restores the damping torque canceled by the high-gain AVR. The PSS function is expensive and is not installed on all excitations system. When the AVR is equipped with a PSS the AVR stability limits are increased far beyond the generator leading Var capability and should not be considered when setting the MEL.

The manual regulator steady-state limit has been retained as the setting criterion for the MEL in many texts, without regard to the type of excitation system provided. This philosophy is rooted in the dominant excitation system configuration that includes one AVR and one manual regulator with automatic transfer to the manual regulator. New digital regulators are available with redundant AVR and manual regulators. The failure of an AVR in such a system results in a transfer to the backup AVR. The manual limit is not applicable on such systems unless the very unlikely concurrent failure of both AVRs is considered.

When the manual regulator limit is arbitrarily applied as a setting criterion, generator operation in the underexcited region can be restricted unnecessarily. At installations where the system is strong, the applicability of the manual steady-state limit is not an issue because the stability limit is outside the generator capability and does not influence the MEL setting. However, on weak systems, the manual limit can be more restrictive than the generator capability and therefore will form the basis for the MEL setting.

11.3 SETTING CRITERIA

The MEL shall be set to prevent operation beyond the leading Var capability of the generator. The MEL and LOF relay characteristics should not overlap. This will ensure that power system swings that produce leading Var transients actuate the MEL before the LOF relay. This does not ensure that the MEL will respond with sufficient speed to prevent a LOF trip for such as swing.

© 2006 by Taylor & Francis Group, LLC

Stability limits are only considered when they are more restrictive than the generator capability curve. Because these limits become more restrictive as the system is weakened, the important question becomes what conditions are considered credible when defining the stability limits. A conservative approach would be to calculate the stability limit assuming one system facility fails while another system facility is out of service for maintenance.

If the most common type of excitation system, one that transfers to a manual regulator in the event of an AVR failure is considered, this criterion gives rise to two credible conditions for stability limits.

1. With the strongest source to the generator HV bus outaged, the second strongest source fails. The AVR dynamic limit defined with two sources out is the operative limit. The MEL should be set to prevent operation beyond this limit. The AVR dynamic limit is chosen because it is more limiting the AVR steady-state limit.
2. With the strongest source to the generator HV bus outaged, the AVR fails. The excitation system will transfer to the manual regulator and the manual regulator steady-state limit is the applicable limit defined with the one source outaged.

If the same excitation system is assumed, but with the AVR equipped with a PSS, the dynamic limit for the first condition will be far in excess of the generator capability and would not affect the MEL setting. The second condition remains valid.

If the excitation system has redundant automatic regulators, but no PSS, the first condition would again dictate the AVR dynamic limit. Since the second case would result in the transfer to the backup AVR with one source out of service. It would be less limiting than the first case, and would not be used.

Another scenario applicable to this system would be the outage of one AVR and the failure of the other. This would be very unlikely considering the designed separation between the primary and backup systems. However, if it occurred, the operable limit would be the manual steady-state limit with the system in a normal configuration.

The multiple outage criteria discussed above are conservative and applicable on strong systems. On systems that are normally weak, this approach may result in a MEL setting that severely restricts leading Var capability during normal operation. In this case, a less conservative single outage approach may be necessary.

There may be rare instances where short-term leading Var requirements may exceed the generator's continuous capability. The recovery period following islanding is an example. The generator's leading Var limit is a thermal limit and the continuous limit can be exceeded for a short period as determined by the manufacturer. In such a situation, the MEL could be utilized as an alarm function to alert an operator of a potentially damaging condition. It then becomes the operator's responsibility to limit this mode of operation to prevent damage.

11.4 GENERATOR LEADING VAR CAPABILITY

The lower portion of the generator capability curve defines the leading Var limit of a generator. Leading Var capabilities for round rotor and salient pole machines differ, because they are set by different physical limitations within the machine. In the salient pole machine, the ampere rating of the stator winding limits leading Vars, while heating in the ends of the stator core material limits the round rotor machine. Figure 11.3 is a generalized capability curve showing the relative limitation for a hydro generator, which is a salient pole machine, a steam-turbine generator, and a gas-turbine generator. The latter two machines, which have significantly less leading Var capability, are round rotor machines.

© 2006 by Taylor & Francis Group, LLC

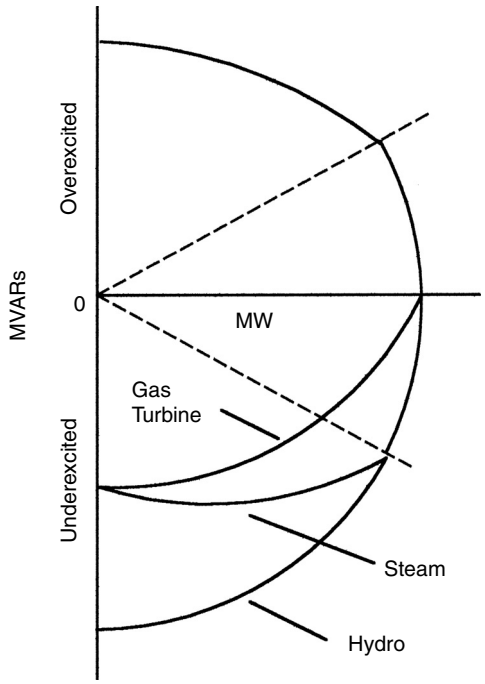


FIGURE 11.3 Generator capability curve.

11.4.1 Stator End-Core Heating in the Round Rotor Generator

Stator end-core heating is caused by leakage airgap flux. Airgap flux is the vector sum of flux produced by load current in the stator windings and the flux produced by the DC current in the rotor winding. The majority of this flux crosses the airgap to link the stator and rotor windings. A portion of this flux does not cross the airgap; instead it exits the end of the stator and links the stator and rotor body as shown in Figure 11.4. This figure is a cross-section of the generator cut along the axis

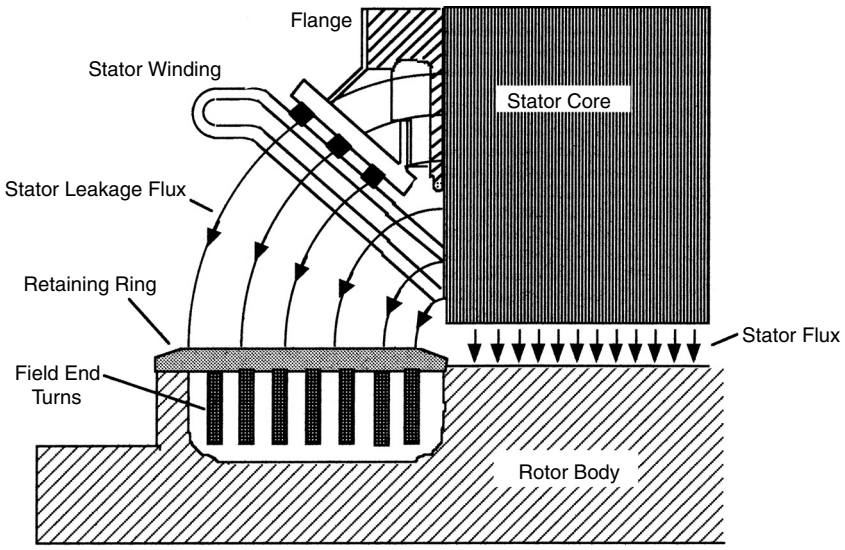


FIGURE 11.4 Stator end-core flux. (From Farnham, S.B., Swarthout, R.W. Field Excitation in Relationto Machine and System Operation, AIEE Transactions, pp. 1215–1223, Dec. 1953. With permission.)

© 2006 by Taylor & Francis Group, LLC

of the rotor. The leakage flux exits the stator at the ends of the stator core through the stator flange and related hardware. It then enters the rotor retaining ring and rotor body from the stator end core and stator flange. The leakage flux rotates around the stator at synchronous speed. The rotation induces eddy currents in all the stator structures it encounters. Because this flux is stationary with respect to the rotor, eddy currents are not induced in rotor structures.

The stator core is constructed of thin sheets of magnetic steel stacked perpendicular to the axis of the rotor. Each sheet is insulated from its neighbor. This laminated construction drastically reducing eddy currents and core heating caused by the eddy currents. Laminations are only effective in eddy current reduction when alternating flux is applied parallel to the laminations. The end-core leakage flux exits the stator parallel to the rotor and perpendicular to the stator laminations. Losses for flux perpendicular to the laminations can be 100 times greater than for flux applied parallel to the plane of the lamination.[2] The high losses confined to the small end-core region can cause rapid temperature rise and damage within minutes. Visible signs of damage would include blueing of metal structures in the end-core region and charring of stator winding insulation at the point where it emerges from the stator.

End-core heating is only a problem when the generator is operating in the underexcited mode, but it is not caused directly by leading Vars. When the generator is operating near full load and rated Var output, the field current is high, causing saturation of the rotor retaining rings. A saturated ring poses a high reluctance, restricting the leakage flux. When the field current is reduced, as would be the case during leading operation, the retaining rings are no longer saturated. The low-reluctance path sharply increases the leakage flux and the associated heating.

In very old machines, the stator end-core limitations can be severe enough to preclude operation near unity power factor. Over the years, manufacturers have developed methods to reduce this limitation. These techniques included nonmagnetic retaining rings, flux shields and changed configuration for the stator end region to minimize perpendicular flux paths. These improvements generally provide a leading Var limit of approximately 60% rated MVA at zero power output and a leading full load power factor capability of 95% or better.

Because the leakage flux is a function of the airgap flux, the leading Var limitation will vary with voltage. Knowledge of this variation is important if damage is to be avoided over the full range of operations. Unfortunately, capability curves published by manufacturers only define the leading limit at rated voltage.

Reference 3 suggests a method of deriving the end-core heating limit and defines how this limit will vary with voltage. The derivation is based on the premise that the end-core leakage flux is proportional to the airgap flux and that heating varies as the square of the flux. Figure 11.5 shows the relation between terminal quantities and the resulting flux. Field flux (ψ_f) leads the equivalent field voltage (E_I) by 90° and stator current flux (Ψ_s) is in phase with stator current. The airgap flux is the vector sum of the field winding flux and stator current flux.

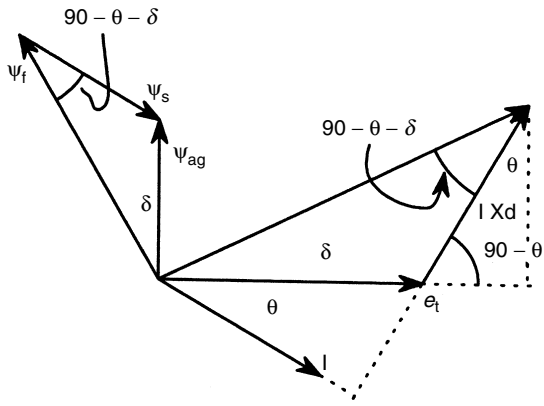


FIGURE 11.5 Generator flux.

© 2006 by Taylor & Francis Group, LLC

Using the law of cosines the airgap flux is:

$$\Psi_{ag}^2 = \Psi_f^2 + \Psi_s^2 - 2\Psi_f^*\Psi_s \cos\left(\frac{\pi}{2} - \delta - \theta\right) \tag{11.3}$$

where δ is the angle between the terminal voltage and the voltage equivalent to the field excitation and θ is the power factor angle.

Redefining flux in terms of current with E directly proportional to field current:

$$\Psi_f = E * N_f \tag{11.4}$$

and

$$\Psi_s = N_s I X_d \tag{11.5}$$

Equation (11.3) can be rewritten in the form:

$$\Psi_{ag}^2 = N_f^2 E^2 + N_s^2 I^2 X_d^2 - 2N_s I X_d * \ N_f E \cos\left(\frac{\pi}{2} - \delta - \theta\right) \tag{11.6}$$

The assumption is that eddy current heating is proportional to the square of the airgap flux density, thus the heating is directly proportional to Ψ_{ag}^2. Using constant k_t, to relate flux to heating the temperature rise can then be written as:

$$T = k_t N_f^2 E^2 + k_t N_s^2 I^2 X_d^2 - 2k_t N_s N_f I X_d * E \cos\left(\frac{\pi}{2} - \delta - \theta\right)$$

Redefining variables and rewriting

$$a = k_t N_f^2 \quad b = k_t N_s^2 \quad c = k_t N_s N_f$$

$$T = aE_I^2 + bI^2 X_d^2 - 2cIX_d E \cos\left(\frac{\pi}{2} - \delta - \theta\right) \tag{11.7}$$

Using the relations derived from the Figure 11.5:

$$E^2 = (e_t \cos(\theta))^2 + (e_t \sin(\theta) + IX_d)^2 \tag{11.8}$$

and

$$e_t^2 = E^2 + (IX_d)^2 - 2EIX_d \cos\left(\frac{\pi}{2} - \delta - \theta\right)$$

Which can be rewritten as:

$$\cos\left(\frac{\pi}{2} - \delta - \theta\right) = \frac{X_d^2 I^2 + E^2 - e_t^2}{2X_d IE} \tag{11.9}$$

Substituting Equation (11.9) then (11.8) into (11.7) gives:

$$T = ae_t^2 + 2(a - c)X_d I e_t \sin(\theta) + (a + b - 2c)X_d^2 I^2 \tag{11.10}$$

Defining

$$\sin(\theta) = \frac{Q}{\sqrt{P^2 + Q^2}} \qquad I = \frac{\sqrt{P^2 + Q^2}}{e_t}$$

© 2006 by Taylor & Francis Group, LLC

And substituting into Equation (11.10)

$$\frac{Te_t^2}{(a+b-2c)X_d^2} = \left[\frac{(a-c)e_t^2}{X_d(a+b-2c)} + Q\right]^2 + \frac{(ab-c^2)e_t^4}{X_d^2(a+b-2c)} + p^2 \tag{11.11}$$

Since a ∗ b = c^2 Equation (11.11) reduces to

$$\frac{T}{(a+b-2c)}\frac{e_t^2}{X_d^2} = \left[\frac{(a-c)}{(a+b-2c)}\frac{e_t^2}{X_d^2} + Q\right]^2 + p^2$$

Redefining constants

$$K_1 = -\frac{c-a}{a+b-2c} \tag{11.12}$$

$$K_2 = \sqrt{\frac{\Delta T}{a+b-2c}} \tag{11.13}$$

ΔT represents the maximum permissible continuous temperature of the end core region.

The end-core-heating limit becomes:

$$K_2^2\frac{e_t^2}{X_d^2} = \left(Q - K_1\frac{e_t^2}{X_d}\right)^2 + P^2 \tag{11.14}$$

The expression for the end-core heating limit is a circle with a center located on the Q-axis and radius as follows:

$$Center\,(P,Q) = \left(0, K_1\frac{e_t^2}{X_d}\right) \qquad Radius = K_2\frac{e_t}{X_d} \tag{11.15}$$

Note that the location of the center varies with the square of the generator terminal voltage, while the radius varies directly with terminal voltage. Thermal constants K_1 and K_2 are unique to each generator.

It is not practical to conduct thermal testing for the purpose of establishing the MEL setting, but the variation of the leading Var capability with voltage can be estimated if the center and radius at rated voltage are derived from the published capability curve. Figure 11.6 compares a calculated curve with the manufacturer's curve for a 0.95 PF machine. The plot also shows leading Var capability is markedly reduced as terminal voltage increases.

11.4.2 Leading Var Capability of a Salient Pole Machine

The limit represented by Equation (11.14) is applicable to round rotor generators. The leading Var portion of the capability curve for a salient pole machine is defined by the ampere rating of the stator. This limit plots on the capability curve as an arc from the origin with radius equal to the ampere rating of the stator times $\sqrt{3}$ of the terminal voltage as plotter in Figure 11.3 for the hydro unit. Salient pole Var capability would therefore vary directly with voltage. This is in contrast to the limitation of the round rotor machine which decreased leading Var capacity with increased voltage.

The significance of the differences between the underexcited Var capability of the salient pole and round rotor machines with respect to voltage variations will be apparent when the MEL voltage characteristic is discussed.

© 2006 by Taylor & Francis Group, LLC

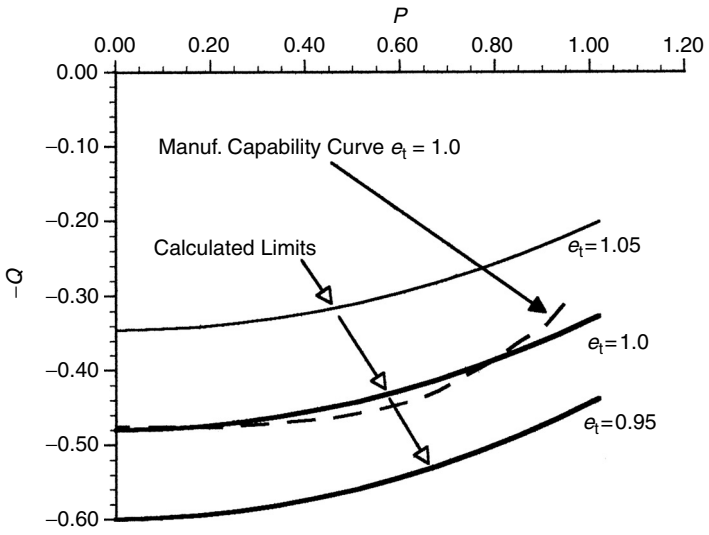


FIGURE 11.6 Calculated end-core thermal limit.

11.5 COORDINATION WITH THE LOF RELAY

Impedance-type LOF relays are applied at the generator terminals to detect a complete failure of the generator excitation in the form of a loss of DC voltage or short circuit. Such a failure will collapse the internal generator voltage and result in Var flow into the generator far in excess of the generator rating. The LOF relay is designed to recognize this condition and trip the generator, usually within one second of the failure.

This type of LOF protection can misoperate when system disturbances caused large transient Var flow into the generator. Coordination of the MEL and LOF characteristic assures that any disturbance that would cause a large influx of Vars into the generator, thus emulating a loss of field, would first actuate the MEL. Coordination is achieved when the LOF characteristic does not infringe on the MEL characteristic, as shown in Figure 11.2. The intent is that as Var flow into the generator increase during the transient the MEL will activate and increase field current to prevent additional Var in-flow and a LOF trip of the generator. Depending on the speed of the MEL circuitry and excitation system, this intent may or may not be met.

The MEL has been shown in general to be ineffective in preventing LOF operation with certain MEL/exciter configurations. The extreme case would include an older MEL design with long time constants in the MEL output circuitry, coupled with an excitation system employing rotating main and pilot exciters. This configuration provides too great a time delay between MEL actuation and the resulting field current increase to prevent a LOF operation.

In such systems it may be possible to adjust the gain and time constants of the MEL and AVR to provide a more rapid response, but this often results in excitation instability in the form of severe terminal voltage and reactive oscillations when the MEL is activated.[4]

High-speed excitation systems with modern MEL designs can provide sufficient response to avert incorrect LOF operations caused by system transients. Dynamic computer simulations are required to confirm the desired MEL/LOF response for a given installation.

The characteristic of impedance-based LOF relaying is described in terms of and $R-X$ diagram. The MEL characteristic is traditionally plotted as a function of Power-Reactive ($P-Q$). If the MEL and LOF characteristics are to be coordinated, they must be plotted to the same parameters. It is customary to convert the LOF setting from the $R-X$ plane to the $P-Q$ plane.

© 2006 by Taylor & Francis Group, LLC

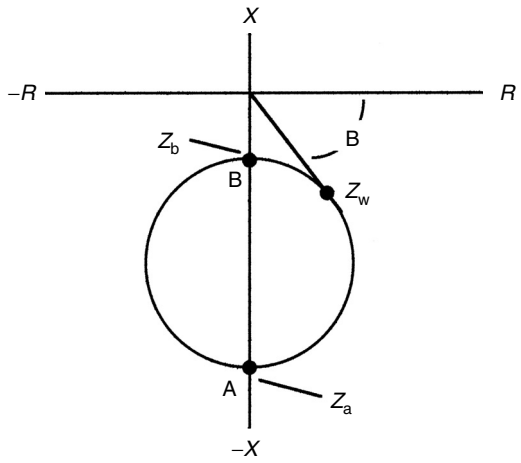


FIGURE 11.7 Loss-of-field relay characteristic on $R-X$ plane.

Converting a point from $R-X$ to $P-Q$ is accomplished using the following:

$$MVA = \frac{kV^2}{Z} \tag{11.16}$$

Conversion of the typical circular LOF characteristic shown in Figure 11.7 to an equivalent circular $P-Q$ characteristic can be accomplished by converting points "A" and "B."

Point $M\text{var}_\text{A}$ (on $P-Q$)

$$M\,\text{var}_\text{A} = \frac{kV^2}{Z_\text{a}} \tag{11.17}$$

Point $M\text{var}_\text{B}$ (on $P-Q$)

$$M\,\text{var}_\text{B} = \frac{kV^2}{Z_\text{b}} \tag{11.18}$$

The resulting points locate the diameter of the equivalent characteristic on the $P-Q$ plane as shown in Figure 11.8. An alternative method of conversion for noncircular characteristics is a

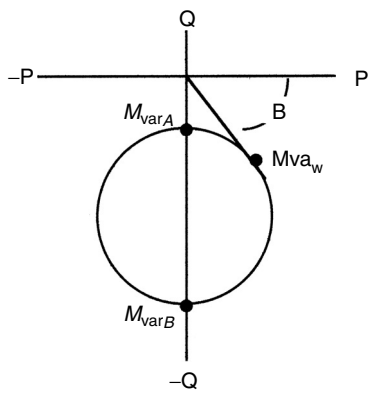


FIGURE 11.8 Loss-of-field characteristic on $P-Q$ plane.

© 2006 by Taylor & Francis Group, LLC

point-by-point conversion. The conversion of point Z_w at angle B to point MVA_w at angle B using Equation (11.16) is as shown in Figure 11.7 and Figure 11.8.

Again note that the coordination shown between the MEL and LOF relay on the $P-Q$ plot, such as shown in Figure 11.2, does not ensure the MEL will prevent misoperation of the LOF relay. This determination must be made from a dynamic simulation of the MEL, excitation system and power system.

11.6 SYSTEM STABILITY LIMITS

Historically, the MEL limit has been set on the basis of the steady-state stability limit with fixed excitation (manual regulator). Protective relay oriented text generally discuss only this limit. It is normally the most restrictive and in many cases it is a proper setting criteria for the MEL as was discussed in Section 11.3, but not always. The AVR dynamic limit is the operative limit when the AVR is in service and it can, in extreme cases, be more restrictive than the manual limit. Because the AVR dynamic limit can be an alternative basis for setting for MEL, the AVR limits will also be presented.

The derivation of the AVR limits is mathematical and provides little insight into the physical reality. Although the solution of the resulting equations yields both the steady-state and dynamic limits applicable to both the AVR and manual regulator, the classical derivation of the manual regulator steady-state limit will be presented first. This derivation provides insight into the concepts involved and offers a quick method of estimating what is typically the most limiting stability condition.

11.6.1 Classical View of Steady-State Stability

A generator would be required to operate in the leading mode (drawing Vars from the power system) to control high system voltage. In this mode, the field current is reduced, thus reducing the internal voltage of the generator. The reduction of internal voltage necessary to reduce system voltage also weakens the forces that hold the generator in synchronism with the power system (reduces synchronizing torque). If the internal voltage is reduced sufficiently, the generator will lose steady-state stability and pull out of step with the grid. Once synchronism is lost, the speed of the rotor flux and stator flux differ, resulting in severe pulsating torque and potentially damaging inducing currents in the rotor structures. The generator must be tripped immediately.

Manual regulator steady-state stability can best be understood by examining the power angle equation that defines the power that the electrical system can accept.

$$P_E = \frac{E_I E_s}{X_d + X_s} \sin\delta + \frac{E_s^2 (X_d - X_q)}{2(X_d + X_s)(X_q + X_s)} \sin 2\delta \tag{11.19}$$

where P_E = electrical power, E_I = voltage behind X_d (Refer to Figure 2.14), E_s = equivalent system voltage, X_d, X_q = d- and q-axes synchronous impedance, X_s = system impedance, and δ = angle between E_I and E_s.

It is customary to ignore the effects of saliency by assuming $X_d = X_q$. The resulting equation represents the generator as a simple voltage behind reactance:

$$P_E = \frac{E_I E_s}{X_d + X_s} \sin\delta \tag{11.20}$$

The power delivered to the electrical system is then proportional to the system and generator voltages and the sine of the angle between them. It is inversely proportional to the impedance between the voltages.

© 2006 by Taylor & Francis Group, LLC

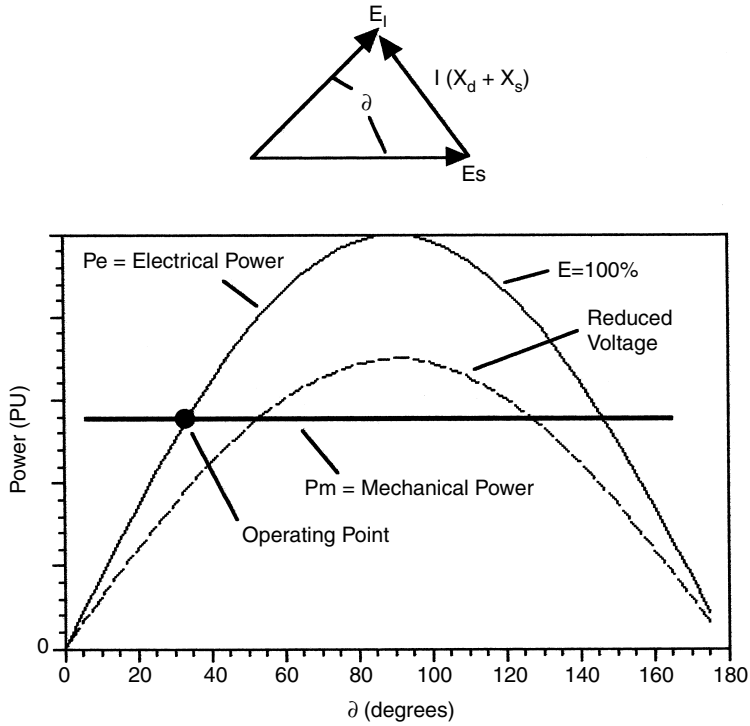


FIGURE 11.9 Power angle curve.

Figure 11.9 is a plot of a power angle curve with the generator excitation fixed by manual regulator control. Thus voltage E_I is constant. The operating point for the system is defined as the point where the mechanical power provided by the prime mover equals the electrical power taken by the electrical system. Note that an increase in mechanical power will necessitate an increased angle between the system and generator voltage.

Mechanical power can increase until the power angle $\delta = 90^\circ$. Any increase in mechanical power beyond this value cannot be absorbed by the electrical system. The excess mechanical energy is expended in accelerating the turbine-generator mass. The shaft speed and, with it, frequency increases above 60 Hz, causing the generator to pull out of step and lose synchronism with the power system.

This loss of steady-state stability can also occur if turbine power is fixed, but the system or generator internal voltage is reduced. This would be the case if the operator were attempting to control a high-voltage condition by reducing the generator field current. The reduction in field will reduce E_I, which in turn reduces the height of the power angle curve as shown by the dotted curve. The power angle will increase as the intersection with the fixed turbine output power moves toward the peak of the curve until the power angle δ reaches 90°. At this point, the mechanical power supplied equals the maximum power the electrical system can accept. Again, any additional reduction in field current will reduce the maximum electrical power below that of the mechanical input power and synchronism will be lost.

A loss of steady-state stability can be a result of operator error during startup. If a unit is placed on line under manual voltage regulator control, the initial field current would be that required for rated voltage at no load. This is typically one-half to one-third the field current required for full load. The resulting power angle curve will have a maximum value of less than rated power output. If the operator fails to increase the field as he loads the Unit, the power angle will increase to the maximum value of 90° and the generator will again pull out of step with the system. Note that

© 2006 by Taylor & Francis Group, LLC

with this scenario, as generator loading is increased, the leading Vars intake of the generator will increase dramatically. Often for this type event the unit will trip by loss of field protection after synchronizm is lost.

11.6.2 Manual Regulator Steady-State Stability Limit

The classical derivation of the steady-state stability limit assumes the generator is operating at fixed excitation on the manual regulator (E_g constant Figure 11.10). The stability limit is found by adjusting system parameters very slowly, reducing the power angle curve, or increasing mechanical power until mechanical input power is equal to the maximum electrical power. The slow change of system parameters is central to the concept of steady-state stability because it eliminates oscillatory parameters and the need for damping. If saliency is neglected, as was the case for Equation (11.20), the stability limit occurs when $\delta = 90^\circ$. If saliency is considered ($X_d \neq X_q$), as in Equation (11.19), the limit will occur at less than 90°.

Obviously, this definition is of little use to operators, because they do not have instrumentation to read system angle or the maximum electrical power. Consequently the limit is expressed in terms of the minimum Var output at the stability limit for a given real power output and generator terminal voltage.

Figure 11.10 defines the system and internal generator voltage in terms of terminal voltage and the in-phase and quadrature components of generator current. These current components relate directly to the real and reactive power at the generator terminals.

$$I_r = \frac{P}{E_t} \tag{11.21}$$

$$I_x = \frac{Q}{E_t} \tag{11.22}$$

With saliency neglected, the stability limit occurs when the angle between the two voltages equals 90°, ($\alpha + \beta = 90^\circ$) or when

$$\tan(\alpha + \beta) = \frac{\tan\alpha + \tan\beta}{1 - \tan\alpha \tan b} = \infty \tag{11.23}$$

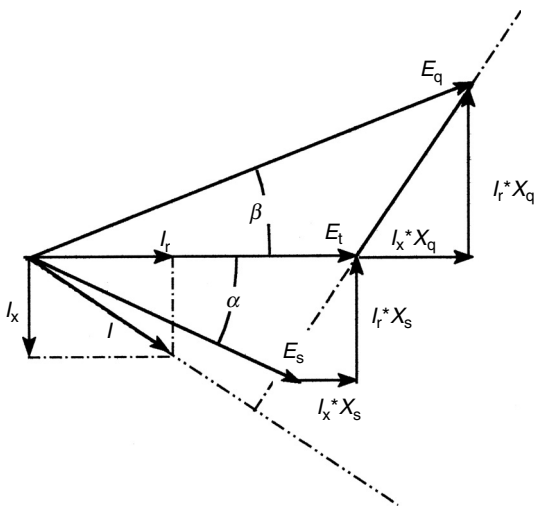


FIGURE 11.10 Generator current voltage.

© 2006 by Taylor & Francis Group, LLC

which occurs when

$$0 = 1 - \tan\alpha \tan\beta \tag{11.24}$$

Defining the internal angles from the figure as follows:

$$\tan\ \beta = \frac{I_r X_q}{E_t + I_x X_q} \tag{11.25}$$

$$\tan\ \alpha = \frac{I_r X_s}{E_t - I_x X_s} \tag{11.26}$$

Substituting

$$0 = 1 - \frac{I_r X_s}{E_t - I_x X_s} \frac{I_r X_q}{E_t + I_s X_q} \tag{11.27}$$

Rearranging

$$\frac{E_t^2}{X_d X_s} E_t^2 = Q^2 + \frac{(-X_d + X_s) Q E_t^2}{X_d X_s} + P^2 \tag{11.28}$$

and completing the squares

$$\left[\frac{E_t^2}{2}\left(\frac{1}{X_d} + \frac{1}{X_s}\right)\right]^2 = \left[\frac{E_t^2}{2}\left(\frac{1}{X_s} - \frac{1}{X_d}\right) + Q\right]^2 + P^2 \tag{11.29}$$

The resulting equation for the manual regulator steady-state limit is that of a circle on the P–Q plane. The circle has center at

$$P = 0, \qquad \frac{E_t^2}{2}\left(\frac{1}{X_s} - \frac{1}{X_d}\right) \tag{11.30}$$

and a radius of

$$R = \frac{E_t^2}{2}\left(\frac{1}{X_d} + \frac{1}{X_s}\right) \tag{11.31}$$

This circle is the stability criterion against which the MEL limit is usually evaluated. Note that, unlike the end-core heating limit characteristic circle (Equation 11.15), both the radius and center vary with the square of the terminal voltage. The limit becomes increasingly restrictive as the system weakens (larger X_s), as shown in Figure 11.11.

11.6.3 Automatic Regulator Stability Limits

The AVR rapidly varies field voltage in response to system conditions. The change in field voltage for a given change in terminal voltage defines the gain of the regulator (k_e). The regulator time constant (T_e) and the generator field time constant determine the speed of the field current response which ultimately determines the response at the generator output terminals. Even a slow acting regulator with low gain will sharply increases synchronizing torque, markedly improving steady-state stability. But at the same time the gain and speed reduce system damping torque. Without sufficient damping torque, minor system oscillations will grow in magnitude until connected generators and tie lines trip.

© 2006 by Taylor & Francis Group, LLC

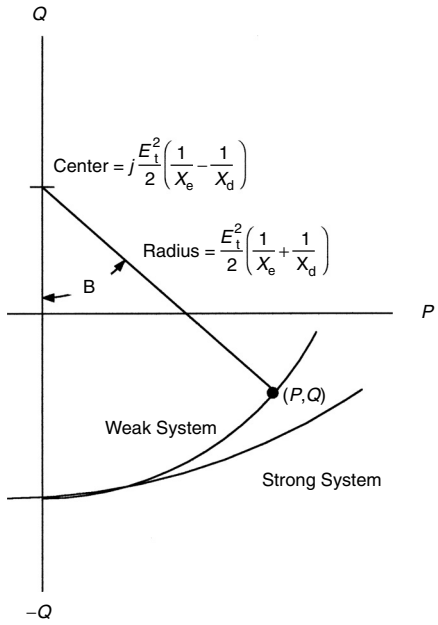


FIGURE 11.11 Circle diagram of manual regulator steady-state limit.

Establishing the steady-state and dynamic stability limits under AVR control is more difficult than establishing the manual regulation shown above, because both involve the interaction between the generator, system, and excitation system.

These interactions are analyzed using the block diagram format customary in control systems design. These diagrams represent complex systems of differential equations and represent both transient and steady-state response. The blocks are defined in terms of the complex frequency domain using the variable s where $s = j\omega$ and ω is the oscillatory frequency of the disturbance. Although the time response is desired, the representation in s has been adopted because it simplifies the solution of the differential equations involved. Reference 5 likened the relation between the time domain and the Laplace complex frequency domain to that of the relationship between real numbers and logarithms. Logarithms allow the more complex mathematical operations such as multiplication and division to be carried out using addition and subtraction. Likewise, the use of Laplace transforms and the complex frequency domain allows the system of differential equations to be represented and solved algebraically.

The method of this analysis and the basic response of a power system can be demonstrated using Figure 11.12. This is a simplified system block diagram for small perturbations taken from Ref. [1].

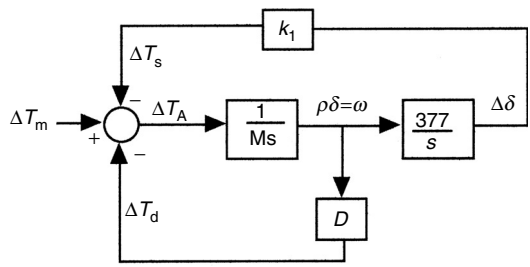


FIGURE 11.12 System block diagram. (From DeMello, F.P., Concordia, C. Concepts of Synchronous Machine Stability as Affected by Excitation Control, IEEE Transactions PAS, Vol. 88, pp. 316–329, April 1969. With permission.)

© 2006 by Taylor & Francis Group, LLC

The diagram relates small changes in mechanical torque (ΔT_m) to the resulting changes in speed ($p\delta$), and rotor angle ($\Delta\delta$). This model does not include a representation of the generator internal circuits or the voltage regulator. The generalized damping effects of the system and generator are represented by a damping term D. The stability of the system is governed by the synchronizing (ΔT_s) and damping (ΔT_d) torque. In the model, k_1 represents the change in electrical torque for a change in rotor angle with constant flux linkages. M represents the mass of the generator and prime mover.

The evaluation of a generator's angular response to a change in mechanical torque is accomplished as follows. Each block element is defined as a frequency domain variable by the (s) term.

$$\Delta T_s(s) = K_1 \Delta\delta(s) \tag{11.32}$$

$$\Delta T_d(s) = D * \omega(s) \tag{11.33}$$

$$\Delta T_A(s) = \Delta T_m(s) - \Delta T_s(s) - \Delta T_d(s) \tag{11.34}$$

$$\omega(s) = T_A(s) * \frac{1}{Ms} \tag{11.35}$$

$$\Delta\delta(s) = \frac{377}{s}\omega(s) \tag{11.36}$$

Substituting Equation (11.32) and Equation (11.33) into Equation (11.34),

$$\Delta T_A = \Delta T_m - K_1 \Delta\delta - D * \omega \tag{11.37}$$

Then, substituting $T_A(s) = sM\omega(s)$ and $\omega(s) = s\Delta\delta(s)/377$ derived from Equation (11.35) and Equation (11.36) into Equation (11.37) and solving for $\Delta\delta(s)$:

$$\Delta\delta(s) = \frac{\Delta T_m(s)}{k_1\left(\dfrac{M}{377k_1}s^2 + \dfrac{D}{377k_1}s + 1\right)} \tag{11.38}$$

This equation represents the change in rotor angle for a change in mechanical torque in the complex frequency domain. The time domain response is found from a lookup table of Laplace transform pairs in any standard reference. The primary difficulty with using the Laplace method to solve differential equations is the immense amount of algebra required to convert equations derived in "s" to the standard forms necessary to use such tables. The transform below can be applied to Equation (11.38)

$$L^{-1}\frac{1}{\left(\dfrac{s^2}{\omega_n^2} + \dfrac{2\xi}{\omega_n}s + 1\right)} = \frac{\omega_n}{\sqrt{1-\xi^2}}\, e^{-\xi\omega_n t}\, \sin\left(\omega_n\sqrt{1-\xi^2}\,t\right) \tag{11.39}$$

The form of the resulting time domain equation provides insight into the power system's response to a disturbance. The rotor angle $\Delta\delta$ varies as an exponentially decaying sinusoidal oscillation. The damping factor (ξ) controls the rate of decay and the frequency of the oscillation. If the damping becomes zero, oscillation is sustained at a fixed magnitude at the natural frequency of the system ω_n. Should damping become negative, the exponential term becomes positive and instability results as the oscillation grows without bounds.

© 2006 by Taylor & Francis Group, LLC

By inspection of Equation (11.38) and Equation (11.39) the natural frequency and damping factor for the simple power system described by Figure 11.12 are

$$\omega_n = \sqrt{\frac{377k_1}{M}} \tag{11.40}$$

$$\xi = \frac{D\omega_n}{754k_1} \tag{11.41}$$

The synchronizing and damping torque produced as a result of the interaction of the generator and system determine the stability of the power system. The boundary of steady-state stability occurs when synchronizing torque is equal to zero. Likewise, the boundary of dynamic stability occurs when damping torque is zero. These stability limits are found by determining the total electrical torque, then resolving the total torque into its synchronizing and damping components. The respective stability limits are then found by determining the power and reactive operating points that result in zero torque for each component.

Figure 11.12 shows that the damping torque is directly related to rotor speed (ω), while synchronizing torque is directly related to change in rotor angle ($\Delta\delta$). Speed is the derivative of the change in rotor position. In the world of Laplace transforms, the $377/s$ box that relates speed ω to $\Delta\delta$ is an integration function ($1/s$); thus, for a sinusoidal input, speed leads $\Delta\delta$ by 90°. It then follows that the synchronizing torque can be identified as the component in phase with $\Delta\delta$ and the damping torque is the component in quadrature with $\Delta\delta$.

The block diagram in Figure 11.13 again taken from Ref. [1] includes the generator d-axis flux linkages, but no voltage regulator. An expression will be derived for the total electrical torque. This torque is then resolved into components in phase with $\Delta\delta$ (synchronizing torque) and torque at quadrature with $\Delta\delta$ (damping torque), from which the respective stability limits can be found.

The individual elements of the system are:

$$\Delta T_a(s) = k_1 \Delta\delta(s) \tag{11.42}$$

$$\Delta T_b(s) = k_2 \frac{k_3}{1 + sk_3 T'_{d0}} E_e(s) \tag{11.43}$$

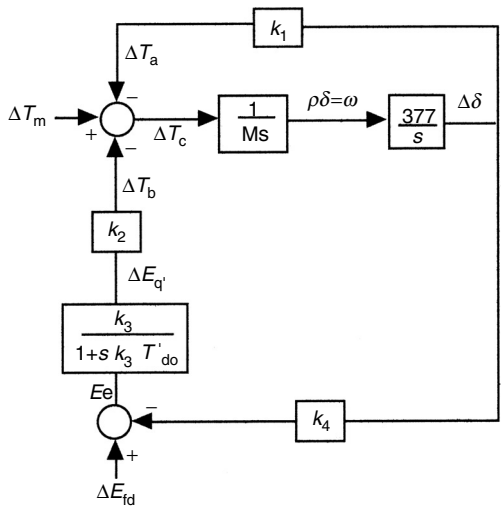


FIGURE 11.13 Block diagram including generator d-axis. (From DeMello, F.P., Concordia, C. Concepts of Synchronous Machine Stability as Affected by Excitation Control, IEEE Transactions PAS, Vol. 88, pp. 316–329, April 1969. With permission.)

© 2006 by Taylor & Francis Group, LLC

$$E_e(s) = \Delta E_{fd}(s) - k_4 \Delta\delta(s) \tag{11.44}$$

$$\Delta T_c(s) = \Delta T_m(s) - \Delta T_a(s) - \Delta T_b(s) \tag{11.45}$$

$$\Delta\delta(s) = \frac{377}{Ms^2}\,\Delta T_c(s) \tag{11.46}$$

The electrical torque is defined as

$$\Delta T_e(s) = \Delta T_a(s) + \Delta T_b(s) \tag{11.47}$$

Substituting expressions for ΔT_a, ΔT_b, and E_e,

$$\Delta T_e = \frac{k_1 \Delta\delta(s)(1 + sk_3 T'_{d0}) + k_2 k_3 [\Delta E_{fd}(s) - k_4 \Delta\delta(s)]}{1 + sk_3 T'_{d0}} \tag{11.48}$$

In the frequency domain $s = j\omega$. This will result in an imaginary term in the denominator of Equation (11.48), which will hinder the resolution of the torque into its synchronizing and damping components. To eliminate the imaginary term in the denominator, both numerator and denominator are multiplied by $1 - sK_3 T'_{d0}$. The resulting equation is:

$$\Delta T_e = \frac{(1 - sk_3 T'_{d0})[k_1 \Delta\delta(s)(1 + sk_3 T'_{d0}) + k_2 k_3 (\Delta E_{fd}(s) - k_4 \Delta\delta(s))]}{1 - s^2 k_3^2 T'^2_{d0}} \tag{11.49}$$

With the manual regulator, $\Delta E_{fd} = 0$, and substituting $s = j\omega$

$$\Delta T_e(s) = \frac{j(T'_{d0}\omega k_2 k_3^2 k_4)\Delta\delta(s) + (k_1 - k_2 k_3 k_4 + T'^2_{d0}\omega^2 k_3^2 k_1)\Delta\delta(s)}{T'^2_{d0}\omega^2 k_3^2 + 1} \tag{11.50}$$

The synchronizing torque is the component that is in phase with $\Delta\delta$.

$$\Delta T(s)_{sync} = \frac{(k_1 - k_2 k_3 k_4 + T'^2_{d0}\omega^2 k_3^2 k_1)\Delta\delta(s)}{T'^2_{d0}\omega^2 k_3^2 + 1} \tag{11.51}$$

The steady-state limit is defined for very slow changes in system parameters; thus, $\omega = 0$ and the steady-state synchronizing becomes

$$\Delta T_{e\,sync}(s) = (k_1 - k_2 k_3 k_4)\Delta\delta(s) \tag{11.52}$$

The damping torque is the component in quadrature with $\Delta\delta$.

$$\Delta T(s)_{damp} = j\frac{T'_{d0}\omega k_2 k_3^2 k_4 \Delta\delta(s)}{T'^2_{d0}\omega^2 k_3^2 + 1} \tag{11.53}$$

The limit of dynamic stability occurs when damping is zero. Under this condition oscillation is at the system natural frequency, which is for practical purposes unchanged from that calculated for the simple power system described by Figure 11.12. Setting ω equal to the natural frequency defined by Equation (11.40), the damping torque at the limit of dynamic stability becomes

$$\Delta T(s)_{damp} = 0 = \frac{jMTd'_0 k_2 k_3^2 k_4 \sqrt{377\frac{K_1}{M}}\Delta\delta}{377 T'^2_{d0} k_3^2 k_1 + M} \tag{11.54}$$

© 2006 by Taylor & Francis Group, LLC

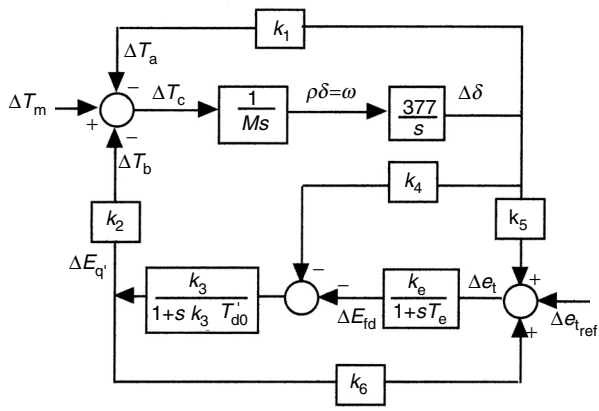


FIGURE 11.14 Block diagram including AVR. (From DeMello, F.P., Concordia, C. Concepts of Synchronous Machine Stability as Affected by Excitation Control, IEEE Transactions PAS, Vol. 88, pp. 316–329, April 1969. With permission.)

The steady-state and dynamic stability limits under manual regulator control would be defined by determining the power and reactive operating points that would set Equation (11.52) and Equation (11.54) equal to zero. We note that this solution of Equation (11.52) will yield the same results as the classical solution Equation (11.29) if saliency is neglected ($X_d = X_q$).

The torque equations for the system under AVR control at the respective stability limits are derived in the same manner from the expanded block diagram in Figure 11.14.

Synchronizing torque under at the steady state limit ($\omega = 0$) under AVR control is:

$$\Delta T(s)_{sync} = \frac{\{k_4 + k_e[k_5 + (k_4 + k_5k_e)k_6k_3]\}k_3k_2\Delta\partial}{[k_3k_6k_e) + 1]^2} \tag{11.55}$$

Damping torque at the dynamic stability limit ($\omega = \omega_n$) under AVR control is:

$$T(s)_{damp} = -\frac{\begin{array}{c} jk_3k_2\{T_e[-k_4k_3T_eT'_{d0}\omega^2 + (-k_5 + k_6k_4k_3)k_e] \\ -(k_4 + k_5k_e)k_3T'_{d0}\}\omega\Delta\partial \end{array}}{[k_3(-T_eT'_{d0}\omega^2 + k_6k_e) + 1]^2 + (T_e + k_3T'_{d0})^2\omega^2} \tag{11.56}$$

Again, the actual power and reactive operating points that define the stability limits are those points that result in zero synchronizing or damping torque as defined by Equation (11.55) and Equation (11.56). This brings us to the reason why these limits are so difficult to determine. Only one of the "k" factors used in the block diagram (k_3) is a constant; all others vary with load. The solution for each limit is a trial and error recalculation of the rather complex "k" factors listed below for each given value of power to find the reactive output that results in zero synchronizing and damping torque. This calculation is repeated for several value of power output through the operating range of the generator.

"k" factors used in the block diagrams are defined as follows[1]:

$$k_1 = \frac{E_{q0}E_0}{A}[r_e \sin\delta_0 + (X_e + X'_d)\cos\delta_0] + \frac{i_{q0}E_0}{A}[(X_q - X'_d)(X_e + X_q)\sin\delta_0 - r_e(X_q - X'_d)\cos\delta_0] \tag{11.57}$$

$$k_2 = \frac{r_eE_{q0}}{A} + i_{q0}\left[1 + \frac{(X_e + X_q)(X_q - X'_d)}{A}\right] \tag{11.58}$$

© 2006 by Taylor & Francis Group, LLC

$$k_3 = \left[1 + \frac{(X_e + X_q)(X_d - X'_d)}{A}\right]^{-1} \tag{11.59}$$

$$k_4 = \frac{E_0(X_d - X'_d)}{A}[(X_e + X_q)\sin\delta_0 - r_e\cos\delta_0] \tag{11.60}$$

$$k_5 = \frac{e_{d0}}{e_{t0}}X_q\left[\frac{r_e E_0\sin\delta_0 + (X_e + X'_d)E_0\cos\delta_0}{A}\right] + \frac{e_{q0}}{e_{t0}}X'_d\left[\frac{r_e E_0\cos\delta_0 - (X_e + X_q)E_0\sin\delta_0}{A}\right] \tag{11.61}$$

$$k_6 = \frac{e_{q0}}{e_{t0}}\left[1 - \frac{X'_d(X_e + X_q)}{A}\right] + \frac{e_{d0}}{e_{t0}}X_q\frac{r_e}{A} \tag{11.62}$$

$$A = r_e^2 + (X_e + X'_d)(X_q + X_e) \tag{11.63}$$

These factors are simplified considerable if resistance is neglected.

In the era of manual calculations, the determination of these limits was very difficult. Fortunately, in the age of personal computers with electronic spreadsheets and iterative solvers, these limits can be determined with relative ease. Appendix C shows the layout for an Excel™ workbook that can be used to calculate steady-state and dynamic limits under AVR and MVR control. This spreadsheet can be downloaded from the publishers webside. On the "data" sheet. Columns A and B are system data input to the spreadsheet. The power values for which the limiting reactive output is to be calculated are entered in column E. Guess values for leading Vars at the limiting condition are entered in column F. Generator parameter columns H through AE are calculated from Equation (11.64) to Equation (11.71) below, and k values from Equation (11.57) to Equation (11.63) above.

The parameters including system voltage E_0, generator terminal voltage e_{t0} and real and reactive currents components I_{p0} and I_{q0}, respectively are used to calculate "k" factors. The equations listed are taken from Ref. [1] and were derived from a standard generator vector diagram similar to Figure 2.14. The "0" subscript indicates steady-state operating "k" factors values. The equations assume lagging Vars (Vars out) are positive.

$$I_{p0} = \frac{p}{e_{t0}}$$

$$I_{g0} = \frac{Q}{e_{t0}}$$

$$E_{q0} = \sqrt{(e_{t0} + I_{q0}X_q)^2 + (I_{p0}X_q)^2} \tag{11.64}$$

$$E_0 = \sqrt{(e_{t0} - I_{p0}r_e - I_{q0}X_e)^2 + (I_{p0}X_e - I_{q0}r_e)^2} \tag{11.65}$$

$$\sin\delta_0 = \frac{e_{t0}I_{p0}(X_q + X_e) - r_e X_q(I_{p0}^2 + I_{q0}^2) - e_{t0}I_{q0}r_e}{E_{q0}E_0} \tag{11.66}$$

$$\cos\delta_0 = e_{t0}\frac{[e_{t0} + I_{q0}(X_q - X_e) - I_{p0}r_e] - X_e X_q(I_{p0}^2 + I_{q0}^2)}{E_{q0}E_0} \tag{11.67}$$

$$i_{q0} = \frac{[I_{p0}(e_{t0} + I_{q0}X_q) - I_{q0}I_{p0}X_q]}{E_{q0}} \tag{11.68}$$

© 2006 by Taylor & Francis Group, LLC

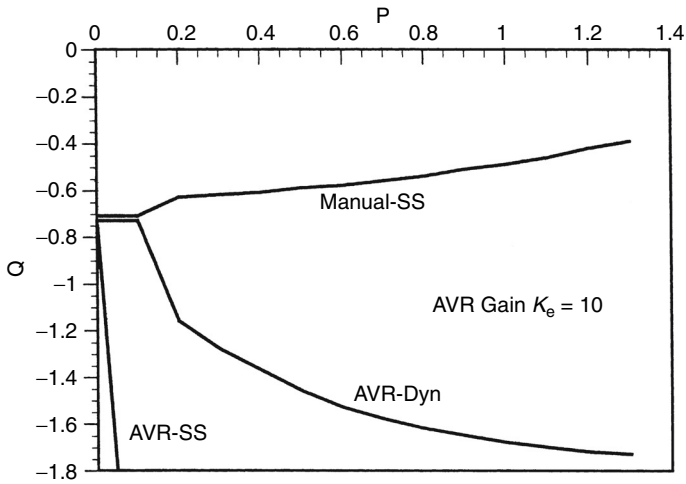


FIGURE 11.15 Manual and AVR stability limits.

$$i_{d0} = \frac{[I_{p0}^2 X_q + I_{q0}(e_{t0} + I_{q0}X_q)]}{E_{q0}} \tag{11.69}$$

$$e_{q0} = e_{t0}[(e_{t0} + I_{q0}X_q)/E_{q0}] \tag{11.70}$$

$$e_{d0} = i_{q0}X_q \tag{11.71}$$

Column Z contains the natural frequencies of the system in radian/sec from Equation (11.40). Note that when $k_1 < 0$ frequency increases with time as can be seen from Equation (11.39) and Equation (11.41). This an unstable condition.

The steady-state and dynamic stability limits are found using Excel's "Goal Seek" tool to find the value of leading reactive (column E) necessary to produce zero synchronizing or damping torque. This process is automated by "zero sync torque" button on the "manual" sheet and the "zero damping/sync" button on the "auto" sheet. On occasions the automatic routine may fall to find a reasonable solution at higher, power levels. In that case individual rows may have to be solved by adjusting guess values on the "data" sheet and using the goal seaking tool to zero synchronous and dynamic torque values on the "manual" or "auto" sheet.

Figure 11.15 plots the manual steady-state limit, and AVR steady-state and dynamic limits for an installation with an AVR gain equal to 10. Note that the manual regulator steady-state limit is not a circle as described by Equation (11.29). This is because the limit calculated from the block diagram includes the effects of saliency ($X_d \neq X_q$). Also note that both AVR limits are far less restrictive than the manual regulator limit. Figure 11.16 demonstrates how, without a power system stabilizer, the stability advantage of the AVR diminishes as gain increases. With regulator gain set at 30, the AVR dynamic limit approaches the manual regulator steady-state limit at full load.

11.7 MEL PROTECTIVE CHARACTERISTIC

Our discussion of MEL design will be limited to the steady-state characteristics that define the protective function. Although MEL circuit gain and time delays are critical to excitation system stability when the MEL is activated, the subject is outside the scope of this text. Insight into the adjustment of these parameters is provided in Ref. [6].

© 2006 by Taylor & Francis Group, LLC

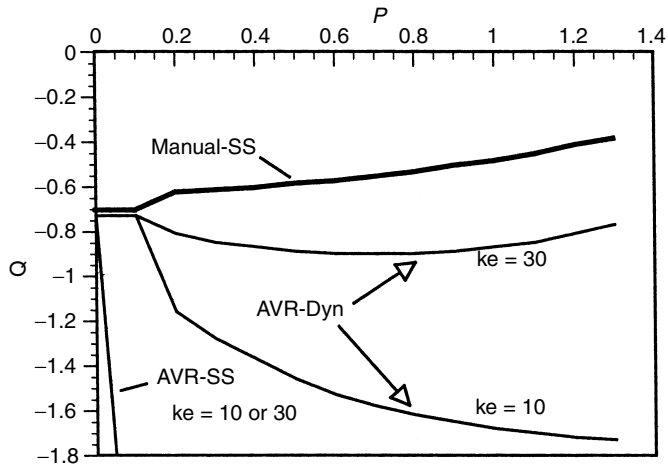


FIGURE 11.16 Effect of AVR gain on stability limits.

Most excitation systems include the MEL function. The individual circuit designs vary among manufacturers, but in general three power-reactive characteristics are offered: a single line, a multiple line and, a circular characteristic. These are shown in Figure 11.17. In older voltage regulators, the characteristic of the MEL is fixed. Some newer solid-state and digital excitation systems provide selectable characteristics.

Because MEL circuit designs are not standardized, generalizations about their response should not be made. Reference 7 has consolidated many of the functional variations in MEL design into three generalized MEL models. These models are intended for use in system stability studies but they provide considerable insight into common design variations and the effects these variations have on settings.

Of particular importance is the variation of the MEL characteristic with voltage. For optimal protection, variations of the MEL characteristic with voltage should match the variations in the Var limitation of the generator. This will be difficult, because we have seen that the voltage variation of the leading Var capability of a round rotor generator is opposite to that of a salient pole machine.

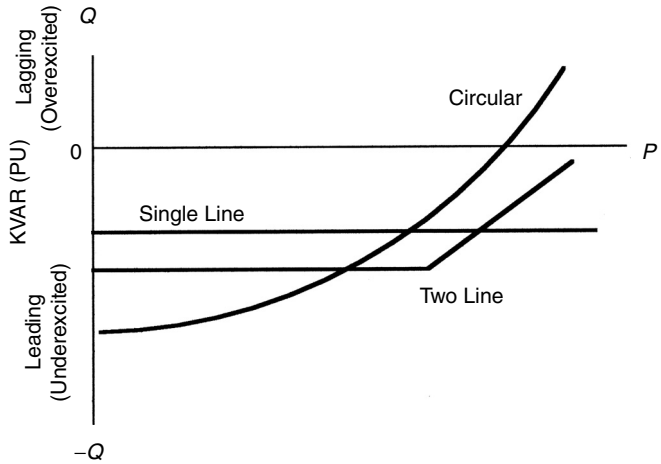


FIGURE 11.17 MEL characteristic.

© 2006 by Taylor & Francis Group, LLC

11.7.1 Straight Line Characteristic: Type UEL2 Model

A partial block diagram for the type UEL2 model is provided in Figure 11.18. Real power (P) and reactive power (Q) along with generator voltage (e_t) are monitored and processed. The resulting signals are summed with a reference voltage. When the resulting error signal (V_{err}) becomes positive, the MEL becomes active and boosts field excitation to prevent any further reduction in Vars.

The constants k_1 and k_2 are provided to simulate the effect of terminal voltage variation on different designs. Setting $k_1 = 0$ makes the power and reactive measurements insensitive to terminal voltage variations. This would be the case if these inputs were derived from power and reactive measuring transducers. If $k_1 = 1$ or 2, the P and Q measurements will vary inversly or inversly by the square of the terminal voltage. A setting of $k_1 = 1$ would be used when in-phase and reactive current measurements are used to simulate P and Q quantities. A setting of $k_1 = 2$ would be appropriate if P and Q quantities are estimated from a voltage generated by load current and a replica impedance. Constant k_2 is set at 0 if terminal voltage is not directly used to bias the characteristic. If $k_2 = 1$ or 2, the MEL setting is biased proportional to e_t or e_t squared, respectively.

We are limiting this discussion to the steady-state characteristic of the MEL. If the power system and connected generators were swinging at a constant frequency, the system would be represented by replacing "s" in the block diagram with $j\omega$, where ω is the oscillatory frequency of the disturbance. In the steady state, there is no oscillation and $j\omega = 0$. Thus, the general block diagram can be reduced to the steady state of the block diagram shown in Figure 11.19 by setting $s = 0$.

Because the limit becomes active when V_{lim} exceeds the reference voltage, the boundary of the MEL characteristic is at

$$0 = V_{lim} - V_{ref} \tag{11.72}$$

If the reference voltage is assumed to be equal to zero, the boundary becomes

$$0 = V_{lim} = A - B - C \tag{11.73}$$

where

$$A = P * e_t^{-k_1} * KUP \tag{11.74}$$

$$B = e_t^{k_2} * KUV \tag{11.75}$$

$$C = Q * e_t^{-k_1} * KUQ \tag{11.76}$$

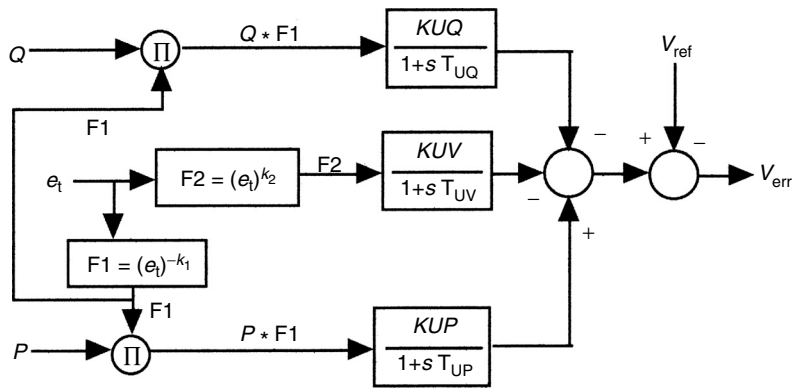


FIGURE 11.18 Type UEL2 block diagram. (From IEEE Task Force on Excitation Limiters, Underexcitation Limiter Models for Power System Stability Studies, IEEE Transactions on Energy Conversion, Vol. 10, No. 3, Sept. 1995. With permission.)

© 2006 by Taylor & Francis Group, LLC

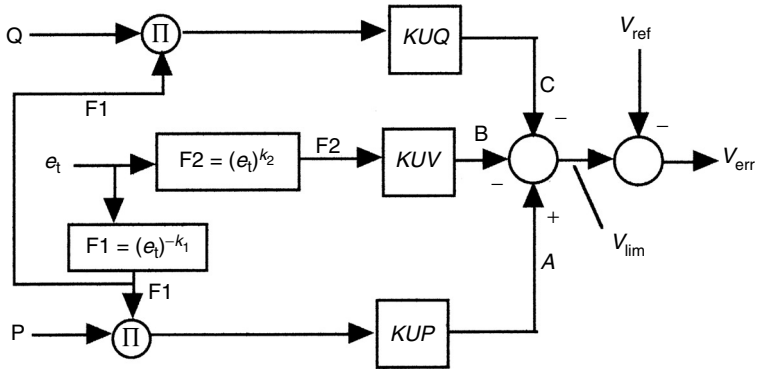


FIGURE 11.19 Type UEL2 steady-state block diagram.[7]

Substituting,

$$0 = P * e_t^{-k_1} * KUP - e_t^{k_2} * KUV - Q * e_t^{-k_1} * KUQ \tag{11.77}$$

Solving for Q, the boundary for steady state operation is at

$$Q = P\frac{KUP}{KUQ} - e_t^{k_1+k_2}\frac{KUV}{KUQ} \tag{11.78}$$

The resulting equation is that of a line with slope KUP/KUQ and offset along the reactive axis equal to KUV/KUQ at rated voltage. The characteristic is plotted in Figure 11.20. Variations in system voltage do not alter the characteristic if both k_1 and k_2 are set at zero. With "k" settings other than zero, the slope will not vary, but reactive axis offset will change with the $(k_1 + k_2)$ power of e_t.

This voltage characteristic favors protection of the salient pole machine, whose underexcited Var capability increases with increased voltage. Figure 11.21 shows a single line MEL setting plotted against the end-core heating limit for a round rotor machine and manual regulator stability limit. The plot is at $e_t = 1.0$.

The setting shown appears to be adequate to prevent operation beyond either the end-core or stability limit. However, this is not the case. At 1.05 pu voltage, the end-core limitation is reduced below the MEL setting. The result is that the end-core is no longer protected. This is

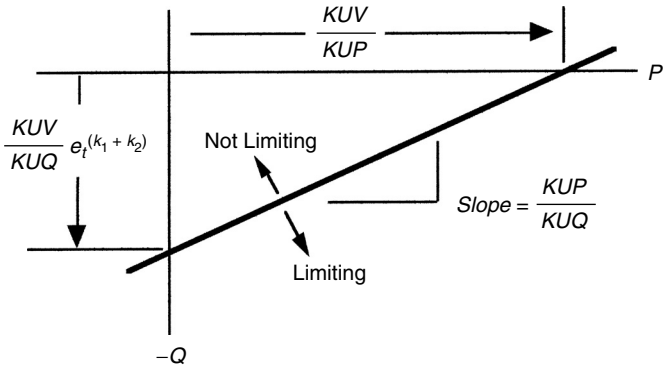


FIGURE 11.20 Single line characteristic. (From IEEE Task Force on Excitation Limiters, Underexcitation Limiter Models for Power System Stability Studies, IEEE Transactions on Energy Conversion, Vol. 10, No. 3, Sept 1995. With permission.)

© 2006 by Taylor & Francis Group, LLC

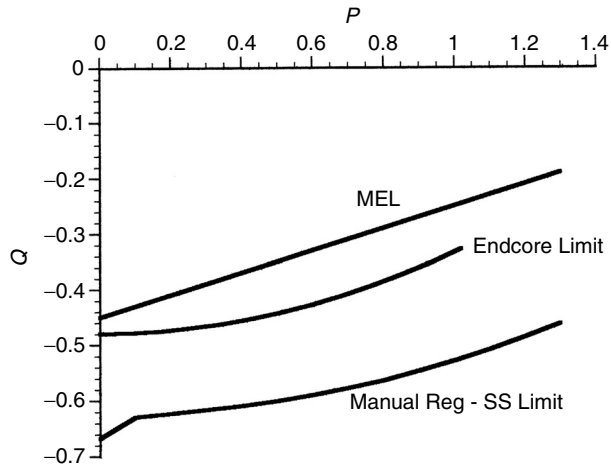


FIGURE 11.21 Single line characteristic with $e_t = 1.0$.

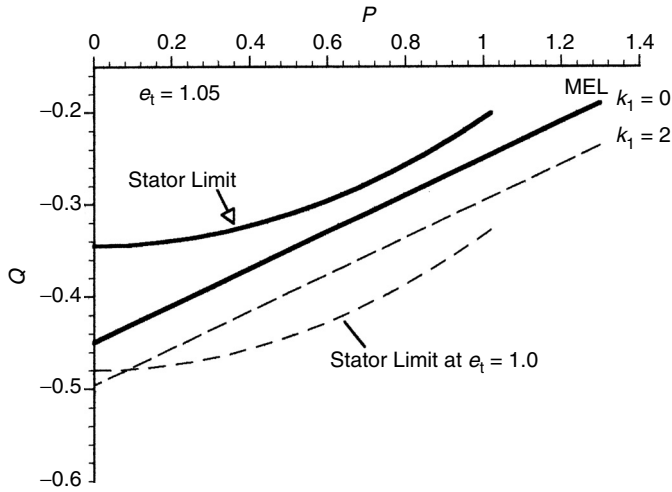


FIGURE 11.22 Single line and stator heating variations with voltage.

shown in Figure 11.22. The MEL characteristic has not been affected by the voltage variation because $k_1 = k_2 = 0$. The loss of protection is greater as the "k" setting increases because the MEL characteristic is offset further into the leading Var region. Likewise, the effectiveness of the MEL to prevent operation in areas of instability is compromised when voltage is reduced to 0.95 pu as is shown in Figure 11.23.

11.7.2 Multisegment Straight Line Model Type UEL3

The characteristic of the multisegment MEL is derived from the partial UEL3 model in Figure 11.24 in the same manner as desired by the single line characteristic. The steady-state response is comprised of multiple single line elements each defined in the form:

$$Q_1 = \frac{KUP_1}{KUQ} P - \frac{KU_{1\text{ref}}}{KUQ} e_t^k \tag{11.79}$$

© 2006 by Taylor & Francis Group, LLC

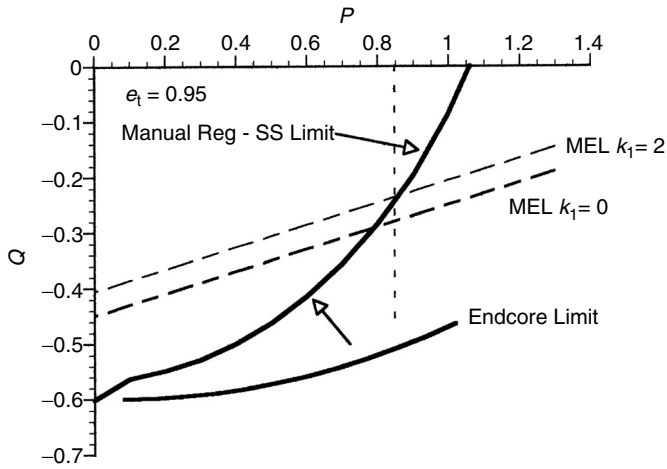


FIGURE 11.23 Single line characteristic with $e_t = 0.95$.

The limit switches between line segments at voltage levels set by VUP_1, VUP_2, and so on, to provide the characteristic shown in Figure 11.25.

11.7.3 Circular Characteristic Type UEL1 Model

The partial block diagram, Figure 11.26, is for a circular characteristic. The bar over the terminal voltage and current indicates vector quantities. The steady-state characteristic is derived in the same manner as the UEL2 model.

$$V_{\text{err}} = VUC - VUR \tag{11.80}$$

$$VUR = |KUR * e_t| \tag{11.81}$$

$$VUC = |KUC * e_t - j^* I_T| \tag{11.82}$$

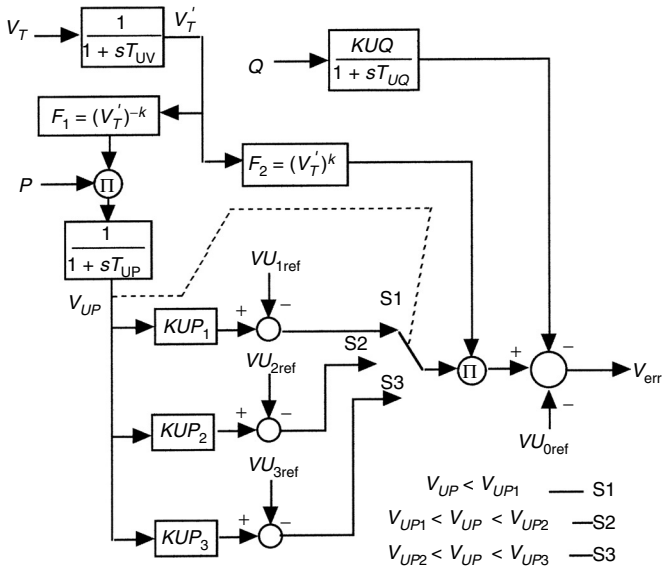


FIGURE 11.24 Type UEL3 block diagram. (From IEEE Task Force on Excitation Limiters, Underexcitation Limiter Models for Power System Stability Studies, IEEE Transactions on Energy Conversion, Vol. 10, No. 3, Sept. 1995. With permission.)

© 2006 by Taylor & Francis Group, LLC

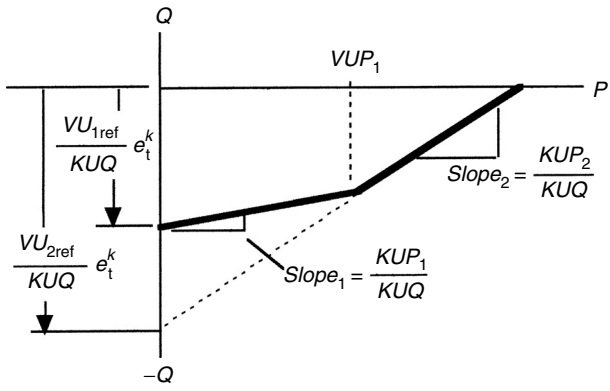


FIGURE 11.25 Multiline characteristic. (From IEEE Task Force on Excitation Limiters, Underexcitation Limiter Models for Power System Stability Studies, IEEE Transactions on Energy Conversion, Vol. 10, No. 3, Sept. 1995. With permission.)

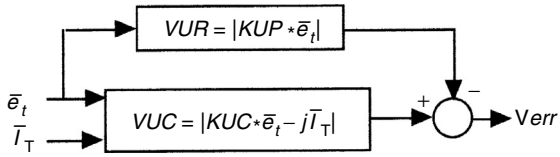


FIGURE 11.26 UEL1 block diagram. (From IEEE Task Force on Excitation Limiters, Underexcitation Limiter Models for Power System Stability Studies, IEEE Transactions on Energy Conversion, Vol. 10, No. 3, Sept. 1995. With permission.)

Substituting,

$$I = \frac{P}{e_t} - j\frac{Q}{e_t} \tag{11.83}$$

the absolute value of VUC becomes

$$VUC = \sqrt{\left(KUC * e_t - \frac{Q}{e_t}\right)^2 + \left(\frac{P}{e_t}\right)^2} \tag{11.84}$$

Substituting *VUC* and *VUR* into Equation (11.80), and setting the reference voltage to zero, the steady state MEL boundary condition is at $V_{err} = 0$ and the resulting boundary equation is

$$(Q - KUC * e_t^2)^2 + P^2 = KUR^2 * e_t^4 \tag{11.85}$$

This equation represents a circle with center and radius:

$$\begin{aligned} Center &= KUC * e_t^2 \\ Radius &= KUR * e_t^2 \end{aligned} \tag{11.86}$$

This characteristic will extend further into the leading Var region as voltage increases a response similar to the steady state and dynamic stability limits but opposite to that of the end-core limit of the round rotor generator. The characteristic favors protection of the salient pole machine and complicates the protection of the round rotor generator.

The circular MEL characteristic is plotted with the end-core and stability limits at unity terminal voltage in Figure 11.27. As with the straight line limit, the setting appears adequate, but again

© 2006 by Taylor & Francis Group, LLC

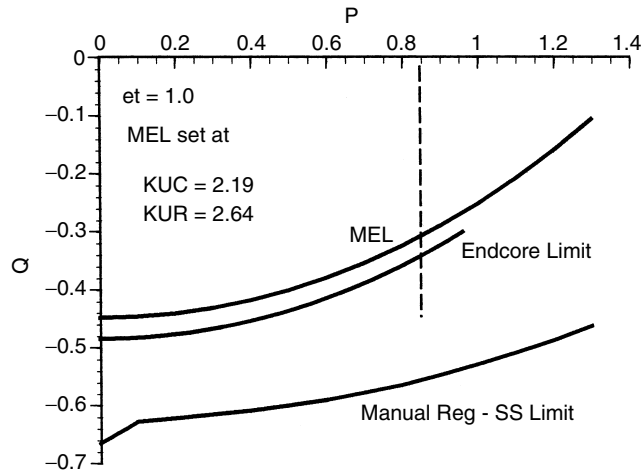


FIGURE 11.27 Circular characteristic at $e_t = 1.0$.

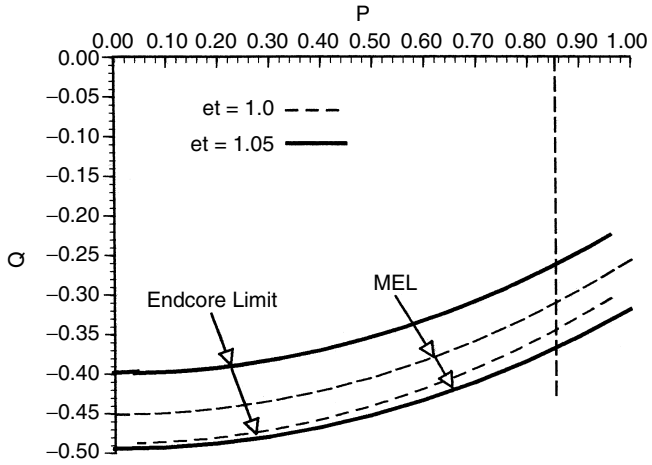


FIGURE 11.28 Circular MEL and stator Var limitation variations with voltage.

at $e_t = 1.05$ end-core protection is lost because of the differing response of the MEL and end-core heating characteristics to the voltage variation. This is shown in Figure 11.28. The chosen setting is only marginally effective in preventing operation outside the manual regulator steady-state limit when operating at 0.95 pu terminal voltage (Figure 11.29).

It becomes apparent that to properly set the MEL, its voltage characteristics must be known. It is also apparent that a MEL voltage characteristic that does not match that of the generator leading Var limit will result in rather restrictive settings if coordination is to be maintained through the full range of operating voltage.

11.8 MEL DYNAMIC PERFORMANCE

11.8.1 Problems with MEL Stability

Although the MEL is often applied to maintain operation within the limits of stability, an ill-tuned MEL will cause instability in the form of severe terminal voltage and reactive oscillations when the

© 2006 by Taylor & Francis Group, LLC

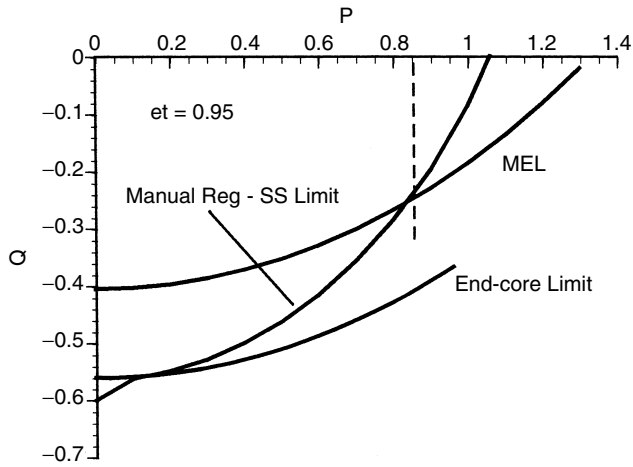


FIGURE 11.29 Circular characteristic with $e_t = 0.95$.

limit is activated. The gain of the MEL and AVR circuitry along with the overall time constant of the excitation system determines system response to the MEL. Older installations are often very sluggish with main and pilot exciters along with long filtering time constants in the MEL itself. Limiters at these installations often produce severe oscillations when activated. Gain reduction and increased delay in the limiter and voltage regulator can stabilize the response. However, these changes tend to render the MEL too slow to effectively maintain stability limits or prevent misoperation of the LOF relay.

Limiters designed with proper damping and feedback can be successfully applied on these and most other systems.[3] Unfortunately, it is necessary to run dynamic system simulations to determine if the AVR and MEL response is adequate to meet these stability and LOF goals.

11.8.2 Interaction with V/Hz

Under normal operation, the terminal voltage of the generator is determined by the AVR setpoint. If system conditions produce leading Vars in excess of the MEL setting, the MEL activates boosting excitation. Terminal voltage will rise above the voltage regulator setpoint to the level necessary to reduce leading Vars below the MEL setpoint. The V/Hz limiter is another auxiliary control circuit within the AVR, which was discussed in Chapter 9. Its function is to prevent damage to the core of the generator and connected transformers caused by excessive flux levels. To accomplish this, the V/Hz limiter initiates excitation reduction when activated. The V/Hz limiter is typically set to operate between 1.05 and 1.2 pu V/Hz. At rated frequency, this translates to 1.05 to 1.2 pu voltage at the generator terminal. If system conditions require that the MEL boost terminal voltage above the V/Hz limiter setting, excitation instability will result as the two limiters alternately boost and reduce excitation. This form of limiter interaction would not be expected during normal system operation, but may occur in a lightly loaded island following a system breakup.

11.8.3 Isolated on Capacitive Load

If a generator becomes isolated on capacitive load, the MEL could cause dangerously high voltage. The condition might result from a large shunt capacitor. It could also occur if a severe disturbance resulted in islanding with lightly loaded, high-voltage transmission lines. Lines 500 KV and above would act as large capacitors when lightly loaded supplying unwanted Vars to the island.

© 2006 by Taylor & Francis Group, LLC

Capacitive load will cause a voltage rise at the generator terminal. The voltage regulator will act to reduce field current, absorb Vars and restore the regulator setpoint voltage. The larger the capacitance, the greater the field current reduction and Var intake necessary to maintain the setpoint voltage. Without the MEL, the field reduction could be sufficient to collapse excitation and actuate the LOF relay, tripping the generator. With MEL control, capacitive load sufficient to activate the MEL will initiate an increase in field current. This action is proper to reduce leading Vars when the generator is connected to a network where other units can absorb the Vars rejected by the MEL. This action is not correct when the generator is isolated on a capacitive load. As the MEL increases field current, the terminal voltage rises and Var output of the capacitor increases by the square of the voltage increase. As leading Vars increases, the MEL continues to increase field in a continuing attempt to reduce leading Vars. If the MEL were unrestrained, the result would be an uncontrolled voltage rise bounded only by the saturation of the generator and transformer cores and protective relaying. At most installations, unstable oscillations would develop as the MEL and V/Hz limiter battle for control as described above.

11.9 MEL APPLICATION ON THE SAMPLE SYSTEM

The sample system is typical of most systems in that the excitation consists of one automatic and one manual regulator. In the event of a failure of the AVR, the system transfers to the manual regulator. The MEL must be set to prevent damage to the end-core region of the stator during periods of underexcited operation (leading Var). At many installations, end-core protection and coordination with the LOF relay are the only considerations for setting the MEL. However, the sample system is connected to a weak power system. This can result in stability limits that are more restrictive than the end-core limit. If this is the case, the stability limits will determine the MEL setting.

The MEL setting required to protect the stator end-core will be determined first. The resulting setting will then be compared to the applicable stability limits and the LOF relay setting.

The AVR is equipped with a two-segment MEL limiter similar to the UEL3 limiter described previously. The characteristic equations for the two-line section are in the form of Equation (11.79).

for $V_{up} \leq V_{up1}$

$$Q = \left(\frac{KUP_1}{KUQ}P - \frac{KU_{1\text{ref}}}{KUQ}e_t^k\right) \tag{11.87}$$

for $V_{up1} \leq V_{up} \leq V_{up2}$

$$Q = \left(\frac{KUP_2}{KUQ}P - \frac{KU_{2\text{ref}}}{KUQ}e_t^k\right)$$

The resulting MEL characteristic is similar to that depicted in Figure 11.25. The inputs to the limiter are watt and Var transducers; thus, these measurements are not affected by terminal voltage and "k" is set equal to 0.

The limiter then has the following characteristics

$$Slope_1 = \frac{KUP_1}{KUQ} \qquad Offset_1 = \frac{KU_{1\text{ref}}}{KUQ} \tag{11.88}$$

$$Slope_2 = \frac{KUP_2}{KUQ} \qquad Offset_2 = \frac{KU_{2\text{ref}}}{KUQ} \tag{11.89}$$

© 2006 by Taylor & Francis Group, LLC

The end-core heating limit is plotted from Equation (11.15) using values of 2.10 and 2.59 pu for the center and radius, respectively. These values were chosen to match the leading Var limit of the manufacturer generator capability curve at rated voltage. The comparison of the two curves is shown in Figure 11.6.

The discussion of the MEL characteristics demonstrated end-core protection becomes more difficult as voltage increases. This is caused by the differing voltage characteristic of the MEL and stator end-core limit. The MEL setting is therefore chosen with the end-core limit at the maximum allowable operating voltage of 1.05 pu.

To facilitate plotting, the end-core limit characteristic can be defined as follows:

$$P = Radius \ \ e_t \sin\beta \tag{11.90}$$

$$Q = Center \ e_t^2 - Radius \ e_t \cos\beta \tag{11.91}$$

where β is an angle measured from the reactive axis to the radius as shown in Figure 11.11. Using this method, the end-core limit is calculated at 1.05 pu voltage as

$$P = 2.59 * 1.05 * \sin\beta \tag{11.92}$$

$$Q = 2.10 * 1.05^2 - 2.59 * 1.05 * \cos\beta \tag{11.93}$$

to give the results in Table 11.1.

The stator end-core limit is plotted at 1.0 and 1.05 pu voltage in Figure 11.30. A tentative MEL characteristic is derived from this plot by laying out a two-line characteristic close to but above the stator limit at 1.05 pu voltage. The resulting characteristic has approximate slopes of near zero and 0.2 and offsets corresponding to 0.3 and 0.36. Settings were then chosen using Equation (11.88) and Equation (11.89) to best fit this characteristic.

The MEL settings obtained are:

$$KUQ = 9$$
$$KUP_1 = 0.3$$
$$KU_{1ref} = 3.42$$
$$KUP_2 = 2.25$$
$$KU_{2ref} = 4$$
$$K = 0$$

The resulting setting is rather restrictive when compared to the stator limit at unity voltage. Note that if the MEL characteristic was voltage sensitive ($k = 1$ or 2), a more restrictive setting would be required.

TABLE 11.1
Calculated values of *P* and *Q*

β (deg)	*P* (pu)	*Q* (pu)
0	0	−0.494
5	0.237	−0.394
10	0.472	−0.363

© 2006 by Taylor & Francis Group, LLC

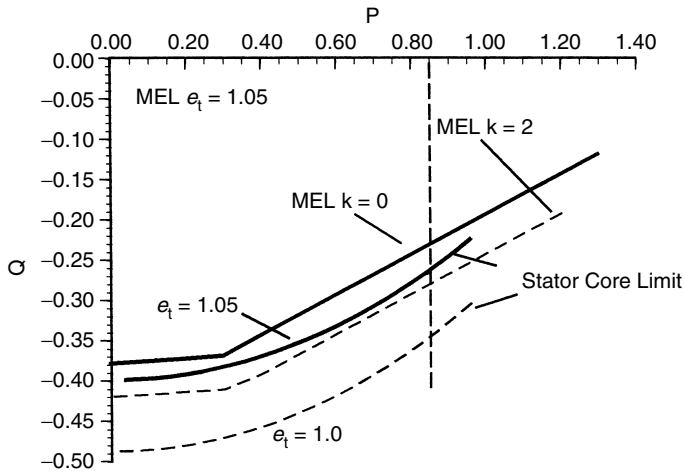


FIGURE 11.30 Stator limit and MEL.

The LOF relay is set with a diameter of 2.7 primary ohms and an offset of 0.178 primary ohms. Relating this setting to Figure 11.7, $Z_a = 2.878\ \Omega$ and $Z_b = 0.178\ \Omega$. Because this MEL characteristic is not sensitive to voltage variations ($k = 0$), the LOF relay characteristic will be plotted at minimum voltage to move the equivalent Point "A" of Figure 11.8 closest to the MEL characteristic.

Converting points Z_a and Z_b to the power-reactive ($P-Q$) plot at rated generator voltage yields:

$$\text{Point Mvar}_B = (13.8\text{KV})^2/(-0.178\Omega) = -1070\,\text{MVar}$$
$$\text{Point Mvar}_A = (13.8\text{KV})^2/(-2.878\Omega) = -66.2\,\text{MVar}$$

In per unit on the generator 104.4 MVA base:

$$\text{Point A} = -1070/104.4 = -10.25$$
$$\text{Point B} = -66.2/104.4 = -0.63$$

From these points, the parametric form of the LOF relay characteristic is derived as follows:

$$\text{Radius} = (10.25 - 0.63)/2 = 4.81$$
$$\text{Center} = -0.63 - 4.81 = -5.44$$

The LOF setting can then be plotted at $e_t = 0.95$ as:

$$P = Radius * e_t^2 \sin\beta$$
$$= 4.81 * 0.95^2 \sin\beta \tag{11.94}$$
$$Q = -Center * e_t^2 + Radius * e_t^2 \cos\beta$$
$$= -5.44 * 0.95^2 + 4.81 * 0.95^2 \cos\beta \tag{11.95}$$

The MEL and LOF settings are plotted in Figure 11.31. The plot shows coordination between the two functions in that the entire LOF circle is below the MEL limit. With this configuration any Var swing into the LOF trip characteristic will first activate the MEL. Of course, this does not

© 2006 by Taylor & Francis Group, LLC

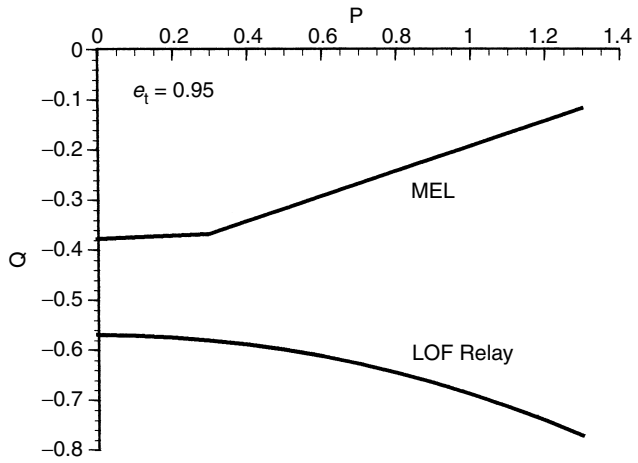


FIGURE 11.31 Loss-of-field relay and MEL at $e_t = 0.95$.

ensure the MEL can prevent a misoperation of the LOF relay. A dynamic simulation would be required to make that determination.

Stability limits will not influence the MEL setting unless they are more limiting than the generator Var capability. The manual regulator steady-state limit is normally the most limiting and is often the only stability limit considered when developing the MEL setting. This approach can be incorrect on a weak system where the AVR dynamic limit may encroach on the generator capability.

The system condition considered when developing stability limits depends on system design and operating philosophies. Many systems are designed to operate with one facility out of service for maintenance or repair and the failure of a second facility. Applying this criteria to the sample system, two conditions are of interest. First, line A (the strongest tie to the sample system bus) is assumed out of service when the AVR fails, transferring excitation control to the manual regulator. Secondly, line A is out of service when line B fails.

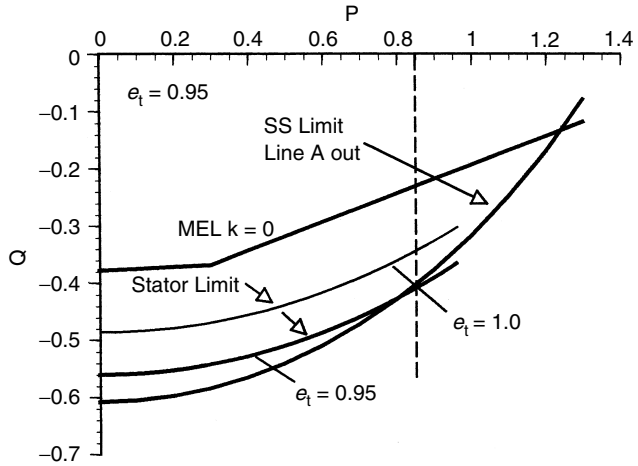


FIGURE 11.32 Manual regulator steady-state limit and MEL.

© 2006 by Taylor & Francis Group, LLC

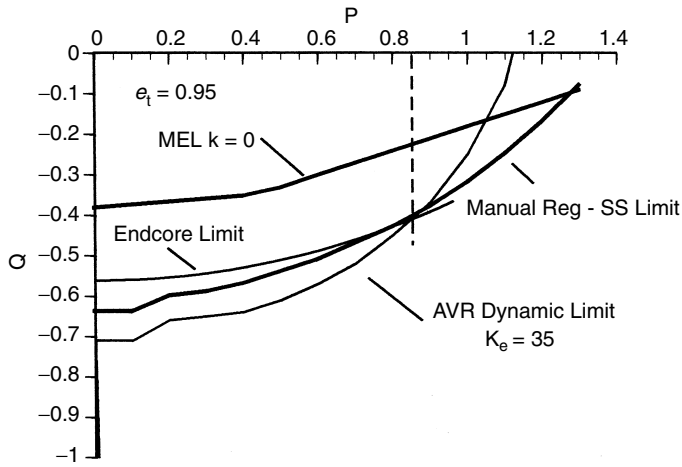


FIGURE 11.33 Sample system stability limits, line A out.

In the first case, the MEL must prevent operation outside the manual regulator steady-state stability limit with line A out of service. In the second case, the MEL must prevent operation beyond the AVR dynamic limit with both lines A and B out of service. As previously stated, the second case is often ignored.

The manual regulator steady-state limit is usually determined using the classical stability limit circle calculated from Equation (11.30) and Equation (11.31). Figure 11.32 plots this limit with line A out against the MEL setting chosen above. Because stability limits are most restrictive, a reduced voltage 0.95 pu terminal voltage is assumed. The figure shows that the MEL setting required for stator end-core protection is adequate to prevent operation beyond the manual regulator limit should the AVR fail with the line outage.

The synchronizing and damping torque evaluations presented in Section 11.6.3 provide a more comprehensive view of the various stability limits. Figure 11.33 plots the manual and AVR limits at

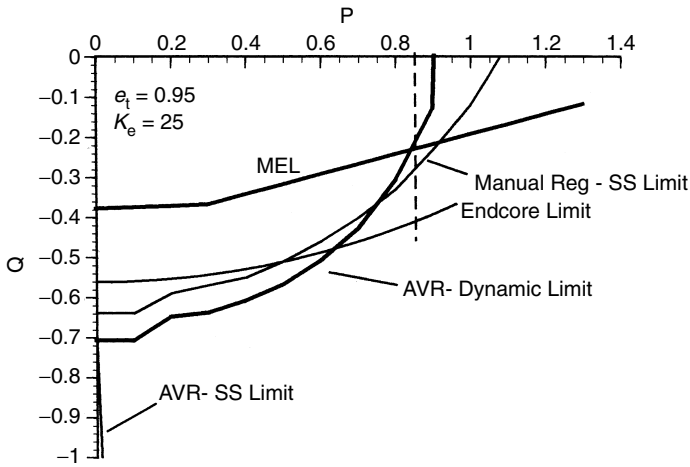


FIGURE 11.34 Sample system stability limits, lines A and B out.

© 2006 by Taylor & Francis Group, LLC

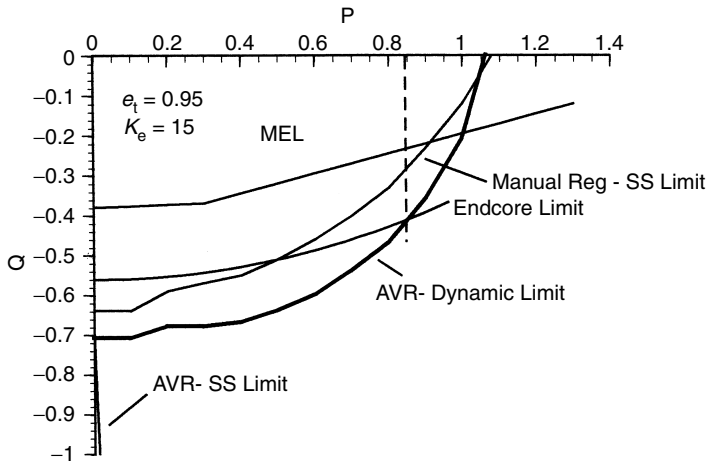


FIGURE 11.35 Sample system stability limits, regulator gain $K_e = 15$.

0.95 pu voltage. The MVR limit has a slightly different characteristic than the previous figure because this limit includes the effect of saliency ($x_d \neq x_g$). Again, the chosen MEL setting is shown to prevent instability in the event of an AVR failure concurrent with the line outage. The plot also validates the assumption that the manual regulator limit is more restrictive than either of the AVR limits. However, because of the weakness of the system and the high AVR gain (KE = 25), the manual steady-state and AVR dynamic limits converge near rated power output (0.85 pu).

The other stability criterion for setting the MEL is that it prevent operation outside the AVR dynamic limit with both line A and line B out. Figure 11.34 shows that this condition is not met. The turbine generator is rated at 85% PF; thus, the maximum power output is 0.85 pu. At maximum power output, the dynamic limit extends above the chosen MEL setting. This is unusual, but it is a result of the very weak system created by the two-line outage and the high AVR gain. The MEL limit could be adjusted upward to prevent operation beyond the dynamic limit at maximum power output, but this will increase the leading Var limitations placed on the generator during normal operations.

An alternative solution would be to reduce gain on the automatic voltage regulator. Figure 11.34 is based on regulator gain $K_e = 25$. By reducing the gain to 15, as shown in Figure 11.35, dynamic stability is improved and the chosen MEL setting is acceptable.

REFERENCES

1. Demello, F. P. and Concordia, C., Concepts of synchronous machine stability as affected by excitation control, *IEEE Trans PAS*, 88, 316–329, 1969.
2. Farnham, S. B. and Swarthout, R. W., Field excitation in relation to machine and system operation. *AIEE Ts*, Vol. 72, PART III, Power Apparatus and Systems 1215–1223, 1953.
3. Choi, S. S. and Jia, X. M., Under excitation limiter and its role in preventing excessive synchronous generator stator end-core heating, *IEEE Trans Power Systems*, 15 (1), 95–101, 2000.
4. Roger Bérubé, G., Les Hajagos, M., and Beaulieu, R. E., A utility prespective on under-excitation limiters, *IEEE Trans Energy Conversion*, 10 (3), 532–537, 1995.

© 2006 by Taylor & Francis Group, LLC

5. IEEE Committee Report. Excitation system dynamic characteristics, IEEE Transactions, Vol. PAS-92, No 1 Jan/Feb, 64–75, 1973.
6. Choi, S. S. and Jia, X. M., A technique for tuning under excitation limiters, *IEEE Trans Power Systems*, 14 (4), 1279–1284, 1999.
7. IEEE Task Force on Excitation Limiters, Underexcitation Limiter Models for Power System Stability Studies, *IEEE Trans Energy Conversion*, 10 (3), 524–531, 1995.

© 2006 by Taylor & Francis Group, LLC

12 Loss of Synchronism

12.1 INTRODUCTION

Normally, all generators within an interconnected power system operate at like frequency with their magnetic poles coupled through interaction with the network. The interconnecting force is elastic, allowing some angular play between generators in response to system disturbances. A loss of synchronism occurs when the bonding force is insufficient to hold a generator or group of generators in step with the rest of the power system. This can occur when equipment outages or low voltage weaken the system or if the force is inadequate to restrain extreme rotor excursions following a system fault or switching.

Once synchronism is lost, the affected generator or generators operate at slightly different frequencies. The difference in frequencies is termed the slip frequency. A generator that pulls out of step ahead of the system with a slip frequency of 4 Hz will be operating at a speed of $1 + \text{slip}/60 = 1.067$ pu or 6.7% overspeed.

The effects of a loss of synchronism can be visualized using the case of a single generator out of step with the system. The system and generator voltage vectors sweep past one another at slip frequency, producing a pulsating current with peak magnitude potentially greater than a three-phase fault at the generator terminals. An out-of-step generator must be rapidly isolated from the power system to prevent damage to the generator, turbine and GSU transformer. The isolation of any asynchronous portion of the system is also required to facilitate system restoration, because synchronism cannot be restored without operator intervention.

There are several schemes available for out-of-step protection. Most detect a loss of synchronism by measuring variations in system impedance. Settings applied to these schemes are critical to system reliability. The schemes must be set to quickly isolate an asynchronous machine, not only to prevent damage, but also to prevent instability from spreading to other portions of the system. Yet, setting must be secure against misoperations. The loss of generating capacity during a disturbance can precipitate a major outage.

After a generator falls out of step, the generator internal voltage will rotate with respect to the system voltage at slip frequency. The resulting current can be expressed as

$$I = \frac{E_g \angle \delta - E_s}{X_g + X_{TR} + Z_s} \tag{12.1}$$

where δ is the changing angle between the generator and system voltage, X_g is the equivalent reactance of the generator, and X_{TR} and Z_s are the GSU transformer and system impedance, respectively. If the generator and system voltages are assumed to be equal, no current will flow when $\delta = 0$ and the system will appear as an open circuit with infinite impedance. As the angle increases, so will the current until the system reaches a separation of 180°. At this point, the driving voltage will be twice normal, the sum of E_g and E_s, and the current will be at a maximum.

Electrically, this condition is identical to that produced by a three-phase fault located one-half the electrical distance to the remote terminal or at $Z = 0.5(X_g + X_{TR} + Z_s)$. This imaginary fault location is called the electrical center of the system. The location of the electrical center denotes the severity of the event with respect to the generator. If the electrical center is located on the transmission network, the three-phase fault it mimics is remote from the generator, producing only moderate stress at the generator. When the electrical center is located in the GSU transformer

© 2006 by Taylor & Francis Group, LLC

or generator itself, it represents an event equivalent to a GSU or generator fault, with severe stress to the local equipment.

The location of the system electrical center is not fixed. It is apparent from Equation (12.1) that the center will move away from the generator as system impedance increases due to equipment outages. The center is also slip dependent because generator reactance varies with slip frequency. In addition, electrical center variation with system and generator voltages will be defined later in the chapter.

12.2 TURBINE GENERATOR DAMAGE

As the electrical center moves from the system into the generator, the current magnitude increases and with it thermal and mechanical stress on the generator and GSU transformer.

On a strong system, the sum of X_T and Z_s can be less than X_g. In this case, the electrical center will lie within the generator and the current at 180° exceeds that of a three-phase fault at the generator terminals. The operative generator reactance during out-of-step events is usually assumed to be X'_d, but with low transformer and system impedance, the current could exceed the subtransient fault current at the generator terminals. This is the maximum current the machine is designed to withstand. The absence of DC offset current during the out-of-step event does lessen the stress from that of the fault case. The point is that as the location of the electrical center moves toward the neutral end of the generator, current induced thermal and mechanical stress can approach design limits. The generator is exposed to these conditions each slip cycle.

In addition to these stresses, the rotational speed difference between the rotor and system will induce currents in the rotor similar to those prodcued by unbalanced stator currents. Prolonged exposure to these currents will cause thermal damage to damper windings, rotor teeth, wedges and the rotor body. Restacking of the stator core will be required. Local hot spots may also damage stator windings.

The current pulsation associated with each slip cycle causes severe torque transients in the turbine generator shaft. This stress is at a maximum during the initial period of each torque pulsation. This is the period when shaft damage normally occurs. The fatigue life of the shaft can be used up after a few pole slip events.[1] If the slip cycle frequency coincide with a natural frequency of one of the shaft sections, shaft failure can result. The severe mechanical and electrical transients associated with an out-of-step event necessitate rapid detection and tripping.

Prolonged asynchronous operation can also cause diode failures within the excitation systems. During each pole slip, these diodes will experience high voltage as they block reversed rotor current. The overvoltage stresses insulation and can result in breakdown.

On the power system, a loss of synchronism by one or more units will result in cyclic voltage fluctuations as generators slip poles. These voltage dips can cause disruption to customers served from the grid. Induction motors may stall and synchronous motors can lose synchronism. Other processes would be disrupted when the voltage dips cause motor contactors to drop out.

12.3 TRANSIENT STABILITY

A loss of synchronism results from some form of system instability.

The loss of steady-state and dynamic stability as discussed in Chapter 11. Although the minimum Var limiter (MVL) is provided to prevent these types of instability, this control device is only available when the automatic voltage regulator (AVR) is in service. When the manual regulator is in service, systems can be vulnerable to these forms of instability.

A generator is most likely to lose transient stability. This is the ability of the system to remain synchronized following an abrupt change such as a fault or switch of a key line. This form of instability is key to the development of out-of-step protection. Unlike steady-state and dynamic stability, the limit of transient stability cannot be defined in terms of operating parameters such

© 2006 by Taylor & Francis Group, LLC

as power and reactive output prior to the loss of synchronism. This is because fault conditions pose the most severe challenge to transient stability and the severity of these events, although influenced by operation conditions, is largely a function of fault location and relay clearing time.

An understanding of transient stability, like steady-state stability, is based on the power angle equation presented in Chapter 11.

$$P_e = \frac{E_g E_s}{Z_T} \sin \delta \tag{12.2}$$

where P_e = electrical power transmitted by the power system, E_g = generator voltage (usually assumed to be voltage behind X'_d for transient stability), E_s = equivalent system voltage, Z_T is the transfer impedance which is the impedance directly between the two voltages, $Z_T = X'_d + X_{TR} + Z_s$, and δ = angle between E_s and E_g.

Figure 12.1 is a plot of the power angle equation for a hypothetical system with two lines in service and with one of those lines switched out. The steady-state operating point is determined by the intersection of the horizontal line representing mechanical power input to the generator shaft (P_m), and the electrical power (P_e) absorbed by the system. The plot shows that to transmit

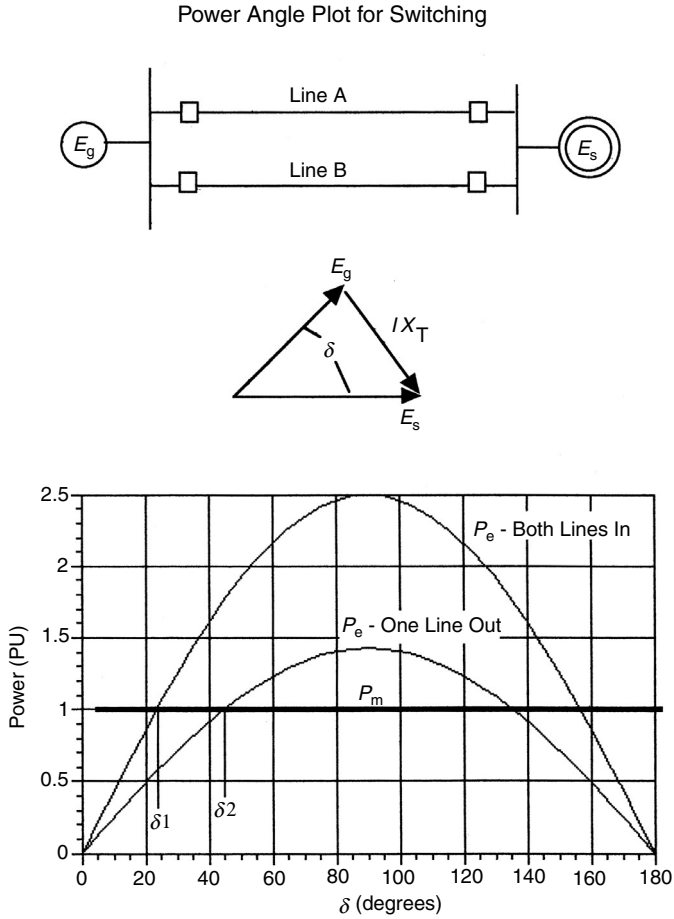


FIGURE 12.1 Power angle plot.

© 2006 by Taylor & Francis Group, LLC

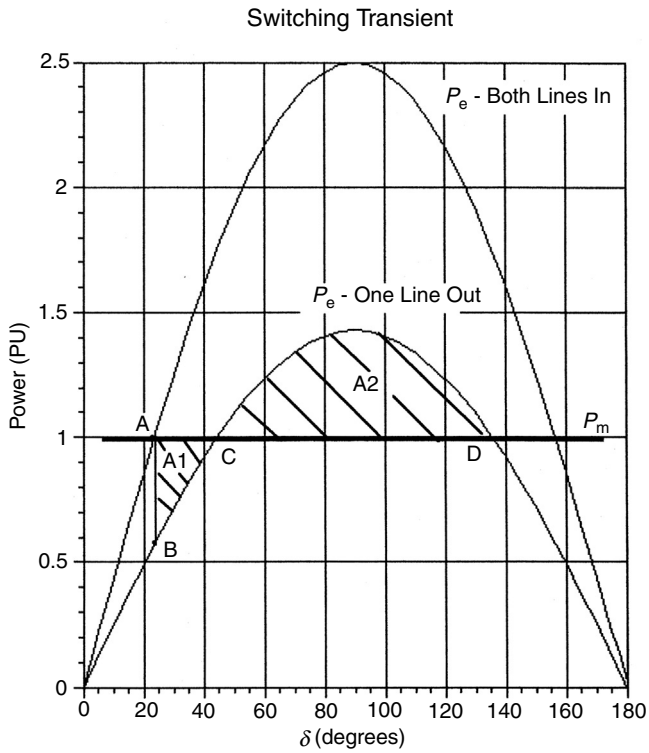


FIGURE 12.2 Power angle with line switching.

1.0 pu power through the electrical system, the angle between the generator and system voltages must be 25°, with both lines in service, and 45° if one line is switched out.

The mechanics of the transient that occurs when a line is switched out is illustrated in Figure 12.2. The unit is initially operating at point A with electrical and mechanical power equal. The switching of the line immediately reduces the electrical power that the system can absorb to the value at point B. The mechanical input power to the generator shaft remains constant. Thus, mechanical power supplied now exceeds the electrical power by the amount A − B. This excess energy acts to accelerate the generator and advance the power angle δ toward the new operting point at 45° (point C). The rotor angle advances through point C because the generator has inertia. After point C, the electrical torque exceeds the mechanical torque and a decelerating torque is produced. Angular speed decreases.

The unit will be stable and remain in synchronism if there is sufficient decelerating torque to prevent the rotor angle from reaching point D. If the swing reaches point D, mechanical torque once again exceeds the electrical torque and the unit will accelerate. This time there is no mechanism to decelerate and the unit will pull out of synchronism. If the system is stable, rotor oscillations about point C will diminish and this point will become the new steady-state operating angle.

System stability can be evaluated from this plot. The total accelerating energy for the switching operation is defined by area 1, the decelerating energy by area 2. Stability exists when A2 > A1.

Analysis of a fault condition is the same as for the switching transient. The amplitude of the power angle curve for a fault condition is markedly reduced from that of the line out condition because a fault dramatically increases the effective transfer impedance X_t between E_g and E_s. To illustrate this increase, refer to the simple network shown in Figure 12.3. Under normal

© 2006 by Taylor & Francis Group, LLC

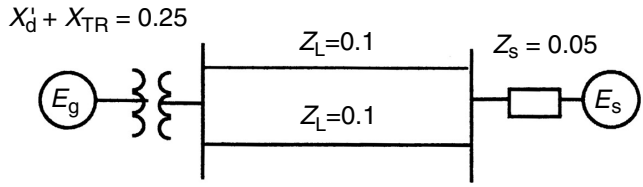


FIGURE 12.3 Transfer impedance, unfaulted network.

conditions, the transfer impedance between the generator internal voltage and the system is given by

$$X_t = X'_d + X_{TR} + 0.5X_l + X_s = 0.35\,\text{pu}$$

Figure 12.4(a) represents a three-phase fault at the midway point of one line. The transfer impedance for this condition is calculated using the basic delta-wye and wye-delta conversions shown in Figure 12.5. The resulting transfer impedance is shown to be 2.0 pu in Figure 12.4(c). This fault represents 570% increase in transfer impedance and an 83% reduction in the amplitude of the power angle curve.

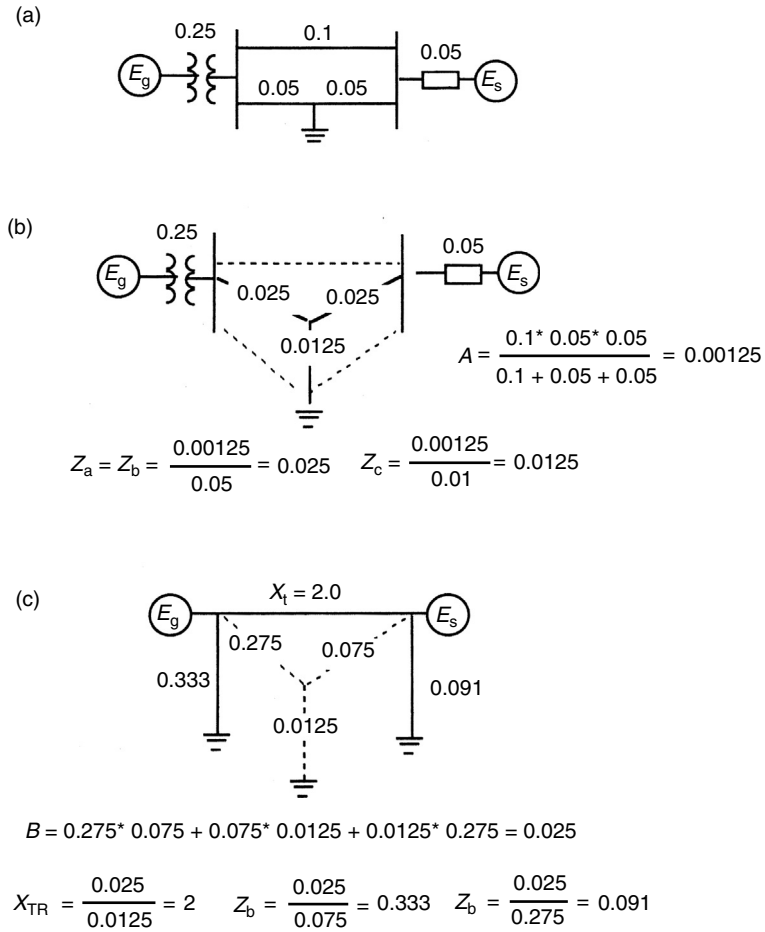
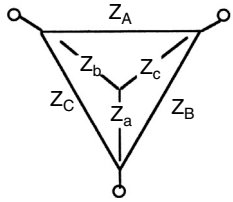


FIGURE 12.4 Transfer impedance, faulted network.

© 2006 by Taylor & Francis Group, LLC



delta to wye

$$A = \frac{Z_A Z_B Z_C}{Z_A + Z_B + Z_C}$$

$$Z_a = \frac{A}{Z_A}$$

$$Z_b = \frac{A}{Z_B}$$

$$Z_c = \frac{A}{Z_C}$$

wye to delta

$$B = Z_a Z_b + Z_b Z_c + Z_c Z_a$$

$$Z_A = \frac{B}{Z_a}$$

$$Z_B = \frac{B}{Z_b}$$

$$Z_C = \frac{B}{Z_c}$$

FIGURE 12.5 Wye-delta and delta-wye conversion.

A three-phase fault at the generator high-voltage bus would yield infinite transfer impedance and a power angle curve with an amplitude of zero. With no electrical power, all the mechanical energy would be expended accelerating the generator.

The power swing analysis for a fault condition is shown in Figure 12.6. The system is initially operating at point O, with electrical and mechanical power equal. A fault occurs on line 2 and the electrical power into the electrical system immediately drops to point A. The excess mechanical power accelerates the rotor to point B. At that time, relaying senses the fault and trips breaker 1, increasing the power transfer capability of the electrical system to C. Later, breaker 2 trips to clear the fault and the electrical power jumps to E.

From the inception of the fault to the opening of breaker 2 at point E, the mechanical power has exceeded the electrical power and the generator has been accelerating. At point E, the fault is cleared and electrical power now exceeds mechanical power to produce decelerating torque. If there is sufficient decelerating energy, the rotor swing will reverse direction before point F is reached and angle δ will decrease. After several diminishing oscillations the generator will settle to the new operating point at J where $P_m = P_e$ with one line out.

If insufficient decelerating energy is available, the rotor will continue to accelerate beyond point F and stability is again lost. As with the switching analysis in Figure 12.2, a stable system exists when decelerating energy exceeds the accelerating energy. This condition is met when $A3 > A1 + A2$.

12.4 OUT-OF-STEP PROTECTION

Prior to the 1960s, electrical centers were normally found on the transmission system and out-of-step protection was provided by line relaying without the need for trip generation. Over the years, the transmission system became stronger. Generator and GSU transformer impedances have increased because improved cooling technology provided greater MVA capacity from physically smaller units. As a result, the electrical centers on many systems have moved into the GSU transformer and the generator itself, significantly increasing stresses on both components. These swings

© 2006 by Taylor & Francis Group, LLC

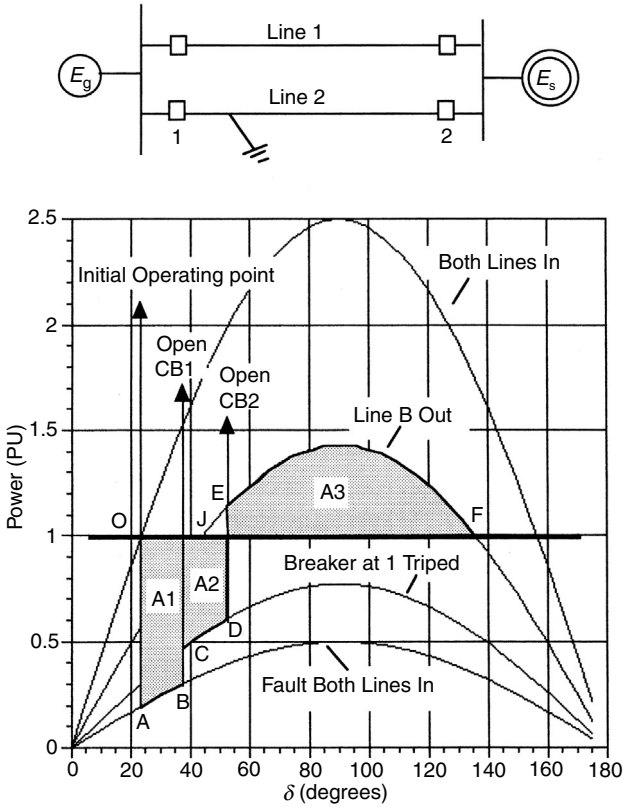


FIGURE 12.6 Power angle plot with fault.

would not be detected by network protection, thus the need for out-of-step protection at the generator.

Out-of-step protection may also be required at the generator if the electrical center is located beyond the GSU on the transmission system, but the transmission relaying is slow or incapable of detecting the out-of-step condition.[2]

Overcurrent relays used for generator protection do not provide reliable loss of synchronism detection. Although currents may be high enough to actuate an overcurrent relay, tripping will depend on the duration of the excess current, which is determined by the slip frequency. The operating time of an overcurrent relay will normally exceed the duration of the current pulse each slip cycle. If the condition persisted for many slip cycles, an electromechanical overcurrent relay might "ratchet" closed and trip the generator. Solid-state and microprocessor relays with fast reset characteristics will not ratchet.

Differential relays will not detect an out-of-step condition because the infeed and outfeed currents within the differential zone are equal.

Following a system disturbance, the generator rotor angle will oscillate as the generator attempts to find a new steady-state operating point. These rotor oscillations produce variations of stator voltage and current. The quotient of these varying quantities represents the dynamic system impedance during the transient as viewed from the generator terminal. The dynamic impedance is also referred to as the "swing impedance" or just "swing."

Distance relays applied at the generator as system backup protection will detect a swing if the swing impedance passes through the trip characteristic. The relay time delay and the speed at which

© 2006 by Taylor & Francis Group, LLC

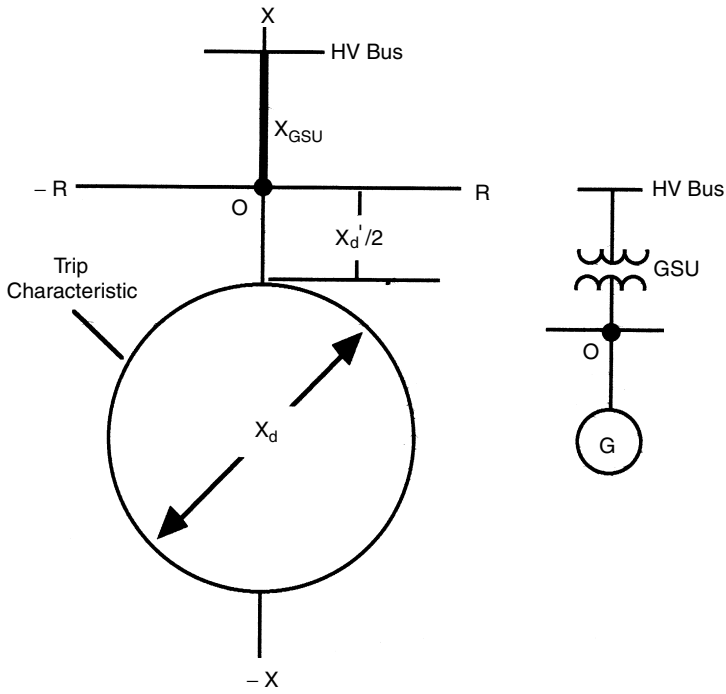


FIGURE 12.7 Loss-of-field relay characteristic.

the apparent system impedance crosses the relay characteristic will determine if tripping is initiated. Normally, the delay required for coordination with network relaying will prevent these schemes from operating during out-of-step events.

Loss-of-field protection is an impedance-based relay scheme applied at the generator terminals to detect the failure of the generator field. Figure 12.7 shows the trip characteristic for one popular LOF configuration. The trip characteristic is set with a time delay. Because this scheme measures the impedance looking into the generator, it cannot detect swings that pass through the GSU transformer. The offset of the characteristic also precludes detection of swings within the generator near the terminals. The trip characteristic will operate for slow-moving swings that linger within its characteristic in excess of the trip delay setting, typically 0.5 sec to 1.0 sec. The bottom line is that the loss-of-field protection may operate for specific out-of-step conditions, but cannot provide standalone out-of-step protection.

Over the years, specialized detection schemes have been developed. Early out-of-step protection schemes counted the current pulsation each time a generator pole slipped (passed through 180° separation with system voltage). Tripping was initiated after a preset number of counts. Now it is recognized that the system impedance viewed from the generator terminals provides a method for the rapid detection of a loss of synchronism. Consequently, out-of-step detection schemes employ impedance-sensing elements and specialized logic to distinguish between a fault condition and a loss of synchronism. In order to apply this type of protection, it is necessary to understand how system impedance varies during a loss of synchronism.

12.5 CLASSICAL SWING IMPEDANCE CHARACTERISTIC

Settings for the various impedance-based detection schemes are derived from a graphical representation of the system impedance trajectory during a loss of synchronism event. An expression for the swing impedance is derived in Ref. [6] from Figure 12.8. The impedance-sensing

© 2006 by Taylor & Francis Group, LLC

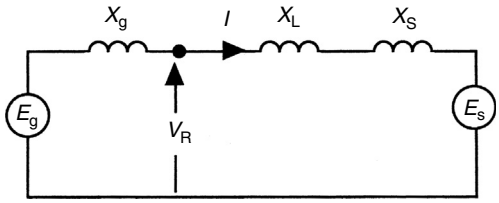


FIGURE 12.8 Equivalent circuit.

element is assumed to be located at the generator monitoring terminal voltage and current. The current has been defined by Equation (12.1) and is repeated here:

$$I = \frac{E_g \angle \delta - E_s}{X_g + X_{TR} + Z_s}$$

The voltage seen by a relay at the generator terminals is then given by

$$V_R = E_g \angle \delta - IX_g \tag{12.3}$$

Substituting for current,

$$V_R = E_g \angle \delta - \frac{E_g \angle \delta - E_s}{X_g + X_{TR} + Z_s} X_g \tag{12.4}$$

Letting $n = E_g/E_s$ and $1\angle\delta = \cos\delta + j\sin\delta$, the generalized equation for the impedance seen by the relay is then

$$Z_R = \frac{V_R}{I} = (X_g + Z_{TR} + Z_s)n\frac{(n - \cos\delta) - j\sin\delta}{(n - \cos\delta)^2 + \sin^2\delta} - X_g \tag{12.5}$$

The equation does not facilitate visitation of the resulting impedance characteristic. Some simplification is required.

Evaluating for the special case where $E_g = E_s$ ($n = 1$) the equation becomes

$$Z_R = \frac{X_g + Z_T + Z_s}{2}\left(1 - j\cot\frac{\delta}{2}\right) - X_g \tag{12.6}$$

Figure 12.9 is a construction for the swing path of Z_R with $n = 1$. The trajectory is a straight line that perpendicularly bisects the line A–B. The distance A−B is the total impedance $(X_g + X_T + Z_s)$ between the two voltages after the fault is cleared or after the switching operation. The origin of the plot is set at the location of the potential transformers that supply the out-of-step relay, normally the generator terminals. This construction is used to set most out-of-step schemes.

If the generator is assumed to be advancing ahead of the system voltage, the apparent system impedance, point P, moves from right to left. An advancing system voltage would result in a path from left to right. Note that the angular separation between E_g and E_s, angle δ, is equal to the separation between lines A–P and B–P. Apparent impedance is plotted at power angles of 60, 90, 120, 180, and 240°. Figure 12.10 shows the construction for these points.

The general case $E_g \neq E_s$ is plotted in Figure 12.11. Here the impedance locus for Z_R becomes a circle centered beyond points A or B. If $E_s > E_g$, the center is beyond A. If $E_g > E_s$ ($n > 1$),

© 2006 by Taylor & Francis Group, LLC

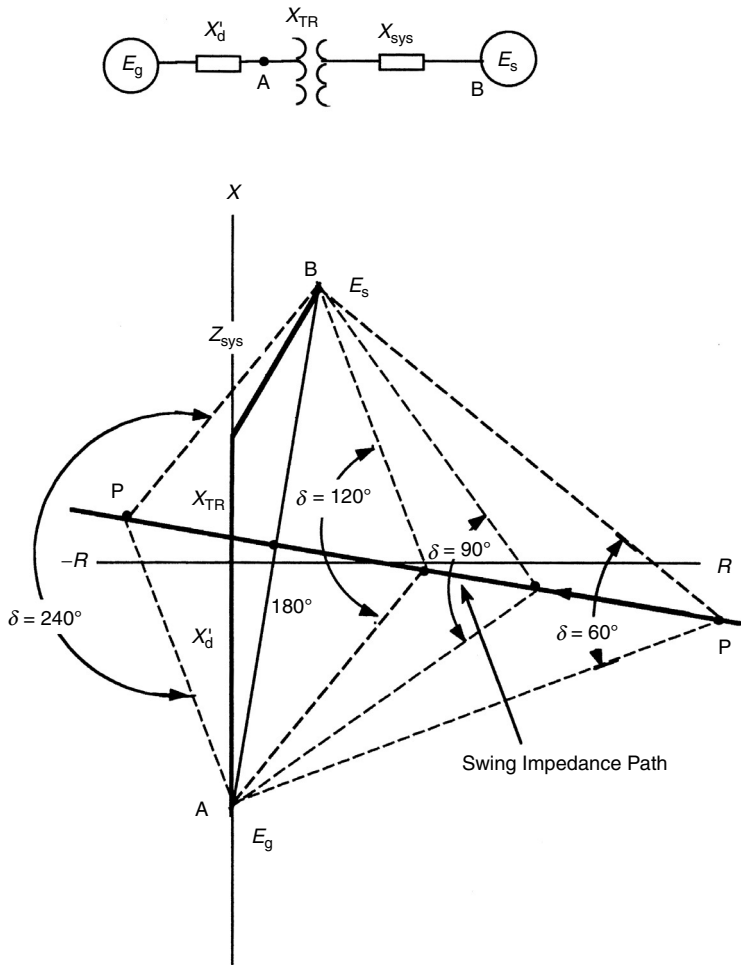


FIGURE 12.9 Apparent impedance swing.

the center is beyond B. Note that a circle plotted through points A, B, and 120° represents all points where the system angle δ equals 120°. Similar circles can be plotted for any system angle. These plots are also used when setting out-of-step protection.

Figure 12.12 shows the construction of the impedance path with $E_g > E_s$ ($n > 1$). Impedance Z_{AB} is the total system impedance and is equal to line A–B. The same construction can be used if $E_s > E_g$ ($n < 1$) by substituting $1/n$ for n and measuring the distance from point A. Figure 12.13 shows the variations in trajectory as n varies. Note the relative dimensions of the swing. The total impedance of the system, Z_{AB}, equals 0.54 pu. The resulting swing diameters vary from 1 to 5 pu.

12.6 DYNAMIC SWING REPRESENTATION

The plots provided in Figure 12.9 and Figure 12.11 are an idealized view of the swing impedance. They provide sufficient insight to estimate out-of-step protection settings, but they do not accurately portray the overall impedance trajectory. These plots consider variation of angle δ, but all other system parameters are held constant. In reality, the swing locus shows the effects of rotor oscillations and are strongly influenced by changes in generator internal voltage. The internal voltage is in turn controlled by the generator constants and the type of excitation, manual or automatic regulation. Other factors that affect the swing impedance characteristic, but are neglected in the

© 2006 by Taylor & Francis Group, LLC

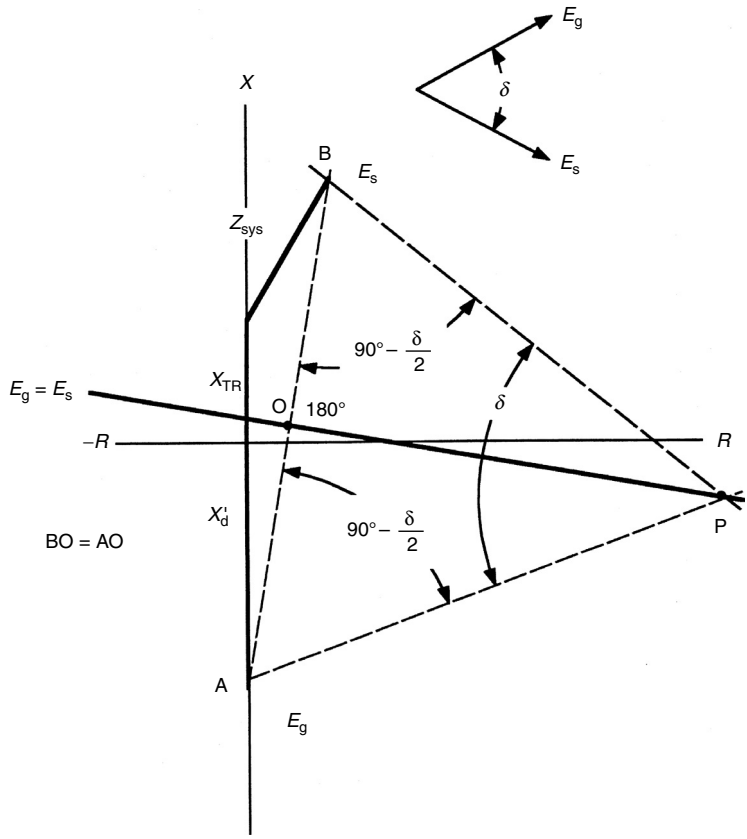


FIGURE 12.10 Swing angle construction.

construction, include governor action, mechanical damping of nearby units, shunt loads, shunt capacitance effects, and generator saliency.

The major limitation of the graphical analysis is that it assumes one generator swinging against a homogenous system. This representation is applicable when the generator under analysis is small with respect to the system and system generators swing together as one unit. For larger units or large-scale disturbances, generators on the system will swing with respect to one another, creating multiple electrical centers and rendering the equivalent system representation invalid. Computer simulations that include modeling of the voltage regulator, governor control, and damping effects of system load in a large area around the study generator are required to obtain accurate impedance plots.

If a system has one or two generators isolated from other machines, swing plots can be derived using the Excel workbook described in Appendix D and available for download from the publisher's website. This workbook models generator d- and q-axes circuits, a simple voltage regulator, and the electromechanical dynamics of rotor oscillations. Swings are initiated by the application of a three-phase fault with a settable clearing time.

The swing trajectories (Figure 12.14 through Figure 12.17) were derived from the Appendix D workbook. They show the shape of swing impedance loci when rotor oscillation and the effects of transients that cause variations of generator internal voltage are included. They also contrast swing variations with manual or automatic voltage regulators in service.

A slow-acting autoregulator will tend to offset the decay in internal voltage to maintain swing diameters nearly constant. On the other hand, a faster acting regulator will increase the internal voltage. If the swing impedance is initially below the R-axis ($n < 1$) the autoregulator will

© 2006 by Taylor & Francis Group, LLC

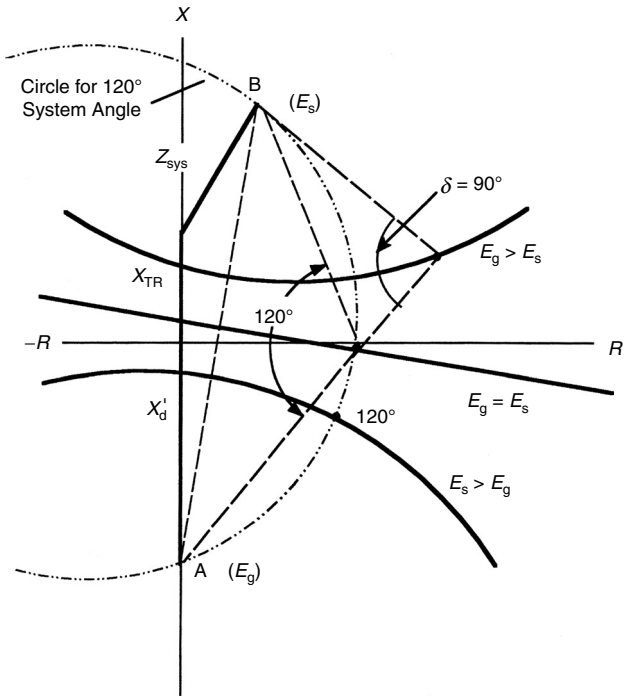


FIGURE 12.11 Swing with dissimilar system and generator voltages.

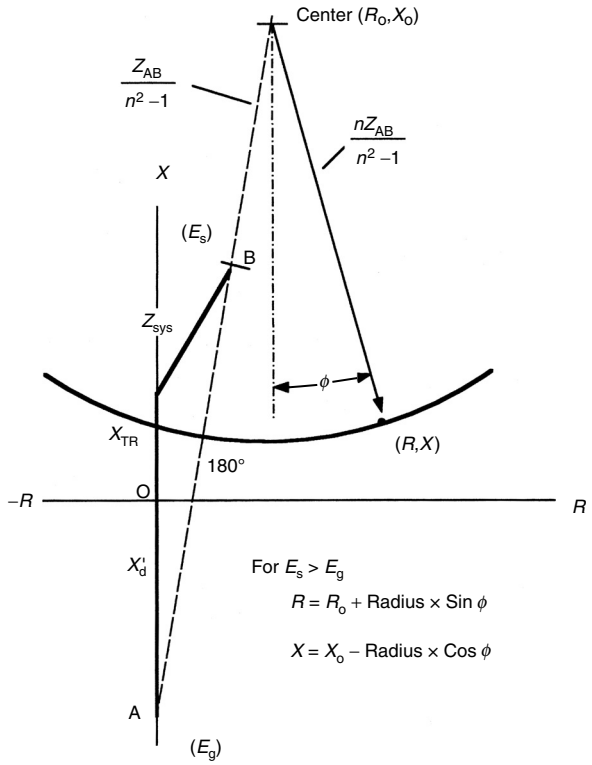


FIGURE 12.12 Construction of swing with $E_s \neq E_g$.

© 2006 by Taylor & Francis Group, LLC

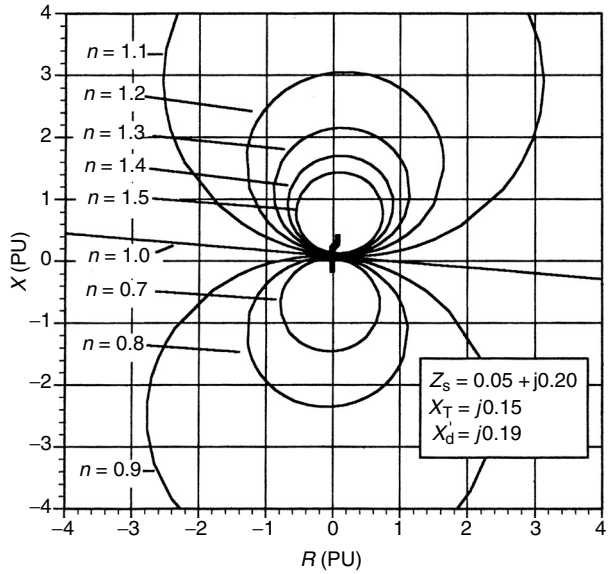


FIGURE 12.13 Swing family.

increase n, thus pushing the electrical center from the generator into the GSU or system. As n increases toward unit, the swing diameter will increase, rendering the swing easier to detect. When n is initially greater than one, the automatic regulation will again increase n, but in this instance regulator action will reduce the trajectory diameter and make it harder to detect. These variations are depicted in Figure 12.13.

Figure 12.14 shows the loci for a stable swing following a fault at the high-voltage terminals of the GSU transformer with manual excitation. Initially, the impedance seen (at $t = 0$) is equivalent to the generator load. When the fault occurs, the impedance immediately jumps to that of the GSU transformer where it remains until the fault is cleared. For the fault shown, clearing occurred in 0.15 sec. During that time, the generator accelerates and rotor angle advanced with respect to

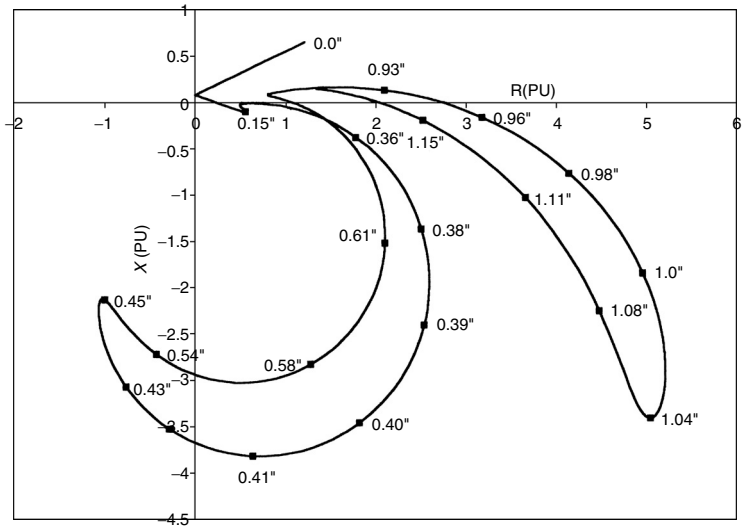


FIGURE 12.14 Stable swing with manual regulator.

© 2006 by Taylor & Francis Group, LLC

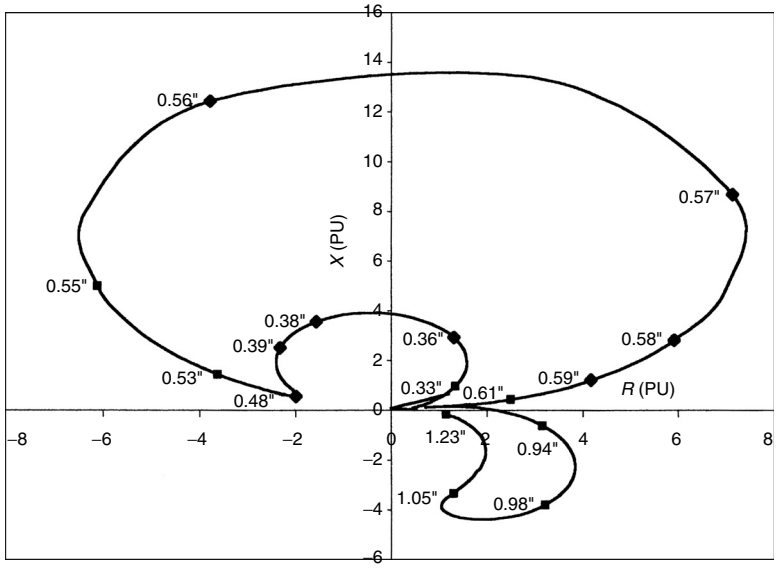


FIGURE 12.15 Stable swing with autoregulator.

the power system. Upon clearing, the impedance seen is a function of the generator internal voltage, the system voltage and the angular displacement between the two. The resulting impedance is plotted at $t = 0.15$ sec. Although the excitation is fixed, the initial transient will demagnetize the airgap, reducing the internal generator voltage. The voltage ratio n is therefore well below unity when the fault clears; thus, the swing radius is centered below the R-axis. The plot shows the increasing diameter of the swing as the generator internal voltage recovers toward its prefault value as set by the manual regulator. This is a stable case not a loss of synchronism because the swing does not cross the axis of the system impedance, Line A–B in Figure 12.9 such a crossing would denote separation of 180° and a pole slip.

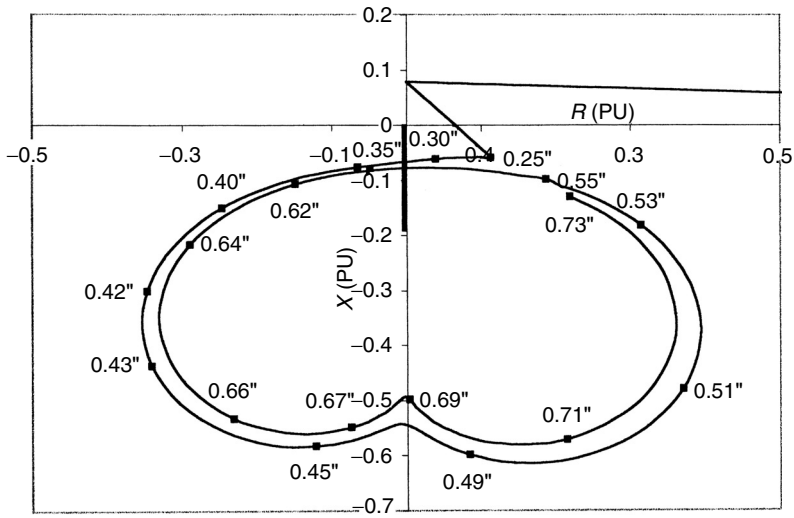


FIGURE 12.16 Unstable swing with manual regulator.

© 2006 by Taylor & Francis Group, LLC

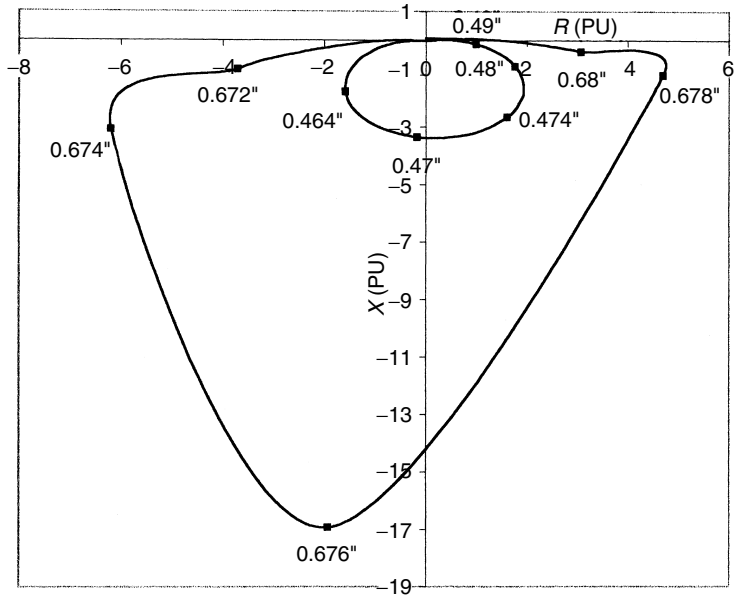


FIGURE 12.17 Unstable swing with autoregulator.

Figure 12.15 plots the same fault as previously described, but with the excitation under the control of a fast-acting automatic voltage regulator. The reduced terminal voltage during the fault and early portions of the swing cause the voltage regulator to initiate a rapid increase in excitation. This boost counter acts on the initial demagnetization and increases the internal generator voltage to the extent that $n > 1$. As a result, the center of the swing radius is located above the R-axis for a portion of the plot. As the transient diminishes, and the terminal voltage recovers, excitation will diminish until $n < 1$ and the center of the swing radius moves below the R-axis. Again this represents a stable case because the swing does not cross the impedance line.

Figure 12.16 and Figure 12.17 represent unstable cases with manual and automatic voltage regulation respectively. Under manual regulator control, the decaying internal voltage causes the swing diameter to decrease each swing cycle. In general, small-diameter swings are more difficult to detect. A manual regulator case tends to produce the "worst case" swings used to define the out-of-step settings. The second plot shows a dramatic increase in swing diameter, which is the result of a high-speed automatic regulator.

12.7 SETTING CONSIDERATION

Improved cooling techniques have increased generator impedance as system impedance declined due to reinforcement. These changes have caused electrical centers to moved from the transmission system into the GSU and the generator itself as seen in Figure 12.16 and Figure 12.17, necessitating the application of out-of-step protection at the generator. A major concern with this application is scheme misoperation for severe but stable swings. Previously, out-of-step protection was applied only on the transmission system and scheme operation did not trip generation. Power system events such as a fault, a sudden loss of a large unit or transmission path can cause severe system perturbations that can challenge out-of-step protection. During such periods of stress, the loss of generator due to the misoperation of a relay scheme can turn a recoverable event into a major system outage. Consequently, an out-of-step trip scheme applied at a generator must not operate for recoverable swings.

© 2006 by Taylor & Francis Group, LLC

During a system transient, the current in the generator and GSU transformer increase as the angular separation between the generator and system increase. At the maximum separation of 180°, current can exceed the level of a three-phase fault at the generator terminals. Repeated application of such high-magnitude currents and severe mechanical torque each slip cycle can damage the turbine, generator, and GSU transformer. Ideally, the out-of-step protection should operate to trip the generator in the first slip cycle before full separation produces peak current.

Unfortunately, the need to prevent tripping for stable swings and the desire for early intervention to limit current conflict. The resulting setting, depending on the specific out-of-step scheme involved, may require compromise. In such cases, generator reliability normally takes precedence and current limitation is the lower priority.

12.7.1 Recoverable Swings

Out-of-step protection must be set to initiate tripping only when a loss of stability is imminent. Following a system disturbance, generator rotors experience angular perturbations as they attempt to adjust a new steady-state operating condition. In a stable system, rotor oscillations are damped. The initial angular displacement is the largest, with each subsequent rotor swing diminished in magnitude until a new steady-state rotor angle is found. As the severity of the disturbance increases, so does the initial angular displacement. There exists a maximum swing angle from which the system cannot recover.

Some out-of-step schemes are designed to operate only after synchronism is lost. Other schemes attempt to actuate before the first pole slip (before 180° separation) at the maximum stable swing angle. In the latter case, settings are difficult to derive. The critical angle and resulting impedance trajectories are not fixed and vary dramatically with system conditions and fault location.

The best way to determine the critical swing angle is to model the system using a transient stability program. The system representation must include system loads, all generators, their voltage regulators and governor controls in a large area surrounding the machines in question. The system would then be tested by applying faults at critical points using maximum anticipated clearing times. These faults would be applied at various load levels, system configurations and generation mix to determine the most severe survivable swing for the unit in question. The impedance loci generated from these test cases would then be used to set the out-of-step relay. Unfortunately, transient stability modeling tools and the time to use them are not available to all and a less accurate method is often adopted.

In the absence of transient stability data, a general assumption is made that a displacement beyond 120° is not recoverable and instability is imminent. Consequently, out-of-step protection is often set to initiate tripping when the impedance loci exceed this value. The graphical construction of the swing loci is then used to determine the location 120° and 240° on the $R-X$ plane. Both are required because a swing may traverse the relay characteristic in either direction.

The minimum system impedance should be used in this calculation, because this will produce the minimum swing diameter. The settings derived should be adequate to accommodate a voltage ratio range n of 0.65 to 1.5. This to cover the decay of internal voltage for machines under manual regulator control and voltage increase for machines under automatic regulator control.

Another factor, which must be considered in any setting derivation, is the variation of generator impedance with slip. Generator impedance, along with the system and GSU transformer reactance, determines the swing trajectory. At zero slip, the equivalent generator impedance would be X_d. At 100% slip $X_g = X''_d$. Studies have shown that the slip for a typical loss of synchronism case is between 50% and 0.33%. This corresponds to a generator impedance variation of from X'_d to $2X'_d$.[3] The X'_d value is typically used to construct the swing loci because lower impedances produce a smaller swing diameter. Setting must allow sufficient margin to capture loci resulting from slower swings with effective generator impedance near $2X'_d$.

© 2006 by Taylor & Francis Group, LLC

12.7.2 Current Limitation

Unfortunately, a high angular setting is required to avoid operation for stable swings. This does not facilitate current limitation. With the out-of-step scheme set to operate at 120° separation, the voltage differences across the system would reach $\sqrt{3}$ rated. This limits current to 86% of the maximum 180° current. If thermal and mechanical stresses are assumed to be a function of current squared, tripping at 120° would reduce generator and GSU transformer stress to 75% of the maximum.

12.7.3 Out-of-Phase Switching Rating for Breakers

The high angular trip setting also imposed significant stress on the circuit breaker used to isolate the generator. Whenever a breaker interrupts current, a high-frequency voltage is developed across the opening contacts to oppose an instantaneous change in current. This is termed the transient recovery voltage (TRV) and has a maximum value equal to two times the difference in voltage imposed on each side of the breaker at the instant of contact parting. On a radial system with a source voltage on one side of the breaker and zero voltage on the outer side, transient recovery voltage has a maximum value of 2.0 pu. On a normal network, the source voltages on either side of the breaker are nearly in phase and, assuming no fault, the TRV would be near zero. Opening a breaker across an out-of-phase network exposed the breaker to a maximum TRV of 4.0 pu voltage across the contacts, a TRV double that normally encountered.

The adverse effect of increased TRV are twofold. When a breaker interrupts, an arc is drawn across the open contacts. Initial interruption of the arc is dependent on the ability of the breaker to cool the arc prior to the first current zero. The thermal energy of the arc is a function of the current and arc voltage (TRV). The increased TRV therefore jeopardizes the initial interruption of current. Assuming the arc is interrupted at the first current zero, the dielectric strength across the opening contacts must establish faster than the transient recovery voltage builds up. If the TRV builds up faster, the arc will restrike across the partially open contacts. The TRV generated by an out-of-phase condition has a faster rate of rise and larger peak value than that normally considered when rating breakers.

IEEE standards consider out-of-phase switching an unusual service condition and do not require breakers to be rated for it. Should a manufacturer choose to provide such a rating, IEEE C37.04-1999 recommends a rating of 25% rated short-circuit current at 180° separation for general use breakers. IEEE standard C37.013-1997, which governs generator breakers, recommends a rating of 50% for the symmetrical short-current rating at a separation at 90° and maximum system voltage. Although most breakers are not assigned an out-of-phase rating, the suggested ratings are considered within the capability of a typical breaker.

Because the out-of-phase current at 180° separation usually exceed 25% of the breaker short-circuit rating, tripping must be delayed until separation is less than 90° or more than 270° to utilize the 50% rating. This limitation must be considered in the design and setting of an out-of-step protection scheme. The switching limit precludes tripping before the first pole slip to limit current.

These constraints could be removed if a breaker is specially designed for out-of-phase switching or a breaker with a higher voltage or higher interrupting ratings is used. This is not normally done.

12.7.4 Swing Velocity

Another consideration is the maximum anticipated swing velocity. Out-of-step detection schemes use timing to differentiate between system impedance changes caused by a fault and those resulting from a swing condition. A fault, for all practical purposes, changes system impedance instantaneously while impedance change during a system transient is constrained by inertia and generator time constants. Scheme timing must detect the fastest swing anticipated. The swing velocity is not

© 2006 by Taylor & Francis Group, LLC

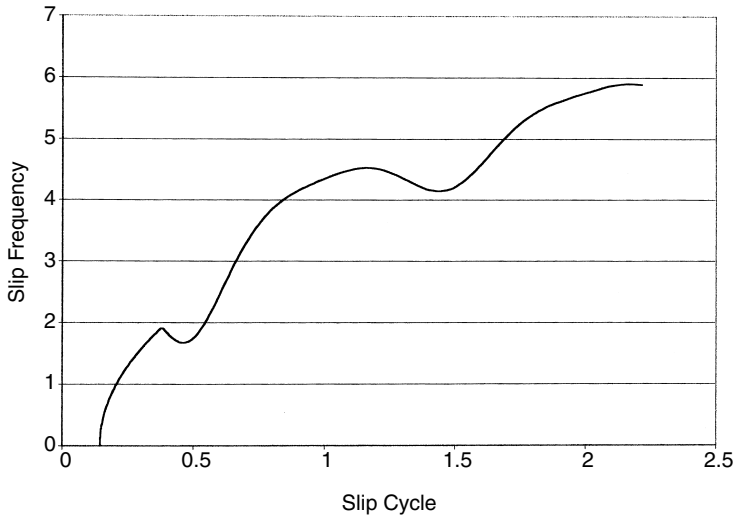


FIGURE 12.18 Slip frequency characteristic.

constant during the slip cycle. The velocity during the first half of the slip cycle is of prime importance because this is the period when out-of-step detection occurs. Reference 2 lists the following average velocities for the first half of the first slip cycle.

Steam units: 1296–1728 deg/sec (3.6–4.8 slip cycles/sec)
Tandem units: 250–400 deg/sec (0.694–1.11 slip cycles/sec)
Compound units: 400–800 deg/sec (1.11–2.22 slip cycles/sec)

A slip frequency characteristic derived from the Appendix D Excel workbook is plotted in Figure 12.18. The plot references slip frequency vs. slip cycle (slip cycle of $1 = 360^{\circ}$). Maximum acceleration occurs after each pole slip at the midpoint of the slip cycle. The slip frequency increases with each slip cycle. This is important because, as will be explained later, for certain fault conditions out-of-step schemes may fail to operate in the first slip cycle. Scheme timing evaluations should therefore consider the slip velocity at the beginning of the second slip cycle. The plot indicates slip less than 5 Hz during this period. This value is a good estimation of the upper limit of slip since it is derived for a light machine ($H = 3$).

12.8 OUT-OF-STEP RELAY: DEVICE 78

There have been various schemes applied for out-of-step protection over the years. The schemes described here are found in electromechanical, solid-state and microprocessor-based designs. The single blinder scheme is the most common. Note that the descriptions provided here are general and specific scheme logic is subject to variation among manufacturers.

12.8.1 Simple Mho Scheme

The simplest form of out-of-step protection uses a standard distance relay (no offset) located at the high-voltage terminals of the GSU transformer as shown in Figure 12.19. The relay is normally set to see the GSU transformer impedance plus the transient reactance (X'_d) of the generator. A characteristic based on this philosophy is shown in Figure 12.20. This setting could fail to detect a slow-moving swing where the generator reactance can approach $2X'_d$. A mho setting based on $2X'_d$ is

© 2006 by Taylor & Francis Group, LLC

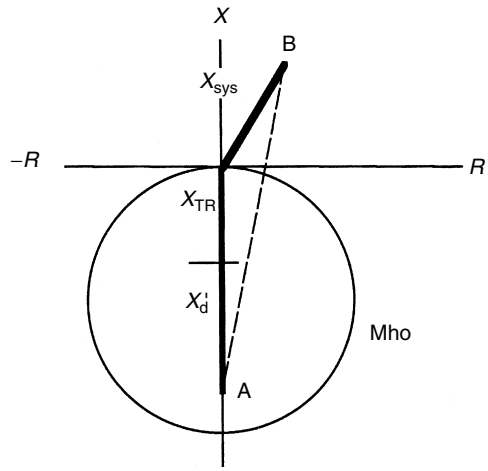


FIGURE 12.19 Mho out-of-step characteristic.

generally not applied. The resulting large characteristic would operate well below the assumed stability limit of 120° and subject the scheme to misoperation for stable swings. Reducing the setting will improve security, but may result in a failure to detect swings with irregular trajectories.[4]

This scheme has the advantage of providing backup fault protection for the generator and GSU transformer. The disadvantage is that the geometry of the mho characteristic makes an ideal out-of-step setting unobtainable. Figure 12.21 shows the boundary of 120° system separation superimposed over the setting to illustrate the problem. The relay is set to initiate tripping at a separation angle of 120° based on the impedance trajectory with $E_g = E_s$ ($n = 1$). It is obvious swing trajectories above the $n = 1$ line can initiate tripping near 180°, subjecting the breaker to a severe out-of-phase switching condition. For swings below the $n = 1$ line, trip initiation can

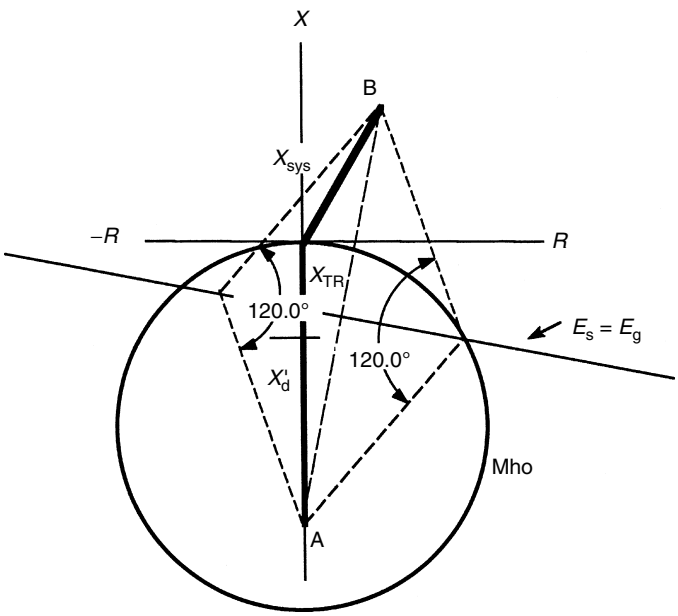


FIGURE 12.20 Mho out-of-step setting.

© 2006 by Taylor & Francis Group, LLC

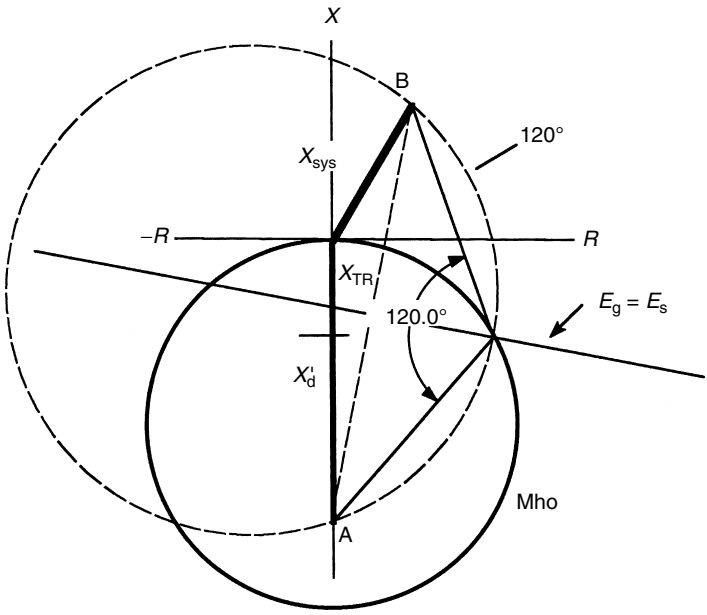


FIGURE 12.21 Mho out-of-step deviation.

occur far below 120°, again rendering the scheme susceptible to misoperation for stable swings. Also note that all swings driven by an advancing system voltage phase angle would enter the characteristic from the left and actuate the scheme for stable swings below 120° separation. Security could be improved by reducing the diameter of the relay trip characteristic, but this reduction will increase the breaker switching angle for trajectories where n is greater than unity.[1] A time delay could be added, but this can result in the failure to detect fast-moving swings. In either case, settings would have to be optimized using actual impedance trajectories obtained from system transient studies.

Although an offset distance relay located at the generator terminals, as shown in Figure 12.22, would appear to have a trip characteristic similar to that of the nonoffset scheme previously described, it does not. The nonoffset relay is inherently directional and will not see faults beyond the GSU terminals. The offset relay must be set short of the GSU high-voltage terminals

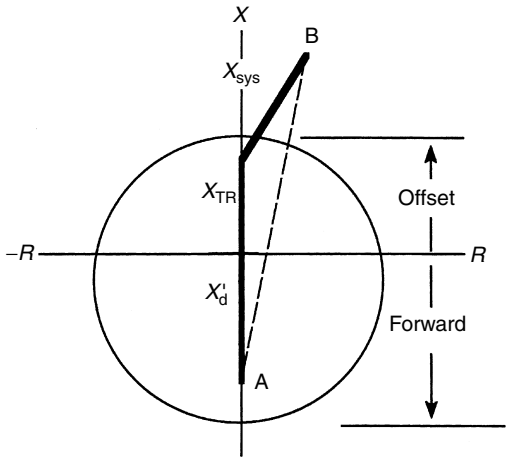


FIGURE 12.22 Offset mho scheme.

© 2006 by Taylor & Francis Group, LLC

to prevent scheme operation for faults on the transmission system near the GSU transformer. The relay could be set to include the GSU high-side terminals, but then a time delay is required for coordination with the transmission line relaying. Both these alternatives render this scheme ineffective for out-of-step protection.

12.8.2 Single Blinder Scheme

This is the most common out-of-step protection scheme. It is a specialized scheme that employs blinders in conjunction with a mho element. A blinder is an impedance-sensing element with a straight-line characteristic when plotted on the $R-X$ plane. The complete impedance characteristic of the scheme is shown in Figure 12.23. It is usually implemented at the generator terminals, but can be applied at the high-voltage terminals of the GSU transformer.

In the figure, the blinder elements are designated B1 and B2, the mho unit, Z_{mo}. The mho element will actuate for faults on the transmission system, but logic is provided to differentiate between a fault and a system swing and to prevent scheme operation for the former.

The system impedance is initially at a load point well outside the mho relay characteristic. If a fault occurred, say at the high-voltage terminals of the GSU transformer, the impedance seen by the scheme will move into the mho characteristic between the blinder units instantaneously. The generator and prime mover have inertia; therefore, the separation angle cannot change instantaneously and a swing will require time to enter the mho characteristic transverse the blinder element and then exit the mho circle. The scheme differentiates between a fault and a swing by timing the actuation of the two blinders. The scheme recognizes a swing condition when the time between actuations exceed a minimum delay set within the relay logic, usually two to four cycles.

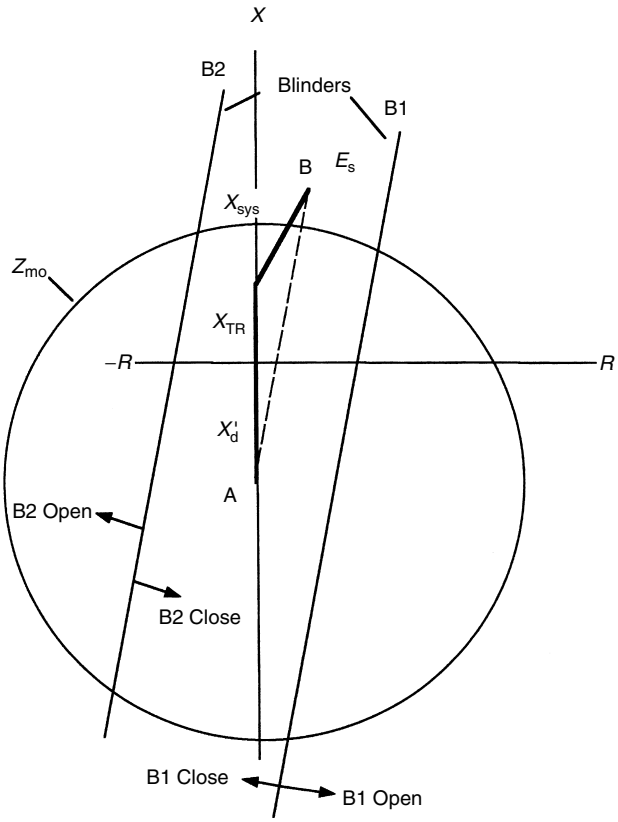


FIGURE 12.23 Single blinder scheme.

© 2006 by Taylor & Francis Group, LLC

The logic must also distinguish between a stable and unstable swing. The single blinder accomplishes this by monitoring the entry and exit path of the swing impedance. For trip initiation, the swing impedance must first enter the Z_{mo} element from outside than traverse both blinders in sequence. Trip initiation can occur after the second blinder actuates, but many schemes delay trip initiation until the swing exits the Z_{mo} characteristic to provide a more favorable angle for breaker interruption. A stable swing will reverse direction and exit the Z_{mo} characteristic from the same quadrant it entered. Consequently, either one blinder would not actuate or the blinder on the entry side would pick up then drop out as the stable swing exits. The out-of-step logic must operate correctly for left-to-right swings, as well as right-to-left swings.

The advantage of this scheme is that it will only operate for an unstable swing. Because both blinders must operate in sequence, the impedance path must exceed the 180° separation. The downside is that the scheme ensures that the generator, prime mover, and GSU transformer are exposed to the maximum out-of-phase current of at least one slip cycle.

Referring to Figure 12.24, the single blinder out-of-step scheme requires several settings. Angles Φ_1, Φ_2, distances D1 and D2, the mho circle offset and forward reach must be set in all schemes. Some relays require a setting for the minimum delay between blinder actuation. In many schemes, this time is fixed within the logic.

A general setting criterion for the single blinder out-of-step trip schemes has been developed from transient stability studies on typical systems.[2] The settings for the mho and blinder elements are as follows:

Φ_1, Φ_2, chosen so blinder characteristic parallels line A–B
Z_{mo} forward reach, chosen to be $2-3 \times X'_d$
Z_{mo} offset, $1.5-2 \times X_{TR}$

The forward reach setting is large to allow for the variation of generator impedance with slip.

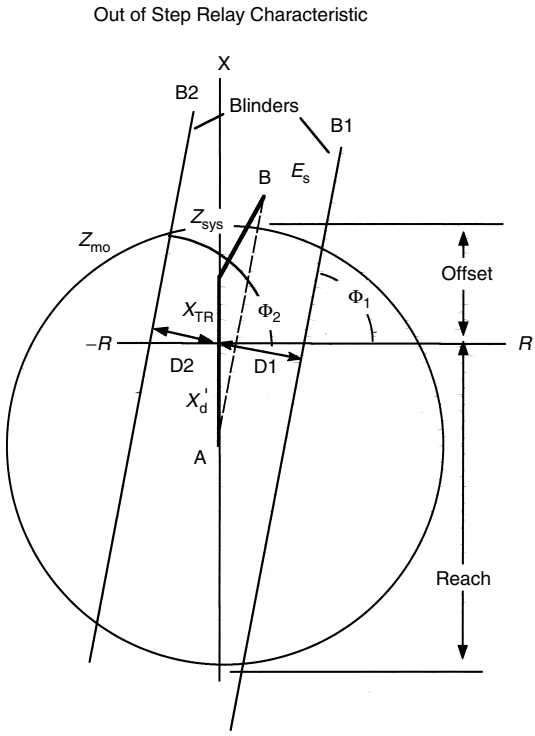


FIGURE 12.24 Single blinder settings.

© 2006 by Taylor & Francis Group, LLC

The blinder displacements along the *R*-axis (distances D1 and D2) are usually set at 120° and 240°, respectively, as shown in Figure 12.25. These settings are not chosen to meet the maximum stable swing criteria of 120° because this scheme will not operate unless the apparent impedance exceeds 180° and a pole has already slipped. The settings are based on scheme timing. The separation between the blinders must be such that the swing impedance at maximum anticipated slip does not actuate the blinders within the minimum allowable time as set by the scheme logic. Using a conservative estimate for the maximum generator slip frequency of five cycles/sec and a four cycle logic delay, the minimum allowable separation becomes $360^\circ \times 5 \times 4/60 = 120^\circ$ between the blinders.

In cases where the system impedance varies with operating modes, the out-of-step relay settings shall be determined using the minimum system impedance value. In many cases, varying system impedance makes little difference in the final setting. However, on a strong system the swing diameter can approach that of the mho element. In this situation it becomes difficult to provide settings that assure proper logic actuation during an out-of-step condition.

After settings are determined using the above criterion, they should be verified by plotting impedance loci derived from computer simulations. The plots should verify that the location of the blinders with respect to the Z_{mo} unit provides the proper operating sequence for all credible impedance trajectories.

Scheme logic that delays tripping until the unstable swing exits the Z_{mo} characteristic is desirable from a breaker duty standpoint. Although breakers are not required to have out-of-phase interrupting rating, it is generally assumed most are capable of opening with a system displacement of 90°. The Z_{mo} setting should be checked to confirm that trip initiations do not occur at more than 90°. If the scheme initiates tripping when the second blinder is actuated (as opposed to when the Z_{mo} element drops out), blinder settings of 90° and 270° should be considered to minimize interrupting duty on the breaker.

Figure 12.26 includes the 90° separation characteristic. The plot shows that the chosen settings can initiate tripping at greater than 90° for swings that pass through the Z_{mo} characteristic just below

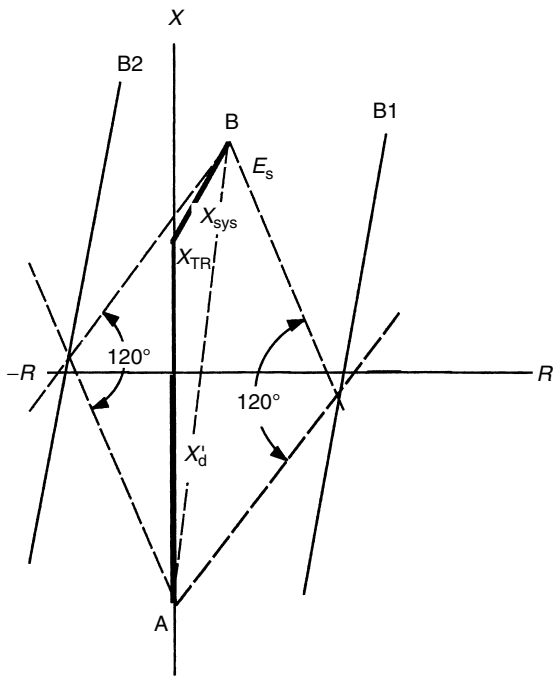


FIGURE 12.25 Blinder angle setting.

© 2006 by Taylor & Francis Group, LLC

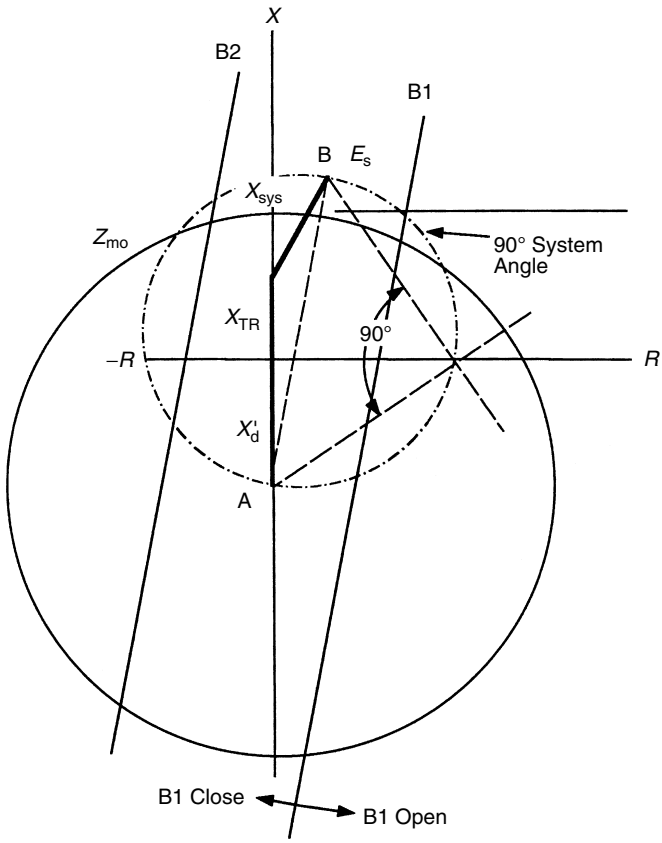


FIGURE 12.26 Blinder with 90° separation.

the intersection with the blinder characteristic. Although the area of vulnerability is small, modification of the out-of-step setting should be considered.

Another approach would be to use simulations to confirm that trajectories do not pass through the areas that challenge the switching capability of a standard breaker. This is not a preferred solution. Simulations cannot include all possible system variables and, with time, system evolution will change the swing characteristic.

12.8.3 Double Blinder

The characteristic of a double blinder scheme is shown in Figure 12.27. This scheme also requires the swing enter the Z_{mo} circle from outside to initiate the logic. Logic times the swing as it crosses the outer (B1) blinder then the inner (B2) blinder. If the time between actuations of these blinders exceeds the minimum required delay, the scheme recognizes the event as a loss of synchronism. Some schemes require that the impedance also remain between the two inner blinders (B2 and A2) for a specific time and may also time the swing's exit from the inner to outer blinder. Most schemes do not initiate a trip until the swing impedance has exited the mho element to assure a more favorable separation angle for breaker operation.

The key difference between the single blinder and double blinder schemes is that after the swing has been recognized, by crossing from the outer to inner blinder with the proper delay, a trip will be initiated regardless of the direction in which the swing exits the characteristic. The single blinder

© 2006 by Taylor & Francis Group, LLC

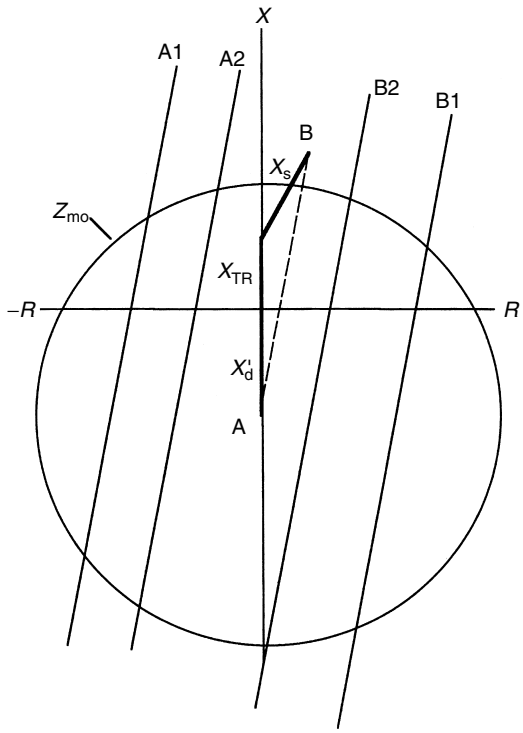


FIGURE 12.27 Double blinder.

scheme will only initiate a trip if the swing exits from the opposite side of the characteristic that it entered.

Consequently, the inner blinder setting is critical in this scheme. It must be set such that it does not actuate for a recoverable swing. This determination can only be made using actual swing loci derived from extensive transient stability studies. Because of this disadvantage, the single blinder scheme is generally favored for out-of-step protection.

In theory, the dual blinder scheme could be applied to trip when the maximum stable swing angle is exceeded via the inner blinder. This would trip the generator before the first pole slip and limit the current-induced stress on the generator and GSU transformer. This is not normally done, because it requires the tripping breaker to have an out-of-phase switching rating or to have an increased interrupting or voltage rating.

The mho element of the dual blinder scheme is set to the same criteria as the mho element used in the single blinder scheme. The forward reach is set two to three times the generator's transient reactance. The offset is set 1.5 to 2 times the GSU transformer reactance. The outer blinders (A1 and B1) must be set with sufficient separation from the inner blinders (A2 and B2) to allow the minimum required logic time to expire between blinder actuations with the maximum anticipated slip frequency. The settings are also constrained by the 90° breaker switching limitation.

12.8.4 Double Lens and Concentric Circle Schemes

The double lens and concentric circle schemes are depicted in Figure 12.28 and Figure 12.29, respectively. Their operation is similar to that of the double blinder scheme without the mho element. In both schemes the inner element must be set to activate only on nonrecoverable swings. The outer elements are set to limit the angle at which breaker opening is initiated.[5]

© 2006 by Taylor & Francis Group, LLC

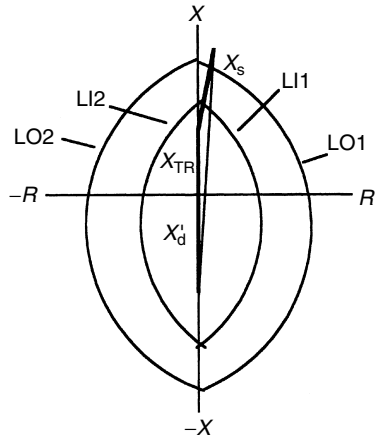


FIGURE 12.28 Double lens scheme.

12.8.5 Detection Problems

The single blinder scheme has a tendency not to operate in the first slip cycle. This usually occurs when the loss of synchronism is initiated by a fault with a clearing time slightly greater than the critical switching time, the critical switching time being the maximum clearing time to retain stability. Figure 12.30 depicts the problem. Assume a three-phase fault occurs at the HV terminals of the GSU transformer. The impedance seen by the scheme, as long as the fault persists, will be that of the GSU transformer alone. When the fault is cleared, the internal generator voltage, the system voltage and the angle of separation between them determine the impedance seen by the scheme. If the fault were cleared instantaneously, the rotor angle with respect to the system would not change. The system impedance would rebound to the initial load point.

As clearing time increases, the rotor angle advances and the impedance seen immediately after fault clearing moves from right to left on the R–X diagram. As long as the initial postfault impedance appears outside the Z_{mo} characteristic, the scheme will actuate in the first slip cycle because the logical requirement that Z_{mo} actuate before the blinder element will be met. Figure 12.30 depicts postfault impedance within the Z_{mo} characteristic. For this condition, the scheme will no longer actuate for the first swing cycle. Tripping will occur on the second slip cycle when the swing

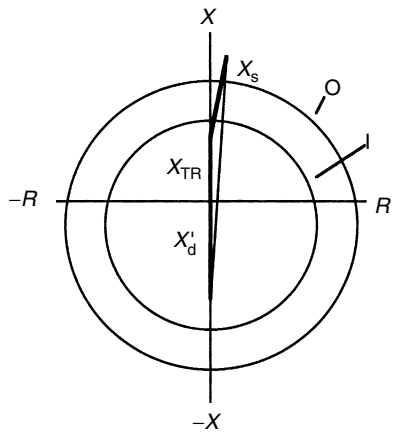


FIGURE 12.29 Concentric circle scheme.

© 2006 by Taylor & Francis Group, LLC

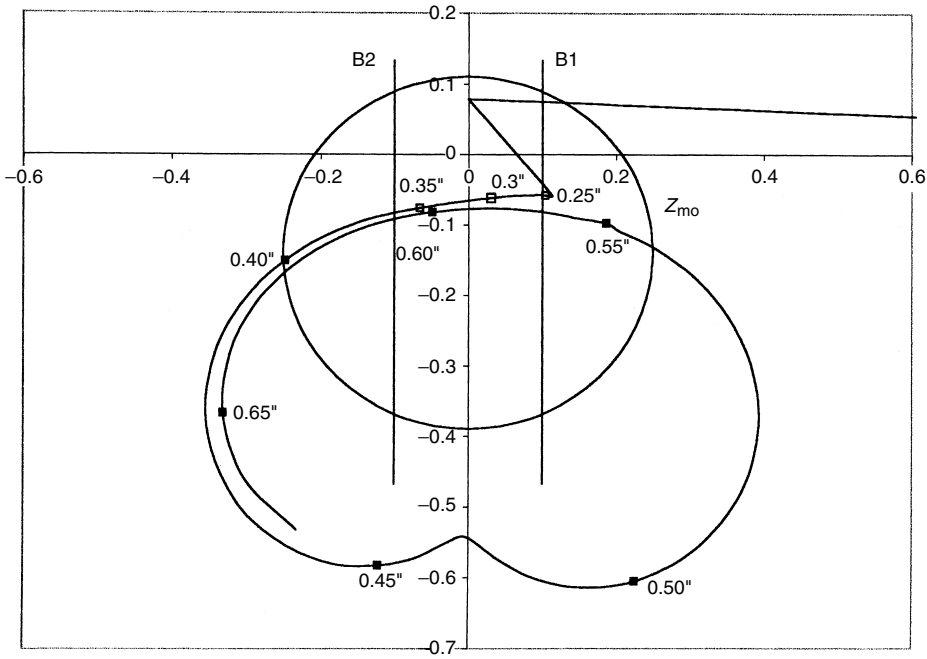


FIGURE 12.30 Single blinder first slip cycle detection failure.

impedance path though the characteristic is not interrupted. The double blinder scheme is also vulnerable to this problem.

Another application problem is encountered with cross-compound installations. At these installations, the high-pressure unit has low inertia, while the low-pressure unit has high inertia. With low system impedance, both units produce normal swing loci similar to Figure 12.11. The low-inertia high pressure unit may complete a slip cycle well before high inertia low pressure unit. In such cases it may be preferable to use the high pressure unit out-of-step relaying to trip both units.

When cross-compound units are connected to a high-impedance system (0.2–0.4 pu), the swing characteristic of each unit becomes irregular and is above the *R*-axis. Neither is suitable for out-of-step detection. In this instance, a composite swing characteristic derived from a summation of both generator currents will resemble the normal out-of-step characteristic and is suitable for out-of-step detection.[2]

12.9 SETTING OUT-OF-STEP ON SAMPLE SYSTEM

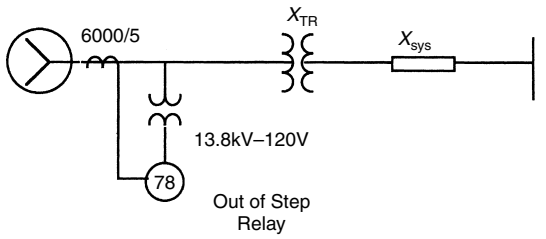
The methodology used to set typical out-of-step protection can be demonstrated using the sample system. It is assumed protection is provided by a single blinder scheme configured as shown in Figure 12.31.

First the system impedances, which are given in per unit on the generator base, must be converted to ohms. The out-of-step relay is located at the generator terminal; therefore, base ohms are calculated at 13.8 kV.

$$I_{FL} = \frac{104{,}000\,\text{kVA}}{\sqrt{3}\ 13.8\,\text{kV}} = 4350\,\text{A}$$

$$Z_{base} = \frac{13{,}800\,\text{V}}{\sqrt{3}\,4350} = 1.83\,\Omega$$

© 2006 by Taylor & Francis Group, LLC



Impedances on generator base 104 MVA 13.8kV

X'_d = 0.196 PU
X_{TR} = 0.07 PU
Z_{sys} = 0.148 PU @ 85° min (normal)
= 0.299 PU @ 75° max (line out)

FIGURE 12.31 Sample system out-of-step protection.

The circuit impedances, as seen at 13.8 kV, become:

$$X'_d = j0.196 \times 1.83\,\Omega = j0.359\,\Omega$$
$$X_{TR} = j0.07 \times 1.83\,\Omega = j0.128\,\Omega$$
$$Z_s = 0.148\angle 85^\circ \times 1.83\,\Omega = 0.271\,\Omega\angle 85^\circ$$

Note that the minimum system impedance is used to determine the setting. Again this is because the lower system impedance produces smaller diameter swing loci, which are generally more difficult to detect.

The values calculated above are in "primary ohms," that is, ohms as seen on the 13.8 kV system. The out-of-step relay will see "secondary ohms," as reflected through the relay PTs and CTs. The relay is set in terms of secondary ohms; it is therefore convenient to convert the system impedances to secondary ohms at this time.

$$Z_{sec} = Z_{prim}\frac{\text{CT ratio}}{\text{PT rato}} \tag{12.7}$$

where CT ratio = 6000/5 = 1200 and PT ratio = 13,800/120 = 115. Converting impedances to secondary ohms:

$$X'_d = 0.359\,\Omega \times \frac{1200}{115} = 3.74\,\Omega(\text{sec})$$
$$X_{TR} = 0.128\,\Omega \times \frac{1200}{115} = 1.34\,\Omega(\text{sec})$$
$$Z_s = 0.27\,\Omega\angle 85^\circ \times \frac{1200}{115} = 2.81\,\Omega\angle 85^\circ(\text{sec})$$

These values are plotted on Figure 12.32. Blinders in a single blinder scheme are typically set at swing angles of 120° and 240° using the straight line approximation of swing trajectory ($n = 1$). These points are chosen to assure that an unstable swing will not traverse the distance between the blinders in less than the minimum allowable time specified by the out-of-step logic (assumed here to be four cycles). This concept was discussed under the description of the single blinder scheme.

The location of points P1 and P2 are determined by plotting lines A–S, B–T, A–U, and B–V at 30° from total impedance line A–B as shown in Figure 12.32.

© 2006 by Taylor & Francis Group, LLC

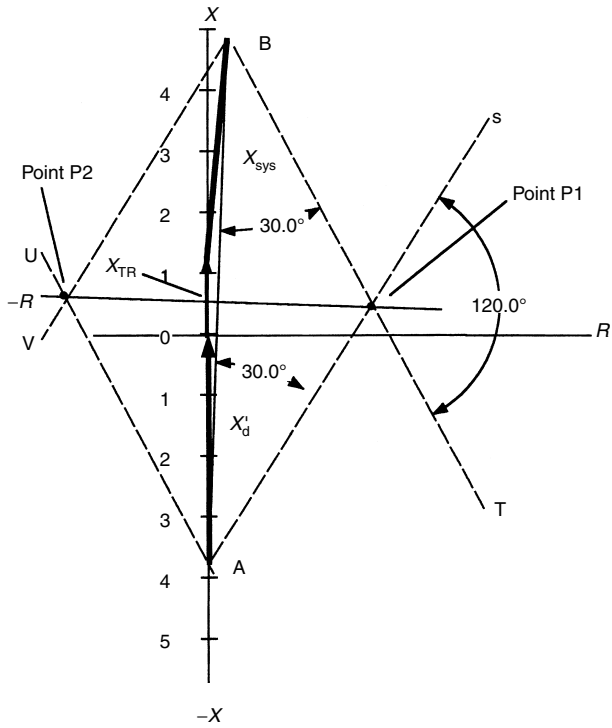


FIGURE 12.32 Sample system impedance plot.

The blinder angle Φ is chosen to parallel line A–B and can be calculated as:

$$\begin{aligned} X'_{\mathrm{d}} &= +j3.74 \\ X_{\mathrm{TR}} &= +j1.34 \\ Z_{\mathrm{s}} &= \underline{0.245 + j2.78} \\ Z_{\mathrm{T}} &= 0.245 + j\,7.86 = 7.86\,\Omega\angle 88^{\circ} \end{aligned}$$

Therefore set Φ_1 and $\Phi_2 = 88^{\circ}$. Depending on the relay type, settings in less than 5° increments may not be possible.

The blinder elements are added in Figure 12.33. These elements are placed through the 120° and 240° points, P1 and P2, and parallel with line A–B at 88°. The blinder distances D1 and D2 are then measured along a perpendicular line from each blinder to the origin (Figure 12.34).

Set D1=2.7 secΩ
Set D2 = 2.35 secΩ

The settings for Z_{mo} are plotted on Figure 12.35. The reach and offset will be set at minimum values (reach $2 \times X'_{\mathrm{d}}$, offset $1.5 \times X_{\mathrm{TR}}$):

$$\begin{aligned} \text{Reach} &= 2 \times X'_{\mathrm{d}} = 2 \times 3.74\,\Omega = 7.48\,\text{sec}\Omega \\ \text{Offset} &= 1.5 \times X_{\mathrm{TR}} = 1.5 \times 1.34\,\Omega = 2.0\,\text{sec}\Omega \end{aligned}$$

After the settings are chosen, impedance loci from system simulations should be plotted over the proposed setting to verify the correct operation of the scheme. Figure 12.36

© 2006 by Taylor & Francis Group, LLC

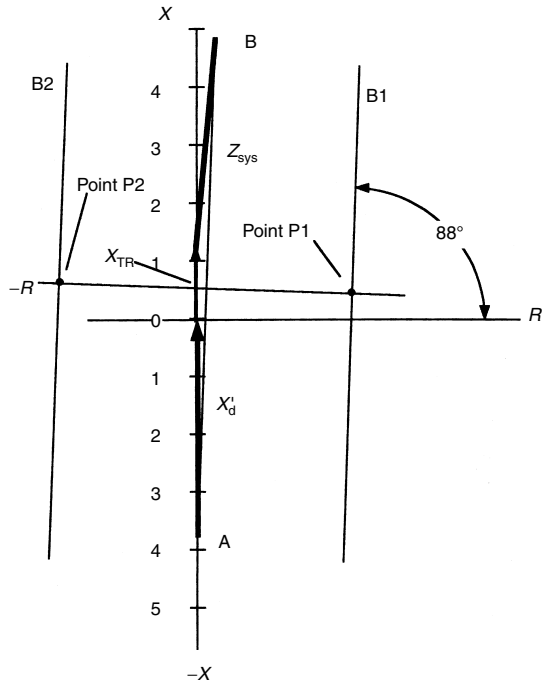


FIGURE 12.33 Sample system, blinders added.

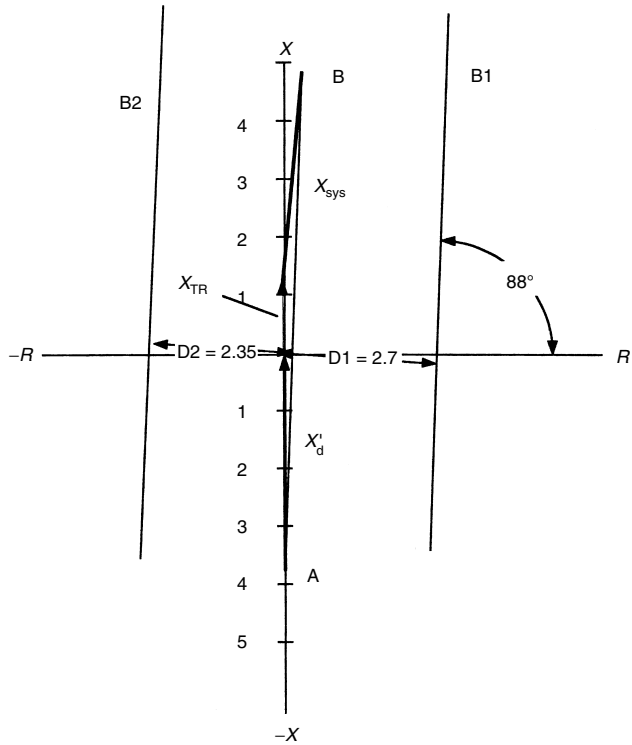


FIGURE 12.34 Sample system blinder settings.

© 2006 by Taylor & Francis Group, LLC

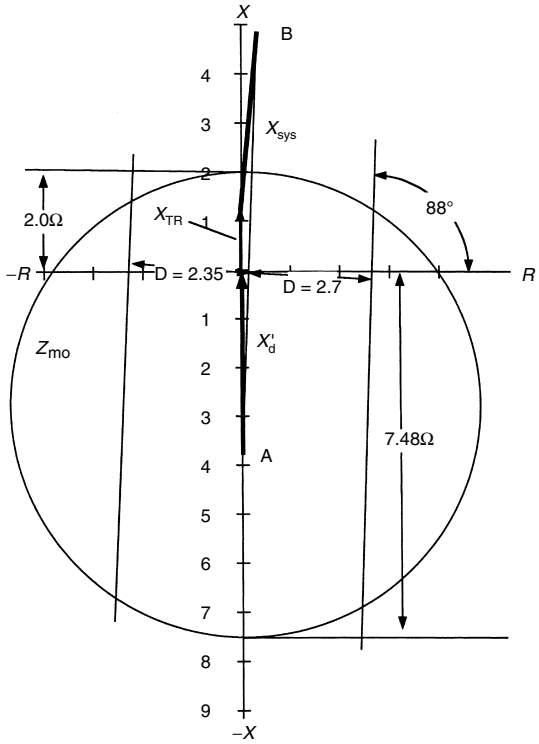


FIGURE 12.35 Sample system mho unit setting.

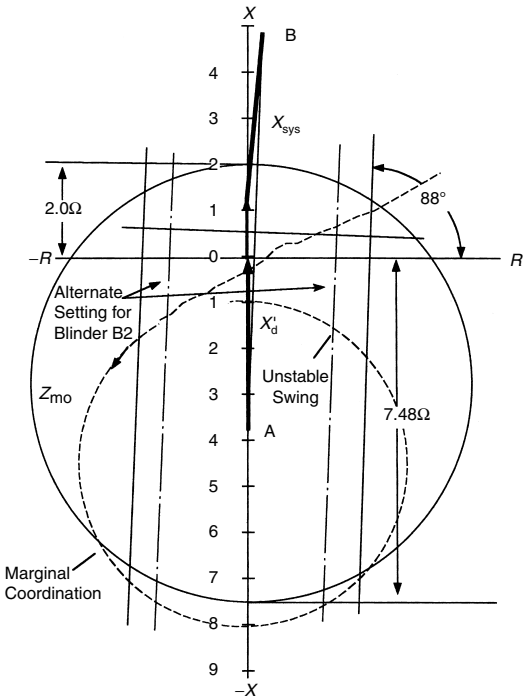


FIGURE 12.36 Verify sample system setting.

© 2006 by Taylor & Francis Group, LLC

demonstrates circumstances that might require the settings to be altered. The small-diameter unstable swing will enter and exit the Z_{mo} unit very close to the blinders. As plotted, the scheme will operate correctly. However, if the swing had a slightly different trajectory, it could cross the blinder B1 before entering the Z_{mo} or recross the B2 blinder before exiting Z_{mo}. In either case, scheme logic would incorrectly interpret this as a stable swing and fail to trip.

The scheme may operate on subsequent slip cycles, but this would subject equipment to increased stress. A larger setting on Z_{mo} may be required. Blinder settings with less than 120° separation could also be considered. This would be contingent on confirming that the fastest anticipated swing would not cross the two blinders in less than the minimum delay set by scheme logic.

The sample system generator breaker does not have an out-of-phase switching rating. It is assumed the breaker will be capable of interrupting 50% of rated current at an angular displacement of 90° between the generator and system voltage. The generator breaker must be rated to interrupt a three-phase fault at the generator terminals. This would require an approximate rating of $1/X''_d$ or $1/0.136 = 7.35$ pu current. The breaker should then have a minimum capability of 3.6 pu current at 90°.

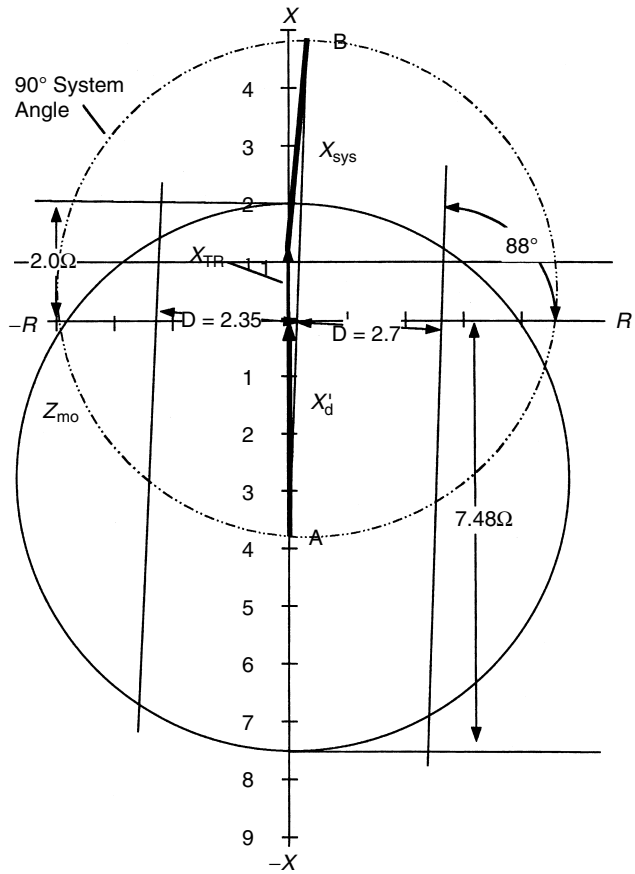


FIGURE 12.37 Sample system setting with 90° switching limit.

© 2006 by Taylor & Francis Group, LLC

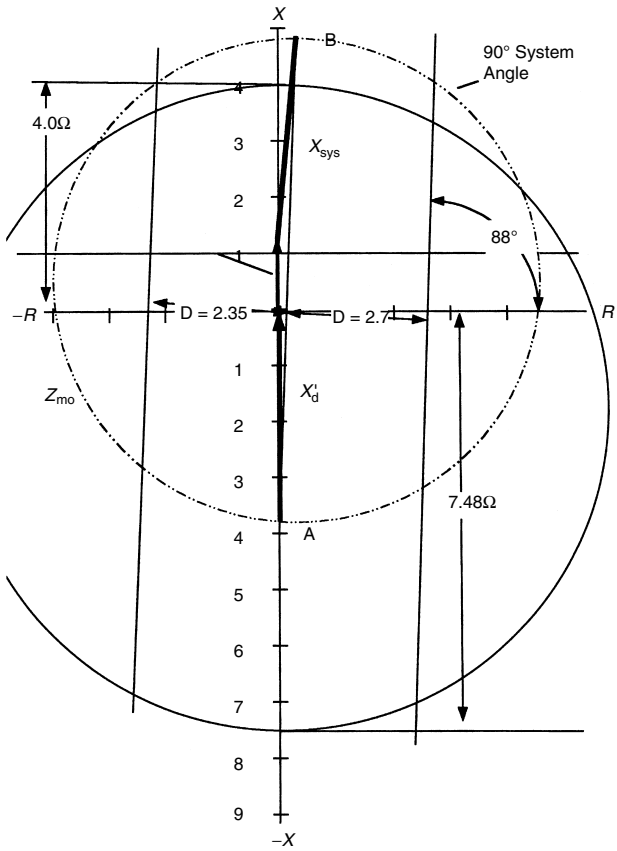


FIGURE 12.38 Revised sample system setting.

The minimum system impedance during an out-of-step event ($X'_d + X_{TR} + Z_s$) is 0.41 pu. The resulting out-of-phase switching current at 90° separation is then approximately

$$I_{90^\circ} = \frac{\sqrt{2}}{0.41} = 3.5\,\text{pu}$$

This is below the estimated switching rating of 3.6 pu.

The out-of-step scheme should not initiate tripping between 90° and 270°. The 90° characteristic circle is plotted over the setting in Figure 12.37. It is clear that switching above 90° is likely.

In an attempt to correct this situation the Z_{mo} offset was increased from 2.0 to 4.0 secΩ in Figure 12.38. This will eliminate the switching problem for the majority of system swings, because most will pass through the unit transformer or very close to it. The revised setting will also improve the scheme reliably for the swing shown in Figure 12.36. The disadvantage is that the generator out-of-step relay now sees swings on most of the transmission system.

REFERENCES

1. Redfern, M. A. and Checksfield, M. J., A new pole slipping protection algorithm for dispersed storage and generation using the equal area criterion, *IEEE Trans Power Delivery*, 10(1), pp. 394–404, 1995.

© 2006 by Taylor & Francis Group, LLC

2. Brady, J., *Out-of-Step Protection for Generators*, GE Publication GER-3179. Schenectady, New York.
3. *Protective Relay Application Guide*, 3rd edition, GEC Measurements, Balding and Mansell UK Limited, London and Wisbech, 1987.
4. Working Group Report, Out of step relaying for generators, *IEEE Trans Power Delivery*, 96(5), 1556–1564, 1977.
5. Smaha, D. W., Out-of-step relay protection of generators, IEEE Tutorial on the Protection of Synchronous Generators, Section 8m 95-TP-102, Power System Relay Committee, 1995.
6. Mason R. C., The art and science of protective relaying GER-3738, General Electric Company, Technology Center Malvern, PA, 1956.

© 2006 by Taylor & Francis Group, LLC

13 Loss of Field Protection

13.1 GENERAL

A loss of field (LOF) occurs when excitation to the generator field winding fails. This may be a result of equipment failure, inadvertent opening of the field breaker, an open or short circuit in the excitation system, or slip ring flashover. Whatever the cause, this condition poses a threat to the generator and to the power system.

The DC current input to the field winding excites the rotor magnetic circuit to establish rotor flux. This flux generates an internal voltage in synchronism with and opposed to the system voltage. When excitation is lost, the rotor current decays at a rate determined by the field circuit time constant. The internal generator voltage will decay at the same rate. Because generator Var output is proportional to the internal generator voltage, Var output also decreases. If the generator is initially supplying Vars to the power system, the Var output will decrease through zero as the generator draws increasing reactive from the power system to replace excitation formerly provided by the field circuit. Var consumption can exceed the generator MVA rating.

The reduction of internal voltage also weakens the magnetic coupling between the rotor and stator. At some point during the decay, the coupling will become too weak to transmit prime-mover output power to the electrical system and the generator will lose synchronism.

This is similar to the loss of steady-state stability discussed in Chapter 11. To visualize the loss of synchronism following a LOF event, we refer once again to the power angle equation:

$$P_e = \frac{E_g E_s}{X_T} \sin \delta \tag{13.1}$$

where P_e = electrical power transmitted to the power system, E_g = generator internal voltage, E_s = equivalent system voltage, X_T = transfer impedance = $X_g + X_{tr} + X_{syst}$, X_g = effective generator reactance, and δ = angle between E_s and E_g.

The effect of the decaying internal generator voltage is to reduce the power angle curve with time as shown in Figure 13.1. The intersection of the power angle curve and the mechanical power output of the turbine define the operating angle of the generator with respect to the system voltage. As the power curve decays, the operating angle increases to maintain equilibrium between mechanical input and electrical output. When the operating angle (δ) reaches 90° electrical power output is at maximum. Field current decay beyond this point renders the generator incapable of transmitting all the mechanical power to the electrical system. The excess mechanical power is dissipated by acceleration of the generator. As speed increases beyond 60 Hz, synchronism is lost.

The generator will continue to accelerate. As speed increases, turbine output decreases as dictated by the droop setting of the governor and electrical power will increase as dictated by the slip-torque characteristic of the power system. Eventually, turbine output and generator electrical power will reach a new equilibrium, with the generator operating above synchronous speed as an induction generator drawing excitation from the power system in the form of Vars.

A loss of synchronism following a field failure is not a high-speed phenomenon. Typically, it will take a fully loaded steam turbine generator several seconds to lose synchronism. Final slip is affected by the droop setting of the governor, system impedance, and initial loading. For a machine initially operating at full load, final slip is typically in the 2 to 5% range. The power output of the induction generator is less than the prefailure power output.

© 2006 by Taylor & Francis Group, LLC

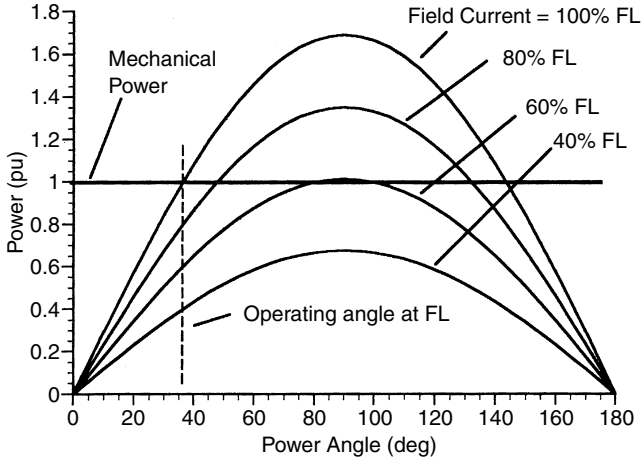


FIGURE 13.1 Power angle plot.

The final or steady-state slip of the induction generator is important because it determines the effective reactance of the generator, which in turn defines the impact of post-LOF operation. A loss of field event can be represented by a series circuit including the generator and GSU transformer reactance and the system impedance. Generator impedance decreases with increased slip and slip increases with initial generator load. Thus, the higher the initial generator load, the greater the asynchronous current and the more severe the consequences to both the generator and the connected power system.

Figure 13.2 and Figure 13.3 depicts a loss of field at the sample system generator. The generator was initially operating near full load with a system impedance (X_s) of 0.2 pu. The plot of generator angle δ shows that synchronism is lost at about 2 sec, after which large cyclic variations are apparent. These oscillations denote operation in the induction generator mode and result from the combined effects of pole slipping, the differing reactance in the d- and q-axes (saliency), and governor action. These cyclic variations are not transitory and are sustained as long as asynchronous operation persists.

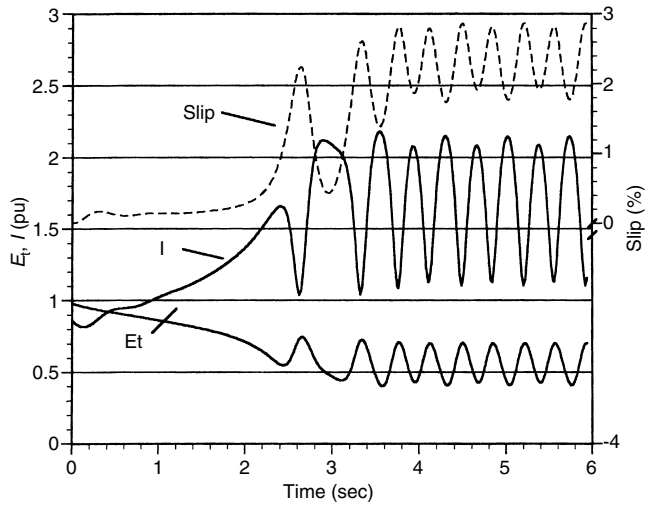


FIGURE 13.2 E_t and I for LOF from full load.

© 2006 by Taylor & Francis Group, LLC

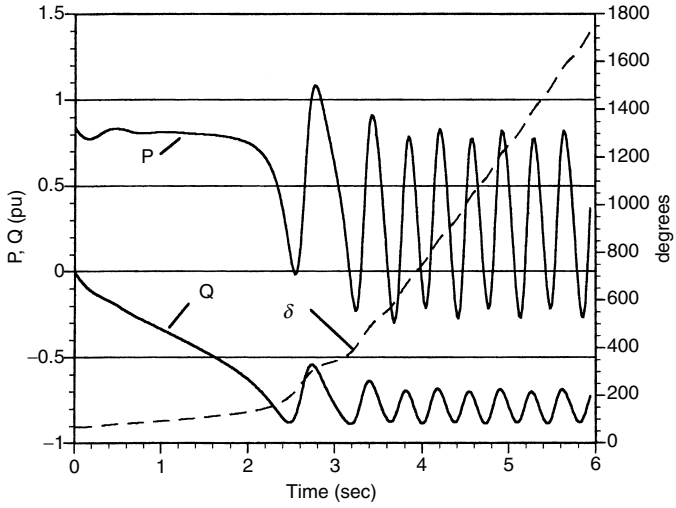


FIGURE 13.3 P, Q, δ for LOF from full load.

The plot also shows that slip is not constant during the slip cycle. Here the variation is between 1.8 and 2.9%. When slip values are quoted, they are average values over the slip cycle. For this case the average slip is 2.4%.

The asynchronous values shown are typical for a fully loaded machine. The average values of power, reactive, terminal voltage, and current during a slip cycle are $P = 0.25$, $Q = -0.79$, $E_t = 0.54$ and $I = 1.64$. It is not apparent from these numbers, but this is a severe event for both the generator and the power system. Although the final average power output is only 0.25 pu, the instantaneous power ranges from $+0.76$ to -0.27 pu, subjecting the generator to mechanical stress associated with a ΔP equal to its rating each slip cycle. The average sustained asynchronous loading is within the MVA rating of the generator, but because the terminal voltage is severely reduced, stator current is well above rated. The current excursions are from 1.14 to 2.13 pu, exposing the stator windings to forces proportional to the square of the current. Thermal damage could result in about 22 sec.

In contrast, Figure 13.4 and Figure 13.5 plot a loss of field for the same system condition, but with the generator initially at 30% rated load. This case shows a much slower decay, approximately 12 sec to lose synchronism, with a final average slip of around 0.3%. The reduction in slip increases the effective generator reactance to approximately double that of the fully loaded machine. The resulting average terminal quantities are less severe than the full load case, with $P = 0.24$, $Q = -0.51$, $E_t = 0.82$ pu, and $I = 0.72$ pu. The most significant difference is the reduced excursions. Although the average power output for both cases is nearly equal, the full load case exposed the generator to a ΔP near unity, while for the light load case ΔP is only 0.29 pu.

These plots were derived from the same spreadsheet (Appendix D) used to generate the out-of-step plots included in Chapter 12. A loss-of-field condition was simulated by setting the switching times beyond the LOF time frame (30 sec) so no fault is initiated or cleared and setting the field voltage limit, $E_{fmax} = 0.01$, to emulate a short at the input to the field circuit.

13.1.1 Other Factors Affecting Loss of Field Severity

The initial generator load is the major factor in determining the potential damage from a LOF event. Variation in system impedance and the mode of excitation failure also have an effect on the final

© 2006 by Taylor & Francis Group, LLC

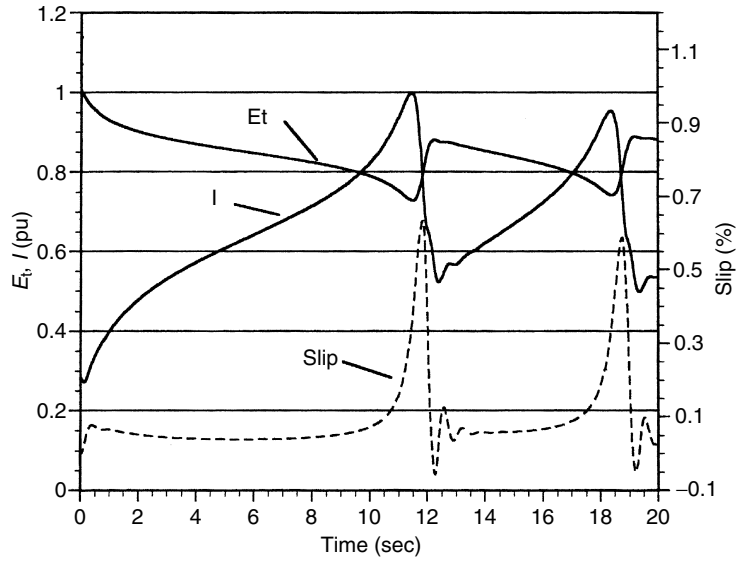


FIGURE 13.4 E_t and I for LOF from light load.

LOF state. A reduction in system reactance will reduce the final slip frequency and increase the power output from the induction generator.

At first glance, a strong power system would appear to offer higher postfailure currents and therefore a greater potential for damage. This is not necessarily true. Because a strong system will result in lower final slip, the effective generator impedance will increase, thereby reducing the stator current. A failure on a strong system may actually produce lower stator currents and be less damaging than a failure on a weak system.

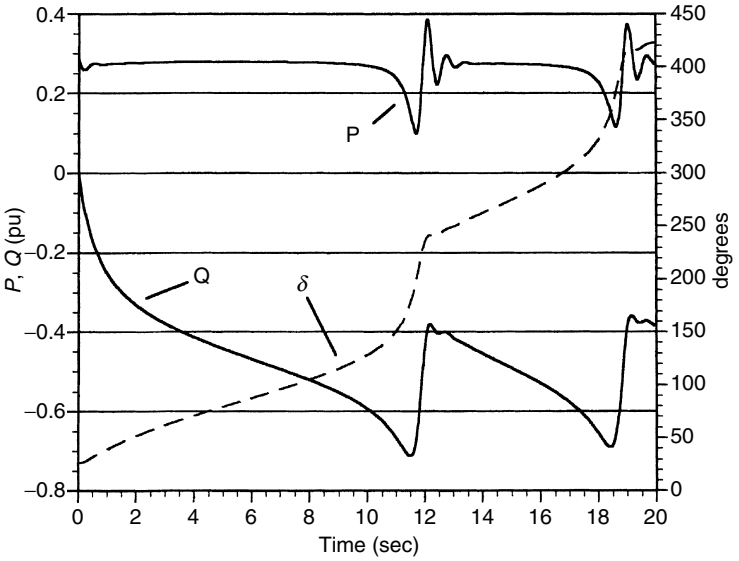


FIGURE 13.5 P, Q, δ for LOF from light load.

© 2006 by Taylor & Francis Group, LLC

A LOF event is more likely to be initiated by a shorted field circuit than an open field circuit. The former will produce higher stator current, larger reactive intake and generally more severe consequences than would be experienced with an open field circuit.[1]

When machines are connected directly to a common bus, the potential for damage increases. As excitation decays on the unit with failed excitation, voltage regulators on healthy machines will initiate full field forcing to support the falling bus voltage. This increases the Var supply to the faulted machine. The situation is aggravated when the units are connected to a strong system. Reference 2 documents a study of two generators connected to a common bus and a moderate-strength power system. In that study, the unit with failed excitation saw a peak MVA loading in excess of 2 pu and peak stator current in excess of 2.5 pu. The healthy unit was also severely stressed with a peak MVA of 1.5 pu and peak current of 2.0 pu.

A LOF on a hydro unit at light load may not result in a loss of synchronism. Hydro generators are salient pole machines and as such can carry up to 25% rated load following a loss of field without a loss synchronism. However, once a salient pole machine loses synchronism, it accelerates rapidly to a high slip. The slower acting hydro governor and the fact that a salient pole machine makes an inefficient induction generator causes this response. If the hydro generator's field is lost near full load, the effects and protection concerns are the same as for steam turbine units.

13.2 SYSTEM IMPACT

A generator operating asynchronously without excitation can consume Vars in the range of 0.4 to 1.9 times the unit nameplate rating as slip increases from near zero to 4%.[1] The impact of the loss of field on the power system is determined by the system's ability to withstand not only the loss of the unit's real and reactive output, but to supply the large Var demand imposed by the faulted generator after the LOF.

A loss of field on a small unit connected to a strong system will produce minimal system impact. On the other hand, if the power system is unable to meet the Var demands of the failed unit, a widespread system outage can result. Initially, excitation on nearby generators will go to full boost to supply reactive to the generator with failed excitation and support the grid voltage. The large Var influx can overload and trip area transmission lines. The adjacent generators cannot maintain ceiling excitation indefinitely without incurring thermal damage to field circuits. If the failed generator is not disconnected, field current limiters on the adjacent units will time out, initiating an immediate reduction in rated field current. The resulting reduction in area Var support is likely to produce severe voltage degradation. System voltage collapse or multimachine instability can result, causing a regional system outage.

Dynamic studies similar to those used in transient stability analysis are required to determine accurately system response to a LOF event. These studies are time-consuming and expensive. A screening technique using a standard load flow can determine where full dynamic studies are required.[3] At the generator of interest, a worst-case LOF event is simulated in load flow by setting the reactive flow into the machine at -1.5 times the nameplate MW rating. If a load flow solves with reasonable system voltages, the system is considered capable of withstanding the LOF event. However, if the solution fails to converge or severely depressed voltage results, the event must then be modeled dynamically to determine if the system can survive the field failure.

13.3 GENERATOR DAMAGE

The assessment of generator damage from an excitation failure has changed since the 1950s when impedance relays came into common use for LOF protection. At that time, it was generally accepted that machines could operate asynchronously following a LOF for at least 2 to 3 min without damage. One 1954 vintage paper related an incident where a 10 MW hydro unit operated as an induction generator for 17 min without apparent damage.[4]

© 2006 by Taylor & Francis Group, LLC

The potential for generator damage following a LOF is dependent on generator design and final slip during asynchronous operation. The adverse effects of unexcited asynchronous operation are high stator current, induced rotor currents, torque pulsations and end-core heating.

Although the asynchronous capabilities are not addressed in standards, modern expectations are much lower, with damage in as little as 10 sec for some instances. This is particularly true of conductor-cooled machines. There are several reasons why the conductor-cooled machine is more vulnerable. The improved cooling techniques employed on this type of machine result in larger MVA ratings from a given physical size. These machines will have higher per-unit impedance and lower inertia then conventionally cooled machines. Because of these characteristics, the conductor-cooled machine will tend to operate at a higher slip. This reduces the equivalent reactance during asynchronous operation, increasing the stator and the induced rotor current. The conductor-cooled machine will also have lower thermal time constants, hence faster temperature rise for a given current than the conventionally cooled machine.

A loss of field from an initial light load condition (30% rated load or less) will terminate at very low slip, 0.1–0.2%. At this low slip, generator damage is unlikely. However, the final slip following a loss of field from full load is much higher, 2–5%, and exposes the generator to damage from all the aforementioned sources.

13.3.1 Stator Winding Overload

The large Var requirements and depressed terminal voltage following a LOF load can give rise to stator current well above rated. Peak currents of 2.5 pu have been reported.[2] Although not related to asynchronous operation directly, ANSI standards C50.12, 13, 14 do define a required short time overload capability for stator windings. This limit is plotted in Figure 4.5.

The full-load LOF event depicted in Figure 13.2 is typical. It produces cyclic stator current with variation between 1.14 and 2.13 pu each slip cycle. Obviously, a direct comparison between the ANSI limit and the cyclic current is not possible. In theory, the stator heating is related to the RMS current over a slip cycle. RMS current is defined as

$$\text{RMS} = \sqrt{\frac{1}{2\pi}\int_0^{2\pi} I^2 \mathrm{d}t} \tag{13.2}$$

The RMS stator current can be calculated from the incremental currents and slip cycle duration determined from the spreadsheet in Appendix D.

The incremental form for RMS current is

$$I_{\text{RMS}} = \sqrt{\frac{1}{T}\sum_0^T I^2 \Delta t} \tag{13.3}$$

where T = period of one slip cycle in seconds.

In the case of the LOF from full load shown in Figure 13.2, the RMS current at final slip was calculated as 1.74 pu. ANSI standards require that this current be limited to 22 sec to prevent winding damage.

A note of caution: in light of the shape of the current waveform shown in Figure 13.2, there may be a temptation to estimate RMS stator current on the basis of an offset sinusoidal waveform ($I = I_{\text{m}} \sin \omega + I_0$). This may be acceptable for the specific condition shown, but this method cannot be applied to all cases. (Sinusoidal approximation would result in $I_{\text{RMS}} = 1.64$ pu for Figure 13.2).

© 2006 by Taylor & Francis Group, LLC

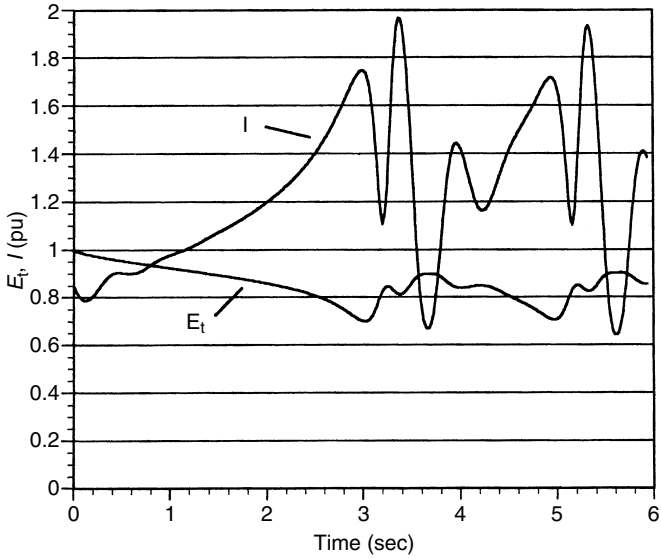


FIGURE 13.6 E_t and I for LOF from full load, strong system.

In reality, the stator waveform cannot be sinusoidal, because slip is not constant through the slip cycle. Figure 13.6 shows the stator current waveform for the same LOF condition depicted in Figure 13.2, but with system reactance reduced from $X_s = 0.2$ to 0.1. Here the stator current variation is far from sinusoidal. The incrementally calculated RMS current for this condition is 1.34 pu. The corresponding stator overload limit for this current is 50 sec from the ANSI standards.

In both these cases, the stator limits alone demonstrate that this machine would not withstand the lengthy asynchronous operation expected of older machines. A comparison of these cases also demonstrates that generator stress can increase with increased system impedance.

13.3.2 Rotor Damage

Rotor damage can also occur as a result of rapid heating caused by currents induced in the rotor. During asynchronous operation, the velocity of the stator magnetic field differs from rotor velocity by the slip frequency. The relative motion of the rotor with respect to the stator field induces potentially damaging currents into rotor structures.

When the LOF is a result of a shorted field circuit, the induced current is divided between the rotor structures and the field winding. This reduces heating in the rotor structures. The magnitude of current induced in the field winding during asynchronous operation is not normally of sufficient magnitude to damage the winding. The induced field current is generally below rated in salient pole machines and only slightly above rated in a few cases with cylindrical rotor machines. If the LOF is a result of an open circuit maximum rotor structure heating will occur also, damaging overvoltage will be induced in the field circuit for all but very low slip events.[1]

In a cylindrical rotor machine, induced currents flow along the length of the rotor body, creating heat in teeth, slot wedges, and, if present, the amortisseur winding. Thermal damage is most likely to occur near the ends of the rotor where currents converge to enter the retaining rings.

In a salient pole machine, induced currents are found in the amortisseur bars located in each pole face.

The rotor heating incurred during asynchronous operation is nearly identical to that described in Chapter 6, resulting from negative-sequence current at the generator terminals. This suggests that rotor withstand time for asynchronous operation can be estimated from the negative-sequence

© 2006 by Taylor & Francis Group, LLC

withstand capability of the generator. The negative-sequence short time limit is defined in terms of K, a constant representing the maximum $I_{2eq}^2 t$ value the machine can withstand. The I_{2eq} term refers to the equivalent RMS per-unit negative-sequence current in the event the current is time variant.

The negative-sequence capabilities of various machine types can be found in the IEEE Protection Guide for AC Generators, IEEE standard C37.102, and are summarized in Chapter 6. These limits, if used directly, yield very conservative withstand times for asynchronous operation. For example, using the effective final slip current derived from Figure 13.2, a salient pole machine ($K = 40$) would have an asynchronous withstand of $40/1.74^2 = 13.2$ sec and for a large conductor-cooled machine ($K = 10$), the withstand would be $10/1.74^2 = 3.3$ sec.

The important difference between negative-sequence heating and heating during asynchronous operation is the frequency of the induced current. Negative-sequence current induces rotor currents at twice synchronous frequency (120 Hz on a 60 Hz system), whereas the frequency of the asynchronously induced rotor current is equal to the slip frequency and is usually less than 5 Hz.

As frequency increases, the skin effect increases the effective resistance of a conductor. The result is that negative-sequence current at 120 Hz produces higher I^2R loss and more heating per amp than does asynchronously induced current at 5 Hz.

Another level of conservatism when applying the $I_2^2 t$ limit directly to asynchronous operation is that the negative-sequence limit does not include the helpful shunting effect of the field winding circuit. The 120 Hz current produced by negative-sequence current does not have sufficient penetration into the rotor slots to induce current into the field winding. Therefore, the negative-sequence limit is, in effect, based on an open field circuit.

The negative-sequence limits are based on the limiting temperature for pole-face amortisseur windings in salient-pole machines and teeth or wedges in round rotor machines with induced current at 120 Hz.[5] Because temperature rise in these components is a result of I^2R losses in the conductive medium, a more realistic estimate of asynchronous limits will require an adjustment of resistance for the lower frequency asynchronous case.

The resistance of any conductor is determined by the resistivity of the conducting material and the effective area through which the current flows. The skin effect forces current flow closer to the circumference of the conductor as frequency increases. This reduces the effective area of the conductor and increases resistance. Resistance is then a function of the depth of current penetration.

Reference 5 relates stator current to temperature rise and penetration depth as:

$$T_{\max} = \frac{CI^2 t}{d^2} \tag{13.4}$$

where $T_{\max}$ = the limiting temperature rise for a component, C = constant for particular machine, I = stator current, t = current duration, and d = depth of current penetration.

In a salient pole machine rotor thermal limits are defined by amortisseur windings which are small conductive bars located in each pole face. These bars, usually copper, are on average 5/8 in. in diameter, spaced several inches apart, and interconnected at the ends. In a cylindrical rotor machine thermal limits are set by slot wedges which are surface components of a conductor with a much larger diameter the rotor itself rotor. The physical differences between these conducting structures result in different treatments for the resistance variation.

For pole-face amortisseurs on a salient pole machine and other small conductors, the penetration depth varies with frequency alone. The variation is influenced by the resistivity of the particular conducting material and the geometry of the conductor. Typically the depth of penetration for a small conductor is assumed to vary proportional to $1/\sqrt{f}$. The negative sequence thermal limit can then be defined in terms of K from Equation (13.4)

$$K = I^2 t = \frac{T_{\max}}{Cf} \tag{13.5}$$

© 2006 by Taylor & Francis Group, LLC

The asynchronous limit expressed in terms of frequency becomes

$$I^2tf = \frac{T_{\max}}{C} = Kf \tag{13.6}$$

Because the negative-sequence limit $K(I_2)$ is defined at 120 Hz, the frequency-dependent limit becomes

$$K(I_2) = \frac{I_2^2 tf}{120} \tag{13.7}$$

If the machine represented in Figure 13.2 were limited by pole-face amortisseur ($K = 40$), the expected rotor withstand for asynchronous operation at 5 Hz slip is estimated at

$$t = \frac{120\,K(I_2)}{I^2 f} = \frac{120 * 40}{1.74^2 * 5} = 317\,\text{sec} \tag{13.8}$$

For a solid surface cylindrical rotor, the depth of penetration also varies inversely with the square root of the frequency. However, for this large diameter configuration the penetration depth is also a function of current magnitude varying directly with the square root of the current:

$$d \propto \sqrt{\frac{I}{f}} \tag{13.9}$$

The cylindrical rotor thermal limit is then defined as

$$I^2 t = \frac{T_{\max} I}{Cf} \tag{3.10}$$

and K becomes

$$K = It = \frac{T_{\max}}{Cf} \tag{13.11}$$

Note that the resulting limitation is a function of It not I^2t. This was recognized when the I_2^2t limit was implemented.[5] To apply an I_2^2t limit to the surface components $K(I2)$ was calculated on the basis of a penetration depth for a fixed 120 Hz current of 4 pu. This current magnitude was assumed to be the practical upper limit for negative-sequence current.

Therefore, $K(I2)$ actually represents

$$K(I_2) = \frac{4Itf}{120} = \frac{T_{\max}}{C} \tag{13.12}$$

Again, if the machine represented in Figure 13.2 were limited by tooth temperature ($K = 10$), the expected withstand for asynchronous operation at 5 Hz slip would be

$$t = \frac{120 * K(I_2)}{4 * If} \tag{13.13}$$

© 2006 by Taylor & Francis Group, LLC

and

$$t = \frac{120 * 10}{4 * 1.74 * 5} = 34.5 \text{ sec } @ \text{ 5 Hz} \tag{13.14}$$

13.3.3 Stator End-Core Damage

A cylindrical-rotor machine can experience thermal damage at the ends of the stator core when operated at reduced field current. This limitation forms the leading Var boundary of the generator capability curve. A loss of field represents the extreme in field current reduction. The mechanism for end-core damage is described in detail in Chapter 11.

A loss of field from full load can result in leading Var loading in excess of the generator's MVA rating. Typically, the generator manufacturer's capability curve limits leading Var intake to about 40 to 60% of the generator rating. The leading Var limitation has been shown to vary inversely with terminal voltage.[6] Although the reduction in terminal voltage that accompanies a LOF markedly increases the Var capability, the increase is insufficient to accommodate a potential 2.0 pu leading Var inflow. The voltage-dependent Var limitation was presented in Chapter 11. The limit is circular on the $P-Q$ plane with the following characteristics:

$$Center(Q, P) = 0, \quad K_1 \frac{e_t^2}{X_d} \quad Radius = K_2 \frac{e_t}{X_d} \tag{13.15}$$

The voltage-dependent leading Var capability of the sample system generator was estimated using this approach. Values for K_1 and K_2 were chosen to approximately reproduce the leading Var limit defined by the generator manufacturer's capability curve at $e_t = 1.0$. The resulting voltage variant limits are plotted in Figure 13.7.

Excessive end-core heating would result in bluing of metallic end-core structure, charring of stator winding insulation and failure of the insulation medium between laminations.

13.3.4 Torque Pulsations

A final consideration is the pulsating torque that originates from the electrical and magnetic differences between the d- and q-axes. Torque pulsation, like other LOF effects, is more severe when the

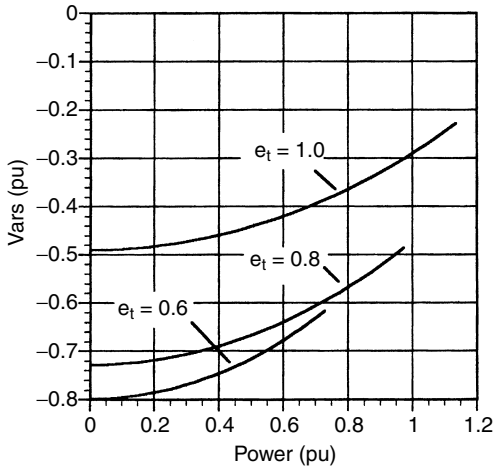


FIGURE 13.7 End-Core limit variation with voltage.

© 2006 by Taylor & Francis Group, LLC

LOF is a result of a shorted field circuit than an open-circuit condition. The torque magnitude associated with a LOF is less severe than that accompanying an out-of-step condition with full excitation, but mechanical damage remains a significant concern following a LOF event.

Asynchronous operation will expose the generator and prime mover to two stress cycles each slip cycle. Fatigue is cumulative, and extended asynchronous operation can consume a considerable portion of the fatigue life of the shaft and associated structures, including the machine foundations. These pulsation are also potentially resonant with shafts, turbine blades and other components.

13.4 LOSS OF FIELD PROTECTION: DEVICE 40

The earliest form of LOF protection employed an undercurrent or undervoltage relay connected in the field circuit. Such schemes would be set to operate a field current or voltage drop below the value required to produce rated output voltage at no load. These schemes must be interlocked to prevent misoperation during startup when the field may be below the setpoint. A trip delay timer is also required to prevent tripping when the voltage regulator rapidly reduces field current in response to an abrupt system change such as clearing a fault.

These schemes have several disadvantages. The undercurrent relay will only detect failures that cause a reduction of current through the relay such as opening of the field breaker. The scheme will not detect loss of field conditions caused by the more likely occurrence of a short circuit. The scheme will, of course, operate when the field circuit breaker is tripped by overload or fault protection, but this sequential operation introduces a considerable time delay. A field undervoltage relay will fail to detect an open circuit downstream of the relay. Also, these relays may not drop out because of AC current induced in the field circuit when the generator is operating asynchronously.

Another scheme that can be applied is a reverse power relay with PT and CT connections altered so the relay senses Vars into the generator. Such a scheme provides good loss of field protection and the reverse power relay is less expensive than a distance relay. The disadvantage is that this scheme does not differentiate well between a loss of field and other system fault conditions.

13.5 DISTANCE RELAY SCHEMES

The modern standard for LOF protection incorporates an impedance-sensing element at the generator terminals.

There are two basic impedance schemes in use today for LOF protection. One scheme initiates tripping whenever a LOF is detected. The other scheme attempts to assess if the LOF is a threat to the power system. If it is not, tripping is delayed to allow the operator time to restore the field and avert a generator trip.

In an instance where the field breaker is inadvertently opened while the generator is online, the field breaker could be reclosed immediately without generator damage. It is not necessary to take the generator offline to resynchronize for this condition, because a long time constant in the field circuit would delay the buildup of the internal generator voltage, thus limiting mechanical transients to acceptable limits.

13.5.1 Distance Scheme 1: Unqualified Trip Scheme

This scheme employs a single mho element connected at the generator terminals oriented to measure impedance looking into the generator and trip with a time delay.

An impedance element cannot detect a failure in the excitation system directly. Instead, it is set to detect the generator's postfailure operation as an induction generator. Following an excitation failure, the field current and the generator internal voltage decay as dictated by the field circuit inductance and resistance. As the internal voltage decreases, Var output goes increasingly leading and the generator eventually loses synchronism with the power system. The generator

© 2006 by Taylor & Francis Group, LLC

will eventually stabilize, operating asynchronously as an induction generator with a constant average slip per slip cycle.

The impedance of a generator operating asynchronously at final slip with no field excitation is unique and can be used to differentiate a LOF event from other power system transients. The magnitude of the asynchronous impedance of the generator varies with slip and slip is a function of initial loading. The initial generator loading therefore determines the apparent generator impedance at final slip.

A LOF event may be initiated by either an open or short circuited field. Although the transient may differ for the two cases the final generator impedance for both cases will be similar.[2]

If an impedance relay is to provide LOF protection over the full range of operation, the relay must be set to detect the impedance presented by the induction generator for a LOF from full load as well as from an initial light load condition. Setting LOF protection is complicated by the fact that the impedance seen by the distance relay at final slip is not a fixed point. The measured impedance will vary between that of the d- and q-axes as the generator slips poles. In addition, the individual axis impedances will vary through each slip cycle as slip varies. Although the average slip through each slip cycle is constant, the instantaneous slip varies, causing variations in axis impedance. The slip variations can be neglected for a conceptual analysis of asynchronous operation.

If the generator is initially operating near full load when the loss of field occurs, the final slip will be high, typically in the 2 to 5% range. At this slip, the individual axis reactances are usually slightly above X'_d and X'_q. Conversely, for a LOF from light initial load, slip will be very low (0.1 to 0.2%) and the axis reactance will be slightly less than X_d and X_q. The reactance measured by the LOF relay as the generator slips poles each slip cycle will then vary between X'_d and X'_q if the generator was initially at full load and between X_d and X_q if initial operation was at light load.

Given that X_d is greater than X_q and that X'_d is less than X'_q, LOF protection must be set to encompass all reactance values between X'_d and X_d if it is to operate for all initial values of generator loading. To meet this criterion, it has become standard practice to set the impedance element for this type of scheme with a diameter of X_d and an offset of $1/2\ X'_d$ as shown in Figure 13.8.

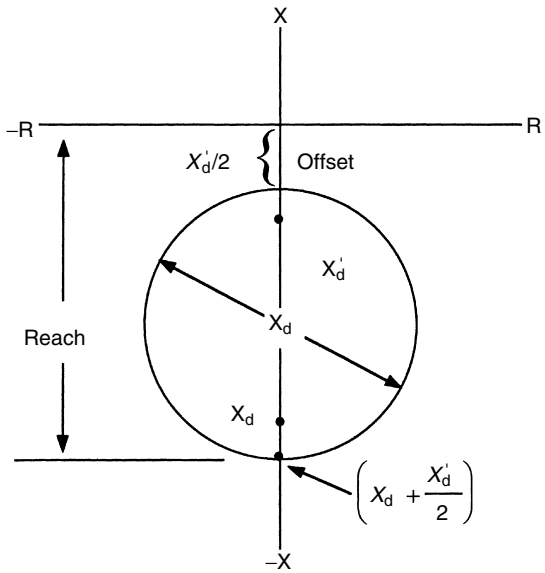


FIGURE 13.8 Typical LOF setting.

© 2006 by Taylor & Francis Group, LLC

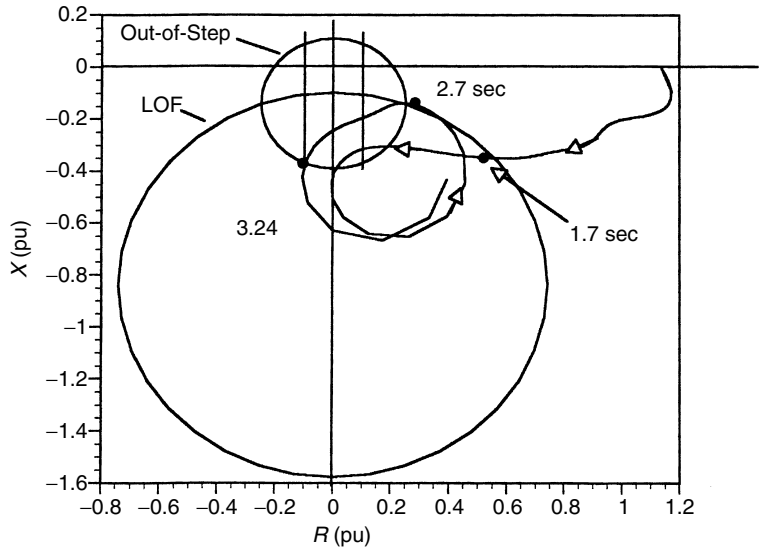


FIGURE 13.9 Impedance locus for LOF from full load.

The impedance loci of the sample system for a loss of field are shown in Figure 13.9 and Figure 13.10. These plots were derived from the spreadsheet described in Appendix D. The LOF condition was simulated by setting the maximum field voltage $E_{fd} = 0.01$ to simulate a shorted field circuit and setting the switching and clearing time to 20 sec so that no fault is initiated or cleared during the simulation.

Figure 13.9 plots a LOF from full load with a moderately strong system ($X_s = 0.2$ pu). The impedance locus requires 1.7 sec for the impedance locus to enter the relay characteristic. This is a bit faster than the 2 to 7 sec considered typical for the full-load case. In contrast, the LOF relay in the lightly loaded case, Figure 13.10, will not actuate until 6.36 sec after the field failure.

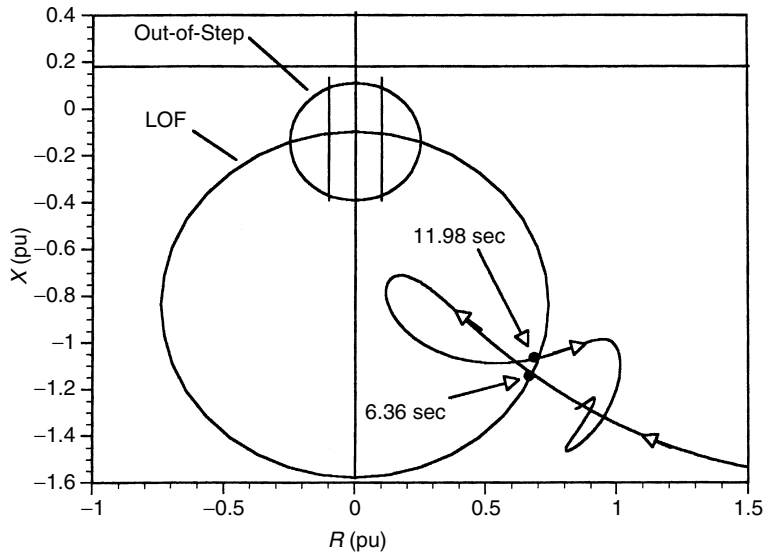


FIGURE 13.10 Impedance locus for LOF from light load.

© 2006 by Taylor & Francis Group, LLC

The longer delay is expected, because accelerating torque is less for the light-load case; thus, changes will take longer. A delay of 7 to 9 sec is considered typical for the light-load case. The faster times are associated with high-impedance systems.

13.5.1.1 Coordination for Stable Swings

Tripping must be delayed to prevent misoperation of stable swings. Power system disturbances such as a fault, the loss of a major generator, or load center can produce severe but stable swings that enter the LOF trip characteristic. This is most likely to occur if the system impedance is low, the generator is initially operating in the leading mode and the manual regulator is in service.[2] The LOF trip delay must exceed the time the stable swing lingers within the LOF characteristic. For a given system configuration, the maximum encroachment time normally occurs when fault clearing equals the critical clearing time. The critical clearing time is the maximum fault clearing time for which the system remains stable.

Figure 13.11 plots the impedance locus for a stable swing initiated by a critical clearing time fault. The swing encroaches on the LOF trip characteristic for 0.32 sec. A time delay of 0.5 sec would be sufficient to prevent misoperation.

A delay of 0.5 sec is usually sufficient to override stable swings, but one- and two-second delays are often applied. The longer delays can jeopardize tripping when a LOF impedance locus exits and reenters the trip characteristic each slip cycle. This situation occurs in Figure 13.12. Here the impedance locus for a LOF event initially enters the trip characteristic in 1.86 sec at A and exits in 3.2 sec at B. A LOF element with a delay greater than 1.34 sec would not respond to the swing. Because the timing of each slip cycle is relatively constant, the relay could also fail to operate on subsequent passes through the characteristic. In this case, the longer delay would result in a failure to trip for a LOF condition.

Ideally the tripping delay should be chosen from dynamic studies that establish the most severe stable swing condition. These studies should consider various system operating configurations, loading and fault types.

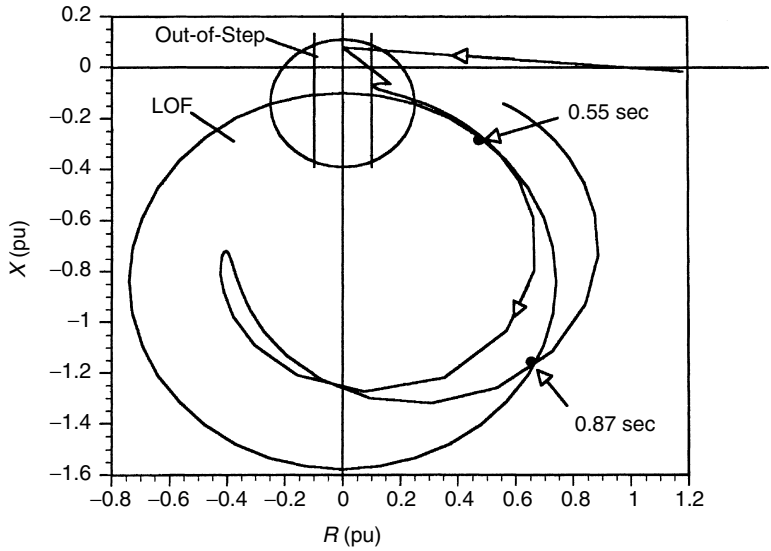


FIGURE 13.11 Stable swing.

© 2006 by Taylor & Francis Group, LLC

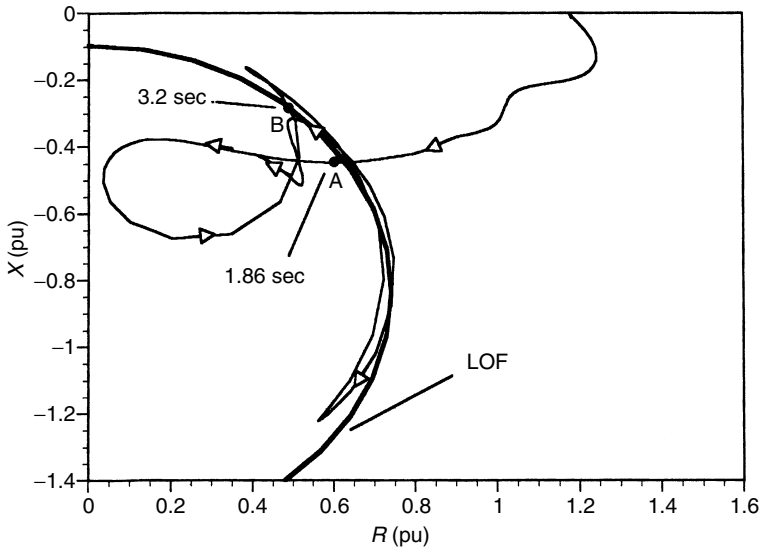


FIGURE 13.12 Impedance locus exit LOF relay.

13.5.1.2 Coordination with Minimum Excitation Limiter and Generator Capability Curve

The minimum excitation limiter (MEL) was discussed in Chapter 11. It is a control function that determines the maximum leading Var intake during normal operation. Should the automatic voltage regulator (AVR) attempt a radical reduction in field current, as might occur in response to high system voltage, the MEL will actuate to prevent additional Var flow into the generator. The MEL is set to prevent operation that would damage the stator end-core or cause loss of steady-state stability.

The MEL and LOF relay should be coordinated such that their characteristics do not overlap. The intent is that the control action of the MEL will prevent leading Var excursions into the LOF characteristic; thus, the MEL would prevent misoperation of the loss-of-field element for system transients.

The MEL characteristic is defined on the $P-Q$ (power-reactive) plane, while the LOF relay is an impedance-sensing device with its characteristic represented on the $R-X$ plane. To assess this coordination, the MEL and LOF relay characteristics must be plotted to common variables.

It is desirable to convert the LOF relay characteristic to the $P-Q$ plane because this facilitates comparison of the LOF setting to the generator capability curve. The conversions are made by choosing impedance points (Z) on the relay characteristic and measure the associated angles ($\emptyset$) between those points and the R-axis. An equivalent kVA point on the $P-Q$ plane equals E_t^2/Z plotted at the angle $\emptyset$ from the P-axis. A point-by-point conversion will allow the transfer of any characteristic between the two planes. This method of transfer was presented in Chapter 11 and Figure 11.7 and Figure 11.8.

The LOF characteristic, the MEL and the generator capability curve are compared on the $P-Q$ plane in Figure 13.13. This plot shows that proper coordination exists between the relay and the MEL. As leading Vars increase, the MEL would be the first to actuate. The MEL would act to prevent any additional increase in Var flow into the generator, thus preventing encroachment on the generator capability, LOF relay characteristic or the steady-state stability limit. If the AVR were out of service, the MEL would also be inoperative. Because the LOF relay characteristic is offset into the $-jX$ region, the relay will not provide backup protection if generator capability or steady-state stability limit were exceeded. This is apparent from the figure.

© 2006 by Taylor & Francis Group, LLC

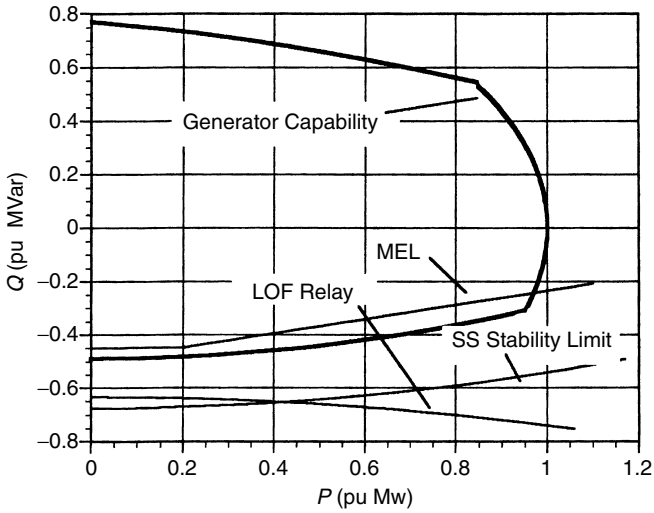


FIGURE 13.13 Coordination with MEL.

Unfortunately, the $P-Q$ plot does not address the dynamic response. When a fast acting MEL is part of a high-speed excitation system, it can act to divert swings from entring the LOF characteristic by rapidly increasing excitation. As excitation increases, the diameter of the swing locus increases, in effect pushing the swing out of the LOF characteristic. Older systems with rotating main and pilot exciters and long time constant MELs respond too slowly to prevent LOF relay actuation.

These older systems can also experience significant undershoot when the MEL is activated during normal operation. The resulting transient can drive the apparent impedance into the LOF characteristic. Dynamic coordination between the MEL and LOF relay is generally not a problem, except as noted with rotating exciters. However, dynamic simulations are required to confirm that the MEL, excitation system and their respective settings provide the desired response. In cases where an undershoot problem exists, a LOF trip delay of 1 to 3 sec may be required to prevent misoperation.[7]

13.5.1.3 Modified Scheme: Two Impedance Elements

The disadvantage with the above scheme is that one trip delay is applied to all LOF events. The delay is set to override stable swings that generally present an impedance trajectory near X_d similar to that of a LOF from light load. The resulting delay between 0.5 and 2.0 sec is then imposed on the most serious LOF events, those that track to X'_d.

A modified version of the previously described scheme adds a second distance element intended to operate for the most severe LOF events. The modified scheme characteristic is shown in Figure 13.14. The intent is that the reach of the inner element into the $-jX$ region is limited such that unstable swings will not enter this characteristic. This being the case, no time delay is required for the inner element and severe LOF events will be tripped immediately when the LOF impedance enters the characteristic.

It has become general practice to set the inner element diameter to 1.0 pu on the generator impedance base. The outer element is set as the single element scheme previously described was set, with diameter X_d. Both elements are set with an offset equal to $1/2X'_d$. With this setting, the inner element will respond to LOF events initiated with the generator operating at approximately 30 to 100% of full load. The aforementioned inner element settings have been adopted because studies and

© 2006 by Taylor & Francis Group, LLC

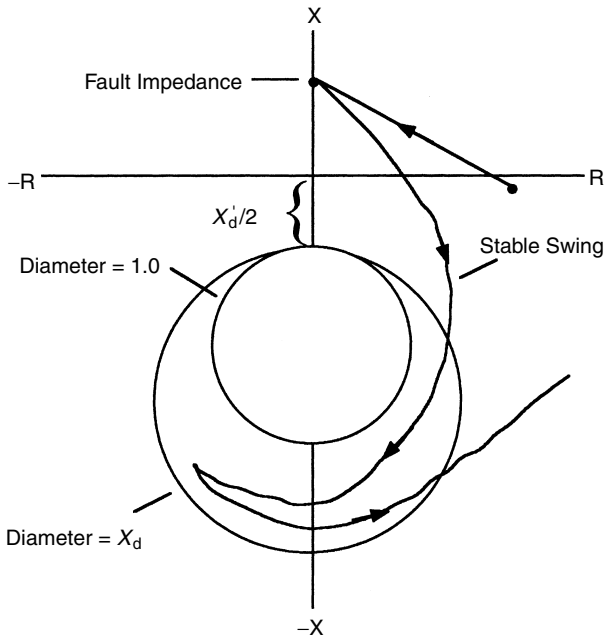


FIGURE 13.14 Scheme 1 with two elements.

experience has shown they are generally immune to stable swing encroachment over a wide range of system conditions.[2] Ideally, transient studies should be run to confirm this. If encroachments are found a reduced diameter or a minimal time delay will be required to prevent misoperation.

In practice, dynamic studies are usually not available. In this instance it is wise to provide some override capability by setting a minimal delay of 0.3 or 0.4 sec on the inner element. Immediate tripping should only be applied when dynamic studies for the specific system have confirmed that stable swings do not enter the trip characteristic and that high-speed tripping is required to prevent system deterioration.

The outer element must be set to detect light-load failures and therefore must encompass X_d. As a result, this element is subject to encroachment by stable swing and must be delayed to avoid misoperation. Because the outer element will respond to less severe excitation failures, a liberal time delay of 1 to 2 sec can be applied without significant impact to system or generator protection. Note that the longer delay is also applicable for the condition shown in Figure 13.12 because the fast-operating inner element would detect the LOF condition.

Microprocessor generator protection packages commonly provide the option for single or dual distance elements for LOF protection. The dual element package is desirable because it provides faster clearing for severe LOF conditions while improving security for stable swings.

The two-element scheme is specifically recommended for locations where the system cannot support the Var requirements of the failed generator and rapid clearing is required to prevent system collapse. The scheme is also recommended at locations where MEL undershoot may cause Var excursions into the LOF relay characteristic. In the latter case, a delay of 1 to 3 sec may be required for the outer element to prevent misoperation.[2]

13.5.2 Distance Scheme 2: Qualified Trip Scheme

This alternative scheme was developed before the high-tech cooling system employed on modern generators. Machines of that period could operate asynchronously without field for

© 2006 by Taylor & Francis Group, LLC

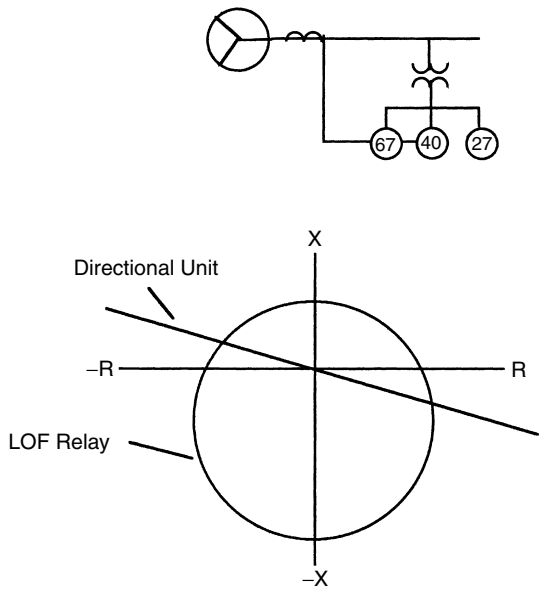


FIGURE 13.15 Scheme 2 with single element.

several minutes. The scheme logic was predicated on the assumption that a LOF event is not immediately damaging to the generator and focuses on system protection. The scheme includes impedance, directional, and undervoltage elements and timers. The scheme's impedance characteristic is shown in Figure 13.15.

A strong power system will supply the Var requirements of the failed unit without significant voltage reduction. A weak system will experience severe voltage degradation with possible loss of stability as a result of the large Var drain imposed by a loss of field. The UV element is intended to differentiate between a strong and a weak system.

A LOF condition is recognized when the impedance locus enters the distance element below the directional unit. If the terminal voltage falls to a level such that the undervoltage unit drops out, it is assumed that the system is incapable of supplying the post-LOF Var requirements and system collapse is imminent. In this instance, tripping is initiated with minimal delay. The minimal delay is that which is necessary to override stable swings that might enter the relay characteristic. The minimum delay should be determined from dynamic studies that consider various system operating configurations, loading, and fault types. If these data are unavailable, which is often the case, a time delay of 0.5 sec is generally adequate to prevent misoperation.

If the UV element does not drop out, the scheme presumes a strong system capable of supplying the Var requirements of the failed unit. An alarm is initiated to alert the operator of the condition and, in most application, the generator is tripped after a delay if the operator has not corrected the problem. Proponents of the scheme have recommended delays ranging from one second to several minutes for this trip, dependent on the type of machine.

13.5.2.1 Trip Delay Considerations

Long delays (several minutes) are intended to facilitate operator intervention to restore excitation and avert a unit trip. This concept is appealing, but involves considerable risk. Long trip delays are a carryover from older vintage machines that were capable of asynchronous operation for extended periods. Machines are now more vulnerable, with damage possible in 10 sec for some machines.

© 2006 by Taylor & Francis Group, LLC

The time delay implemented when the undervoltage unit does not drop out is typically set at 60 sec. This is predicated on the assumption that severe events will drop out the undervoltage element, which is typically set at 80% voltage. Experience has shown this to be true for most cases. However, situations can arise such that the undervoltage element set in this manner will not respond to a loss of field from full load. In these cases, the delay should be reduced from 60 sec to about 1.0 sec, or Scheme 1 should be implemented.

13.5.2.2 Criteria for Setting Mho Characteristic

The impedance element of this scheme is set to operate when leading Var flow exceeds generator capability. The setting is also coordinated with the MEL, and the steady-state stability limit. This is accomplished by replotting the aforementioned curves on the $R-X$ plane. This replot is the inverse of the $R-X$ to $P-Q$ plane conversion described for Scheme 1.

A point-by-point calculation is required to transfer the generator capability curve and MEL characteristic to the $R-X$ plane. The manual regulator steady-state stability limit can be plotted directly if system reactance X_s and X_d are known. On the $R-X$ plane, the steady-state limit is a circle with the following parameters:

$$\text{Center} = \frac{-j(X_d - X_s)}{2} \quad \text{Radius} = \frac{X_d + X_s}{2} \tag{13.16}$$

Ideally, the trip characteristic of the LOF relay is set to allow full utilization of the leading Var capability of the generator. The relay should actuate to initiate an alarm and tripping when operation exceeds the generator leading Var limit or approaches the SS stability limit. Figure 13.16 shows the desired coordination on the $R-X$ plane.

Note that real and reactive power increase as the distance from the origin increases on the $P-Q$ plane while the opposite is true on the $R-X$ plot. Operating points inside the generator capability curve on the $P-Q$ plane are within the generator rating, while operation outside the capability plot on the $R-X$ plane are within rating.

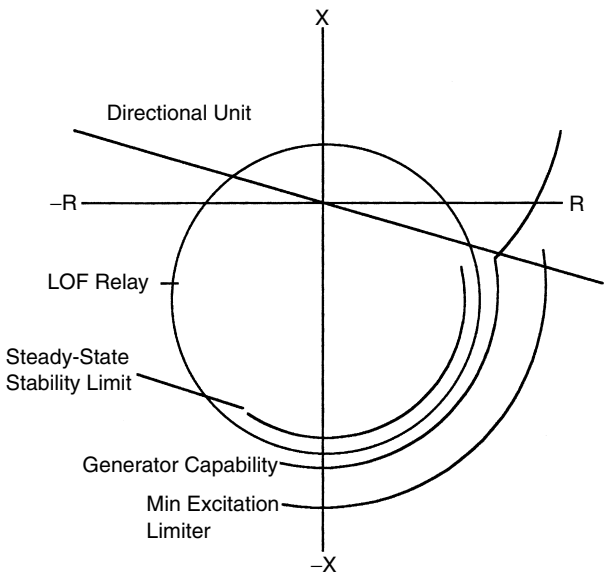


FIGURE 13.16 Scheme 2 coordination.

© 2006 by Taylor & Francis Group, LLC

It is important to note that, regardless of the configuration of the Var capability or stability limits, the trip characteristic must encompass both X'_d and X_d if the LOF relay is to provide protection over the full range of generator loading condition.

Normally, the MEL will inhibit operation beyond the generator's leading Var capability or near the stability limit. However, when the automatic regulator is out of service, the MEL is inoperative. In this instance, the stated setting strategy will provide an alarm to alert the operator in the event of excess leading Vars or infringement of the stability limit. A unit trip will result if the situation is not corrected. This is an advantage over Scheme 1, which does not provide this type of backup protection when the MEL is out of service.

Fulfilling this ideal is complicated by the voltage variant nature of the generator leading Var capability and the fixed LOF and steady-state stability characteristics on the $R-X$ plane. A method of estimating variations of end-core capability with voltage was presented in Chapter 11. (The stator end-core determines the leading capability.) Using this method, end-core capability increases as terminal voltage decreases. Figure 13.17 shows a LOF characteristic and steady-state stability limit plotted against the generator end-core capability at 0.95 and 1.0 pu terminal voltage.

The orientation of the stability limit and the LOF characteristics are independent of voltage on the $R-X$ plane. However, the location of the generator's leading Var capability will vary significantly with voltage. The figure shows that a LOF relay cannot be set to provide complete protection and allow full utilization of the available leading Var capability. A setting chosen on the basis of the generator's maximum Var capability ($e_t = 0.95$ pu) will provide limited protection at higher operating voltages. Conversely, a LOF setting chosen to provide full protection at the maximum operating voltages will sharply limit leading Var capability at reduced voltage.

The setting chosen in Figure 13.17 is based on maximum utilization ($e_t = 0.95$ pu). The reduced protection at higher voltages is not considered a significant problem, because operation

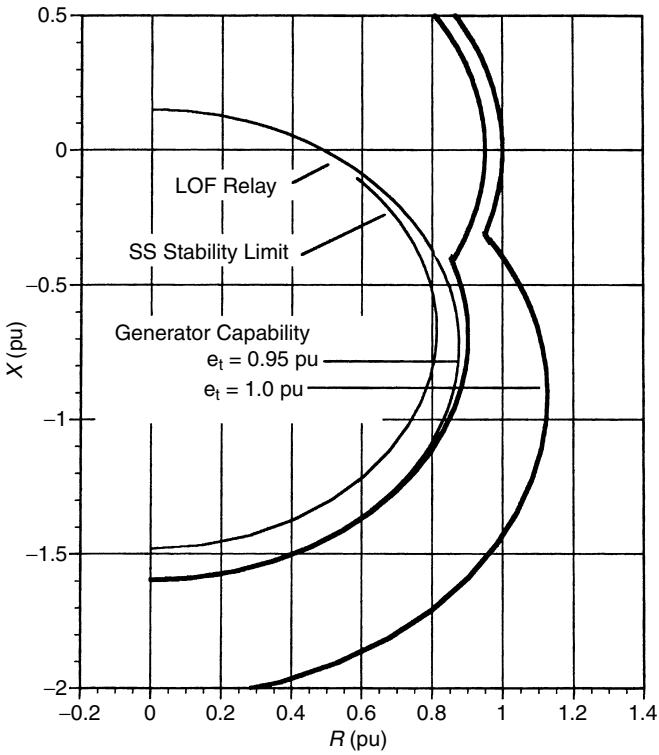


FIGURE 13.17 $R-X$ plane LOF, end-core limit at $e_t = 0.9.5$ and 1.0 pu.

© 2006 by Taylor & Francis Group, LLC

with high leading Vars is normally associated with reduced terminal voltage. Also, the automatic voltage regulator would normally be in service and the MEL would prevent operation in excess of generator capabilities.

To achieve the desired trip characteristic, it is necessary to extend the reach of the impedance element beyond the generator terminals, as is the case in Figure 13.17. The directional unit is provided to prevent tripping in this area. Without the directional unit, tripping could occur for system faults near the unit transformer.

13.5.2.3 Undervoltage Element

The undervoltage element is intended to predict system ability to withstand the LOF event. In theory, the undervoltage element should be set at the maximum voltage at which stability could be lost or a voltage collapse would occur. Attempts to define such a voltage threshold would require a tremendous amount of dynamic analysis and, in the end, an ideal setting may not be obtainable. As a practical alternative, a loss of field from full load will generally result in terminal voltage less than 70%. Therefore, the undervoltage element is typically set to drop out at 80% nominal voltage.

13.5.2.4 Modified Scheme

As with Scheme 1, a second impedance element can be added to enhance protection. The two-zone scheme has a trip characteristic as shown in Figure 13.18. The inner element is set identical to the outer element of Scheme 1 with an offset of $X_d'/2$ and a diameter of X_d. The inner element provides fast tripping for field failures over the full range of generator loading. The outer element is set as previously described for the single element Scheme 2 and is intended to respond to excess leading Vars and partial LOF conditions.

The outer characteristic is supervised by the undervoltage element; the inner characteristic is not. As with Scheme 1, the minimum delays should be determined from dynamic studies that define the maximum time a stable swing will linger within a trip characteristic. In lieu of these studies, inner element tripping is typically initiated in 0.5 sec. The outer element is typically set to trip in 1.0 sec if the undervoltagae element drops out and 60 sec if it does not.

13.5.2.5 Special Consideration for Bussed Generators

Units that are bussed together at their terminal require some special considerations. When one unit loses excitation, the remaining bussed machine(s) and the connected system will provide very strong support for the terminal voltage. This can prevent dropout of an undervoltage element set at 80%. Therefore, it is recommended that the dropout setting for the undervoltage element should be increased to 87% nominal voltage when multiple units are connected directly to a common bus.[8]

The bussed arrangement also increases the potential for generator damage by increasing the stator current during the LOF event. Reference 2 included a case study of a system with two machines bussed together and connected to a strong system through a single transformer. The stator current in the machine with the failed excitation approached a peak value of 2.5 pu. Clearly, machines that are connected to a common bus should have a two-zone LOF protection scheme to obtain the fastest possible clearing. It is also recommended that the outer element trip delay for cases where the undervoltage element does not drop out should be reduced to 10 sec for a directly cooled machine and 25 sec for an indirectly cooled machine.[8]

The response of other units connected to the same bus as the unit with failed excitation will depend on system impedance and which voltage regulator is in service. If the automatic regulator is in service and the connected power system is strong, the units with sound excitation may continue operation without loss of stability.

© 2006 by Taylor & Francis Group, LLC

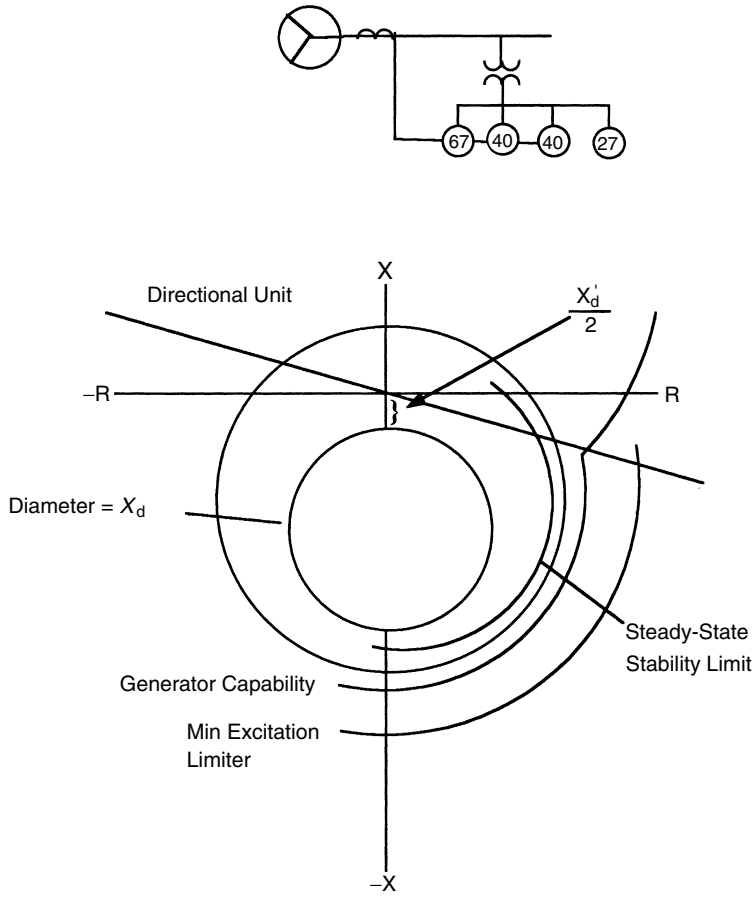


FIGURE 13.18 Scheme 2, dual element.

13.6 OTHER CAUSES FOR LOF RELAY OPERATIONS

Up to this point, we have considered LOF events caused by shorted or open field circuits. However, a legitimate LOF operation can result from other causes.

13.6.1 Operator Error on Startup

Assume that a unit is coming on line. The automatic regulator is unavailable and the operator must use the manual regulator for startup. The unit is synchronized and begins ramping up MW load. At about 60% load, the unit trips by LOF relay. A complete check of the excitation system and the LOF relay finds no problem. What happened?

The answer is the unit lost steady-state stability because the operator failed to manually increase field as the unit was loaded. The LOF relay operated when the out-of-step impedance locus entered its characteristic. This is not an uncommon operator error. On startup, the field must be initially adjusted such that the generator no-load voltage equals the system voltage, $e_t = 1.0$ pu voltage, to allow synchronization.

The electrical power output of a generator is given by the power angle equation (13.1). After synchronization with manual regulation, E_g is fixed at 1.0 pu. This is approximately 40% the value required at full-load. The maximum value of the power angle curve (Figure 13.1), would be 0.6 pu.

© 2006 by Taylor & Francis Group, LLC

If the operator fails to increase field as he increases MW loading the generator will be incapable of delivering power in excess of 0.6 pu to the electrical system. When turbine power input is increased above this point, the energy is expended, accelerating the generator above synchronous speed and out of synchronism with the system.

As MW load is being increased, with fixed excitation the generator Var loading will become increasingly leading. When synchronism is lost, operation will be far into the leading Var region. This will cause the impedance locus of the swing to intersect the LOF relay characteristic and trip the unit.

13.6.2 Frequency-Sensitive Excitation Systems

Figure 13.19 is typical for an exciter driven from the generator shaft. The load line represents a plot of the total field circuit resistance, including the controlling resistance of the voltage regulator. The intersection of the load line and the exciter characteristic determine generator field voltage and current.

Exciter output is directly proportional to flux times speed and shaft speed varies with generator frequency. The figure shows the reduction in exciter output as the voltage at the intersection point decreases frequently. If the automatic regulator where in service during such an event the slope of the load line would be reduced to increase field current and maintain terminal voltage. If the manual regulator where in service the same action would be taken to maintain field current at its preset value. The reduction in field current and voltage can be much greater than the reduction in frequency dependent on the slope of the load line. A large field current reduction will significantly reduce the power angle curve for the generator and can cause a loss of steady-state stability with LOF relay actuation as described in the preceding section.

The frequency decay can be such that load line parallels the exciter characteristic. This is shown in Figure 13.19 with frequency reduced to 55 Hz. If this happens, there is no intersection point for the two curves and the only stable operating point will be near the origin. A LOF trip will result when excitation collapses.

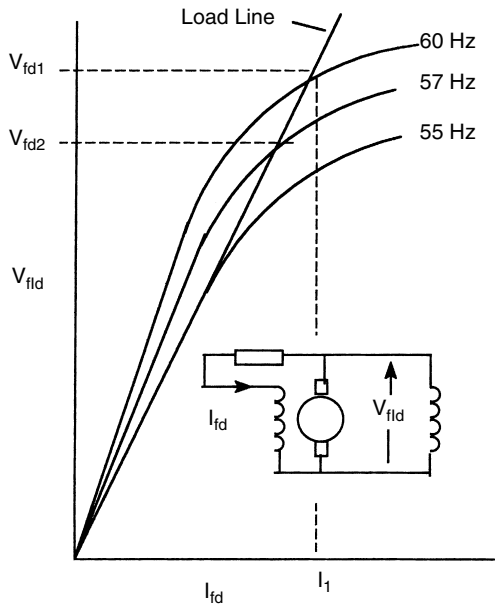


FIGURE 13.19 Shunt field exciter.

© 2006 by Taylor & Francis Group, LLC

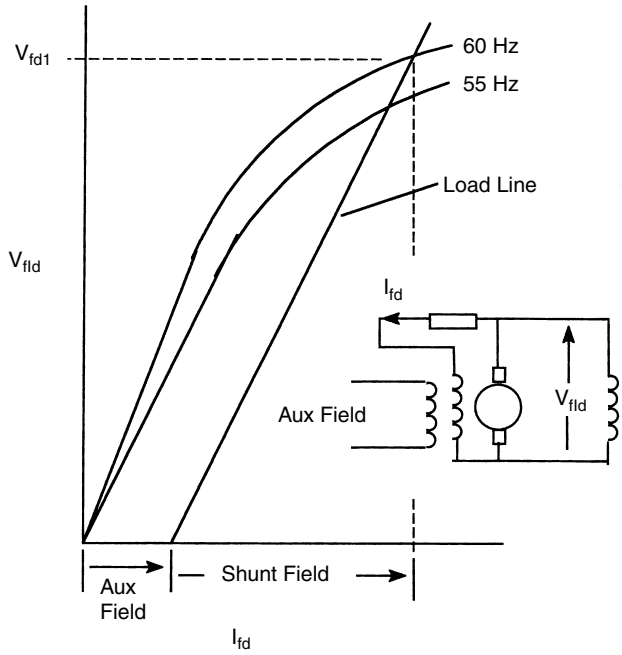


FIGURE 13.20 Exciter with boost/buck auxiliary field winding.

Excitation collapse is more likely under manual regulator control then under automatic regulator control. Field current under manual regulator control is limited to a maximum value slightly above that required for full load. Under automatic control field forcing current of 1.2 to 1.5 times rated field current are permitted. The results is that under automatic regulator control a lower load line slope is permitted. This will facilitating stable operation at a lower frequency than is permitted by the slope of the manual regulator load line.

A similar failure will occur with an excitation system that employs a boost/buck auxiliary field for control as shown in Figure 13.20. The loss of the automatic regulator will remove the auxiliary field, immediately shifting the load line to the left. At reduced frequency, this can trigger a severe reduction in excitation, causing a loss of stability or field collapse.

13.7 LOF RELAYS DURING SYSTEM DISTURBANCES

During the infamous Northeast Disturbance of November 9, 1965, 16% of the total system capacity tripped by LOF relaying. During the PJM Disturbance of June 5, 1967, LOF relay operations resulted in the loss of 28% of the total system capacity.[9] These relays were in general set to the same criterion recommended in this chapter. The large number of trips cast considerable doubt on LOF setting philosophy and the relay application itself.

At the time of these events, rotating exciters and electromechanical LOF relays were the norm. The frequency response of this equipment was a key factor in LOF tripping during the disturbances. Both events lasted in excess of 10 min. Initially, as with most disturbances, system voltage was reduced by the initiating event. Units operating with AVRs boost excitation to increase Var output and support the decaying system voltage. Overloads cause tie lines to trips, forming islands. Some islands formed with excess generation, others with deficient generation. Islands with excess generation tended toward high voltage and frequency in excess of 60 Hz. Generation-deficient islands tended to operate with reduced voltage and low frequency. During portions of the June 5 event, frequency is believed to have been below 56 Hz.

© 2006 by Taylor & Francis Group, LLC

The postmortem on the event concluded that nearly all the LOF trips occurred when the associated generators were on manual regulations. Some units were initially in operation in this mode, but many units were tripped to manual regulation by protective functions described in Chapter 8 or operator action after prolonged field forcing threatened to thermally damage field circuits. Machines initially on automatic regulation were tripped by LOF relays immediately after transfer to manual regulation as a result of the collapse of excitation precipitated by reduced frequency. Others tripped because the reduced excitation available from the manual regulator was not sufficient to maintain steady-state stability. The generator was tripped when out-of-step impedance swing passed through the LOF characteristic.

The frequency response of the electromechanical LOF relays contributed to the LOF relay detection of out-of-step conditions. Figure 13.21 and Figure 13.22 show the frequency response of two manufacturer's LOF relays that were commonly in use on both systems when the disturbances occurred. Both characteristics roll toward the *R*-axis with reduced frequency. Figure 13.22 includes partial plots of the idealized out-of-step swing impedance with reduced generator voltage. The plot shows swing loci are more prone to enter the frequency-distorted LOF characteristic.

A subsequent report by the IEEE on the disturbances endorsed the application of LOF relays and the setting philosophies. The report concludes that the relay operations did not aggravate the scope of the disturbance because, in general, the LOF relay trips occurred on units that had already lost stability or suffered excitation collapse. The report also concluded that the relays did provide protection during the events. The report recognized that LOF settings are generally derived from rule of thumb and recommended that settings should be derived from dynamic studies.

We note that the response of today's power system would be much different than that of the 1960s. System security has been improved by the application of automatic load-shedding schemes. These schemes activate when system frequency begins to decay. They rapidly shed load and reestablish a balance between system load and generation. Load shedding will significantly reduce the frequency excursions during major system disturbances. Also, many rotating excitation systems have been replaced with static systems that are more frequency-tolerant. Electromechanical schemes are continually being replaced with microprocessor schemes that are insensitive to frequency variations in the range seen during the subject disturbances.

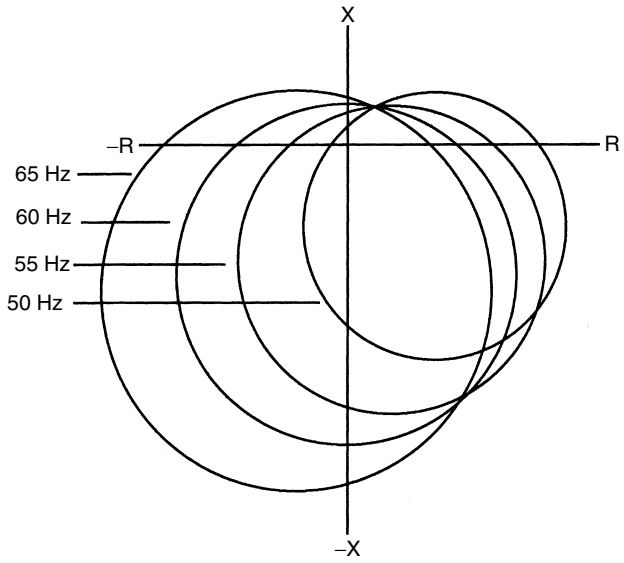


FIGURE 13.21 Frequency Response of LOF relay A. (From Darron H.G., Koepfinger J.K., Mather J.R., Pusche P.A., The Influence of Generator Loss of Excitation on Bulk Power System Reliability IEEE Transactions PAS-94, No 5, Sep/Oct 1975, pp. 1473–1481 IEEE. With permission.)

© 2006 by Taylor & Francis Group, LLC

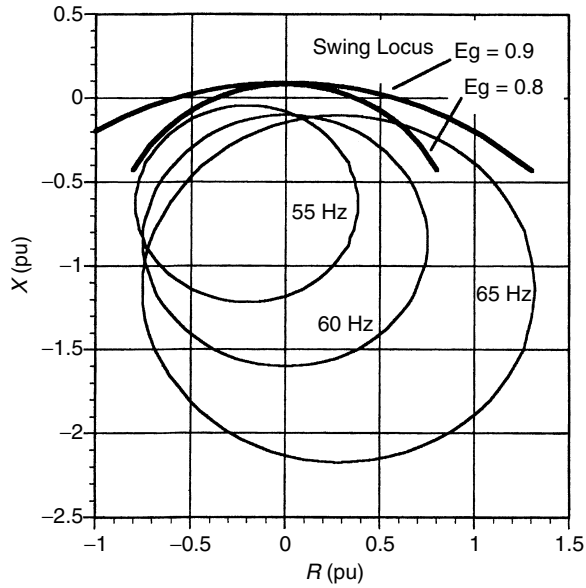


FIGURE 13.22 Frequency response of LOF relay B with swing locus.

13.8 SPECIAL CONSIDERATIONS FOR HYDRO UNITS

Hydro units are often run as synchronous condensers. Loss of field relays set as previously described may experience incorrect operations in this mode of operation if the Var loading is near the rating of the generator. This problem can be eliminated if the LOF relays are supervised by undervoltage relays set at 90 to 95% rated voltage.

Another hydro unit concern is load rejection that can cause unit speed and frequency to exceed 200% until the governor regains control. This might occur as a result of islanding during a system breakup or as a result of a load rejection. Electromechanical LOF relay characteristics are frequency-dependent. The maximum torque angle shifts to the fourth quadrant and diameter increases of 200 to 300% have been reported during overspeed. The altered characteristic may lead to misoperation on line charging current during overfrequency events.

To avoid this problem, the loss of field relay on hydro units could again be supervised by an undervoltage relay set at the 90 to 95% rated voltage previously suggested or an overfrequency relay set at 110% rated frequency.

13.9 APPLICATION OF THE LOF ON THE SAMPLE SYSTEM

The Loss of Field protection for the sample system generator will be provided using a multifunction microprocessor generator protection relay. The relay provides the option of implementing either Scheme 1 or Scheme 2 protection as described in Section 13.5.

Both schemes provide rapid clearing for severe LOF events. The trip characteristic of Scheme 2 is configured to the leading Var capability of the generator and provides backup protection for the stator end-core. Normally, the AVR is in service and the MEL will prevent operations that threaten the generator's leading Var capability or steady-state stability limit. However, when the automatic regulator is out of service, the MEL is inoperative. Scheme 2 will provide an alarm if Var loading exceeds the generator's leading Var capability or approaches the stability limit. If the condition is severe enough to depress system voltage to the extent that the scheme's undervoltage element drops out, tripping is initiated with minimal time delay. If the condition is not severe enough to

© 2006 by Taylor & Francis Group, LLC

drop out the undervoltage element, tripping is delayed to allow the operator a brief period to intervene and avert a trip.

The trip characteristic of Scheme 1 is not configured to the generator capability and will not provide effective backup protection for excessive leading Vars. The reduced sensitivity of Scheme 1 makes it less prone to misoperations for stable swings. Also, Scheme 1 is not dependent on voltage constraints, as in Scheme 2, and provides direct tripping for all LOF conditions.

13.9.1 Application of Scheme 1 on the Sample System Generator

This protection is shown in Figure 13.23 and the trip characteristic for the scheme with two impedance elements is shown in Figure 13.14.

Two setpoints are usually required for each distance element, the offset and the diameter. Some LOF elements also require a setting for the maximum torque angle (MTA). This is the angular distance from the R-axis to the center of the circular characteristic. Because the LOF characteristic centers on the X-axis, MTA $= 90^\circ$.

A time delay setting is required for the outer element to override stable swings that enter the characteristic. The inner element can be allowed to trip without a delay if there is confidence that no stable swings will enter its characteristic. Lacking this confidence, a minimal delay of 0.3 to 0.4 sec should be applied.

The conventional settings for Scheme 1 are:

Outer element

Diameter $= X_d = 1.48$ pu

Offset $= \frac{1}{2}X'_d = 0.196/2 = 0.098$ pu

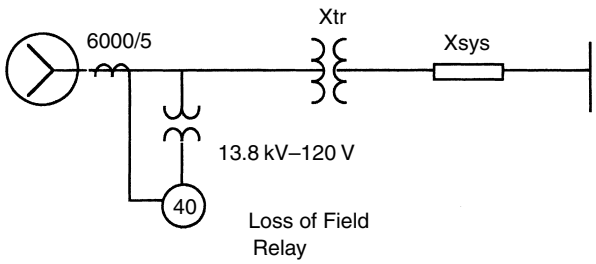
Time delay $= 1.0$ sec

Inner element

Diameter $= 1.0$ pu

Offset $= \frac{1}{2}X'_d = 0.098$ pu

Time delay $= 0.4$ sec



Impedances on generator base 104 MVA 13.8 kV

$X_d = 1.48$ pu
$X'_d = 0.196$ pu
$X_{tr} = 0.07$ pu
Zsyst = 0.078 pu @ 85° min (normal)
= 0.225 pu @ 75° max (line out)

FIGURE 13.23 Sample system Scheme 1 installation.

© 2006 by Taylor & Francis Group, LLC

The LOF settings should not infringe on the generator's leading Var capability. Also, the MEL should be set to prevent Var loading that would encroach on the LOF relay trip characteristic. To assess this coordination, all must be plotted on the $P-Q$ plane.

The leading Var capability of the generator is voltage-dependent. Capacity increases with reduced terminal voltage. Therefore, to ensure utilization of the full leading Var capability, the LOF setting should be coordinated with a capability curve derived at 0.95 pu voltage. This is the minimum allowable operating voltage for a generator.

The leading Var capability on the $P-Q$ plane can be estimated using equations from Chapter 11.

$$P = Radius\ e_t \sin\beta \tag{11.90}$$

$$Q = Center\ \epsilon_t^2 - Radius\ e_t \cos\beta \tag{11.91}$$

The values of "*Radius*" and "*Center*" are chosen to provide a calculated capability curve at $e_t = 1.0$ that matches the manufacturer's capability curve. For the sample system generator, "*Radius*" and "*Center*" were chosen as 2.59 and 2.10, respectively.

The impedance settings of the LOF relay derived above must be converted to the $P-Q$ plane. This process was described in Chapter 11. An impedance point at an angle θ from the R-axis will plot as a kVA point at angle θ from the P-axis. The per unit magnitude of the equivalent kVA point is given as

$$\text{kVA} = \frac{e_t^2}{Z} \tag{13.17}$$

The circular characteristic of the impedance element on the $R-X$ plane will translate to a circular characteristic on the $P-Q$ plane. Because the center of the impedance characteristic is located on the X-axis, the center on the $P-Q$ plane will be on the Q-axis. Thus, the $P-Q$ characteristic of the relay can be determine by converting only the offset and reach points to the $P-Q$ plane. The $P-Q$ characteristic of the LOF element is then drawn as a circle with its center on the Q-axis, halfway between the converted offset and reach points.

Converting the outer element to the $P-Q$ plane at $e_t = 0.95$ pu:

Outer element
- Offset (Z) $= -0.098$ pu (Z)
- Offset (kVar) $= -0.95^2/0.098 = -9.2$ pu
- Reach (Z) = offset + diameter $= -0.098 - 1.48 = -1.57$ pu
- Reach (kVar) $= -0.95^2/1.57$ pu $= -0.58$ pu

The outer characteristic plots as a circle on the $P-Q$ plane with its diameter on the Q-axis passing through points -9.2 pu kVar and -0.58 pu kVar.

The inner element will only respond to severe leading Var excursion and would not be expected to conflict with the leading Var capability or the MEL setting. The Q-axis intersections for the inner element are at:

Inner element
- Offset (kVA) = same as the outer element $= -9.2$ pu
- Reach (Z) = offset + diameter $= -0.098 - 1.0 = -1.098$ pu
- Reach (kVar) $= -0.952/1.098$ pu $= -0.82$ pu

© 2006 by Taylor & Francis Group, LLC

The steady-state stability limit is plotted on the $P-Q$ plane using Equation (11.30) and (11.31) with $e_t = 0.95$. Note that when plotting the stability limit, the system impedance must be expressed on the same base as the LOF settings, which is the generator base.

Figure 13.13 is a plot of the sample system with the proposed settings. The plot shows that the desired coordination between the LOF element, MEL and Var capability is achieved. Note that because the LOF characteristic is offset into the negative reactance region, the relay does not provide effective protection for the end-core region.

An impedance element normally requires settings in terms of secondary ohms, not in per-unit impedance as is given above. Secondary ohms are primary or power system ohms as viewed from the secondary of the relay PTs and CTs.

To convert the setting to secondary ohms, the per-unit settings must first be converted to primary ohms. Because the per-unit settings are expressed on the generator base system, base ohms must be calculated from the generator base MVA = 104 and base kV = 13.8. Base ohms are then

$$Z_{\text{Base}} = \frac{Genk\text{V}^2}{Gen\text{MVA}} = \frac{13.8^2}{104} = 1.83\,\Omega$$

Primary ohms are converted to secondary ohms used:

$$Z_{\text{sec}} = Z_{\text{prim}} \frac{CT \text{ ratio}}{PT \text{ ratio}} \tag{13.18}$$

From Figure 13.23, PT and CT ratios are

PT = 13,800/120 V = 115/1
CT = 6000/5 = 1200/1

The secondary ohm settings are then:

Outer element
Diameter = 1.48 pu * 1.83 * 1200/115 = 28.3 sec ohm
Offset = 0.098 pu * 1.83 * 1200/115 = 1.87 sec ohm
Time delay = 1.0 sec

Inner element
Diameter = 1.0 pu * 1.83 * 1200/115 = 19.1 sec ohm
Offset = same
Time delay = 0.4 sec

13.9.1.1 Setting Review against Dynamic Data

These settings have been derived using a rule-of-thumb approach. Ideally, the derived settings should be compared to worst-case swing data derived from dynamic simulations. The comparison should ensure that the chosen delays are adequate to prevent misoperation for stable swings and confirm that the settings will detect LOF events with varying system conditions. Dynamic data are generally not available and, in most practical circumstances, the rule-of-thumb settings are implemented. Although the spreadsheet provided in Appendix D is not a substitute for such studies, it can be used to evaluate settings for one or two generators isolated from other machines such as the sample system generator. The following analysis is intended to give some insight into the response of these settings to actual dynamic system conditions.

© 2006 by Taylor & Francis Group, LLC

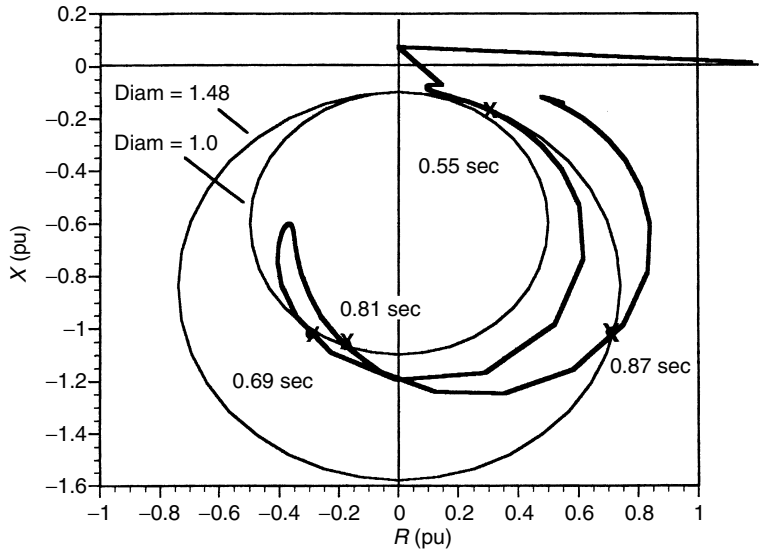


FIGURE 13.24 Stable swing locus for sample system Scheme 1.

Figure 13.24 was derived from the aforementioned spreadsheet. It plots a swing initiated by a three-phase fault at the high side of the GSU with the generator on manual regulator and minimum system impedance (all lines in service). Initially, the generator was operating near full load with Vars leading. The fault duration was set equal to the critical clearing time. This is the maximum fault clearing time for which the system is stable. These conditions generally provide the maximum swing encroachment times within the LOF characteristic.

The plot shows the swing is within the outer element for 0.32 sec confirming that the 1.0 sec delay chosen for this element is adequate. The plot also shows that the swing encroaches on the inner element for 0.12 sec. This confirms that the 0.4 sec delay chosen for the inner element is adequate, but also shows that a 0.3 sec time could also be used. Here is an example of where the application of instantaneous tripping via the inner element as advocated by some would result in an incorrect relay operation.

13.9.2 Application of Scheme 2 on the Sample System Generator

The trip characteristic for Scheme 2 with two impedance elements is shown in Figure 13.18. As with Scheme 1, two setpoints are required for each distance element, the offset and the diameter. Some relays may also require a setting for the maximum torque angle, which would be 90°. Settings are also required for the undervoltage element and three timers. One timer is for the inner element. Two timers are related to the outer element and the state of the undervoltage element.

The impedance settings for the inner element of Scheme 2 are identical to the outer element of Scheme 1: diamater $= X_d$ with offset $= X'_d/2$. On most systems, a delay of 1.0 sec is adequate to override stable swings that enter the relay characteristic.

Inner element
- Diameter $= X_d = 1.48$ pu
- Offset $= 1/2\ X'_d = 0.196/2 = 0.098$ pu
- Time delay $= 1.0$ sec

© 2006 by Taylor & Francis Group, LLC

The outer element is set just beyond the generator's leading Var capability. Because the leading Var limit is inversely proportional to voltage, it should again be plotted at the generator's minimum operation voltage, 0.95 pu, to take advantage of the increased capability at the lower voltage.

Because the LOF element is set in ohms, it is necessary to plot the generator leading Var capability, MEL and steady-state stability limit on the $R-X$ plane using the technique's described in Chapter 11. The steady-state stability limit can be plotted directly on the $R-X$ plane using Equation (13.17).

Figure 13.17 shows the results of this plot for the sample system generator. The plot includes the selected setting for the outer LOF element. The setting was chosen to permit full utilization of the leading Var capability of the generator at 0.95 pu voltage. Remember that on the $R-X$ plane, loading increases with proximity to the origin. Included on the plot is the leading Var capability at 1.0 pu voltage. It is apparent that protection provided by the LOF element diminishes as terminal voltage increases. The outer characteristic chosen has a diameter of 1.75 pu with an offset of 0.15 pu. The voltage element is typically set at 80% nominal voltage for single generator installations such as this. There are two trip delay times for the outer element. If the undervoltage element does not drop out, indicating a strong system capable of supporting the Var requirements of the failed generator, the delay is typically set at 60 sec. If the undervoltage element drops out, indicating a severe LOF event, the trip time is typically set at 1.0 sec.

Without the benefit of dynamic data, the final settings for Scheme 2 are then:

Inner element

Diameter $= 1.48 \text{ pu} * 1.83 * 1200/115 = 28.3$ sec ohm
Offset $= 0.098 \text{ pu} * 1.83 * 1200/115 = -1.87$ sec ohm
Time delay $= 1.0$ sec

Outer Element

Diameter $= 1.75 \text{ pu} * 1.83 * 1200/115 = 33.4$ sec ohm
Offset $= 0.15 \text{ pu} * 0.133 * 1200/115 = +2.86$ sec ohm
Time delay with UV element Drop Out $= 1.0$ sec
Time delay without UV element Drop Out $= 60$ sec

Undervoltage element $= 80\%$ nominal $= 96$ V dropout

13.9.2.1 Setting Review against Dynamic Data

The chosen settings should be tested against swing data from a dynamic simulation. Figure 13.25 plots the maximum encroachment swing against the Scheme 2 settings. The plot shows that the more sensitive setting applied to the outer element of Scheme 2 increases the encroachment time to 0.89 sec compared to 0.32 sec for Scheme 1 (Figure 13.24). The plot confirms that a standard one-second time delay is adequate to override the swing. However, because the voltage recovers to 80% nominal in 0.6 sec, as shown in Figure 13.26, the undervoltage element will picks up to disable the 1.0 sec trip timer. The scheme will actually be timed against on a 60 sec timer.

The encroachment on the inner Scheme 2 element is identical to that of the outer element of Scheme 1, 0.32 sec as shown in Figure 13.24. The encroachment is the same because the settings are identical. The 1.0 sec delay is again adequate to prevent misoperation.

Figure 13.27 plots a loss of field from full load with the sample system significantly weakened by the outage of the strongest tie line. This condition will tend to produce high slip, which is a more damaging condition for the generator than the lower slip associated with a strong system.

© 2006 by Taylor & Francis Group, LLC

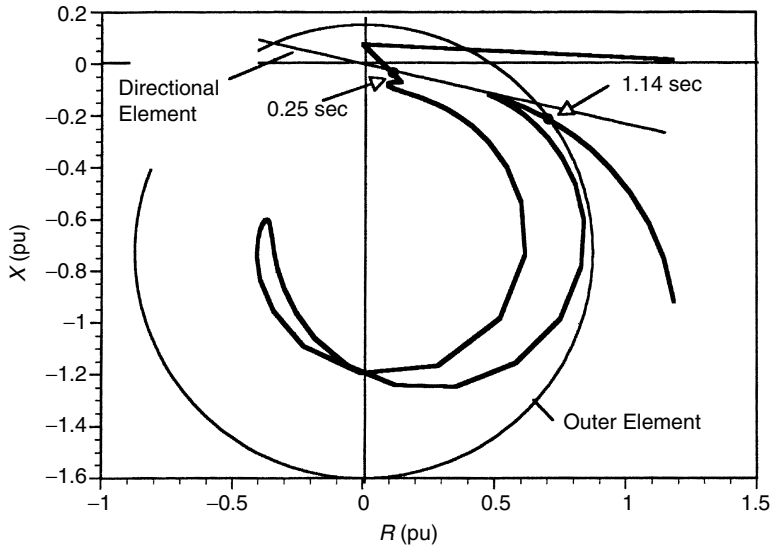


FIGURE 13.25 Stable swing locus sample system Scheme 2.

From the figure, the impedance locus will enter the outer characteristic in 0.90 sec and the inner characteristic in 1.48 sec. The generator current and voltage are plotted in Figure 13.28. The undervoltage element that controls the timing of the outer element will drop out in approximately 1.25 sec (80% voltage) and initiate the 1.0 sec timer. The unit will trip via the inner characteristic, which is not controlled by the UV unit, in $1.48 + 1.0 = 2.48$ sec after the field was lost.

A LOF from full load was also evaluated for a strong system (all lines in service). The impedance locus for this condition is shown in Figure 13.29. The plot shows that the inner element will trip the generator $1.68 + 1.0 = 2.68$ sec after the LOF occurs.

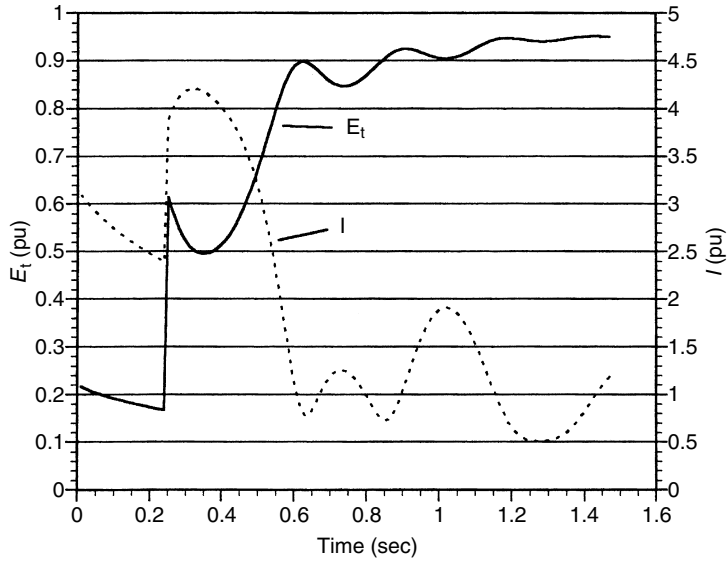


FIGURE 13.26 Voltage and current during stable swing.

© 2006 by Taylor & Francis Group, LLC

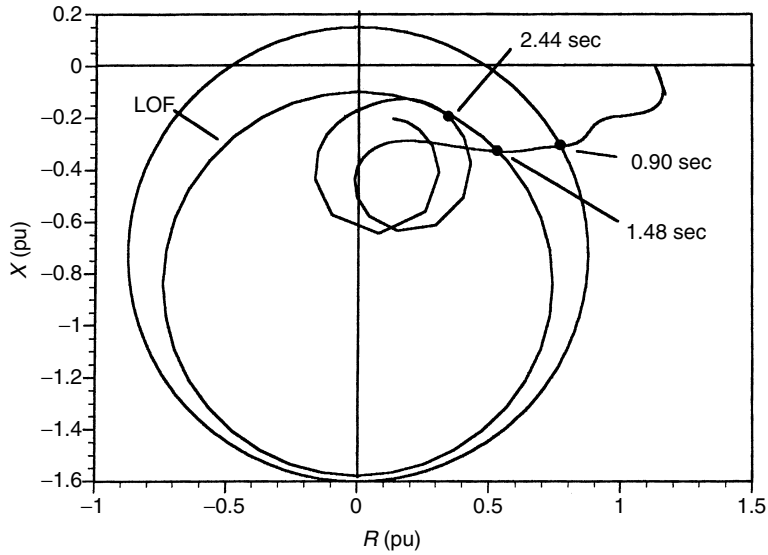


FIGURE 13.27 Sample system LOF high system *Z*, swing.

It is worth noting that been Scheme 2 had applied with a single element, the outcome would have been markedly different. Current and voltage for this event are plotted in Figure 13.30. The undervoltage element is set for 80% dropout. The outer element trip time is 60 sec without undervoltage dropout and 1.0 sec with undervoltage dropout. The plot shows that voltage is only depressed below an undervoltage element dropout of 0.32 sec and remains above 80% voltage for 1.94 sec each slip cycle. These times would not permit either the 1.0 sec or the 60 sec trip timer to actuate. The result is a failure to trip.

The current waveform is cyclic over a 2.26 sec period. The RMS current over this period was calculated to be 1.46 pu using the incremental currents generated from the Appendix D spreadsheet

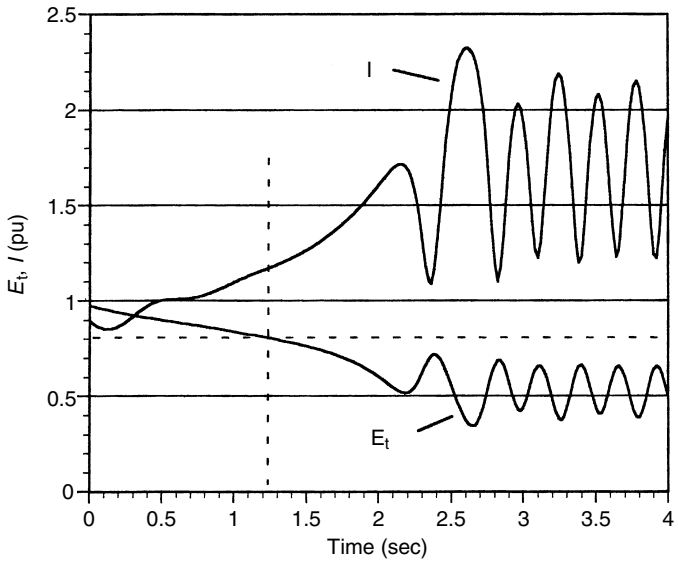


FIGURE 13.28 Sample system LOF high *Z*, E_t and *I*.

© 2006 by Taylor & Francis Group, LLC

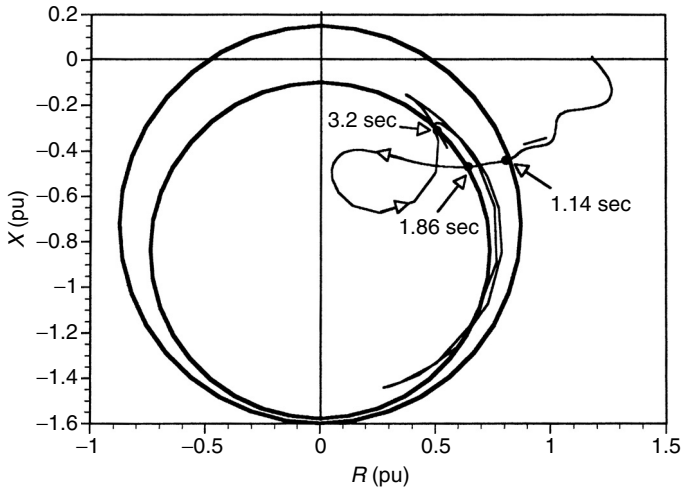


FIGURE 13.29 Sample system LOF low system *Z*, swing.

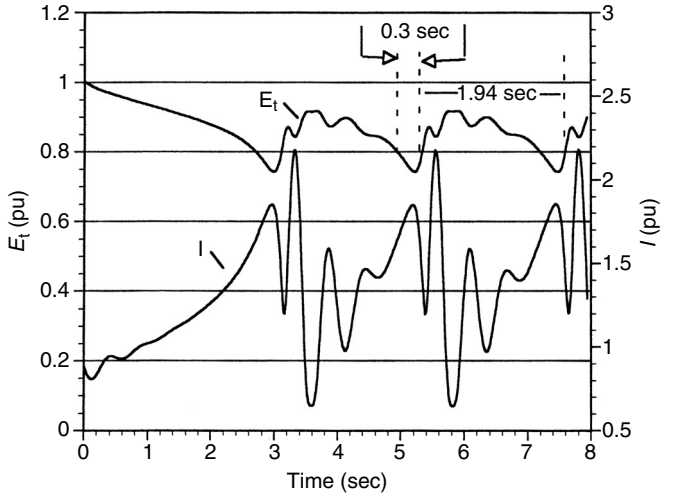


FIGURE 13.30 Sample system LOF low system *Z*, E_t and *I*.

and Equation (13.3). The stator short-time thermal capability for this current, from IEEE C37.102, is about 40 sec. The single-element scheme had been applied with standard settings, the generator would not have been protected for a LOF when all lines are in service, which is the normal configuration.

REFERENCES

1. Seetharaman, C. K., Verma, S. P. and El-Serafi, A. M., Operation of synchronous generators in the asynchronous mode, *IEEE Trans Power Apparatus and Systems*, 928–939, 1974.
2. Brady, J., Loss of excitation protection for modern synchronous generators, *IEEE Trans Power Apparatus and Systems*, 94 (5), 1457–1463, 1975.

© 2006 by Taylor & Francis Group, LLC

3. Darron, H. G., Koepfinger, J. K., Mather, J. R. and Pusche, P. A., The influence of generator loss of excitation on bulk power system reliability, *IEEE Trans Power Apparatus and Systems*, 94 (5), 1473–1481, 1975.
4. Tremaine, R. L. and Blackburn J. L., Loss-of-excitation protection for synchronous machines, *AIEE Transactions PAS*, 73 Part III, 765–772, 1954.
5. Alger, P. L., Franklin, R. F., Kilbourne, C. E. and McLure, J. B., Short circuit capabilities of synchronous machines for unbalanced faults, *AIEE Trans.*, 72, Part III, 394–403, 1953.
6. Choi, S. S. and Jia, X. M., Under excitation limiter and its role in prevention excess synchronous generator stator end-core heating, *IEEE Trans.*, 15 (1), 95–101, 2000.
7. Bérubé, R. G., Hajagos Les, M., and Beaulieu, R. E., A utilities perspective on under-excitation limiters, *IEEE Trans Energy and Conversion*, 10 (3), 532–537, 1995.
8. ABB Power, T&D Company, *Protective Relaying Theory and Applications*, Marcel Dekker, New York, 1994, 111–116.
9. Mackenzie, W. F., Imnof, U. A., Dewey, C., Emmerling, E. J., Freer, F. H., Horowitz, S. H. and Wagner C. L., "Loss-of-field relay operation during system disturbances, working group report June 1991 IEEE Transactions vol PAS-94 No. 5 Sept/Oct 1975, 1464–1472.

© 2006 by Taylor & Francis Group, LLC

14 Synchronization Protection

14.1 INTRODUCTION

Generators are removed from service and reconnected to the power system for various reasons: variations in load, maintenance and emergency outages, to name a few. Each time that a generator is returned to service it must be synchronized with the power system before the interconnecting breaker can be closed. Synchronizing is the act of matching the magnitude and frequency of the generator and system voltage and bringing the two voltages into phase alignment. A failure to properly synchronize can result in electrical and mechanical transients that can damage the generator, prime mover, GSU transformer, and severely perturbate the power system.

The potential severity of an out-of-phase closure is dependent on the strength of the system to which the generator is being synchronized. The stronger the system, the larger the potential out-of-phase current. Designs that interconnect multiple generators directly to a common bus would support more severe closures than designs that interconnect individual generators through a transformer.

Synchronizing is routinely accomplished along with the many other activities required to return a generator to service. Synchronizing equipment only gains prominence when protective functions associated with the synchronizing logic delay a unit's return to service, or, in the more odious case, when operation errors or equipment malfunctions result in severe nonsynchronous closure. The latter case can be very expensive.

Figure 14.1 is a vector representation of the variables associated with synchronizing. System voltage E_s and speed (frequency) are set by the power system. System frequency is very tightly controlled, usually within 0.005 Hz of nominal. System voltage will vary, but should not stray beyond $\pm 5\%$ of nominal during normal operations. With the machine disconnected from the power system generator voltage and speed are controlled by the plant operator or plant automatic control equipment.

During the synchronizing process, the generator and system frequency will differ. If the generator is assumed to be at a higher speed than the system, the generator voltage would be visualized on the vector diagram rotating about the fixed system voltage in a counterclockwise direction. The phase angle δ and voltage difference ΔE between the generator and system will vary at slip frequency, slip frequency being the difference between the generator frequency and system frequency.

Ideally, the generator and system voltages on either side of the open synchronizing breaker should be equal in magnitude and frequency and in perfect phase alignment at the instant of breaker closure. A perfect synchronizing would result in no electrical or mechanical system transients, hence no stress to the generator or system. In practice, both the electrical and mechanical systems are tolerant of small deviations from the ideal and synchronizing is often performed with an intentional mismatch of frequency and voltage.

Breaker closure is normally initiated with a small positive slip (the generator speed slightly greater than the system) and with generator voltage slightly higher and leading that of the system. This produces an initial power and reactive flow out of the generator. A power outflow assures antimotoring protection will not operate following breaker closure. An elevated generator voltage avoids a voltage dip and Var drain on the power system on synchronizing.

14.2 DAMAGE

Out-of-phase closing can result in damage to generator, prime mover and the associated GSU transformer. Magnetic forces created by high synchronizing current can loosen windings and

© 2006 by Taylor & Francis Group, LLC

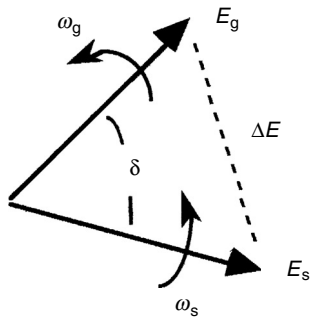


FIGURE 14.1 Synchronizing variables.

laminations in the GSU transformer and generator. Torsional stress imposed on the mechanical system can cause slippage of couplings, bearing misalignment, and fatigue damage to the shaft and turbine blades.[1] Increased shaft vibration following and out-of-phase closure or any other torsional event is a symptom of coupling or bearing movement.

14.2.1 Transformer Damage

The high current associated with severe out-of-phase closures produces both thermal and mechanical stress in a transformer. Thermal damage is not an issue, because high synchronizing current is limited to a few seconds and given the large thermal time constant of the transformer, temperature rise will not be excessive. The primary threat to the transformer is mechanical stress to the windings, which is proportional to the square of the current.

14.2.1.1 Maximum Withstand Current

Standards do not define out-of-phase withstand capabilities for transformers directly, but they do specify the peak asymmetrical current magnitude a transformer must withstand without damage. This current is defined in IEEE Std C57.12.00-2000. For Category III and IV transformers (larger than 5 MA, three-phase) the required withstand current is equivalent to a three-phase fault on the transformer leads with a specified source impedance. Numerically, the required symmetrical withstand current is specified as

$$I_{SC} = \frac{1.0}{Z_T + Z_s} \tag{14.1}$$

where Z_T and Z_s are the transformer and source impedance in per unit, both referenced to the transformer MVA base. The standard includes an asymmetrical factor, K, to account for the DC component.

The K factor is defined as

$$K = \sqrt{2}\left\{1 + \left[e^{-(\phi+\frac{\pi}{2})\frac{r}{X}}\right]\sin\phi\right\} \tag{14.2}$$

where X/r = reactance to resistance ratio of the total impedance to the transformer low side and $\phi = \arctan(X/r)$.

The source impedance (Z_s) used in Equation (14.1) is either a minimum source impedance specified in the purchase specification for the transformer or if no value is specified the appropriate value from Table 14.1 or Table 14.2 of the standard.

As an example, the sample system transformer is a 97 MVA 67/13.8 kV unit with $Z = 6.5\%$. Because no source impedance was specified when the transformer was purchased an estimate of the

© 2006 by Taylor & Francis Group, LLC

TABLE 14.1
System Impedance

Maximum System Voltage (kV)	System Fault Capacity	
	K_a (RMS)	MVA
Below 48.3	—	4,300
48.3	54	4,300
72.5	82	9,800
121.0	126	25,100
145.0	160	38,200
169.0	100	27,900
242.0	126	50,200
362.0	84	50,200
550.0	80	69,300
800.0	80	97,000

Source: IEEE Std C57.12.00-2000, IEEE Standard General Requirements for Liquid-Immersed Distribution Power, and Regulating Transformers.

peak asymmetrical current capability of the transformer can be made by using the source impedance for a 72.5 kV system from Table 14.1. The 9800 MVA fault capacity represents an impedance of $97/9800 = 0.0099$ pu on the transformer base. Assuming an overall X/r ratio of 50 ($K = 2.74$). The peak RMS current the sample system transformer must withstand is then

$$I_{\text{peak}} = 2.74 \frac{1.0}{0.065 + 0.0099} 36.6\,\text{pu}$$

14.2.1.2 Maximum Synchronizing Current

The synchronizing current is a function of the voltage across the open breaker at the instant of closure and the total system impedance. If the generator and system are both at the rated frequency prior to closure, the AC component of current at synchronizing is expressed as

$$I_{\text{AC}} = \frac{\sqrt{E_s^2 + E_g^2 - 2E_s E_g \cos\delta}}{X_d'' + Z_{\text{tr}} + Z_s} \tag{14.3}$$

The abrupt current change caused by an out-of-phase closing is governed by the same constraints as a fault conditions, namely current in, and an inductive circuit cannot change instantaneously. Therefore, synchronizing current will be asymmetrical, offset by a DC current component.

At the most severe closing angle, 180° out-of-phase, the peak RMS asymmetrical current can be written as

$$I_{\text{peak}} = \frac{2.0K}{X_d'' + Z_{\text{tr}} + Z_s} \tag{14.4}$$

For the sample system X_d'', X_s and Z_{tr} are 0.136, 0.078, and 0.065 pu, respectively, on the transformer's 97 MVA base. Assuming a worst case X/r value of 200, the maximum peak closing current for the sample system is

© 2006 by Taylor & Francis Group, LLC

$$I_{\text{peak}} = \frac{2.0 * 2.8}{0.136 + 0.065 + 0.078} = 20.1 \text{ pu}$$

This current is well below the peak current capability of the transformer (36.6 pu). This is generally the case. The reverse is true only when the sum of the system and generator subtransient reactance approach the transformer impedance.

A larger peak current can occur at closure if the generator is at a significantly lower frequency than system as would occur if the synchronizing breaker was closed after the unit was taken off line and is decelerating. The peak current with the generator speed less than that of the system can be estimated using the following equation from Ref. 2:

$$I_{\text{MaxPeak}} = \frac{2.83}{Z_1}\left(1 + \frac{E_g}{f_g}\right) \tag{14.5}$$

where Z_1 = total circuit impedance $X''_d + Z_{tr} + Z_s f_g$ = generator frequency per unit. This equation assumes the system is at rated voltage and frequency.

After closure, both the AC and DC components of current develop torque to pull the generator and system into phase alignment. If the generator is leading the system voltage, decelerating torque will be created to slow the generator. Conversely, synchronizing with the generator lagging the system will result in accelerating torque. In either case, synchronizing current will decay as a function of the electrical time constants and the inertia of the generator and prime mover, which governs the rate of acceleration or deceleration to phase alignment.

At high slip, it will require more than one slip cycle for the generator to accelerate to system frequency. As a result, the generator may slip poles several times. Each slip cycle will include a full out-of-phase current excursion as defined by Equation (14.3). The peak current value during each slip cycle will be less than a maximum closing current at 180° because there will be no DC component ($K = 1.0$) during the slip cycle.

14.2.2 Generator Damage

The issue of generator damage is far more complex. Again, standards to not specifically address synchronizing capabilities, but do require that a generator withstand a current equivalent to a maximum three-phase fault at the stator terminals with the generator at rated load, power factor, and with terminal voltage at 105%.[3,4] In the case of the sample system generator, the maximum three-phase fault current under these conditions is 8.32 pu (as calculated in Chapter 2).

The three-phase fault current can be applied as the maximum withstand limit when assessing generator winding durability for an out-of-phase event. This is because windings are subject to deformation that is directly related to the current magnitude alone. Unfortunately, the fault current criteria is not applicable to the mechanical system. There is no direct relationship between the magnitude of stator current and torque imposed on the shaft by electrical system transients. This would appear contrary to logic, because in the electrical system, power increases with current. However, shaft dynamics are far more complex and do not directly relate to any one variable.

14.2.2.1 Shaft Torque

All electrical system disturbances such as line switching, faults, load rejections, automatic line reclosing, and synchronizing out-of-phase cause a sudden change in the electrical torque imposed across the air gap onto the generator rotor. Although the magnitude of the electrical

© 2006 by Taylor & Francis Group, LLC

torque is a function of current, the response of the mechanical system is strongly influenced by form of the electrical torque, which can have three unique components, unidirectional, 60 Hz and 120 Hz.

The unidirectional torque component is proportional to the change in fundamental (60 cycle) current and voltage. This component appears as a change in the average shaft torque. Any sudden electrical disturbance will create a decaying component of current at the natural frequency of the electrical system. If the electrical system is without capacitors, the natural frequency will be DC. The interactions of this unidirectional current with the generator's rotating flux produce a decaying 60 Hz component of torque that acts on the rotor. If the electrical disturbance is a result of an unbalanced fault, the resulting negative-sequence current will produce a 120 Hz torque that will be sustained for the duration of the disturbance.

Figure 14.2 shows a typical turbine generator shaft system. The dynamic model for the shaft includes the mass of each major rotating element (generator, exciter, low- and high-pressure turbine, gearing in the case of gas turbines). Shaft sections are represented as weightless torsional springs interconnecting the masses. A shaft system will normally have the same number of natural frequencies as it has shaft sections. The mass distribution and the stiffness of the connecting shaft sections determine the natural frequencies.

When perturbed by an electrical disturbance, the shaft exhibits torsional vibration at all natural frequencies. Each natural mode exhibits a unique sensitivity to individual component of electrical torque and each type of electrical disturbance generates a unique mix of electrical torque components. Hence, there is large diversity in shaft response to different system disturbances.

Each mass will have unique motion dictated by the sum of the vibratory modes at its location. The interconnecting shaft sections experience strain as the masses on each end of the section move independently. The greater the difference in motions, the greater the strain.

Because standards require generators to withstand the effects of sustained three-phase fault current without damage, one would assume that this would represent the most severe service condition. However, this is not the case for the rotating components in the drive train. A three-phase fault at the generator terminal produces only moderate shaft stress when compared to other system disturbances. Automatic reclosing and out-of-phase synchronizing produce much higher shaft torque. As a benchmark, a three-phase fault produces electrical torque roughly equivalent to synchronizing 60° out-of-phase.[5] One reason for this is the fact that large generator shafts show a particular sensitivity to the unidirectional torque component that is more prevalent in the latter two cases.

The analysis of shaft torque is accomplished by solving differential equations that describe transient electrical torque produced by the generator and the response of the spring mass model used to describe the shaft system. The Mathcad™ worksheet included as Appendix E performs

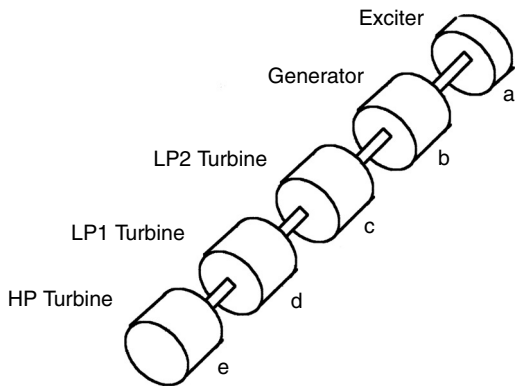


FIGURE 14.2 Turbine generator shaft.

© 2006 by Taylor & Francis Group, LLC

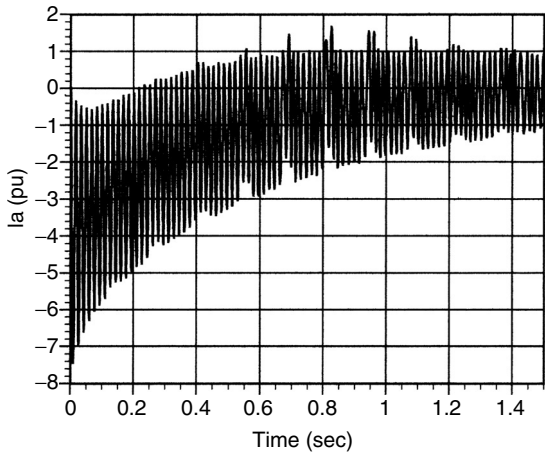


FIGURE 14.3 Three-phase stator fault current.

these calculations and was used to simulate shaft torsion and stator current transients following a three-phase fault and out-of-phase closure. This worksheet demonstrates modeling for the both d- and q-axes circuits of a generator and a five-mass shaft model. The sheet also shows the derivation of shaft natural frequencies as a function of the individual rotating masses and shaft stiffness and is available for down load from the publishers webside.

Figure 14.3 through Figure 14.8 are output from the Appendix E worksheet. They compare a three-phase fault at the stator terminals with no initial load on the generator to synchronizing with the generator leading the system by 120°. Synchronizing near 120° out-of-phase produces a more severe torsional duty than does a 180° closure. Also, a closure with the generator leading the system by 120° is normally more severe than a closure with the generator lagging the system by the same angle.

Figure 14.3 and Figure 14.6 represent stator current for the three-phase fault condition and the out-of-phase closure, respectively. These figures show that the three-phase fault current is larger and sustained longer than that of the torsionally more severe out-of-phase closure. The electrical torques produced by these conditions are plotted in Figure 14.4 and Figure 14.7. Both

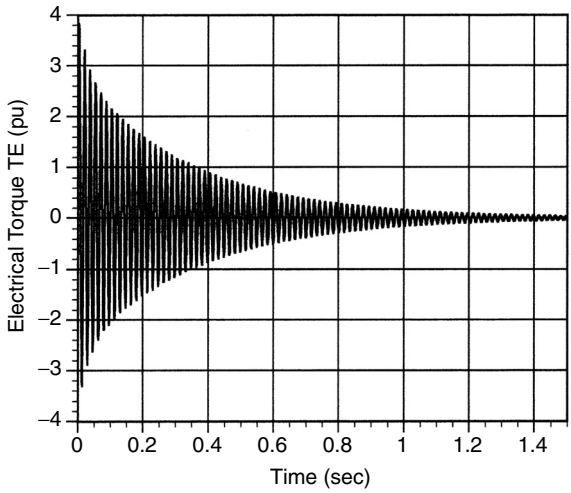


FIGURE 14.4 Three-phase electrical torque.

© 2006 by Taylor & Francis Group, LLC

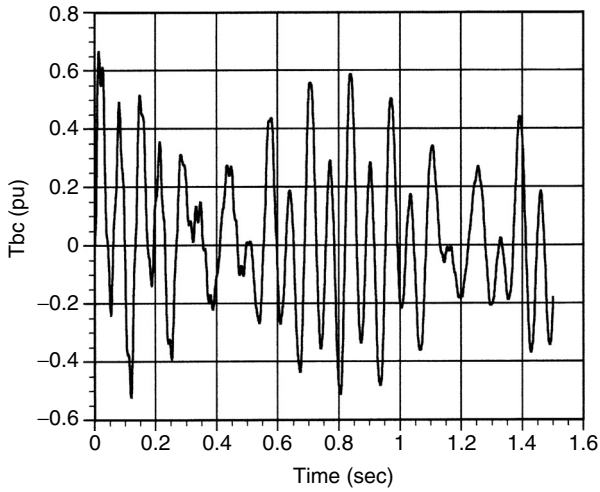


FIGURE 14.5 Shaft section b–c torque for three-phase fault.

conditions yield similar peak-to-peak torque magnitudes, but electrical torque from the out-of-phase closure (Figure 14.7) has a much larger unidirectional component.

The erratic nature of the shaft torque is apparent in Figure 14.5 and Figure 14.8. Maximum torque usually appears in the shaft section between the generator and prime mover, shaft section b–c from Figure 14.2. This is the case for both conditions studied. The resulting peak shaft torque for the out-of-phase event is 2.8 times rated torque and about four times the peak torque produced by the three-phase fault. Figure 14.8 includes the torsional response of the shaft section c–d for comparison. The torsion in this section is not as severe, but is significantly above rated torque.

14.2.2.2 Fatigue Damage

Although peak shaft torque values during a transient give an indication of the severity of the event, torque magnitude alone does not quantify damage. Damage is measured as a percentage of fatigue life lost during the event. This damage is cumulative. The fatigue life of a shaft section is expressed

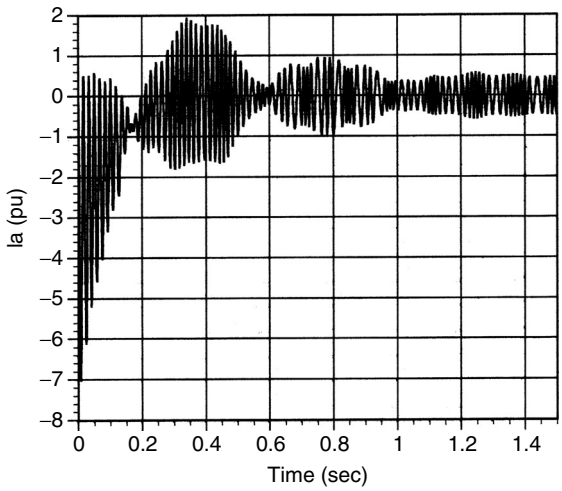


FIGURE 14.6 Out-of-phase closing current (120°).

© 2006 by Taylor & Francis Group, LLC

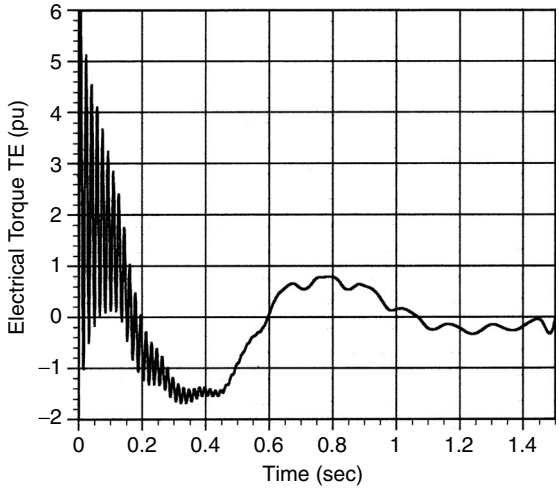


FIGURE 14.7 Electrical torque for 120° closing.

by a stress–life curve like Figure 14.9. This plot relates the number of stress cycles a material can withstand at each value of stress. These curves normally define the end of life at the onset of cracking. This occurs well before the shaft would shear. The number of tolerable stress cycles increases as stress decreases. The stress value at the point where the curve becomes asymptotic to the x-axis is known as the fatigue limit. It is assumed that stress below this value does not produce loss of life. Because stress is a measure of force per unit area, the stress in each shaft section is not only a function of shaft torque, but also diameter.

The fatigue life expended for each torsional event is primarily a function of stress magnitude, but it is also a function of the number of stress cycles imposed by the event. Oscillations in the shaft system, like any other vibratory system, will diminish with time as a function of system damping. The primary torsional damping components are steam-damping, windage, shaft material hysteresis, bearing oil film damping, and electrical damping.[6] Unfortunately, these elements produce very poor damping. At no load, which would be the applicable case for out-of-phase synchronizing, the damping time constant would be in a range of 8 to 30 sec.[7] Once torsional oscillations are initiated

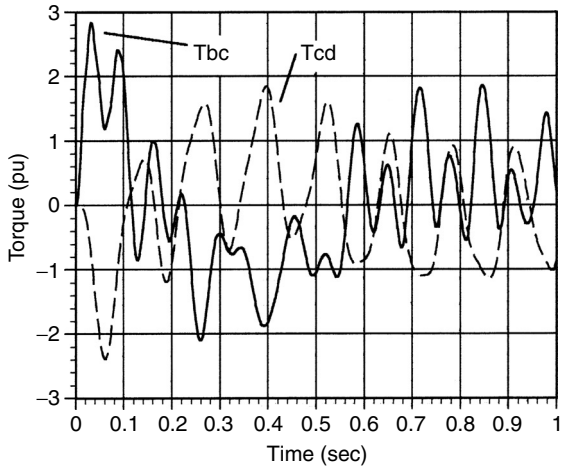


FIGURE 14.8 Shaft sections b–c and c–d torque for 120° closing.

© 2006 by Taylor & Francis Group, LLC

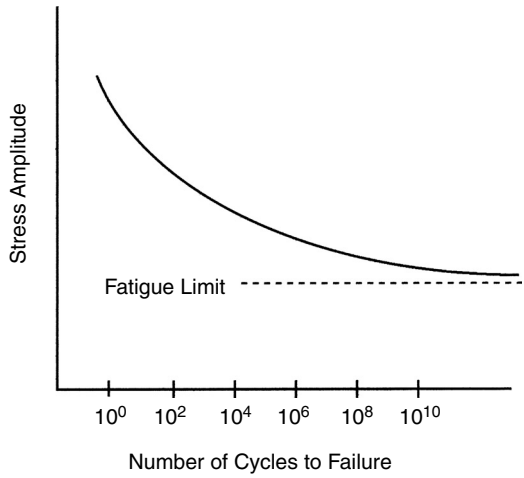


FIGURE 14.9 Life-cycle curve.

in the shaft by an out-of-phase synchronizing, they can persist for over 30 sec. Each torque excursion above the fatigue limit adds to the loss of life.[8]

A quantitative determination of loss of life for an event requires that each torque excursion following a disturbance be assigned a percent loss of life from the life-cycle curve. The loss of life for the event would then be the loss-of-life sum for all torque excursions until torque magnitude decays below the fatigue limit. This evaluation is convoluted because the life-cycle curve is derived from tests in which stress cycles are symmetrical. Because torsional excursion following power system disturbances are offset by unidirectional torque, they do not match the test condition. Complex methods of equivalentizing the actual torque cycle to the test condition must be employed to produce actual loss-of-life data.[9]

14.2.2.3 Relative Damage Assessment

The diversity of shaft damage for various system transients is shown in Figure 14.10. These data are taken from Ref. 10. It is the result of studies on two large steam-turbine generators at 1800 and 3600 rpm. A loss of life equal to 100% indicates that crack initiation is possible. The dark portions of the indicating bars show the range of damage for the specific units studied. The white extensions to the bar are estimates of the overall range of damage with different machine dimensions and system parameters. Because of the wide spectrum of parameters that influence loss of life, these data should be viewed as qualitative ranking of event severity, not as a basis for loss-of-life evaluation.

This figure shows that an out-of-phase closure can be one of the most severe events to which a shaft can be exposed. Also notable is the relative loss of life for the three-phase fault at the generator terminals with no interconnected system. This is the maximum stator current condition specified by standards and produces only moderate loss of life.

The loss of life incurred from an out-of-phase incident increases with slip frequency. When a closure occurs with the system and generator at significantly different speeds, the generator must accelerate or decelerate to match the system. The inertia of the generator and prime mover will determine the time necessary for this transition. With a substantial initial speed difference, several slip cycles may be required to make this transition. Each slip cycle will impose an additional torque component at slip frequency onto the rotor. Figure 14.11 shows synchronizing with the same initial voltage difference across the open breaker as existed for the synchronizing depicted by

© 2006 by Taylor & Francis Group, LLC

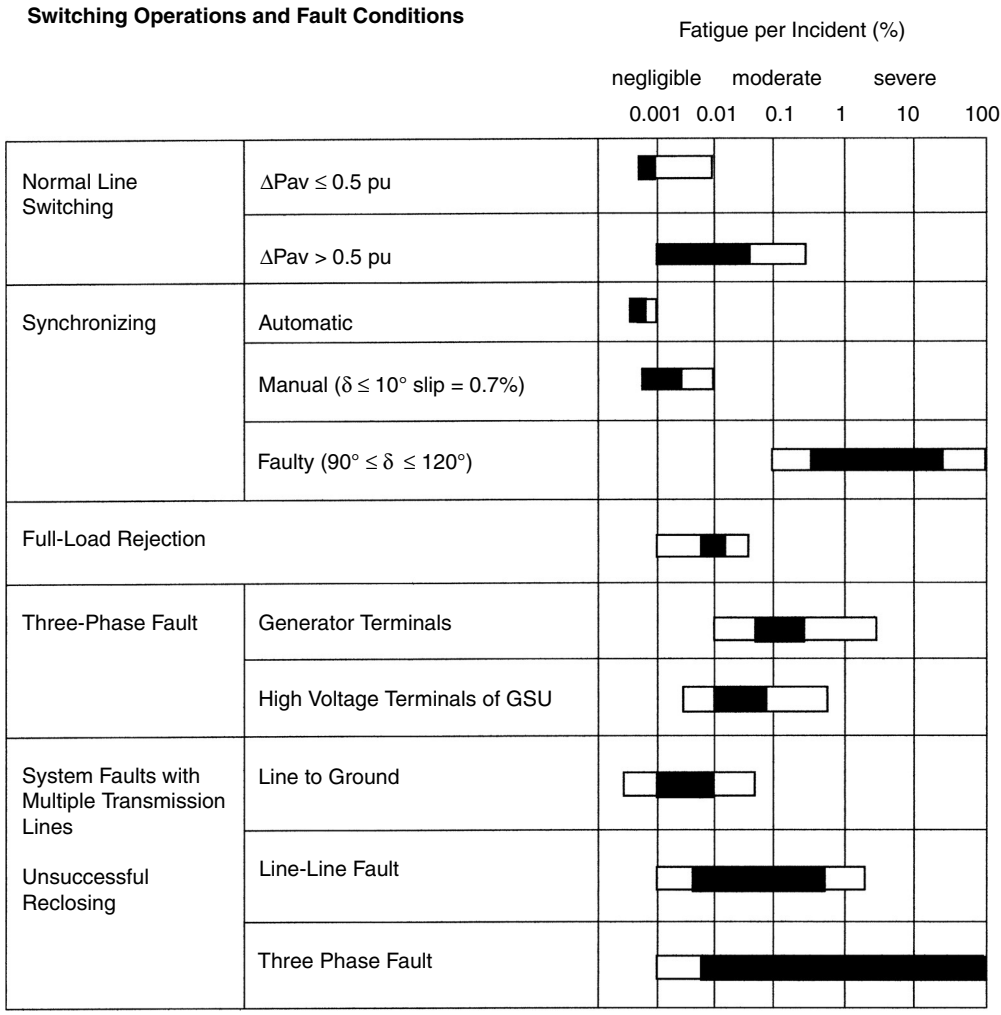


FIGURE 14.10 Fatigue for switching and fault conditions. (From Joyce, J.S., Kluig, T., and Lambercht, D., Torsional fatigue of turbine-generator shafts caused by different electrical system faults and switching operations, *IEEE Transactions*, Vol. PAS-97, Sept/Oct, 1978, pp. 1965–1973.)

Figure 14.6, except for in this instance the generator was assumed to be at 95% rated speed. The increased severity is obvious. One study reported that closure with a slip frequency of 0.5 Hz produces stress roughly equivalent to a closure 15° out-of-phase.[11] Slip frequency could approach the value of the lowest natural shaft frequency. If this occurred, the resulting shaft stress would be much greater, with shaft shear a possibility.

14.2.2.4 Considerations for Gas Turbines and Hydro Units

It is important to note that although most of the material presented above was derived for steam-turbine installations, this discussion is valid for gas turbines and hydro installations.[12] Modeling a gas turbine differs from a steam turbine in that the gas turbine and generator are connected through gearing. This necessitates adjustment of the per unit mass and per unit stiffness to reference the generator shaft revolutions per minute. In hydro units shaft torque may be less of a problem because the inertia of the water turbine is low compared to that of the generator itself; thus, the generator rotor dissipates much of the electrical torque.[5]

© 2006 by Taylor & Francis Group, LLC

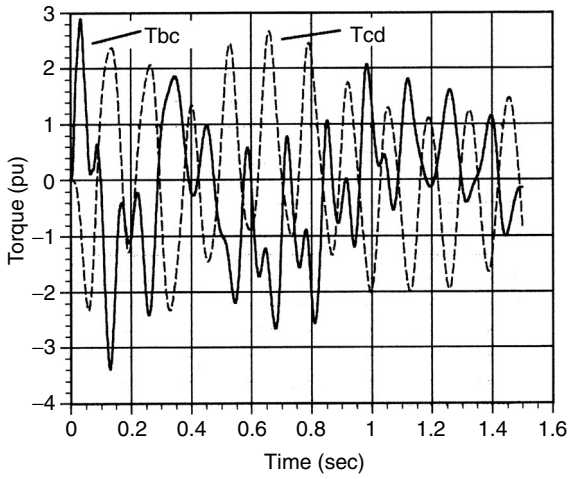


FIGURE 14.11 Out-of-phase closing with generator at 95% speed.

14.2.3 Breaker Considerations

A final consideration is breaker interruption following an out-of-phase closure. Breakers are designed to interrupt at current zeros, that is, when the instantaneous current is zero. The stator current following out-of-phase synchronizing includes decaying AC and DC components just as the generator fault currents described in Chapter 2. Following a fault at the generator terminals, system parameters can be such that the AC component decays faster than the DC component. The resulting waveform can be completely offset above or below the x-axis. Current zeros are then delayed a few cycles as determined by the decay of the DC component. This is evident in Figure 2.1, where the first current zero occurs about 10 cycles into the fault.

Fortunately, when a breaker is called upon to interrupt fault current under these circumstances, the arc voltage developed across the parting breaker contacts normally adds sufficient resistance into the circuit to drastically reduce the time constant for the DC component. The resulting rapid decay of the DC component restores current zeros to permit interruption. Typically, opening of the first pole of the breaker reduces the DC component to about 25% of its preopening value.

Out-of-phase synchronizing can also generate delayed current zeros, but the mechanism is somewhat different. Like the fault current case, current zeros are lost when the DC offset exceeds the AC component. For the fault condition, this constraint was met when the exponential decay of the AC component exceeded the decay of the DC component. In the case of out-of-phase synchronizing, the decay of the AC component is primarily a function of the rotor acceleration or deceleration.

If speed and voltage are precisely matched prior to synchronizing, the AC component of synchronizing current is solely a function of the displacement angle between the generator and system as defined by Equation (14.3). At the instant of closure, the synchronizing current produces electrical torque that acts to reduce the displacement angle. A rapid alignment hastens the decay of the AC component. An example of the resulting current waveforms is given in Figure 14.12. This figure depicts phase currents for a 60° closure with matched voltage and frequency. Current zeros are delayed in C-phase for 0.16 sec. Zeros initially exist in the A and B phases, but are lost with the rapid reduction of the AC component as the generator and system reach phase alignment. A closure near 60° results in a shorter time to phase alignment and in this case provides a greater delay in zero crossings than did a closure at 120°. The condition worsens significantly if generator speed differs from that of the system, as shown in Figure 14.13.

From a breaker standpoint, the out-of-phase condition is more severe than the loss of zeros for a fault condition. In the fault case, the resistive arc voltage inserted into the circuit when

© 2006 by Taylor & Francis Group, LLC

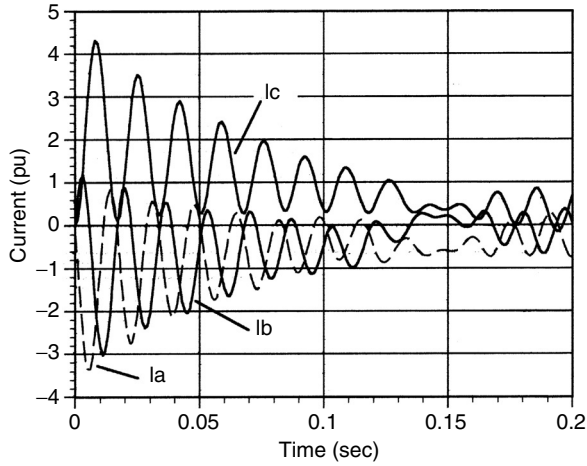


FIGURE 14.12 Stator current for 60° closure slip = 0.0.

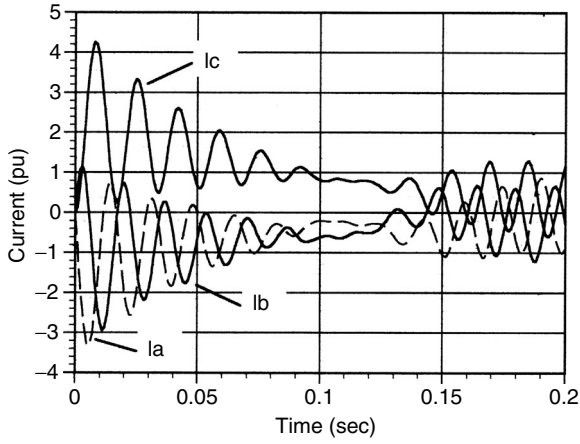


FIGURE 14.13 Stator current for 60° closure slip = 0.01.

the breaker contacts open sharply reduces the time constant of the DC component, effectively forcing current zeros. This mechanism is not effective in restoring current zeros for the out-of phase case.

Out-of-phase closures can actuate high-speed protective functions such as the "inadvertent energization" function, which will be discussed in the next chapter. If such relaying initiates a breaker opening during a period divorced of zeros, severe breaker damage can result. Such cases require individual analysis. Key factors are the current magnitude and the time after trip initiation that the breaker's arc extinguishing mechanism remains active. Typically, this would not exceed two or three cycles. In the case of a vacuum breaker, thermal damage can occur in the same time frame.

14.3 SYNCHRONIZING METHODS

Synchronizing methods fall into two general classifications, manual synchronizing and automatic synchronizing. During a manual synchronizing, the operator adjusts generator speed and voltage,

© 2006 by Taylor & Francis Group, LLC

and initiates the breaker closure command. In its pure form, manual synchronizing is accomplished by the operator without aid or constraint. Current practice is to supervise manual synchronizing with protective functions to prevent out-of-phase closures that would result from operator error. Sophisticated protective functions with settable parameters have become an integral part of both automatic and manual synchronizing schemes.

For the first 40 yr of the power industry, synchronizing was entrusted to the skill of a well-trained operator. Such responsibility would not be delegated to an automatic scheme that could malfunction and initiate a disastrous out-of-phase closure. However, as generator size increased and designs became more efficient, both electrical and mechanical systems became less tolerant of the bumpy synchronization of impatient or inattentive operators. A less-tolerant design is reflected by the tight limits now placed on closing angle, voltage difference and slip frequency by manufacturers.

Plant complexity also increased dramatically, putting more demands on the operating staff and diverting the operator from the once sacred act of synchronizing. These changes and the catastrophic damage resulting from some operator misjudgments led to the evolution of synchronizing equipment from unrestricted operator-controlled to the fully automated hands-off synchronizing schemes that have now become commonplace.

Plants are designed with both manual and automatic synchronizing equipment. The intent is that the automatic system is preferred and the manual system is used only when the automatic system is unavailable. However, in practice, the method actually implemented is dependent on individual plant philosophy and, in some cases, the level of frustration with the automatic synchronizing equipment.

14.3.1 Manual Synchronizing

Synchronizing equipment has come a long way from the dark lamp synchronizer used in the early days of parallel generator operation. This method used lamps connected across like phases of the open breaker. Two voltmeters were used, one to measure system voltage and the other to measure generator voltage. First the operator would bring the generator near rated speed using the governor controls. He then would adjust the voltage regulator to match the generator voltage to system voltage. The operator would then watch the lamps. The lamps pulsed as the generator voltage rotated with respect to the system voltage at slip frequency. The lamp would be at maximum brilliance when the generator and system were completely out of phase (180° displacement) and completely extinguished when the two voltages were in phase (zero degree displacement) with identical magnitudes. The operator would then make final adjustments to the generator speed until the light pulsations were very slow. This is indicative of a very close speed match between system and generator frequency. The operator would initiate a breaker close when the lamps were dark, indicating matching voltages and phase alignment.

Obviously, this system is not perfect. The maximum rate of pulsation, which determines the frequency difference at closure, is a matter of operator judgment or, in some cases, operator impatience. Also, the lights will go out at some minimum voltage for luminescence not at zero voltage. There is also a delay between the initiation of the close signal and the actual breaker closure.

The dark lamp method of synchronizing is certainly an inexpensive design. However, the potential for damage from a major out-of-phase closure or reduced service life due to repeated hard closures has led to the development of more secure synchronizing schemes.

Manual synchronizing equipment in current use is depicted in Figure 14.14. System and generator voltage equality is still determined from metering provided on each side of the synchronizing breaker. The frequency and phase angle match between the two systems is now determined by observation of a synchroscope, as shown in Figure 14.15. If the generator frequency exceeds the system frequency, the indicator on the scope will rotate in a clockwise direction. If the generator frequency is below that of the power system, rotation will be in the counterclockwise direction.

© 2006 by Taylor & Francis Group, LLC

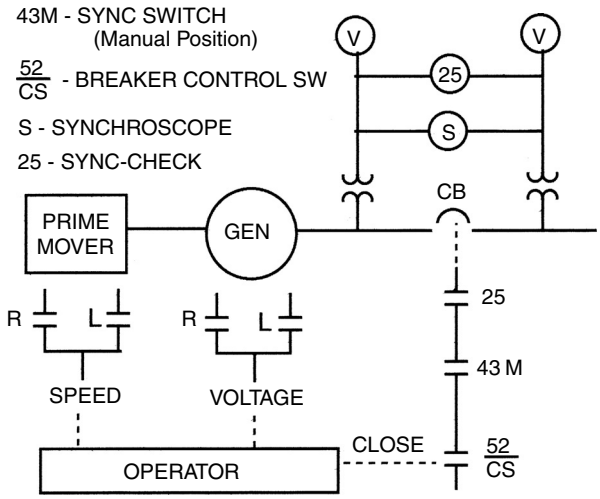


FIGURE 14.14 Manual synchronizing.

The speed of rotation is indicative of the frequency difference (slip) between the two systems. The position of the scope also indicates the instantaneous phase displacement between the two voltages. At the 12:00 position, voltages are in phase. At the 2:00 position, the two voltages would be $360 * 2/12 = 60^\circ$ apart.

To gain a feel for the synchronizing process, assume a generator manufacturer specifies synchronizing must be within $\pm 10^\circ$ of the in-phase (zero degree) position with slip less than ± 0.067 Hz. The slip limitation translates to a maximum scope speed of less than one revolution in 15 sec ($1/0.067 = 14.9$ sec). The angular limit of $\pm 10^\circ$ requires the operator to initiate breaker closure when the synchroscope indicator is between one-third of the distance from 12:00 to 11:00 and one-third the distance from 12:00 to 1:00 ($10/360 * 12 = 0.33$).

In a pure manual synchronizing scheme, the operator initiates an unsupervised close command to the breaker from the breaker control switch. This operator-only design has become nearly extinct. Now, at a minimum, manual mode closing is supervised by a sync-check relay (Device 25) in series with the control switch. The sync-check relay measures the phase angle between the generator and system voltage. The relay will close its contact only when the voltages are within a preset angular limit, which is typically 10° or less either side of the in-phase position for a generator application, and slip is within a preset limit. Much larger angular settings are used for transmission line application. This design retains the operator's control over closing, but prevents him from making a gross out-of-phase closure.

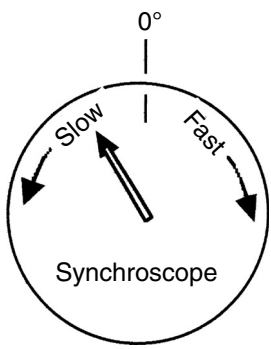


FIGURE 14.15 Synchroscope.

© 2006 by Taylor & Francis Group, LLC

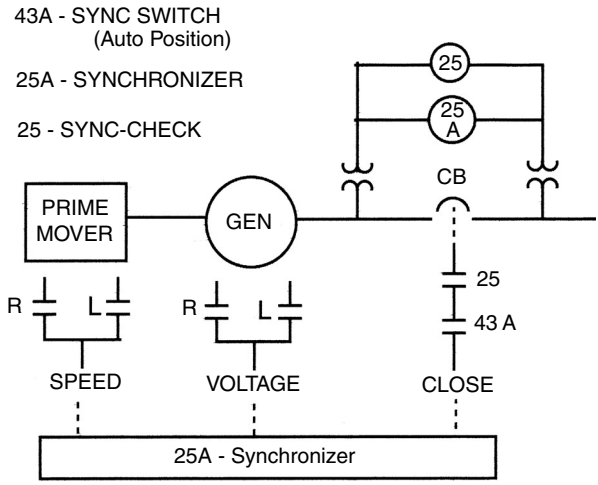


FIGURE 14.16 Automatic synchronizing.

14.3.2 Automatic Synchronizing

Automatic synchronizers perform all the monitoring and control functions necessary to synchronize the generator and close the breaker without operator intervention, as illustrated in Figure 14.16. The operator controls the initial startup and early acceleration of the generator. As the generator accelerates, voltage rises. At about of 70 to 80% rated voltage, the automatic synchronizer is capable of measuring generator frequency and takes control of the synchronizing. The autosynchronizer actuates the governor and voltage regulator to meet slip, voltage magnitude and phase angle limits set within the synchronizer. When operating parameters are within the preset limits, the synchronizer issues a close command to the synchronizing breaker.

Depending on the type of synchronizer, a breaker close signal may be generated as soon as all parameters fall within the predefined limits. Most electronic synchronizers are of the anticipatory type, when all limits are satisfied the synchronizer will use real-time slip measurements and the breaker closing time to calculate the close initiation angle necessary to produce a closure at the zero degree position. At the calculated angle, the synchronizer issues the close command. Anticipatory synchronizers require some minimum system slip to operate. State-of-the-art synchronizers can operate with slip as low as 0.0001 Hz. This equates to one synchroscope revolution in 2.8 h.

Speed matching to this accuracy is not normally achieved. Although such a close match is ideal for a bumpless synchronization, at this slip breaker closing will be delayed about 5 min for every 10° the generator voltage must travel to reach the in-phase position. Most anticipatory synchronizers issue a bump pulse to the governor if voltage is within acceptable closure limits but slip is very low. Implementation of this feature accepts the slight increase in slip to expedite breaker closing.

Automatic synchronizers include a variety of settable closing limit parameters to assure safe synchronization. However, these limits are useless if the synchronizer itself malfunctions. To prevent damage from this type of failure, the breaker close command from the automatic synchronizer (Device 25A) is normally supervised by a sync-check relay (Device 25) as shown in Figure 14.16. This is often the same sync-check relay that supervises manual synchronizing.

14.4 SYNCHRONISM CHECK RELAYS (DEVICE 25)

The sync-check relay is applied in series with breaker closing signals initiated by the operator or automatic synchronizing equipment. Traditionally, the relay only provided verification that slip

© 2006 by Taylor & Francis Group, LLC

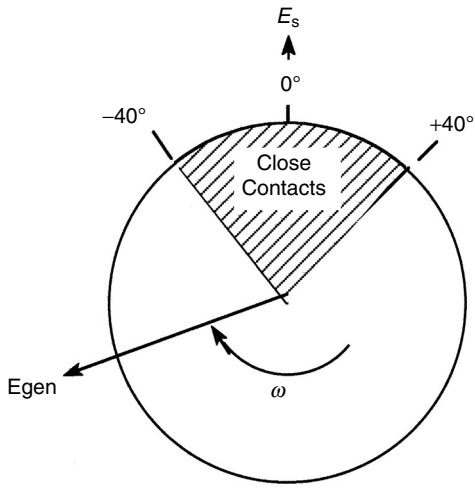


FIGURE 14.17 Closing angle.

and phase angle were within preset limits. The advent of microprocessor technology has greatly expanded the complexity and the level of supervision provided by this function. These advanced capabilities will be discussed later. However, we will first look at attributes that are common to all synch-check applications.

All sync-check relays are set for a maximum closing angle. This defines the maximum deviation either side of the zero degree position for which the relay will close its contacts. For instance, if a relay is set for 40°, the relay will close its contacts with voltage $\pm 40^\circ$ from the in-phase position as shown in Figure 14.17. In other words, the 40° setting will allow closure with the generator leading or lagging the system voltage by up to 40°.

All sync-check functions also limit the maximum slip frequency for breaker closure, but the way this is accomplished differs for electro-mechanical and microprocessor relays.

All sync-check functions require potential on both inputs to operate. If the generator is required to supply load while isolated from the power system, or to restore the power system following regional outage (black start), it will be necessary to close the synchronizing breaker into a deenergized bus. This requires additional logic. A switch could be used to bypass the sync-check contact in the breaker closing circuit. However, such a switch, if left in the wrong position during normal operation, would negate the sync-check function with potentially disastrous results. Instead, the logic shown in Figure 14.18 is often used. Undervoltage element Device 27 and overvoltage Device 59 operate to confirm a dead bus and normal generator voltage. Under these conditions, generator voltage is applied to both sync-check relay inputs to allow a breaker closure.

14.4.1 Electromechanical Sync-Check Relays

Electromechanical sync-check relays use the induction disk principle, with two sets of coils acting on the disk. Operating torque proportional to the vector sum of the two input voltages is produced by one set of coils. The other coil set produces restraining torque in proportion to the vector difference of the voltages. The assembly also includes a restraint spring and drag magnet. The generalized torque equation for the electromechanical sync-check relay is given by:

$$T = K_o|(V_x + V_y)^2| - K_R|(V_x - V_y)^2| - T_s \tag{14.6}$$

where T = torque applied to the disk, K_o = operating torque constant, K_R = restraint torque constant, V_x, V_y = input voltages, and T_s = restraint spring torque.

© 2006 by Taylor & Francis Group, LLC

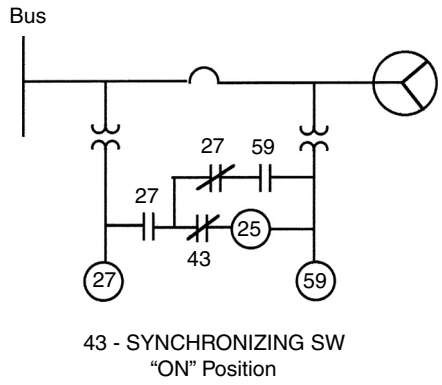


FIGURE 14.18 Dead bus closing logic.

The maximum closing angle is set by adjusting the operating and restraint constants K_o and K_R such that net torque is zero at the desired angle. Manufacturers claim accuracy of ± 3 or 4° for these relays, but closing angle settings are normally in 10° increments.

From the torque equation, it is obvious that relay operation is not only a function of phasing but also voltage magnitude. The published closing angle for this type of relay is obtained with rated voltage on both inputs. At reduced voltage, operating torque is reduced and a smaller angle is required to close the relay contacts. A typical voltage vs. closing angle curve for an electromechanical sync-check relay is plotted in Figure 14.19. The plot assumes rated voltage is applied on one input and reduced voltage on the other input.

Relay operating time is primarily dependent on the operating torque applied to the disk and the time dial setting, but the drag magnet, and spring tension are also factors. The operating time is important because it establishes the maximum slip frequency for which this relay will operate.

In practice, the frequencies of the generator and system are not equal prior to synchronizing. Some slip is always present. The sync-check relay monitors the relative phase position of the two voltages and initiates relay timing when the voltages are within the angular setting window. If the relay is to operate, slip must be such that the voltages remain within the operating angle window until the relay times out. If the slip frequency is too high, the voltages will exit the relay characteristic before timing is complete, thus preventing a breaker closure.

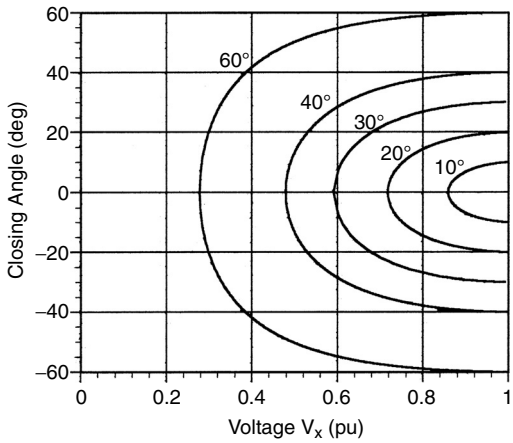


FIGURE 14.19 Electromechanical relay voltage vs. closing angle.

© 2006 by Taylor & Francis Group, LLC

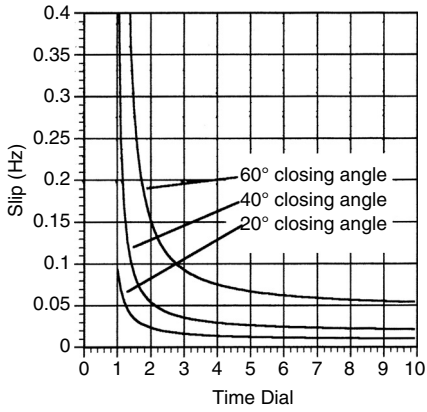


FIGURE 14.20 Time dial vs. maximum slip.

Ideally, the relationship between operating time and allowable slip frequency is

$$Slip(\text{Hz}) = \frac{2 * \delta_{\text{set}}}{(360 * t)} \tag{14.7}$$

where t = time delay, and δ_{set} = relay angular setting which is one half of the angular operating window. A relay set at 10° with a 0.5 sec delay theoretically will not operate if the slip is greater than $2 * 10/(360 * 0.5) = 0.11$ Hz. Unfortunately, the relationship between the time delay setting and maximum slip is not straightforward when applied to an electromagnetic relay. The torque applied to the induction disk varies with phase angle. As a result, the operating time is a function of slip and a direct computation of maximum slip is not possible. Instead, the maximum slip for contact closure is set using slip vs. time dial curves provided by the relay manufacturer. Such a plot is shown in Figure 14.20.

Electromechanical sync-check relays should not be applied such that both inputs are continuously energized. This will result in vibration that will, over time, damage the relay. Instead, one relay input should be connected through the contact of the synchronizing switch (Device 43) that closes when synchronizing is activated, as shown in Figure 14.18.

14.4.2 Electronic-Based Sync-Check Relays

Solid-state and microprocessor technology has allowed the development of algorithms to monitor a host of voltage and frequency conditions pertinent to safe synchronization. The most important of these is the direct slip calculation afforded by many microprocessor-based relays. The following are features offered by various electronic synch-check relay manufacturers:

- Phase angle supervision
- Slip frequency limitation
  - Angle-time limit (similar to electromechanical relay)
  - Minimum/maximum slip frequency limits (Direct slip measurement)
- Anticipatory close initiation
- Minimum and maximum voltage limits
- Maximum difference voltage
- Generator voltage priority check
- PT phase angle compensation
- Voltage magnitude compensation
- Built-in dead bus logic

© 2006 by Taylor & Francis Group, LLC

The supervision afforded by these relays may appear excessive, but is in line with synchronizing specifications provided by turbine-generator suppliers and with current operating philosophy. Synchronizing guidelines provided by generator manufacturers can include not only closing angle and slip limitations, but also maximum voltage difference and, in some cases, a maximum positive and negative slip is specified.

14.4.2.1 Phase Angle Supervision

This function is obviously not unique to electronic-based sync-check relays, but an accuracy of $\pm 1^\circ$ is. Electromagnetic relays claim accuracy to 3 or 4°. The operating time for electronic-based relays is also much faster than their electromechanical counterparts.

14.4.2.2 Slip Frequency Limitation

An important advantage provided by electronic relays is improved implementation of the maximum slip limitation. Two methods of slip calculation are employed by electronic relays. The time-angle method used by electromechanical relays has been copied by some solid-state relay designs. The advantage found in electronic-based relays, aside from accuracy, is that timing is independent of system conditions. This allows the maximum slip to be computed directly from Equation (14.7). If such a relay is set at 10° and breaker closure is to be inhibited if slip exceeds 0.1 Hz, the required delay for the relay is calculated directly as

$$2 * 10/(360 * 0.11) = 0.50 \,\text{sec}$$

The disadvantage of the time-angle method of slip detection is that closing is always delayed, even when the voltages are in ideal alignment.

Microprocessor technology has permitted the direct measurement of real-time slip. This is a major advancement in synchronizing control. The slip frequency limit in relays with this capability is set directly in terms of hertz. These relays often allow a permissive range of synchronizing slip to be defined by offering maximum and minimum slip settings. This slip window is necessary when manufacturer recommendations include positive or negative slip stipulations. As an example, the acceptable range of synchronizing slip might be specified as 0 to +0.1 Hz or −0.08 to 0 Hz. Directly slip frequency measurement also allows the relay to provide a permissive close signal immediately when the slip criteria are met.

14.4.2.3 Anticipatory Close Initiation

This feature is fairly standard on relays that calculate slip directly. It allows the relay to initiate a closing signal to the synchronizing breaker in advance of the zero degree position such that breaker closure occurs at zero degrees. Settings for a relay equipped with this feature must include the closing circuit delay time, which is the summation of the breaker closing time, the sync-check relay delay and any other close circuit delays. The initiating angle is calculated as

$$\delta(\text{deg}) = 360 * Slip(\text{Hz})t \tag{14.8}$$

where t = close circuit delay time and slip = real time slip calculated by the relay. Generally, microprocessor-based relays can effect a closure within $\pm 0.5^\circ$ of the in-phase position.

14.4.2.4 Minimum and Maximum Voltage Limits

The maximum and minimum voltage limits define the permissible range of system and generator voltages for synchronizing. The system and generator limits are usually independant settings.

© 2006 by Taylor & Francis Group, LLC

14.4.2.5 Maximum Voltage Difference

This setting limits the maximum absolute magnitude difference between the generator and system voltage.

14.4.2.6 Generator Voltage Priority

This setting is a binary True or False setting. If set True, the generator voltage must exceed the system voltage to allow breaker closure. The option assures Var flow out of the generator upon synchronization, thus avoiding a voltage dip on the system.

14.4.2.7 PT Phase Angle Compensation

A synchronizing relay must obtain potential from both sides of the synchronizing breaker. In the interest of economy, these voltages may be derived from opposite sides of the GSU transformer (Figure 14.21). If the transformer is connected wye-delta, such voltages will have a 30° phase displacement from one another. Compensation is necessary if these voltages are to be used for synchronization. This compensation has traditionally been accomplished using appropriately connected auxiliary PTs. Now, many microprocessor relays include settable compensation to rotate the voltage vectors internally, eliminating the need for auxiliary PTs. This feature simplifies wiring and reduces insulation cost, but it also has the potential to cause an out-of-phase synchronization if an incorrect setting is applied.

14.4.2.8 Voltage Magnitude Compensation

Ideally, the magnitude of the two voltage inputs to the sync-check should be equal when the generator terminal voltage and system bus voltages are equal. Unfortunately, this is often not the case. Slight differences in PT ratio or PT burden (load) will produce different secondary voltages with identical primary voltages. Electronic-based relays often include settable input multipliers or settable PT ratios that can be used by the relay to adjust for these differences. When settable PT ratios are used, voltage matching is then based on the calculated primary circuit voltages, not the secondary voltage at the relay input.

Figure 14.21 illustrates a configuration where this correction is extremely useful. With potential taken from either side of the GSU transformer, regardless of the care taken in matching the high-voltage and generator PT ratios, the voltage at the synchronizing equipment is dependent on the voltage tap setting of the GSU transformer. If the secondary synchronizing voltages were perfectly matched with the GSU on, say the nominal tap, a tap change necessitated by system condition would result in a 2.5% mismatch. When this generator is synchronized, we say the generator terminal voltage is adjusted to match the bus voltage, but, in reality, it is the secondary voltages that are

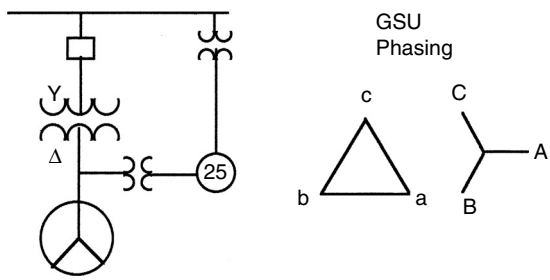


FIGURE 14.21 Phasing of potential circuit.

© 2006 by Taylor & Francis Group, LLC

matched. If unresolved, the aforementioned 2.5% secondary error will cause an equivalent primary voltage error across the open breaker prior to synchronizing.

One caution when applying correction for voltage drop in the potential circuit: the correction is only effective if the voltage drop is constant. If potential circuit loading varies with operating conditions, ideal correction is unobtainable. At installations where CCVTs (Capacitor Coupled Voltage Transformers) are used, output voltage can be burden sensitive making these circuits unsuitable as a source of synchronizing potential.

14.4.2.9 Built-In Dead Bus Logic

If enabled, this feature allows the synchronizing breaker to energize a dead bus. The logic mimics that shown in Figure 14.18. When dead bus logic is enabled, setting are required for functions 27 and 59. The relay will permit a breaker closure without a synchronism check if the bus voltage is below the dropout setting of function 27 and the generator voltage is above the pickup setting of function 59.

14.5 AUTOMATIC SYNCHRONIZER (DEVICE 25A)

The automatic synchronizer replaces the operator in the synchronizing process. It provides the speed and voltage control necessary to bring the unit to a frequency, voltage and phase angle match with the power system and them initiate a breaker close command. Many synchronizer settings are similar to those required for the sync-check elements, namely:

Phase angle limit
Slip frequency limit
Minimum and maximum voltage limits
Maximum difference voltage limit

The difference here is that in the synchronizer, voltage and frequency settings define the bandwidth for the frequency and voltage control functions provided by the synchronizer. Microprocessor-based synchronizers may also include auxiliary features found in sophisticated sync-check relays, such as:

Generator voltage priority check
Anticipatory close initiation
PT phase angle compensation
Voltage magnitude compensation

14.5.1 Speed Control

For many years the addition of autosynchronizing was not a guaranteed operational improvement. Some voltage control problems occurred, but speed control had been the main issue.

Speed control of a generator is an important aspect of manual and automatic synchronizing. The limit of a generator's speed control defines the limit of sync-check and autosynchronizer settings. Touchy governor controls with overshoot and poor damping make close frequency control very difficult and time-consuming. Likewise, slowly responding systems test operator patience. In either case, poor control is not compatible with small closing angle or low slip settings on synchronizing equipment.

These control problems are caused by response lags in the system. A major delay in speed control is caused by the large inertia of the generator and prime mover. Other lags are introduced

© 2006 by Taylor & Francis Group, LLC

by delay in the governor controls, steam pressure buildup, operating time of fuel racks, and steam valves. Hydro units are particularly vulnerable to control problems because of the large inertia of the water wheel and the inertia of water in the long penstock.

14.5.2 Frequency Modulation Speed Control

Older autosynchronizing equipment often incited the worst speed control behavior because of the control method employed. A fundamental principle of control system design is proportionality. The amount of correction applied to a system should be proportional to the deviation from the desired operating point. Older speed matching equipment often accomplished proportionality by applying a fixed-duration corrective pulse to the governor each slip cycle, as illustrated in Figure 14.22.

The greater the slip, the more often the pulses. This is called frequency modulation control. It is easy to implement, but it often produces a system prone to excess overshoot and hunting because it does not accommodate system lags.

If the slip frequency were 3 Hz three corrective pulses would be issued to the governor each second. Assuming the generator speed is slow, each pulse would initiate a boost in energy input to the prime mover. After 10 sec, 30 boost pulses have been given, but because of lags the generator is just beginning to respond to the first boost. As the generator accelerates, boost pulses continue at a reduced rate until speed reaches the lower limit of the control bandwidth. The pulses stop, but acceleration continues because the backlog of boost pulses has produced excess input energy. Overshoot occurs as speed exceeds the upper limit of the speed bandwidth. Now, retarding pulses begin and increase in frequency as slip increases, eventually slowing the generator and producing undershoot. This process is depicted in Figure 14.23.

After what can be minutes of hunting, the system damps to near synchronizing speed and the second problem with this method of control becomes evident. At low slip there would still be only one pulse per slip cycle with the same duration as the initial pulses, while at a slip of, say, 0.1 Hz, there would be only one brief pulse every 10 sec. The result is a very long wait to reach final synchronizing speed.

These control problems are often resolved by widening the slip bandwidth on the synchronizer to give the automatic equipment a bigger target or by a return to manual synchronizing.

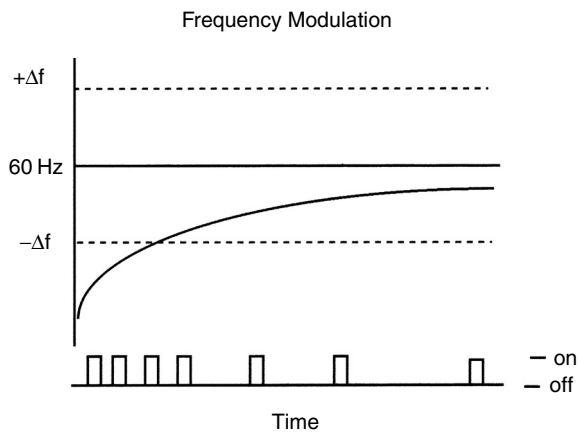


FIGURE 14.22 Frequency modulation.

© 2006 by Taylor & Francis Group, LLC

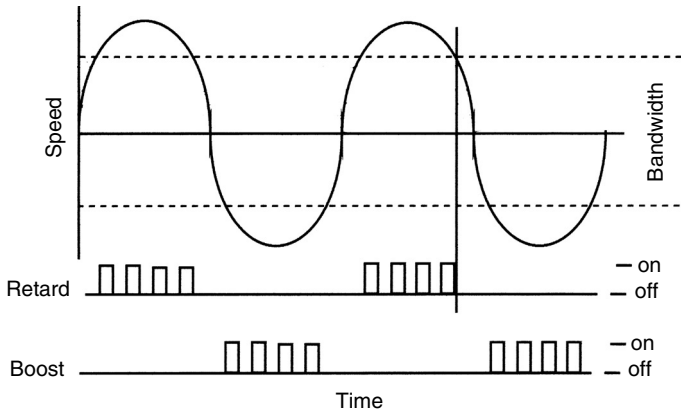


FIGURE 14.23 Hunting with frequency modulation.

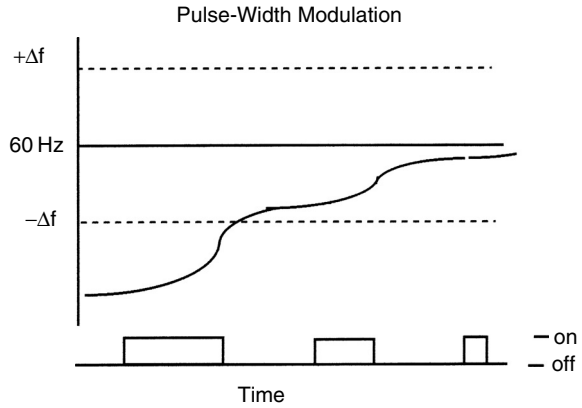


FIGURE 14.24 Pulse width modulation.

14.5.3 Pulse Width Modulation Speed Control

The reason manual synchronizing was a better option is that skilled operators apply the principle of proportionality in a different manner. They vary the duration of the pulse, not the frequency — the greater the slip, the longer the pulse. The operator would then wait for the system to stabilize before another pulse was initiated. This method, known as pulse width modulation, is shown in Figure 14.24. A proportionality constant is set in the synchronizer to vary the pulse width as a function of slip. The duration of pulse off time is set to allow system response to the preceding pulse. Pulse width modulation provides a fast method to speed control because it accommodates system lag and is now used by most autosynchronizing equipment.

14.6 SLOW BREAKER PROTECTION

Both manual and automatic synchronizing are dependent on prompt breaker response following a close initiation. There have been a number of incidents where breakers have displayed closing times far in excess of their design values, resulting in out-of-phase closures.

© 2006 by Taylor & Francis Group, LLC

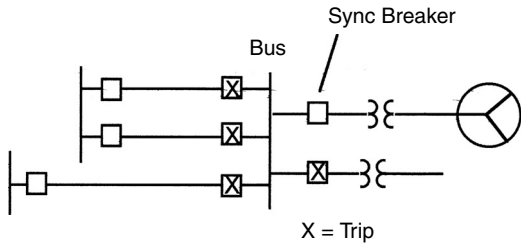


FIGURE 14.25 Slow CB close tripping.

Slow closing may be a result of faulty lubrication, corrosion, inadequate control voltage, or problems with solenoids, coils, or the latch mechanism. Breakers normally require 5 to 15 cycles to close. During a slow close event, a breaker may require seconds to close.[13] A three-second delay with 0.07 Hz slip would result in a closure at 76° out of phase. These incidents are more likely after the breaker has been in the open position for an extended period of time. One of the precautionary measures that can be taken to prevent such closure is to exercise the breaker prior to synchronizing. This is only possible if the generator can be isolated for the test closure.

A slow close defeats all the redundancy and technology built into the synchronizing schemes previously discussed. Consequently, delayed close protection is now being applied at many installations. A major constraint on slow-close protection is that once a close signal is given, the breaker must complete the close operation before it can be tripped. Opening a partially closed breaker could result in a catastrophic failure; therefore, slow-close protection must trip all breakers adjacent to the synchronizing breaker, as shown in Figure 14.25. Slow breaker protection is usually implemented through the trip circuit of the bus differential or the synchronizing breaker's breaker failure scheme.

Slow-close protection has several forms. The simplest is a timer actuated when the close signal is initiated. If closure does not occur within the set interval, a slow close is declared, tripping all adjacent breakers. More advanced schemes are incorporated into microprocessor-based sync-check relays. These schemes monitor the closing angle. If, after a close initiation, closure does not occur prior to a set maximum close angle, a trip is initiated. Advanced schemes usually include a monitor function that times each breaker closure and alarms without a trip if the operating time is greater than normal, but not long enough to cause damage. The intent is to alert the operator so that maintenance can then be scheduled to correct the problem.

14.7 SETTINGS

The sync-check and automatic synchronizers should be set within the limits recommended by the turbine-generator manufacturer. A typical recommendation might be for a maximum closing angle of $\pm 10°$, maximum voltage difference of 0 to +5% and a maximum slip of 0.067 Hz.[1]

To optimize protection, minimum settings should be applied. Setting a 1.0° closure angle with a max slip of 0.001 Hz would guarantee a bumpless synchronizing. However, there are practical limits to how tightly closing parameters can be controlled. The maximum slip setting must not exceed the control capability of the governor and speed matching system. Older controllers that use pulse frequency modulation and hydro units are prone to poor speed control and would require larger angle and maximum slip settings.

If control considerations could be ignored, 0.001 Hz and 1.0° closure settings would pose other problems. First, it would be very difficult for the operator to initiate a closure within a 1.0° window on the synchroscope. Undoubtedly, the answer would be to hold the breaker control switch in the "close" position and allow the sync relay to close the breaker when the angle entered the relay close characteristic. Also, these settings would delay synchronizing because at 0.001 slip, one revolution

© 2006 by Taylor & Francis Group, LLC

of the synchroscope takes 16 min. This translates to a minute wait for every 20° to reach the in-phase position.

14.8 SYNCHRONIZING EQUIPMENT ON THE SAMPLE SYSTEM

We will assume new manual and automatic synchronizing equipment is being installed on the sample system. Synchronizing potential is taken from the 69 kV bus and generator terminal (Figure 14.26). Both auto and manual synchronizing will be supervised by a microprocessor-based sync-check relay with the control logic shown in Figure 14.27.

The turbine-generator manufacturer has provided the following synchronizing limits: $\pm 10^\circ$ closing angle, maximum voltage differential of 5% and a maximum slip of 0.07 Hz. The closing time for the synchronizing breaker is six cycles.

The sync-check relay has the following settable functions and settings:

Closing angle (0–90°)
Max slip (0.001–0.10 Hz)
Minimum voltage limits (50–120 V)
Maximum voltage limits (80–140 V)
Maximum difference voltage (0–25 V)

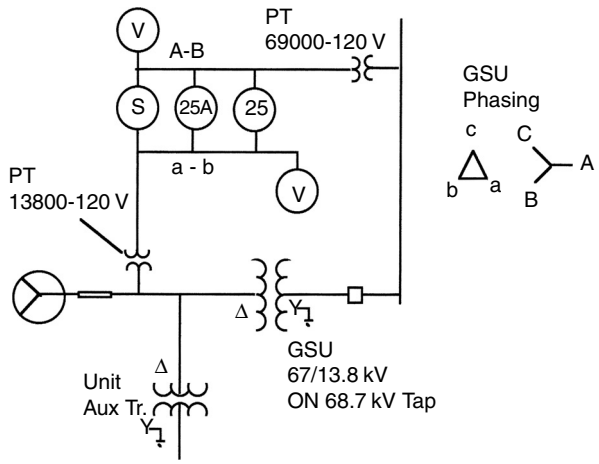


FIGURE 14.26 Sample system synchronizing.

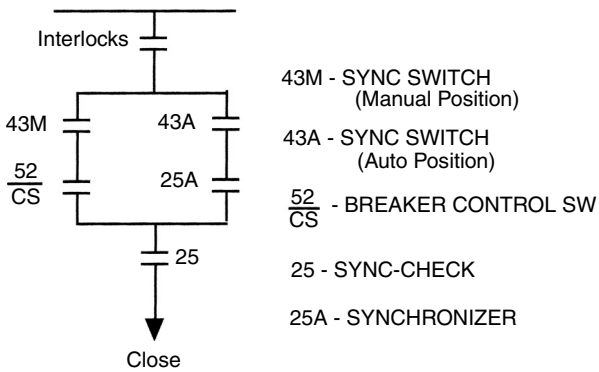


FIGURE 14.27 Sample system sync control.

© 2006 by Taylor & Francis Group, LLC

PT phase angle compensation ($\pm 90^\circ$)
Voltage magnitude compensation (0.5–2.0)
Dead bus closing (enable/disable)
    27 — Dead bus voltage (0–120 V)
    59 — Live line voltage (80–140 V)
Anticipatory close initiation (enable/disable)
    Breaker close time (0–30 cycles)
    Slow close trip actuation

The autosynchronizer has the following functions and settings:

PT phase angle compensation ($\pm 90^\circ$)
Voltage magnitude compensation (0.5–2.0)
Closing angle (0–90°)
Max slip (0.001–0.10 Hz)
Minimum voltage limits (50–140 V)
Maximum voltage limits (80–140 V)
Maximum difference voltage (0–30 V)
Anticipatory close initiation (enable/disable)
    Breaker close time (0–30 cycles)
    Slow close trip actuation

14.8.1 Input Circuit Settings

The first consideration is the potential circuit. Figure 14.26 shows a–b phase potential from the 69 kV bus and generator terminals that will be used for synchronizing. These voltages are not in phase. The 69 kV A–B phase voltage leads generator a–b phase voltage by 30° as a result of the wye-delta connection of the GSU transformer. These voltages would normally be unsuitable for synchronizing, but because both the sync-check and autosynchronizing relay have angle compensation features, the relays can compensate for the phasing shift internally. The relays being installed compensate the bus potential input. The phase compensation on each relay must then be set at -30° to shift the bus voltage in phase with the generator-side voltage.

$$\text{Set bus-side phase angle compensation} = -30^\circ$$

If the relay was designed to compensate the input used for generator voltage a $+30^\circ$ setting would be required. If the chosen relays did not have phase angle compensation, delta-wye auxiliary PTs could be installed to provide the same -30° correction. Alternatively, 69 kV phase-to-neutral voltage could be used in conjunction with a generator phase-to-phase voltage, say 69 kV A-phase with generator voltage a–b. This combination would produce a proper phase relationship, but the voltage magnitudes would differ and an auxiliary PT would be required to compensate.

At rated generator voltage the generator side of the synchronizing circuit, voltage would be:

$$V_{\text{Gen}} = 13{,}800 * 120/13{,}800 = 120\,\text{V}$$

The voltage applied to the bus-side circuit is dependent on the GSU transformer ratio as well as the PT ratio. With the GSU transformer on the 68.7 kV tap, the bus-side synchronizing voltage becomes

$$V_{\text{Bus}} = 13{,}800 * 68{,}700/13{,}800 * 120/69{,}000 = 119.5\,\text{V}$$

© 2006 by Taylor & Francis Group, LLC

Additional voltage errors due to voltage drop will occur when potential circuits are heavily loaded or as a result of long cable runs. On the sample system, a drop of 1.0 V is anticipated in the PT and long cable run from the switchyard to the synchronizing equipment. This drop will be constant for all modes of operation.

Considering both the ratio error and voltage drop, the synchronizing circuit will see an error of 1.5 secondary volts (1.3%) when the actual differential voltage across the synchronizing breaker is zero. Conversely, when the two secondary voltages input to the automatic synchronizer are perfectly matched, there will be a 518 V ($0.013 * 69{,}000/\sqrt{3}$) differential across the open breaker. This is tolerable, but should system changes require a GSU tap change to the 67.0 kV tap, the bus-side voltage with the synchronizing breaker closed would drop to 115.5 V, producing a 3.8% differential between the voltages applied to the synchronizer. The voltage across the open breaker with secondary voltages to the synchronizer matched would rise to nearly 1500 V. In the latter case, the voltage mismatch must be corrected.

The electronic relays provide methods to compensate for mismatch in the synchronizing potential circuit. The relays being installed on the sample system use a magnitude correction, which is applied to the bus voltage input of the relay. The correction factor required for the existing case (GSU on the 68.7 kV tap and 1.0 V drop in the bus-side leads) is

$$RCF = \frac{120}{119.5 - 1.0} = 1.013$$

The phase angle and voltage magnitude correction factors are set on both the sync-check and automatic synchronizer.

The sync-check relay will supervise the autosynchronizer function; therefore, settings for the autosynchronizer will be determined first.

14.8.2 Autosynchronizer Settings

The generator manufacturer's recommendations provide maximum limits for closing parameters. Because each synchronizing stresses the mechanical and electrical components to some extent, the autosynchronizer should be set to initiate breaker closure with the minimum difference between generator and system frequency, voltage, and phase angle as is practical. The practical limit for these settings is dictated by the response of the speed and voltage control equipment. Sluggish response or hunting in either speed or voltage control will force wider tolerance in the associated settings.

In lieu of manufacturer's recommendations, a slip frequency limit of 0.10 is often used. This setting generally provides satisfactory performance for nonhydro units with modern speed control systems. Using this as a benchmark, we will not attempt to set the maximum slip frequency limit on the sample system synchronizer below the manufacturer's recommendations of 0.07 Hz. A lower slip limit would reduce stress on the unit, but may be beyond the capability of the speed control of the equipment. Also the relative stress imposed by automatic synchronizing is very low, as shown in Figure 14.10. Therefore, the stress reduction achieved by reducing the slip setting below the manufacturer's recommendation will not be significant. After commissioning, when the response of the speed control is known, it may be possible to reduce the slip setting.

Set maximum slip = 0.07 Hz

The autosynchronizer close circuit delay time consists of five cycles for the synchronizer closing circuit and six cycles delay for the breaker. This delay of 11 cycles must be set in the autosynchronizer. This delay is used by the relay to calculate the close initiation time necessary to produce an in-phase closure. The auto synchronizer used on the sample system offers the

© 2006 by Taylor & Francis Group, LLC

anticipatory close feature as an option. To use this function it must be enabled. Settings for this function are then:

Anticipatory close initiation — Enable
Breaker closing circuit time (11 cycles)

With the maximum slip limit and closing delay known, the closing angle window can be set. Assuming the generator is at the maximum allowable slip frequency and the breaker is to close its contacts when the generator and system voltage are in phase, the close signal must be initiated at a specific angle before the in-phase position. That angle is calculated from Equation (14.8) as:

$$\begin{aligned}\delta(\text{Ideal}) &= 360 * Slip(\text{Hz})t \\ &= 360 * 0.07 * (0.083 + 0.10) = 4.6^\circ\end{aligned}$$

This being the case, the closing angle window must be set wider than $\pm 4.6^\circ$. Allowing some margin we will set the permissive angle at $\pm 6.0^\circ$.

Set the synchronizer angular limit at $= \pm 6.0^\circ$

The manufacturer limits the voltage differential between the system and generator to a maximum of 5%. Each synchronizer input is 120 V nominal. (The bus input was adjusted to this value using a voltage correction factor.) The manufacturer's allowance is then $120 * 0.05 = 6$ V differential. The voltage regulator is capable of holding voltage within 1%, so a 2.5% (3 V) limit is obtainable and will be used.

Set max voltage differential = 3.0 V

The minimum and maximum synchronizing voltage limits for the sample system generator will be set at 95 to 105% rated voltage. These values represent a generator's allowable operating voltage range as defined by standards. Based on the nominal secondary voltage of 120 V, these limits would be set as:

Gen max voltage $= 1.05 \times 120 = 126$ secondary volts
Gen min voltage $= 0.95 \times 120 = 114$ secondary volts

The bus voltage is preferred to be lower than the generator voltage at synchronizing to prevent a flow of Vars into the generator. Therefore, a lower voltage limit is provided for the bus:

Bus max voltage = 126 secondary volts
Bus min voltage $= 0.9 \times 120 = 108$ secondary volts

14.8.3 Sync-Check Relay

The sync-check function provides a backup protective function during both manual and automatic synchronizing. As such, the sync-check function must prevent any closure that is potentially damaging to the generator and prime mover. Also, settings applied to the sync-check must not interfere with either synchronizing mode. Therefore, the function should be set with the widest possible limits that meet the protective requirement. In keeping with this philosophy, the maximum slip, closing angle, and voltage differential limits prescribed by the manufacturer will be set in the relay.

© 2006 by Taylor & Francis Group, LLC

Maximum slip = 0.07 Hz
Maximum closing angle = $\pm 10^{\circ}$
Maximum voltage differential = 6 secondary volts (5%)

The minimum and maximum voltage settings for the sync-check relay will determine the voltage window for manual synchronizing and should be set to the same criteria as those of the automatic synchronizer.

Gen max voltage = $1.05 \times 120 = 126$ secondary volts
Gen min voltage = $0.95 \times 120 = 114$ secondary volts
Bus max voltage = 126 secondary volts
Bus min voltage = $0.9 \times 120 = 108$ secondary volts

The sync-check relay applied on the sample system generator includes an anticipatory close function similar to that of the automatic synchronizer. This function would be highly desirable in the manual synchronizing mode, but because the sync-check relay supervises the auto-synchronizer, this implementation may result in closing contact coordination problems between the two relays. The anticipatory close signal initiated by either device is normally a pulse of limited duration. Therefore, the anticipatory function of the sync-check relay cannot be enabled unless concurrent closure of the sync-check and automatic synchronizer contacts can be assured.

The devices applied on the sample system maintain contact closure for 0.5 sec. At maximum slip of 0.07 Hz, it will take 14.3 (1/0.07 Hz) sec to complete one slip cycle. A delay of 0.5 sec would relate to contact closure for $0.5 * 360/14.3 = 12.6^{\circ}$ at maximum slip. Given that these devices can initiate closure within $\pm 0.5^{\circ}$ of zero, the 12° window would appear more than adequate to allow implementation of the anticipatory close function.

The operating time for the sync-check relay output contact is four cycles and the breaker will require six cycles to close following an initiation.

Anticipatory close initiation — Enable
Breaker closing circuit time (10 cycles)

The final settings are for the live line and dead bus detection. The sample system generator would be required to energize the 69 kV bus for a "black start" of the transmission system following a major regional system outage. Under this scenario, the normal closing circuit for the 69 kV breaker would not be active because the sync-check function will not actuate without potential on both inputs. The dead bus and live source functions are equivalent to device 27 and 59, respectively, in Figure 14.18. The live bus element (59) is set to assure source voltage is normal. The dead bus element is set to assure the bus is dead and a synchronism check is not required.

Dead bus closing (Enable)
27 — dead bus voltage = 0.20×120 V = 24 V
59 — live line voltage = 0.95×120 V = 114 V

14.8.4 Slow Close Protection

Slow close protection will use two timers. One timer will actuate the 69 kV bus differential lockout relay to trip all breakers adjacent to the synchronizing breaker. The other timer will initiate an alarm. The scheme logic is shown in Figure 14.28.

The time delay setting chosen for 62SC should initiate tripping before the angle of late closure becomes a threat to the turbine-generator. The setting chosen must also allow sufficient margin to avoid false operation, because actuation of the scheme will outage the 69 kV bus.

© 2006 by Taylor & Francis Group, LLC

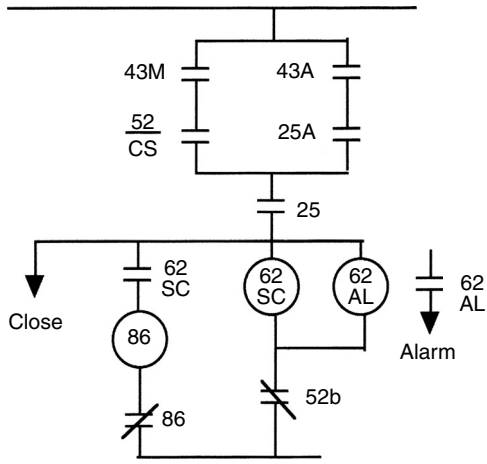


FIGURE 14.28 Slow close protection.

The generator manufacturer has recommended limiting the closing angle to a maximum of $\pm 10^\circ$ for routine synchronizing. This is based on cumulative damage and a target loss-of-fatigue life over the life of the unit. The design of the turbine-generator allows for rare torsional events such as out-of-phase closures that far exceed the 10° limitation. A setting equivalent to a 20° closure would not result in significant loss-of-fatigue life considering the rarity of a slow close event.

The time delay associated with a 20° closure is determined as follows. Actuation of the close circuit would not occur with slip greater than 0.07 Hz, because this is the slip limit set in both the sync-check and autosynchronizer. At this slip, the time required for a 20° closure is calculated from Equation (14.8) as

$$t = \delta/(360 * Slip)$$
$$= 20^\circ/(360 * 0.07) = 0.79 \text{ sec}$$

Set slow close trip delay at = 0.8 sec.

The generator breaker specifications list a closing time of six cycles following initiation. The timer 62AL will initiate and alarm if the operating time during a closure exceeds the design value. With a nominal time operating time of six cycles, a 12–18-cycle delay would be appropriate for this alarm.

At maximum this would represent a late closure of:

$$\delta = 360 * 0.07 * 18\,\text{cy}/60\,\text{cy} = 7.6^\circ$$

which is within the desired 10° window and there for harmless to the generator

Set slow close alarm delay at = 18 cycles (0.30 sec).

REFERENCES

1. *IEEE Guide to for AC Generator Protection* C37.102-1995, IEEE, New York, 1996.
2. Nelson, P. Q. and Benko, I. S., Determination of transient inrush current in power transformers due to out-of-phase occurrences, Paper 70 TP 710-PWR, *IEEE Summer Power Meeting and EHV Conference*. Los Angeles, CA, July 12–17, 1970.

© 2006 by Taylor & Francis Group, LLC

3. *ANSI C50.12 American National Standards Requirement for Salient-Pole Synchronous Generators and Generator/Motors for Hydraulic Turbine Applications*, IEEE, 1996.
4. *ANSI C50.13 American National Standards Requirement for Rotating Electric Machinery — Cylindrical Rotor Synchronous Generators*, IEEE, 1996.
5. Stone, M. and Kilgore, L. A. Transient torques in synchronous machines, *AIEE Trans* 52, 942–952, 1933.
6. Walker, D. N., Adams, S. L., and Placek, R. J., Torsional vibrations and fatigue of turbine-generator shafts, *IEEE Trans Power Apparatus and Systems*, PAS-100 (11), 4373, 1981.
7. Jackson, M. C., Umans, S. D., Dunlop, R. D., Horowitz, S. H., and Parikh, A. C., Turbine-generator shaft torques and fatigue: Part 1 — simulation methods and fatigure analysis, *IEEE Trans Power Apparatus and Systems*, PAS-98 (6), 2299, 2307, 1979.
8. Ramey, D. G., Effects of electrical disturbances on turbine-generator unit life expectancy, Westinghouse Electric Corporation, Presented at the *Steam Turbine-Generator Symposium*, Charlotte, North Carolina, October 4–5, 1978.
9. Jackson, M. C. and Umans, S. D., Turbine-generator torque and fatigue: Part III — Refinements to fatigue model and test results, *IEEE Trans Power Apparatus and Systems*, PAS-99 (3), 1259–1268, 1980.
10. Joyce, J. S., Kluig, T., and Lambercht, D., Torsional fatigue of turbine-generator shafts caused by different electrical system faults and switching operations, *IEEE Trans Power Apparatus and Systems*, PAS-97, 519, 1978.
11. United States Department of the Interior, Bureau of Reclamation, Denver Colorado, *Power O and M Bulletin*, 27, 1957.
12. Krause, P. C., Hollopeter, W. C., Triezenberg, D. M., and Rasche, P. A., Shaft torque during out-of-phase synchronization, *IEEE Trans Power Apparatus and Systems*, PAS-96 (43), 1318–1323, 1977.
13. Gross, L. C., Anderson, S., and Young, R. C., *Avoid Generator and System Damage Due to a Slow Synchronizing Breaker*, Schweitzer Engineering Laboratories, Inc. Publication, Pullman, WA 99163.
14. IEEE Std C57. 12.00-2000 IEEE Standard General Requirements for Liquid-Immersed Distribution, Power, and Regulating Transformers, New York, 2000.

© 2006 by Taylor & Francis Group, LLC

15 Accidental Energization Protection

15.1 INTRODUCTION

An accidental energization occurs whenever an offline generator is unintentionally connected to the power system. Generator damage reported from these incidents has ranged from none to the complete distraction. The simplest form of accidental energization is an erroneous closure of the generator breaker. The most common scenarios involve closing a generator disconnect switch at a ring bus or breaker-and-a-half switchyards or a flashover across contacts of the open synchronizing breaker.

At ring bus (Figure 15.1) and breaker-and-a-half switchyards (Figure 15.2), it is common practice to open disconnect switches to isolate the generator after it is taken out of service. The switchyard breakers are then closed to reestablish the normal redundant conducting paths afforded by these switchyard configurations. Station designs provide interlocks to prevent closure of the disconnect switch when the source breakers are closed, but experience has shown such energization still occurs.

A breaker flashover occurs when the insulating medium between one or more of the open contacts of the synchronizing breaker fails, causing the breaker poles to arc over and thus energizing the generator.

A generator can also be energized via a back feed from the unit auxiliary transformer. This energization does not typically result in damage because the current is very low at 0.1 to 0.2 per unit.[1]

Energizations from a breaker are three-phase events. Switch energizations can be either three-phase or single-phase depending on the type of disconnect switch. Breaker flashovers are considered single- or two-phase events because the probability of a three-phase flashover is extremely low. The number of phases involved in an energization not only affects the severity of the event, but also determines which protective devices can detect the condition. Many protective functions are specifically designed to respond to either multiphase or single-phase events.

A single-phase energization at the generator (Figure 15.3) is not of concern at most installations because the ground path includes the generator grounding resistance, which limits current to less than 20 A. The single-phase energization of interest is from the high-voltage side of the GSU transformer, as shown in Figure 15.4. Closure of a single-phase switch or a flashover imposes single-phase voltage E_A on one high-voltage terminal of the GSU transformer, which in turn imposes a single-phase voltage E_{ab} on the generator. Here, the current is not limited by the grounding impedance and can approach that of the three-phase energization.

15.2 GENERATOR STATE AT ENERGIZATION

The offline machine can have many different states during the course of an outage and an accidental energization could occur at any time. The state of the machine not only affects the severity of the event and the response of the protective scheme, but it also affects how the generator is modeled when calculating energization currents and voltages.

When the generator is taken out of service, it is disconnected from the power system and allowed to coast down. The field excitation may be removed immediately after disconnecting from the system or it may be retained for a period of time.

© 2006 by Taylor & Francis Group, LLC

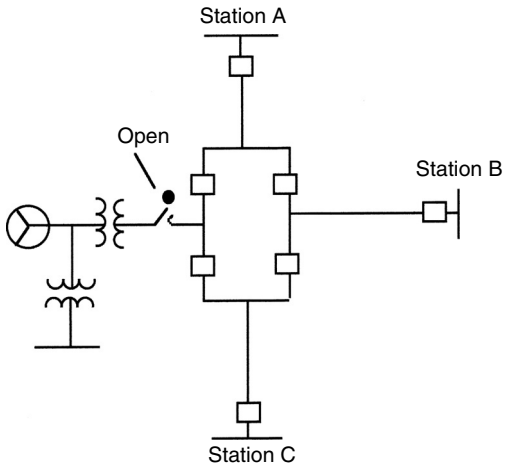


FIGURE 15.1 Ring bus.

The coast down period may last an hour or more. When speed has decayed to a very low value, the unit is placed on turning gear. The turning gear maintains rotation of the turbine-generator at 2 to 60 rpm to allow the shaft to cool without bowing. When cool down is complete, the machine is taken off the turning gear and remains at rest until unit restart.

Often after shutdown PTs associated with protective functions are removed from service as a safety precaution. This disables protective functions with voltage inputs. Other protective functions may be blocked to prevent erroneous trip signals initiated at the out-of-service generator from tripping the closed generator breakers in the switchyard (ring bus and breaker-and-a-half configurations).

Prior to restart, protective functions would be returned to service. The unit would again be placed on turning gear to remove any bowing that may have occurred during the shutdown. The time on turning gear is dependent on the duration of the shutdown; 10 hours or more would be typical. The unit would then begin to ramp up to synchronizing speed. This process can take several hours depending on the type unit. Field excitation is normally applied when the generator is very near synchronous speed. After final voltage, a speed matching the generator would be returned to service by resynchronizing to the power system.

The number of possible variations of generator status and energizing modes is mind-boggling. However, protective analysis and scheme designs have evolved into two categories termed inadvertent energization and open breaker flashover (OBF). Inadvertent energization has come to refer to

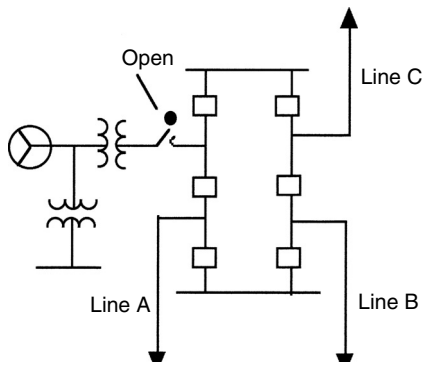


FIGURE 15.2 Breaker-and-a-half.

© 2006 by Taylor & Francis Group, LLC

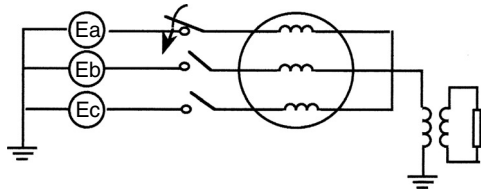


FIGURE 15.3 Simple single-phase energization.

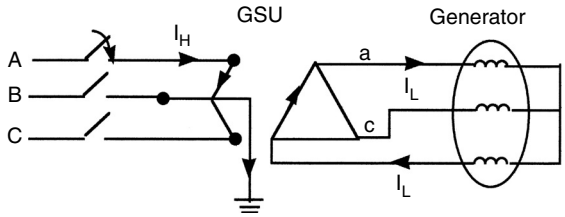


FIGURE 15.4 High-side single-phase energization.

an energization from standstill without field excitation. An open breaker flashover is an energization with field excitation applied and is generally assumed to occur with the generator near rated speed. These two conditions tend to bracket the potential hazards to equipment and the current/voltage excursions available for detection.

15.3 INADVERTENT ENERGIZATION

A generator is at standstill without field excitation a majority of time during an outage, making this the most likely initial condition for energizing. The lengthy acceleration period following such an energization maximizes thermal stress to the generator. This type of energization would be a three-phase event if energized from a breaker or gang-operated switch or a single-phase if energized from a single-phase disconnect.

When a generator is energized without field excitation, it responds as an induction motor starting across the line. Rotating machines produce torque as a result of an interaction between flux produced in the stator and that produced by the rotor. A synchronous generator employs an external current source to excite a rotor winding and create rotor flux. When energized without field excitation, the generator becomes an induction machine. The rotating stator field induces current into the rotor and that induced current produces the rotor flux necessary to create shaft torque. To induce current into the rotor, there must be a speed differential between the stator magnetic field, which travels at synchronous speed, and the rotor. Hence, an induction machine under load cannot operate at synchronous speed. The speed difference between the stator magnetic field and the rotor is quantified as slip.

$$slip = \frac{RPM_{\text{sync}} - RPM_{\text{rotor}}}{RPM_{\text{sync}}} \tag{15.1}$$

The frequency of the current induced in the rotor is directly related to rotor speed through slip.

$$f_{\text{rotor}} = s^* f_{\text{synchronous}} \tag{15.2}$$

The rotor circuits that conduct the induced current have both resistive and inductive components; therefore, the frequency of the induced current determines the circuit impedance,

© 2006 by Taylor & Francis Group, LLC

current magnitude and the phase angle of the rotor flux with respect to the stator flux. These parameters determine generator phase current and torque when starting as a motor. In fact, all the generator parameters during starting are a function of rotor speed. The lower the rotor speed, the higher the frequency of the induced rotor current. As shown by Equation (15.2), at standstill (slip = 1), the frequency of the induced rotor current will be equal to system frequency.

As frequency increases, current flowing in a conductor is forced closer to the outer surface by the skin effect. At standstill, this phenomenon forces the 60 Hz induced current into paths at the surface of rotor. These are the same paths followed by the 120 Hz current induced in the rotor by negative-sequence current associated with unbalanced stator currents. Consequently, the negative-sequence impedance of the generator closely approximates the generator impedance at standstill and at all values of high slip.

$$Z_{\text{start}} = R_2 + jX_2 \tag{15.3}$$

15.3.1 Initial Current for a Three-Phase Energization from Standstill

An energization from a balanced three-phase source produces only positive-sequence current. The simplified positive-sequence equivalent circuit for a motor (Figure 15.5) demonstrates the relationship between the equivalent motor impedance and slip. In this figure, R_s, X_s, and R_r, X_r represent stator and rotor resistance and reactance, respectively.

Upon energization, at standstill (slip = 1) the total generator impedance ($R_s + R_r + X_s + X_r$) is minimum and approximately equal to $R_2 + jX_2$, its negative-sequence impedance. As the generator accelerates, slip decreases, causing current to decreases as the R_r/s term increases. Because rotor resistance (R_r) is small, the variation of the R_r/s term has minimal impact on current until near rated speed when slip is very small. The result is that current remains nearly constant at its initial high value through most of the acceleration period.

The starting time is dependent on the total rotating inertia and the accelerating torque. Because the combined inertia of generator and prime mover is high, and because a generator makes a poor motor, accelerating times can exceed a minute. A typical acceleration time–current plot is shown in Figure 15.6. This curve shape is characteristic for induction motor starting.

The initial three-phase energizing current is easily calculated from Figure 15.5, substituting the generator's negative-sequence impedance for the motor impedance and setting slip = 1:

$$I_{\text{start}} = \frac{E_{\text{sys}}}{Z_{\text{ex}} + R_2 + X_2} \tag{15.4}$$

where $Z_{1\text{ex}}$ = total positive-sequence system Z to the generator terminals.

15.3.2 Single-Phase Energization from Standstill

The phase-to-neutral energization at the high-voltage side of the GSU shown Figure 15.4 imposes a single phase-to-phase voltage on the generator. A generator energized from a single-phase source will again respond as an induction motor. However, a motor's response to a single-phase

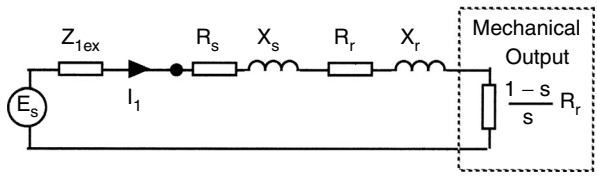


FIGURE 15.5 Induction motor positive-sequence equivalent circuit.

© 2006 by Taylor & Francis Group, LLC

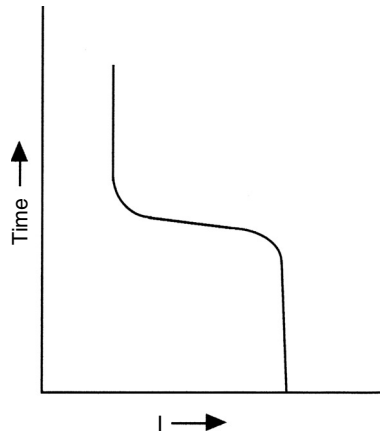


FIGURE 15.6 Time vs. current during acceleration.

energization is markedly different than to a three-phase energization, because negative-sequence current is now present. Figure 15.7 is a simplified negative-sequence equivalent circuit for a motor. Note that the negative-sequence impedance of the motor differs from the positive sequence.

The output torque of a motor is the summation of both positive- and negative-sequence torques. Positive-sequence torque is that which is produced by positive-sequence current and is the load driving torque. Negative-sequence torque is created by negative-sequence current and opposes the positive-sequence torque. The per unit output torque developed at the motor shaft is equal to the total power input to the rotor

$$\begin{aligned} T_{\text{shaft}} &= I_1^2\left[R_{\text{r}} + \frac{1-s}{s}R_{\text{r}}\right] - I_2^2\left[R_{\text{r}} - \frac{1-s}{2-s}R_{\text{r}}\right] \\ &= I_1^2\frac{R_{\text{r}}}{s} - I_2^2\frac{R_{\text{r}}}{2-s} \end{aligned} \tag{15.5}$$

With current in only one high-voltage phase, symmetrical component theory dictates that positive-sequence current must equal negative-sequence current ($I_1 = I_2$). Substituting this equality into Equation (15.5), the torque output of the generator for a single-phase energization becomes

$$\begin{aligned} T_{\text{shaft}} &= I_1^2 R_{\text{r}}\left(\frac{1}{s} - \frac{1}{2-s}\right) \\ &= I_1^2 R_{\text{r}}\left(\frac{2(1-s)}{s(2-s)}\right) \end{aligned} \tag{15.6}$$

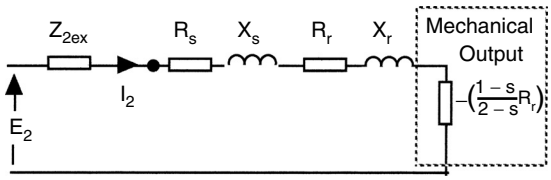


FIGURE 15.7 Induction motor negative-sequence equivalent circuit.

© 2006 by Taylor & Francis Group, LLC

This equation shows that if the single-phase energization occurs with the generator at standstill (slip = 1.0), no net torque is developed and the generator will remain at rest. If there is initial rotation (slip $\neq$ 1.0), a net output torque will be developed. The magnitude of the torque is a function of the initial rotor speed and current. Current is in turn a function of system stiffness. If a generator experiences a single-phase energization at low speed, torque output will be very low. The generator will accelerate if the initial torque is sufficient to overcome losses, but acceleration may be extremely slow.

15.3.3 Initial Current for a Single-Phase Energization at Standstill

A complete sequence diagram for a high-voltage single-phase energization is shown in Figure 15.8. Symmetrical component theory requires equality of positive-, negative- and zero-sequence current for a single-phase event ($I_1 = I_2 = I_0$). The diagram is constructed to maintain this equality. The diagram represents the generator using the slip-dependent positive- and negative-sequence motor equivalent circuits. The diagram includes ideal $\pm 30^\circ$ phase shift transformers to represent the effect of the wye-delta GSU transformer. The inclusion of the phase shift is necessary if delta-side currents are to be calculated.

The secondary (high-voltage) winding of a GSU transformer normally leads the primary (generator) winding. For this configuration, the positive-sequence delta-side quantities are shifted by -30° and negative-sequence quantities are shifted $+30^\circ$. The delta connection also removes zero-sequence quantities from the generator side of the transformer.

The sequence diagram can be simplified if only wye-side currents are to be calculated and the generator is assumed to be at standstill (slip = 1.0). These assumptions allow the removal of the phase shift transformers and representation of the generator by its locked rotor impedance ($R_2 + jX_2$). The simplified version of the diagram is shown in Figure 15.9.

From this diagram it is apparent that

$$I_1 = \frac{E_s}{Z_{1sys} + Z_{2sys} + Z_{0sys} + 3Z_{tr} + 2(R_2 + X_2)} \tag{15.7}$$

Phase currents on either side of the GSU transformer will be calculated for varied conditions throughout this chapter. The method of calculation will be the same for all conditions. Phase currents on the wye side of the GSU transformer are calculated using the standard symmetrical

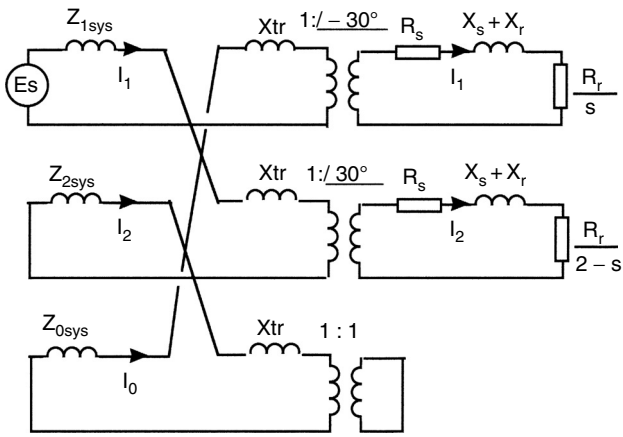


FIGURE 15.8 Sequence diagram for HV single-phase energization.

© 2006 by Taylor & Francis Group, LLC

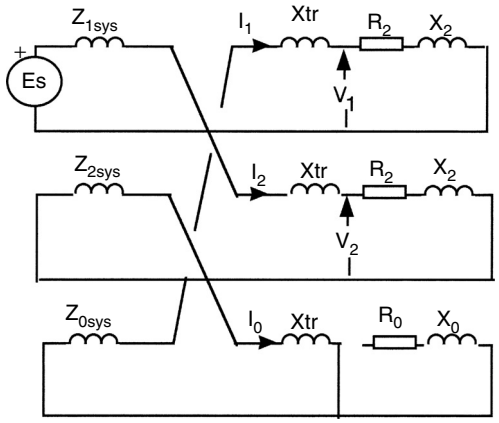


FIGURE 15.9 Simplified sequence for HV single-phase energization.

component transforms below for an ABC rotation:

$$\begin{aligned} I_A &= I_1 + I_2 + I_0 \\ I_B &= I_1 a^2 + I_2 a + I_0 \\ I_C &= I_1 a + I_2 a^2 + I_0 \end{aligned} \tag{15.8}$$

where $a = 1\angle 120^\circ$ and $a^2 = 1\angle 240^\circ$.

The transforms for generator-side currents are derived from Equations (15.8) by including the appropriate 30° shift of positive- and negative-sequence currents and the removal of zero-sequence current. The resulting transforms are:

$$\begin{aligned} I_a &= I_1\angle -30^\circ + I_2\angle 30^\circ \\ I_b &= I_1 a^2\angle -30^\circ + I_2 a\angle 30^\circ \\ I_c &= I_1 a\angle -30^\circ + I_2 a^2\angle 30^\circ \end{aligned} \tag{15.9}$$

Equations (15.8) and (15.9) are generalized equations applicable to any symmetrical component calculations. Phase currents for specific fault conditions are found by substituting sequence currents derived for the fault condition of interest.

For any single-phase energization, $I_1 = I_2 = I_0$. Substituting this constraint into Equations (15.8), the high-side currents become

$$\begin{aligned} I_A &= I_1 + I_2 + I_0 = 3 * I_1 \\ I_B &= I_1 a^2 + I_2 a + I_0 = 0 \\ I_C &= I_1 a + I_2 a^2 + I_0 = 0 \end{aligned} \tag{15.10}$$

Assuming $Z_{1sys} = Z_{2sys}$ and substituting the expression for positive-sequence current specific to this energization, Equation (15.7), into Equation (15.10), the high-side phase current can be written as

$$I_a = \frac{3E_s}{2Z_{1sys} + Z_{0sys} + 3Z_{tr} + 2(R_2 + X_2)} \tag{15.11}$$

© 2006 by Taylor & Francis Group, LLC

Phase currents at the generator terminals are defined from Equation (15.9) and the single-phase constraint $I_1 = I_2$:

$$\begin{aligned} I_a &= I_1\angle -30^\circ + I_2\angle 30^\circ = \sqrt{3}I_1 \\ I_b &= I_1 a^2\angle -30^\circ + I_2 a\angle 30^\circ = -\sqrt{3}I_1 \\ I_c &= I_1 a\angle -30^\circ + I_2 a^2\angle 30^\circ = 0 \end{aligned} \tag{15.12}$$

15.4 BREAKER FLASHOVER

A breaker flashover is the result of a dielectric failure at the contacts of the open synchronizing breaker and is a concern with nonoil breakers. Such a failure could occur as a result of a loss of insulating medium pressure. A flashover is most likely to occur just prior to synchronizing or immediately after the generator is tripped offline. In either case, the generator would have field excitation applied and would be at rated voltage, but not quite at synchronous speed. The difference between generator and system frequency would cause the voltage across the open breaker to vary between zero and two times the phase-to-neutral voltage, severely stressing the dielectric at the contacts. The voltage variation would be at slip frequency. Although theoretically any number of poles can flash, a three-phase event is extremely unlikely and the most popular open breaker flashover protection schemes are designed to detect the failure of only one or two poles.

Depressurization of the insulation system does not guarantee a flashover. If a gas breaker loses pressure in such a way that one atmosphere of gas remains between the open contacts, a breaker can withstand the 2 pu voltage for a time sufficient to take it out of service in an orderly fashion. However, if the failure is on an air breaker or the gas between the contacts is displaced by air, a flashover is probable.

15.4.1 Initial Single-Phase Flashover Current

Because field excitation is applied, the generator responds to a flashover as it would to an out-of-phase synchronization. At the instant of energization, the generator exhibits positive-sequence impedance equivalent to its subtransient reactance (X''_d).

Figure 15.10 is a sequence network connection representing conditions immediately after a single-phase flashover. The connection is similar to that for single-phase energization

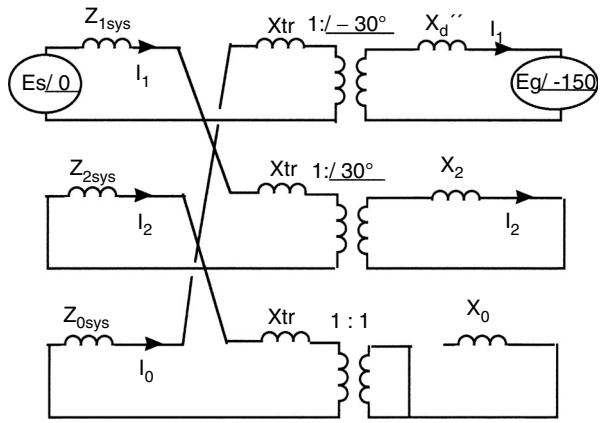


FIGURE 15.10 Single-phase HV energization with field.

© 2006 by Taylor & Francis Group, LLC

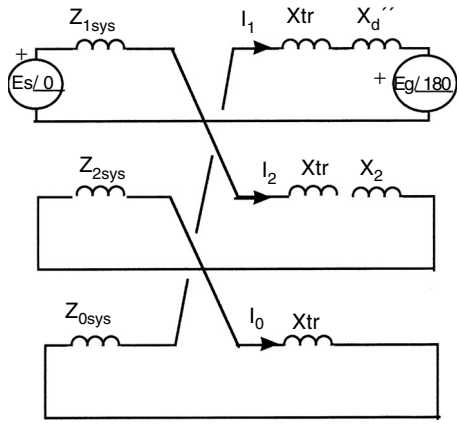


FIGURE 15.11 Simplified sequence diagram for HV energization with field.

(Figure 15.8), except that the motor equivalent impedance is replaced by X''_d and internal voltage E_g in the positive sequence and X_2 in the negative sequence.

A displacement of 180° produces maximum stress on the breaker dielectric and maximum initial current. Obviously, a flashover at a lower phase displacement would result in a lower current for detection, but because dielectric failure is a deterioration over time, not an instantaneous occurrence, failure would be expected at the point of maximum stress, 180° separation.

A simplified sequence diagram representative of current at the high-voltage side of the GSU is presented in Figure 15.11. If the equality $Z_{1sys} = Z_{2sys}$ is assumed, the positive-sequence current for a single-phase flashover at 180° displacement can be written as

$$I_1 = \frac{(E_s + E_g)}{2Z_{1sys} + Z_{0sys} + 3Z_{tr} + X''_d + X_2} \tag{15.13}$$

Phase currents for the single-phase flashover are calculated from the positive-sequence current using the same symmetrical component methodology applied in Section 15.3.3. Hence, wye-side phase currents are given by Equation (15.10) as

$$\begin{aligned} I_A &= I_1 + I_2 + I_0 = 3 * I_1 \\ I_B &= I_1 a^2 + I_2 a + I_0 = 0 \\ I_C &= I_1 a + I_2 a^2 + I_0 = 0 \end{aligned} \tag{15.10}$$

Also, generator-side phase currents are again given by Equation (15.12)

$$\begin{aligned} I_a &= I_1 \angle -30^\circ + I_2 \angle 30^\circ = \sqrt{3} I_1 \\ I_b &= I_1 a^2 \angle -30^\circ + I_2 a \angle 30^\circ = -\sqrt{3} I_1 \\ I_c &= I_1 a \angle -30^\circ + I_2 a^2 \angle 30^\circ = 0 \end{aligned} \tag{15.12}$$

15.4.2 Initial Current for Two-Phase Flashover

Figure 15.12 is the sequence diagram for a two-phase flashover at the high-voltage side of the GSU transformer. Note that this condition is represented by the parallel of the negative and zero sequence

© 2006 by Taylor & Francis Group, LLC

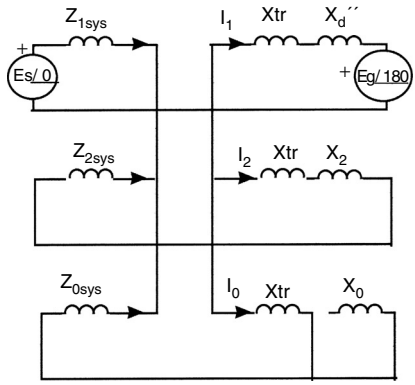


FIGURE 15.12 Two-phase flashover.

circuits in series with the positive sequence circuit. Letting

$$\begin{aligned} Z_1 &= Z_{1\text{sys}} + X_{\text{tr}} + X''_{\text{d}} \\ Z_2 &= Z_{1\text{sys}} + X_{\text{tr}} + X_2 \\ Z_0 &= Z_{0\text{sys}} + X_{\text{tr}} \end{aligned} \tag{15.14}$$

positive-sequence current at the instant of flashover is equal to

$$I_1 = \frac{E_{\text{s}}\angle 0^\circ - E_{\text{g}}\angle \partial}{Z_1 + \left(\dfrac{Z_2 Z_0}{Z_2 + Z_0}\right)} \tag{15.15}$$

The relationships between the sequence currents are

$$I_{\text{A}} = I_1 + I_2 + I_0 = 0 \tag{15.16}$$

$$I_0 = -I_1 \frac{Z_2}{Z_2 + Z_0} \qquad I_2 = -I_1 \frac{Z_0}{Z_2 + Z_0} \tag{15.17}$$

Open breaker flashover protection schemes often employ overcurrent elements in the neutral of the GSU transformer. Such a relay would see current equivalent to

$$3I_0 = 3I_1 \frac{Z_2}{Z_2 + Z_0} I_{\text{base}} \tag{15.18}$$

The 69 kV phase currents are found by substituting the per unit sequence currents from Equation (15.15) and Equation (15.17) into Equation (15.8):

$$\begin{aligned} I_{\text{a}}(\text{amps}) &= (I_1 + I_2 + I_0) I_{\text{base}} = 0 \\ I_{\text{b}} &= (I_1 a^2 + I_2 a + I_0) * I_{\text{base}} \\ I_{\text{c}} &= (I_1 a + I_2 a^2 + I_0) * I_{\text{base}} \end{aligned} \tag{15.19}$$

Phase current at the generator terminal is again calculated by substituting sequence currents from Equations (15.15) and (15.17) into Equation (15.9).

© 2006 by Taylor & Francis Group, LLC

15.5 DYNAMIC ANALYSIS OF THREE-PHASE ENERGIZATION FROM STANDSTILL

A dynamic analysis of the accelerating transient is not necessary to set commonly used inadvertent energization protection schemes, as will be shown in the example calculations for the sample system generator. The following development of a current vs. time plot for the acceleration period is intended to provide insight into the electrical and mechanical aspects of the transient. It may also prove useful when investigating actual events and assessing potential damage.

As previously stated, the response of a generator to an energization from standstill is identical to that of an induction motor starting across the line. Dynamic analysis of the starting condition is routinely carried out for motors (refer to Chapter 16), but is more difficult for a generator because data available for a motor such as speed torque and speed current curves are not available for the generator. These motor parameters must be derived from generator data.

The derivation will be based on the two-axis representation of the generator introduced in Chapter 2. The d- and q-axes represent the principal magnetic circuits within the generator. The d-axis circuit represents the magnetic circuits aligned with rotor field winding. The q-axis is perpendicular to the d-axis and is aligned between the poles.

System phase voltages can be resolved into component voltages that align with these axes. Axis currents are then calculated by equating these d- and q-axes components of system voltage to expressions that define the same voltages in terms of the generator's internal electrical dynamics.

15.5.1 System Voltage Impressed on d- and q-Axes

System phase quantities are related to the generator d- and q-axes by transforms derived by R. H. Park. These transforms, Equation (15.20), and their inverse transforms, Equations (15.21), have become the bases for rotating machine analyses. In these transforms, the Y terms can represent current, voltage or flux; ω_r represents rotor speed.

Defining axis quantities in terms of phase quantities:

$$\begin{bmatrix} Y_d \\ Y_q \end{bmatrix} = \frac{2}{3} \begin{bmatrix} \cos(\omega_r t) & \cos\left(\omega_r t - \frac{2\pi}{3}\right) & \cos\left(\omega_r t + \frac{2\pi}{3}\right) \\ -\sin(\omega_r t) & -\sin\left(\omega_r t - \frac{2\pi}{3}\right) & -\sin\left(\omega_r t + \frac{2\pi}{3}\right) \end{bmatrix} * \begin{bmatrix} Y_a \\ Y_b \\ Y_c \end{bmatrix} \tag{15.20}$$

The inverse transforms define phase quantities in terms of axis quantities:

$$\begin{bmatrix} Y_a \\ Y_b \\ Y_c \end{bmatrix} = \begin{bmatrix} \cos(\omega_r t) & -\sin(\omega_r t) \\ \cos\left(\omega_r t - \frac{2\pi}{3}\right) & -\sin\left(\omega_r t - \frac{2\pi}{3}\right) \\ \cos\left(\omega_r t - \frac{4\pi}{3}\right) & -\sin\left(\omega_r t - \frac{4\pi}{3}\right) \end{bmatrix} * \begin{bmatrix} Y_d \\ Y_q \end{bmatrix} \tag{15.21}$$

Assuming balanced three-phase voltages of frequency ω_e are applied to the stator

$$\begin{aligned} e_a &= E\sin(\omega_e t) \\ e_b &= E\sin\left(\omega_e t - \frac{2\pi}{3}\right) \\ e_c &= E\sin\left(\omega_e t + \frac{2\pi}{3}\right) \end{aligned} \tag{15.22}$$

and rotor speed $\omega_r \neq \omega_e$

© 2006 by Taylor & Francis Group, LLC

the voltages impressed on the d- and q-axes by the power system are found by substituting Equation set (15.22) into Equation (15.20). The resulting d- and q-axes component voltages are found to be sinusoidal, varying at slip frequency:

$$\begin{aligned} e_{\mathrm{d}} &= E\sin(\omega_{\mathrm{s}}t) \\ e_{\mathrm{q}} &= -E\cos(\omega_{\mathrm{s}}t) \\ \omega_{\mathrm{e}} &= \text{ power system velocity} = 2\pi f \\ \omega_{\mathrm{s}} &= \text{slip velocity} = \omega_{\mathrm{e}} - \omega_{\mathrm{r}} \end{aligned} \tag{15.23}$$

15.5.2 Axis Voltages Produced by Generator

Opposing the axis voltages imposed by the system are axis voltages developed within the generator. Expressions for these internal voltages can be derived from Equation (15.24), which defines the voltage produced by a stator winding. Because balanced conditions are being assumed, we can evaluate voltage in one phase. The voltage produced in the "a" phase winding is a function of the flux change in the winding and the resistive drop in the coil:

$$e_{\mathrm{a}} = \frac{\mathrm{d}}{\mathrm{d}t}\psi_{\mathrm{a}} - i_{\mathrm{a}}r \tag{15.24}$$

where ψ_{d} = "a" phase flux and r = stator and system resistance. From the Park Equation set (15.21), the "a" phase voltage can be defined in terms of d- and q-axes quantities:

$$e_{\mathrm{a}} = \left[\left(\frac{\mathrm{d}}{\mathrm{d}t}\psi_{\mathrm{d}} - i_{\mathrm{d}}r\right)\cos(\omega_{\mathrm{r}}t) - \left(\frac{\mathrm{d}}{\mathrm{d}t}\psi_{\mathrm{q}} - i_{\mathrm{q}}r\right)\sin(\omega_{\mathrm{r}}t)\right] \tag{15.25}$$

where ψ_{d},ψ_{q} = d- and q-axes fluxes, i_{d}, i_{q} = d- and q-axes currents, and ω_{r} = rotor speed.

After differentiating $\frac{\mathrm{d}}{\mathrm{d}t}\psi_{\mathrm{d}}\cos(\omega_{\mathrm{r}})$ and $\frac{\mathrm{d}}{\mathrm{d}t}\psi_{\mathrm{q}}\sin(\omega_{\mathrm{r}})$ becomes

$$e_{\mathrm{a}} = \left[\left(\frac{\mathrm{d}}{\mathrm{d}t}\psi_{\mathrm{d}} - \omega_{\mathrm{r}}\psi_{\mathrm{q}} - i_{\mathrm{d}}r\right)\cos(\omega_{\mathrm{r}}t) - \left(\frac{\mathrm{d}}{\mathrm{d}t}\psi_{\mathrm{q}} + \omega_{\mathrm{r}}\psi_{\mathrm{d}} - i_{\mathrm{q}}r\right)\sin(\omega_{\mathrm{r}}t)\right] \tag{15.26}$$

which, by comparison with Equation (15.21), yields the conclusion that:

$$\begin{aligned} e_{\mathrm{d}} &= \frac{\mathrm{d}}{\mathrm{d}t}\psi_{\mathrm{d}} - \omega_{\mathrm{r}}\psi_{\mathrm{q}} - i_{\mathrm{d}}r \\ e_{\mathrm{q}} &= \frac{\mathrm{d}}{\mathrm{d}t}\psi_{\mathrm{q}} + \omega_{\mathrm{r}}\psi_{\mathrm{d}} - i_{\mathrm{q}}r \end{aligned} \tag{15.27}$$

These equations are derived in standard machine text[2] and show that the axis voltages produced within the generator include one component that is a function of rotor speed and a second component that is a function of the rate of flux change.

15.5.3 Derivation of Axis Currents

Flux is the product of current and inductance. The total system d- and q-axes flux in Equation set (15.27) are given as

$$\psi_{\mathrm{d}} = -i_{\mathrm{d}}L_{\mathrm{de}} \qquad \psi_{\mathrm{q}} = -i_{\mathrm{q}}L_{\mathrm{qe}} \tag{15.28}$$

© 2006 by Taylor & Francis Group, LLC

The inductances L_{de} and L_{qe} are the sum of the generator axis inductance and L_e, the inductance external to the generator:

$$L_{de} = L_e + L_{dz} \qquad L_{qe} = L_e + L_{qz} \tag{15.29}$$

The generator d- and q-axes inductances are designated as L_{dz} and L_{qz} because they are slip frequency dependent complex quantities ($L - jR$). The treatment of the axis impedance will be discussed in detail later.

Equations defining the axis currents can now be derived by substituting Equations (15.23) and (15.29) into Equation (15.27), resulting in the following:

$$E\sin(\omega_s t) = -\frac{d}{dt} i_d L_{de} + \omega_r i_q L_{qe} - r i_d \tag{15.30}$$

$$-E\cos(\omega_s t) = -\frac{d}{dt} i_q L_{qe} - \omega_r i_d L_{de} - r i_q \tag{15.31}$$

If the transient components of axis current are ignored, the steady-state current components can be found using phasor analysis. Phasor equations are established by replacing the time derivative with j times the rate of change, which in this case is the slip speed $j\omega_s$. Phasor values are chosen for e_d and e_q to maintain the e_d leads e_q relationship established by Equation (15.23). The resulting equations are:

$$\begin{aligned} E &= -j\omega_s I_d L_{de} + \omega_r I_q L_{qe} - r i_d \\ -jE &= -j\omega_s I_q L_{qe} - \omega_r I_d L_{de} - r i_d \end{aligned} \tag{15.32}$$

Solving for I_d and I_q yields

$$\begin{aligned} \hat{I}_d &= \frac{E\,[j(\omega_r - \omega_s)L_{qe} - r]}{r^2 + L_{de}L_{qe}(\omega_r^2 - \omega_s^2) + jr(L_{de} + L_{qe})\omega_s} \\ \hat{I}_q &= \frac{E[L_{de}(\omega_r - \omega_s) + jr]}{r^2 + L_{de}L_{qe}(\omega_r^2 - \omega_s^2) + jr(L_{de} + L_{qe})\omega_s} \end{aligned} \tag{15.33}$$

In order to define phase current and torque, these currents are expressed in time-variant form:

$$\begin{aligned} I_d &= I_d \sin(\omega_s t + \theta_d) \\ I_q &= I_q \sin(\omega_s t + \theta_q) \end{aligned} \tag{15.34}$$

where I_d and I_q are the absolute magnitudes of $\hat{I}_d$ and $\hat{I}_d$ from Equation set (15.33) and θ_d and θ_q are the angles associated with each complex current from the same equation set. Note that although both axis currents are designated as sine functions, they are actually at right angles to one another because θ_d and θ_q are at right angles.

Phase current is obtained by substituting Equations (15.34) into the Park inverse transform Equation (15.21):

$$\begin{aligned} i_a &= i_d \cos(\omega_r t) - i_q \sin(\omega_r t) \\ &= I_d \sin(\omega_s t + \theta_d)\cos(\omega_r t) - I_q \sin(\omega_s t + \theta_q)\sin(\omega_r t) \end{aligned} \tag{15.35}$$

© 2006 by Taylor & Francis Group, LLC

Reduction by trigonometric identities reveals two components of current. One component is at system frequency and the other at twice slip frequency.

$$\begin{aligned} i_a &= i_a(\omega_e) + i_a(2\omega_s) \\ i_a(\omega_e) &= \frac{1}{2}[I_d \sin(\theta_d + \omega_e t) + I_q \cos(\theta_q + \omega_e t)] \\ i_a(2\omega_s) &= \frac{1}{2}\{I_d \sin[\theta_d + (\omega_e - 2\omega_r)t] - I_q \cos[\theta_q + (\omega_e - 2\omega_r)t]\} \end{aligned} \tag{15.36}$$

If stator and system resistance are neglected, $\theta_d = \pi/2$ and $\theta_q = 0$ and these expressions reduce to

$$i_a(\omega_e) = \frac{1}{2}[-(I_d + I_q)\sin(\omega_e t)] \tag{15.37}$$

$$i_a(2\omega_s) = \frac{1}{2}\{(I_q - I_d)\sin[(\omega_e - 2\omega_r)t]\} \tag{15.38}$$

It is obvious that the latter term is a result of saliency, that is, the difference between the d- and q-axes circuit impedance.

15.5.4 Defining Generator Shaft Torque

The basic equation for the electrical torque developed by a rotating machine is given as

$$T_e = \psi_{dg} i_q - \psi_{qg} i_d \tag{15.39}$$

where ψ_{dg} and ψ_{qg} are the axis flux *at the generator terminals*:

$$\begin{aligned} \psi_{dg} &= -L_d i_d \\ \psi_{qg} &= -L_q i_q \end{aligned} \tag{15.40}$$

Expressing the flux in time-variant terms, the equations become

$$\begin{aligned} \psi_{dg} &= -|L_d| I_d \sin(\omega_s t + \theta_d + \theta_{Ld}) \\ \psi_{qg} &= -|L_q| I_q \sin(\omega_s t + \theta_q + \theta_{Lq}) \end{aligned} \tag{15.41}$$

where θ_{Ld} and θ_{Lq} are angles associated with complex inductances L_d and L_q. Substituting Equations (15.41) into Equation (15.39), the torque equation resolves into two components:

$$T_e = \frac{1}{2} I_d I_q [-|L_d| \cos(\theta_d - \theta_q + \theta_{Ld}) + |L_q| \cos(\theta_q - \theta_d + \theta_{Lq})] \tag{15.42}$$

$$T_e(\text{Puls}) = \frac{1}{2} I_d I_q [|L_d| \cos(\theta_d + \theta_q + \theta_{Ld} + 2\omega_s t) - |L_q| \cos(\theta_q + \theta_d + \theta_{Lq} + 2\omega_s t)] \tag{15.43}$$

The first is a nontime-varying torque with a fixed average value over time. This torque produces acceleration. The second component is a pulsating torque generated by the difference between d- and q-axes impedances. This component has a frequency twice the slip frequency and is symmetrical about the time axis. This symmetry results in an average torque equal to zero. Therefore, this component cannot contribute to acceleration, but these torque pulsations can add significantly to shaft stress during acceleration.

© 2006 by Taylor & Francis Group, LLC

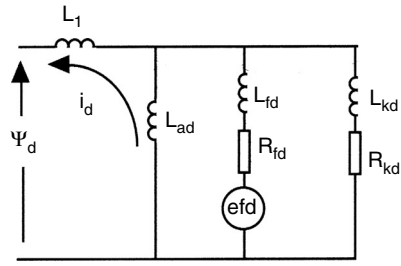


FIGURE 15.13 d-Axis equivalent circuit.

15.5.5 D- AND Q-AXES CIRCUIT IMPEDANCE

The above derivation treated the axis circuits as a fixed inductance for convenience, but this representation is inadequate. Figure 15.13 and Figure 15.14 are circuits commonly used to represent d- and q-axes magnetic paths. These circuits contain resistive and inductive components. The axis inductances L_d and L_q, which appear in the torque and current equations derived above, are representative of the impedance seen looking into the terminals of the respective axis circuits. The frequency of the axis voltages impressed on these circuits is equal to slip frequency. During acceleration, this frequency will vary from rated frequency for an energizing at standstill to near zero (DC) when the rotor reaches a final operating speed nearly equal to synchronous speed. With this variation in frequency, axis impedance will increase from subtransient to synchronous; this variation must be accounted for in the calculation.

The inductance of each axis at a given slip frequency can be derived from the equivalent circuits in Figure 15.13 and Figure 15.14 by replacing each inductive element with its equivalent reactance at the frequency in question ($X = jL\omega_s$). A series/parallel impedance reduction would yield the axis impedance at the given value of slip. Using the d-axis as an example

$$\begin{aligned} Z_d(\omega_s) &= R + j\omega_s L_l + \frac{1}{\left(\frac{1}{j\omega_s L_{ad}}\right) + \left(\frac{1}{R_{fd} + j\omega_s L_{fd}}\right) + \left(\frac{1}{R_{kd} + j\omega_s L_{kd}}\right)} \\ &= Reqv(\omega_s)_d + jXeqv(\omega_s)_d \end{aligned} \tag{15.44}$$

Because reactance is defined as $X = j\omega L$, the equivalent axis inductance becomes:

$$L_d(\omega_s) \frac{= Reqv_d(\omega_s) + jXeqv_d(\omega_s)}{j\omega_s} = L_d(\omega_s) - j\frac{Reqv_d(\omega_s)}{\omega_s} \tag{15.45}$$

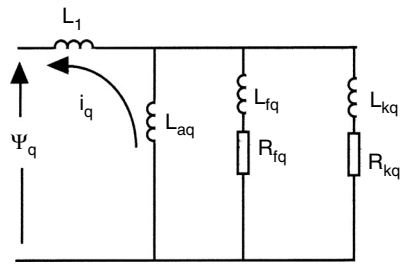


FIGURE 15.14 q-Axis equivalent circuit.

© 2006 by Taylor & Francis Group, LLC

The result is a complex inductance defined at each specific value of slip used in the starting time calculation. A similar reduction would be required for the q-axis.

A problem with this approach is that the reactive and resistive elements of the equivalent axis circuits cannot be determined directly from tests and are not included with standard generator data sheets. These network components can be derived from standard data as was done in Appendix E, but this process is time-consuming.

Alternatively, the same axis inductances are derived from standard generator data using equations derived in Ref. 2:

$$L_{\mathrm{d}}(\omega_{\mathrm{s}}) = \frac{L_{\mathrm{d}}\left(1 + j\frac{T'_{\mathrm{do}}}{t_{\mathrm{base}}}\frac{L'_{\mathrm{d}}}{L_{\mathrm{d}}}\omega_{\mathrm{s}}\right)\left(1 + j\frac{T''_{\mathrm{do}}}{t_{\mathrm{base}}}\frac{L''_{\mathrm{d}}}{L'_{\mathrm{d}}}\omega_{\mathrm{s}}\right)}{\left(1 + j\frac{T'_{\mathrm{do}}}{t_{\mathrm{base}}}\omega_{\mathrm{s}}\right)\left(1 + j\frac{T''_{\mathrm{do}}}{t_{\mathrm{base}}}\omega_{\mathrm{s}}\right)} \tag{15.46}$$

$$L_{\mathrm{q}}(\omega_{\mathrm{s}}) = \frac{L_{\mathrm{q}}\left(1 + j\frac{T'_{\mathrm{qo}}}{t_{\mathrm{base}}}\frac{L'_{\mathrm{q}}}{L_{\mathrm{q}}}\omega_{\mathrm{s}}\right)\left(1 + j\frac{T''_{\mathrm{qo}}}{t_{\mathrm{base}}}\frac{L''_{\mathrm{q}}}{L'_{\mathrm{q}}}\omega_{\mathrm{s}}\right)}{\left(1 + j\frac{T'_{\mathrm{qo}}}{t_{\mathrm{base}}}\omega_{\mathrm{s}}\right)\left(1 + j\frac{T''_{\mathrm{qo}}}{t_{\mathrm{base}}}\omega_{\mathrm{s}}\right)} \tag{15.47}$$

These equations are written for per unit quantities. As such the per unit values of inductance used in the equations, L_{d}, L'_{d}, L_{q}, and so on, are numerically equivalent to the per unit values of X_{d}, X'_{d}, X_{q} provided on standard generator data sheets. The time constants are entered in seconds; the division by base time establishes per unit time. Base time equals $t_{\mathrm{base}} = 1/2\pi f$.

Often, data are not provided for the transient paths in the q-axis. In that case, Equation (15.47) is applied as

$$L_{\mathrm{q}}(\omega_{\mathrm{s}}) = \frac{L_{\mathrm{q}}\left(1 + j\frac{T''_{\mathrm{qo}}}{t_{\mathrm{base}}}\frac{L''_{\mathrm{q}}}{L_{\mathrm{q}}}\omega_{\mathrm{s}}\right)}{\left(1 + j\frac{T''_{\mathrm{qo}}}{t_{\mathrm{base}}}\omega_{\mathrm{s}}\right)} \tag{15.48}$$

Substituting data for the sample system generator into these equations for the standstill condition where $\omega_{\mathrm{s}} = 1.0$ pu (60 Hz), axis inductances are

$$\begin{aligned} L_{\mathrm{dz}} &= 0.136 - j0.00545 \\ L_{\mathrm{qz}} &= 0.132 - j0.013 \end{aligned} \tag{15.49}$$

Two things are of note: first the fact that the standstill inductances of 0.136 and 0.132 are equivalent to X''_{d} and X''_{q}, respectively. This is expected, because the high slip mimics the rapid rate of change apparent at the inception of a short circuit where X''_{d} and X''_{q} are also representative of the generator impedance. We also note that impedance at standstill is often approximated by the generator negative-sequence reactance, which is $X_2 = (X''_{\mathrm{d}} + X''_{\mathrm{q}})/2$.

The second notable feature of Equation (15.49) is the presumed negligible resistive component. In fact, this component is anything but negligible. Motor torque is derived from the angular displacement between axis current and flux. If the axis circuits are represented as a pure inductance by neglecting the resistive component, no torque is produced. To illustrate this, the electrical torque

© 2006 by Taylor & Francis Group, LLC

equation, Equation (15.42), can be simplified by neglecting stator and system resistance $r = 0$. With that assumption, $\theta_d = \pi/2$ and $\theta_q = 0$ and the torque resolves to

$$T_e(\text{Av}) = \frac{1}{2} I_d I_q [|L_d| \sin(\theta_{Ld}) + |L_q| \sin(\theta_{Lq})] \tag{15.50}$$

If the d- and q-axes are assumed to be pure inductance their values become

$$L_d = L_d + j0 \qquad L_q = L_q + j0 \tag{15.51}$$

Substituting θ_{Ld} and θ_{Lq} equal to zero into Equation (15.42), electrical torque becomes zero, which is incorrect.

Calculation of the starting transient requires a complex slip variant representation of the d-and q-axes circuit inductances. Generator torque during the acceleration period is then calculated from torque Equation (15.42) using complex values for L_{dz} and L_{qz} at each value of slip derived from Equations (15.46) and (15.47).

15.5.6 Acceleration

Now that the electrical torque is known, the accelerating time can be derived for the torque equation:

$$T_{acc} = I\alpha = I\frac{d\omega_r}{dt} \tag{15.52}$$

where T_{acc} = accelerating torque, I = inertia, t = time, α = acceleration, and ω_r = angular rotor velocity. Accelerating torque is the difference between the electrical torque developed by the generator acting as a motor and the torque load on the shaft. In the case of inadvertent energizing, the only shaft loading results from rotational losses such as friction and windage, which are negligible. The torque equation can be rewritten in incremental form, neglecting shaft losses to yield the time increment for a given chance in speed.

$$\Delta t = \frac{I}{T_e}(\omega_{r2} - \omega_{r1}) \tag{15.53}$$

This equation can be applied to a point-by-point calculation of time for incremental rotor speed changes from zero at energization to near synchronous speed. The torque at each value of speed is calculated from Equation (15.42). The incremental time calculation should use the average electrical torque over the interval. That is the average of the electrical torque at the beginning of the interval (ω_1) and the end of the interval (ω_2):

$$T_{e-av} = \frac{T_{e-\omega 2} + T_{e-\omega 1}}{2} \tag{15.54}$$

Inertia of the generator and prime mover may be given in terms of H (seconds) or Wk^2 (lb-ft^2). In the former case, Δt for each increment of speed can be calculated in seconds directly from per unit quantities as

$$\Delta t = \frac{2H}{T_{e-av}}(\omega_2 - \omega_1)\,\text{sec} \tag{15.55}$$

© 2006 by Taylor & Francis Group, LLC

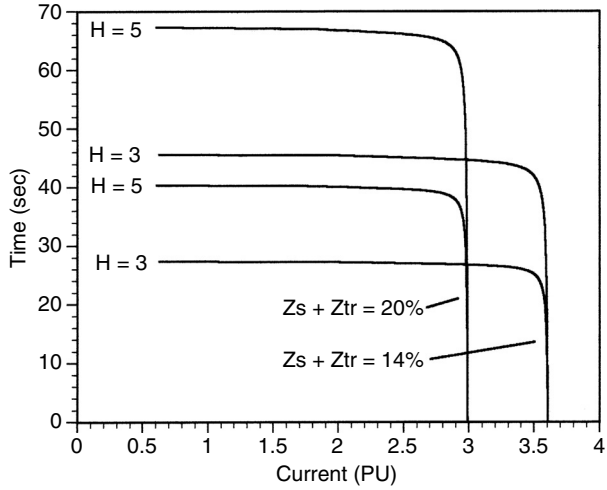


FIGURE 15.15 Generator acceleration.

In the latter case, unit conversions are required to obtain

$$\Delta t = \frac{Wk^2(\omega_2 - \omega_1)}{308 T_{e-av} T_{base}} \text{ sec} \tag{15.56}$$

with ω in RPM and torque in per unit and the base torque equal to

$$T_{base} = 7.04 \times 10^6 \frac{MVA_{base}}{RPM_{rated}} \text{ (ft-lb)} \tag{15.57}$$

Applying this analysis, Figure 15.15 plots the starting characteristic of the sample system generator with varied values of inertia and combined system and transformer impedance. These plots provide some insight into the variation of acceleration time with starting parameters. Appendix E is a mathcad work book which performs the starting calculation just described.

15.6 GENERATOR DAMAGE

If a generator does not have field excitation, when it is energized it behaves as an induction motor started across the line. A three-phase energization at standstill or turning gear speed would result in significant inrush current and a prolonged period of acceleration. A three-phase energization from a strong system would typically result in phase current in a range of three to four times rated, while on a weak system current magnitude can be as low as one to two times rated.[3]

The accelerating characteristic of an induction motor is such that current magnitude remains near the high initial value through most of the accelerating period, which in the case of a generator energization can last from tens of seconds to minutes. This characteristic produces severe thermal stress in both the stator windings and the rotor.

15.6.1 Rotor Heating

The generator rotor experiences excessive heating during the acceleration period because it is not designed for starting duty. The magnetic field produced by the stator current rotates at synchronous speed. During normal operation, the generator rotor also rotates at synchronous speed and the

© 2006 by Taylor & Francis Group, LLC

relative velocity between the stator field and the rotor is zero. With no relative motion between the two, no current is induced into the rotor. During the acceleration period, there is a large speed differential and high-magnitude current is induced.

The rotor of an induction motor is designed with low-impedance conducting paths to accommodate these induced currents. A generator lacks these low-impedance paths, forcing the induced currents into the rotor body, wedges, teeth and retaining rings of a round rotor machine. Induced current paths are illustrated in Figure 6.4. These paths are not designed to conduct current and have significant resistance. The I^2R losses along these paths produce rapid temperature rise in the rotor structures that can cause damage in seconds. This heating is most severe at the ends of the rotor where currents converge to pass from the wedges and teeth into the retaining rings and back.

On salient pole machines the induced rotor current will flow in the amortisseur bars located on the pole faces. If these damper bars are not interconnected between pole faces, the induced current also flows down one pole through the dovetail that connects the poles to the hub of the rotor and up the adjacent pole structure. Damage in a salient pole machine would most likely occur where the amortisseur winding contacts the pole and in the dovetail of machines without connected amortisseurs.

Standards do not address generator withstand capabilities for accidental energization events, but the thermal damage described above is similar to that caused by the negative-sequence current as discussed in Chapter 6. Consequently, the negative-sequence current withstand capability of the rotor expressed in terms of $K = I_2^2 t$ is used to estimate the time until the onset of rotor damage during the acceleration.[3]

When a generator is operating at synchronous speed, positive-sequence current produces flux rotating at synchronous speed with the rotor and negative-sequence current produces flux at synchronous speed, but with rotation opposed to that of the rotor. Hence, positive-sequence current induces no current in the rotor, while negative-sequence current induces rotor current at double frequency. The result is that rotor heating during normal operation is solely a result of negative-sequence current. This is the condition for which the negative-sequence $I_2^2 t$ limit is defined.

At standstill, both positive- and negative-sequence currents induce current into the rotor at system frequency, but with opposed rotation ($+\omega$, $-\omega$). With equal frequency, the skin effect and effective resistance for each component will also be equal, allowing the negative-sequence limit to be rewritten as

$$K = (I_1^2 + I_2^2)t \tag{15.58}$$

The safe stall time at locked rotor calculated from the above equation is used to estimate the permissible acceleration time for the generator. However, this method is more empirical than theoretical.

First, the treatment of the negative-sequence limit is not universal. Reference 3 recommends using the square of the per unit generator phase current in place of the $I_1^2 + I_2^2$ term in Equation (15.58).

Also, the $I_2^2 t$ limit is based on heating caused by double frequency current induced in the rotor by negative-sequence current with the generator at rated speed. The skin effect forces current flow closer to the surface of a conductor as frequency increases. Thus, current densities at the surface of the rotor body, wedges, teeth and amortisseur windings are greater at higher frequency. This increases the effective resistance, and higher resistance causes more heating. In short, the 120 Hz current induced in rotor structures by negative-sequence current at rated speed produces more heat per amp than the 60 Hz current induced at standstill. If heating is considered directly proportional to frequency, rotor capability at standstill would be twice the $I_2^2 t$ limit. Also, the frequency of the current induced during starting would decrease from 60 Hz to near DC as the rotor accelerates, further reducing the heating during the acceleration period. These points imply that the

© 2006 by Taylor & Francis Group, LLC

accelerating capability of the generator is much greater than indicated by the I_2^2t limit, but this is not true. The negative-sequence limit represents the overall thermal capacity of the rotor. During starting, failures are most likely caused by local heating at the points of contact between the rotor body, wedges and retaining rings.

During normal operation of a round rotor machine, rotor velocity imposes considerable clamping force on the wedges holding them tight against the rotor slots and retaining rings. This reduces contact resistance and minimizes resistance at the points of contact between the wedges and other rotor structures. When energized from standstill, the loose contact between these surfaces promotes arcing and heat concentrated at the point of arc. The local heating can be severe enough to melt slot and wedge material, resulting in mechanical failure of the wedge and winding support system. This failure may occur before the generalized thermal damage predicted by the I_2^2t limit occurs, and could occur as the generator accelerates during the energization event or at some late date during normal operation. Such a failure would send debris into the air gap and stator, which has the potential to destroy the generator.

For a salient pole machine, local heating at the interface between the damper bar and the pole face can be more severe for the standstill case because of reduced ventilation and higher induced current.

Although the I_2^2t limit may be an imperfect gage of generator starting capability, it does provide a method of quantifying the severity of starting events. Figure 15.16 plots the accumulated I_2^2t for three-phase energization with varied system impedance and inertia. The plot shows the speed at which damage can occur. Even machines with I_2^2t limits of 30 and 40 can be damaged in seconds. The plot also shows that the initial rate of rise of I_2^2t is determined solely by the system impedance.

15.6.2 Other Considerations

The required short time overload capability of the stator winding is defined in ANSI standard C50.13-1989 and plotted in Figure 4.15. The standard only defines short time capability up to 2.26× full load current and requires a 10 sec withstand at this value. If a generator is assumed to have maximum short time negative-sequence capability ($I_2^2t = 40$), and relating rotor heating during acceleration to the square of stator current as prescribed by reference [3] the rotor withstand time at 2.26 pu current would be $40/(2.26)^2 = 7.8$ sec. This comparison demonstrates why stator windings are not considered limiting for an energization from standstill.

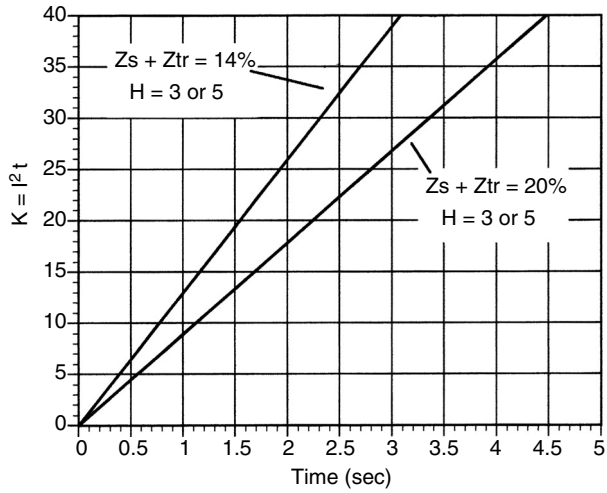


FIGURE 15.16 Accumulated I_2^2t.

© 2006 by Taylor & Francis Group, LLC

Generator field windings are not threatened by an energization at standstill because the high frequency of the induced current during acceleration prevents current penetration into the bottom of the slots where the windings are located until the end of the acceleration period.

The severity of an energization with excitation applied is dependent on the phase angle between the generator and system at the instant of closure and system stiffness. A large angular displacement will result in transient current far in excess of those experienced for an energizing without field. The thermal stress associated with such an energization is dependent on generator speed. If the energization occurs near rated speed, the acceleration time will be minimal and thermal stress to the generator will be negligible.

15.7 TURBINE DAMAGE

When a generator is energized from standstill, one of the most critical items is bearing protection. With the generator at rest, lube oil pumps will be shut down and the lack of oil will cause bearings to damage very quickly as the unit accelerates. Bearing protection necessitates high-speed tripping. If the unit were on, turning gear oil pumps would be in service, but damage to the turning gear may result.

Other areas of potential turbine damage would be similar to those a prime mover would experience during a motoring event, as described in Chapter 7. Steam turbines rely on steam to cool blade tips and equalize heating. A unit at standstill would not have a steam supply. Accelerating such a unit to near rated speed could cause damaging heat and erosion at the ends of the long blades of the low-pressure turbine. Localized heating can result in physical distortion of structures and rubbing of moving parts.

Hydro units can suffer damage to the water wheel due to cavitation. This is a phenomenon that occurs when the waterwheel is immersed but does not have sufficient pressure at the inlet. The generator acts as a pump, but low pressure behind the blades causes an explosive formation of small steam bubbles that chip metal from the blades.

Hydro units are salient pole machines and can have a significant difference in d- and q-axes impedances. This difference will produce the pulsating torque described by Equation (15.43). These pulsations will severely stress the shaft, couplings and support structures during acceleration.

Gas turbines are usually connected to the generator through gearing. This gearing may be designed to drive in only one direction by machining only one side of the gear tooth to carry load. An energization from the power system will drive from the generator to the turbine, hence damaging the gear teeth.

A three-phase energization will impose impact torque on the generator rotor that is transmitted to the connecting shafts, bearings and couplings. An energization without field excitation applied will result in reduced torque excursions when compared to a case with field excitation applied. The initial torque is less severe for the former case because rotor flux, a component of shaft torque, must build up after energization.

An energization with field applied is in effect an out-of-phase synchronization. The severity of this event is dependent on the initial speed, the angular difference between the generator and system, and system stiffness. Shaft torsional excursions in excess of three times rated can occur as a result of a three-phase event. The torsional oscillation from such an event can persist for 30 sec with each individual torsional excursion adding to the total loss of fatigue life in the shaft. A single- or two-phase out-of-phase synchronizing, as could occur for a breaker flashover, will produce less torsional stress than the three-phase case.

The loss of life will be significantly increased if there is a large frequency differential between the generator and system at the time of closure. The greater the speed differential, the more slip cycles the unit will have to endure before pulling into phase alignment with the system. Each slip cycle represents a major torque excursion at 180° separation. Shaft loss of life and torsional oscillations were discussed in Chapter 14.

© 2006 by Taylor & Francis Group, LLC

Severe torsional stress is also possible from events that produce very low accelerating torque. During normal startup, the generator accelerates from zero to synchronous speed, passing through one or more of the shaft system natural frequencies. Damage is avoided by accelerating through each critical speed fast enough to avoid exciting the natural modes. A single-phase energization or a three-phase energization from a very weak source such as the unit auxiliary transformer will result in very slow passage through critical speeds. This can allow natural modes to excite, resulting in mechanical damage to the shaft, bearings, couplings and turbine blades.

15.8 ENERGIZATION PROTECTION

The two most common energization events are energizations at standstill, and breaker pole flashovers. In the first case, an energization at standstill from a strong system will result in an initial current of three to four times rated and voltage of 50 to 70%. On a weak system, current can be as low as one to two times rated with voltage at 20 to 40%. Because of the starting characteristic of an induction motor, current and voltage are maintained near their initial values through most of the accelerating period, providing ample opportunity for relay operation.

This is not the case for a breaker flashover, which requires a high-speed trip scheme. Flashover is most likely to occur just prior to synchronization or just after the unit is taken offline. In either case, the generator speed would be very near synchronous speed. A flashover would cause the generator to pull into synchronism with the system quickly, rapidly reducing the high initial flashover current and allowing little time for a protective scheme to activate.

Relaying that detects a breaker flashover provides no protection if that relay merely attempts to trip the flashed breaker because that breaker is already open. To clear a flashover, the trip relay must initiate the breaker failure scheme of the flashed breaker. The breaker failure scheme will in turn initiate tripping of all breakers adjacent the flashed breaker.

At stations with single breaker terminations as shown in Figure 14.25, a flashover is cleared by tripping local breakers. At stations where breakers terminate multiple circuits, a remote terminal must be opened. An example is shown in Figure 15.17. To clear a flashover of breaker "B" a protective relay must detect the fault and initiate the "B" breaker's breaker failure (BF) scheme. The BF scheme will then trip breaker "C" locally and initiate a direct transfer trip signal over a communication channel to the remote station instructing breaker "D" to open the deenergizing faulted breaker "B".

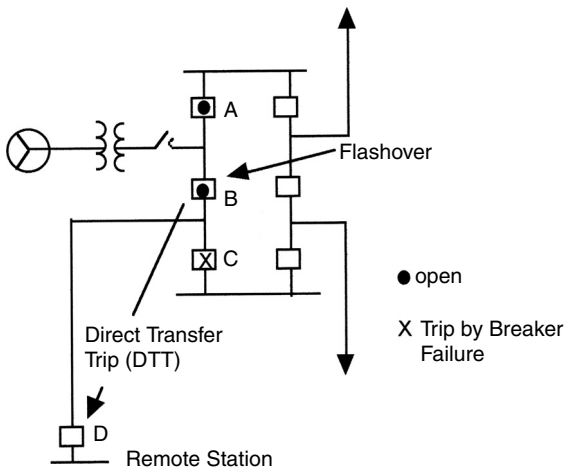


FIGURE 15.17 Direct transfer trip clearing.

© 2006 by Taylor & Francis Group, LLC

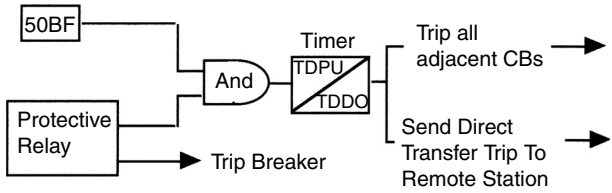


FIGURE 15.18 Breaker failure logic.

Figure 15.18 shows logic typical for a breaker failure scheme. A protective function must first detect the fault or the breaker flashover and attempt to trip the breaker in question. At the same time the relay initiates tripping, it initiates the breaker failure timer. This timer is set a few cycles longer than the maximum time necessary to initiate trip logic, open the breaker, and reset the trip logic after the breaker opens. For a normal operation the breaker will open, interrupting the current and causing the instantaneous fault detector relay (50BF) to drop out. Dropout of the fault detector will stop the timer and prevent scheme operation. If the breaker fails to open or opens but fails to interrupt the current, the fault detector will remain picked up. The timer will time out, initiating a trip of all local and remote breakers adjacent to the faulted breaker. It is therefore necessary that both the breaker failure current detector (50BF) and a protective element detect the breaker flashover current.

Another problem rises when a flashover occurs on a breaker terminating a long HV or EHV line. These lines are highly capacitive when unloaded and supply Vars to the connected system. When a breaker failure operation opens the remote terminal, the faulted breaker, generator and line charging capacitance become elements in a series circuit. Even if the generator field breaker is tripped, the capacitance can provide sufficient excitation to maintain generator voltage near rated during coast down, thus adding to damage caused by the initial event.

15.9 PROTECTION PROVIDED BY NATIVE SCHEMES

A generator is adorned with a myriad of protective functions such as loss-of-field, antimotoring, and negative-sequence current, to name a few. Although these functions are installed for other conditions, several are capable of providing limited energization protection. Unfortunately, these protective elements may be intentionally or accidentally disabled when the generator is offline.

15.9.1 Loss-of-Field Relay: Device 40

Loss-of-field relaying is provided to detect failure of the circuitry that supplies excitation to the generator field winding during operation. A three-phase energization from standstill without field excitation is equivalent to an across the line start of a large induction motor and is characterized by a large flow of reactive power into the generator. A true loss-of-field condition is also characterized by a large Var inflow. It would seem logical that loss-of-field protection would also detect an energization at standstill, but this is not always the case.

There are two basic loss-of-field protection schemes in use today. Both schemes employ impedance-sensing elements at the generator terminals, connected to measure impedance looking into the generator. Only one of these schemes can provide reliable detection for an energization at standstill. Neither scheme provides reliable flashover protection.

A legitimate LOF is a balanced three-phase event; consequently, LOF protection schemes normally monitor only one phase pair. Also, the impedance elements used in these schemes are not designed to respond to phase-to-neutral quantities. For these reasons, the LOF schemes discussed below will not provide reliable detection for a single-phase energization or single-phase breaker flashovers.

© 2006 by Taylor & Francis Group, LLC

15.9.1.1 LOF Scheme 1

The first scheme may employ one or two impedance elements. Both impedance characteristics are set with an offset from the R axis equal to half the transient reactance of the generator ($X'_d/2$) as shown in Figure 15.19. Tripping is initiated when the generator impedance falls inside either relay's characteristic circle. The trip delay for the inner circle is typically set between instantaneous and 0.5 sec. Tripping via the outer characteristic is typically delayed 1.0 sec or more.

When energized at standstill, the generator exhibits locked rotor reactance approximately equal to its negative-sequence impedance. Because the negative-sequence impedance and X'_d, which determines the offset of the LOF characteristic, are of comparable magnitude, the locked rotor impedance of the generator (X_2) falls just inside the trip characteristic with little margin. This is shown in Figure 15.19. Sensing errors and inaccuracies in data used to establish the LOF setting can result in a relay failure to detect the initial locked rotor condition. If this occurs, tripping can be delayed for a considerable portion of the acceleration period because the impedance of the accelerating generator, as with any induction motor, will remain nearly constant through a significant portion of the acceleration period. As speed increases, generator impedance will eventually move through the trip characteristic. If the relay fails to detect the initial condition, the delayed tripping may result in rotor damage.

The energization protection afforded by this LOF scheme could be significantly improved by reducing the offset of the trip characteristic and eliminating the trip delay. Such modifications would be disastrous to reliability, because the offset and delay are specifically chosen to prevent the LOF element from misoperation for stable transients such as power system faults.

15.9.1.2 LOF Scheme 2

The second LOF scheme in common usage is depicted in Figure 15.20. This scheme includes a directional element, undervoltage element and one or two impedance-sensing elements. If only one impedance element is used it is the outer element set just within the generator capability as plotted on the $R-X$ plane. An impedance element set in this manner is offset in the $+jX$ direction, allowing the trip characteristic to encompass the origin. Tripping is supervised by directional and undervoltage elements. The directional element limits tripping to the $-jX$ portion of the impedance plane. The intent of the scheme is to differentiate between a LOF on a strong and one on a weak power system. A LOF on a weak system will cause a severe voltage drop and necessitate rapid

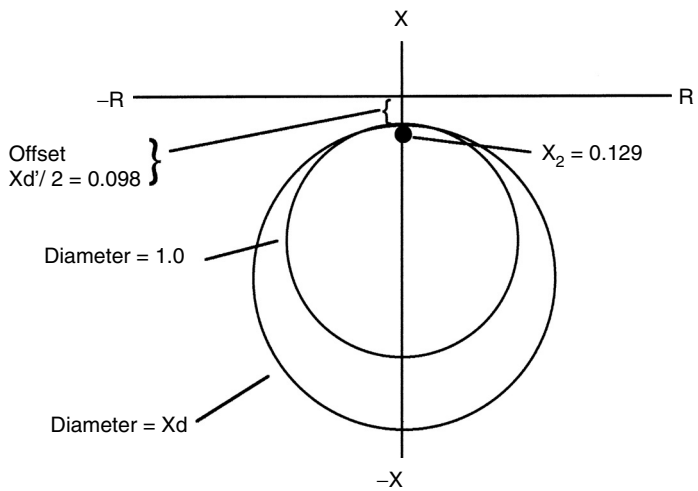


FIGURE 15.19 Scheme 1 loss-of-field characteristic.

© 2006 by Taylor & Francis Group, LLC

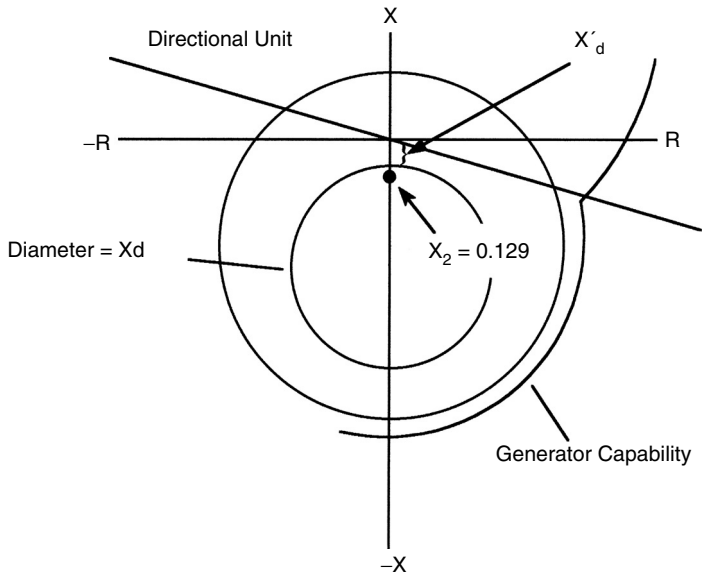


FIGURE 15.20 Scheme 2 loss-of-field characteristic.

tripping. A LOF on a strong system will not jeopardize the system and tripping is delayed. Typically, the undervoltage element is set at 80% rated voltage and tripping delays are 1.0 sec when the UV element drops out and 10 to 60 sec when it does not.

A second impedance element can be added to provide rapid tripping of severe LOF events. This element plots inside the characteristic of the element previously described. It is set similar to the inside element of LOF Scheme 1. It has an offset of $X'_d/2$ and a diameter equal to X_d. It is not supervised by the UV element and is typically set with a delay of 0.25 to 0.5 sec.

This scheme will provide protection for an energization at standstill. The outer element incorporates the $-jX$ axis about the origin and will detect the generator's locked rotor impedance of X_2. This element is supervised by the voltage element, which is normally set to drop out at around 80% voltage. Assuming that an energization depresses the voltage below the undervoltage element setpoint, tripping will be initiated via the scheme's weak system timer, which is typically set around one second. This fast clearing should provide protection for the generator rotor. Of course, if the generator were connected to a very strong system, voltage during energization could remain above the undervoltage setpoint. Tripping would then be through the strong system timer (10 to 60 sec delay). Damage would be expected with the longer delay.

15.9.2 Backup Distance Protection: Device 21

Impedance relays are often applied at the generator terminals to provide backup protection for faults beyond the generator terminals and on the transmission system. This application requires that the relays measure impedance from the generator terminal looking into the power system. Certain types of distance relay can be set with a reverse looking offset. This offset can be adjusted to include impedance equivalent to the negative-sequence impedance of the generator, thus allowing the relay to detect the initial energization at standstill. Figure 15.21 depicts such a setting.

This element provides a backup protection function and must be delayed to allow primary protection schemes at the generator and on the transmission system to operate. Generally this will necessitate a 0.5 to 1.5 sec trip delay. Successful application of an impedance element for standstill protection requires that the offset setting provides sufficient margin to assure that the increasing generator impedance remains within the trip characteristic until the relay times out.

© 2006 by Taylor & Francis Group, LLC

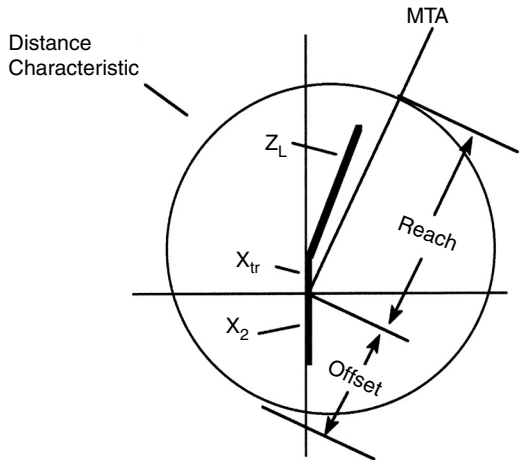


FIGURE 15.21 Backup distance relay.

A distance element at the generator terminals can detect both a three-phase and single-phase energization at standstill. This is not intuitive, because the wye-delta connection of the GSU transformer distorts the current and voltage input to the relay for a single-phase event. The subsequent derivation will show that the relay measured the same initial impedance for a single-phase and three-phase standstill energization.

Distance protection is provided by three distance elements, each measuring voltage and current for a phase pair:

$$\begin{aligned} Z_{ab} &= \frac{V_a - V_b}{I_a - I_b} \\ Z_{bc} &= \frac{V_b - V_c}{I_b - I_c} \\ Z_{ca} &= \frac{V_c - V_a}{I_c - I_a} \end{aligned} \tag{15.59}$$

The phase current and voltages at the relay are found in the usual manner by the inclusion of the $\pm 30^\circ$ phase shift and deletion of zero-sequence quantities to account for the effects of the wye-delta connection of the GSU transformer. The resulting phase equations are:

$$\begin{aligned} V_a &= V_1\angle -30^\circ + V_2\angle 30^\circ \qquad I_a = I_1\angle -30^\circ + I_2\angle 30^\circ \\ V_b &= V_1a^2\angle -30^\circ + V_2a\angle 30^\circ \qquad I_b = I_1a^2\angle -30^\circ + I_2a\angle 30^\circ \\ V_c &= V_1a\angle -30^\circ + V_2a^2\angle 30^\circ \qquad I_c = I_1a\angle -30^\circ + I_2a^2\angle 30^\circ \end{aligned} \tag{15.60}$$

These current and voltage equations are applicable to any condition. Sequence currents and voltages specific to the single-phase event in question are derived from Figure 15.9.

$$V_1 = I_1X_g \qquad V_2 = I_2X_2 \tag{15.61}$$

where X_g = positive-sequence reactance of the generator.

© 2006 by Taylor & Francis Group, LLC

Substituting values from Equation (15.61) and Equation (15.60) into Equation (15.59) and imposing the constraint that $I_1 = I_2$, the measured impedances are found to be

$$\begin{aligned} Z_{ab} &= 1/2(X_2 + X_g) \\ Z_{bc} &= 1/2(X_2 + X_g) + j\frac{\sqrt{3}}{2}(X_2 - X_g) \\ Z_{ca} &= 1/2(X_2 + X_g) + j\frac{\sqrt{3}}{2}(-X_2 + X_g) \end{aligned} \tag{15.62}$$

For the standstill case, generator reactance $X_g = X_2$ and all three elements measure the impedance as X_2, the same as the three-phase case.

As with any scheme, the energization protection afforded is determined by a comparison of the relay operating time against the rotor damage time for the specific event under study.

15.9.3 Voltage Restraint/Voltage Control Relays: Device 51V

These relays are often applied at the generator terminals as an alternate to distance relays for backup protection. Voltage-controlled elements include an overcurrent element and a supervising voltage element. The overcurrent element is set to operate below rated generator current, but operation is inhibited when voltage is above the setting of the voltage element.

The overcurrent pickup of a voltage-restrained element is typically set to operate between 125 and 175% rated generator current at rated voltage. The pickup current of this relay decreases with generator terminal voltage. A typical pickup vs. voltage characteristic for a voltage restraint relay is plotted in Figure 4.3. At 50% rated voltage, the overcurrent element depicted operates at half the current necessary for operation at rated voltage.

A three-phase energization at standstill typically results in an initial current between one and four times rated generator current and voltage depressed to 20 to 70% rated. These conditions would be detectable by either type of voltage-supervised relay.

Single-phase energizations are more difficult to detect because the per unit phase current on the generator side of the transformer, where the voltage-supervised relays are located, is only 58% of that on the switchyard side. This effect is apparent from a comparison of Equation (15.10) and Equation (15.12) and is the result of the wye-delta connection of the GSU transformer. The voltage-supervised relay should detect a single-phase energization at the majority of installations, but calculations should confirm that relay current and voltage reduction are sufficient to actuate the relay. This calculation would use the same methodology applied to current and voltage calculations for the distance relay in Section 15.9.2.

Voltage-supervised relays are backup relays and must have sufficient time delay to allow coordination with primary transmission line protection. This will necessitate a trip delay typically between 0.5 and 1.5 sec. Again, the protection provided by the voltage-supervised relay for a standstill energization is determined from a comparison of the relay trip time and the rotor damage time.

Neither type of voltage-supervised relay would be expected to provide protection for a flashover, because the coordination time delay would likely override current and voltage transient.

15.9.4 Motoring Protection: Device 32

Motoring protection is provided by a power-sensing relay at the generator terminals connected to measure power flow into the generator. Motoring protection will trip the generator in the event the prime mover ceases to drive the generator. During an actual motoring condition, the generator acts as a synchronous motor supplying unit losses including friction and windage. The motoring

© 2006 by Taylor & Francis Group, LLC

protection must be set to detect these losses. An energization at standstill would not initially include the rotational losses, but higher electrical losses during the acceleration period would be expected because of the increased current. Consequently, the motoring relay should detect a three-phase energization at standstill.

Motoring is a balanced three-phase condition and many motoring elements measure only one set of phase-to-phase quantities to calculate the motoring power. Such a relay would not sense a single-phase energization evolving phases to which it is not connected.

The power input to the generator during a three-phase energization can be calculated in per unit as

$$P_{3\text{ph}} = 3I_1^2 R_2 \tag{15.63}$$

The energization current would be calculated from Equation (15.4).

Although this relay would likely detect the energization the trip delay associated with the motoring function is in the 30 to 60 sec range — much too long to protect the accelerating generator. Also, some motoring relays use an inverse-time voltage relay to provide the trip delay. Relays of this design require about 50% rated voltage to activate the timer and will not function for energization from a weak system where voltage may be depressed to 20 to 40% of rated.

15.9.5 Negative-Sequence Current Protection: Device 46

Negative-sequence current protection is routinely provided to protect the generator rotor from excessive heating resulting from 120 Hz current induced into the rotor body and structure by an unbalanced stator current. This protection could sense the negative-sequence current associated with single-phase and two-phase energization, but would be insensitive to a three-phase energization.

The short time negative-sequence current capability of a generator is expressed in terms of its I_2^2t limit, which appears on standard generator data sheets. The time–current characteristic of the negative-sequence relay is typically set slightly below the I_2^2t limit of the generator. This coordination provides protection for the rotor during normal operation when rotor heating is attributed to negative-sequence current. However, at standstill and during acceleration, both positive- and negative-sequence currents contribute to rotor heating as described by Equation (15.58).

A single-phase energization at standstill will produce equal positive- and negative-sequence currents and no acceleration. At standstill, positive- and negative-sequence currents contribute equally to rotor heating and the time–current characteristic of a negative-sequence relay would have to be set less than half the generator's I_2^2t limit to provide protection for this case.

A faster trip characteristic may be required for a two-phase energization. In this case, positive-sequence current would exceed negative-sequence current. The ratio of positive- to negative-sequence current is a function of the negative- and zero-sequence impedance of the generator and connected system, as shown in Figure 15.12. To complicate matters, the rotor heating caused by the positive-sequence current will decrease as the rotor accelerates.

There are two types of negative-sequence relay in use. The first is electromechanical time overcurrent relays, which were designed as backup protection for system faults. These relays lack sensitivity and usually require about 0.6 pu negative-sequence current (based on generator rating) to actuate. Also, the time–current characteristics of such a relay are not an exact match to the generator's negative-sequence capability, which complicates their application. Newer solid-state and microprocessor negative-sequence elements are sensitive down to the negative sequence capability of the generator and have characteristics that match the I_2^2t capability of the generator.

A single-phase energization initiated from the high-voltage side of the GSU is depicted in Figure 15.4. The negative-sequence component of current at the generator terminal for this condition would be equal to the line current at the generator divided by $\sqrt{3}$. Generally, the

© 2006 by Taylor & Francis Group, LLC

electromechanical relay can be set to provide sufficient sensitivity to detect single-phase energization on a strong system. These relays may not detect the same energization on a weak system or a two-phase energization and should be assessed on an individual basis. The solid-state and microprocessor relays have sufficient sensitivity to detect both these conditions.

15.9.6 Backup Ground Relay: Device 51N

Many installations include a time delay ground relay connected to a CT in the neutral of the GSU transformer. This relay is intended to trip the GSU and generator if transmission line primary ground fault protection fails to operate. This scheme is capable of detecting single- and two-phase energizations, but each installation must be checked to confirm that existing settings provide the required sensitivity. Because this relay performs a backup function, it is set with sufficient time delay to allow primary line relaying to operate. The required delay can result in tripping being too slow to prevent damage during energization and will render the relay ineffective for protection for a breaker flashover.

15.10 DEDICATED ENERGIZATION PROTECTION

It is apparent that native schemes do not provide adequate protection for energization events. These schemes are either too slow or lack sensitivity. Another major disadvantage with these schemes is that they are associated with online protections and as such are routinely removed from service during shutdown. These schemes are also disabled unintentionally when the generator relay voltage transformer fuses are removed or when schemes are tested or modified during a generator outage. For these reasons, it has become standard practice to install dedicated "inadvertent energization" and "open breaker flashover" schemes.

Dedicated schemes should trip the appropriate high-voltage switchyard breakers, the generator field breaker and the breaker(s) at the low side of unit auxiliary transformer. The schemes should also be designed with control circuitry segregated from online protection to assure these schemes are not disabled during unit shutdown.

15.10.1 Dedicated Inadvertent Energization Schemes

These schemes are intended to detect an energization that occurs with the generator at standstill. Such energization would be the result of a breaker, gang-operated, or single-phase disconnect switch closure. Consequently, an inadvertent energization scheme must detect both three-phase and single-phase events. The scheme shown in Figure 15.22 is armed when the generator is taken offline and all three-phase voltage elements drop out. These elements are typically set about 85% nominal voltage. Arming is delayed 2 to 5 sec by the delayed pickup of the timer. This delay is necessary to ensure that the scheme is not activated by voltage dips associated with system faults. Once armed, tripping is initiated without delay if any one of the phase instantaneous overcurrent elements actuate. Overcurrent elements are normally set about 50% of the minimum anticipated energization current. The minimum current is usually a result of a single-phase energization.

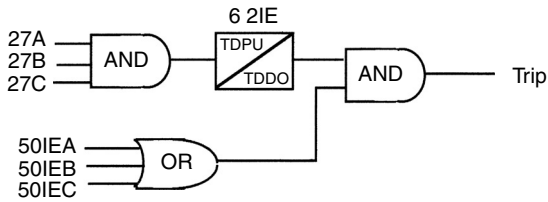


FIGURE 15.22 Inadvertent energization: Scheme 1.

© 2006 by Taylor & Francis Group, LLC

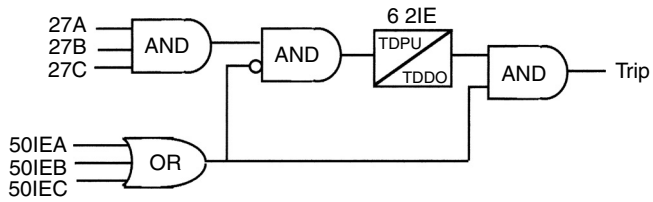


FIGURE 15.23 Inadvertent energization: Scheme 2.

The scheme is taken out of service automatically when the generator is returned to service and the terminal voltage rises above the undervoltage element settings. Deactivation of the scheme is delayed 10 to 15 cycles by the delayed dropout of the timer. This delay is required to assure the scheme will operate for an actual energization, which would also reset the undervoltage elements. Because this scheme deactivates before the generator reaches rated voltage, it will not provide breaker flashover protection.

There are many scheme variations. The scheme shown in Figure 15.23 is similar to the above scheme, but provides increased security against false actuation by including logic that requires the dropout of overcurrent and voltage elements to arm.

The scheme in Figure 15.24 uses an underfrequency element to arm. By setting the underfrequency element below the minimum frequency anticipated for a system event, say 55 Hz, a delay in arming the scheme is not required. The underfrequency element used in this scheme must remain asserted when the element is deenergized to maintain scheme operability during shutdown. This requirement makes the scheme vulnerable to false activation if potential to the UF element is lost. For this reason the scheme is supervised by a fuse failure (Device 60) element to block scheme operation in the event a PT fuse fails. A delay in disabling the scheme is again required to assure scheme operation when an actual energization resets the underfrequency relay. Because this scheme is only active at reduced frequency, it will not be in service when open breaker flashovers are most likely.

Dedicated impedance elements have been applied for inadvertent energization protection. One such scheme is shown in Figure 15.25. The distance element is oriented to measure impedance looking into the generator. The element is set to detect the transformer plus generator standstill impedance ($X_{tr} + X_2$) plus margin. This scheme would be in service regardless of the generator's status. During normal operations the scheme provides backup fault protection with tripping delayed to coordinate with primary protection relays. An impedance element set in this manner will detect power system swings and may require an additional delay to avoid misoperation for stable swings. Stability studies are required to assess this. A time delay in excess of a second may be required to meet these criteria. When the generator is offline, as indicated by the position of the generator disconnect switch, tripping is immediate.

In the application shown, tripping is supervised by an instantaneous overcurrent unit set above maximum load. This feature will prevent scheme operation for a loss of potential to the distance relay. Such a loss could cause the distance relay to close its contacts, actuating the scheme.

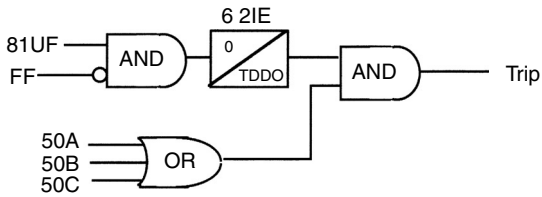


FIGURE 15.24 Inadvertent energization: Scheme 3.

© 2006 by Taylor & Francis Group, LLC

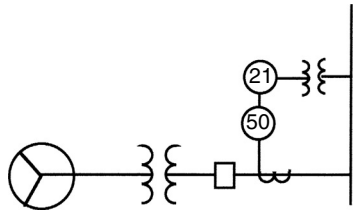


FIGURE 15.25 Inadvertent energization: Scheme 4.

15.10.2 Dedicated Breaker Flashover Protection

Breaker flashover protection is prescribed of air and gas breakers. Most flashovers involve only one breaker pole, but two-pole events are reported. A three-phase flashover is conceivable, but extremely improbable and open breaker flashover (OBF) schemes are typically not designed to sense three-phase flashover. Inadvertent energization schemes focus on energization with the generator shut down. These schemes are not in service just prior to synchronizing and immediately after the unit is taken offline; hence, they are not operable when flashover is most likely. The native solid-state negative-sequence relaying at the generator can detect an OBF condition and initiate breaker failure logic, but clearing may be too slow because of the inherent delay in the negative-sequence function.

More rapid clearing is provided by the dedicated OBF scheme. Because any OBF scheme must initiate the breaker failure logic to open all breakers adjacent to the faulted breaker, the modified breaker failure scheme shown in Figure 15.26 has become a preferred form of OBF protection. The scheme shown is for breaker A. A similar scheme would be required for breaker B. The upper portion of the scheme is standard breaker failure (BF) logic. The lower portion is placed in service by a 52b switch when breaker A is taken out of service. Both the 50N and the breaker failure fault detector (50BF) must have sufficient sensitivity to detect the flashover. If a flashover occurs, tripping of all adjacent breakers is initiated within a few cycles, as dictated by the pickup delay of the breaker failure timer.

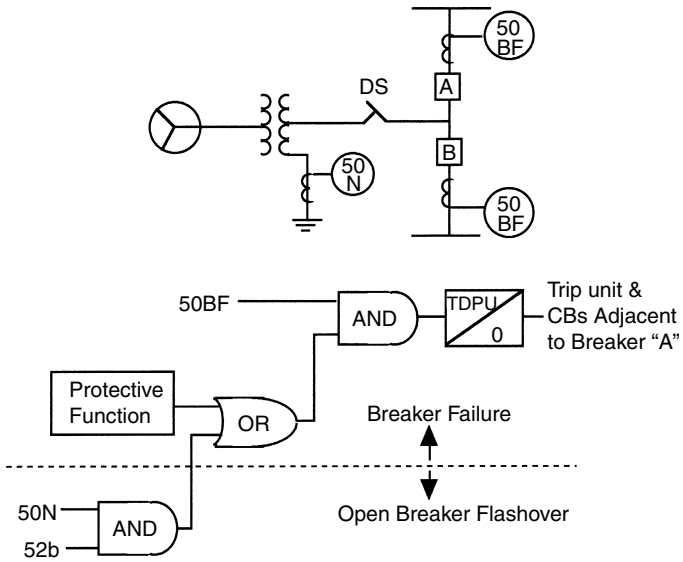


FIGURE 15.26 Open breaker flashover/breaker failure scheme.

© 2006 by Taylor & Francis Group, LLC

15.11 APPLYING ENERGIZATION PROTECTION ON THE SAMPLE SYSTEM

Assume the sample system generator protection is being upgraded by the addition of dedicated inadvertent energization and open breaker flashover schemes. The placement of the current detectors for these schemes is shown in Figure 15.27. The OBF scheme logic is shown in Figure 15.28. This scheme is similar to Figure 15.26, except the BF fault detector on the sample system scheme consists of two-phase and one ground element. The inadvertent energization scheme logic is shown in Figure 15.22.

The relay elements used are as follows:

- The instantaneous elements of the inadvertent energization, 50IE A, B and C, have a range of 1–12 secondary amps, settable in 0.1 increments. The scheme timer, 62IE, has a settable range of 1–5 sec on pickup and 0.1 to 2 sec on dropout.
- The open breaker flashover current detector 50N is a solid-state instantaneous element with a range of 0.5–5.0 secondary amps.
- The breaker failure fault detector has three instantaneous elements: A and C phase elements and one ground element. The phase elements have a range of 2–8 A. The ground element range is 0.5–2.5 A.

15.11.1 Inadvertent Energization Scheme Settings

The inadvertent energization scheme is intended to operate for energizations when the generator is at rest. Such energization would be caused by accidental closure of the high-voltage breaker or the disconnect switch. A breaker closure would result in a three-phase energization, while a switch closure would produce either three-phase or single-phase energization depending on the type of switch. Consequently, the current detectors in the inadvertent energization scheme must be capable of detecting both conditions.

When energized at standstill, the generator will display positive-sequence impedance closely approximated by its negative-sequence impedance. The initial three-phase energization current is calculated using sample system data from Chapter 1, Generator data sheet Appendix A, and Equation (15.4) neglecting R_2.

$$I_1(\text{start}) = \frac{E_{\text{sys}}}{X_{\text{sys}} + X_{\text{tr}} + X_2}$$

$$= \frac{1.0}{0.078 + 0.07 + 0.129} = 3.61 \text{ pu}$$

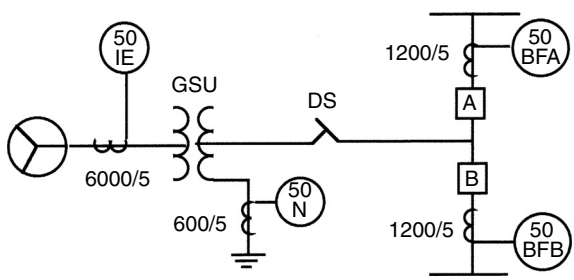


FIGURE 15.27 Energization protection on sample system.

© 2006 by Taylor & Francis Group, LLC

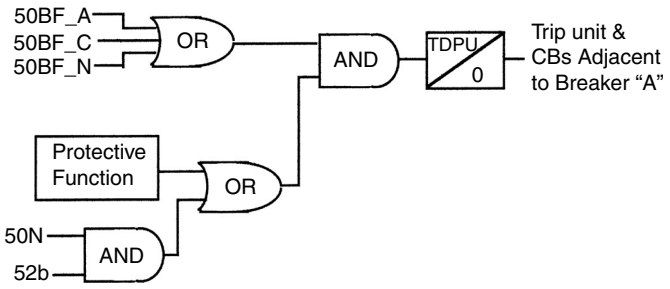


FIGURE 15.28 Sample system OBF scheme.

or, in terms of amps

$$I_1 = I_{\text{base}} * I_{1_\text{PU}}$$
$$= \frac{kVA_{\text{base}}}{\sqrt{3}kV_{\text{base}}} 3.61$$

Since impedances are on the generator base current at the high-voltage terminals of the GSU is

$$I_1 = \frac{104{,}400}{\sqrt{3}\ \ 69\,\text{kV}} 3.61 = 3153\,\text{A@}69\,\text{kV}$$

Current at the generator terminals is then:

$$I_1 = \frac{104{,}400}{\sqrt{3}\ \ 13.8\,\text{kV}} 3.61 = 15{,}768\,\text{A@}13.8\,\text{kV}$$

The initial single-phase energization currents are calculated as follows. The positive-sequence energization current is found from Equation (15.7):

$$I_1 = \frac{E_s}{Z_{1\text{sys}} + Z_{2\text{sys}} + Z_{0\text{sys}} + 3Z_{\text{tr}} + 2X_2}$$
$$= \frac{1.0}{0.078 + 0.078 + 0.23 + 3(0.07) + 2(0.129)}$$
$$= 1.17\ \text{pu}$$

Current at the high-voltage terminals of the GSU transformer are found from Equation (15.8) and the constraint that $I_1 = I_2 = I_0$. This yields

$$I_a(\text{amps}) = (I_1 + I_2 + I_0)I_{\text{base}}$$
$$= 3 * 874\,\text{A} * 1.17 = 3068\,\text{A}$$
$$I_b = (I_1 a^2 + I_2 a + I_0) * I_{\text{base}} = 0$$
$$I_c = (I_1 a + I_2 a^2 + I_0) * I_{\text{base}} = 0$$

Current at the generator terminals is found by including the $\pm 30^\circ$ phase shift imposed on the negative- and positive-sequence currents respectively by the wye-delta connection of the GSU

© 2006 by Taylor & Francis Group, LLC

transformer, Equation (15.9).

$$\begin{aligned} I_A &= (I_1\angle -30^\circ + I_2\angle 30^\circ) * I_{base} \\ &= (1.17\angle -30^\circ + 1.17\angle 30^\circ) * 4368\ A \\ &= 8851\ A\angle 0 \end{aligned}$$

$$\begin{aligned} I_B &= (I_1 a^2\angle -30^\circ + I_2 a\angle 30^\circ) * I_{base} \\ &= (1.17\angle 210^\circ + 1.17\angle 150^\circ) * 4368\ A \\ &= 8851\angle 180^\circ \end{aligned}$$

$$\begin{aligned} I_C &= (I_1 a\angle -30^\circ + I_2 a^2\angle 30^\circ) * I_{base} \\ &= (1.17\angle 90^\circ + 1.17\angle 270^\circ) * 4368\ A = 0 \end{aligned}$$

Clearly, the phase-to-ground case produces the minimum energizing current and is therefore chosen as the basis for the instantaneous element settings. The 50IE should be set no higher than 50% the minimum energization current. The 50IE setting is then calculated as:

6000/5 CTs

Maximum setting = 8851 × 0.5 = 4426 primary amps
Secondary amps = 4426 A * 5/6000 = 3.69 A
Setting 50IE: 3.6 secondary amps = 4320 primary amps

The time delay pickup of timer 62IE sets the delay in arming the scheme after the generator is taken offline and the 27 element dropout. This setting is not critical, but must allow sufficient time to override voltage transients caused by system faults that would drop out the 27 elements and erroneously arm the scheme. The transmission lines adjacent to the sample system generator employ two-zone step-distance phase protection and time and instantaneous overcurrent ground protection. The time delay on the second zone phase protection is 0.5 sec, so both ends of a faulted line would clear in less than a second. Although the overcurrent ground protection could take several seconds to clear, a ground fault would not drop out all three 27 elements to arm the scheme. A delay on arming of 2.0 sec should be more than sufficient.

Note that if the scheme portrayed in Figure 15.23 had been used, this delay would not be required. Arming of that scheme requires three phases of both 50IE and 27 elements to drop out. If 50IE were reset to a pickup value below generator full load current, arming could not occur with the generator online.

The delay in dropout for 62IE is critical because it must maintain the trip path when the 27 elements reset following an actual inadvertent energization. A delay of 15 cycles (0.25 sec) is adequate to maintain the required contact coordination.

During an energization from standstill, generator damage would likely occur in the generator rotor as a result of induced currents. The generator's negative-sequence short time capability ($K = I_2^2 t$) is an indicator of rotor thermal capability and can be used to estimate time to the onset of damage. The data sheet for the sample system generator (Appendix A) lists an $I_2^2 t$ limit equal to 30. At standstill, both positive- and negative-sequence currents contribute equally to rotor heating and the time until damage is estimated as

$$t = \frac{K}{I_1^2 + I_2^2}$$

For the instance under study, a three-phase energization produces a positive-sequence current of 3.61 pu, while a single-phase energization produces positive- and negative-sequence currents each with a magnitude of 1.17 pu. The resulting withstand times are as follows.

© 2006 by Taylor & Francis Group, LLC

For the three-phase case:

$$t = \frac{30}{3.61^2} = 2.3 \text{ sec}$$

For the single-phase case:

$$t = \frac{30}{1.17^2 + 1.17^2} = 10.9 \text{ sec}$$

15.11.2 Open Breaker Flashover

An open breaker flashover represents a dielectric failure across one or more open breaker poles. A breaker flashover is most likely for a single-pole flashover, but two-pole flashovers have been reported. A three-phase flashover is considered extremely unlikely and not considered a credible event for protection. The OBF schemes employ only ground current detectors, making the scheme insensitive to a three-phase flashover. The scheme being installed at the sample system generator uses an instantaneous overcurrent element in the neutral of the GSU transformer (50N) to detect the flashover as shown in Figure 15.26. This element measures three times the zero-sequence current ($3*I_0$) and should be set no greater than 50% the minimum $3I_0$ flashover current.

With field applied at the time of flashover, the generator is represented by an internal voltage proportional to the field excitation and its subtransient reactance (X''_d) in the positive sequence and X_2 in the negative sequence. A flashover is an out-of-phase synchronizing and the initial current is a function of the generator and system voltages, the phase difference at closure, and the total circuit impedance. A flashover is assumed to occur at the point of maximum insulation stress, 180° separation. The minimum relay current would be expected for a single-phase flashover, but both single-phase and two-phase flashover currents will be analyzed to confirm this assumption.

15.11.2.1 Initial Current for Single-Phase Flashover

The calculation of single-phase flashover current is discussed in Section 15.4.1 The sample system positive-sequence current is calculated from Equation (15.13), with the generator at 180°:

$$\begin{aligned} I_1 &= \frac{E_s\angle 0^\circ - E_g\angle 180^\circ}{2Z_{1sys} + Z_{0sys} + 3Z_{tr} + X''_d + X_2} \\ &= \frac{2.0}{2(0.078) + 0.23 + 3(0.07) + 0.136 + 0.129} \\ &= 2.32 \text{ pu} \end{aligned}$$

For the single-phase case, $I_1 = I_2 = I_0$, and the relay current at the neutral of the GSU transformer is

$$\begin{aligned} 3I_0 &= 3I_1 * I_{base} \\ &= 3 * 2.32 * 874 \text{ A} = 6080 \text{ A} \end{aligned}$$

and 69 kV phase currents from Equation (15.8) are

$$\begin{aligned} I_a(\text{amps}) &= (I_1 + I_2 + I_0)I_{base} \\ &= 3 * 874 \text{ A} * 2.32 = 6080 \text{ A} \\ I_b &= (I_1 a^2 + I_2 a + I_0) * I_{base} = 0 \\ I_c &= (I_1 a + I_2 a^2 + I_0) * I_{base} = 0 \end{aligned}$$

© 2006 by Taylor & Francis Group, LLC

Current at the generator terminals is calculated from Equation (15.9) as

$$\begin{aligned} I_A &= (I_1\angle -30^\circ + I_2\angle 30^\circ) * I_{base} \\ &= (2.32\angle -30^\circ + 2.32\angle 30^\circ) * 4368\,A \\ &= 17{,}552\,A\angle 0 \\ I_B &= (I_1 a^2\angle -30^\circ + I_2 a\angle 30^\circ) * I_{base} \\ &= (2.32\angle 210^\circ + 2.321\angle 150^\circ) * 4368\,A \\ &= 17{,}552\angle 180^\circ \\ I_C &= (I_1 a\angle -30^\circ + I_2 a^2\angle 30^\circ) * I_{base} \\ &= (2.32\angle 90^\circ + 2.32\angle 270^\circ) * 4368\,A \\ &= 0 \end{aligned}$$

15.11.2.2 Initial Current for Two-Phase Flashover

The two-phase flashover calculation is described in Section 15.4.1. Sample system impedances are

$$\begin{aligned} Z_1 &= Z_{1sys} + X_{tr} + X''_d \\ &= 0.078 + 0.07 + 0.136 = 0.284 \\ Z_2 &= Z_{1sys} + X_{tr} + X_2 \\ &= 0.078 + 0.07 + 0.129 = 0.277 \\ Z_0 &= Z_{0sys} + X_{tr} \\ &= 0.23 + 0.07 = 0.30 \end{aligned}$$

Referring to Equation (15.13) and Figure 15.12, positive-sequence current is

$$\begin{aligned} I_1 &= \frac{E_s\angle 0^\circ - E_g\angle 180^\circ}{Z_1 + \left(\frac{Z_2 Z_0}{Z_2+Z_0}\right)} \\ &= \frac{2}{0.284 + \left(\frac{0.277*0.3}{0.277+0.3}\right)} = 4.67 \end{aligned}$$

Negative- and zero-sequence currents are calculated for Equations (15.17) as

$$I_0 = -I_1\frac{Z_2}{Z_2+Z_0} = -4.67\frac{0.227}{0.227+0.3} = -2.01$$

$$I_2 = -I_1\frac{Z_0}{Z_2+Z_0} = -4.67\frac{0.3}{0.227+0.3} = -2.66$$

The relay current is $3I_0$, so

$$3I_0 = 3 * 2.01 * 874\,A = -5270\,A$$

© 2006 by Taylor & Francis Group, LLC

69 kV phase currents are calculated by substituting the sequence currents into Equation (15.8):

$$\begin{aligned} I_a(\text{amps}) &= (I_1 + I_2 + I_0) I_{\text{base}} \\ &= (4.67 - 2.66 - 2.01) * 874\,\text{A} = 0 \\ I_b &= (I_1 a^2 + I_2 a + I_0) * I_{\text{base}} \\ &= (4.67a^2 - 2.66a - 2.01) * 874\,\text{A} \\ &= 6142\,\text{A}\angle -115^\circ \\ I_c &= (I_1 a + I_2 a^2 + I_0) * I_{\text{base}} \\ &= (4.67a - 2.66a^2 - 2.01) * 874\,\text{A} \\ &= 6142\,\text{A}\angle 115^\circ \end{aligned}$$

Currents at the generator terminals are derived from Equation (15.12), which account for the wye-delta configuration of the GSU transformer:

$$\begin{aligned} I_A &= (I_1\angle -30^\circ + I_2\angle 30^\circ) * I_{\text{base}} \\ &= (4.67\angle -30^\circ - 2.66\angle 30^\circ) * 4368\,\text{A} \\ &= 17{,}723\ \text{A}\angle -64.6 \\ I_B &= (I_1\, a^2\angle -30^\circ + I_2 a\angle 30^\circ) * I_{\text{base}} \\ &= (4.67\angle 210^\circ - 2.26\angle 150^\circ) * 4368\,\text{A} \\ &= 17{,}723\ \text{A}\angle -115.4^\circ \\ I_C &= (I_1\, a\angle -30^\circ + I_2 a^2\angle 30^\circ) * I_{\text{base}} \\ &= (4.67\angle 90^\circ - 2.66\angle 270^\circ) * 4368\,\text{A} \\ &= 32{,}017\,\text{A}\angle 90^\circ \end{aligned}$$

15.11.2.3 Setting the OBF Fault Detector (50N)

As anticipated, the phase-to-ground case produces the minimum relay current and will be the basis for the current detector settings. The 50N should be set no higher than 50%, the minimum flashover current. The 50N setting is then calculates as:

600/5 CTs

Maximum setting = 6080 × 0.5 = 3040 primary amps
Secondary amps = 3040 A*5/600 = 25.3 A
Setting 50N: 25.0 secondary amps = 3000 primary amps

REFERENCES

1. IEEE C37.102-1995, *IEEE Guide for AC Generator Protection*, IEEE, New York, 1996.
2. deMello, F. P., *Course Notes, Electrical Machine Dynamics I*, Power Technologies Inc, Schenectady, NY, July 1974 Revision.
3. Inadvertent energizing protection of synchronous generators, IEEE Report, *IEEE Trans Power Delivery*, 4 (2), 965, 1989.

© 2006 by Taylor & Francis Group, LLC

16 Motor Protection

16.1 INTRODUCTION

Motor protection is a vast subject. Our intent is to limit discussion to the dominant application at generating plants, induction motors. This chapter is primarily dedicated to protection of the motors themselves, but does include topics on phase and ground fault protection.

Motors may drive continuous loads such as fans and pumps, or time-variant loads like crushers or boring mills. In either case, proper motor protection is contingent upon a sound motor application that match motor capability to the driven load. Motors with similar horsepower rating have different torque and thermal characteristics. Likewise, loads with similar horsepower requirements have varied torque and inertial specifications. These characteristics must be suitably matched for proper operation. Misapplication often appears as protective device problems such as nuisance tripping and recuring failures. Consequently, a significant portion of this chapter is dedicated to motor/load compatibility.

Motors are subject to damage from both mechanical and electrical abnormalities. Damage generally results from overheating internal motor components. Manufacturers provided motor short time capabilities in the form of thermal limit curves. Protective device applications and settings are constrained by the thermal limits and the motor starting characteristic. Overcurrent elements are commonly applied for motor protection. These must be set to operate with sufficient speed to prevent motor damage, but must also have sufficient delay to override the starting current transients. Figure 16.1 shows an overcurrent element in the desired configuration between motor thermal capability and the starting transient.

A basic difficulty with the application of overcurrent elements for motor protection is that the graphic coordination of Figure 16.1 is invalid for the time-varying starting current. The fact that the starting trace lies below the relay characteristic and below the thermal limit does not ensure that the relay will not actuate during the start or that the start is within the capability of the motor. In this chapter, techniques are developed to assess relay response and motor capability with time-variant currents. These currents may be starting currents or load cycle current.

Protection becomes more difficult as starting time increases. The greater the starting time, the more difficult it is to thread the relay characteristic between the start and the thermal limit curves. Starting time increases with increased rotating inertia and with decreased starting voltage.

In the past, motor protection was hampered by electromechanical technology. Of all the protective relaying specialties, motor protection has benefited the most from microprocessor technology. This advance has allowed the implementation of thermal algorithms that can be configured to individual motors using standard motor data. Two such algorithms will be discussed.

16.2 MOTOR CHARACTERISTICS AND REPRESENTATION

Before motor protection can be discussed in detail, we must establish a basic understanding of motor theory and operation. One way to accomplish this is to develop an equivalent circuit for a motor.

16.2.1 Classical Motor Equivalent Circuit

A three-phase induction motor consists of a rotor and a stator. The stator is the stationary structure with phase windings distributed 120 electrical degrees apart around its parameter. The rotor of a

© 2006 by Taylor & Francis Group, LLC

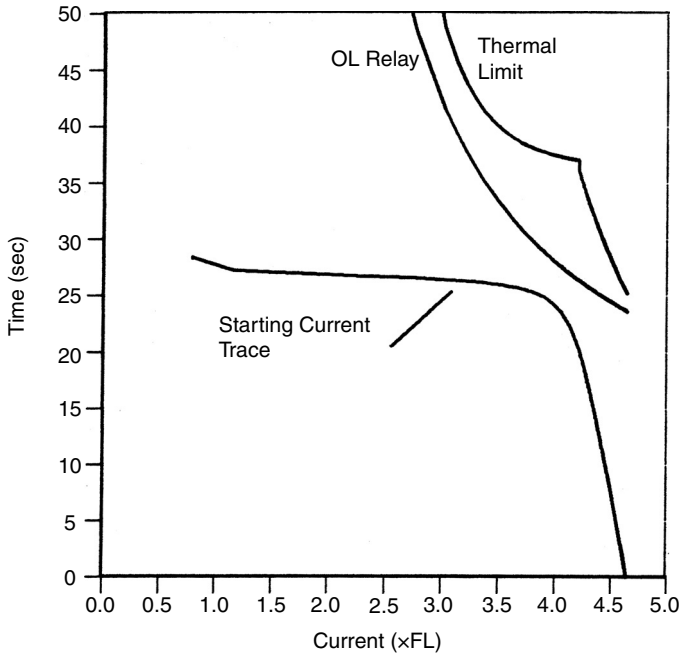


FIGURE 16.1 Motor starting time–current characteristic.

wound rotor motor has wound coils of similar number and placement as the stator winding. In an induction motor, the rotor has conductive bars placed longitudinally along the circumference. These bars are electrically connected at the ends to form conductive paths that act as windings. Figure 16.2 illustrates the stator winding and, in the case of an induction motor, the pseudo rotor windings.

When energized, each stator winding produces flux in phase with the phase current. In a balanced three-phase system, the currents sum to zero. It would seem that the same would be true of the flux produced by these currents. In fact, if the windings were aligned tip to tail, the net flux would be zero, but because each phase winding is physically distributed around the stator, each displaced 120 electrical degrees from the other, a net stator flux is created. The resulting magnetic flux would have a north and south pole; hence, a motor with one three-phase coil group would be termed a two-pole machine.

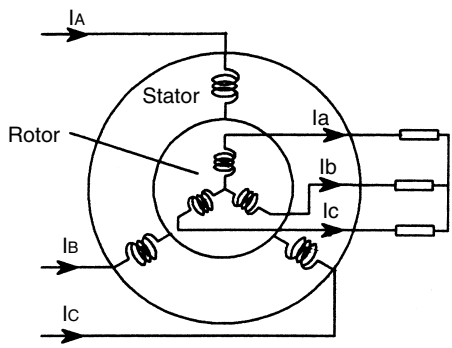


FIGURE 16.2 Stator and rotor windings.

© 2006 by Taylor & Francis Group, LLC

A stator may have several sets of phase windings adjacent to one another distributed about the stator perimeter. Each phase grouping would produce its one resultant flux. A motor with two groups of phase coils would be a four-pole machine.

The synchronous speed of a motor is listed on the motor nameplate. This is the speed at which the resultant stator flux circles the inner circumference of the stator. The synchronous speed of the motor is calculated as:

$$RPM_{\text{sync}} = \frac{120 * f}{p} \tag{16.1}$$

where $f =$ frequency of the applied voltage and $p =$ number of poles. The rotor lies within the opening of the stator separated from the stator by an air gap. The relationship between the stator and rotor is similar to the primary and secondary windings of a transformer. This relationship is more easily understood when the motor is at standstill, as would be the case at starting.

The circuit in Figure 16.3 represents a motor under locked rotor conditions. With the rotor at standstill, the stator flux passes over the rotor and the rotor winding at synchronous speed, inducing a voltage into the stationary rotor winding. The magnitude of the induced rotor voltage is determined by the turn ratio of the stator to rotor windings (N_S/N_R). The frequency of the induced current will equal that of the stator line current.

The locked rotor current in the stator phases is determined by stator impedance plus the rotor circuit impedance as viewed from the stator winding. Transformer theory dictates that the rotor (secondary) impedance is reflected to the stator (primary) winding by using the square of the turn ratio. The locked rotor impedance of the motor as viewed from the stator winding is then:

$$Z_{\text{LR}} = R_{\text{s}} + jX_{\text{s}} + n^2(R_{\text{r}} + jX_{\text{r}}) \tag{16.2}$$

and the locked rotor current in the stator becomes $I_{\text{LR}} = E/Z_{\text{LR}}$.

Although the inclusion of an equivalent turns ratio in the locked rotor model is physically correct and does illustrate the difference in current and voltage magnitudes between the stator and rotor circuits, this model has little practical value. Induction motor parameters are generally determined by test. Because the rotor is inaccessible from a test standpoint, motor parameters are determined from the stator terminals and conversion of rotor circuit values is not necessary. Motor equivalents are then, by convention, drawn with rotor impedance reflected to the stator. With this convention, the effective turn ratio becomes unity.

The current induced in the rotor circuit generates a rotor flux that interacts with the stator flux to produce torque. In the starting case, this torque acts to accelerate the rotor and driven load.

When the rotor is in motion, the transformer analogy becomes more complex. First the induced rotor voltage is no longer directly proportional to the turns ratio. In any transformer the voltage

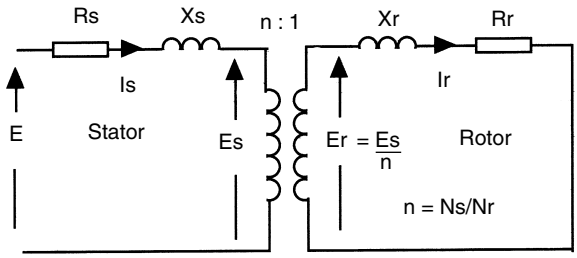


FIGURE 16.3 Equivalent motor circuit with locked rotor.

© 2006 by Taylor & Francis Group, LLC

induced in a winding is proportional to the rate of flux change and the number of turns in that winding. For a normal transformer the primary and secondary voltages are then

$$E_{\text{prim}} \propto N_{\text{prim}} \frac{d\Psi}{dt} \qquad E_{\text{sec}} \propto N_{\text{sec}} \frac{d\Psi}{dt}$$

Because the core flux Ψ is common to both primary and secondary windings, the voltage relation for a normal transformer reduces to

$$\frac{E_{\text{prim}}}{E_{\text{sec}}} = \frac{N_{\text{prim}}}{N_{\text{sec}}}$$

This is the relation used in the locked rotor circuit. However, when the rotor is in motion, the rate of flux change in the rotor winding is equal to the angular speed difference between the stator field (at synchronous speed) and the rotor. This speed difference is generally expressed in terns of per unit slip, which is defined as:

$$s = \frac{RPM_{\text{sync}} - RPM_{\text{rotor}}}{RPM_{\text{sync}}} \tag{16.3}$$

The magnitude of the voltage induced into the rotor and the frequency of the induced voltage and current become functions of slip.

$$E_{\text{r}} = s * E_{\text{stator}} \qquad f_{\text{rot}} = s * f_{\text{stator}} \tag{16.4}$$

The variation in rotor frequency causes variations in rotor circuit impedance

$$Z_{\text{r}} = R_r + j * 2\pi f_{\text{r}} L_{\text{r}}$$

At locked rotor, slip $= 1$, and the rotor exhibits 60 Hz reactance. Expressing X_{r} in terms of the locked rotor value, the slip-dependent rotor impedance becomes:

$$Z_{\text{r}} = R_{\text{r}} + jsX_{\text{r}}$$

The circuit in Figure 16.4 incorporates these slip-dependent terms to form a generalized representation of the motor. Because rotor resistance and reactance are displayed as equivalents seen from the stator winding, the transformer turns ratio is equal to unity.

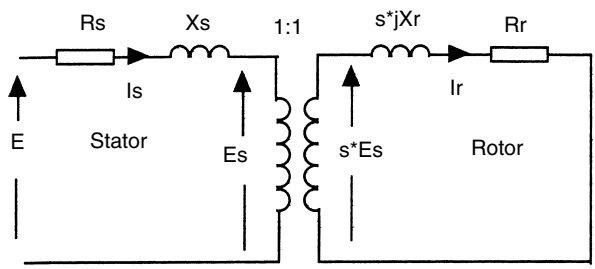


FIGURE 16.4 Motor circuit with rotor in motion.

© 2006 by Taylor & Francis Group, LLC

The rotor current is then equal to

$$I_r = \frac{E_r}{Z_r} = \frac{sE_s}{R_r + jsX_r} = \frac{E_s}{\left(\frac{R_r}{s}\right) + jX_r} \tag{16.5}$$

Because the rotor voltage and rotor reactance each vary directly with slip, the reactance appears as a constant while the resistance, which is constant, appears to vary with slip. The turns ratio of the equivalent transformer is unity; hence, stator and rotor current are equivalent and motor current can be written as:

$$I_s = \frac{E}{\left(\frac{R_r}{s}\right) + R_s + j(X_s + X_r)} \tag{16.6}$$

This relationship gives rise to the classical equivalent circuit depicted in most motor texts and shown in Figure 16.5. The circuit includes the current I_m, which is the magnetizing current required by the stator core. This is a high-reactance path; typically, I_m is about 40% of the motor full-load current.

An alternate motor circuit commonly used separates motor losses from the mechanical output. From the equivalent circuit derived above, the total power input to the rotor is:

$$P_r = I_r^2 \frac{R_r}{s} \tag{16.7}$$

This power input includes power lost in the rotor $I_2^2 R_r$ and power delivered to the mechanical load. Solving for mechanical power,

$$P_r = I_r^2 \frac{R_r}{s} = I_r^2 R_r + P_M$$
$$P_M = I_r^2 R_r \left(\frac{1-s}{s}\right) \tag{16.8}$$

The separation of motor losses $I_r^2 R_r$ from mechanical losses $R_r(1-s)I_r^2/s$ is shown in Figure 16.6.

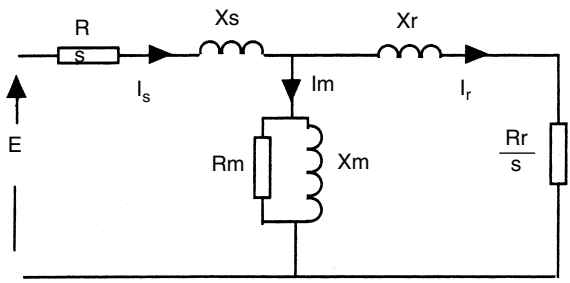


FIGURE 16.5 Motor equivalent circuits.

© 2006 by Taylor & Francis Group, LLC

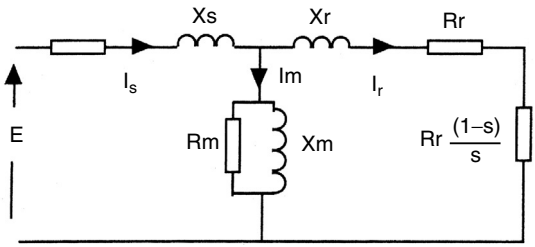


FIGURE 16.6 Motor equivalent circuit with mechanical load separated.

16.2.1.1 Motor Torque

Motor torque (T) is derived from the power equation $P = \omega T$ and the rotor power Equation (16.7). Substituting and solving for torque yields:

$$T = I_r^2 \frac{R_r}{s\omega}$$

The question is what speed to use, ω_{sync} of the rotating stator field or rotor speed ω_r? The answer is ω_{sync}.

$$T = \frac{I_r^2 R_r}{s\omega_{sync}}$$

Torque is produced by the interaction of stator and rotor flux. The velocity of stator flux is ω_{sync}. The velocity of the rotor-produced flux is the velocity of the rotor, $\omega_r = (1 - s)\omega_{sync}$, plus the velocity of the flux produced by the induced rotor current, $s^*\omega_{sync}$. The resulting velocity for the rotor flux is $(1 - s)\ \omega_{sync} + s\omega_{sync} = \omega_{sync}$. The rotor and stator flux are at the same velocity, ω_{sync}.

In fact, useful torque cannot be produced if flux velocities differ. Under such a condition, the angular distance between the stator and rotor flux would vary cyclically with time. Positive torque would be developed in one-half of the slip cycle and negative torque for the other half. The result would be a net average torque equal to zero.

In the pu system $\omega_{sync} = 1.0$; thus

$$T = \frac{I_r^2 R_r}{s} \tag{16.9}$$

This also shows that in the per unit system torque is numerically equivalent to the per unit power input to the rotor.

An alternate approach is to defining output torque from the mechanical output power Figure 16.6.

$$\begin{aligned} P_M &= \omega_r T \\ T &= \frac{P_M}{\omega_r} \\ T &= I_r^2 R_r \frac{(1 - s)}{s\omega_r} \end{aligned} \tag{16.10}$$

© 2006 by Taylor & Francis Group, LLC

Because $\omega_{rot} = (1 - s)$, per unit torque is:

$$T = I_r^2 R_r \frac{(1-s)}{s} \frac{1}{1-s} = \frac{I_2^2 R}{s} \tag{16.11}$$

as was derived above.

Multiplying per unit torque calculated above by the base torque for the motor yields torque in physical units.

$$T_{Base}(\text{ ft} - \text{lb}) = \frac{5250\,\text{HP}}{RPM}\text{sync rpm}$$

16.3 MOTOR RATINGS

A motor is not an ideal device. In the process of converting electrical energy to mechanical energy, losses occur within the motor. These include mechanical losses such as friction and windage, core magnetic losses, stray load losses, and I^2R losses in the rotor and stator. All these losses produce heat within the motor. Heat deteriorates insulation and can causes deformation, mechanical stress and fatigue on other components. As shaft load increases, so do losses and component temperature. The motor designer chooses materials and constructions to minimize the temperature rise under load. The temperature of any component within the motor is equal to the temperature rise due to loading plus the temperature of the motor environment (ambient temperature).

The expected service life of each motor component is inversely proportional to its operating temperature. A motor is assigned a horsepower rating to meet a desired service life with the operating temperatures that result from the given rating and the design ambient temperature.

Insulation is the component defining rated motor output. There are several classifications of electrical insulation; each class has a specific maximum continuous operating temperature assigned to it. These maximum temperatures are chosen to provide a long service life. Insulation technology is not an exact science and specific life expectancies are not included with the insulation temperature rating, but a 15 to 20 year life is generally assumed. For temperatures around the rated temperature, a generally accepted rule of thumb is that insulation life is halved for every 10°C rise in operating temperature and doubled for every 10°C reduction in temperature.

Under the NEMA (National Electrical Manufacturers Association) rating system, motors are assigned continuous HP ratings on the basis of temperature rise under load with an ambient temperature of 40°C. A motor with Class B insulation (rated for 135°C) could be rated for a continuous horsepower output that produces a temperature rise of 95°C (135°–40°C). A motor rated in this manner would theoretical have a service life equal to that of the insulation. However, because of the many variables associated with insulation aging, the actual in-service life of a given motor may vary widely from the insulation life benchmark.

There are several problems with this simplistic approach to motor ratings. The first is very basic; how is the HP output at which a 95°C rise occurs determined. A motor is a very complex thermodynamics system not amenable to precise mathematical modeling; therefore, a determination of temperature rise requires testing. Another problem is that motor heating is not homogenous. Insulation temperature at the motor "hot spot" must be limited to 95°C, but the location of the hot spot is not known.

The NEMA approach is to base the rating on the "observable" temperature rise. Two specified methods of temperature measurement are used: "by resistance" or "by embedded detector." The hot spot temperature is then estimated using an empirical correction, which is dependent on the method of temperature measurement and the motor under test.

Temperature measurement by resistance is accomplished by recording the stator winding resistance at ambient temperature and again after the loaded motor has reached thermal equilibrium.

© 2006 by Taylor & Francis Group, LLC

TABLE 16.1
Maximum Observable Temperature Rise for Motors in °C[a]

Motor Rating	Temperature Measurement	Insulation Class A	B	F	H
Max insulation temp		105	130	155	180
Max allowable rise (from 40°C ambient)		65	90	115	140
Through 1500 HP	RTD[b]	70	90	115	140
Over 1500 HP					
Below 7 kV	RTD	65	85	110	135
Above 7 kV	RTD	60	80	105	125
All ratings	Resistance	60	80	105	125

[a]Service factor = 1.0 (MG-1 20.8.1).

[b]Resistance temperature detector.

Knowing the initial ambient temperature, the hot and cold resistance and the material from which the coil was constructed (copper/aluminum), the *average* temperature rise of the winding can be calculated.

The second method is more direct. Embedded temperature detectors are placed in the stator winding slots when the motor is constructed. Slot temperature would be expected to be close to the actual hot spot temperature.

Table 16.1 assumes an ambient temperature of 40°C and summarizes the allowable observable temperature rise for large NEMA rated motors. The table allows for a 10–15° difference between the average temperature measured by the resistance method and the actual winding hot spot temperature. For smaller low voltage motors the RTD measurement is assumed equal to the hot spot. For larger high voltage motors with reduced thermal conductivity and thicker slot insulation 5°–10° are allowed.

Note that the use of Type A insulation has been generally abandoned in favor of the newer higher temperature insulation systems.

A motor may also be specified with a temperature rise less than the insulation maximum temperature. Motors are specified for type F (155°C) insulation and a 90°C temperature rise by resistance temperature detector (RTD). The purchaser of this motor is looking for extended life. This motor will operated 25°C below the rating for type F insulation. Using the 10°C rule this will increase motor life by:

$$2^{\frac{25}{10}} = 5.6 \text{ times}$$

16.3.1 Rated Voltage and Frequency

The temperature rise of a motor under load is not only a function of the mechanical load connected to the shaft, but also the electrical input to the motor. Operation below rated voltage will require higher current to meet the motor's output power requirement. Increased current generates higher I^2R losses and increased heat.

Operation above rated voltage reduces running current and I^2R heating, but increases core losses. Operation below rated frequency will reduce core losses but also reduce running speed and cooling airflow, possibly producing a net temperature increase. Operation at increased

© 2006 by Taylor & Francis Group, LLC

frequency improves cooling, but also increases core losses, again potentially increase motor temperature.

It is apparent that if temperature limits are to be maintained, the range of electrical input quantities must be bounded. The NEMA standard stipulates that the thermal limits of Table 16.1 are applicable with the following input variations:

- Voltage variation of $\pm 10\%$ rated voltage with frequency held at its rated value
- $\pm 5\%$ rated frequency with voltage held at its rated value
- A combined variation of voltage and frequency such that the sum of the absolute values of frequency and voltage variation does not exceed 10% is also permitted if the frequency variation does not exceed 5%

These parameters set the electrical boundaries for normal operation.

16.3.2 Service Factor

A motor rated from the above parameters has a service factor of 1.0. Motors can be purchased with a service factor greater than 1.0. A motor with a 1.15 service factor can operate continuously at 115% of its nameplate HP rating if frequency and voltage are maintained at 100% of their rated values. Motors with NEMA 1.15 service factor are allowed a temperature rise 10°C higher than 1.0 service factor (SF) motors. Using the 10°C rule, these motors, if continuously operated at the service factor load, have about half the service life of a 1.0 SF motor and less if motor voltage and frequency deviate from rated.

A service factor greater than unity should not be used to reduce the nameplate horsepower required for a continuous load. The use of a service factor rating would be advised to cover infrequent load peak.

16.4 MOTOR CHARACTERISTICS

In the course of applying and setting protective relays, it becomes necessary to evaluate starting and operation under various mechanical load, voltage and source impedance conditions. Motor speed–torque, speed–current and speed–power factor curves along with mechanical load data form the basis for these evaluations. Typical motor torque, current and power factor curves are shown in Figure 16.7.

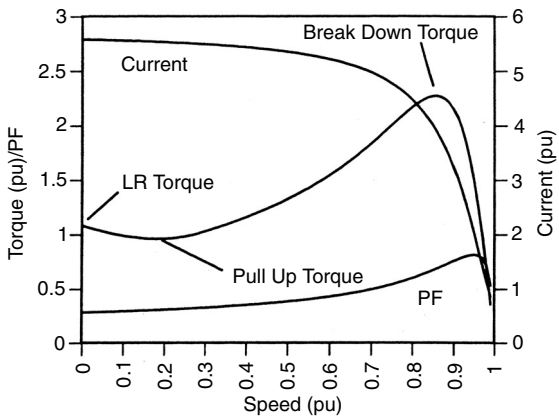


FIGURE 16.7 Motor speed–current, torque and PF curves.

© 2006 by Taylor & Francis Group, LLC

16.4.1 Motor Current

Motor current is at a maximum at locked rotor (zero speed). Upon starting, motor current remains near the locked rotor value until speed reaches 80 to 90% of rated speed, then decreases rapidly. The reason for this is evident from the motor equivalent circuit (Figure 16.5). At high slip (low speed) the R_r/s term is small and motor current is primarily determined by motor reactance X_s and X_r. Above 80% speed, the decrease in slip is rapid and nonlinear, causing the R_r/s to become the dominant circuit parameter, rapidly reducing current.

The shape of the speed–current curve gives rise to the distinctive starting time–current characteristic shown in Figure 16.1. This inverted "L" starting characteristic is common to all motors. Typically high starting current persists through 90% of the acceleration period, challenging both overcurrent protection and motor thermal limits.

Locked rotor current for most motors is about six times rated current, but this value can vary dramatically with motor design. The locked rotor current for a specific motor is determined from the locked rotor code stamped on the motor nameplate or from a data sheet for the motor in question. NEMA locked rotor codes are given in Table 16.2.

Locked rotor codes are based on rated motor voltage at the motor terminals and include no consideration for supply circuit impedance.

A 460 V, 500 HP, locked rotor code F motor with rated voltage at its terminal would have a maximum locked rotor current of:

$$I_{LR} = \frac{5.6\dfrac{\text{kVA}}{\text{HP}} * 500\,\text{HP}}{\sqrt{3}\ 0.460} = 3514\,\text{A}$$

If this motor were to be started from a 480 V source, the maximum locked rotor current would be 3514 A $*$ 480 V/460 V $=$ 3667 A.

16.4.2 Speed–Torque Curves

Motor speed–torque characteristics vary with motor design; hence, the torque characteristics of two motors with identical horsepower ratings can be significantly different. This is important because motor torque characteristics must be matched to the torque requirements of the driven load. There

TABLE 16.2
Locked Rotor Currents

NEMA Code Letter	Maximum Locked Rotor kVA/HP	NEMA Code Letter	Maximum Locked Rotor kVA/HP
A	3.15	L	10.0
B	3.55	M	11.2
C	4.0	N	12.5
D	4.5	P	14.0
E	5.0	R	16.0
F	5.6	S	18.0
G	6.3	T	20.0
H	7.1	U	22.4
J	8.0	V	Above 22.4
K	9.0		

© 2006 by Taylor & Francis Group, LLC

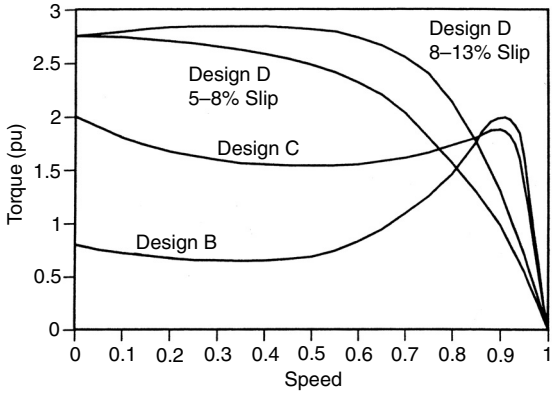


FIGURE 16.8 NEMA designs B, C, and D.

are several critical points on the torque curve, which are referenced by standard nomenclature. These points are labeled on Figure 16.7.

Locked-rotor torque: the torque developed with the rotor at rest and rated voltage and frequency at the motor terminals
Pull-up torque: the minimum torque developed during the period of acceleration from rest to the speed at which breakdown torque occurs
Breakdown torque: the maximum torque that a motor will develop with rated voltage at rated frequency
Full load torque: The torque output when the motor is operating at rated horsepower and rated full load speed

Small and medium motors built to NEMA specifications are designated as NEMA design B, C or D motors based on their torque characteristics. Figure 16.8 depicts torque curves for these NEMA design designations. Torque specifications for motors over 200 HP of these designs are shown in Table 16.3. NEMA large motors are not given design letters but are designate as "standard" and "high torque" motors based on Table 16.4.

TABLE 16.3
Torque Specifications for NEMA Design Codes

NEMA Design	Locked Rotor Torque	Pull-Up Torque	Breakdown Torque	Locked Rotor Current
B	70–120%	65–100%	175–200%	600–700%
	For fans, blowers, centrifugal pumps and compressors; applications with low starting torque			
C	200%	140%	190%	600–700%
	Conveyors, crushers, reciprocating pumps and compressors; applications that start under load			
D	275%			600–700%
	High peak loads with or without flywheels, punch presses, shears, elevators, extractors, hoists			

© 2006 by Taylor & Francis Group, LLC

TABLE 16.4
NEMA Large Motor Torque Designations

	Locked Rotor Torque	Pull-Up Torque	Breakdown Torque
Standard torque	60%	60%	175%
High torque	200%	150%	190%

16.5 MOTOR APPLICATIONS

A successful motor application involves more than meeting the horsepower requirements of the driven load. The motor must also be compatible with the torque and inertial requirements of the driven load.

16.5.1 Horsepower Rating

Motors that drive fixed load such as a fan or pump are sized on the basis of their horsepower rating. Economics dictates that the lowest standard horsepower rating in excess of the load requirement be applied. In cases where infrequent load excursions occur, a lower horsepower motor might be applicable if the excursions are within the motor service factor rating.

Many motors drive time-varying load such as crushers, hoists, and boring mills. In these applications, loading typically varies dramatically over a load cycle. Motors used in these applications are sized on the basis of thermal capacity. This means that the smallest motor that has sufficient torque to meet the peak load requirement without overheating is installed.

One method to assess motor heating is the RMS horsepower over the duty cycle. Remember that alternating current is expressed in RMS amperes, which is the heating equivalent of the same magnitude of direct current amperes.

$$HP_{\text{RMS}} = \sqrt{\frac{HP_1^2 * t_1 + HP_2^2 * t_2 + \cdots + \cdots}{t_1 + t_2 + \cdots + \cdots}} \tag{16.12}$$

Given the duty cycle shown in Figure 16.9, the RMS horsepower required is calculated as

$$HP_{\text{RMS}} = \sqrt{\frac{340^2 * 10 + 900^2 * 6 + 450^2 * 15}{10 + 6 + 15}} = 540\,\text{HP}$$

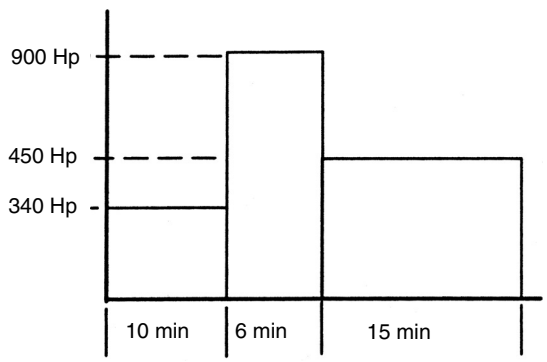


FIGURE 16.9 Cyclic load.

© 2006 by Taylor & Francis Group, LLC

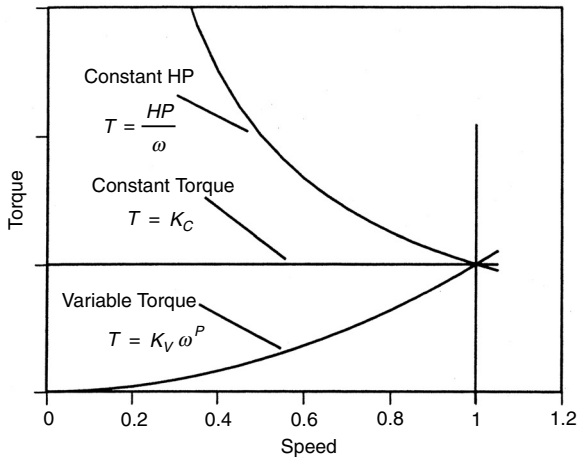


FIGURE 16.10 Load characteristics.

The closest standard motor rating above this value is 600 HP. To meet the torque requirements with a 15% margin, the 600 HP motor must have a breakdown torque in excess of 1.15* 900/600 = 1.72 × its full-load torque rating.

16.5.2 Matching Motor and Load Torque Characteristics

Mechanical loads can be broadly classified into three types, constant torque, variable torque and constant horsepower. Most applications like fans and centrifugal pumps are variable-torque loads with torque varying as the square (or some other power) of speed. Conveyors, hoists, and cranes are examples of loads that exhibit a constant torque at all speeds. Power is a function of torque × speed; consequently, a constant horsepower load would have infinite torque at starting. Motors driving such loads start with the load uncoupled. Figure 16.10 plots speed–torque curves for these three load types.

Figure 16.11 plots a fixed and variable torque load against the speed–torque characteristic of a NEMA Design B motor having locked rotor torque of 115% rated. Both loads are within the motor

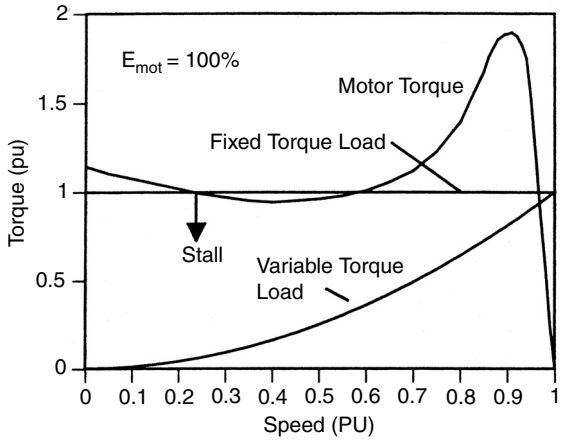


FIGURE 16.11 Motor and load torque.

© 2006 by Taylor & Francis Group, LLC

rating at rated speed. If a motor is to accelerate a load, it must produce torque in excess of the load–torque characteristic. This motor would not be successful accelerating the fixed-torque load because torque and load cross at about 20% speed. Acceleration would not continue beyond this point and the motor would stall resulting in sustained motor current approximately equal to locked rotor current. The motor would suffer severe thermal damage in less than a minute if overcurrent protection failed to operate. In the case of the variable-torque load, motor torque comfortably exceeds the load torque at all speeds up to normal operating speed; hence, acceleration would be accomplished. This comparison demonstrates why NEMA B motors are applied with variable-torque loads such as fans and centrifugal pumps and compressors and not cranes and hoists.

NEMA design C and D motors have significantly higher starting torque and are applied when equipment is started under load or for high inertia loads. Although the starting torque of these motors can be more than twice that of Design B motors, high starting torque does not guarantee a successful start.

Assume that a design C motor with 200% starting toque is being considered to drive the fixed-torque load from the previous example. The manufacturer's speed–torque curve (Figure 16.12), shows that the motor's pull-up torque (minimum torque output between locked rotor and breakdown torque) for this motor is 154% rated, well above the torque required by the load. However, motor torque varies with the square of voltage and the motor speed–torque curve provided is plotted assuming rated voltage at the motor terminal.

Under actual service conditions, the motor terminal voltage is depressed during starting. Figure 16.7 shows that motor current is maximum and power factor is minimum at starting. Both these conditions increase the voltage drop through the power system serving the motor. The actual starting voltage will depend on the size of the motor, the prestart system voltage and the impedance of the electrical supply to the motor.

Assuming that the starting voltage at this motor drops to 80% of the rated motor voltage (not the bus rating), the torque curve must be reduced by 64% (0.80^2) as shown in Figure 16.12. At 80% voltage, the pull-up torque is reduced to 98% and the motor again stalls near 30% speed. If the motor were started on a slightly stronger system, the voltage drop would be less severe and output torque would be adequate to avoid a stall. However, with motor torque low, starting time will be long and a long acceleration time increases motor heating. When acceleration time becomes excessive, a motor may be damaged during starting. General methods for assessing motor accelerating capability are presented in Section 16.8.

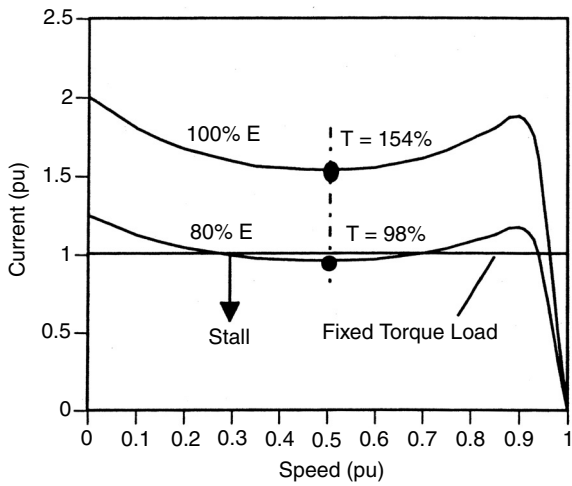


FIGURE 16.12 Speed–torque and speed–current at reduced voltage.

© 2006 by Taylor & Francis Group, LLC

16.5.3 Inertial Capability of NEMA Motors

Motor heating during acceleration is a function of load torque, the inertia of the rotating system being accelerated, and voltage. Motors built to NEMA standards must be capable of accelerating as a minimum the load inertia specified in NEMA standard MG-1. For "large" NEMA induction motors with a "standard torque" characteristic, the required load inertia is defined in terms of Wk^2 (ft-lb^2) by the equation below:

$$Wk^2_{\text{Load}} = A\left[\frac{H\text{p}^{0.95}}{\left(\frac{RPM}{1000}\right)^{2.4}}\right] - 0.0685\left[\frac{H\text{p}^{1.5}}{\left(\frac{RPM}{1000}\right)^{1.8}}\right] \text{ft} - \text{lb}^2$$

where $A = 24$ for 300 to 1800 RPM motors inclusive, and $A = 27$ for 3600 RPM motors. Large induction motors designated as "high torque" motors are only required to accelerate half the Wk^2 derived from this equation. The MG-1 standard also tabulates Wk^2 limits for small and medium motors.

All MG-1 inertia specification presume: (1) load torque varies as the square of the speed, in other words a fan or centrifugal pump applications, and (2) load torque at rated speed does not exceed the motor full load rating. NEMA motors meet these requirements with terminal voltage variation of $\pm 10\%$ of rated.

If load inertia exceeds the specified value or the load–torque characteristic is more demanding, motor damage may occur during starting. For such applications, the motor manufacturer must be consulted to determine if a specific starting application is within the motor's capabilities. Often, motors have inertial capability in excess of the minimum NEMA requirements.

16.6 MOTOR STARTING

The starting duty imposed by the driven load is a major consideration when choosing a drive motor and when assessing motor protection. Starting time can range from less than a second to nearly a minute dependent on the combined inertia of the motor and driven load, the torque characteristics of both load and drive motor, and the impedance of the electrical supply to the motor. The accelerating time is indicative of the severity of the starting duty imposed on the motor.

At the instant of starting, motor current is typically six times rated current. The nature of the starting transient is shown in Figure 16.1. Current diminishes as motor speed increases, but current remains near the locked rotor value for most of the acceleration period. The large heat input over a short time cannot be dissipated through the motor structures and results in a rapid temperature rise. The longer the starting transient persists, the higher the temperature. A motor will be damaged if maximum temperature limitations for materials within the motor are exceeded; consequently, a motor is limited as to the load it can accelerate.

Starting studies are performed to determine the time–current and/or time–voltage profile of the starting transient. The time–current data are used to assess motor heating and relay performance. Voltage data reflect the start impact on plant running loads. The impedance of the electrical system supplying a motor reduces motor starting current and voltage while increases acceleration time and motor heating.

16.6.1 System Voltage Degradation during Starting

A small- to medium-sized motor connected to a strong power system will create a negligible voltage dip when starting. However, large motors or a weak system can result in severe voltage dips. It is considered good design practice to maintain 80% voltage or better at the motor terminal when starting.

© 2006 by Taylor & Francis Group, LLC

The mechanical load to which the motor is connected determines the shaft power a motor must deliver. When voltage at a running motor is reduced, current must increase to meet load requirements. Figure 16.13 is a magnified view of a fixed torque load plotted against the speed–torque and speed–current characteristics of a motor with 100% and 80% rated voltage applied at its terminals. At rated voltage, load torque intersect the motor torque curve at point A, the motor operates at 0.965 pu speed and rated current. At 80% voltage, motor torque is reduced by the square of the voltage reduction and the motor must slow to near 0.94 pu speed to intercept the load torque curve at point B. Although the current curve is reduced in proportion to the voltage reduction, the reduction in speed produces a net increase in motor current to about 1.3 pu. Figure 16.14 shows a typical variation of current with voltage for a running motor.

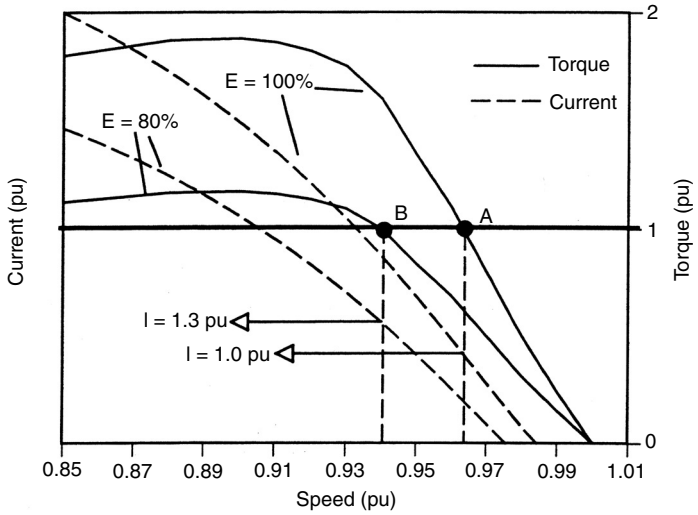


FIGURE 16.13 Motor current at reduced voltage.

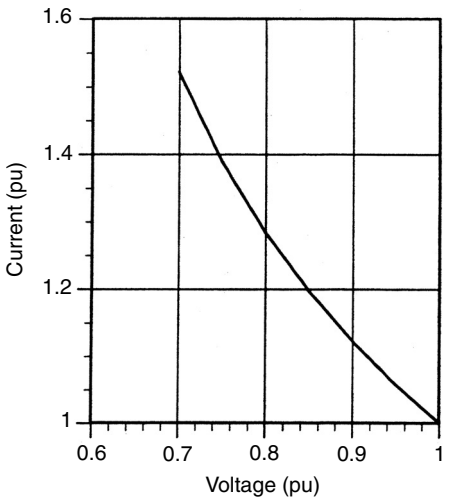


FIGURE 16.14 Running current vs. voltage.

© 2006 by Taylor & Francis Group, LLC

The inverse relationship between motor voltage and running current has several negative impacts on systems with a large percentage of motor load such as plant auxiliary systems. When a large motor starts from a bus that is supplying a group of running motors, the voltage drop is amplified by increased current and decreased power factor at the running motors. Hence, starting a motor from a bus with significant running motor load will produce a larger voltage drop than an isolated start of the same motor.

Setpoints for bus and source transformer overcurrent protection must allow for starting and increased running current. The worst-case scenario would be a voltage collapse occurring as a result of the start of a large motor. Most motors have a breakdown torque in the order of two times rated torque. At 70% voltage, the breakdown torque of such a motor would be equal to rated torque ($200\%*0.7^2 = 100\%$) and the motor would just meet its output torque rating. If the start of a large motor and the increased loading from running motors pulls the bus voltage down to near this value, running motors may be unable to meet their load requirements and will stall. The cumulative locked rotor currents from the starting and stalled motors can cause an unrecoverable voltage collapse. Undervoltage or overload protection must them operate to trip the bus and prevent damage to the connected motors and supply circuit.

16.6.2 Starting Time Calculation

The majority of installations will not require starting calculations to choose or set motor protection. These calculations are usually required for problem installations and when existing equipment is modified (change of motor or driven load).

At new installations, the motor vendor will provide a starting time–current plot if given the torque characteristic and inertia of the driven load. These plots are calculated at rated terminal voltage and fixed values of reduced terminal voltage as requested. If plots are requested at a fixed terminal voltage equal to the actual initial starting voltage, those plots generally provide adequate data to choose and set motor protection. This is true because during an actual start, terminal voltage will recover as speed increases; thus, start times calculated with fixed terminal voltage are longer than would actually occur.

The starting calculations described in the following sections would be used to include the effects of supply system impedance to more accurately define the starting time–current characteristic or to derive a time–voltage profile for the motor and supply bus.

Motor starting time can be derived from the expression for angular acceleration:

$$\alpha = \frac{\mathrm{d}\omega}{\mathrm{d}t} = \frac{T_{\mathrm{acc}}}{I} \tag{16.13}$$

where α = angular acceleration, $\mathrm{d}\omega$ = change in speed, $\mathrm{d}t$ = change in time, I = rotating inertia, and T_{acc} = accelerating torque $(T_{\mathrm{M}} - T_{\mathrm{L}})$, T_{M} = torque produced by the motor, T_{L} = torque required by the load.

Figure 16.15 plots motor and load speed–torque curves. The accelerating torque at any given speed is the difference between the two curves. Where the motor and load torque curves cross, acceleration ceases and a stable operating point is established. This would be expected near rated speed for the motor.

The motor starting time is calculated by defining the accelerating torque at many small speed increments between locked rotor and the running speed. The time required for each incremental speed change is calculated from the incremental form of Equation (16.13).

$$\Delta t = I\frac{\Delta\omega}{T_{\mathrm{acc}_n}}$$

© 2006 by Taylor & Francis Group, LLC

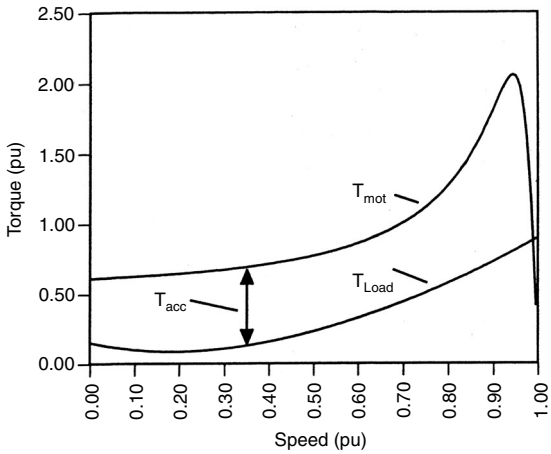


FIGURE 16.15 Acceleration torque.

If speed (ω) and accelerating torque (T_{acc}) are expressed in per unit on the motor base and inertia in lb-ft^2, the time in seconds for each speed increment (ω_{n-1} to ω_n) becomes

$$\Delta t = Wk^2 \frac{(\omega_n - \omega_{n-1})RPM_{sync}}{308 * T_{acc_n} T_{base}} \tag{16.14}$$

where base torque is

$$T_{base} = \frac{5250}{HP_{rated} * RPM_{FL}} \tag{16.15}$$

The acceleration torque used in the equation is the average over the speed increment. The total starting time is then the sum of the speed increment times.

16.6.3 Motor Model for Starting Studies

Motor starting studies are dynamic and require motor impedance and torque at small increments of speed from standstill to near rated speed. An electrical equivalent motor circuit is generally used to derive these values. In theory, data could be extracted from the manufacturer's curves on a point-by-point basis. However, with the number of data points required and the difficulty in reading them, this is impractical. Also, the use of an equivalent electrical circuit for the motor facilitates inclusion of supply impedance to the starting calculation.

Unfortunately, for most motor designs, the classical equivalent circuit as shown in Figure 16.5 will not replicate published speed–torque, current and power factor data. Figure 16.16 compares manufacturer's speed–torque and speed–current data for a 600 HP motor with curves calculated from the classical model. This model assumes rotor resistance and reactance equal to their locked rotor values. The poor correlation between the curves is obvious.

The major flaw with the classical equivalent circuit is that it assumes constant rotor resistance and reactance (R_r, X_r). In most practical motor designs, these parameters vary with slip. (The classical equivalent includes the slip variant term R_r/s, but for most motors the R_r term is not constant, such that in a practical motor the R_r/s term becomes $R_r(s)/s$.)

These variations are caused by the skin effect, which forces current flow closer to the surface of a conductor as the frequency of the current increases. This decreases the effective area of the

© 2006 by Taylor & Francis Group, LLC

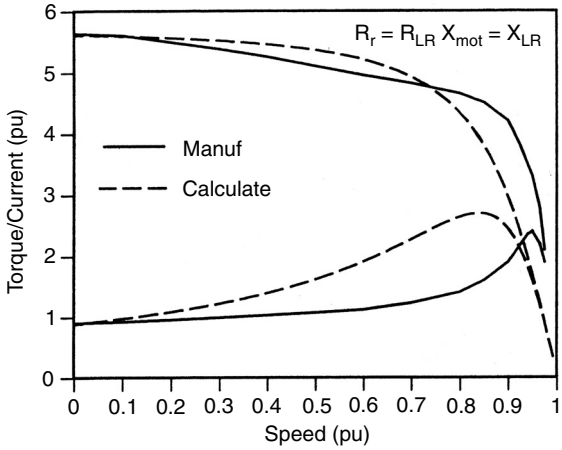


FIGURE 16.16 Characteristic of a fixed rotor impedance model.

conductor, which increases resistance. In a motor, the conductors and, rotor bars respond in the same manner. Reactance is also affected by the change in current distribution.

At locked rotor, slip equals 1.0, and the frequency of the induced rotor current, from Equation (16.4), is equal to that of the line current, 60 Hz. Assuming a motor has a synchronous speed of 1800 RPM and full load speeds of 1750 RPM, slip at full load is then $(1800-1750)/1800 = 0.028$. The frequency of rotor current at rated speed is then 60 Hz $\times$ 0.28 = 1.68 Hz. Typically, the ratio of rotor resistance at locked rotor to that at full load is about 3:1.

The reduction of rotor resistance with speed is desirable. High resistance at locked rotor increases starting torque, which is a desirable characteristic. However, a high-resistance rotor will result in high slip and poor efficiency at rated speed. Conversely, low rotor resistance will reduce full-load slip and improve running efficiency, but significantly reduces starting torque. Motor designers manipulate the change in rotor resistance with deep bar and double squirrel-cage rotor designs to produce speed–torque characteristics required for a given motor application. The deep-bar design uses thin rotor bars that extend deep into the rotor. The double squirrel-cage design employs two bars per slot, the outer bar having higher resistance than the inner bar.

There are several methods used to model the speed variant rotor impedance. One method is the double rotor model shown in Figure 16.17. The two slip variant circuits attempt to emulate the inner and outer current flow paths in the rotor. This circuit can significantly improve the accuracy of calculated speed–torque and speed–current curves if appropriate R and X values can be determined. In some instances, these values are available from the motor manufacturer. Iterative techniques are

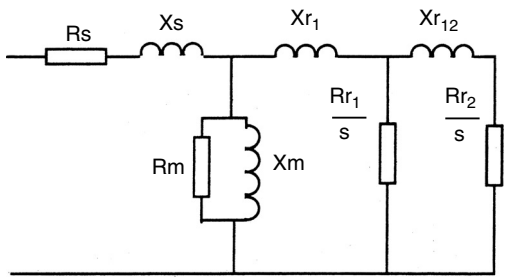


FIGURE 16.17 Double rotor motor model.

© 2006 by Taylor & Francis Group, LLC

also available to calculate circuit parameters for this model from published speed–torque, current and power factor curves,[1] but these methods are impractical if not computerized.

This text will use an alternative representation that assumes rotor resistance and reactance are a linear function of slip, as described below.

$$R_r(s) = (R_{r_{LR}} - R_{r_{NL}})s + R_{r_{NL}} \tag{16.16}$$

$$X_{mot}(s) = (X_{mot_{LR}} - X_{mot_{NL}})s + X_{mot_{NL}} \tag{16.17}$$

where $R_{r_{LR}}$, $R_{r_{NL}}$ = No-load and locked rotor resistance and $X_{mot_{NL}}$, $X_{mot_{LR}}$ = No-load and locked motor reactance $= X_s + X_r$.

This rotor representation will be incorporated into an equivalent circuit similar to that of Figure 16.5, but with the magnetizing branch neglected. The circuit used is shown in Figure 16.18.

We note that there are many different methods and assumptions that can be used to derive resistance and reactance values for the equivalent circuit. However, from this author's experience, none of these variations will produce calculated current, torque, or power factor curves that match the manufactures data. In fact, we have seen manufactures data that defied mathematical justification.

Our goal here is to develop a model that provides a reasonable match to the published data. The model being developed is intended for use in a starting study; therefore, it should provide the best fit with published curves at speeds between locked rotor and the speed at which breakdown torque occurs to this end. The following derivation of motor constants is intended to provide circuit parameters that return locked rotor and breakdown torque equivalent to the given motor data. Because the representation is not critical near rated load, the no-load rotor reactance will be manipulated to shape the calculated speed–torque and speed–current curves to the data.

A motor model will be derived for a 600 HP motor with the following specifications:

Synchronous speed, $RPM_{sync} = 1800$
Speed at full load, $RPM_{FL} = 1777$
Rated voltage, $E_{rated} = 4000$ V
Full-load current, $I_{FL} = 78$ A
Locked rotor current, $I_{LR} = 439$ A ($5.628 \times$ FL)
Power factor at LR, $PF_{LR} = 0.22$
Torque at locked rotor, $T_{LR} = 0.9$ pu
Breakdown torque, $T_{max} = 2.4$ pu

The motor model will use a base current equal to the motor full-load running current and a base voltage equal to motor rated voltage:

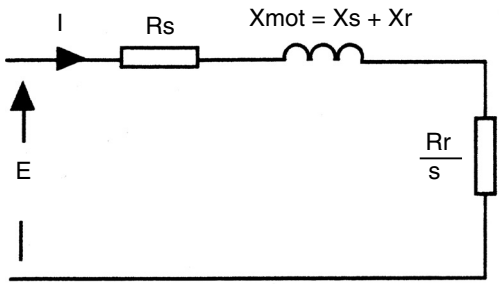


FIGURE 16.18 Motor model for dynamic studies.

© 2006 by Taylor & Francis Group, LLC

$I_{base} = 78$ A
$V_{base} = 4000$ V

At locked rotor, motor resistance and reactance in per unit are

$$Z_{LR} = \frac{E_{rated}}{I_{LR}} = \frac{1}{5.628} \angle \arccos(0.22)$$
$$= 0.1777 \text{ pu } \angle 77.29^\circ$$

At locked rotor, slip = 1, and from the equivalent circuit, Figure 16.5, motor resistance and reactance become

$$R_{mot_{LR}} = R_s + R_{r_{LR}}$$
$$= 0.1777 \cos(77.29^\circ) = 0.0391 \text{ pu}$$
$$X_{mot_{LR}} = X_s + X_{rot_{LR}}$$
$$= 0.177 \sin(77.29^\circ) = 0.1733 \text{ pu}$$

Rotor resistance at any speed can be calculated from the torque and rotor current using Equation (16.18) below:

$$T = \frac{R_r(s)}{s} I^2 \tag{16.18}$$

At locked rotor

$$R_{r(LR)} = \frac{T_{LR}}{I_{LR}^2} = \frac{0.9}{5.63^2} = 0.0284 \text{ pu}$$

At full load, torque and current are 1.0 pu and the per unit rotor resistance must equal the slip at full load:

$$T_{FL} = \frac{R_{r(FL)}}{s_{FL}} I_{FL}^2$$
$$R_{r(FL)} = s_{FL}$$

or

$$s_{FL} = \frac{RPM_{sync} - RPM_{FL}}{RPM_{sync}}$$
$$= \frac{1800 - 1777}{1800} = 0.0128 \text{ pu}$$
$$R_{r(FL)} = 0.0128$$

Stator resistance can be determined from locked rotor data:

$$R_s = R_{mot_{LR}} - R_{r_{LR}}$$
$$= 0.0391 - 0.0284 = 0.0107$$

© 2006 by Taylor & Francis Group, LLC

With rotor resistance known, at locked rotor and at full load the no-load rotor resistance can be calculated from Equation (16.16):

$$\begin{aligned} R_{r_{NL}} &= \frac{R_{r_{FL}} - s_{FL}R_{r_{LR}}}{1 - s_{FL}} \\ &= \frac{0.0128 - 0.0128 * 0.0284}{1 - 0.0128} = 0.0126 \end{aligned} \tag{16.19}$$

If the motor model is to produce the maximum torque equivalent to the motor data the model must be derived on this basis. Maximum torque occurs when power transfer to the rotor is maximum. The point of maximum power transfer for any electrical system occurs when source impedance ($\sqrt{R_s^2 + (X_r + X_s)^2}$) equals the load impedance (R_r/s). In the case of the simplified motor equivalent, Figure 16.18, circuit maximum power transfer occurs when

$$\frac{R_{r_{mt}}}{s_{mt}} = \sqrt{R_s^2 + (X_{r_{mt}} + X_s)^2} \tag{16.20}$$

Also at maximum torque;

$$T_{mt} = \frac{R_{r_{mt}}}{s_{mt}} I_{mt}^2 \tag{16.21}$$

Rearranging Equation (16.21) and substituting into Equation (16.20)

$$\begin{aligned} \frac{R_{r_{mt}}}{s_{mt}} &= \frac{T_{mt}}{I_{mt}^2} \\ \frac{T_{mt}}{I_{mt}^2} &= \sqrt{R_s^2 + (X_{r_{mt}} + X_s)^2} \end{aligned} \tag{16.22}$$

Solving for motor reactance at maximum torque

$$X_{mot_{mt}} = X_{r_{mt}} + X_s = \sqrt{\left(\frac{T_{mt}}{I_{mt}^2}\right)^2 - R_s^2} \tag{16.23}$$

Motor current at maximum torque is:

$$I_{mt} = \frac{E_m}{\sqrt{\left(\frac{R_{r_{mt}}}{s_{mt}} + R_s\right)^2 + X_{mot_{mt}}}} \tag{16.24}$$

Substituting Equation (16.23) into Equation (16.24), the expression for current at breakdown torque becomes

$$I_{mt} = \sqrt{2\frac{T_{mt}^2}{E_m - 2R_s T_{mt}}} \tag{16.25}$$

© 2006 by Taylor & Francis Group, LLC

With motor voltage at rated ($E_m = 1.0$), the current at breakdown torque for the subject motor is

$$I_{mt} = \sqrt{2\frac{2.4^2}{1 - 2 * 0.0107 * 2.4}} = 3.485 \text{ pu}$$

Then, from Equation (16.16) and Equation (16.21)

$$T_{mt} = \frac{(R_{r_{LR}} - R_{r_{NL}})s_{mt} + R_{r_{NL}}}{s_{NL}} I_{mt}^2$$

Solving for s_{mt}

$$\begin{aligned} s_{mt} &= \frac{R_{r_{NL}} I_{mot_{mt}^2}}{T_{mt} - (R_{r_{LR}} - R_{r_{NL}})I_{mt}^2} \\ &= \frac{0.0126 * 3.485^2}{2.4 - (0.0284 - 0.0126) * 3.485^2} = 0.0693 \text{ pu} \end{aligned}$$

From Equation (16.23)

$$X_{mot_{mt}} = \sqrt{\left(\frac{2.4}{3.485^2}\right)^2 - 0.0107^2} = 0.1974$$

Then, $X_{mot_{NL}}$ can be calculated from Equation (16.17):

$$\begin{aligned} X_{mot_{NL}} &= \frac{X_{mot_{mt}} - Slip_{mt} X_{mot_{LR}}}{1 - Slip_{mt}} \\ &= \frac{0.1974 - 0.0693 * 0.1733}{1 - 0.0693} = 0.1992 \end{aligned}$$

Using the circuit parameters found above, motor current and torque can now be calculated as a function of slip using the equations below:

$$I = \frac{E_m}{\sqrt{\left(\frac{R_r(s)}{s} + R_s\right)^2 + X_{mot(s)}{}^2}} \tag{16.26}$$

$$T_{mot} = \frac{R_r(s)}{s} I^2$$

The fit between the calculated and published current and torque curves varies from motor to motor. Figure 16.19 compares the speed–torque and speed–current curves provided by the manufacturer with those calculated using the equivalent circuit in Figure 16.18 and the parameters derived above, which includes the calculated value of $R_{r_{NL}} = 0.0126$. The torque and current curve fit is much improved over the fixed rotor impedance model depicted in Figure 16.16, but significant error remains in the torque curve. The torque fit can be improved by trial and error variation of $R_{r_{NL}}$. Figure 16.19 shows the close fit obtained with $R_{r_{NL}} = 0.008$ and all other parameters held at the previously calculated values. The latter representation will be use to model this motor.

Summarizing the circuit values used in the equivalent circuit:

$R_{r_{NL}} = 0.008$ pu

© 2006 by Taylor & Francis Group, LLC

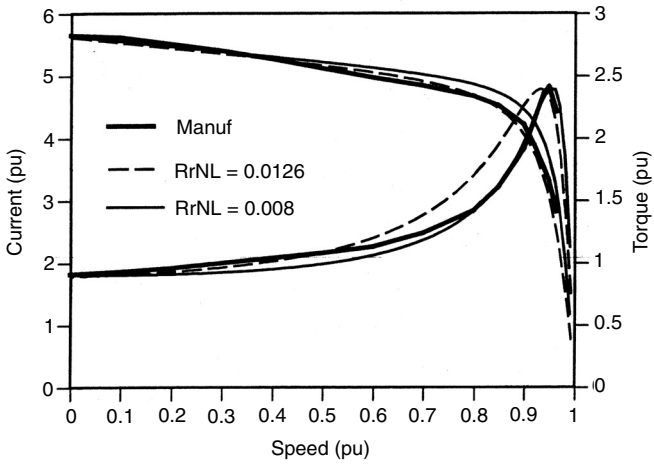


FIGURE 16.19 Comparisons of calculated speed–torque and speed–current curves.

$R_{r_{LR}} = 0.0284\,\text{pu}$
$X_{mot_{NL}} = 0.1992\,\text{pu}$
$X_{mot_{LR}} = 0.1733\,\text{pu}$
$R_s = 0.0107\,\text{pu}$
$s_{mt} = 0.0693$

and the variable

$$\begin{aligned} R_r(s) &= (R_{r_{LR}} - R_{r_{NL}})s + R_{r_{NL}} \\ &= (0.0284 - 0.008) * s + 0.008 \\ &= 0.0204 * s + 0.008 \\ X_{mot}(s) &= (X_{mot_{LR}} - X_{mot_{NL}})s + X_{mot_{NL}} \\ &= (0.1733 - 0.1992)s + 0.1992 \\ &= -0.0259 * s + 0.1992 \end{aligned}$$

16.6.4 Starting Calculation Example

This example assumes that the 600 HP motor modeled above is driving a large fan. The fan full-load torque is 60% of the motor rating. Motor and load characteristics for a similar system are provided in Figure 16.15. The combined motor and fan inertia is 4332 lb-ft^2. The fan torque curve includes an estimated breakaway torque of 15%. This is the torque required to initiate rotation. The per unit fan torque curve with breakaway is represented as

$$\begin{aligned} T_L &= (1-\omega)^5 T_{ba} + \omega^2 T_{FL} \\ &= (1-\omega)^5 0.15 + \omega^2 0.6 \end{aligned} \tag{16.27}$$

Normally, a large fan such as this is started with dampers closed or vanes set to minimal air flow (unloaded). This can reduce the torque at rated speed to 25% of the normal running value. The high inertia and high starting torque for this fan makes the starting duty for the example motor significantly more severe than would be seen at a typical installation.

The starting calculation is a point-by-point calculation of motor current, motor torque and accelerating torque at speed increments between locked rotor and running speed. The smaller

© 2006 by Taylor & Francis Group, LLC

the speed increments the better the accuracy. This example will use 0.005 pu speed increments. Equation (16.28) below defines the time required for each speed increment. The starting time is then the sum of the time increments for each speed interval.

The base torque for this drive motor is calculate form Equation (16.15) as

$$T_{\text{base}} = \frac{600\,\text{HP} * 5250}{1777\,\text{RPM}} = 1773\ \text{ft-lb}$$

Substituting base torque, inertia and speed decrement values into Equation (16.14), the incremental time equation for any interval "$n-1$ to n" reduces to:

$$\begin{aligned}\Delta t_{\text{n}} &= Wk^2\,\frac{(\omega_{\text{n}} - \omega_{\text{n}-1})RPM_{\text{sync}}}{308 * T_{\text{acc}_{\text{n}}} T_{\text{base}}} \\ &= 4332\,\text{lb-ft}^2 * \frac{0.005 * 1800\,\text{RPM}}{308 * 1773 * T_{\text{acc}_{\text{n}}}} \\ \Delta t_{\text{n}} &= \frac{0.0714}{T_{\text{acc}_{\text{n}}}}\ \text{sec}\end{aligned} \tag{16.28}$$

The accelerating torque used in the above equation is the average accelerating torque for the interval and is calculated as

$$T_{\text{acc}_{\text{av}}} = \frac{(T_{\text{m}_{\text{n}}} - T_{\text{L}_{\text{n}}}) + (T_{\text{m}_{\text{n}-1}} - T_{\text{L}_{\text{n}-1}})}{2} \tag{16.29}$$

where $(T_{\text{m}_{\text{n}-1}} - T_{\text{L}_{\text{n}-1}})$ is the accelerating torque at the beginning of the speed increment and $(T_{\text{m}_{\text{n}}} - T_{\text{L}_{\text{n}}})$ is the accelerating torque at the end of the increment.

The acceleration torque is a function of motor voltage. The three-phase 4.16 kV fault current at the motor location is 1520 A with an X/R ratio of 5.6. This is indicative of the impedance of the supply circuit to the motor and is required data if the starting calculation is to include the effect system impedance and reduced terminal voltage on motor torque and current.

The source impedance to the motor is then:

$$\begin{aligned}Z_{\text{sys}} &= \frac{4160\,V}{\sqrt{3} * 1520\,\text{A}}\ \text{at arctan(5.6)} \\ &= 1.578\,\Omega\angle 79.8^{\circ}\end{aligned}$$

It is convenient to represent the source impedance as a per unit value, but it must be referenced to the same base impedance as the motor model. The motor model was derived using base current equal to the motor full-load current (78 A) and base voltage equal to rated motor voltage (4 kV); the base impedance on the motor base for the model is then

$$Z_{\text{base}} = \frac{4000\,\text{V}}{\sqrt{3} * 78\,\text{A}} = 29.61\,\Omega$$

© 2006 by Taylor & Francis Group, LLC

The source impedance per unit source impedance is then

$$Z_{\text{sys}} = \frac{1.578\,\Omega}{29.61\,\Omega} = 0.0533 \text{ pu at } 79.8^\circ$$
$$= 0.0094 + j.0525$$

Motor locked rotor current and power factor are 5.63 pu (429 A/78 A) and 0.22, respectively. Motor impedance at starting is then

$$Z_{\text{LR}} = \frac{E}{I_{\text{LR}}} = \frac{1.0}{5.63\angle \arccos(0.22)}$$
$$= 0.1776 \text{ pu at } 77.3^\circ$$

If the motor bus is operating at 4160 V prior to starting, it is 4160/4000 V = 1.04 pu on the motor voltage base. Upon starting, motor voltage will drop to:

$$E_{\text{m}} = E_{\text{sys}} * \left| \frac{Z_{\text{mot}}}{Z_{\text{mot}} + Z_{\text{sys}}} \right|$$
$$= 1.04 \left| \frac{0.177\angle 77.3^\circ}{0.177\angle 77.3^\circ + 0.0533\angle 79.8^\circ} \right|$$
$$= 0.80 \text{ pu}$$

Motor starting voltage is reduced to 80% rated motor voltage at the instant of starting. This voltage reduction will reduce the starting current to 80% of the rated voltage value and reduce starting torque to 64% ($0.80^2 = 0.64$) of the rated voltage value.

Per unit current at each speed is calculated from the sum of system impedance and the slip-dependent motor impedance as defined by I_{m}:

$$I_{\text{m}} = \frac{E_{\text{m}}}{\sqrt{\left(\frac{R_{\text{r}}(s)_{\text{n}}}{Slip_{\text{n}}} + R_{\text{s}} + R_{\text{sys}}\right)^2 + (X_{\text{mot}}(s)_n + X_{\text{sys}})^2}} \tag{16.30}$$

Table 16.5 demonstrates the calculation of the starting characteristic using the example data and motor equivalent. The resulting start time is 25.6 sec.

16.6.5 Effect of Load Torque Characteristic

The starting duty of a motor is strongly influenced by the torque characteristic of the driven load. Driven loads generally fall into three classifications, constant torque, variable torque or constant horsepower, which are plotted in Figure 16.10. Examples of these load types are given in Table 16.6.

Because constant-horsepower applications would require infinite torque at starting, motors driving these loads are started unloaded. This reduces starting concerns to constant- and variable-torque load types. The torque of a variable-torque load usually varies with the square of speed ($T \propto \omega^2$), but other exponents may apply. The starting duty imposed on a motor by a load is proportional to the inertia and the area under the load speed–torque curve. Using this benchmark, for a given inertia, a constant-torque load will result in a longer start time and greater rotor heating than a variable-torque load.

© 2006 by Taylor & Francis Group, LLC

TABLE 16.5
Starting Time Calculation

Speed (pu)	I_{mot} (pu)[a]	T_{motor} (pu)[b]	T_{load} (pu)[c]	$T_{acc} = T_m - T_L$	T_{acc} average[d]	ΔSpeed (pu)	Δt (sec)[e]	$t = \Sigma\Delta t$ (sec)
0	4.504	0.5762	0.1500	0.4262				0
					0.4282	0.005	0.1667	
0.005	4.501	0.5764	0.1463	0.4301				0.167
					0.4320	0.005	0.1653	
0.01	4.498	0.5766	0.1427	0.4339				0.332
					0.4357	0.005	0.1639	
0.015	4.496	0.5767	0.1392	0.4375				0.496
0.980	2.053	1.7717	0.5762	1.195				25.62
					1.0706	0.005	0.0667	
0.985	1.661	1.5282	0.5821	0.9461				25.687

Equations used: [a]Equation (16.30); [b]Equations (16.16, 16.18); [c]Equation (16.27); [d]Equation (16.29); [e]Equation (16.28).

TABLE 16.6
Mechanical load types

Constant Torque	Variable Torque	Constant Horsepower
Conveyors	Fans	Lathes
Hoists	Centrifugal pumps	Drills
Cranes	Centrifugal compressors	Reeling applications
Elevators		
Reciprocating compressors		

The torque at the end of the acceleration period may not equal the full-load torque for which the motor is applied. Large fans, for example, may have adjustable dampers or vanes and are started with the dampers closed or vanes at minimum pitch. As a result, there is little air flow during starting this can reduce the torque at rated speed after the start to 25% of rated torque ($K_V = 0.25$ in Figure 16.10). These initial settings are made to reduce the starting duty on the drive motor. After the fan reaches rated speed, dampers are opened to bring the fan to rated load.

16.6.5.1 Centrifugal Pumps

The starting characteristic of a centrifugal pump can vary dramatically with pump design and the hydraulic system to which the pump is connected. A typical fluid system is shown in Figure 16.20. Flow is directly proportional to pump speed. The torque required by the pump relates directly to the head (pressure) the pump produces. Head is often expressed in feet. A 10 ft head represents pressure necessary to force a column of liquid, usually water, 10 ft up a standpipe.

The head required by the fluid system has several components, velocity head, friction head and static head. Static head is backpressure as would occur if liquid were pumped to a higher elevation and is the difference between the suction and discharge liquid elevation as shown in Figure 16.20. Static head is a fixed pressure, not varying with flow. It may also result if liquid is pumped into a

© 2006 by Taylor & Francis Group, LLC

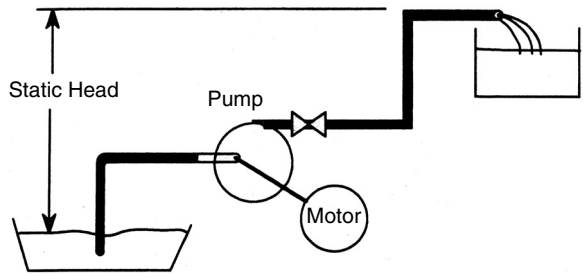


FIGURE 16.20 Pump hydraulic system.

pressurized container. Friction head is the pressure necessary to overcome flow losses in the piping and fittings. Velocity head represents the kinetic energy of the fluid and may be neglected in the analysis of some systems. Both friction and velocity heads are expressed in feet and both vary with the square of flow (or pump speed). For the purpose of this discussion, the sum of friction and velocity head will be referred to as friction head. The variation of head with flow for a typical fluid system is shown in Figure 16.21.

Pumps are classified into three categories, with vaguely defined boundaries between the classifications. Axial-flow pumps have propeller-like impellers that drive fluid forward, radial-flow pumps have more scoop-like impellers that force liquid outward. Mixed-flow pumps include various combinations of both flow paths.

The most significant difference between pump designs from a starting perspective is the torque required at no flow. When a pump is started with a closed discharge valve pump, torque increase as the square of speed from zero to the pump's "no flow" torque value. Typical characteristics for radial-, mixed- and, axial-flow pumps are shown in Figure 16.22 through Figure 16.24, respectively.[2] The no-flow torque, *T*nf, can vary from less than 50 to near 220% rated torque, depending on the type pump. Note that "rated" flow, head, and torque for a pump are defined at the point of maximum pump efficiency with the pump at rated speed and are not necessarily the flow, head and torque at which the pump is normally operated.

The above representation neglects the breakaway torque required at zero speed. This initial torque can be up to 15% of rated torque, but decreases rapidly after rotation begins. Breakaway torque is assumed to decay at the fifth power of speed in the starting calculation example. The same equation can be applied to a pump start.

$$T_L = (1 - \omega)^5 T_{ba} + \omega^2 T_{nf} \tag{16.31}$$

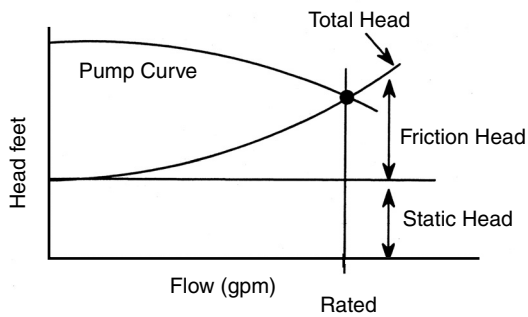


FIGURE 16.21 Head vs. flow.

© 2006 by Taylor & Francis Group, LLC

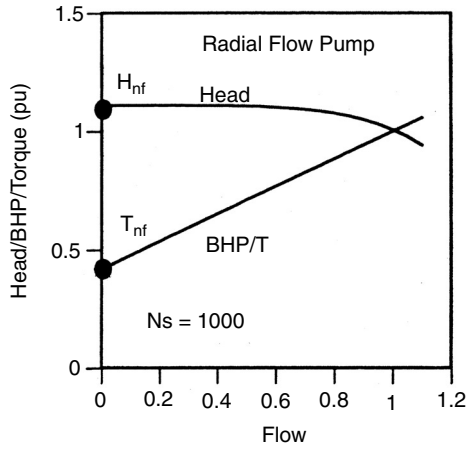


FIGURE 16.22 Radial-flow pump.

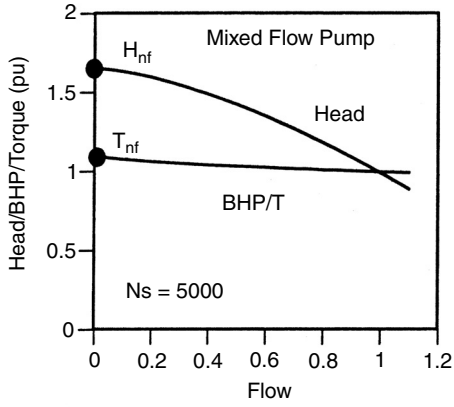


FIGURE 16.23 Mixed-flow pump.

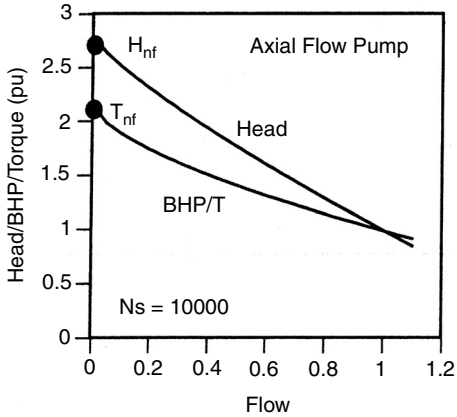


FIGURE 16.24 Axialry-flow pump.

© 2006 by Taylor & Francis Group, LLC

Neglecting breakaway torque, Figure 16.25 compares starting speed–torque characteristics for various pump designs expressed in terms of pump "specific speed." The specific speed of a pump is a performance indicator that provides a more definitive distinction of pump performance than the axial, mixed and radial flow designation. If a pump were physically scaled down to a size that would provide 1.0 gpm at 1.0 ft head, the required operating speed for that model pump is its specific speed. The specific speed is calculated as

$$N_s = \frac{RPM * Q^{1/2}}{H^{3/4}}$$

where N_s = specific speed (RPM), Q = flow (gpm), and H = head per stage (ft). In the above equation, all the values are taken at the point of maximum pump efficiency on the pump characteristic curve.

Pumps with similar specific speeds have similar operating characteristics, regardless of their physical resemblance. There is no formal defined boundary between pump designations, but approximate groupings are as follows: radial-flow pumps are pumps with specific speeds up to about 3000 RPM, mixed-flow pumps have speeds from 3000 to 6000 RPM, and pumps above 6000 RPM are considered axial-flow pumps.

Generally, radial-flow pumps are started with a close discharge valve. Pumps with specific speeds below about 4500 RPM have no-flow torque requirements that are less than rated flow. A closed valve start for these pumps reduces motor starting duty. Closed valve starting may be required by the hydraulic system. Any system with a static head would drain by back flow through the pump upon pump shutdown if valving where not closed or a check valve installed.

Pumps with higher specific speeds are normally started with open valves or the valves open as the pump starts. This is necessary to reduce motor starting duty and relieve stress in the hydraulic system. Figure 16.25 shows that the NEMA design B motor (the dashed speed torque curve), will not start an axial-flow pump with a specific speed of 10,000 RPM if the discharge valve is closed. The motor stalls at the intersection of the speed torque curves near 55% speed.

A second problem with closed valve starting of high specific speed pumps is system pressure. As can be seen in Figure 16.24, these pumps are capable of producing over 2.5 times rated head

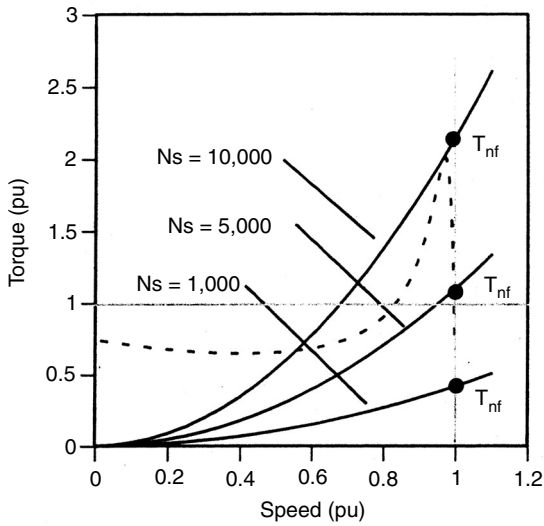


FIGURE 16.25 No-flow speed–torque for axial, mixed, and radial-flow pumps.

© 2006 by Taylor & Francis Group, LLC

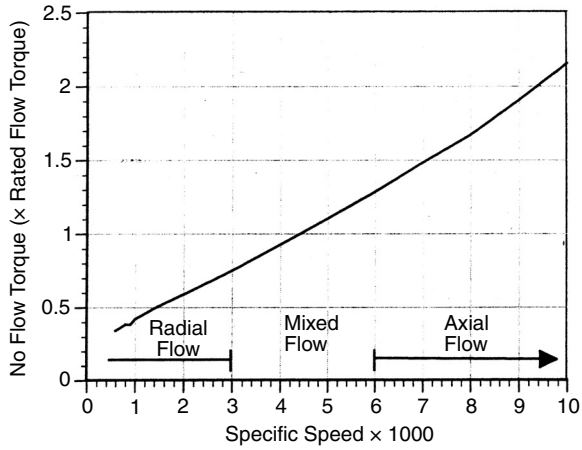


FIGURE 16.26 No-flow torque vs. specific speed.

(pressure) under no flow conditions. The hydraulic system between the pump and the valve must be designed to withstand this pressure for a closed valve start.

Figure 16.26 plots typical values of no-flow torque at rated pump speed as a function of pump specific speed.[3] This plot can be used to estimate the no-flow torque when a performance curve is not available.

When a pump is started with an open discharge valve, the pump's starting speed–torque curve is determined by the running load on the pump, the system static head, and pump no-flow head and torque. A pump starting without static head would present a speed–torque characteristic varying from zero to rated load as a function of speed squared, similar to that of a fan:

$$T_p = T_{FL} * \omega^2$$

If a static head exists, it will exert a constant backpressure on the pump. A check valve is required to prevent a back flow through the pump when the pump is shut down. During a pump start, flow cannot begin until pump head exceeds the static head. Until flow begins, a pump will exhibit the speed–torque characteristic identical to that of the closed discharge case.

As an example, assume a system has a static head equal to 40% rated. The driving pump is a radial flow pump ($N_s = 1500$) with a no-flow head of 1.15 rated and a no-flow torque of 0.5× rated. At full flow, the pump torque equals rated motor torque.

Head varies with the square of speed:

$$H_\omega = H_{FL}\left(\frac{\omega}{\omega_{FL}}\right)^2 \tag{16.32}$$

For the example system, flow will begin when pump speed reaches 59% ($\omega_{flow} = 0.59$).

$$\omega_{flow} = \sqrt{\frac{H_{static}}{H_{nf}}} = \sqrt{\frac{0.4}{1.15}} = 0.59\,\text{pu}$$

From zero speed to ω_{flow}, pump torque is a function of the pump no-flow torque, in this case $T_p = 0.5\omega^2$. Once flow begins, the torque increases to its running value, which is assumed to be 1.0 pu. Figure 16.27 plots the speed–torque characteristics for the system for both no-flow and

© 2006 by Taylor & Francis Group, LLC

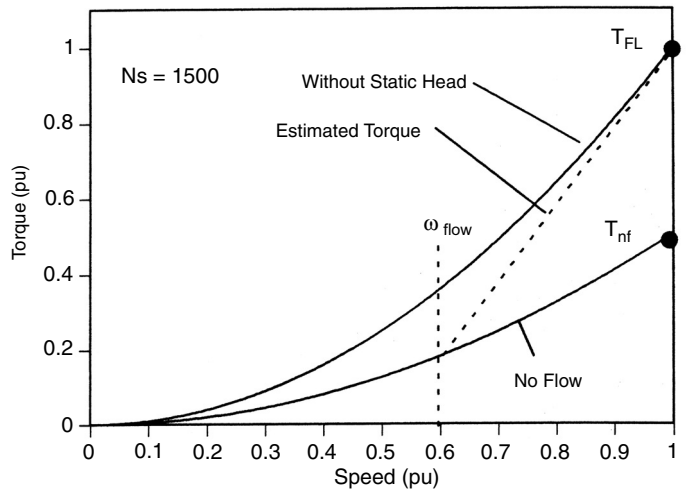


FIGURE 16.27 Start axial-flow pump with open discharge valve.

no static-head conditions. The actual speed–torque characteristic for 40% static head is estimated by a linear connection from torque when flow begins to rated flow torque.

The plot in Figure 16.28 presents a markedly different starting characteristic. This system also has a static head equal to 40% the rated pump head. However, this plot is for an axial-flow pump ($N_s = 10{,}000$), with much higher no-flow parameters than the previous plot. The axial-flow pump has a no-flow head of 2.79 × rated and a no-flow torque of 2.15 × rated.

The preflow torque characteristic for this system ($T_P = 2.15\omega^2$) is much more severe than for the radial flow case and higher no-flow head initiates flow earlier, at 38% speed.

$$\omega_{\text{flow}} = \sqrt{\frac{H_{\text{static}}}{H_{\text{nf}}}} = \sqrt{\frac{0.4}{2.79}} = 0.38\,\text{pu}$$

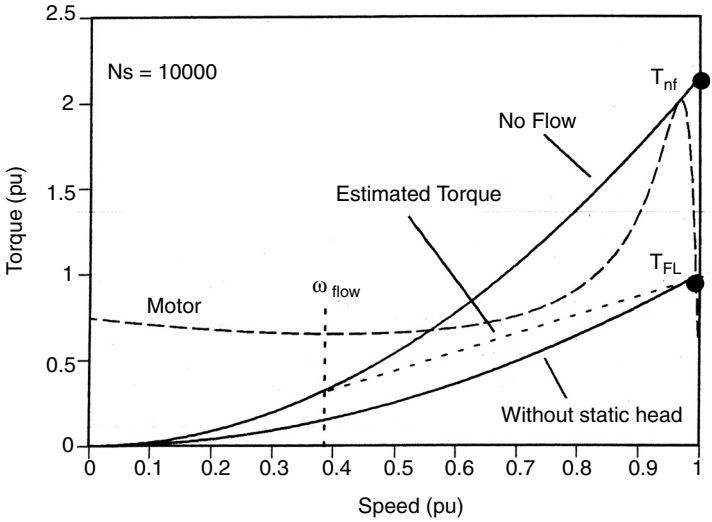


FIGURE 16.28 Effect of acceleration head on pump torque.

© 2006 by Taylor & Francis Group, LLC

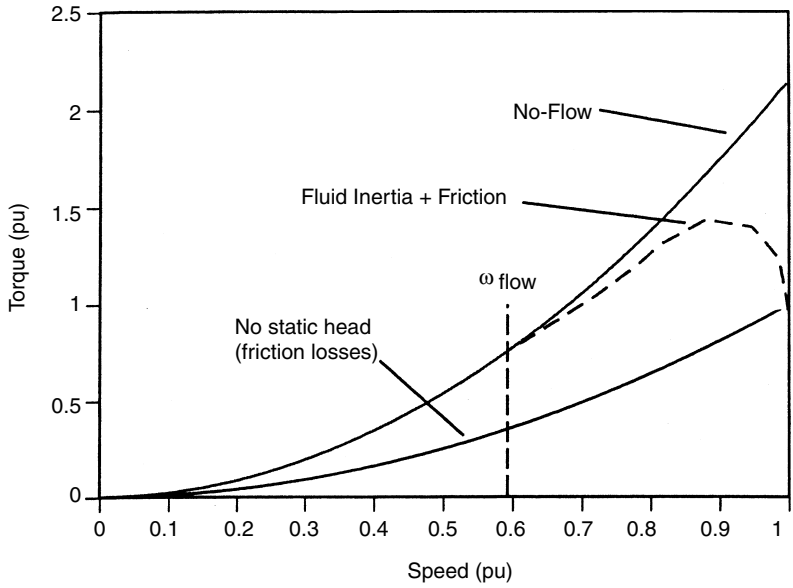


FIGURE 16.29 Flow with hydraulic friction.

The pump's starting speed–torque characteristic is again estimated by a linear connection from the initial flow torque to the rated flow torque.

The overall starting speed–torque curve for the axial-flow pump is more demanding than that of the radial-flow pump as indicated by the greater area under the axial-flow pump's speed torque characteristic. A comparison of starting times for the pumps in the preceding examples driving the same hydraulic system and driven by the same motor yields starting time for the axial-flow pump 70% greater than that of the radial-flow pump.

Figure 16.28 also shows that larger static head, one that would delay flow beyond about 55% speed, would actually stall the NEMA B drive motor depicted. Such an installation would require a design C motor.

In both the radial and axial start cases, the pump torque after flow begins is a function of fluid and pump dynamics. However, for most systems, the torque in this region can be approximated with a straight line connecting the no-flow torque at ω_{flow} to the running torque at rated speed, as shown in the previous figures. In some large systems, particularly those driven by high head pumps (high specific speed pumps), the linear approximation of the torque trajectory may be optimistic. Such systems can generate a large acceleration head to accelerate liquid in the system. The acceleration head would increase the pump torque as shown in Figure 16.29.

16.6.6 Rotor Heating during Acceleration

At any point during the acceleration period, all the power transmitted to the rotor across the airgap is consumed either by the mechanical load or by losses in the rotor structure and windings. The motor equivalent circuit in Figure 16.6 separates mechanical load ($I^2\ R_r(1-s)/s$) from rotor losses ($I^2\ R_r$). Aside from torque limitations, the accelerating capability of most motors is limited by heating in the rotor. This rise is a result of I^2R losses in the R_r element of the equivalent circuit.

© 2006 by Taylor & Francis Group, LLC

The total power input to the rotor is the mechanical load plus rotor losses:

$$P_{\text{rot}} = I_{\text{r}}^2 R_{\text{r}} + I_{\text{r}}^2 R_{\text{r}} \frac{(1-s)}{s} \tag{16.33}$$

The acceleration period begins at slip = 1.0 (speed = 0). At this point there is no mechanical output and all the power delivered to the rotor must be consumed by the R_{r} element and applied to heat the rotor bars and end rings. As the rotor begins to move the $(1-s)/s$ term begins to increase and rotor input power divides between the mechanical load and rotor heating. At the end of the acceleration period, nearly all the input power is consumed by mechanical load and rotor losses are minimal.

A derivation of the rotor losses provides insight into factors that affect rotor heating during the acceleration period. The instantaneous power loss at any given rotor speed ω_{r} is

$$P_{\text{r}_{\text{loss}}} = P_{\text{r}_{\text{developed}}} - P_{\text{acceleration}} - P_{\text{Load}}$$

or

$$P_{\text{r}_{\text{Loss}}} = T_{\text{m}}\omega_{\text{s}} - T_{\text{acc}}\omega_{\text{r}} - T_{\text{L}}\omega_{\text{r}}$$

Because the accelerating torque is the difference between the motor torque and the load torque, the equation can be rewritten as

$$P_{\text{r}_{\text{loss}}} = T_{\text{m}}(\omega_{\text{s}} - \omega_{\text{r}})$$

Rotor heating during the acceleration period is then the sum of the instantaneous losses as the rotor accelerates from zero to rated speed:

$$P_{\text{r}_{\text{Loss}}} = \int T_{\text{m}}(\omega_{\text{s}} - \omega_{\text{r}})\,\text{d}t$$

Defining dt from the Equation (16.13) for rotary acceleration

$$T_{\text{acc}} = T_{\text{m}} - T_{\text{L}} = I\frac{\text{d}\omega_{\text{r}}}{\text{d}t}$$

where I = inertia of motor and driven load,

$$\text{d}t = \frac{I}{(T_m - T_L)}\,\text{d}\omega_{\text{r}}$$

Substituting

$$\begin{aligned} P_{\text{r}_{\text{Loss}}} &= I\int_0^{\omega_{\text{s}}} \frac{T_{\text{m}}}{(T_{\text{m}} - T_{\text{L}})}(\omega_{\text{s}} - \omega_{\text{r}})\,\text{d}\omega_{\text{r}} \\ &= I\frac{T_{\text{m}}}{(T_{\text{m}} - T_{\text{L}})}\left(\omega_{\text{s}}^2 - \frac{1}{2}\omega_{\text{s}}^2\right) \end{aligned}$$

© 2006 by Taylor & Francis Group, LLC

The resulting expression for rotor heating losses over the acceleration period reduces to

$$P_{r_{Loss}} = \frac{1}{2} I \omega_s^2 \frac{T_m}{(T_m - T_L)} \tag{16.34}$$

The expression shows that with no load torque, the rotor heating would be equal to half the rotational energy stored in the mechanical system after the start.

$$P_{r_{Loss}} = \frac{1}{2} I \omega_s^2 \tag{16.35}$$

For this case, the duration of the acceleration time has no bearing on rotor heating. However, with the addition of load torque, rotor heating increases as the accelerating torque term $(T_m - T_L)$ decreases.[4] It is intuitive that heating should increase with load torque. What may not be intuitive without Equation (16.34) is that a reduction of the starting voltage and the resulting reduction in motor torque not only increases starting time, but will also increase motor heating.

The point to remember is that rotor heating is directly proportional to load inertia and inversely proportional to the accelerating torque. Accelerating time varies in the same manner, so anything that increases the starting time increases motor heating.

16.7 MOTOR OVERLOAD PROTECTION

Overcurrent protection is intended to prevent thermal damage. A motor may suffer thermal damage as a result of overloads, stalling caused by mechanical failure, or operator error. Thermal damage may also result from repeated starts or unbalanced current. In each instance, damage results when one or more internal motor components exceeds its design temperature limit. Damage to motor insulation can range from minor loss of life to complete failure, depending on the severity and duration of the temperature excursion. Excess temperature can also cause mechanical damage due to thermal expansion. Rotor components such as bars and end rings are vulnerable to this damage.

Temperature rise within a motor for these conditions is primarily a function of I^2R losses. Because temperature increases with current, it is logical to apply overcurrent elements with inverse time–current characteristics. The motor overcurrent applications are complicated by the complexity of motor thermal characteristics and the time-varying nature of current experienced during starting and when the motor drives a time-varying load.

16.7.1 Motor Thermal Limit Curves

If a motor is to be protected, its overload capabilities must be know. The motor manufacturer provides this information in the form of a *thermal limit curve*. This plot is prepared in accordance with IEEE 620-1996, which requires only that it include safe times for three conditions: running overloads, locked rotor and acceleration. Typical thermal limit curves are shown in Figure 16.30.

Although thermal limit curves are prepared in accordance with IEEE 620, the standard only defines the physical configuration of the plot and requires that the three overload conditions be represented. The standard provides no technical basis for calculating these limits. Curves provided are then based on each manufacture's interpretation of the three conditions and his experience. The loss of life represented by these curves is therefore indeterminate and presumable inconsistent.

These curves are usually plotted with the motor at full-load operating temperature (hot) just prior to the overload condition. Cold curves, with the motor initially unloaded and at ambient temperature, may also be provided. When plotted for a hot motor, the resulting overload and locked rotor times would be applicable following prolonged continuous operation at full load. The hot

© 2006 by Taylor & Francis Group, LLC

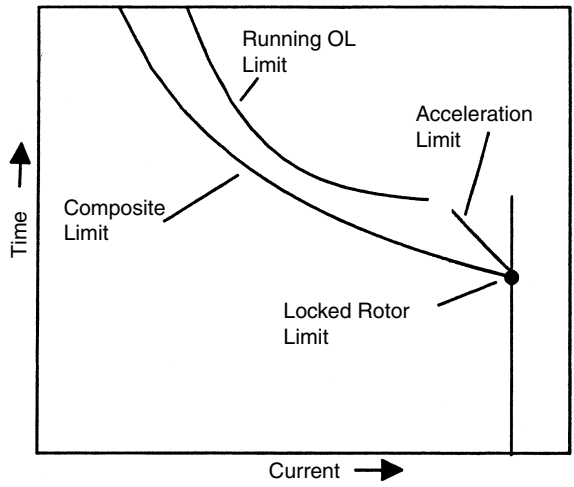


FIGURE 16.30 Typical thermal limit curves.

acceleration limit would be applicable for immediate restart following a shutdown from full load. Both hot and cold curves are normally based on a 40°C ambient temperature.

The running overload potion of the curve extends from rated or service factor current to a current level comparable with the breakdown torque of the motor (approximately 60% of the locked rotor current). The acceleration limit portion extends from the breakdown torque current level to locked rotor current.

The running overload portion represents small to moderate overloads applied while the motor is operating near rated speed. The large thermal storage capacity of the motor and the near normal ventilation facilitated by normal air flow through the air gap allows these overloads to persist for several minutes without significant temperature rise. Most motors are limited by stator insulation temperature in this region of operation.

The locked rotor condition is the most severe that a motor must endure. Current for this condition is typically six times greater than normal, and line frequency current is induced into the rotor, as opposed to the near DC rotor current at rated speed. At higher frequencies, current is forced to the outer circumference of the rotor by the skin effect. The high current density increases the effective rotor resistance to as much as three times that at rated speed (DC) operation.

The I^2R heating in the rotor during locked rotor is then approximately $6^2 \times 3$ or 108 times more severe than during normal operation. This enormous heat input to the rotor cannot be dissipated. The result is a rapid temperature rise that can damage rotor components, typically in 10 to 30 sec. The stator winding is also subject to six times rated current, but stator resistance is not affected by rotor speed; hence, stator heating during locked rotor is only 6^2 or 36 times greater than normal. This explains why most motors are rotor limited at locked rotor and during acceleration.

The rotor of a squirrel-cage motor does not have insulation. Rotor temperature limits are defined by heat-induced mechanical deformation and the resulting stress in the rotor bars and end rings. Locked rotor and stalls are infrequent and are considered an emergency condition by motor designers. Higher temperatures are allowed for these conditions than are allowed for starting. This is based on the recognition that the higher loss of fatigue life per locked rotor incident will not appreciably reduce the motor's service life because of the infrequent occurrence of this event.

Rotor temperature limits vary among manufacturers. Papers report bar temperature limits from 240 to 390°C for locked rotor and stall conditions; 300°C is a typical limit. End ring limits are much lower at 80 to 160°C; 80°C is typical.

© 2006 by Taylor & Francis Group, LLC

Thermal limit curves may present running, accelerating and locked rotor limits separately or as a composite curve as shown in Figure 16.30. The starting time for most motor applications is less than the motor safe time at locked rotor. For these applications, the acceleration limit is not critical. When manufacturers provide thermal limit curves for such applications, the limit is usually a composite of the running overload and locked rotor limits. A curve drawn to include these points would be conservative in the area of the acceleration limit. Motors applied to high-inertia loads may have starting times in excess of their safe stall time. In these applications, the three limits must be displayed separately to demonstrate the full starting capability of the motor.

Although IEEE Standard 620 does not describe the derivation or application of the acceleration thermal limit (ATL) curves, the ATLs plotted in 620 and in the IEEE Guide to AC Motor Protection, C37.96-2000, resemble the ATL curves discussed in Refs 5 and 6. The ATL curves presented in those references plot running current and the associated maximum allowable operating time for a motor operating at fixed speeds between locked rotor and the speed at which breakdown torque occurs.

When a motor starts, acceleration continues as long as motor torque exceeds the torque required by the driven load. Acceleration ceases at the point where the motor and load speed–torque curves intersect. The speed at intersection becomes the operating speed for the motor. Normally, this intersection occurs near the full-load speed of the motor. However, under abnormal conditions, load torque may be increased due to mechanical failure or operator error or motor torque may be reduced by low system voltage. Either case may result in a failure to accelerate, with the torque intersection point well below rated speed as was shown in Figure 16.11.

Operation at reduced speed produces high running current with reduced ventilation and will eventually result in motor damage. Each current and time point on the ATL curve represents the operating current and safe time for a specific stall speed along the motor's speed–torque curve. Because torque and current are voltage-dependent a unique ATL exists for every value of motor terminal voltage.

Both the locked rotor and acceleration portions of the thermal limit curve are voltage-dependent and are usually plotted at the same voltages that motor starting current is plotted, typically 100%, 90% or 80% rated voltage. If these limits are known for one voltage they can be estimated for other voltages.

During locked rotor, critical temperatures are reached very quickly and heat loss to the surroundings is generally not considered when analyzing temperature rise for this condition. With this assumption, rotor temperature rise is proportional to I^2t. The I^2t value derived from the safe stall time and associated locked rotor current is then a constant representative of the limiting rotor temperature and can be used to define the safe stall time at any other voltages. Figure 16.31 is a thermal limit curve with the accelerating and locked rotor limits plotted at 100% voltage.

The safe stall time is 8.0 sec at a rated voltage locked rotor current of 6.5 pu amps. The limiting I^2t is then $6.5^2 * 8 = 338$, which plots as a straight line on a log–log plot. At 80% voltage, the locked rotor current is 80% of its rated voltage value (neglecting the effect of saturation). The safe stall time at 80% voltage is $338/(6.5*0.8)^2 = 12.5$ sec as plotted in the figure.

Every value of motor terminal voltage generates a unique ATL curve. If heat loss is neglected, these curves also plot as straight lines on a log–log plot and are parallel to one another. Note that not all manufacturers plot curves in this manner. If the curves match the theoretical configuration, it is then possible to derive the ATL curve for any voltage if one ATL is known.

Each ATL plots motor current and withstand at varied speeds including locked rotor. It follows then that the ATL for every value of terminal voltage must intersect the locked rotor I^2t limit plot. Figure 16.32 demonstrates how the ATL at 80% voltage can be estimated from the 100% voltage ATL curve. Locate the point where the locked rotor current at the reduced voltage of interest intersects the locked rotor I^2t limit. A line drawn through that point and parallel to the known ATL establishes the ATL at the reduced voltage.

© 2006 by Taylor & Francis Group, LLC

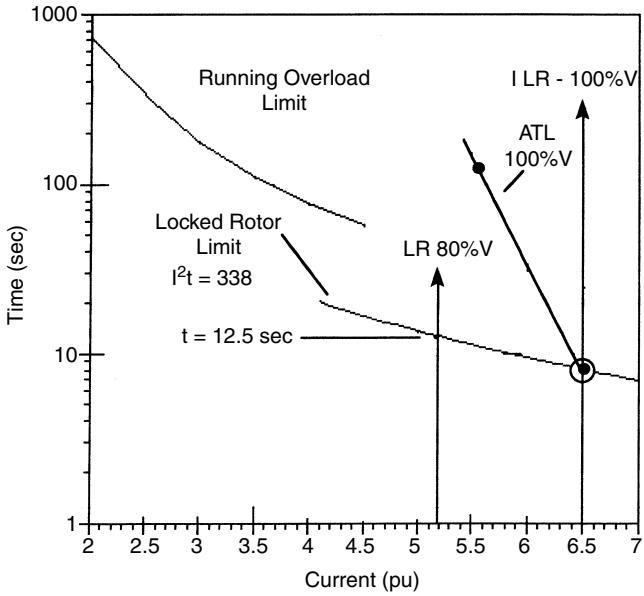


FIGURE 16.31 Acceleration limit at 100% voltage.

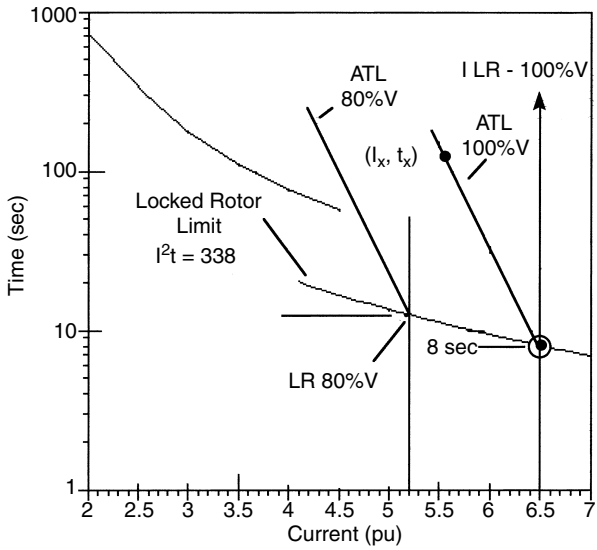


FIGURE 16.32 Accelerating limit 80% voltage CC.

16.7.2 Overcurrent Coordination

Motor overload protection is achieved when the overcurrent trip element actuates before limiting temperatures are exceeded. However, the overcurrent trip delay is constrained by the starting current transient in that the trip device must provide sufficient delay to allow the motor to accelerate. Figure 16.1 depicts the desired configuration of limit, trip and starting characteristics. However such graphic comparison of time–current characteristics can provide a distorted view of protection and coordination. Starting current below the trip characteristic and thermal limit does not guarantee the relay will override the start or that the start is within motor thermal capability.

© 2006 by Taylor & Francis Group, LLC

The reason for this is that thermal limit curves and trip device characteristics represent timing points associated with fixed values of current while the starting current trace represents a dynamic change of current with time. Consequently, the thermal limit and trip characteristics are not directly comparable with the starting current plot. A comparison of time–current characteristics is only valid at constant current. Thus, the plot accurately shows coordination between the trip and limit curve for locked rotor and overloads of constant magnitude. However, the ability of the overcurrent element to override the starting transient or the motor's thermal capability with respect to the starting duty are both technically indeterminate from the plot.

Admittedly, plots similar to Figure 16.1 are commonly used to depict motor protection. Such representations of the coordination between the thermal limit curve and overcurrent protection trip characteristic are justified for motors that drive a fixed load such as a fan or pump, because most conceivable overload conditions would be of constant current magnitude. Although the representation of the starting current on the plots is dubious, various texts provide recommended minimum time margins between the starting current and the trip device characteristic to assure successful starting.

IEEE Standard C37.96-2000 recommends a minimum margin between the starting current and the relay characteristic of 2 sec for starts of 5 to 10 sec in duration and 5 sec for starts in the 40 to 50 sec range. Required margins are voltage and relay characteristic dependent. The stated margins are quoted for 100% voltage starting and are not adequate for reduced-voltage starts. Time margins are discussed in Sections 16.7.6.3 and 16.7.7.2.

For starts lasting 25 sec or less, trip elements will override the starting transient if margins equal to or greater than those listed in Table 16.10 or Table 16.12 are maintained between the relay characteristic and the starting current trace. If the start time exceeds 25 sec, or different relay characteristics are used, relay response to the starting current must be calculated on a point-by-point basis as described in Section 16.7.6.3 and Section 16.7.7.2.

To assess overcurrent element response to time-varying current, whether resulting from starting or a cyclic load, a dynamic analysis is required. The analytical method employed here is a point-by-point solution using data from the starting calculation in Section 16.6.4 and unique dynamic models for disk and thermal overcurrent elements. As will be shown, disk and thermal elements adjusted to have similar time–current characteristics respond in a similar manner to the starting transient. However, the response of the two elements to time-varying load can be radically different depending on the shape of the load cycle. Because the motor thermal limit curve, like the relay time current curve, is derived from fixed current data, a similar dynamic analysis is required to assess motor capability during starting and time-variant loading.

At most installations, the accelerating duty does not challenge motor capability and the overcurrent trip characteristic can be set between the starting current transient and limit curve, maintaining a margin well in excess of that recommended. In such situations, a dynamic analysis may not be required. Problems arise when dealing with high inertia loads and/or low starting voltage. In these applications, the starting current transient will approach the limit curve, and in severe cases it is not possible to configure a single overcurrent trip characteristic to override the start and protect the motor. These applications required specialized trip schemes that will be discussed later.

16.7.3 Thermal vs. Disk Elements

There are two basic forms of overcurrent protection: disk elements and thermal elements. Disk elements include electromechanical elements that operate on the induction disk principles and electronic elements that mimic them. Disk elements are characterized by a minimum trip current setting that defines a distinct boundary between operation and nonoperation. The element is unresponsive to current below the minimum trip current. When current is above the trip setting, operation is inevitable. The operating time of the element is determined solely by the magnitude of the overload current.

© 2006 by Taylor & Francis Group, LLC

Thermal elements are designed to simulate a thermal system responding exponentially to current in both actuation and reset modes. This is an attempt to match the exponential heating and cooling characteristics of the protected motor. These elements have an ultimate trip current setting that is similar to the minimum trip current of the disk element. However, unlike the disk element, the operating time of a thermal element is determined not only by the overload current, but also the operating current prior to the overload. Trip time for a given overload current decreases as the preoverload current increases.

This is easy to visualize with older thermal elements. Before the advent of electronic relays, thermal elements were constructed using heating coils and bimetallic contacts or melting alloys. Tripping occurred when the relay reached the temperature necessary to deflect the contacts or melt the alloy. Obviously, the initial operating current of the motor will determine the initial temperature of the relay. The higher the initial temperature the faster the trip temperature is reached for a given overload. Solid-state thermal elements, although more sophisticated, emulate heater-driven units and have an equivalent response.

Thermal element response corresponds with that of a motor. A motor operating at light load (cold) will tolerate a subsequent overload for a significantly longer time than it would following initial operation at rated load (hot). The ability of the thermal element to adjust its characteristic to the initial thermal state of the motor is often referred to as "thermal memory," and is the primary difference between disk and thermal elements.

Because a thermal element adjusts with motor operating current, it should provide better protection than a disk element. The disk element will have the same trip time for a given overload following unloaded operation as it would following full-load operation.

A primary example of the advantage of thermal memory is starting. Disk elements provide little protection for repetative starting. The cooling time for a motor at standstill can be hours, while a disk element will reset in less than a minute. Consequently, a disk element will reset between consecutive starts, while the motor experiences little cooling during the same period. The trip time and resulting motor temperature rise will be the same for each failed start attempt, allowing motor temperature to ratchet to damaging levels.

In theory, a thermal element with heating and cooling constants matching the motor would accumulate heat in proportion to the motor and could be set to operate before motor damage occurred. However, in the past, thermal elements were implemented using electromechanical technology, which limited their effectiveness.

Relays of this design have one heating and one cooling characteristic, which are not adjustable. The single heating characteristic cannot match motor thermal characteristics in all modes of operation. In the running overload portion of the thermal limit curve, heat input to the motor is moderate and temperature rise is limited by heat dissipation to neighboring components within the motor. The thermodynamics of the acceleration and locked rotor portions of the limit curve are quite different. Heat input during these conditions is very high, and limiting temperatures are reached in a fraction of the thermal time constant. In effect, for the seconds required in reaching limiting temperature, little or no heat is dissipated to surrounding materials. Consequently, thermal elements configured to the running overload portion of the limit curve are usually too slow to provide protection during acceleration and locked rotor.

Also, the single cooling mode of electromechanical-based thermal elements severely limited their effectiveness during multiple starts. Motor cooling times when running compared with stopped vary dramatically. When a motor is successfully started, airflow through the air gap provides cooling of motor components. Airflow is severely reduced during spin down and nonexistent when stopped. Typically, the cooling time constant for a stopped motor can be 10 to 15 times greater than the running cooling time constant. An increase from 15 min to 225 min would be typical. A single relay cooling characteristic that is chosen for the running conditions would, like the disk element, reset between starts and permit motor temperatures to increase beyond acceptable limits.

© 2006 by Taylor & Francis Group, LLC

Only recently, with the advent of microprocessor-based relaying, has thermal-based protection become dominant for large motor protection. These protection systems use more sophisticated algorithms to more closely track motor temperature and avoid many of the problems experienced by their electromechanical predecessors. Many microprocessor-based thermal elements also monitor the severe heating effects of unbalanced phase currents.

16.7.4 Time Overcurrent Trip Settings

The time overcurrent trip settings are constrained by the National Electric Code. The maximum overcurrent pickup allowed for motors with a service factors of 1.15 or greater and motors marked with a rise not over 40°C is 125% the full-load current. All other motors shall have a maximum overcurrent trip setting of 115% full-load current or less. The code states that if protection so set is unable to carry motor load or start the motor, the next higher setting can be used. The increased settings are constrained as follows: settings shall not exceed 140% motor full-load current for motors with a service factor of 1.15 or greater and motors marked with a rise not over 40°C; increased setting shall not exceed 130% of full load for all other motors.

Motors operated at rated load (service factor = 1.0) will draw the full load current stamped on the motor nameplate at rated voltage. NEMA standards permit such motors to operation continuously at voltage that varies ±10% from rated. At 90% rated voltage, the same motor will draw 1.1 times the nameplate current. A trip setting of 1.15 times rated current would allow the motor to operate at 90% voltage with a 5% margin.

Assuming the same motor has a 1.15 service factor and was operating at service factor load, the current would be 1.15 times the nameplate full-load current. If the 5% margin is retained, a setting of 1.2 times rated full-load current should be used. Note that no allowance is made for reduced voltage at service factor load because the service factor rating is only valid at rated voltage.

Ideally, the minimum trip current should be set just above the continuous current that produces the maximum allowable temperature rise. If temperature rise data are available, the minimum trip current can be based on insulation temperature limitation. For example, assume a motor with Class B insulation has a temperature rise of 65°C at rated load. At a standard ambient of 40°C, this motor would operate at 105°C, which is 25°C below the hot spot temperature allowed for type B insulation. Because temperature is a function of $I^2 R$ losses, minimum trip for this motor could be set at

$$I_{trip} = \sqrt{\frac{130^\circ\text{C}}{105^\circ\text{C}}} = 1.11\, I_{\text{FL}} \tag{16.36}$$

16.7.5 Duty Cycle Motor Protection

Overcurrent element setpoints are chosen by comparing relay characteristics to motor thermal limitations. This strategy assumes that the relay responds to the same current responsible for heating. This presumption is valid for motors driving continuous loads, but is not true for motors driving time-variant loads. In both cases, motor heating is directly proportional to the square of the effective RMS current over the load cycle, but neither the disk nor thermal elements respond directly to this value. These elements are more responsive to current variations during the load cycle.

Motors applied to constant mechanical loads are chosen on the basis of rated horsepower. An overload is clearly defined as current in excess of rated full-load or service factor current. Protection is easily provided by setting the actuation current of the overcurrent element slightly above the magnitude of the maximum allowable continuous current of the motor.

© 2006 by Taylor & Francis Group, LLC

Crushers, cranes, and boring machines are examples of fluctuating mechanical loads. In these applications, load typically varies from light to severe overload during a load cycle. Motor temperature rises during load cycle peaks and cools during light load intervals. The maximum temperature of any motor component is a function of the magnitude and duration of the load perturbations and the heating and cooling time constants of the protected motor.

Motors applied to time-varying loads are sized on the basis of thermal capability, not horsepower rating. In Section 16.5.1 a motor was sized thermally using the equivalent RMS horsepower of the load cycle. For duty cycle motors, an overload exists when the RMS equivalent current calculated over the load cycle exceeds the motor rated current. Hence, an overload can result not only from increased current magnitude but also from changes in the duration of peak and light load excursions during the load cycle.

Neither disk nor thermal elements respond directly to the RMS value of current. When motor current is continuous, both motor heating and relay response relate directly to the current magnitude. However, as the current profile changes from flat to time-varying, the relation between load cycle RMS current and relay response becomes nonlinear. Disk elements become relatively insensitive to a high RMS current resulting from large short-duration load peaks and provide poor overload protection for that profile. Thermal elements become more sensitive to the same profile and will tend to misoperate for load cycles of this type that are within motor capability. Techniques to evaluate disk and thermal element response to a load cycle are derived below.

16.7.6 Induction Disk Operating Characteristics

Disk and thermal elements exhibit unique steady state and transient responses. To understand these differences, their respective characteristics will be derived from their operating principles.

An induction disk element is constructed with a stationary electromagnet mounted perpendicular to and near the circumference of a thin aluminum disk. The disk has a thin shaft through its center. The shaft mounted on bearings allowing the disk to rotate freely. When alternating current energizes the electromagnet, current is induced in the disk, which in turn produces a magnetic field. The interaction of the two magnetic fields results in torque and rotation of the disk. The minimum current in the electromagnet necessary to produce disk motion is controlled by a restraint spring, while the speed of rotation is controlled by a permanent magnet (drag magnet), also mounted at the circumference of the disk. As disk speed increases, the drag magnet induces current in the disk, which produces a magnetic field and torque that act to oppose the speed increase.

A full mathematical representation of the induction disk relay is given in Ref. 7 as:

$$K_I I^p = m\frac{\mathrm{d}^2\theta}{\mathrm{d}^2 t} + K_\mathrm{d}\frac{\mathrm{d}\theta}{\mathrm{d}t} + \frac{\tau_F - \tau_\mathrm{s}}{\theta_\mathrm{max}}\theta + \tau_\mathrm{s} \tag{16.37}$$

where p = constant relating current to torque, I = current input to electromagnet, θ = disk travel, θ_max = maximum disk travel, K_I = constant relating current to torque, m = moment of inertia of disk assemply, K_d = drag magnet damping factor, τ_F = spring force at max travel, and τ_S = spring force at inital position. Because disk inertia is small and the disk is shaped slightly spiral to produce increased torque to offset the relatively small increase in spring torque from τ_S to τ_F, disk dynamics are closely approximated by

$$K_I I^p = K_\mathrm{d}\frac{\mathrm{d}\theta}{\mathrm{d}t} + \tau_\mathrm{s} \tag{16.38}$$

© 2006 by Taylor & Francis Group, LLC

Rewriting with current expressed in terms of multiples of the pickup current (I_p)

$$M = \frac{I}{I_p} = \text{multiples of pickup current } I_P$$

$$K_I(MI_p)^p = K_d\frac{d\theta}{dt} + \tau_s \tag{16.39}$$

At minimum pickup, current, $M = 1$ and disk speed is near zero. Then

$$K_I I_p^p = \tau_s$$

Substituting into Equation (16.39):

$$\tau_s(M^p - 1) = K_d\frac{d\theta}{dt} \tag{16.40}$$

Solving for θ,

$$\theta = \int_0^t \frac{\tau_s}{K_d}(M^p - 1)\,dt$$

and integrating with constant current,

$$\theta = \frac{\tau_s}{K_d}(M^p - 1)t$$

The element initiates a trip when disk rotation $\theta = \theta_{trip}$. For constant current, the time–current characteristic for the disk element is then

$$t_{trip} = \frac{\left(\frac{\theta_{trip}K_d}{\tau_s}\right)}{(M^p - 1)} \tag{16.41}$$

Or, presenting the relay trip time in a more familiar form,

$$t_{trip} = \frac{A}{(M^p - 1)} \tag{16.42}$$

In theory, this equation is applicable for constant current with $M > 1$ and $M < 1$, which define operate and reset states for the relay. In the equation, "A" is equivalent to the relay reset time. Assuming that the relay has operated ($\theta = \theta_{trip}$) and current is removed from the relay the disk rotation to reset will now equal -θ_{trip} and the reset time will be

$$t_r = \frac{-A}{(0 - 1)} = A \tag{16.43}$$

The relay characteristic is adjusted by varying the pickup current (I_p) and time dial. The latter adjustment changes the distance the disk must travel (θ_{trip}) and the reset time (A).

This relay has no response when current is below the minimum pickup setting. When current rises above the pickup setting, a trip will occur in the time prescribed by the time dial setting.

© 2006 by Taylor & Francis Group, LLC

Hence, these elements have only two states, "Reset" or "Operating," and can not adjust to the changing thermal state of the motor.

16.7.6.1 Dynamic Characteristic of the Disk Element

The response of a disk element to time-varying current is evaluated using an incremental form:

$$\theta_n = \overline{\omega}_n \Delta t + \theta_{n-1} \tag{16.44}$$

Disk velocity ω can be derived from Equation (16.40) as

$$\omega = \frac{\mathrm{d}\theta}{\mathrm{d}t} = \frac{\tau_\mathrm{s}}{K_\mathrm{d}}(M^p - 1) \tag{16.45}$$

Disk velocity will be a function of current and will differ at the beginning and end of the interval. The average velocity over the interval is estimated by using the average multiple of pickup over the interval.

$$\begin{aligned} \overline{M}_n &= \text{average multiple over the interval} \\ &= \frac{(I_n + I_{n-1})}{2I_\text{pickup}} \end{aligned} \tag{16.46}$$

Substituting Equation (16.45) and Equation (16.46) into Equation (16.44):

$$\theta_n = \frac{\tau_\mathrm{s}}{K_d}(\overline{M}_n^p - 1)\Delta t + \theta_{n-1} \tag{16.47}$$

A trip is indicated when $\theta_\mathrm{n} = \theta_\mathrm{trip}$. By dividing each side of Equation (16.47) by θ_trip, relay response is expressed as *%_Trip*. Relay operation occurs when $\%_Trip_\mathrm{n} = 100$

$$\%_Trip_n = \frac{\theta_n}{\theta_\text{trip}} = \frac{\tau_\mathrm{s}}{K_\mathrm{d}\theta_\text{trip}}(\overline{M}_n^p - 1)\Delta t * 100 + \frac{\theta_0}{\theta_\text{trip}} * 100$$

$$\%_Trip_n = \frac{100 * (\overline{M}_n^p - 1)\Delta t}{A} + \%_Trip_{n-1}$$

Substituting Equation (16.42), the final incremental form becomes

$$\%_Trip_n = \frac{\Delta t * 100}{t_\text{trip}(\overline{M_n})} + \%_Trip_{n-1} \tag{16.48}$$

where $t_\text{trip}(\overline{M_n})$ is the operating time of the relay at the average multiple of pickup for the interval.

16.7.6.2 Practical Disk Element Model

Before applying the disk relay equations, some modifications are required to move from the theoretical to the practical. Electromechanical relay characteristics are shaped by magnetic saturation as well as the rotating system parameters used to derive the disk equations. Also, the reset time of a practical relay element will not equal the "*A*" parameter of Equation (16.43). To include these effects and provide a basis for the comparison, inverse, very inverse, and extremely inverse

© 2006 by Taylor & Francis Group, LLC

TABLE 16.7
Disk Relay Constant[7]

Characteristic	*A*	*B*	*p*	t_r
Inverse	0.0515	0.1140	0.020	4.85
Very inverse	19.61	0.491	2.00	21.6
Extremely inverse	28.2	0.1217	2.00	29.1

Source: IEEE Std C37.112-1996(2001R), IEEE Standard Inverse Time Characteristic Equations of Overcurrent Relays. With permission.

time–current characteristic relay representations from IEEE Standard C37.112–2000 will be used (Table 16.7).

From the standard,

$$t_{\text{trip}} = \left(\frac{A}{M^p - 1} + B\right)\frac{TD}{5} \tag{16.49}$$

$$t_{\text{reset}} = \left(\frac{t_r}{M^2 - 1}\right)\frac{TD}{5} \tag{16.50}$$

The standard defines parameters for the midrange time dial of three characteristics. The parameters of Table 16.7 apply to the #5 TD position on a (1–10) TD relay. In the following examples, TD settings above 10 are required to override the starting inrush.

With these modifications Equation (16.42) and Equation (16.43) are replaced by relay trip and reset Equation (16.49) and Equation (16.50). The dynamic response Equation (16.48) remains valid, but relay operating time is now derived from Equation (16.49). A comparison of the three relay characteristics is provided in Figure 16.33.

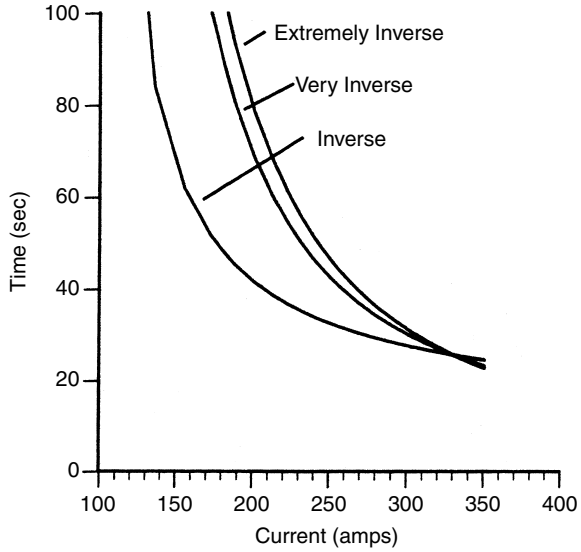


FIGURE 16.33 Overcurrent element characteristics.

© 2006 by Taylor & Francis Group, LLC

16.7.6.3 Disk Element Response to Starting Current

In Section 16.6.4, the starting characteristic of a 600 HP motor driving a high-inertia fan load was calculated. The system impedance reduced initial terminal voltage to 80% for rated motor voltage. The resulting starting time was 26 sec. Figure 16.1 plots this starting transient with the motor's hot thermal limit, and a disk relay characteristic. The disk element shown is set for a pickup of 94 A (1.2 × motor full-load current) at time dial = 60 with an inverse characteristic as defined from Equation (16.49) and Table 16.7.

$$t_{\text{trip}} = \left[\frac{0.0515}{\left(\frac{I}{94\text{ A}}\right)^{0.02} - 1} + 0.114\right]\frac{TD}{5}, \quad TD = 60$$

The dynamic response of this disk element is calculated in Table 16.8 using Equation (16.48, 16.49) and the starting current–time points derived in Section 16.6.4.

In the table, relay current is equal to the motor per unit current times motor full-load current (78 A).

The table shows that the relay reaches 99.7% of trip, indicating that this is the minimum time dial setting that will override the start. This setting was chosen so that the minimum time margin between the relay characteristic and the starting current trace could be determined. By benchmarking the margin required, it might be possible to confirm coordination from time-current plots, thus avoiding the point-by-point dynamic analysis.

If actual settings were being derived, a higher time dial would be desired to provide a safety margin during the start. The maximum time dial setting would be constrained by the hot thermal limit curve.

The relay response calculation was repeated for inverse, very inverse, and extremely inverse characteristics, all set at 94 A pickup, and the minimum time dial for starting. Table 16.9 summarizes the time margins required between the start current and relay characteristic for each

TABLE 16.8
Disk Element Response to Starting Current

Speed (pu)	$t = \Sigma\Delta t$ (sec)	I_{mot} (pu)	I_{relay} (A)	I_{relay} (average)[a]	t_{relay} (sec)[b]	Δt (sec)	C $\Delta Trip$%	% *Trip*
0	0	4.504	351.27					0
				351.17	24.505	0.1667	0.680	
0.005	0.167	4.501	351.07					0.680
				350.97	24.516	0.1653	0.674	
0.01	0.332	4.498	350.87					1.354
				350.77	24.526	0.1639	0.668	
0.015	0.496	4.496	350.67					2.022
0.980	25.62	2.053	160.12					99.62
				144.84	72.53	0.0667	0.092	
0.985	25.687	1.661	129.57					99.71

Equations used: [a]Equation (16.46); [b]Equation (16.49); [c]Equation (16.48).

© 2006 by Taylor & Francis Group, LLC

TABLE 16.9
Disk Element Starting Margins with Circuit Impedance

Characteristic	TD	%Trip	Minimum Margin to Start Current
Inverse	60	99.8	3.30
Very inverse	57.8	99.4	5.27
Extremely inverse	49.4	99.0	6.02

TD, time dial.

characteristic. The table shows that a margin of slightly in excess of 6 sec is required for the very inverse characteristic.

The above analysis included system impedance that reduced the initial motor voltage to 80% of rated. This representation takes advantage of the fact that motor voltage rises as the motor accelerates. Often as a matter of convenience acceleration calculation, assume constant voltage at the motor terminals.

Table 16.10 compares required time margins for the same motor with acceleration time calculated with fixed voltages of 100 and 80% at the motor terminals. A comparison of the 80% impedance-based and 80% fixed voltage cases demonstrates that the more rigorous impedance-based starting calculation reduced the required margin by 1.1 to 1.6 sec.

16.7.6.4 Disk Element Response to Cyclic Load

Disk element response to time-varying load is analyzed using the same point-by-point solution employed for the starting analysis. The only difference is that a time-varying load would typically include current excursions above and below the element's trip setting. Relay response in terms of relay *%_Trip* is again calculated from Equation (16.48) as above:

$$\%_Trip_{\mathrm{n}} = \frac{\Delta t * 100}{t_{\mathrm{relay}}(\overline{\mathrm{M}})} + \%_Trip_{n-1} \tag{16.48}$$

but:

For $M > 1$, $t_{\mathrm{relay}}(M) = t_{\mathrm{trip}}(M)$ is calculated from Equation (16.49)
For $M < 1$, $t_{\mathrm{relay}}(M) = t_{\mathrm{reset}}(M)$ is calculated from Equation (16.50) and represents a negative *%_Trip*.

TABLE 16.10
Disk Element Starting Margins with Fixed Terminal Voltage

Characteristic	Fixed Voltage	TD	%Trip	Minimum Margin to Start Current
Inverse	100%	41.6	99.7	2.24
	80%	62.5	99.7	4.47
Very inverse	100%	47.8	99.8	3.47
	80%	59.0	99.7	6.83
Extremely inverse	100%	44.7	99.8	4.11
	80%	50.0	99.7	7.66

© 2006 by Taylor & Francis Group, LLC

This methodology is applicable to any load profile, but provides no insight into a disk element's protection shortfall with respect to cyclic loads.

With overloads of constant magnitude, there is a direct relationship between relay characteristics and motor heating, but when time-varying loads are involved, this direct relationship is lost. Motor heating is now directly proportional to the square of the equivalent RMS current calculated over the load cycle, while disk element response to a time-varying load is influenced by load cycle shape.

Consider the simple load cycle shown in Figure 16.34. During the overload portion of the load cycle, disk motion is in the trip direction and in the reset direction during the light load portion. The disk element is on the verge of operation when overload current, light load current, overload duration and light load duration are such that disk rotation in both the operate and reset modes are equal.

Disk rotation is found from the relay timing equations:

$$t_{\text{trip}} = \left(\frac{A}{M_{\text{OL}}^{p} - 1} + B\right)\frac{TD}{5} \quad A = K_0\ \theta_{\text{trip}}$$

$$t_{\text{reset}} = \left(\frac{t_{\text{r}}}{M_{\text{Rst}}^{2} - 1}\right)\frac{TD}{5} \quad t_{\text{r}} = Kr\ \theta_{\text{reset}}$$

Substituting the load cycle times and currents and solving for disk travel in both the trip and reset modes,

$$\theta_{\text{trip}} = \frac{1}{K_0}\left(\frac{5 * t_{\text{OL}}}{TD} - B\right)(M_{\text{OL}}^{p} - 1)$$

$$\theta_{\text{reset}} = \frac{1}{K_{\text{r}}}(M_{\text{Rst}}^{2} - 1) * t_{\text{Rst}}\frac{5}{TD}$$

where t_{OL} = duration of the overload portion of the load cycle, t_{Rst} = duration of the light load portion of the load cycle, M_{OL} = multiple of trip current during overload portion of the load cycle, and M_{Rst} = multiple of trip current during light load portion of the load cycle. If disk travel to trip is set to unity ($\theta = 1.0$) it is apparent that $k_0 = A$ as $k_{\text{r}} = t_{\text{r}}$.

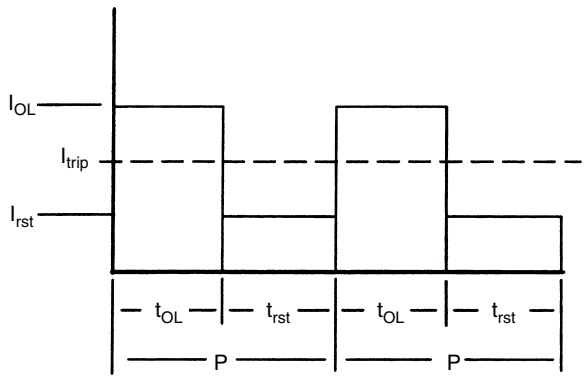


FIGURE 16.34 Load cycle for relay evaluation.

© 2006 by Taylor & Francis Group, LLC

Defining the trip and reset times in terms of the period of the load cycle

$$t_{OL} = x * P \tag{16.51}$$

$$t_{Rst} = (1 - x) * P \tag{16.52}$$

where P = duration of the load cycle and, x = portion of the load cycle in overload. Setting trip and reset rotation equal

$$\frac{1}{A}\left(\frac{5xP}{TD} - B\right)(M_{OL}^{p} - 1) = \frac{1}{t_r}(M_{Rst}^{2} - 1) * (1 - x) * P\,\frac{5}{TD}$$

Defining D as the ratio of the load period to time dial setting

$$D = P/TD \tag{16.53}$$

Solving for the minimum value overload current (M_{OL}) necessary to operate the relay for a given value of light load current M_{Rst}:

$$K = 1 - \frac{5 * A(1 - x)D(M_{Rst}^{2} - 1)}{t_r(5xD - B)} \tag{16.54}$$

$$M_{OL} = e^{\ln(K)/p} \tag{16.55}$$

Figure 16.35 is plotted from Equation (16.54) and Equation (16.55) for a disk element with a very inverse-time characteristic as defined by the parameters from Table 16.7. The figure shows that the shorter the duration of the overload segment, the greater the overload current required to operate the relay. This is logical, because the shorter the "on" time, the larger the overload current required to cause disk travel to the trip position. Motor heating during the load cycle is directly related to the

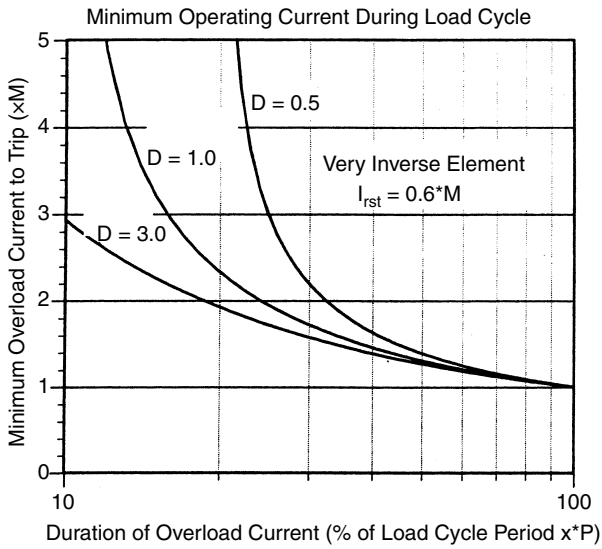


FIGURE 16.35 Cyclic overload current for very inverse relay.

© 2006 by Taylor & Francis Group, LLC

equivalent RMS current over the load cycle. The RMS current defined for the two-segment load cycle is:

$$I_{\text{RMS}} = \sqrt{\frac{I_{\text{OL}}^2\, t_{\text{OL}} + I_{\text{Rst}}^2 t_{\text{Rst}}}{t_{\text{OL}} + t_{\text{Rst}}}}$$

which, from Equations (16.51) and (16.52), can be rewritten as

$$I_{\text{RMS}} = \sqrt{\frac{I_{\text{OL}}^2\, xP + I_{\text{Rst}}^2 (1-x)P}{P}}$$

which resolves to

$$I_{\text{RMS}} = \sqrt{I_{\text{OL}}^2\, x + I_{\text{Rst}}^2 (1-x)} \tag{16.56}$$

In terms of relay pickup currents

$$I_{\text{RMS}} = \sqrt{(I_{\text{p}} M_{\text{OL}})^2 x + (I_{\text{P}} M_{\text{Rst}})^2 (1-x)}$$

and with relay pickup equal to 1.0 pu

$$I_{\text{RMS}} = \sqrt{M_{\text{OL}}^2 x + M_{\text{Rst}}^2 (1-x)}$$

Substituting Equation (16.55) into RMS current Equation (16.56) yields the relay minimum trip current in terms of load cycle RMS (heating) current. Figure 16.36 through Figure 16.38 plot the variation of RMS trip current against overload duration (x) for inverse, very inverse and extremely inverse disk elements.

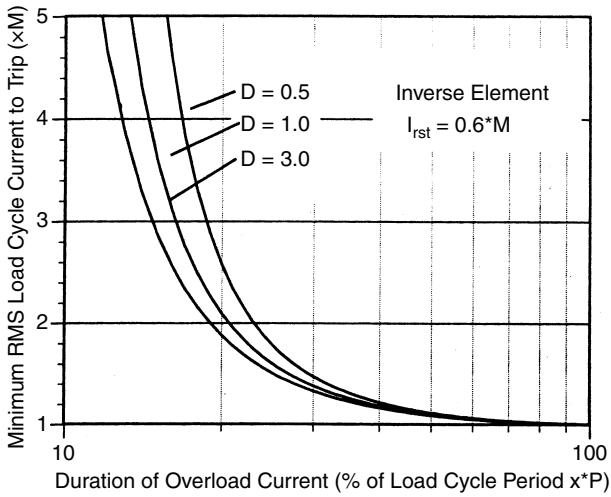


FIGURE 16.36 Inverse-time element RMS response.

© 2006 by Taylor & Francis Group, LLC

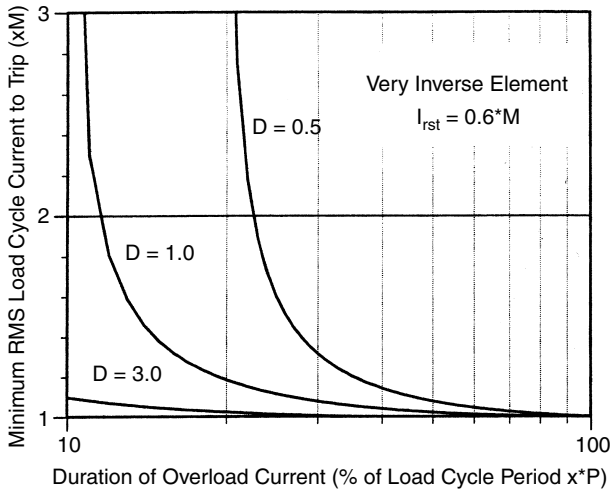


FIGURE 16.37 Very inverse time element RMS response.

All elements require RMS current in excess of their set point (1.0 per unit) to operate. This tendency to underprotect increases dramatically for the inverse and very inverse elements as the overload duration decreases. In the case of the inverse element, with overload duration below 15% of the load cycle, RMS current above 4 pu is necessary to actuate the element. The unity trip setting is intended to limit motor heating to a relative value of $1.0^2 = 1.0$. With 4.0 pu RMS current required to operate, heating will be 8.0 per unit (4.0^2 pu RMS), the intended value at the trip point.

16.7.7 Basic Thermal Element

The characteristic for a basic thermal overcurrent element is derived from an idealized thermal model in Figure 16.39. Power is applied to a mass (m) with specific heat (S). Heat dissipation is

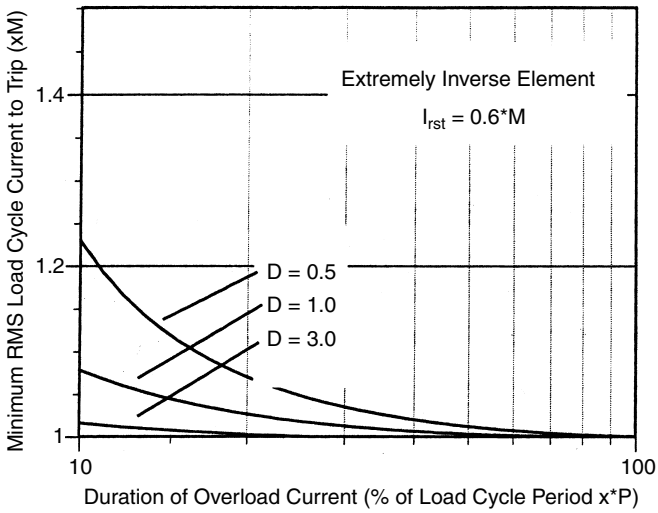


FIGURE 16.38 Extremely inverse time element RMS response.

© 2006 by Taylor & Francis Group, LLC

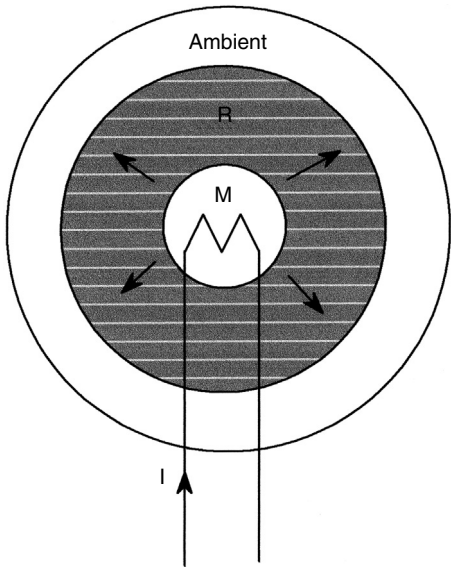


FIGURE 16.39 Simple thermal model.

restrained by thermal resistance (R). The rate of temperature change is proportional to power input minus losses:

$$Power\ input - Losses = S * m \frac{\mathrm{d}\theta}{\mathrm{d}t}$$

where $\mathrm{d}\theta =$ the change in temperature.

In the case of a motor, input power is in the form of I^2r losses dissipated in the rotor and stator. Heat is lost through transfer from motor internal components to ambient air[8]:

$$I^2r - \frac{(T - T_\mathrm{a})}{R_\mathrm{T}} = S * m * \frac{\mathrm{d}\theta}{\mathrm{d}t} \tag{16.57}$$

where $T - T_\mathrm{a} =$ temperature difference between heated motor component and ambient air, $R_\mathrm{T} =$ thermal resistance of material between internal motor component and ambient air, and $S * m =$ specific heat of heated motor component $\times$ mass of that component.

If temperature is defined as the rise above ambient temperature and $i * m$, which is constant for any given component, is defined as C_T the thermal capacitance, the thermal balance can be rewritten as

$$I^2r - \frac{T}{R_\mathrm{T}} = C_\mathrm{T} * \frac{\mathrm{d}\theta}{\mathrm{d}t} \tag{16.58}$$

Solving this first-order differential equation with constant current, temperature is given as

$$\theta = RI^2r(1 - e^{-t/R_\mathrm{T}C_\mathrm{T}}) \tag{16.59}$$

From this equation two things are apparent; first the term $R_\mathrm{T} * C_\mathrm{T}$ is the thermal time constant for the system and, secondly, for every value of current there exists a unique final operating temperature.

© 2006 by Taylor & Francis Group, LLC

If the motor initially operates at current I_0, until a thermal equilibrium is reached ($t = \infty$) the operating temperature of the motor will be

$$\theta_0 = RI_0^2 r$$

Rewriting Equation (16.59) to include the effects of initial operation at current I_0 prior to the application of overload current I, and expressing the resultant temperature in terms of an equivalent heating current.

$$I_\theta^2 = (I^2 - I_0^2)(1 - e^{-t/\tau_T}) + I_0^2 \tag{16.60}$$

The thermal element is set to actuate when the calculated equivalent temperature, now defined in terms of I_ϕ, equals a preset trip equivalent temperature $I_\theta = I_{\text{trip}}$. The value of I_{trip} is then equivalent to the minimum pickup current for the disk element. Solving for time, the resulting equation defines the time–current characteristic of a thermal overcurrent element as

$$t = \tau_T \ln\left(\frac{I^2 - I_0^2}{I^2 - I_{\text{trip}}^2}\right) \tag{16.61}$$

Note that the trip time is dependent on both the overload current (I) and the initial operating current I_0. This dependence on the initial operating current gives rise to the element's so-called "thermal memory." Figure 16.40 demonstrates the advantage of the thermal trip using the 600 HP motor from the starting calculation in Section 16.6.4. The thermal element is set assuming motor operation at full load. The ultimate trip current (I_{trip}) is set at 1.2 times full load current (94 A) and the thermal element time constant is chosen to coordinate with the "hot" thermal limit curve with I_0 equal to full load of 78 A.

This motor actually drives a fan load that is 60% of the motor rating. Therefore, motor initial running current is 47 A and the thermal limit curve would increase because of the reduced operating

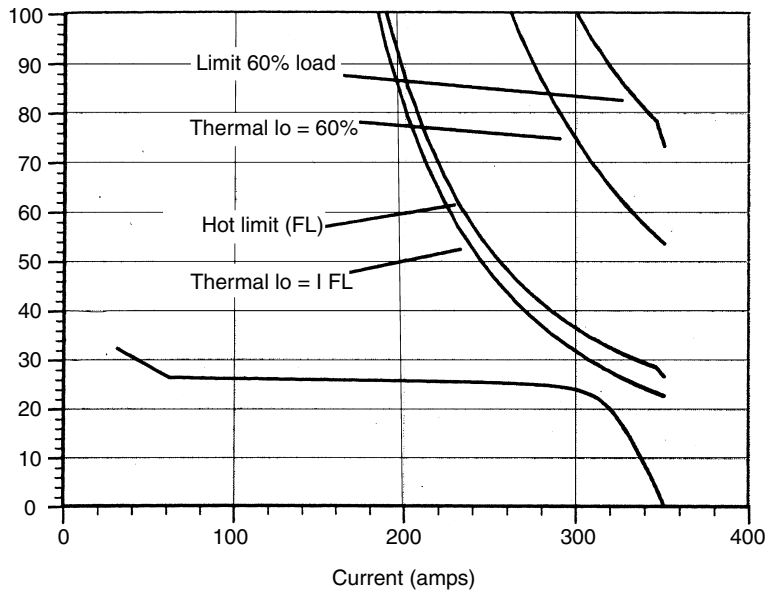


FIGURE 16.40 Thermal element response to initial load.

© 2006 by Taylor & Francis Group, LLC

temperature. The figure shows that at the reduced running current, the thermal element characteristic shifts upward to match the shift in the thermal limit curve at reduced load. The overall effect is that the relay shift allows utilization of more of the increased short time overload capability of the motor.

Equation (16.60) and Equation (16.61) do not precisely describe the response of electromechanical-based thermal elements that employ heaters. The ideal thermal model used to derive these equations defines temperature rise at the heat source with one heat transfer path to ambient air. In the relay, heat must be transferred from the heating element to a bimetallic contact or melting alloy. This transfer introduces a delay between a current excursion and thermal element response. The delay is most apparent as thermal overshoot, which may cause this type of relay to trip inappropriately after a successful start. The relay also has multiple heat transfer paths, which alter its response from that of the ideal model, particularly in the cooling mode.

With the development of electronic relays, it becomes possible to precisely implement the thermal algorithm. It might appear that such a thermal element would provide ideal motor protection for any driven load. In theory, a thermal element with a thermal time constant equal to that of the protected motor would "track" the rise and fall of motor temperature with constant or fluctuating load and during starting.

Unfortunately, this ideal match between the thermal element and motor is not possible because the simple model from which the thermal element was derived is inadequate to describe the complexities of motor heating. One basic problem is evident from the thermal limit curve, which includes three unique thermal characteristics: running overload, acceleration, and locked rotor. Each requires a unique thermal model. In the running overload portion of the limit curve, heat input to the motor is at a moderate rate and temperature rise is controlled by heat dissipation to neighboring components and ambient air. At locked rotor and initially during starting, heat input to the motor is very high and temperature rise is so rapid that heat transfer has little effect. During acceleration, a transitional model that includes the effects of cooling air flow and rotor resistance change with speed is required. In short, a single time constant thermal element cannot replicate motor behavior over the full range of overload.

The ideal thermal model used to develop the thermal element is most representative of the running overload portion of the limit curve in that both are dependent on heat transfer. However, even if the application of the thermal element is limited to the running overload portion of the limit curve, the relay cannot track motor temperature. The thermal element characteristic is derived for the idealized thermal system shown in Figure 16.39. This system has a single heat source and a single path for heat dissipation. It is represented by an algorithm with a single thermal time constant. A motor has multiple heat sources and multiple thermal conduction paths[9] as shown in Figure 16.41. The resulting motor thermal model requires multiple heating and cooling time constants to describe the thermal interactions between all structures within the motor. Each structure also exhibits a unique limiting temperature. The resulting expression for temperature rise of a given motor component would be in the form:

$$\theta_{sc} = \theta_F - k_1 e^{-t/\tau_1} - k_2 e^{-t/\tau_2} - k_3 e^{-t/\tau_3} - k_4 e^{-t/\tau_4} \tag{16.62}$$

Figure 16.42 is a comparison of the response of the single time constant model and a multitime constant motor model for a step increase in loading. It is apparent that the thermal element will tend to overestimate motor temperature. Generally, differences between the motor and thermal element cooling characteristics are even more pronounced than for the heating curve. In the cooling mode, the thermal elements tend to reset much faster than the protected motor cools. The overall result is that the thermal elements tend to overprotect during starting and when applied to fluctuating loads. This can result in incorrect tripping for either condition. The too rapid reset of a thermal element will allow premature restart of the motor, which will lead to damage when repeatedly restarted.

© 2006 by Taylor & Francis Group, LLC

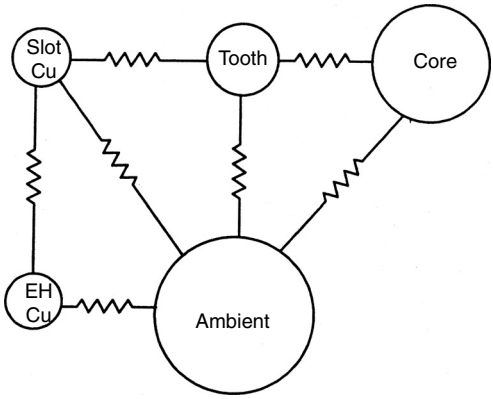


FIGURE 16.41 Motor thermal model. (From Boothman, D.R., Elgar, E.C., Rehder, R.H., and Wooddall, R.J. Thermal Tracking – A Rational Approach to Motor Protection, IEEE Transactions on Power Apparatus and Systems, July-August 1974, p. 1335. With permission.)

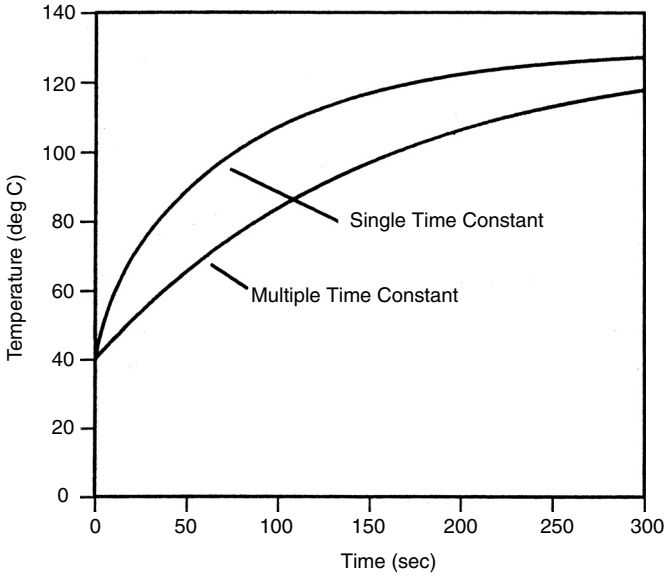


FIGURE 16.42 Thermal response of motor single and multitime constant (RTD). (From Boothman, D.R., Elgar, E.C., Rehder, R.H., and Wooddall, R.J. Thermal Tracking – A Rational Approach to Motor Protection, IEEE Transactions on Power Apparatus and Systems, July-August 1974, p. 1335. With permission.)

16.7.7.1 Dynamic Characteristic of the Thermal Element

The characteristic equation of a thermal element with time was previously derived and presented as Equation (16.60).

$$I_\theta^2 = (I^2 - I_0^2)(1 - e^{-t/\tau_T}) + I_0^2 \tag{16.60}$$

The I_θ^2 term is proportional to temperature. To apply a point slope solution, the equation is rewritten in incremental form:

$$I\theta_n^2 = m_n \Delta t + I\theta_{n-1}^2 \tag{16.63}$$

© 2006 by Taylor & Francis Group, LLC

Term m_n is the rate of change of I_θ^2 with time, which is the derivative of Equation (16.60) with respect to time:

$$m = \frac{d}{dt}\left[(I^2 - I_0^2)(1 - e^{-t/\tau_T}) + I_0^2\right]$$
$$= \frac{(I^2 - I_0^2)}{\tau_T} e^{-t/\tau_T}$$

With the inclusion of the slope, the incremental form becomes

$$I\theta_n^2 = \frac{(I_{n-1}^2 - I\theta_{n-1}^2)}{\tau_T} e^{-\Delta t/\tau_T} \Delta t + I\theta_{n-1}^2$$

If the numerical solution uses time steps that are small with respect to the time constant, the e term approaches unity and the equation reduces to

$$I\theta_n^2 = \frac{(I_{n-1}^2 - I\theta_{n-1}^2)}{\tau_T} \Delta t + I\theta_{n-1}^2 \tag{16.64}$$

which rendering the slope constant over small time intervals.

Because tripping occurs when $I_{\theta_n}^2 = I_{trip}^2$, trip element response can be expressed in terms of *%_Trip* by dividing both sides of Equation (16.64) by I_{trip}^2

$$\%Trip_n = \left(\frac{I_{n-1}^2 * 100}{I_{trip}^2} - \%Trip_{n-1}\right) \frac{\Delta t}{\tau_T} + \%Trip_{n-1} \tag{16.65}$$

Relay operation will occur when $\%Trip = 100$.

16.7.7.2 Thermal Element Response to Starting Current

The starting characteristic derived for a 600 HP motor in Section 16.6.4 is again used to evaluate relay response to the starting transient.

The dynamic response of the thermal element is calculated using Equation (16.65) and the starting current–time points derived in Section 16.6.4. The starting calculation assumes a start immediately after a stop with the motor initially operating at 47 A ($I_0 = 47$ A). The relay is set to trip at 1.2 times rated motor current ($1.2 \times 78 = 94$ A). The relay time constant was chosen to be the minimum value that would allow a start ($\tau = 402$). This value was chosen so that the minimum time margin between the thermal element characteristic and the starting current trace could be determined. Knowledge of the required margin may allow confirmation of the thermal element starting capability from time–current characteristic plots, directly eliminating the need for point-by-point dynamic calculation. For an actual setting calculation, a larger time constant would have been chosen to allow a safety margin.

The thermal memory of the element must be included in the calculation. Because the start is assumed to occur immediately after a stop, the relay will not reset and remains at the prestop trip state, which is

$$\%Trip_{t=0} = 100 * I_0^2/I_{trip}^2 = 100 * 47\,A^2/94\,A^2 = 25\%$$

© 2006 by Taylor & Francis Group, LLC

TABLE 16.11
Thermal Element Response to Starting Current

A Speed (pu)	B $t = \Sigma\Delta t$ (sec)	C I_{relay} (A)	D $100 * I_{rly}2/I_{trip}2$	E Δt (sec)	F (D−G) $\Delta t/\tau$	G[a] %Trip
0	0	351.27				25
			1396.45	0.1667	0.568	
0.005	0.167	351.07				25.57
			1394.86	0.1653	0.563	
0.01	0.332	350.87				26.13
			1393.03	0.1639	0.557	
0.015	0.496					26.69
0.980	25.62	160.12				99.76
			147.57	0.0667	0.0316	
0.985	25.687	129.57				99.79

[a] Equations 16.55.

Relay response is tabulated in Table 16.11. In the above case, terminal voltage is initially reduced to 80% by action of circuit impedance, but recovers as the motor accelerates. A comparison of the required starting margin for that case and starts of the same motor with 80 and 100% fixed voltage at the motor terminals during the start is presented in Table 16.12. These times are comparable with those of the extremely inverse disk element, which might be expected because the time–current characteristics for the two are very similar.

It is apparent that, although the thermal element operating principle differs from that of the disk element, the two elements respond to starting current in a similar manner.

16.7.7.3 Thermal Element Response to Cyclic Load

The responses of disk and thermal elements to time-varying current are quite different. A point-by-point application of Equation (16.65) could be used to analyze thermal element response to any time-varying current. To gain insight into the protective characteristic of the thermal element we will again evaluate the load cycle present in Figure 16.34.

As with the disk element analyses, it is assumed that the current in the first load cycle segment is above the relay setpoint (I_{trip}) and below the trip setting in the second segment. The virtual temperature of the relay (expressed in terms of I^2) will rise to I_h^2 at the end of the first load segment of the cycle and fall to I_L^2 at the end of the second segment.

TABLE 16.12
Thermal Element starting Margins with Fixed Terminal Voltage

Starting Condition	Minimum Margins	τ
100% voltage fixed	4.8 sec	377
80% voltage by impedance	6.02 sec	402
80% voltage fixed	8.4 sec	404

© 2006 by Taylor & Francis Group, LLC

In overload segment

$$I_h^2 = (I_{OL}^2 - I_L^2) * (1 - e^{-t_{OL}/\tau}) + I_L^2 \tag{16.66}$$

In light load segment

$$I_L^2 = (I_{Rst}^2 - I_h^2) * (1 - e^{-t_{Rst}/\tau}) + I_h^2 \tag{16.67}$$

In a trip situation, I_h^2 will ratchet up each load cycle until the trip temperature (I_{trip}^2) is reached. A trip initiation is dependent on the last load cycle prior to trip. In that load cycle

$$I_{trip}^2 = (I_{OL}^2 - I_L^2) * (1 - e^{-t_{OL}/\tau}) + I_L^2 \tag{16.68}$$

Setting I_h equal to I_{trip}, substituting Equation (16.67) into Equation (16.68) and solving for I_{OL} yields

$$I_{OL} = \sqrt{\frac{I_{trip}^2(1 - e^{-(t_{OL}+t_{Rst})/\tau}) - I_{Rst}^2(e^{-t_{OL}/\tau} - e^{-(t_{OL}+t_{Rst})/\tau})}{1 - e^{-t_{OL}/\tau}}} \tag{16.69}$$

Defining the load segment times in terms of the load segment period (P) and redefining D in terms of element time constant.

$$t_{OL} = x * P \qquad t_{Rst} = (1 - x) * P \qquad D = \frac{P}{\tau}$$

Substituting these into Equation (16.69)

$$I_{OL} = \sqrt{\frac{I_{trip}^2(1 - e^{-D}) - I_{Rst}^2(e^{-xD} - e^{-D})}{1 - e^{-xD}}} \tag{16.70}$$

The resulting expression yields the first segment overload current necessary to produce a relay operation for a given second segment light load current as a function of the load cycle period. Figure 16.43 plots this relationship with variation of the overload segment duration.

The parameter that is directly related to protection is the load cycle RMS equivalent current (heating current) required to initiate a thermal unit trip. This value is calculated from Equation (16.56) and plotted in Figure 16.44. The thermal element will actuate with RMS current below its trip setting. This tendency to overprotect increases as overload duration decreases and will lead to misoperation for load cycles within the capability of the motor. The thermal element response is in direct contrast to that of the disk element, which tends not to operate for load cycles that are damaging to the motor.

16.8 MULTIFUNCTION MICROPROCESSOR RELAYS

In recent years, microprocessor-based protection has become the standard for large motor protection. Microprocessor relays provide a complete complement of motor protection functions in one box. This includes fault and thermal protection. Some relays also provide control functions.

Because these relays are mathematically based, they are not constrained by the physical limitations of their electromechanical predecessors. This has allowed the development of many new and more sophisticated thermal protection algorithms. Microprocessor motor protection packages may

© 2006 by Taylor & Francis Group, LLC

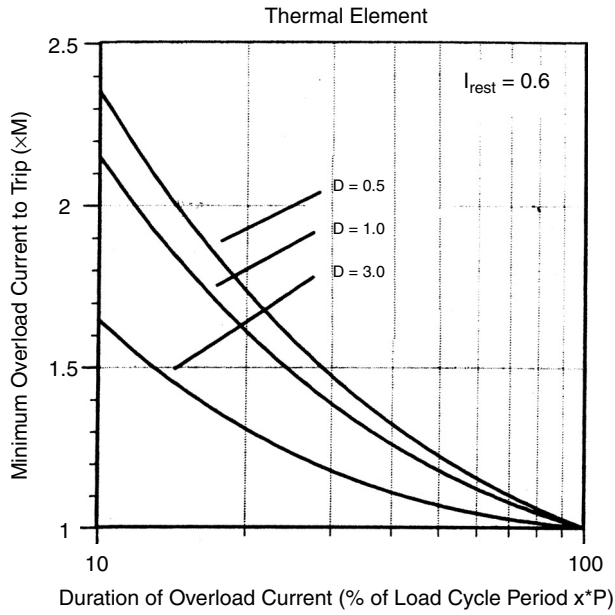


FIGURE 16.43 Cyclic overload current for thermal element.

include advanced thermal elements and/or algorithms that mimic traditional thermal and disk elements. The electronic versions of traditional elements are improved over the originals. Electronic reproductions of a disk element do not have mechanical overtravel, and electronic thermal elements allow settable thermal time constants and do not suffer from thermal overshot.

Microprocessor thermal models may including enhancements such as separate heating and cooling thermal time constants, heating caused by unbalanced current, real-time stator temperature

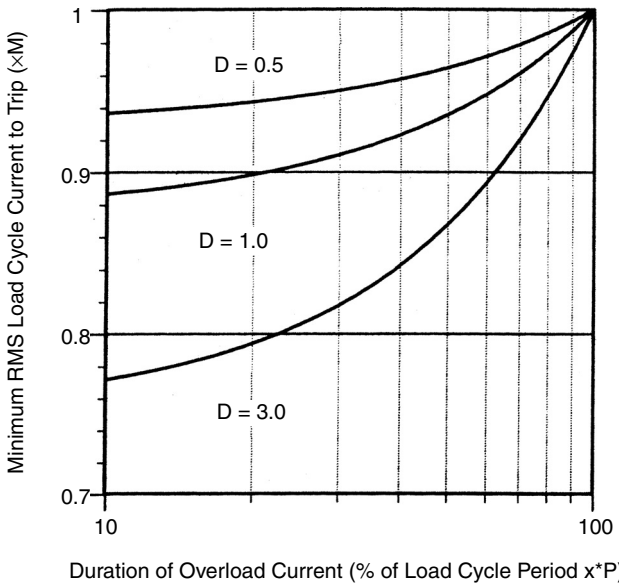


FIGURE 16.44 Thermal element RMS response.

© 2006 by Taylor & Francis Group, LLC

input to the relay via RTDs, to name a few. These advancements have significantly improved protection afforded to the motor. However, the basic thermal model used in microprocessor protection remains the ideal single time constant model, described in Figure 16.39.

Although current electronic technology will support the solution of multitime constant thermal models required for accurate dynamic temperature tracking, Equation (16.62), the data necessary to implement such models are not available. Consequently, microprocessor-based thermal algorithm are limited by and designed around available data.

It is not practical to discuss all variation of thermal protection implemented in myriad microprocessor relays on the market today, so two have been chosen. Although these schemes are derived as protection algorithms they are also useful tools for evaluating motor starting and load cycle capability.

16.8.1 Thermal Model Protection Scheme

The first protection scheme is an adaptation of the traditional thermal element.[10,11] It uses locked rotor data to define the motor thermal limit and the parameters to implement two thermal models. One model is applicable for light to moderate overload and the other for severe overloads. The scheme switches to the severe overload model when current exceeds 2.5 times full-load current. Both models are derived from the ideal thermal system depicted in Figure 16.39 and quantified by Equation (16.58).

In this treatment of the thermal model, rotor resistance R_r is a variable with slip. If input current (I) is to be expressed as a multiple of rated load current, the resulting input power must also reference input power at rated load. This is accomplished by dividing input power by R_0 (rotor resistance at rated load). The resulting expression is given below.

$$\frac{I^2 R_r}{R_0} - \frac{\theta}{R_T} = C_T * \frac{d\theta}{dt} \tag{16.71}$$

During light and moderate overload conditions, heat input to the motor is moderate and temperature rise is limited by heat dissipation to neighboring components and ambient air as determined by the θ/R_T term.

Temperature variation is derived from the same point-slope methodology used in the dynamic evaluation of disk and traditional thermal elements. The rate of temperature change for a given thermal input (I^2r) is derived from the incremental form of Equation (16.71) above:

$$\frac{\Delta\theta}{\Delta t} = \frac{I^2 R_r}{C_T R_0} - \frac{\theta_0}{R_T C_T} \tag{16.72}$$

and temperature is calculated as the initial temperature plus the incremental change:

$$\theta_n = \left[\frac{I_{n-1}^2 R_{r_{n-1}}}{C_T R_0} - \frac{\theta_{n-1}}{R_T C_T}\right]\Delta t + \theta_{n-1}$$

During severe overload conditions such as a locked rotor, the rate of energy input to the system is much greater than the system's ability to dissipate the resulting heat. In terms of Equation (16.71), the θ/R_T term becomes negligible with respect to the I^2R_r term, reducing the thermal balance equation to:

$$\frac{I^2 R_r}{R_0} = C_T * \frac{d\theta}{dt} \tag{16.73}$$

© 2006 by Taylor & Francis Group, LLC

Temperature for severe overload in incremental form becomes:

$$\theta_n = \frac{I_{n-1}^2 R_{r_{n-1}}}{C_T R_0} \Delta t + \theta_{n-1} \tag{16.74}$$

where θ_n = temperature at end of interval n, θ_{n-1} = temperature at beginning of interval n, R_{r_n} = rotor resistance at time interval n as calculated from Equation (16.16), C_T = thermal capacitance, R_0 = rotor resistance at rated speed, and I_{heat} = current at time interval n.

16.8.1.1 Derivation of Model Parameters

To implement these models, the equivalent thermal capacitance (C_T) and thermal resistance (R_T) must be determined. A conservative value for C_T is found by neglecting heat transfer and solving Euation (16.73) for temperature rise:

$$\begin{aligned} \theta &= \frac{R_r/R_0}{C_T} I^2 \int_0^t dt \\ &= \frac{R_r/R_0}{C_T} I^2 t \end{aligned} \tag{16.75}$$

Motor data typically include locked rotor current and safe stall times t_a and t_{op}, which represent the times required for the motor to reach limiting temperature with the motor initially at ambient temperature (cold) and with the motor at rated-load operating temperature (hot), respectively. With heat loss neglected, temperature can be expressed in terms of I_2t; thus, the locked rotor data become indicative of motor temperature limitations.

With no initial load "cold," the limiting temperature would equal $\theta_{Lim} = \theta_{LR_Rise} + \theta_{Ambient}$. If the limiting temperature were defined in terms of rise above ambient and expressed in terms of I_2t, the limiting temperature becomes:

$$\theta_{Lim} = I_{LR}^2 t_a \tag{16.76}$$

Substituting into Equation (16.75) and solving for CT,

$$\theta_{Lim} = I_{LR}^2 t_a = \frac{R_r}{C_T R_0} I_{LR}^2 t_a$$

and

$$C_T = \frac{R_r}{R_0} \tag{16.77}$$

If speed variant rotor resist is considered, CT becomes

$$C_{T_n} = \frac{R_{r_n}}{R_0} \tag{16.78}$$

© 2006 by Taylor & Francis Group, LLC

R_T is used in the light to moderate overload model and is defined in terms of operating temperature at rated load as follows. The formal solution to Equation (16.71) is

$$\theta = R_T I^2 \frac{R_r}{R_0} + \left(\theta_0 - R_T I^2 \frac{R_r}{R_0}\right) e^{-t/R_t C_T} \tag{16.79}$$

If the motor is assumed to run continuously at rated load, the motor will be at normal operating temperature, $\theta = \theta_{Rise_FL}$. Substituting rated load conditions ($t = \infty$, $I =$ 1 pu, and $R_r = R_0$) into Equation (16.78), the equation reduces to

$$R_T = \theta_{Rise_FL} \tag{16.80}$$

Operating temperature at rated load is also derived from the safe stall data and Equation (16.76). The safe stall limit from full load temperature is

$$\theta_{Lim} = \theta_{Rise_LR} + \theta_{Rise_FL} = I_{LR}^2 t_a$$

or

$$I_{LR}^2 t_a = I_{LR}^2 t_{op} + \theta_{Rise_FL}$$
$$\theta_{Rise_FL} = I_{LR}^2 (t_a - t_{op})$$

and from Equation (16.80)

$$R_T = \theta_{Rise_FL} = I_{LR}^2 (t_a - t_{op}) \tag{16.81}$$

Most microprocessor elements express temperature in terms of percent of thermal capacity used. This is equal to percent of limiting temperature ($I_{LR}^2\ t_a$). With this modification, the thermal equations are as follows.

For light to moderate overload $I < 2.5 \times I_{LR}$:

$$\%TC_n = \left[\frac{I_{n-1}^2 * 100}{I_{LR}^2 t_a} - \frac{\%TC_{n-1} R_0}{R_T R_{r_{n-1}}}\right] \Delta t + \%TC_{n-1} \tag{16.82}$$

where

$$R_T = I_{LR}^2 (t_a - t_{op})$$

For severe overload $I \geq 2.5 \times I_{LR}$

$$\%TC_n = I_{n-1}^2 \frac{\Delta t}{I_{LR}^2 t_a} 100 + \%TC_{n-1} \tag{16.83}$$

If the motor is initially unloaded, the initial thermal state of the motor is $\%\ TC_0 = 0$. If the motor is operating under load prior to the overload, the initial condition can be found from Equation (16.82).

© 2006 by Taylor & Francis Group, LLC

The model reaches steady state %TC when

$$0 = \frac{I_{n-1}^2 * 100}{I_{LR}^2\, t_a} - \frac{\%TC_{n-1}\, R_0}{R_T R_{r_{n-1}}}$$

Near rated speed, $R_r = R_0$ and the steady-state thermal capacity at I_0 reduces to

$$\%TC_0 = \frac{R_T I_0^2}{I_{LR}^2\, t_a} 100 = \frac{(t_a - t_{op})}{t_a} * I_0^2 \tag{16.84}$$

As a side note, many texts reference the thermal capacity used at rated load in terms of the "hot to cold ratio," which is the safe stall time at rated load divided by the safe stall time at no load, t_{op}/t_a. From the above equation, the thermal capacity used at rated load ($I_0 = 1$) can be expressed in terms of the hot/cold ratio:

$$\%TC_0 = \frac{(t_a - t_{op})}{t_a} 100 = \left(1 - \frac{t_{op}}{t_a}\right) * 100 \tag{16.85}$$

16.8.1.2 Scheme Application Example

Data needed to applying this scheme to the 600 HP motor used in the starting analysis are given in Section 16.6.4.

The following data would be required for the 600 HP motor:

t_a (cold) = 20 sec
t_{op}(hot) = 17 sec
$I_{LR} = 5.63 \times I_{FL}$

$$R_T = I_{LR}^2(t_a - t_{op}) = 5.63^2(20 - 17) = 95.0$$

Calculated data from Section 16.6.3:

$R_0 = 0.008$
$R_{LR} = 0.0284$

Rotor resistance variation with slip is defined by Equation (16.16)

$$\begin{aligned} R_{r_n} &= (R_{r_{LR}} - R_{r_{NL}})s_n + R_{r_{NL}} \\ &= 0.0204 * s + 0.008 \end{aligned}$$

Assuming that the motor is operating at rated load, the initial %TC used is taken from Equation (16.84)

$$\%TC_0 = \left(1 - \frac{t_{op}}{t_a}\right) * 100 = \left(1 - \frac{17}{20}\right) * 100 = 15\%$$

© 2006 by Taylor & Francis Group, LLC

TABLE 16.13
Thermal Capability Used: $I > 2.5 \times FL$

A Speed (pu)	B Δt (sec)	C $t = \Sigma\Delta t$ (sec)	D I_{mot} (pu)	E $100 * \Delta t * D^2/633.9$	F $\Delta Trip\%$	G $\%Trip$
0		0	4.504			15
	0.1919			0.614	0.614	
0.005		0.192	4.501			15.61
	0.190			0.607	0.607	
0.01		0.382	4.498			16.22
	0.1882			0.600	0.600	
0.015		0.570	4.495			16.82

Applying these values to Equation (16.82) and Equation (16.83) for light to moderate overload $I < 2.5 \times I_{LR}$

$$\%TC_n = \left[\frac{\overline{I_n}^2 100}{633.9} - \frac{0.008\ \%TC_{n-1}}{95R_{r_n}}\right]\Delta t + \%TC_{n-1}$$

For severe overload, $I \geq 2.5 \times I_{LR}$

$$\%TC_n = \overline{I_n}^2 \frac{\Delta t}{633.9} 100 + \%TC_{n-1}$$

Samples of the point-by-point calculations are shown in Table 16.13 and Table 16.14.

The motor reaches 87.29% of its thermal capability during the above start. Circuit impedance limits the initial starting voltage for the above start to 80%. Voltage improves as the motor accelerates.

Rotor heating increases as the margin between load and motor torque curves is reduced by the reduced starting voltage, Equation (16.34). Table 16.15 compares thermal capacity used for a start of the same motor as above with several values of constant voltage at the motor terminals.

16.8.2 Thermal Limit Based Protection Scheme

An alternative overload protection scheme uses a replica of the thermal limit curve to define motor capability. This curve is configured in the relay using various overcurrent elements to match the

TABLE 16.14
Thermal Capability Used, $I < 2.5 \times FL$

A Speed (pu)	B Δt (sec)	C $t = \Sigma\Delta t$ (sec)	D I_{mot} (pu)	E R_r	F $D^2 * 100/633.9$	G $0.0128I/95R_r$	H $(F - G) * \Delta t$	I $\%Trip$
0.960		25.62	2.415	0.01323				87.291
	0.061				0.920	0.889	0.00189	
0.965		25.681	2.223	0.01315				87.293
	0.067				0.779	0.894	−0.0077	
0.970		25.748	2.002	0.01307				87.285

© 2006 by Taylor & Francis Group, LLC

TABLE 16.15
Thermal Capacity Variation with Constant Starting Voltage

Starting Voltage	% Thermal Capacity Used
100%	81.7
80%	88.1
75%	90.9

motor limit curve or by inputting points from the limit curve in a data table. Each point on the stored limit curve would presumably represents the time necessary for a component to reach maximum design temperature (100% thermal capacity). Because motor limit curve is plotted for fixed current values, it cannot be directly compared to fluctuation load or transient starting current; again, an incremental analysis is required.

If heat loss is neglected motor temperature rise is maximized and can be expressed in terms of I^2t as per Equation (16.74).

$$\theta_{\mathrm{n}} = KI_{\mathrm{n}-1}^2 Rr_n \Delta t + \theta_{\mathrm{n}-1}$$

The temperature limit at any given current can be expressed in terms of $I_{\mathrm{n}}^2\, t_{\mathrm{Lim}_n}$, where t_{Lim_n} is the maximum safe operating time at current I_n, with both points taken from the thermal limit curve.

$$\theta_{\mathrm{Lim_n}} = KI_n^2 Rr_n t_{\mathrm{Lim}_n}$$

The percent thermal limit used by the motor at the end of each time interval is then calculated as:

$$\begin{aligned} \%TC_{\mathrm{OL}_n} &= \frac{\theta_{n-1}}{\theta_{\mathrm{Lim}_{n-1}}} 100 + \%TL_{n-1} \\ &= \frac{\Delta t}{t_{\mathrm{Lim}}(\overline{I_{n-1}^2})} 100 + \%TL_{n-1} \end{aligned} \tag{16.86}$$

where $\overline{I_{n-1}}$ represents the average current over the time interval. Note that this representation is identical to that used to evaluate a disk element.

Equation (16.86) is only applicable for currents represented on the thermal limit curve (overload conditions). When current drops below rated, cooling is dependent on the applicable motor cooling time constant. During the cooling period, thermal capacity used would vary as defined by:

$$\%TC = (\%TC_{\mathrm{start}} - \%TC_{\mathrm{final}}) e^{\frac{-t}{\tau_{\mathrm{cool}}}} + \%TC_{\mathrm{final}} \tag{16.87}$$

where $\%TC$ = thermal capacity used at time t, $\%TC_{\mathrm{start}}$ = thermal capacity at the beginning of the cooling interval, $\%TC_{\mathrm{final}}$ = steady-state thermal capacity used with continuous operation at

© 2006 by Taylor & Francis Group, LLC

current I. The thermal capacity used with steady-state operation at current I can be estimated from the hot/cold ratio as

$$\%TC_{\text{final}} = I^2 * \left(1 - \frac{t_{\text{op}}}{t_{\text{a}}}\right) * 100 \tag{16.88}$$

Converting to incremental form in the same manner used for Equation (16.64), Equation (16.87) becomes

$$\%TC_n = -\frac{(\%TC_{n-1} - \%TC_{\text{final}_{n-1}})}{\tau_{\text{cool}}}\Delta t + \%TC_{n-1} \tag{16.89}$$

Thermal cooling constants applied to Equation (16.89) will differ significantly for a running motor and a stopped motor; typical values are 15 minutes running and 225 minutes stopped. Specific values should be obtained from the motor manufacturer, but this is not always possible. In some cases, thermal time constants may be gleaned from starting limitations imposed on the motor. For instance, assume a motor is allowed only two consecutive starts cold. After two failed starts, a 120 minute delay is required before another start can be attempted.

If two consecutive starts are allowed, each start would consume 50% of the thermal capacity and 120 minutes are required to cool to allow another start. From Equation (16.85)

$$50\% = (100\% - 0\%)e^{\frac{-120}{\tau_{\text{stop}}}} + 0\%$$

Solving for τ_{stop}

$$\tau_{\text{stop}} = -\frac{120}{\ln(50/100)} = 173 \text{ min}$$

If the same motor is allow two consecutive starts and then a minimum run of 15 minutes before another start, the running cooling time constant would be estimated as follows:

$$100\% = (50\% + 50\%)e^{\frac{-15}{\tau_{\text{run}}}} + 50\%$$

$$\tau_{\text{run}} = \frac{15}{\ln(50/100)} = 22 \text{ min}$$

16.8.2.1 Application of Thermal Limit Based Scheme

To apply this algorithm, it is necessary to establish a mathematical model for the thermal damage curve. The limit may be presented as one continuous curve or running overload and acceleration limits may be shown separately (Figure 16.30). The running overload portions of the limit curve for the 600 HP motor can be closely approximated using the disk element model. This is not always the case.

Parameters for the disk equation can be found using a Mathcad curve fit algorithm as follows. The disk characteristic equation is

$$t_{\text{trip}} = \left(\frac{A}{M^p - 1} + B\right)$$

© 2006 by Taylor & Francis Group, LLC

Data points from the running overload portion of the limit curve are input to matrix Data_Hot. The Mathcad function "genfit" uses the derivative of each unknown A, b, D with respect to time fit the curve. These are input via function F(x,b).

Running overload limit data

Column 1 = current (xFL)
Column 2 = time (sec)

$$\text{Data 2:} \begin{pmatrix} 2 & 167 \\ 3.0 & 60 \\ 3.5 & 44 \\ 4.25 & 30 \\ 5.35 & 22 \end{pmatrix}$$

Derivatives

$$\text{Vx} := \text{Data 2}^{\langle 0 \rangle}$$
$$\text{Vy} := \text{Data 2}^{\langle 1 \rangle}$$
$$\text{V}_g = \begin{pmatrix} 200 \\ 2 \\ 100 \end{pmatrix}$$

$$\text{F}(x, a) := \begin{bmatrix} \dfrac{a_0}{x^{a_1} - 1} + a_2 \\ \dfrac{1}{(x^{a_1} - 1)} \\ \dfrac{-a_0}{(x^{a_1} - 1)^2} \cdot X^{a_1} \cdot \ln(x) \\ 1 \end{bmatrix}$$

$$\text{P} := \text{genfit (Vx, Vy, Vg, F)}$$

$$\text{t(I)} := \frac{P_0}{I^{P_1} - 1} + P_2 \qquad \text{P} = \begin{pmatrix} 752.161 \\ 2.542 \\ 11.037 \end{pmatrix}$$

The resulting approximation of the overload portion of the curve is then:

$$t_{\text{OL}_{\text{limit}}} = \left(\frac{752.16}{M^{2.542} - 1} + 11.037 \right) \tag{16.90}$$

The acceleration limit is voltage-dependent as described in Section16.7.1. The following mathematical treatment of this dependence assumes the accelerating limit is represented as shown in Figure 16.32, linear on log-log plot with different voltage-specific limits parallel.

The fact that the limit plots as a straight line on the log-log plot indicates the limit is of the form:

$$t = \frac{C_r}{I^m} \tag{16.91}$$

Referring to Figure 16.32, at 100% voltage the acceleration limit curve extends from the safe stall point (I_{LR}, t_{LR}) to point (I_x,t_x). From these points, the value of exponent m is derived.

Because each point lies on the limit curve each must satisfy:

$$C_r = I^m t$$

Rewriting and subtracting

$$\begin{aligned} \log(C_r) &= m \log(I_{LR}) + \log(t_{LR}) \\ \log(C_r) &= m \log(I_x) + \log(t_x) \\ \hline 0 &= m[\log(I_{LR}) - \log(I_x)] + \log(t_{LR}) - \log(t_x) \end{aligned}$$

© 2006 by Taylor & Francis Group, LLC

Subtracting and solving for m yields

$$m = \frac{\log(t_x/t_{LR})}{\log(I_{LR}/I_x)} \tag{16.92}$$

The parallel variations of the acceleration limit curve are generated by different values for constant C. At 100% voltage the acceleration limit curve passes through points (I_{LR}, t_{LR}) thus, $C_{100\%}$ is then:

$$C_{100\%} = I_{LR}^m t_{LR}$$

At voltages other than 100% the value of C can be derived from the fact that the acceleration limit curve must cross the I^2t locked rotor limit as shown in the Figure 16.32. Locked rotor current is directly proportional to the voltage variation. At reduced terminal voltage V_r (in per unit of rated motor voltage) the safe stall time becomes

$$t_r = \frac{I_{LR}^2 t_{LR}}{(I_{LR} V_r)^2} = \frac{t_{LR}}{V_r^2}$$

Solving for C at reduced voltage:

$$\begin{aligned} C_r &= I_r^m t_r \\ &= (I_{LR} V_r)^m * \frac{t_{LR}}{V_r^2} = I_{LR}^m t_{LR} V_r^{m-2} \end{aligned} \tag{16.93}$$

Applying this to the 600 HP motor data where:

$$\begin{aligned} I_{LR} &= 5.63 \\ t_{LR}(\text{hot}) &= 17 \text{ sec} \\ I_x &= 5.35 x I_{FL} \\ t_x &= 22 \text{ sec} \end{aligned}$$

from Equation (16.92) $m = 5.05$ and the acceleration limit for the 600 HP motor expressed as a function of voltage becomes:

$$C_r = I_{LR}^{5.05} t_{LR} V_r^{5.05-2} \tag{16.94}$$

Using overload and acceleration limits derived above, Equation (16.90), Equation (16.91), and Equation (16.94), the thermal capacity used during the start was 83%. This computation was conservative in that it used the hot limit curve even though the motor was not running at rated load prior to the start. The evaluation also assumed an acceleration limit at 80% voltage throughout the start, recognizing that voltage actually recovers during the transient.

One would expect that similar results would be obtained using the cold limit and adding the thermal capacity used by initial operation at rated load. This is not the case and said alternate analysis yielded 75% thermal capacity usage during the start. The discrepancy accentuates the fact that published thermal limit curves are born out of a mixture of theory and judgment.

© 2006 by Taylor & Francis Group, LLC

16.8.3 Unbalanced Current Protection

Phase current unbalance can significantly increase heating in the rotor. This topic is covered in Section 16.13. For now it is sufficient to say that motor current can be resolved into several components. A motor operating with equal magnitude phase currents each displaced by 120°, is operating with only a positive-sequence component. Phase current unbalance, either in magnitude or phase displacement, generates a negative-sequence component of current. Most microprocessor relays include the heating effect of this component into the thermal models developed in Section 16.8.1 and 16.8.2. This is accomplished by replacing heat in the I^2R_r term:

$$(I^2_{\text{pos}_n} + kI^2_{\text{neg}_n})R_{\text{pos}_n}$$

The k term is the ratio of negative- to positive-sequence rotor resistance. This value is typically 3 to 5.

16.9 SPECIAL SCHEMES FOR DIFFICULT STARTS

Most motors start quickly. Start times do not approach the safe stall time at locked rotor. Consequently, an overcurrent element can be set between the thermal limit curve and the starting current trace with sufficient margin on either side to assure starting and provide protection over the full range of motor operation.

Motors driving high-inertial loads, such on induced or forced draft fans, present application problems for both disk and thermal elements. Starting times increase as rotating inertia increases and starting voltage decreases. Motor heating also increases with increased starting time. In sever cases, start times will exceed the locked rotor time and it is not possible to properly position an overcurrent characteristic above the starting current trace with sufficient margin to permit starting while remaining completely below the thermal limit curve as is required for protection (Figure 16.45).

Microprocessor-based protection is less likely to experience nuisance tripping because this overload protection is based on the thermal capacity of the protected motor. In theory, operation of such a scheme would imply the start was outside the motor capability. Note that the thermal

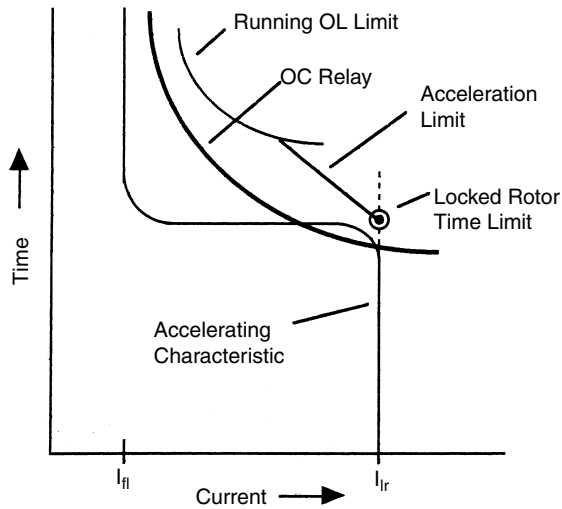


FIGURE 16.45 Hard start.

© 2006 by Taylor & Francis Group, LLC

model scheme described in Section 16.8.1 is conservative in its estimate of capacity and may be prone to misoperation for starts very close to motor capacity.

For disk or thermal overcurrent elements, there are two basic special schemes used for these problems installations. One scheme employs two overcurrent elements, one with an inverse characteristic covering the overload portion of the limit curve and a very inverse or extremely inverse element covering the acceleration and locked rotor portion. The advantage here is that the combined overcurrent characteristic will more closely match the contour of the limit curve, thus reducing the areas of overprotection that result when applying a single element.

The inverse element would be set as typical overcurrent protection, 115 to 125% rated motor current, while the second element would be set at about half the locked rotor current. A plot of the dual overcurrent schemes is shown in Figure 16.46. This scheme optimizes the starting capacity of the overcurrent protection, but will not override all problematic starts.

The second scheme retains the single overcurrent element, but this element is intended only to provide protection should the motor fail to start, that is, the rotor fails to turn. The overcurrent element is blocked after rotation is confirmed, but before the element can initiate a false trip. In the most basic application of this scheme, the overcurrent element would be removed from service by a speed switch set at about 20% rated speed. This implementation will not provide protection should the motor begin rotation, but fail to accelerate to rated speed. Such a stall will occur should the motor and load torque curves intersect at a point other than rated speed. This would result from mechanical failures that increase load torque or motor malfunctions or low voltage that reduce motor torque.

Limited stall protection can be provided if blocking can be deferred until motor speed has surpassed the point of minimum separation between motor and load torque curves. The location of this point of minimum accelerating torque is dependent on the shape of the two curves, but can be within 20% of rated speed. In such cases, blocking may occur to late to avoid the false trip and limited stall protection is not obtainable.

An alternative to a speed switch blocking would be an instantaneous overcurrent element or an impedance relay. In the course of a successful acceleration, motor current will decrease from a locked rotor value to a running value. This change is predictable with speed and can be used to block the trip element.

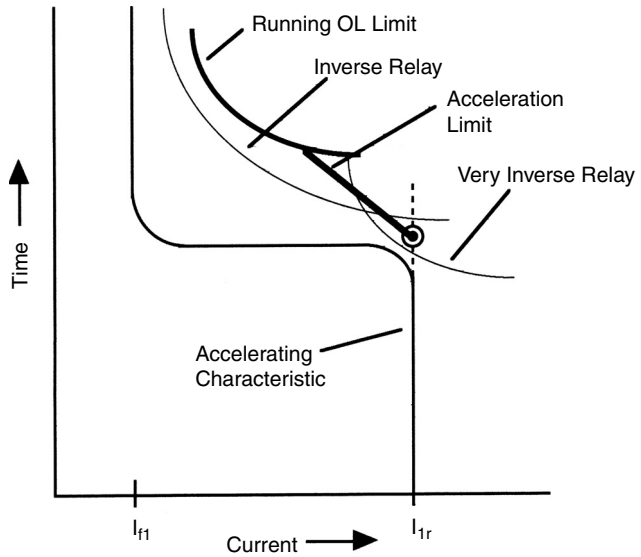


FIGURE 16.46 Dual overcurrent protection.

© 2006 by Taylor & Francis Group, LLC

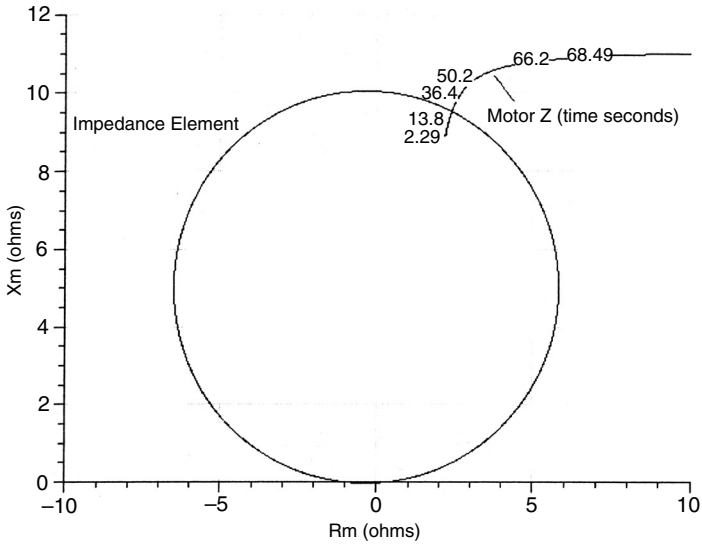


FIGURE 16.47 Impedance element.

When an instantaneous element is used, it must be of a "high dropout" design, meaning that the current at which the relay will drop out is no less than 95% of the current required to actuate the relay. This is necessary to ensure that the relay will quickly reset at the desired current level.

If a large motor is started under varying system conditions, an instantaneous blocking relay may be difficult to set, because starting currents will vary with system configuration. Motor impedance is less influenced by these variations. An impedance relay looking into the motor can also initiate blocking. The relay would be set to actuate upon starting and reset as impedance increases with speed. Figure 16.47 illustrates a typical impedance trajectory during starting. The motor shown displays increased R and X with increased speed; some motors exhibit nearly constant X with increasing R.

Although impedance–speed profiles can be calculated from standard motor data sheets, field tests are usually required to confirm impedance relay settings. Dynamic interaction between the drive motor and the driven system, particularly hydraulic systems, can cause unanticipated irregularities in both the current and impedance characteristic.[6] Motor starting impedance can also vary with starting voltage due to saturating.

16.10 DIRECT TEMPERATURE MEASUREMENT

In most motors, the running overload capability is defined by stator insulation temperature. Direct sensing of stator temperature provides an additional method of stator protection in this portion of the capability curve. Direct temperature sensing also provides protection for conditions not sensed by overcurrent elements such a reduced ventilation of high ambient temperature.

Typically, six to nine sensors (two to three per phase) are placed around the stator of motors 1500 HP and larger. These sensors are located in the stator slots between stator coils as shown in Figure 16.48. The sensors are placed at locations where the motor designer anticipates maximum winding temperature. The sensors may be resistance temperature detectors (RTDs) or thermocouples. The RTDs are devices with precise resistance vs. temperature characteristics. Thermocouples are bimetallic junctions, which generate a voltage proportional to junction temperature.

© 2006 by Taylor & Francis Group, LLC

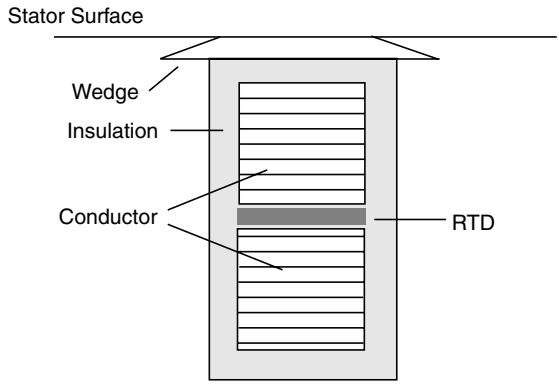


FIGURE 16.48 RTD placement. (From Boothman, D.R., Elgar, E.C., Rehder, R.H., and Wooddall, R.J. Thermal Tracking – A Rational Approach to Motor Protection, IEEE Transactions on Power Apparatus and Systems, July-August 1974, p. 1335. With permission.)

Because the detectors are in contact with the winding insulation, not the winding conductors themselves, the temperature measured will be a few degrees less than the maximum temperature. This temperature differential is a function of motor size and design voltage. NEMA horsepower ratings are based on RTD or thermocouple measurement. The NEMA rating structure assumes sensor temperature equal to the hot spot temperature of the winding for motors 1500 HP and below. Above 1500 HP, the temperature differential becomes voltage related. The higher the motor rated voltage, the thicker the insulation to ground on each coil. Above 1500 HP, a 5°C temperature differential between the measured temperature and the winding hot spot is assumed for motors rated 7 kV and below above 7 kV a 10°C differential is assumed.

Stator temperature monitors may be implemented to trip, alarm or both. Trip settings should not exceed the maximum rated temperature for the insulation system used and are typically set within the NEMA 0–10°C allowance. Alarms are typically set 10°C above the full-load temperature rise plus the maximum ambient temperature, but not above the rated temperature for the insulation system.

As an example, assume a motor with class F insulation (rated 155°C) and a specified 90°C rise at full load is operated with an ambient temperature of 40°C. The maximum operating temperature would be 90 + 40 = 130°C. An appropriate alarm setting would be 140°C. A trip setting from 145 to 155°C could be chosen. For this installation, a conservative 145°C trip can be chosen. The motor manufacturer should be consulted when trip or alarm settings are chosen.

Obviously, if a motor has the maximum temperature rise permitted by the insulation class and operated at an ambient temperature of 40°C, the resulting trip setting will permit operation above the maximum insulation temperature. If the class F insulated motor in the previous example were rated 13 kV the hotspot allowance would be 10°C. A stator monitor set with a 5°C margin actuated at 160°C (155°C+ 5°C) could allow operation with a hotspot temperature of 170°C (160°C+ 10°C hotspot allowance).

On large machines, temperature sensors are only effective where winding temperature changes at a slow rate. Figure 16.49 demonstrates the close coordination between hot spot and sensor temperature as a motor heats during full-load operation. Severe overloads cause stator-winding temperature to rise rapidly, but heat transfer to the sensor is delayed by the thermal resistance and capacitance of the winding, insulation and core material. A typical thermal time constant for heat transfer from the stator winding to sensor is 30–60 sec.[9] As a result, the sensor may respond too slowly to prevent damage. This is demonstrated by Figure 16.50, which depicts stator temperature variation for a 20 sec locked rotor event.

Direct stator temperature measurement is, of course, not an effective protection strategy for conditions that are rotor limited, such as locked rotor and during acceleration.

© 2006 by Taylor & Francis Group, LLC

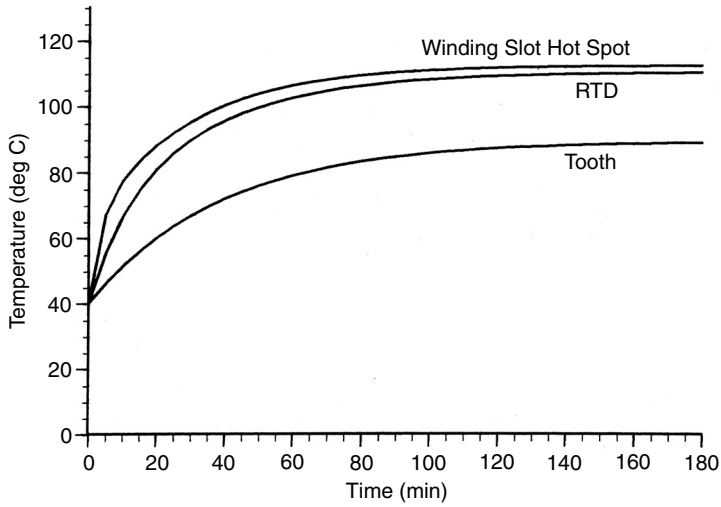


FIGURE 16.49 RTD response to slow load change. (From Boothman, D.R., Elgar, E.C., Rehder, R.H., and Wooddall, R.J. Thermal Tracking – A Rational Approach to Motor Protection, IEEE Transactions on Power Apparatus and Systems, July-August 1974, p. 1335. With permission.)

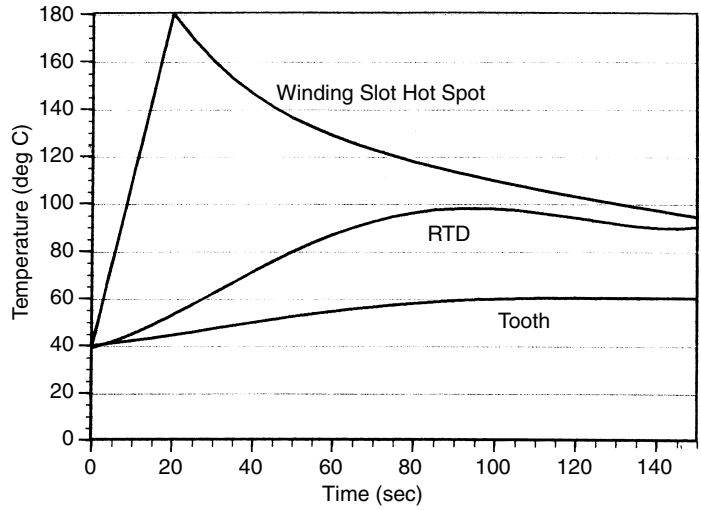


FIGURE 16.50 RTD response to rapid load change. (From Boothman, D.R., Elgar, E.C., Rehder, R.H., and Wooddall, R.J. Thermal Tracking – A Rational Approach to Motor Protection, IEEE Transactions on Power Apparatus and Systems, July-August 1974, p. 1335. With permission.)

16.11 PHASE FAULT PROTECTION

Short-circuit protection for phase faults is normally provided by instantaneous overcurrent relays. These elements are intended to respond to high-magnitude phase-to- phase and three-phase faults in the motor winding, motor cable or starter, if so equipped.

The instantaneous relay must be set above the starting inrush current. This includes considerations for 6 to 15 cycles of asymmetrical current. A setting of 1.65 to 1.9 times locked rotor current is generally sufficient to avoid nuisance trips, but the manufacture's instruction for a given relay should be

© 2006 by Taylor & Francis Group, LLC

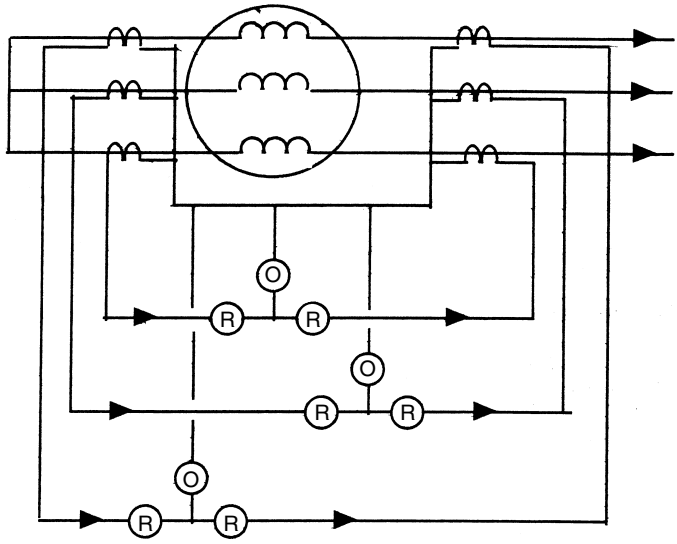


FIGURE 16.51 Differential protection.

followed. This setting will also prevent misoperation of the instantaneous elements for faults on the motor supply system. A running motor develops an internal voltage similar to that of a generator. The motor supplies fault current for a few cycles as the motor's internal magnetic field collapses.

Reduced settings of 1.2 to 1.3 times locked rotor current are applicable for cup and inverse instantaneous elements. Cup-type elements are significantly more expensive than standard hinge-type units, but are, by design, unresponsive to the DC component of asymmetric current. Some electronic relays include inverse instantaneous elements that have a diminishing time delay with increased current. These are intended to override the DC component of the asymmetrical current. Microprocessor based relays typically have filtering that removes the DC component and facilitate reduced settings.

The motor locked rotor current can be obtained from data sheets or from the starting code on the motor's nameplate. The NEMA starting codes define the starting kVA/HP at rated voltage and are listed in Table 16.2.

Instantaneous relays should be set to detect the minimum three-phase fault current at the motor terminals with a 300% margin. In cases where a large motor is connected to a relatively weak system, the locked rotor current can approach the fault current. It may not be possible to meet the 300% criteria. A rule of thumb is that if the motor kVA (approx. equivalent to HP) is less than one-half the supply transformer's kVA rating, instantaneous relays can be used.

If instantaneous relays cannot be used, differential relays are an alternative. Figure 16.51 is a typical differential connection. For very large motors, a differential scheme may be justified in conjunction with phase instantaneous overcurrent (OC) relays because of the increased fault sensitivity for failures within the motor. This scheme is functionally equivalent to the generator differential scheme discussed in Chapter 3 and the same concerns about CT mismatch apply.

The self-balancing differential scheme shown in Figure 16.52 is often applied in conjunction with instantaneous overcurrent relays on medium-sized motor installations because of the improved sensitivity for motor faults.

16.11.1 Cable Protection

The short-circuit protection provided a cable is defined by the cable insulation. Instantaneous elements should provide protection to the cable insulation in the event of a bolted fault at the

© 2006 by Taylor & Francis Group, LLC

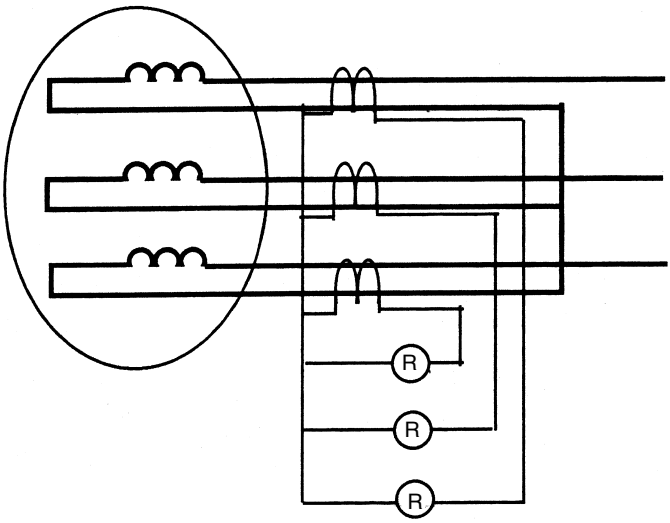


FIGURE 16.52 Self-balancing differential relay.

motor terminals. In the event of a low-magnitude fault, clearing must be initiated by the disk or thermal time overcurrent element.

Cable insulation protection is more a function of system design than settings. The fault clearing time for an instantaneous element is generally fixed at four to six cycles (One cycle for the relay and three to five cycles for the breaker to open). Cable protection is contingent on the installation of sufficiently large cable to withstand the maximum system fault condition for four to six cycle as shown in Figure 16.53. The insulation damage curve should also lie above the time-delayed overcurrent element so that protection is also provided for restricted faults.

Cable protection is achieved when the fault clearing time does not exceed the cable insulation withstand time as defined by the Insulated Power Engineers Association (ICEA) equations below.[12]

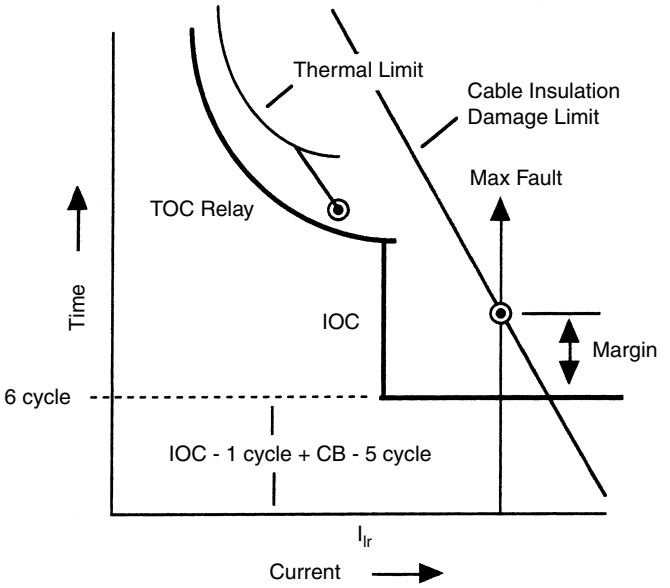


FIGURE 16.53 Conductor protection.

© 2006 by Taylor & Francis Group, LLC

TABLE 16.16
Insulation Temperature Limits

Insulation Type	Maximum Operating Temperature T_o (°C)	Maximum Short-Circuit Temperature T_f (°C)
Rubber	75	200
Rubber	90	250
Silicone rubber	125	250
Thermoplastic	60, 75, 90	150
Paper	85	200
Varnished cloth	85	200

Cable insulation withstand for copper conductor:

$$\left(\frac{I}{CM}\right)^2 t = 0.0297 \log\left(\frac{T_f + 234}{T_o + 234}\right) \tag{16.95}$$

For aluminum conductor:

$$\left(\frac{I}{CM}\right)^2 t = 0.0125 \log\left(\frac{T_f + 228}{T_o + 228}\right) \tag{16.96}$$

where t = insulation withstand time for at current I, I = short-circuit current in amps, CM = area in circular mils, T_o = Maximum operating temperature of conductor, and T_f = maximum short-circuit temperature. Both the maximum operating temperature and the maximum short-circuit temperature are defined by the insulation type and are listed in Table 16.16.

Many electronic motor protection relays include provisions to time delay the instantaneous element. This delay would be used to override the initial asymmetry of the starting transient and permit a reduced pickup setting. The implementation of such a delay would be contingent on coordination with the cable damage curve.

16.11.2 Upstream Coordination

The setting of the instantaneous element at the motor will impact on coordination with upstream protection. As motor size increases and/or as starting times increase, the operating time of the motor overcurrent protection increases and can approach that of the overcurrent protection on the main incoming breaker at the motor supply bus. Figure 16.54 shows that there are two critical coordination points. One point is at maximum fault current, where upstream protection must have sufficient delay to allow the instantaneous element at the motor to operate. An instantaneous element will require about a cycle to operate and actual fault clearing will require an additional three to five cycles of breaker interrupting time. A 12-cycle safety margin should include yielding a minimum upstream overcurrent operating time of 16 to 18 cycles depending on the breaker speed. This value is applicable to electronic upstream relays. If the upstream element is an electromechanical disk element, an additional six-cycle margin should be added for overtravel. The inertia of the disk, although small, cause the disk to continue rotation for a short time after current ceases.

The second critical coordination point is at a fault current just below the setting of the motor instantaneous element. At this current, the time–current, curves of the motor overcurrent protection and

© 2006 by Taylor & Francis Group, LLC

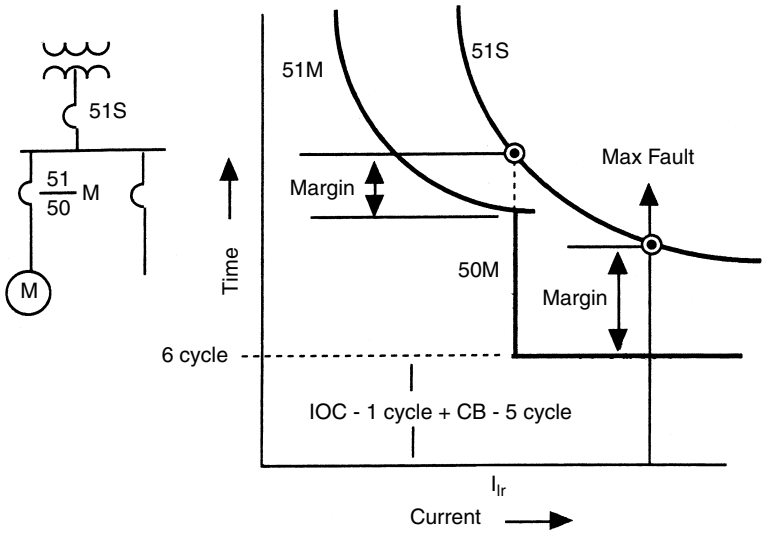


FIGURE 16.54 Motor circuit coordination.

upstream overcurrent protection must coordinate. The minimum margin between the curves is defined by the same constraints as above, circuit breaker clearing time three to five cycles, plus a safety margin of 12 cycles for a 15- to 17-cycle margin if the upstream device is electronic based. If the upstream device is electromechanical, an additional six cycles are required between the curves for relay overtravel.

16.12 GROUND FAULT PROTECTION

On a solidly grounded system, the ground fault protection can be provided by a time overcurrent relay residually connected in the phase CT circuit as shown in Figure 16.55. Inverse or short time relay characteristic curves are recommended. Residually connected instantaneous relays are not advised. During motor starting and when the motor backfeeds into a fault, differences in the individual phase CTs and their connected circuits will lead to unequal saturation of the phase CTs, as discussed in Chapter 5. The resulting error current in the neutral CT circuit can cause misoperation of residually connected relays. Time overcurrent relays can override the backfeed conditions, but must be set above the error currents during starting. A typical pickup setting for the

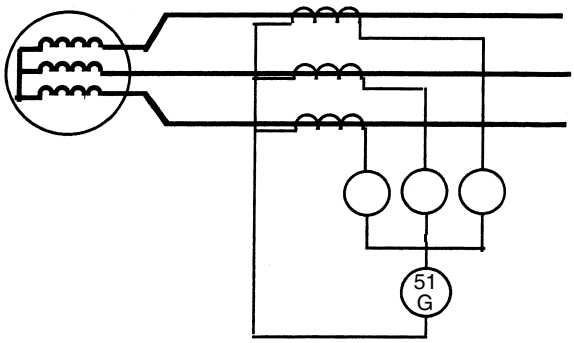


FIGURE 16.55 Residual ground relay.

© 2006 by Taylor & Francis Group, LLC

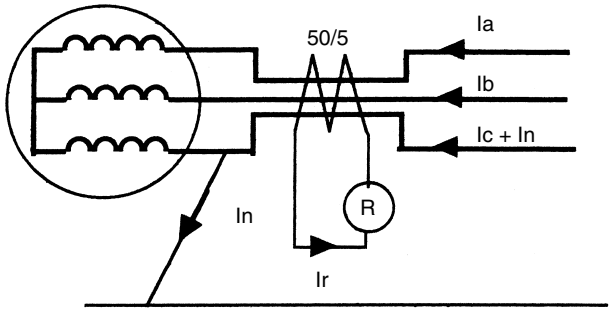


FIGURE 16.56 Window CT.

time overcurrent ground relay on a motor feeder is 50 to 80% of the phase relay setting, with the time dial at the #1 position.

Low-resistance grounding is often used on 2.4 to 15 kV systems. Ground protection is provided using time or instantaneous relays connected to a window CT as shown in Figure 16.56. Current in the CT is:

$$I_r = (I_A + I_B + I_C + I_n)\frac{5}{50}$$

Because the phase currents sum to zero, current in the relay is

$$I_r = I_n \frac{5}{50}$$

This scheme provides fast clearing at low cost. Because all three phases pass through the single CT, the flux of the individual phases cancel and no erroneous current is transmitted to the relay. This allows very sensitive settings. The scheme has two limitations. It is not applicable for large motors because multiple large cables will not fit through the CT. Also, these window CTs have a very low accuracy class (C10) and as such can produce limited secondary voltage. The burden (impedance) of the CT secondary circuit and the maximum ground fault current must be such that the CT does not saturate to the extent that the relay will not operate.

Saturation can also cause slow timing of time overcurrent relays; this can result in miscoordination with upstream relays. We note that low-range electromechanical disk relays (0.5–2.5 amp), as an example, have high burdens, which increase saturation and exacerbate slow timing. This is why instantaneous elements are usually applied in this scheme. When purchased as stand alone protection relay/CT combination used in this scheme is often sold as a set, the manufacturer having matched the relay and CT for optimum performance on a system with a specified range of ground fault current. Slow timing is not associated with electronic time overcurrent elements because these relays have very low CT burdens.

Improper installations of grounds frequently cause window CT schemes to misoperate. Figure 16.57(a) shows the correct methods of grounding a neutral or cable sheath. The neutral or sheath current must not enter into the relay. By looping the neutral or sheath back through the CT and grounding once on the incoming side of the CT, the neutral current cancels itself. Figure 16.57(b) and Figure 16.57(c) show the effects of incorrect installation. In Figure 16.57(b) the *A* phase ground fault current returns through the improperly grounded neutral conductor. Neutral and phase currents cancel in the CT and the fault is undetected. In Figure 16.57(c) a ground fault at a remote location from the protected motor, possibly at a different voltage level, flows in the multiple grounded neutral or sheath and trips the motor.

© 2006 by Taylor & Francis Group, LLC

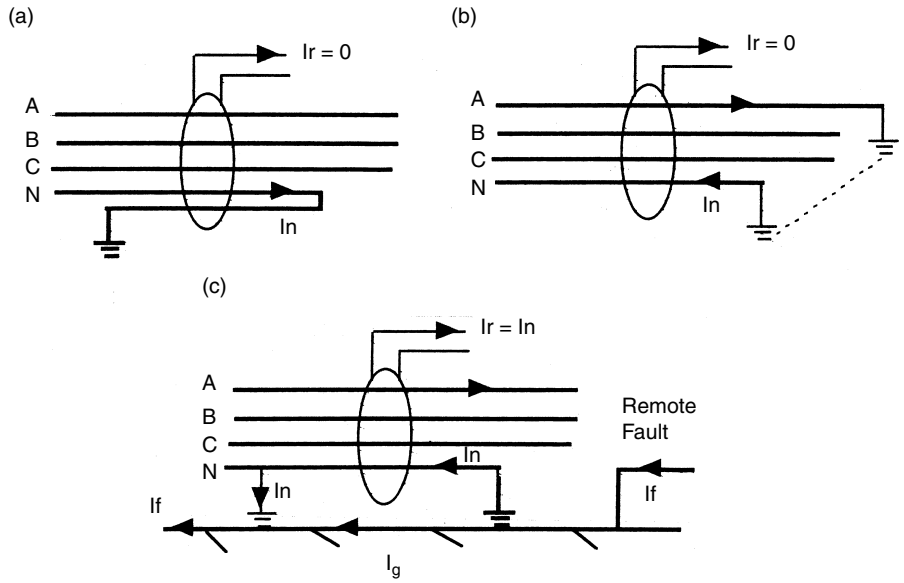


FIGURE 16.57 Window CT installation. (a) Correct installation, (b) Relay will not operate for fault, and (c) Relay trips for remote fault.

Typical settings for the window CT ground scheme are 4 to 12 primary amps. If surge capacitors are installed at the motor terminals, the capacitor inrush current must be considered in the pickup setting calculation if instantaneous relays are used. The window CT scheme just described can also be used on high-resistance grounded systems. Aspects of ground fault protection were also discussed in Chapter 5.

16.13 PHASE UNBALANCED PROTECTION

Unbalanced phase current causes increased heating in the high-current stator winding(s) and in the rotor. Stator windings generally do not experience significant temperature rise because heat transfer within the stator is usually good, allowing heat in the high-current winding(s) to dissipate to the stator iron associated with the low-current winding(s). As such, overall temperature rise in the stator tends toward a value indicative of the average value of phase current. Only in cases of severe unbalance in large motors where heat transfer between windings is hindered by distance and/or insulation would stator temperature be a concern.

Unbalanced phase current will cause significant temperature rise in the rotors. NEMA standards include derating factors for motors with voltage unbalance between 1.0 and 5%. NEMA defines unbalance as

$$\%Unbal_{\text{NEMA}} = \frac{\text{Max voltage deviaton from average}}{\text{Average voltage}} \times 100$$

Derating factors vary from 99% at 1% unbalance, 95% at 2% unbalance and 75% at 5% unbalance. Motor operation is not recommended above 5% unbalance. The NEMA voltage unbalance approximates the negative-sequence component of phase voltage. Negative-sequence voltage gives rise to negative-sequence current, which is the quantity that actually produces the increased rotor heating.

© 2006 by Taylor & Francis Group, LLC

A motor operating with equal magnitude phase currents, each displaced by 120°, is operating with only positive-sequence current. This is the ideal operating mode. Phase current unbalance. either in magnitude or phase displacement, generates a negative-sequence component of current. Chapter 6 includes a method that can be used to calculated negative-sequence current if magnitude and phase angle are known for all three phases.

The negative-sequence current produces significantly more heating per amp than does positive-sequence current. Negative-sequence quantities have a phase rotation opposed to that of the rotor; consequently, negative-sequence voltage induces double frequency (120 Hz) current in the rotor. The high frequency current is forced to the surface of the rotor conductors. This "skin effect" increases the effective resistance of the rotor circuit, which in turn increases I^2R losses and heating. An induction motor is somewhat more tolerant of the induced 120 Hz rotor current than a synchronous generator, because a motor rotor must be designed to circulate induced rotor current during normal operation.

Standards do not provide continuous or short time negative-sequence limitations for motors as are provided for generators. However, a short time limit of $I_2^2\, t = 40$ is suggested as a conservative estimate.

The combined heating effect of both positive- and negative-sequence current is represented as an equivalent heating current:

$$I_{eq-heat} = \sqrt{I_1^2 + kI_2^2} \tag{16.97}$$

where k represents the increased negative-sequence rotor resistance due to the skin effect

$$k = \frac{R_{r_2}}{R_{r_1}} = \frac{175}{I_{\mathrm{LR}}^2}(\text{conservative estimate})$$

and I_1 = positive-sequence current (pu), I_2 = negative-sequence current (pu), R_{r_1} = Positive−Sequence Rotor Resistance (pu), R_{r_2} = negative-sequence rotor resistance (pu), and Relative heating is a function of the square of the equivalent heating current

$$\text{Relative heating} = I_1^2 + kI_2^2 \tag{16.98}$$

The negative-sequence equivalent circuit for a motor is shown in Figure 16.58. Note that negative-sequence rotor resistance varies with $1/(2 - \text{slip})$ as opposed to $(1/\text{slip})$ in the positive sequence, (Figure 16.5). In the positive sequence, rotor resistance and reactance are assumed to

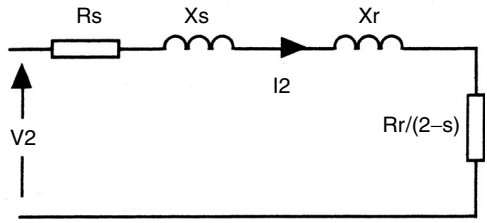


FIGURE 16.58 Negative-sequence circuit.

© 2006 by Taylor & Francis Group, LLC

vary linearly with slip and are given by Equation (16.16) and Equation (16.17)

$$R_{r_P}(s) = (R_{r_{LR}} - R_{r_{NL}})s + R_{r_{NL}}$$
$$X_{r_P}(s) = (X_{r_{LR}} - X_{r_{NL}})s + X_{r_{NL}}$$

Assuming the same linear relationship in the negative sequence,

$$R_{r_N}(s) = (R_{r_{LR}} - R_{r_{NL}}) * (2 - s) + R_{r_{NL}} \quad (16.99)$$
$$X_{r_N}(s) = (X_{r_{LR}} - X_{r_{NL}}) * (2 - s) + X_{r_{NL}} \quad (16.100)$$

In Section 16.6.3, the locked rotor and no-load rotor resistances where calculated for a 600 HP motor

$$R_{r_{NL}} = 0.008\,\text{pu} \quad Rr_{LR} = 0.0284\,\text{pu}$$

For this motor, $R_{r_{LR}} = 3.55R_{r_{NL}}$; substituting this into Equation (16.99) and setting $s = 0$ to approximate rated speed yields:

$$k = \frac{R_{r_N}}{R_{r_P}} = 6.1 \quad (\text{at } s = 0)$$

Typically, the locked rotor resistance is close to five times the no-load rotor resistance, which would yield $k = 5$.

A small negative-sequence voltage will produce large negative-sequence currents. The per unit negative-sequence impedance of a motor is approximately equal to the starting impedance. For a typical motor with a starting inrush of six times rated current,

$$Z_2 = \frac{1}{I_{LR}} = \frac{1}{6} = 0.167\ \text{pu}$$

Assuming a 5% negative-sequence voltage exists at the motor terminals, the resulting motor negative-sequence current would be

$$I_2 = \frac{V_2}{Z_2} = \frac{0.05}{0.167} = 0.30\ \text{pu}$$

From the above equation, a 5% negative-sequence voltage produces 30% negative-sequence current, which in turn, would produce 30% increase in rotor heating with $k = 6.1$.

Heating is not the only detrimental effect: negative-sequence torque is also produced. Positive-sequence torque is produced by positive-sequence current and is the basis for motor ratings. Negative-sequence torque opposes positive-sequence torque, reducing the available output torque of a motor. From the negative-sequence circuit diagram, negative-sequence torque in per unit is

$$T_{neg} = -\frac{I_2^2 R_{r_N}(s)}{2 - s}$$

At rated load, the torque reduction caused by negative-sequence current is minimal with respect to the positive-sequence torque, increasing slightly as speed decreases.

The most severe unbalanced condition for a motor is an open-phase condition. The sequence diagram for this condition is provided in Figure 16.59. When a phase opens, the positive-sequence

© 2006 by Taylor & Francis Group, LLC

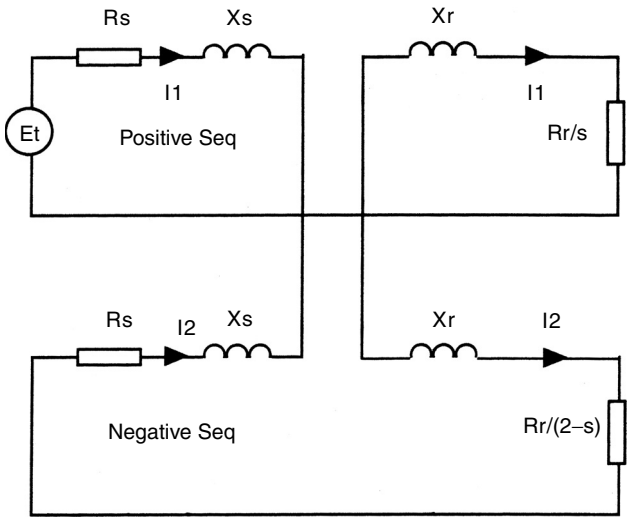


FIGURE 16.59 Open-phase sequence connection.

current essentially remains at the pre failure value, which is the initial load current. The negative-sequence current created by the open phase is approximately equal to but opposite in direction to, the positive-sequence current. The resulting current in the intact phases is usually between 170 and 200% of the pre failure value. (The conversion of sequence quantities to phase quantities was discussed in Chapter 4.) If the motor is running at the time of the failure, the motor will usually continue to run unless the remaining single-phase voltage is low or the mechanical load on the motor is above 80% nameplate. A motor will not start with an open phase. At standstill (slip $= 1$), positive- and negative-sequence rotor resistances are equal and positive- and negative-sequence currents are equal in magnitude, but opposed in direction. These conditions produce positive- and negative-sequence torques that are equal and opposed, yielding a net starting torque equal to zero.

16.13.1 Current and Voltage Unbalanced Relays

In the electromechanical and solid-state world unbalanced protection is provided by phase-balancing or negative-sequence relays. Microprocessor-based relays use a negative-sequence current bias in their thermal models.

The phase-balance relay compares individual phase quantities, and when the difference between phases exceeds the setpoint, the relay operates. Current-actuated versions of this type of relay are available with 1.0 A sensitivity and can detect an open-phase condition if the prefailure load on the motor is 0.6 A or more in the relay. These relays do not measure the damaging quantity, the negative-sequence current, and cannot be set to match the motor thermal limits. This type of relay tends to be too sensitive and overprotects the motor.

Negative-sequence current relays have an advantage over the phase-balance relay in that they measure the damaging quantity directly. They are also far less dependent on motor loading to detect a damaging condition than are phase-balance relays. These relays are typically set to operate at 15% negative-sequence current.

Both current detecting relays, the phase-balance and negative-sequence, should be applied to individual motor circuits as opposed to application at the main breaker supplying a motor bus. Neither type of relay will detect an open phase on a feeder to a small individual motor if applied at the incoming breaker of the motor supply bus. Also, if balanced nonmotor load is a significant portion of the bus loading, open-phase detection, particularly for smaller motors, will be

© 2006 by Taylor & Francis Group, LLC

jeopardized, because such a load will tend to balance phase current at the relay for an open phase downstream of the relay.

The voltage versions of the above relays are usually applied at the bus supplying a group of motors. They provide protection for an open phase that occurs between the relay and the power source. They do not provide this protection for open phases between the relay and the motors themselves.

All the aforementioned forms of unbalance detection shall trip with a time delay to avoid nascence tripping for external system faults.

Microprocessor relays employ thermal models for overload protection. These models were described in Section 16.8. Unbalanced protection is provided by including heating effects of negative-sequence current in the thermal model. The combined heating effect of both the balanced and unbalanced components of phase current (positive- and negative-sequence current, respectively) are represented by the equivalent heating current defined in Equation (16.97). By substituting this equivalent current into the thermal model of Equation (16.82), Equation (16.83), or Equation (16.86), the models become representative of the combined heating effects of both sequence components. We note that the response of the thermal models closely approximates the thermal limit defined by the NEMA derating factors when $k = 8$.

16.14 SAMPLE SETTING CALCULATIONS

A 3000 HP motor is to be used to drive a large fan. The supply is from a 13.8 kV auxiliary bus with overcurrent protection at the incoming breaker. The auxiliary bus is supplied from a 20 MVA 230/13.8 kV transformer with 10% impedance. A maximum three-phase short circuit at the station 230 kV bus is 10,000 MVA. The system configuration is shown in Figure 16.60.

The intent is to protect the motor using an inverse time (51M) and instantaneous (50N) element supplied for 200/5 CTs.

Motor data:

3000 HP
Rated voltage = 13.2 kV
Sync speed = 1200 RPM

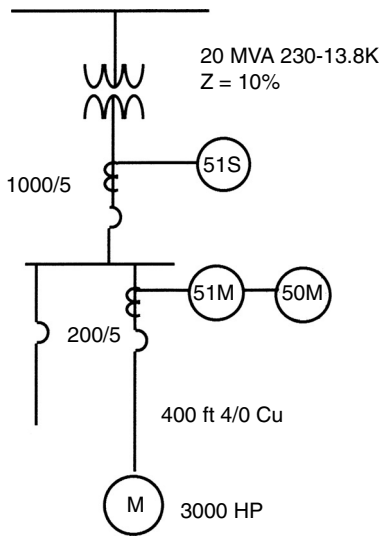


FIGURE 16.60 Motor installation online.

© 2006 by Taylor & Francis Group, LLC

Full load speed = 1190 RPM
$I_{FL} = 117$ A
$I_{LR} = 833$ A
$PF_{LR} = 0.14$
Torque at LR = 1.49 pu
Breakdown Torque = 3.4 pu
Motor $Wk^2 = 1{,}0751$ lb-ft^2
Safe stall time cold = 38
Safe stall time hot = 32

Fan data:

HP at full 1190 RPM = 2850 HP (95% motor)
Breakaway torque = 450 HP (15% motor)
$Wk^2 = 170{,}000$ lb-ft^2

The upstream from the motor breaker is an auxiliary bus. Bus differential relaying protects the auxiliary bus. The source transformer breaker is equipped with phase overcurrent relays (51S) that provide backup protection for the bus and the feeders emanating from the auxiliary bus. The overcurrent protection at the incoming breaker is as follows:

51S

Phase TOC = 5.0 A–1000 PA – TD# 20
Very inverse (2–6 A)
1000/5 CTs,

16.14.1 Set Device 51 Operating Current

The time overcurrent trip settings are constrained by the National Electric Code. The maximum overcurrent pickup allowed for motors with a service factors of 1.15 or greater and motors marked with a rise not over 40°C is 125% the full-load current. All other motors are allowed a maximum overcurrent trip setting of 115% full-load current. The 3000 HP motor has a service factor of 1.0 and is not marked with a temperature rise. Thus, the overcurrent trip should be limited to 115% full-load current or 134.5 A (1.15 × 117 A). With 200/5 CT on the motor circuit, the maximum relay tap setting wound only be 134.5A × 5/200 = 3.36 A. Unfortunately, the only tap settings available on the relay are (2.0, 2.5, 3.0, 3.5, 4.0, 5.0, 6.0 A). Set on the 3.0 A tap (120 primary amps), the trip point would be 3 A above full-load current. This is an insufficient margin. The NEC allowed settings at the next available value to be used if the prescribed setting will not carry the load or permit starting provided the increased setting does not exceed 130% full load for motors with service factors less than 1.15. This constraint would permit a setting of 152 A (1.3 × 117 A).

Set the pickup of the motor of Device 51 at 3.5 A = 140 primary amps (PA)

16.14.2 Set Device 50 Operating Current

The phase instantaneous trip is typically set 165 to 190% the locked rotor current. The minimum setting would then be 1.65 × 833A = 1374 A. With 200/5 CTs, this corresponds to a relay tap of 1374 A × 5/200 = 34.35 A. Rounding off to 35 A, the proposed setting is 35 A × 200/5 = 1400 A.

© 2006 by Taylor & Francis Group, LLC

The instantaneous element provides protection for high-magnitude faults on the motor and motor circuit. The setting should detect the maximum available fault on the motor circuit with a minimum of 300% coverage.

16.14.3 Checking the Maximum Three-Phase Fault Current at the Motor

The supply transformer is a 20 MVA 230/13.8 kV transformer with 10% impedance. Converting the 230 kV short-circuit MVA to per-unit impedance on the transformer MVA base:

$$\begin{aligned} Z_{\text{bu}} &= \text{MVA transformer/MVA short circuit} \\ &= 20/10{,}000 = 0.002 \text{ pu on } 20\,\text{MVA base} \end{aligned}$$

The impedance of the cable 400 ft 4/0 cu cable from the auxiliary bus to the motor is

$$Z_{\text{cab}} = 0.025 + j0.02\,\Omega$$

Converting the cable impedance to percent on transformer 20 MVA and 13.8 kV base:

$$I_{\text{base}} = \frac{20{,}000\,\text{kVA}}{\sqrt{3} * 13.8\,\text{kV}} = 836.7\,\text{A}$$

$$E_{\text{base}} = \frac{13,800}{\sqrt{3}} = 7967\,\text{V}$$

$$Z_{\text{base}} = \frac{E_{\text{base}}}{I_{\text{base}}} = \frac{7967\,\text{V}}{836.7\,\text{A}} = 9.52\,\Omega$$

$$Z_{\text{cab}}(\text{pu}) = \frac{0.025 + j0.02\,\Omega}{9.52\,\Omega} = 0.0026 + j0.0021 \text{ pu (20 MVA base)}$$

The maximum three-phase fault current at the motor is calculated as:

$$\begin{aligned} Z_{\text{BU}}(230\,\text{kV}) &= \quad + j0.002\,\text{pu} \\ Z_{\text{trans}} &= \quad + j0.100\,\text{pu} \\ Z_{\text{cab}} &= 0.0026 + j0.002\,\text{pu} \\ \hline Z_{\text{total}} \quad & 0.0026 + j0.104 = 0.104\,\text{pu} \quad \angle 88.6^{\circ}(20\,\text{MVA base}) \end{aligned}$$

$$I_{\text{max}} = \frac{E}{Z_{\text{total}}} I_{\text{base}}$$

$$= \frac{1.0}{0.104} * 836\,\text{A} = 8038\,\text{A}$$

Checking coverage with the proposed 1400 A setting;

$$\textit{Coverage} = \frac{8038\,\text{A}}{1400\,\text{A}} = 5.74 \qquad \textit{Coverage} > 3 \rightarrow \text{OK}$$

Set the pickup of Device 50 at 35 A = 1400 A

© 2006 by Taylor & Francis Group, LLC

16.14.4 Device 51 Time Delay

The time overcurrent trip must have sufficient time delay to override the starting inrush, yet act with sufficient speed to prevent motor damage in the event of an overload or stall. The first step is to define an electrical model for the motor. The model will then be used to calculate a time-current plot for the starting transient.

Motor parameters were calculated from the data listed for the 3000 HP motor using the methodology of Section 16.6.3. A comparison of the calculated and vendor supplied speed–torque and speed–current curves, (Figure 16.61) shows close correlation between the torque curves and disagreement between current traces. The figure also shows that the correlation of current is improved with some sacrifice of torque correlator by altering the value of the no-load rotor resistance from the calculated value of 0.00815 pu. to a value of 0.012 pu. The adjusted value is used in the motor model.

The starting calculation is performed as shown in Section 16.6.4. The impedance of the electrical supply to the motor is included in this calculation. The per unit impedance of the supply was calculated above, but that value was on a 20 MVA base. The value must be converted to the motor base for use in the starting calculation.

The per unit source impedance was derived on the transformer 20 MVA, 13.8 kV base (base ohms = 9.52).

$$Z_{sys} = 0.104\,\text{pu}\angle 88.6^\circ \times 9.52\,\Omega = 0.990\,\Omega\angle 88.6^\circ$$

Base ohms for the motor are:

$$Z_{base} = \frac{13{,}200}{\sqrt{3}\ 117\text{A}} = 65.1\Omega$$

$$Z_{sys} = 0.990/65.1\ \angle 88.6 = 0.0152\,\text{pu}\ \angle 88.6^\circ\ \text{(on motor base)}$$

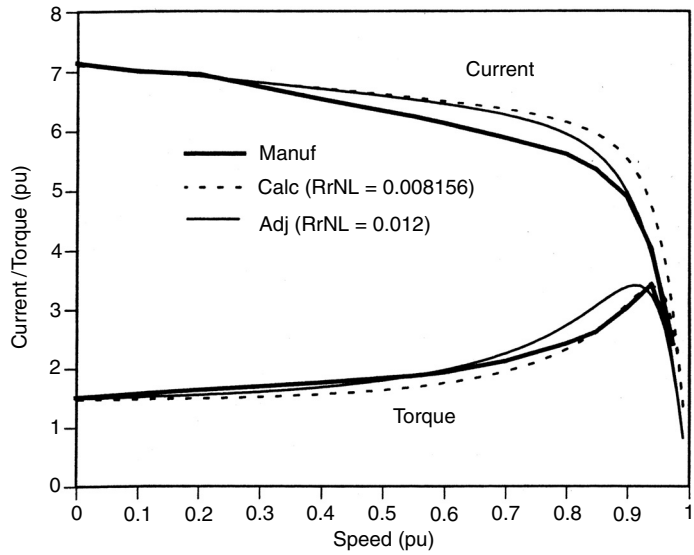


FIGURE 16.61 Manufacturer's data vs. calculated.

© 2006 by Taylor & Francis Group, LLC

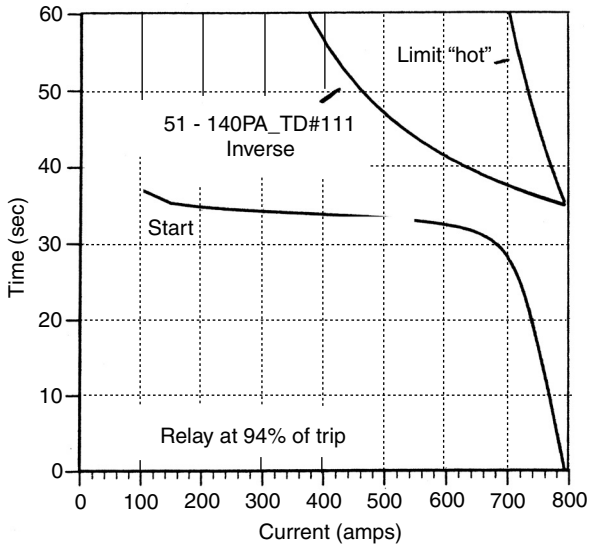


FIGURE 16.62 Starting current vs. inverse overcurrent relay.

With this impedance included, the starting time-current characteristic is as shown in Figure 16.62. The plot includes the thermal limit curve for the motor at operating temperature (the "hot" curve) and the inverse-time disk element

Device 51 set at: 4.0 A–140PA–TD# 111 200/5CTs

The response of the inverse element to the starting transient was evaluated using the dynamic point-slope technique from Section 16.7.6.3. The relay reached 94% of trip, indicating it would overide the start. This setting will also protect the motor, because it is below the thermal limit current at all points. However the setting provides very little margin over the start and has only a 0.4 sec margin to the thermal limit curve at locked rotor.

Both the starting and protection margins can be improved if two disk elements, an inverse and a very inverse element, are installed to better match the thermal limit curve.

Figure 16.63 shows that the combined characteristic of the two elements more closely follows the contour of the limit curve, thus reducing the areas of overprotection. The elements plotted are set as follows:

51M Inverse: 3.5 A–140 PA–TD# 220
51M Very inverse: 13.0 A–520 PA–TD# 10

The inverse and very inverse elements reaches 46% trip and 86% trip, respectively, during the start. The very inverse element provides a margin of 5.4 sec to the thermal limit at locked rotor. Overall, the two-element scheme provides improved starting security and protection margins over the single-element scheme and should be implemented.

16.14.5 Coordination with Upstream Protection

The settings chosen for the motor circuit must coordinate with the source breaker and should provide protection to the insulation on the cable supplying the motor. Figure 16.64 plots motor protection relays against overcurrent relays at the source bus. The insulation damage curve for the 4/0 cu

© 2006 by Taylor & Francis Group, LLC

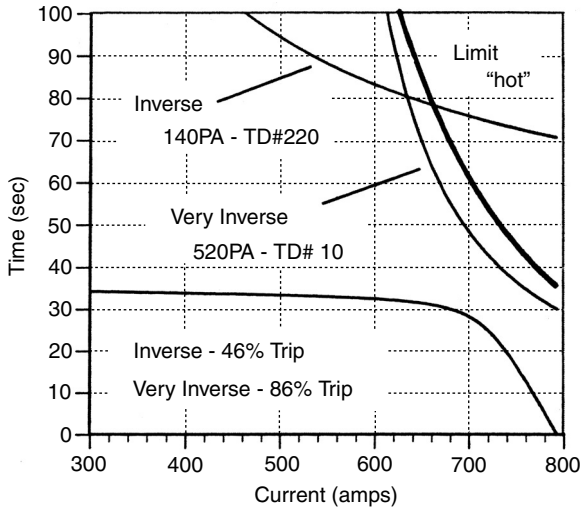


FIGURE 16.63 Dual overcurrent scheme.

motor cable is also plotted. The cable damage curve is plotted from Equation (16.95) and the operating and maximum temperature limits for thermoplastic insulation from Table 16.16.

The dotted lines show the critical points for coordination between the motor protection and the source overcurrent relay. Point A must be greater than the fault clearing time for an instantaneous element operation. The minimum time delay is:

CB operating time = 5 cycles
Inst relay = 1 cycle
Margin = 6 cycles
Total = 12 cycles = 0.1 sec

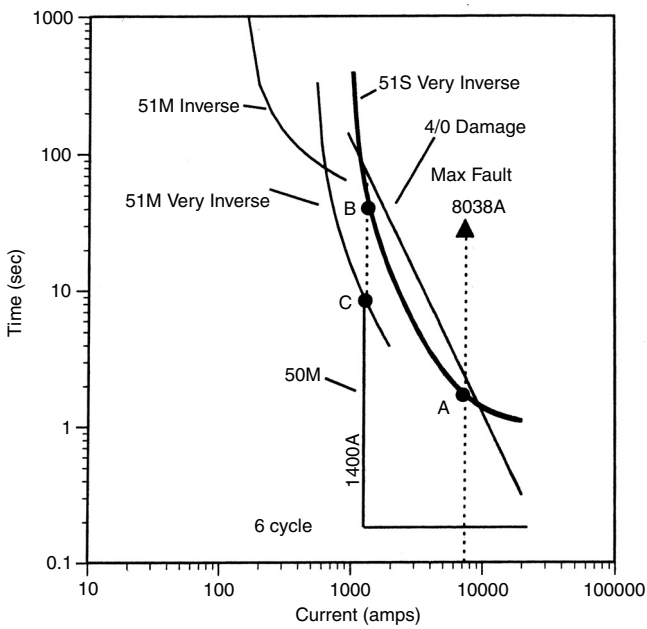


FIGURE 16.64 Coordination with source breaker.

© 2006 by Taylor & Francis Group, LLC

If the upstream relay is electromechanical, an additional six cycles should be added to allow for overtravel after the fault is cleared. It is apparent from the plot that this requirement is met.

The second point for coordination is at the operating current of the motor instantaneous element. Motor and backup overcurrent elements must coordinate at this current. Above this current, motor faults are cleared rapidly, about six cycles, by the motor instantaneous relay. The minimum distance between motor and backup overcurrent curves, points B and C, is calculated as:

CB clearing time = 5 cycles
Margin = 12 cycles
Total = 17 cycles = 0.28 sec

Again, if the upstream relay is electromechanical, an additional six cycles are required for overtravel. The figure shows ample time margins exist at these points. The plot also shows the overload and instantaneous settings chosen for the motor provide protection for the 4/0 cable.

REFERENCES

1. Johnson, B. K. and Wills, J. R., Tailoring induction motor analytical models to fit known motor performance characteristics and satisfy particular study needs, Paper 91 WM135-4 PWRS, presented at the *IEEE/PES 1991 Winter Meeting*, New York, February 3–7, 1991.
2. Messina, J. P., Consider starting conditions before specifying propeller pumps, Worthington Pump International, Power Engineering, pp. 58–60, January 1973.
3. Wiegand, H. A. and Eddy, L. B., Characteristics of centrifugal pumps and compressors which affect the motor driver under transient conditions, *AIEE Trans. Part II Applications and Industry*, 79, 150, 1960.
4. Picozzi, V. J., Factors influencing starting duty of large induction motors, *AIEE Trans. III-A, Power Apparatus and Systems*, 401, 1959.
5. Eliasen, A. N., High-inertia drive motor and their starting characteristics, *IEEE Trans. on Power Applications and Systems*, 99(4), 1472–1482, 1980.
6. Eliasen, A. N., The protection of high-inertia drive motors during abnormal starting conditions, *IEEE Trans. on Power Applications and Systems*, 99(4), 1483–1492, 1980.
7. IEEE Std C37.112-1996(2001R), *IEEE Standard Inverse Time Characteristic Equations of Overcurrent Relays*, IEEE, New York, 1997.
8. Zocholl, S. E. and Benmouyal, G., *Using Thermal Limit Curves to Define Thermal Models of Induction Motors*, Schweitzer Engineering Laboratories, Inc, Pullman, WA, 2001.
9. Boothman, D.R., Elgar, E.C., Rehder, R.H., and Wooddall, R.J., Thermal tracking – A rational approach to motor protection, *IEEE Trans. Power Apparatus and Systems*, 1335, 1974.
10. Zocholl, S. E., Schweitzer III, E. O., and Aligar-Zegarra, A., Thermal protection of induction motors enhanced by interactive electrical and thermal models, *IEEE Trans. Power Apparatus and Systems*, 103, 1749, 1984.
11. Zocholl, S. E., *Comparing Motor Thermal Models*, Schweitzer Engineering Laboratories, Inc, Pullman, WA, 2004.
12. IEEE Std 242-1986, *IEEE Recommended Practices for Protection and Coordination of Industrial and Commercial Power Systems* (Buff Book), IEEE, New York, 1990.

© 2006 by Taylor & Francis Group, LLC

Appendix A: Generator Data Sheet

104,400 KVA, 3600 RPM, 13800 Volt, 0.85 PF, 30 PSIG, 46.0 C H2, 86740 KW, 4368 Amp, 0.58 SCR, 375 FLD Volts, Wye Conn

Reactance Data—(Per Unit)	Direct Axis	Quadrature Axis
Synchronous	$X_d = 1.48$	$X_q = 1.42$
Transient	$X'_d = 0.196$	$X'_q = 0.484$
Subtransient	$X''_d = 0.136$	$X''_q = 0.132$
Negative Sequence	$X_2 = 0.129$	
Zero Sequence	$X_0 = 0.066$	
Leakage	$X_{lm} = 0.14$	

Field Time Constant Data—(Seconds at 125°C)

Open Circuit	$T'_{d0} = 3.59$	$T'_{q0} = 0.312$
Open Circuit Subtransient	$T''_{d0} = 0.033$	$T''_{q0} = 0.084$
3PH Short circuit Transient	$T'_d = 0.476$	$T'_q = 0.102$
3PH Short circuit Subtransient	$T'' = 0.023$	$T''_q = 0.023$
L–L Short circuit Transient	$T'_{d2} = 0.727$	
L–N Short circuit Transient	$T'_{d1} = 0.84$	

Armature DC Component Time Constant Data—(Seconds at 100°C)

Three phase short circuit	$T_{a3} = 0.239$
L–L Short Circuit	$T_{a2} = 0.239$
L–N Short Circuit	$T_{a1} = 0.200$

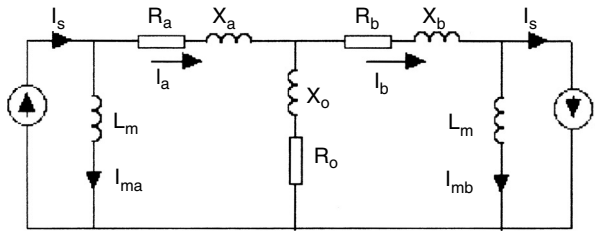
Rotor Short-Time Thermal Capacity, I_2^2t	= 30
Turbine-Generator Combined Inertia Constant, H	= 3.09 Kw sec/Kva
Three Phase Armature Winding Capacitance	= 0.947 Microfarads
Armature Winding DC Resistance (per phase)	= 0.00262 Ohms 100°C
Field winding DC Resistance	= 0.308 Ohms 25°C
Field Current at Rated KVA, Arm Volts, PF	= 848.8 Amp
Field Current at Rated KVA, Arm Volts, PF = 0	= 1017 Amp

© 2006 by Taylor & Francis Group, LLC

Appendix B: CT Performance in Differential Relay Circuits

This mathcad worksheet available for download at www.taylorandfrancis.com. This worksheet was developed on mathcad 2001i and may require backward compatibility enabled to run. This worksheet calculates currents in a differentially connected CTs circuit. Quantities requiring input are underlined. The worksheet will calculate currents for faults internal or external to the differential zone of protection.

When an external analysis is being carried out, the external analysis solve block and differential current equation must be toggled "ON" and the internal analysis solve block and differential current equations must be toggled "OFF". The reverse is true if an internal analysis is required.



Circuit Quantities in Ohms and Henrys:

$R_a \equiv 5.8$ $R_b \equiv 3.0$ $R_0 \equiv 0$
$L_a \equiv 0$ $L_b \equiv 0$ $L_0 = 0$
Ideal Secondary Current = I primary/N $= Im \equiv 30$ RMS
DC Component Time Constant (L/R) for primary Ckt $\tau = 0.24$ sec
Frequency = $f \equiv 60$ $\omega \equiv 2.\pi \cdot f$

FOURIER FILTER

Harmonic being detected $h := 1$
Sampling rate, samples per cycle = sample $\equiv 24$
Number of data points per sample Pts_Sample $\equiv 2$

Note the "sample" and "Pts_sample" determine Δt. The value of Δt must be less than the smallest circuit time constant to prevent numerical instability in the solution. If the solver gives an erratic output current for the CTs, try increasing the "Pts_sample" to reduce Δt.

$$\Delta t := \frac{(1/f)}{sample \cdot Pts_Sample} \qquad \Delta t = 3.472 \cdot 10^{-4} \text{ sec}$$

© 2006 by Taylor & Francis Group, LLC

Total number of points calculated $K \equiv 200$

$$\text{Duration of simulation} = \Delta t \cdot K = 0.069\,\text{sec}$$

SECONDARY CIRCUIT CURRENT CALCULATION

ORIGIN: $= -1$

$$k \equiv 1 \ldots K \qquad t_k := \Delta t \cdot k$$

Expression for secondary current

$$Is_k := \sqrt{2}\,Im \cdot \left[e^{(-t_k/\tau)} - \cos(\omega \cdot t_k)\right]$$
$$Iso_k := Is_{k-1} \qquad \Delta Is_k := Is_k - Is_{k-1}$$

CURRENT TRANSFORMER MODEL

The CTs are modeled using the Frolich equation. This is an empirical approximation of the S-shaped B–H curve. This model does not include a representation of residual flux or hysteres's.

The Frolich:

$$B = \frac{H}{c + b \cdot |H|}$$

where H = amp-turns/meter of core length and B = flux in weber/m^2 (Tesla).

$$H = \frac{I \cdot N}{d}$$

where I = current, d = length of core in meters, and N = number of turns.

The coefficients are calculated for the maximum permeability of the core and the saturation flux of the core. The constant "c" determines the slope and "b" determines the saturation flux of the empirical B–H curve.

$$c = \frac{1}{\mu_i \cdot \mu_0} \qquad b = \frac{1 - 1/\sqrt{\mu_i}}{B_{sat}}$$

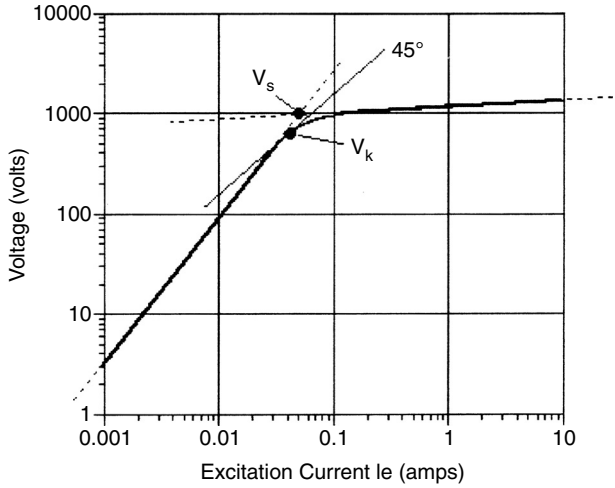
where μ_i = initial relative permeability, μ_0 = permeability of free space = $4\pi \times 10^{-7}$, and B_{sat} = saturation flux density.

The relative permeability of the core is the chanage in flux density (B) per change in H (amp-turns per unit length). It is nonlinear because the CT is being analyzed at high levels of excitation, the maximum permeability is used.

The point of maximum permeability can be found from the excitation curve by plotting the magnetizing impedance of the core. Divide the secondary voltage by the corresponding exciting current. The result is a plot of the magnetizing impedance. Maximum permeability occurs at the maximum impedance.

© 2006 by Taylor & Francis Group, LLC

This point will lie at or near the knee-point voltage of the excitation curve. The knee-point voltage, v_k, is at the point tangent to the 45° slope of the excitation curve.



Knowing the maximum magnetizing impedance, the maximum permeability can be calculated from the maximum inductance $L_m = X/2\pi f$ and the equation below.

The magnetizing inductance of the CT core is:

$$L_m = \frac{\mu_0 \cdot \mu_r \cdot N^2 \cdot A}{d}$$

where L_m = Henrys, N = number of turns, A = core area in m^2, d = core length in m, and $\mu_o \equiv 4 \cdot \pi \cdot 10^{-7}$ and where the permeability is

$$\mu_r \cdot \mu_0 = \frac{dB}{dH}$$

In the circuit model the value of the nonlinear magnetizing inductance of a CT is calculated from the slope of the B–H curve (dB/dH) at each level of excitation.

The saturation flux of a CT core is typically 1.8 Tesla (Wb/m^2) or about 125,000 lines per square inch. The saturation flux for a specific CT is calculated from the saturation voltage, shown as V_s on the above excitation curve.

$$B = \frac{\sqrt{2} \cdot V_s}{N \cdot A \cdot \omega}$$

where B = flux density (Webers/m^2), V_S = saturation voltage in RMS volts, and A = effective core area in meters.

CT MODE DATA

CTA Data

Secondary turns (for 1200/5 $N = 240$): $N_a \equiv 1200$ turns
Effective core area in meters sq: $A_a \equiv 0.0011\ m^2$
Length of magnetic path in meters: $d_a \equiv 0.58$ m

© 2006 by Taylor & Francis Group, LLC

Saturation voltage (RMS): $V_{sa} \equiv 600$ V
Knee-point voltage (RMS): $V_{ka} \equiv 550$ V
Excitation current at V_k: $I_{eka} \equiv 0.04$ A

Calculated values:

$$B_{sata} \equiv \frac{\sqrt{2} \cdot V_{sa}}{N_a \cdot A_a \cdot \omega} \qquad B_{sata} = 1.705\,\text{Tesla}$$

$$L_{max_a} \equiv \frac{V_{ka}}{I_{eka} \cdot \omega} \qquad L_{max_a} = 36.473\,\text{Henrys}$$

$$\mu_{a_i} \equiv \frac{L_{max_a} \cdot d_a}{N_a^2 \cdot A_a \mu_o} \qquad \mu_{a_i} = 1.063 \cdot 10^4$$

$$c_a \equiv \frac{1}{\mu_0 \cdot \mu_{a_i}} \qquad b_a \equiv \frac{[1 - (1/\sqrt{\mu_{a_i}})]}{B_{sata}} \qquad k_a \equiv \frac{N_a}{d_a}$$

CTB Data

Secondary turns (for 1200/5 $N = 240$): $N_b \equiv 1200$ turns
Effective core area in meters sq: $A_b \equiv 0.0012$ m^2
Length of magnetic path in meters: $d_b \equiv 0.55$ m
Saturation voltage (RMS): $V_{sb} \equiv 700$ V
Knee-point voltage (RMS): $V_{kb} \equiv 650$ V
Excitation current at V_k: $I_{ekb} \equiv 0.04$ A

Calculated values:

$$B_{satb} \equiv \frac{\sqrt{2} \cdot V_{sb}}{N_b \cdot A_b \cdot \omega} \qquad B_{satb} = 1.824\,\text{Tesla}$$

$$L_{max_b} \equiv \frac{V_{kb}}{I_{ekb}\omega} \qquad L_{max_b} = 43.104\,\text{Henrys}$$

$$\mu_{b_i} \equiv \frac{L_{max_b} \cdot d_b}{N_b^2 \cdot A_b \mu_0} \qquad \mu_{bi} = 1.092 \cdot 10^4$$

$$c_b \equiv \frac{1}{\mu_0 \cdot \mu_{bi}} \qquad b_b \equiv \frac{(1 - (1/\sqrt{\mu_{bi}}))}{B_{satb}} \qquad k_b \equiv \frac{N_b}{d_b}$$

Simulation of CT core inductance:

$$L_{ma}(I_1, I_2) \equiv \frac{N_a^2 \cdot A_a}{d_a} \cdot \left[\left(\frac{I_2 \cdot k_a}{c_a + b_a \cdot |k_a \cdot I_2|} - \frac{I_1 \cdot k_a}{c_a + b_a \cdot |k_a \cdot I_1|} \right) \cdot \frac{1}{(I_2 - I_1) \cdot k_a} \right]$$

$$L_{mb}(I_1, I_2) \equiv \frac{N_b^2 \cdot A_b}{d_b} \cdot \left[\left(\frac{I_2 \cdot k_b}{c_b + b_b \cdot |k_b \cdot I_2|} - \frac{I_1 \cdot k_b}{c_b + b_b \cdot |k_b \cdot I_1|} \right) \cdot \frac{1}{(I_2 - I_1) \cdot k_b} \right]$$

© 2006 by Taylor & Francis Group, LLC

CIRCUIT EQUATIONS SOLUTION

Circuit solutions are accomplished using Mathcad Solve blocks. This worksheet includes two solve blocks, one for internal faults and one for external faults. They are preceded by the statement "GIVEN." The desired solve block is chosen using the "Toggle Equation" command form the Math Menu. To solve for external faults, select the "Given" command preceding the internal fault solve block and toggle it off. Also toggle off the "FricFac" statement at the end of the unused solve block.

It is also necessary to toggle "ON" the I_d current equation for the external fault and toggle "OFF" the I_d equation for the internal fault condition.

Calculation for External Fault

Using Mathcad Solver to evaluate circuit equations

$$I_{maga_k} := 0 \qquad I_{magb_0} := 0 \qquad V_{og_0} := 0$$
$$V_0 := 0 \qquad I_{ma} := 0 \qquad I_{mb} := 0$$

■ **TOGGLE "ON" THIS "GIVEN" FOR EXTERNAL FAULT**

Given

$$V_0 = \frac{L_0 \cdot (I_{ma0} - I_{mb0}) + (R_0 \cdot \Delta t + L_0) \cdot (I_{mb} - I_{ma})}{\Delta t}$$

$$I_{ma} = I_{ma0} + \frac{R_a \cdot \Delta t \cdot (I_{s0} - I_{ma0}) + (R_a \cdot \Delta t + L_a) \cdot \Delta I_s + \Delta t \cdot V_0}{R_a \cdot \Delta t + L_a + |L_{ma}(I_{mao}, I_{ma})|}$$

$$I_{mb} = I_{mb0} + \frac{R_b \cdot \Delta t \cdot (I_{s0} - I_{mb0}) + (R_b \cdot \Delta t + L_b) \cdot \Delta I_s - \Delta t \cdot V_0}{R_b \cdot \Delta t + L_b + |L_{mb}(I_{mb0}, I_{mb})|}$$

$$V_0 = \frac{-(L_a + L_{ma}(I_{ma0}, I_{ma})) \cdot I_{ma0} - R_a \cdot \Delta t \cdot I_{s0} - (R_a \cdot \Delta t + L_a) \cdot \Delta I_s + (R_a \cdot \Delta t + L_a + L_{ma}(I_{ma0}, I_{ma})) \cdot I_{ma}}{\Delta t}$$

$$V_0 = \frac{(L_b + L_{mb}(I_{mb0}, I_{mb})) \cdot I_{mb0} + R_b \cdot \Delta t \cdot I_{s0} + (R_b \cdot \Delta t + L_b) \cdot \Delta I_s - (R_b \cdot \Delta t + L_b + L_{mb}(I_{mb0}, I_{mb})) \cdot I_{mb}}{\Delta t}$$

$$\text{FricFac}\ (I_{s0}, \Delta I_s, I_{ma0}, I_{mb0}) := \text{Minerr}\ (I_{ma}, I_{mb}, V_0)$$

■ **TOGGLE ON FOR EXTERNAL FAULT**

Calculation for Internal Fault

■ **TOGGLE "ON" THIS "GIVEN" FOR INTERNAL FAULT**

Given

$$V_0 = \frac{L_0 \cdot (I_{ma0} - I_{mb0}) + 2 \cdot R_0 \cdot \Delta t \cdot I_{s0} + (R_0 \cdot \Delta t + L_0) \cdot (2 \cdot \Delta I_s - I_{ma} - I_{mb})}{\Delta t}$$

$$I_{ma} = I_{ma0} + \frac{-R_a \cdot \Delta t \cdot I_{ma0} + R_a \cdot \Delta t \cdot I_{s0} + (R_a \cdot \Delta t + L_a) \cdot \Delta I_s + \Delta t \cdot V_0}{R_a \cdot \Delta t + L_a + |L_{ma}(I_{ma0}, I_{ma})|}$$

© 2006 by Taylor & Francis Group, LLC

$$I_{mb} = I_{mb0} + \frac{-R_b \cdot \Delta t \cdot I_{mb0} + R_b \cdot \Delta t \cdot I_{s0} + (R_b \cdot \Delta t + L_b) \cdot \Delta I_s + \Delta t \cdot V_0}{R_b \cdot \Delta t + L_b + |L_{mb}(I_{mb0}, I_{mb})|}$$

$$V_0 = \frac{-(L_a + L_{ma}(I_{ma0}, I_{ma})) \cdot I_{ma0} - R_a \cdot \Delta t \cdot I_{s0} - (R_a \cdot \Delta t + L_a) \cdot \Delta I_s + (R_a \cdot \Delta t + L_a + L_{ma}(I_{ma0}, I_{ma})) \cdot I_{ma}}{\Delta t}$$

$$V_0 = \frac{-(L_b + L_{mb}(I_{mb0}, I_{mb})) \cdot I_{mb0} - R_b \cdot \Delta t \cdot I_{s0} - (R_b \cdot \Delta t + L_b) \cdot \Delta I_s + (R_b \cdot \Delta t + L_b + L_{mb}(I_{mb0}, I_{mb})) \cdot I_{mb}}{\Delta t}$$

■ TOGGLE ON FOR INTERNAL FAULT

$$\text{FricFac}\ (I_{s0}, \Delta I_s, I_{ma0}, I_{mb0} := \text{Minerr}\ (I_{ma}, I_{mb}, V_0)$$

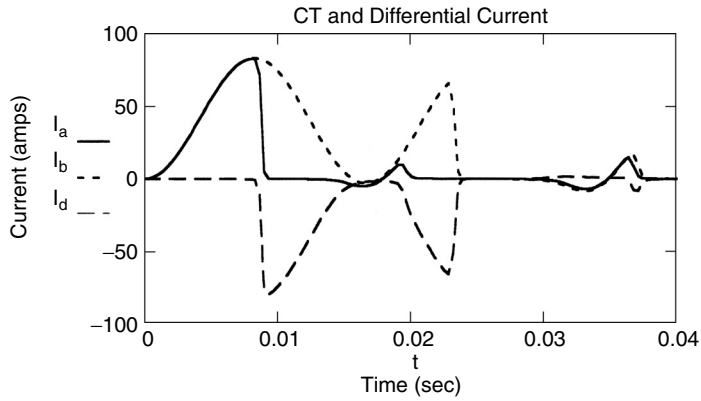
$$\begin{bmatrix} I_{magak} \\ I_{magbk} \\ V_{ogk} \end{bmatrix} := \text{FricFac}\ (I_{sok}, \Delta I_{sk}, I_{magak-1}, I_{magk-1})$$

$$I_{ak} := I_{sk} - I_{magak} \quad I_{bk} := I_{sk} - I_{magbk} \quad L_k = L_{mb}(I_{magbk}, I_{magbk-1})$$

Differential Current Equations

Turn On for External Faults $I_{d_k} := I_{magbk} - I_{magak}$

Turn On for Internal Faults $I_{d_k} := I_{ak} + I_{bk}$ ■



Filter Model Using Mathcad Programmable

A Fourier filter is assumed. The filter's output is two variables *Ys* and *Yc* which are the real and imaginary components of the harmonic being evaluated. Mathematically the two

© 2006 by Taylor & Francis Group, LLC

components are:

$$Ys = \frac{2}{sample} \cdot \sum_{n=1}^{sample-1} I_{dn} \cdot \sin(n \cdot \omega \cdot h \cdot \Delta t)$$

$$Yc = \frac{2}{sample} \cdot \left[\frac{I_{d0}}{2} + \frac{I_{dsample}}{2} + \sum_{n=1}^{sample-1} I_{dn} \cdot \cos(n \cdot \omega \cdot h \cdot \Delta t) \right]$$

$$Q := \text{floor}\left(\frac{K}{Pts_Sample} \right)$$

$Ih(I) :=$ for $n \in 0..Q$

$Isam_n \leftarrow I_{n \cdot Pts_Sample}$

$Ys \leftarrow 0$

$Yc \leftarrow 0$

$L \leftarrow sample$

for $g \in 0..L$

$S_g \leftarrow 0$

for $m \in 0..Q$

$m = 0$ if $S_m \leftarrow Isam_0$

$Y_0 \leftarrow 0$

$m > 0$ if for $j \in L..1$

$S_j \leftarrow S_{j-1}$

$S_0 \leftarrow Isam_m$

$$Ys \leftarrow \frac{2}{L} \cdot \left[\sum_{n=1}^{L-1} \left[S_n \cdot \sin\left[(n) \cdot h \cdot \omega \cdot \Delta t \cdot Pts_Sample \right] \right] \right]$$

$$Yc \leftarrow \frac{2}{L} \cdot \left[\frac{S_0}{2} + \frac{S_L}{2} + \sum_{n=1}^{L-1} S_n \cdot \cos\left[(n) \cdot h \cdot \omega \cdot \Delta t \cdot Pts_Sample \right] \right]$$

$$Y_m \leftarrow \sqrt{Ys^2 + Yc^2}$$

$$\theta_m \leftarrow \text{atan}\left(\frac{Ys}{Yc} \right)$$

for $m \in 0..Q$

$nn \leftarrow Pts_Sample \cdot m$

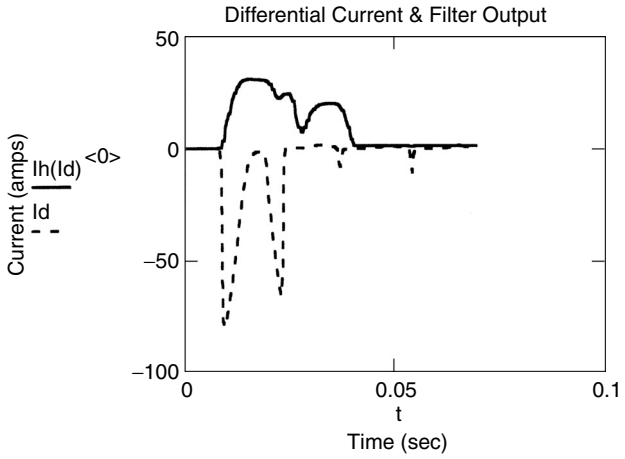
for $i \in 0.\ Pts_Sample - 1$

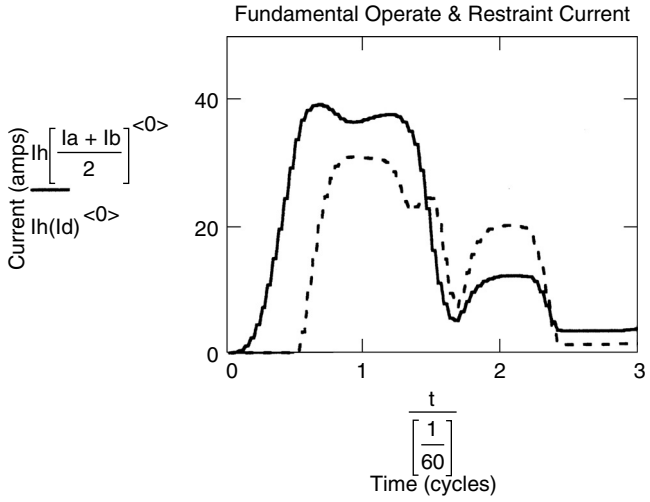
$Io_{(nn+i),0} \leftarrow Y_m$

$Io_{(nn+i),1} \leftarrow \theta_m \cdot 57.3$

Io

© 2006 by Taylor & Francis Group, LLC





© 2006 by Taylor & Francis Group, LLC

Appendix C: Dynamic and Steady State Stability Limits

The following worksheet is available for download at www.taylorandfrancis.com

© 2006 by Taylor & Francis Group, LLC

Data

	A	B	C	D	E	F	G	H	I	J	K	L	M	N	O
1					P	Q-guess		Ipo	Iqo	Eqo	Eo	Sin DELo	Cos DELo	Iqaxo	Idaxo
2					0	–0.78		0	–0.776	0.101	1.11635135	0.000	–1.000	0.000	0.776
3					0.1	–5.00		0	–5.000	6.100	1.750	0.000	–1.000	0.000	5.000
4	et =	1			0.2	–184.70		0.2	–184.704	261.279	28.706	0.000	–1.000	0.001	184.704
5	Xd =	1.48			0.3	–297.06		0.3	–297.062	420.828	45.559	0.000	–1.000	0.001	297.062
6	Xd' =	0.196			0.4	–772.88		0.4	–772.879	1096.488	116.932	0.000	–1.000	0.000	772.879
7	Xq =	1.42			0.5	–1248.10		0.5	–1248.096	1771.297	188.214	0.000	–1.000	0.000	1248.096
8	Xe =	0.15	System X		0.6	–1247.21		0.6	–1247.211	1770.040	188.082	0.000	–1.000	0.000	1247.211
9	Re =	0			0.7	–2014.61		0.7	–2014.610	2859.746	303.192	0.000	–1.000	0.000	2014.610
10	Ke =	25			0.8	–3254.82		0.8	–3254.820	4620.844	489.223	0.000	–1.000	0.000	3254.820
11					0.9	–3251.24		0.9	–3251.240	4615.761	488.686	0.000	–1.000	0.000	3251.240
12	Rsh	1E+35	Shunt load		1	–5252.42		1	–5252.416	7457.431	788.862	0.000	–1.000	0.000	5252.416
13	Xsh	0			1.1	–5245.27		1.1	–5245.266	7447.278	787.790	0.000	–1.000	0.000	5245.267
14	H =	3.09			1.2	–5237.44		1.2	–5237.440	7436.164	786.616	0.000	–1.000	0.000	5237.440
15	Tdo'=	3.59			1.3	3.41		1.3	3.414	6.132	0.525	0.633	0.774	0.212	3.647
16	Te =	0.05	Exciter TC												
17						–5									
18								Leading Vars <0							
19	Req=	0.000													
20	Xeq =	0.150													
21															
22	A=	0.543													
23															
24	Qo=	–0.78													
25															
26															
27															
28															
29															
30															
31															
32															
33															

Derivation of steady state and dynamic limits are taken from "Concepts of Synchronous Machine Stability as Affected by Excitation Control" F.P. Demello. IEEE Transactions PAS April 1969. This sheet contains data for both the manual and auto reg calculations. Enter data then first use button "Zero Syn Torque" then button "Zero Damping/Sync" to set synchronizing and damping torque's to zero thus defining the limits. The P & Q values used for this calc are taken from Columns E & F on this sheet then copied to the "auto" and "Manual" sheets. P & Q values on other sheets are not used in the calculation.

The automatic solver may not find reasonable solutions at higher power values. It may be necessary to manually enter guess values for Q in Column F and use the Excel's "Goal Seek" tool for individual rows that do not solve properly.

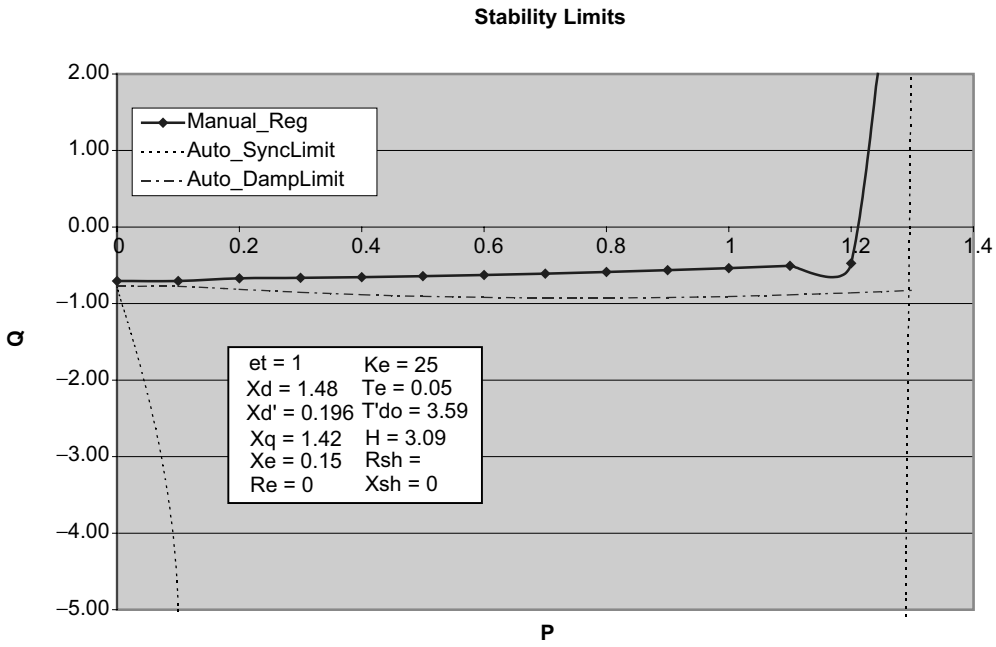
© 2006 by Taylor & Francis Group, LLC

Data (*Continued*)

	P	Q	R	S	T	U	V	W	X	Y	Z	AA	AB	AC	AD	AE
1	eqo	edo		K1	K2	K3	K4	K5	K6		Nat Freq	Denom		Damp Num	Sync	Damp
2	–1.000	0.000		–0.07214293	0.0000	0.2123	0.0000	0.0000	–0.4335		0	1.691595		0	–0.07214	0
3	–1.000	0.000		–6.7994	0.0000	0.2123	0.0000	0.0000	–0.4335		0	1.691595		0	–6.79936	0
4	–1.000	0.001		–4777.1751	0.0035	0.2123	0.0045	–0.0275	–0.4335		0	1.691592		0	–4777.18	0
5	–1.000	0.001		–12211.8536	0.0032	0.2123	0.0042	–0.0411	–0.4335		0	1.691592		0	–12211.9	0
6	–1.000	0.001		–81665.2429	0.0017	0.2123	0.0021	–0.0545	–0.4335		0	1.691595		0	–81665.2	0
7	–1.000	0.000		–212346.2102	0.0013	0.2123	0.0016	–0.0680	–0.4335		0	1.691595		0	–212346	0
8	–1.000	0.000		–212045.8154	0.0015	0.2123	0.0020	–0.0816	–0.4335		0	1.691595		0	–212046	0
9	–1.000	0.000		–552261.6810	0.0011	0.2123	0.0014	–0.0951	–0.4335		0	1.691595		0	–552262	0
10	–1.000	0.000		–1439887.1794	0.0008	0.2123	0.0010	–0.1086	–0.4335		0	1.691595		0	–1439887	0
11	–1.000	0.000		–1436724.7143	0.0009	0.2123	0.0011	–0.1222	–0.4335		0	1.691595		0	–1436725	0
12	–1.000	0.000		–3747061.6235	0.0006	0.2123	0.0008	–0.1357	–0.4335		0	1.691595		0	–3747062	0
13	–1.000	0.000		–3736873.4877	0.0007	0.2123	0.0009	–0.1493	–0.4335		0	1.691595		0	–3736873	0
14	–1.000	0.000		–3725736.1197	0.0007	0.2123	0.0009	–0.1629	–0.4335		0	1.691595		0	–3725736	0
15	0.954	0.301		1.8377	0.9620	0.2123	1.2352	–0.0691	0.4134		10.58802	75.08682		3.5257927	1.820977	–0.00959
16																
17																
18																
19						et = 1	Ke = 25									
20						Xd = 1.48	Te = 0.05									
21						Xd' = 0.196	H = 3.09									
22						Xq = 1.42	T'do = 3.59									
23						Xe = 0.15										
24						Re = 0										
25						Rsh =										
26						Xsh = 0										
27																
28																
29																
30																
31																
32																
33																

© 2006 by Taylor & Francis Group, LLC

Chart 1



Manual Reg

	A	B	C	D	E	F	G	H	I	J	K	L	M
1			P	Q		K1–K2K3K4							
2			0	–0.70		–0.00061							
3			0.1	–0.70		–0.00042							
4			0.2	–0.67		0.000157							
5			0.3	–0.66		2.24E–05							
6			0.4	–0.65		4.44E–06							
7			0.5	–0.64		–3.7E–06							
8			0.6	–0.63		–1E–05							
9			0.7	–0.61		–1.5E–05							
10			0.8	–0.59		–2E–05							
11			0.9	–0.56		–2.4E–05							
12			1	–0.54		–2.7E–05							
13			1.1	–0.51		–3.1E–05							
14			1.2	–0.47		–3.5E–05							
15			1.3	6.43		0.000839							
16													
17													
18													
19													
20													
21													
22													
23													
24													
25													
26													
27													
28													
29													

Zero Sync Torque

The steady state limit with the manual regulator in service is defined by the synchronizing power coefficient K1–K2*K3*K4. The limit is reached when K1–K2*K3*K4 =0

Use Zero Sync Torque button to set sync torque to zero. Columns C and D give steady state limit.

© 2006 by Taylor & Francis Group, LLC

Sheet 1

	A	B	C	D	E	F	G	H	I	J	K	L
1	et =	0.95	Manual	P	Q		Auto	P	Q–Syn=0	Auto	P	Q–Damp=0
2	Xd =	1.48		0	–0.63619		SSLIM	0	–0.63558	dynam	0	–1
3	Xd' =	0.196		0.1	–0.61007			0.1	–0.86624		0.1	–1
4	Xq =	1.42		0.2	–0.6039			0.2	–0.99547		0.2	–1.09718
5	Xe =	0.15		0.3	–0.59616			0.3	–1.09539		0.3	–1.25733
6	Re =	0		0.4	–0.58579			0.4	–1.17788		0.4	–1.31
7	Ke =	30		0.5	–0.57256			0.5	–1.2472		0.5	–0.77201
8				0.6	–0.55507			0.6	–1.30665		0.6	–0.77299
9	Rsh	1E+35		0.7	–0.53505			0.7	–1.35765		0.7	–0.76616
10	Xsh	0		0.8	–0.51181			0.8	–1.40138		0.8	–0.75157
11	H =	3.09		0.9	–0.48527			0.9	–1.43861		0.9	–0.72909
12	Tdo'=	3.59		1	–0.45536			1	–1.47025		1	–0.69847
13	Te =	0.05		1.1	–0.42197			1.1	–1.49663		1.1	–0.65929
14				1.2	–0.385			1.2	–1.51759		1.2	–0.61089
15				1.3	–0.34443			1.3	–1.53408		1.3	–0.55236
16												
17												
18	et =	1	Manual	P	Q		Auto	P	Q–Syn=0	Auto	P	Q–Damp=0
19	Xd =	1.48		0	–0.70482		SSLIM	0	–0.70439	dynam	0	–1
20	Xd' =	0.196		0.1	–0.67694			0.1	–0.94469		0.1	–1
21	Xq =	1.42		0.2	–0.67078			0.2	–1.08051		0.2	–1.18939
22	Xe =	0.15		0.3	–0.66277			0.3	–1.18634		0.3	–1.31
23	Re =	0		0.4	–0.65394			0.4	–1.27429		0.4	–0.8441
24	Ke =	30		0.5	–0.64161			0.5	–1.34925		0.5	–0.85783
25				0.6	–0.6266			0.6	–1.41404		0.6	–0.8642
26	Rsh	1E+35		0.7	–0.60887			0.7	–1.47044		0.7	–0.86345
27	Xsh	0		0.8	–0.58838			0.8	–1.51955		0.8	–0.85572
28	H =	3.09		0.9	–0.56368			0.9	–1.56225		0.9	–0.84102
29	Tdo'=	3.59		1	–0.53689			1	–1.59917		1	–0.81926
30	Te =	0.05		1.1	–0.50704			1.1	–1.63099		1.1	–0.79025
31				1.2	–0.47405			1.2	–1.65792		1.2	–0.75367
32				1.3	–0.43785			1.3	–1.68019		1.3	–0.70907
33												
34												
35	et =	0.95	Manual	P	Q		Auto	P	Q–Syn=0	Auto	P	Q–Damp=0
36	Xd =	1.48		0	–0.63558		SSLIM	0	–0.63561	dynam	0	–1
37	Xd' =	0.196		0.1	–0.60874			0.1	–0.82272		0.1	–1
38	Xq =	1.42		0.2	–0.59884			0.2	–0.92518		0.2	–1.0128
39	Xe =	0.295		0.3	–0.58549			0.3	–1.00113		0.3	–1.11
40	Re =	0		0.4	–0.56577			0.4	–1.0605		0.4	–1.28874
41	Ke =	30		0.5	–0.54045			0.5	–1.10693		0.5	–1.31
42				0.6	–0.50905			0.6	–1.14315		0.6	–1.31
43	Rsh	1E+35		0.7	–0.47126			0.7	–1.17061		0.7	–1.41523
44	Xsh	0		0.8	–0.42667			0.8	–1.1902		0.8	–0.48286
45	H =	3.09		0.9	–0.37474			0.9	–1.20275		0.9	–0.40142
46	Tdo'=	3.59		1	–0.31332			1	–1.20835		1	–0.29491
47	Te =	0.05		1.1	–0.2435			1.1	–1.2078		1.1	–0.14889
48				1.2	–0.16309			1.2	–1.20121		1.2	0.088974
49				1.3	–0.07023			1.3	–1.18885		1.3	5.063517
50												
51												
52	et =	1	Manual	P	Q		Auto	P	Q–Syn=0	Auto	P	Q–Damp=0
53	Xd =	1.48		0	–0.70421		SSLIM	0	–0.70473	dynam	0	–1
54	Xd' =	0.196		0.1	–0.67509			0.1	–0.90018		0.1	–1
55	Xq =	1.42		0.2	–0.66618			0.2	–1.00874		0.2	–1.11
56	Xe =	0.295		0.3	–0.6536			0.3	–1.09057		0.3	–1.29667
57	Re =	0		0.4	–0.63609			0.4	–1.1554		0.4	–1.31
58	Ke =	30		0.5	–0.61348			0.5	–1.20751		0.5	–0.71377
59				0.6	–0.58569			0.6	–1.24948		0.6	–0.68586
60	Rsh	1E+35		0.7	–0.5514			0.7	–1.28274		0.7	–0.64708
61	Xsh	0		0.8	–0.51168			0.8	–1.30829		0.8	–0.59627
62	H =	3.09		0.9	–0.46564			0.9	–1.32685		0.9	–0.53154
63	Tdo'=	3.59		1	–0.41279			1	–1.33909		1	–0.4499
64	Te =	0.05		1.1	–0.35222			1.1	–1.34498		1.1	–0.34605
65				1.2	–0.28348			1.2	–1.34526		1.2	–0.20935
66				1.3	–0.20669			1.3	–1.34002		1.3	–0.01058
67												
68												
69												
70	1		Manual	P	Q		Auto	P	Q–Syn=0	Auto	P	Q–Damp=0
71	1.48			0	–0.70472		SSLIM	0	–0.70521	dynam	0	–1
72	0.196			0.1	–0.67398			0.1	–0.87303		0.1	–1
73	1.42			0.2	–0.66117			0.2	–0.96342		0.2	–1.09758
74	0.47	System X		0.3	–0.64347			0.3	–1.02817		0.3	–1.20502
75	0			0.4	–0.6181			0.4	–1.07653		0.4	–1.31
76	30			0.5	–0.58357			0.5	–1.11192		0.5	–1.31
77				0.6	–0.54089			0.6	–1.13671		0.6	–1.31
78	1E+35	Shunt load		0.7	–0.48861			0.7	–1.1523		0.7	–0.51302
79	0			0.8	–0.4255			0.8	–1.15929		0.8	–0.41477
80	3.09			0.9	–0.34982			0.9	–1.15852		0.9	–0.27523
81	3.59			1	–0.25626			1	–1.15034		1	–0.03068
82	0.05	Exciter TC		1.1	–0.14304			1.1	–1.13488		1.1	2.891
83				1.2	0.00156			1.2	–1.11258		1.2	2.028496
84				1.3	0.199542			1.3	–1.08376		1.3	3.10856

© 2006 by Taylor & Francis Group, LLC

Auto

	A	B	C	D	E	F	G	H	I	J	K	L	M	N
1			P	Q		D	f(damp)		T_sync	T_dam		Q-Damp=0	Q-Syn=0	Min Q
2			0	–0.77568		1.691595	0		–3E-75	0		–0.78	–0.78	–0.77568
3			0.1	–0.77568		1.691595	0		–1.1E-71	0		–0.78	–5.00	–0.77568
4			0.2	–0.81496		1.691592	0		–0.00072	0		–0.81	–184.70	–0.81496
5			0.3	–0.85391		1.691592	0		–0.001	0		–0.85	–297.06	–0.85391
6			0.4	–0.88382		1.691595	0		–0.00068	0		–0.88	–772.88	–0.88382
7			0.5	–0.90557		1.691595	0		–0.00065	0		–0.91	–1248.10	–0.90557
8			0.6	–0.91974		1.691595	0		–0.00094	0		–0.92	–1247.21	–0.91974
9			0.7	–0.92676		1.691595	0		–0.00079	0		–0.93	–2014.61	–0.92676
10			0.8	–0.9269		1.691595	0		–0.00064	0		–0.93	–3254.82	–0.9269
11			0.9	–0.9203		1.691595	0		–0.00081	0		–0.92	–3251.24	–0.9203
12			1	–0.90701		1.691595	0		–0.00062	0		–0.91	–5252.42	–0.90701
13			1.1	–0.88698		1.691595	0		–0.00075	0		–0.89	–5245.27	–0.88698
14			1.2	–0.86009		1.691595	0		–0.0009	0		–0.86	–5237.44	–0.86009
15			1.3	3.413651		75.08682	3.525792687		–8.4E-05	–0.009588633		–0.83	3.41	3.413651
16														
17														
18						Zero Damping/ Sync								
19														
20														
21														
22														
23														
24														
25														
26														
27														
28														
29														
30														
31														
32														
33														

$$\Delta T_{sync}(Fld) = -\frac{\left\{k_4 + k_e\left[k_5 + (k_4 + k_5 k_e)k_6 k_3\right]\right\}k_3 k_2}{(k_6 k_3 k_e + 1)^2}\Delta\delta$$

$$f(damp) = \{T_e[(-K_4 K_3 T_e T'_{do}\omega_n^2) + (-k_5 + K_6 K_4 K_3)K_e] - (k_4 + K_5 K_e)K_3 T'_{do}\}\omega_n$$

$$D = (-K_3 T_e T'_{do}\omega_n^2 + K_6 K_3 K_e + 1)^2 + (T_e + K_3 T'_{do})^2\omega_n^2$$

$$\Delta T_{damp} = -\frac{K_2 K_3\left[f(famp)\right]}{D}\Delta\delta$$

When the auto regulator is in service the field induced portion of the synchronizing torque becomes more positive as regulator gain increases (Ke). This maintains positive synchronizing torque for higher leading PF. But the increase in gain reduces the damping torque hence the system will become unstable due to increasing oscillations. The result is that steady state stability is no longer the operational limit. Dynamic stability now limits operation in the leading mode. The dynamic stability limit is defined by zero damping torque. Use "Zero Damping/Sync button to set Tsync and Tdamp to zero.

Columns L and M give steady state and dynamic limiting values of Q for the auto regulator.

© 2006 by Taylor & Francis Group, LLC

Appendix D: Swing Impedance Locus Calculation Using Excel®

The following describes an Excel workbook that will calculate swing impedance trajectories. This workbook is available for download at www.taylorandfrancis.com. The workbook is intended for the representation of one or two generators that are electrically distant from other machines as shown on the "Input" sheet.

The workbook has nine worksheets.

- *"Input" sheet:* This is the entry point for all data required for the swing calculation. On the download sheet all data entry locations are shown in gray. Data relating to the out-of-step relay setting is entered on the "Set_GA" and "Set_GB" sheets.
- *"Initial" sheet:* All initial conditions are calculated on this sheet. This includes prefault, faulted and postfault network admittances. The sheet contains a macro-powered button to calculate initial internal generator currents, voltages, along with the initial rotor angles.
- *"GenA" and "GenB" sheets:* These sheets calculate internal generator parameters including the impedance locus for each machine on the system MVA base.
- *"Network" sheet:* This sheet solves the network equations for generator and system currents. It also resolves the generator currents into their d- and q-axes components.
- *"Set_GA" and "Set_GB" sheets:* Out-of-step relay setting data is entered on these sheets. These sheets convert the impedance locus calculated on the "GenA" and "GenB" sheets to per unit values on the generator's base MVA. These sheets also calculate the points needed to plot the out-of-step relay characteristic for each generator on that generator's base MVA.
- *"Plot GA" and "Plot GB" sheets:* this sheets plot the swing impedance against out-of-step and loss-of-field relay characteristics

A printout of the "Input" and "GA Plot" sheets are attached.

Before the spreadsheet can be run, the following Excel features must be activated.

Add-ins (under the "Tools" menu)
Solver
Analysis ToolPack (contains complex math functions)
Iteration (a calculation option under "Preferences" on the "Tools" menu)
Solver.xls (retrieved from "Library" folder in "Office" folder). Solver.xls is accessed via "References" under the Visual Basic "Tools" menu

SOME TIPS ON USING THE WORKBOOK

Depending on the computer the macro associated with the "Initialize" button may run very slowly if used with the complete notebook. Speed is dramatically improved if a copy of the workbook is made and all but the "Input" and "Initial" sheets are deleted from the copy. With the real notebook closed, use this "Initialize" button in the copy workbook to establish the initial angles. Then cut and

© 2006 by Taylor & Francis Group, LLC

past these angles (Cells I:14, 1:16) of the "Initialize" sheet into the real workbook. Do not forget to make the input data change that necessitated the initialization in the real notebook first.

The sheets are set up for two generators. If only one generator is to be simulated, enter a large value for transformer impedance (Xtrb = 400), inertia (H = 60) and the exciter time constant (Te = 70) of the machine not being modeled.

BACKGROUND ON CALCULATIONS

The equations used in the workbook are taken from Kimbark's texts.[1,2] Calculation of the swing locus involves the solution of three categories of equations. The network equations determine the current in each machine, based on network impedance, rotor position, and the internal voltage magnitude of each generator. Note that the rotor angle denotes the position of the generator's q-axis. The machine equations determine the instantaneous power output and internal voltage magnitude as a function of generator current, rotor position and time. Swing equations relate the change in rotor angle to generator instantaneous output power and time.

Network Equations (on "Network" Sheet)

The basic network equations used are from Ref. 1 and are shown below.

$$I_a = Y_{aa} eh_a \angle \delta_a + Y_{ab} eh_2 \angle \delta_b + Y_{as} eh_s \angle \delta_s$$
$$I_b = Y_{ab} eh_a \angle \delta_a + Y_{bb} eh_b \angle \delta_b + Y_{bs} eh_s \angle \delta_s$$
$$I_s = Y_{as} eh_a \angle \delta_a + Y_{bs} eh_b \angle \delta_b + Y_{ss} eh_s \angle \delta_s$$

where I_a, I_b = generator currents, I_s = system current, eh_a, eh_b = equivalent generator internal voltage, $\angle\delta_a$, $\angle\delta_b$, and $\angle\delta_s$ = angle of respective voltage (rotor and q-axis angle).

The self-admittances Y_{aa}, Y_{bb}, and Y_{ss} and mutual admittances Y_{ab}, Y_{as}, and Y_{bs} must be derived for prefault, faulted and postfault conditions. All the elements in the above equation are complex.

A detailed explanation of the derivation and use of network admittances is given in Ref. 1, beginning on page 81.

The first step in the solution is to establish initial (prefault) network and generator parameters, including initial rotor angles. These values are calculated from initial MW load and operating voltage of the system and each unit along with the prefault network admittances. A calculation demonstrating the derivation of initial generator d- and q-axes components was presented in Chapter 2 in Section 2.9.1. The "Initial" worksheet includes a macro-powered button to solve for the initial conditions. Initial conditions must be recalculated using the "Initialize" button each time generator loading, terminal voltage or system prefault impedance are changed.

Once these steady-state parameters are established the workbook uses the iterative solver to satisfy conditions at each time step. The network admittances used at a given time step are set by the "status" column of the "Network" sheet. The status cell indicates prefault, faulted, or postfault conditions, as dictated by the times entered in the "fault on" and "fault off" cells of the "Input" sheet.

The equivalent internal generator voltage used in the network equations, E_n, is a hypothetical voltage inside the generator defined behind an arbitrary reactance X_h.

$$e_h = e_t + IX_h$$

Within the generator, e_h must be defined in terms of the e'_q and e'_d. These voltages represent the field flux linkages that are assumed to be constant during each interval of the solution of the generator equations. Because the terminal voltage is composed of a q-axis component e_{qt} and a d-axis

© 2006 by Taylor & Francis Group, LLC

component e_{dt} as defined below,

$$e_{qt} = e'_q - I_d X'_d \qquad e_{dt} = e'_d + I_q X'_q$$

e_h can then be defined as

$$e_{qh} = e'_q + I_d(X_h - X'_d) \qquad e_{dh} = e'_d + I_q(X'_q - X_h)$$

The value of X_h is arbitrary; for the workbook, X_h has been set equal to X_d; thus, e_h becomes

$$e_{qh} = e'_q + I_d(X_d - X'_d) \qquad e_{dh} = e'_d + I_q(X'_q - X_d)$$

and

$$e_h = \sqrt{e_{qh}^2 + e_{dh}^2}$$

Note, because internal voltage e_h is defined as the voltage behind X_d, the circuit admittances must include X_d as the internal impedance for each generator.

The solution to the network equation yields the current at each generator. These currents must be resolved into their d- and q-axes components for use in the generator equations. The axis components are a function of the angle between the current and the q-axis (rotor) and are resolved as follows:

$$I_q = \text{Real}\left(\frac{I_a \angle \theta_a}{1 \angle \delta_a}\right) \qquad I_d = \text{Imag}\left(\frac{I_a \angle \theta_a}{1 \angle \delta_a}\right)$$

where $\angle\theta_a$ = angle of current from network equations and $\angle\delta_a$ = rotor angle (q-axis).

Generator Equations ("Gen A" and "Gen B" Worksheets)

The generator equations are taken from Kimbark, Volumes I and III, and are in incremental form. These equations are listed below. The (n) designation defines a value at the end of interval "n," while (o) designates a value at the beginning of the same interval. An (av) indicates a value at the midpoint of the interval.

Columns D and P

$\Delta\delta$ is the change in rotor angle and angle of the q-axis

$$\Delta\delta(n) = \Delta\delta(o) + \frac{\Delta t^2}{M} P_{ACC}(o)$$

M = Inertial Constant (MegJoules-sec)

$$= \frac{H * \text{MVA}_{gen}}{\pi f * \text{MVA}_{sys}}$$

H = generator inertia constant on the generator MVA base (MVA_{gen})

© 2006 by Taylor & Francis Group, LLC

Columns E and F

$\Delta P_{Mec}Gov$ is the mechanical output of the turbine. The simple governor shown at the bottom of the "input" sheet controls the mechanical output of the turbine as a function of speed (ω). Solving the block diagram the Lapace expression for the transfer function is:

$$\frac{\Delta P_{Mec}Gov(s)}{\Delta\omega(s)} = \frac{1+sT_2}{(1+sT_1)(1+sT_3)R}$$

The response to a step function would be:

$$\Delta P_{Mec}Gov(s) = \frac{1+sT_2}{(1+sT_1)(1+sT_3)R}\frac{\Delta\omega(s)}{s}$$

The time domain equivalent function is then:

$$\Delta P_{Mec}Gov = \left(1+\frac{T_1-T_2}{T_3-T_4}e^{t/T_1} - \frac{T_3-T_2}{T_3-T_1}e^{-t/T_1}\right)\frac{\Delta\omega}{R}$$

In incremental form, the slope at the beginning of the interval is approximately equal to the time coefficient in the exponent.

$$\Delta P_{Mec}Gov_n = \left[1+\left(\frac{T_1-T_2}{T_3-T_1}\right)\frac{\Delta t}{T_1} - \left(\frac{T_3-T_2}{T_3-T_1}\right)\frac{\Delta t}{T_3}\right]\frac{1}{R}$$

The "If" statement in Column F prevents negative power output.

Columns G and V

e'_q is the voltage behind X'_d'.

$$\begin{aligned} e'_q(n) &= e'_q(n) + \Delta e'_q \\ &= \frac{E_{fd}(av) - EI(n)}{T'_{d0} + \left(\frac{EI(n)}{e'_q}\right)\Delta t/2} \end{aligned}$$

Columns H and X

e'_d is the voltage behind X'_q

$$e'_d(n) = e'_{d(0)} - \frac{EI(n)\Delta t}{T'_{q0} + \left(\frac{EI(n)}{e'_{d(n)}}\right)\frac{\Delta t}{2}}$$

Columns I and J

I_q and I_d are the d and q-axis component currents. These component currents are derived on the "network" worksheet using the network equations as described above.

© 2006 by Taylor & Francis Group, LLC

Columns L and M

e_{qt}, e_{dt} are the d and q-axis components of the terminal voltage.

$$e_{qt} = e'_q - I_d X'_d \qquad e_{dt} = e'_d + I_q X'_q$$

Column N

P_e = electrical power

$$P_e = e_{qt} I_q + e_{dt} I_d$$

Column O

P_{acc} = accelerating power. Accelerating power is the difference between the mechanical power input to the generator and the electrical power (P_e) taken by the electrical system.

The accelerating power is equal to:

$$P_{acc} = P_M - P_e$$

At points of discontinuity such as where the fault is applied or cleared the accelerating power is taken as the average power for the instant before and after the discontinuity.

$$P_{acc}(n) = \frac{P_{acc}(o) + P_{acc}(n)}{2}$$

Column R

e_t = the magnitude of generator terminal voltage

$$e_t = \sqrt{e_{qt}^2 + e_{dt}^2}$$

Column S

E_I = the voltage behind Xd

$$E_I = e'_q + I_d(X_d - X'_d)$$

Column T

Δe_{fd} = change in field voltage

$$\Delta e_{fd}(n) = [et_{set} - et(av)]K_e \frac{\Delta t}{T_e + \frac{\Delta t}{2}}$$

e_t (set) equals the voltage regulator set point. This is taken as the initial terminal voltage from the "input" sheet.

Column U

E_{fd} = Voltage applied to field by excitation system

$$E_{fd}(n) = E_{fd}(o) + \Delta e_{fd}$$

© 2006 by Taylor & Francis Group, LLC

The field voltage is constrained by the $E_{fd}(max)$ and $E_{fd}(min)$ settings on the "input" sheet. The maximum limit should be set equivalent on the per-unit ceilin voltage. The minimum limit is usually set at 0. If a value of less than 0 is used to allow simulation of agbridge rectifier applying negative voltage to the field (inverting), the workbook contains no mechanism to preclude the calculation of negative field current a condition that can not actually exist.

Column W

E_d = The voltage behind X_q

$$E_d = e'_d + I_q(X'_q - X_q)$$

Column Z

e_t = Generator terminal voltage in complex form.

Column AA

I_t = Generator current

$$I_t = \sqrt{I_d^r + I_q^2}$$

Columns AB

Z = Complex swing impedance locus

$$Z = \frac{e_t\angle}{I_t\angle}$$

Columns AC and AD

R,X = real and reactive components of Z

$$R = \mathrm{Re}al(Z) \qquad X = \mathrm{Im}ag(Z)$$

REFERENCES

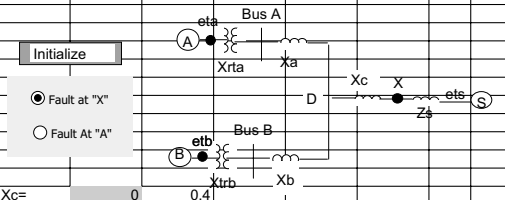
1. Kimbark, E.W., *Power System Stability, Vol. I, Elements of Stability Calcualtions*, John Wiley & Sons, Inc., New York, 1948.
2. Kimbark, E.W., *Power System Stability, Vol. III, Synchronous Machines*, John Wiley & Sons Inc., New York, 1956.

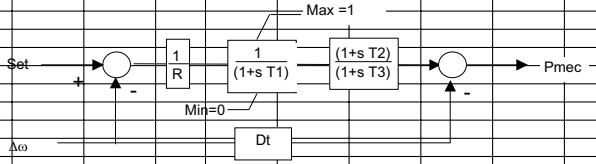
The following are selected sheets from the Swing Locus Spreadsheet.

© 2006 by Taylor & Francis Group, LLC

Input

	A	B	C	D	E	F	G	H	I	J	K	L	M	N	O	P	Q	R
1	Read First																	
2	Fault on=	0	sec.		Δt =	0.01	sec.											
3	Fault off =	0.25	sec.															
4																		
5	Initial System		MVA Base =		100													
6																		
7	eta =	1		etb =	1													
8	Pa =	0.88		Pb =	0													
9																		
10	Xtra =	0.07		Xtrb =	400													
11	Xa =	0		Xb =	0													
12	Ra =	0		Rb =	0													
13																		
14	ets =	1.01		Xs =	0.078		Xc=	0	0.4									
15	Xs =			Rs =	0		Rc=	0	0.3									
16	Rs =								-0.4									
17																		
18	System Z with Fault cleared (on System MVA base)																	
19	Xtra =	0.07		Xtrb =	400		Xs =	0.078		Xc=	0							
20	Xa =	0		Xb =	0		Rs =	0		Rc=	0							
21	Ra =	0		Rb =	0													
22																		
23	GenA																	
24	MVA base =	104		Ha =	3		Tdo'=	3.59	sec	R=	0.04				On 100 MVA Base			
25	Xd =	1.48		Te =	100		Tqo'=	0.31	sec	T1=	0.5	sec			Xd =	1.423077	Ma=	0.016552
26	Xd' =	0.196		ke=	20					T2=	2.1	sec			Xd' =	0.188462		
27	Xq =	1.42		Efdmax	4					T3=	7	sec			Xq =	1.365385		
28	Xq' =	0.464		Efdmin	0										Xq' =	0.446154		
29	Gen B																	
30	MVA base =	50		Hb =	60		Tdo'=	6.1	sec	R=	0.04				On 100 MVA Base			
31	Xd =	2.1		Te =	70		Tqo'=	0.27	sec	T1=	0.5	sec			Xd =	4.2	Mb =	0.159155
32	Xd' =	0.17		ke=	20					T2=	2.1	sec			Xd' =	0.34		
33	Xq =	1.83		Efdmax	2.2					T3=	7	sec			Xq =	3.66		
34	Xq' =	0.2		Efdmin	0										Xq' =	0.4		
35																		
36																		
37	Governor																	
38																		
39																		
40																		
41																		
42																		
43																		
44																		
45																		
46																		
47																		
48																		
49																		
50																		
51																		
52																		
53																		
54																		
55																		





R = Droop or 1/gain

T1 = Steam Bowl Time Constant 0.5sec typical

T2 = Numerator Time Constant 2.1 sec typical

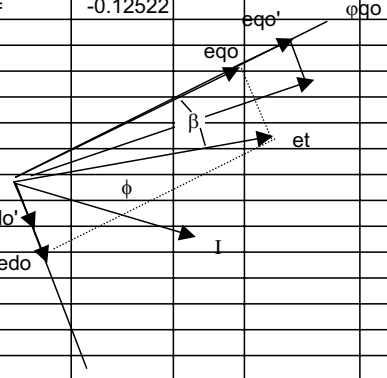
T3 = Reheater Time Constant 7.0 sec typical

Dt = Turbine Damping Coefficient, 0 typical

© 2006 by Taylor & Francis Group, LLC

Initial

	A	B	C	D	E	F	G	H	I	J	K	L	M	N
1														
2	Normal System						Mag	Ang						
3		ZaD=	7E-002i		Yab(-yab)=	1.31744605	0.001317	1.5707963						
4		ZbD=	400i		Yas(-yas)=	6.75613364	6.756134	1.5707963						
5		ZsD=	7.8E-002i		Ybs(-bs)=	1.18232338	0.001182	1.5707963						
6		Znum=	-59.20546		Yaa=	-6.7574510	6.757451	-1.570796						
7					Ybb=	-2.4997694	0.0025	-1.570796						
8					Yss=	-6.7573159	6.757316	-1.570796						
9														
10														
11														
12	Solved initial Network													
13					Data	Calc			calc(rad)	deg				
14	eta =	1		Pa=	0.88	0.88		δa =	0.129311	7.409				
15	etb =	1		Pb =	0	3.611E-08		δb =	0.067848	3.887				
16	ets =	1.01		Ps =		-0.88		δs =	0	0				
17					Sum	1.887E-15								
18								Qa=	0.010588					
19			Leading Vars +,Lagging Vars -					Qb=	6.59E-06					
20								Qs=	-0.12522					
21														
22														
23	Initial Generator A			Initial Generator B										
24														
25	Ira =	0.88		Irb =	0									
26	Ixa =	-0.01059		Ixb =	-6.6E-06									
27	Iao=	0.880064		Ibo=	6.59E-06									
28	ϕao=	-0.68934		ϕbo=	-90									
29	β oa =	49.82566		β ob =	0									
30	eqo =	0.645116		eqo =	1									
31	edo=	0.764085		edo=	0									
32	Ido=	0.679225		Ido=	6.59E-06									
33	Iqo=	0.559612		Iqo=	4.04E-22									
34	eqo'=	0.773123		eqo'=	1.000002									
35	edo'=	0.514412		edo'=	-1.6E-22									
36														



© 2006 by Taylor & Francis Group, LLC

Initial (*Continued*)

	A	B	C	D	E	F	G	H	I	J	K	L	M	N
37	φ qo=	57.23461		φ qo=	3.887415									
38	ehq=	0.418414660313362+0.650114591258489j												
39	ehd=	0.432565937238708-0.278400042279472j												
40	eh =	0.85098059755207+0.371714548979017j					0.514412							
41														
42														
43	Network Bus X Faulted +Xd						Network Bus A Faulted +Xd							
44	ZaD=	1.49307692307692j					ZAD=	0						
45	ZbD=	404.2j					ZbD=	404.2j			Fault on X	1		
46	ZxD=	7.8E-002j					ZsD=	7.8E-002j						
47	Znum=	-635.145752307691					Znum=	-31.5276			Used on Network Sheet			
48														
49	Yab(-yab)=	1.22806457756508E-		0.0001	1.570796		Yab(-yab)=	0			Yab(-yab)=	1.22806457756508E-004j		
50	Yas(-yas)=	0		0			Yas(-yas)=	0			Yas(-yas)=	0		
51	Yaf(-yaf)=	0.636389361861289j		0.6364	1.570796		Yaf(-yaf)=	0.66975785677486j			Yaf(-yaf)=	0.66975785677486j		
52	Ybs(-bs)=	0		0			Ybs(-bs)=	0			Ybs(-bs)=	0		
53	Ybf(-ybf)=	2.35076266770593E-		0.0024	1.570796		Ybf(-ybf)=	2.4740227610094E-003j			Ybf(-ybf)=	2.4740227610094E-003j		
54	Ysf(-Ysf)=	12.8205128205128j		12.821	1.570796		Ysf(-Ysf)=	12.8205128205128j			Ysf(-Ysf)=	12.8205128205128j		
55	Yaa=	-0.636512168319046j		0.6365	-1.5708		Yaa=	-0.66975785677486j			Yaa=	-0.66975785677486j		
56	Ybb=	-2.47356912546244E		0.0025	-1.5708		Ybb=	-2.4740227610094E-003j			Ybb=	-2.4740227610094E-003j		
57	Yss=	-12.8205128205128j		12.821	-1.5708		Yss=	-12.8205128205128j			Yss=	-12.8205128205128j		
58	Yff=	-13.4592529450418j		13.459	-1.5708		Yff=	-13.4927447000487j			Yff=	-13.4927447000487j		
59														
60														
61														
62	Fault cleared +Xd													
63	ZAD=	1.49307692307692j												
64	ZbD=	404.2j												
65	ZsD=	7.8E-002j												
66	Znum=	-635.145752307691												
67														
68	Yab(-yab)=	1.22806457756508E-004j												
69	Yas(-yas)=	0.636389361861289j												
70	Yaf(-yaf)=	0												
71	Ybs(-bs)=	2.35076266770593E-003j												

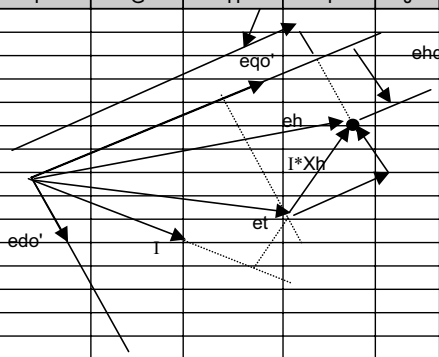
ehq = eqo'+(Xh-Xd')*Id @ φqo

(*continued*)

© 2006 by Taylor & Francis Group, LLC

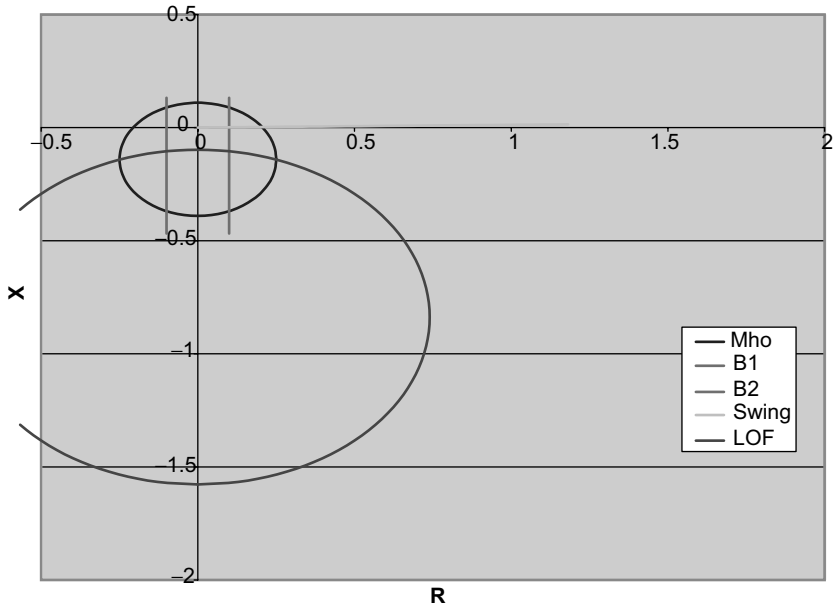
Initial (*Continued*)

	A	B	C	D	E	F	G	H	I	J	K	L	M	N
72	Ybf(-ybf)=	0												
73	Ysf(-Ysf)=	0												
74	Yaa=	-0.636512168319046j												
75	Ybb=	-2.47356912546244E-003j												
76	Yss=	-0.638740124528995j												
77	Yff=	0												
78														
79														
80														
81	Normal System + Xd													
82		ZaD=	1.49307692307692j											
83		ZbD=	404.2j											
84		ZsD=	7.8E-002j											
85		Znum=	-635.145752307691											
86				Mag										
87		Yab(-yab)=	1.2280645	0.0001										
88		Yas(-yas)=	0.6363893	0.6364										
89		Yaf(-yaf)=	0	0										
90		Ybs(-bs)=	2.3507626	0.0024										
91		Ybf(-ybf)=	0	0										
92		Ysf(-Ysf)=	0	0										
93		Yaa=	-0.636512	0.6365										
94		Ybb=	-2.473569	0.0025										
95		Yss=	-0.638740	0.6387										
96		Yff=	0	0										
97														
98														
99	Governor													
100		Pmec= (Set-DW)*[1+(T1-T2)e^ -t/T1/(T3-T2)-(T3-T2)e^ -t/T3/(T3-T1)]/R												
101														
102	GenA													
103		(T1-T2)/(T3-T1)=		-0.2462										
104		(T3-T2)(T3-T1)=		0.7538										
105		SetA =		0.0352										
106														
107														
108	GenB													
109		(T1-T2)/(T3-T1)=		-0.2462										
110		(T3-T2)(T3-T1)=		0.7538										
111		SetA =		0										

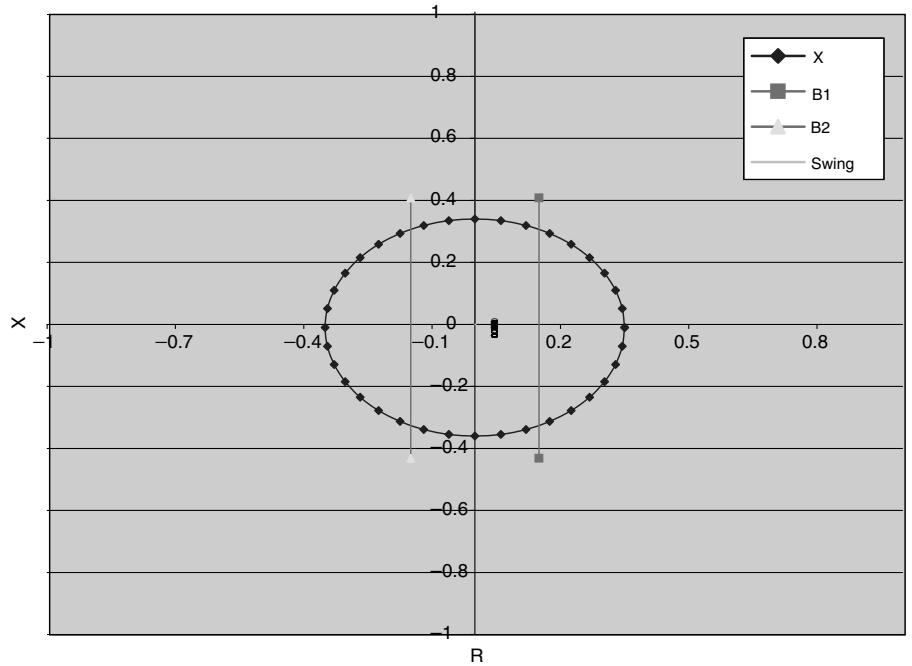


© 2006 by Taylor & Francis Group, LLC

Plot GA



Plot GB



© 2006 by Taylor & Francis Group, LLC

Appendix E: Generator Shaft Torsional Transients

This worksheet calculates the torsional response of a shaft system to an out-of-phase synchronizing. The gray boxes denote input data. The closing conditions are set by manipulating values eag and ΔE. A three-phase fault is simulated by settting Es = 0. The fault is applied on the system side of impedance Zs.

This worksheet is available for download at http://www.taylorandfrancis.com/

Initial conditions

System Voltage

$$Ea = \sqrt{2} \cdot Es \cdot \sin(\omega_s \cdot t + \theta s0), \quad f := 60 \quad Es := 1$$

Generator

$$Eag = \sqrt{2} \cdot et \cdot \sin\left(\omega_{ge} \cdot t + \theta g0\right)$$

$et := 1.0$ $P := 0$ $Q := 0$ Vars out are + Initial generator speed $\omega g_{pu} := 1.0$

Simulation Time

$tsim := 0.5$	This is the duration of the simulation in seconds.
$tswitch := 0.15$	Time until generator CB opens. At this time, electrical torque applied to the shaft is set to zero, thus simulating the mechanical system response to a CB trips. The electrical system response is not simulated. Electrical equations continue to solve as if the CB is closed.

Define Instant of Closure t = 0

Set instantaneous generator voltage at closure $eag := -1.22$

Set instantaneous voltage difference at closure $\Delta E = Eag - Ea$ at $t = 0$ $\Delta E := -2.44$

$$\omega_s := 2 \cdot \pi \cdot f \qquad \omega_{ge} := 2 \cdot \pi \cdot f \cdot \omega g_{pu}$$

Calculate t = 0 parameters

$$\theta g0 := \operatorname{asin}\left(\frac{-eag}{\sqrt{2} \cdot et}\right) \quad \theta s0 := \operatorname{if}\left(Es = 0, -\frac{\pi}{2}, \operatorname{asin}\left(\frac{2 \cdot et \cdot \sin(\theta g0) + \sqrt{2}\Delta E}{2 \cdot Es}\right)\right)$$

$$Eag(t) := -\sqrt{2} \cdot et \cdot \sin\left(\omega_{ge} t + \theta g0\right) \quad Ea(t) := -\sqrt{2} \cdot Es \cdot \sin(\omega_s \cdot t + \theta s0)$$

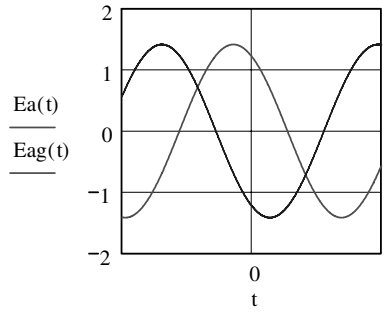
© 2006 by Taylor & Francis Group, LLC

$\theta s0 = -59.618$ deg

$\theta g0 = 59.618$ deg

$Ea(0) = 1.22$

$Eag(0) = -1.22$



Closing Angle

$$\theta g0 - \theta s0 = 119.235 \text{ deg}$$

Electrical Data Input

System

$Zsys := 0.00787$ pu $\theta sys := 84.3$ deg $MVA_{system} := 100$

GSU Transformer

$Ztr := 0.0105$ pu TR X/R Ratio $XR := 52$ $MVA_{TR} := 100$

Generator Data

$MVA_B := 955$ $V_B := 22$ Kv $RPM := 1800$

Reactance (pu)

$Xd := 1.594$ $Xq := 1.544$ $XI := 0.155$

$Xd' := 0.366$ $Xq' := 0.955$

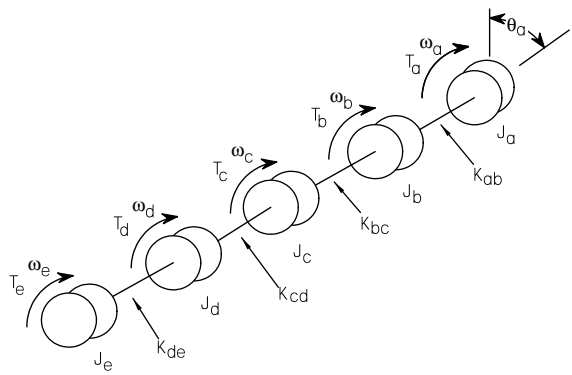
$Xd'' := 0.256$ $Xq'' := 0.251$

Time Constants (sec)

$Td0' := 6.53$ $Tq0' := 1.5$ $Ta := 0.46$

$Td0'' := 0.05$ $Tq0'' := 0.133$

Mechanical System Data



The mechanical system is represented as a spring-mass system. The model includes self and mutual damping terms for each mass. Self damping terms would result from rotational losses such as windage and friction. Mutual damping would result from torsional losses in the connecting shafts.

© 2006 by Taylor & Francis Group, LLC

Inertia

J_Unit := 2 Set J_Unit as follows:

= 1 if lbm-ft^2, = 2 if lbf-ft-sec^2, = 3 if kg-m^2,

= 4 if Per unit

Ja := 1249 Jc := 47473 Je := 10370 Jb := 38223 Jd := 47362

Stiffness of Connecting Shafts

K_Unit := 1 Set K_unit as follows:

= 1 if lbf-ft, = 2 if Newton-Meters,

= 3 if Per Unit

$K_{a_b} := 222.5 \cdot 10^6$ $K_{b_c} := 173 \cdot 10^6$ $K_{c_d} := 90.83 \cdot 10^6$ $K_{d_e} := 74.42 \cdot 10^6$

Damping Factors

These represent the self and mutual damping factors for each mass element and interconnecting shaft. These are not the modal damping factors.

D_Unit := 3 Set D_unit as follows:

= 1 if lbf-ft-sec, = 2 if Newton-Meters-sec,

= 3 if Per unit

Self Damping Terms

Da := 0 Db := 0 Dc := 0 Dd := 0 De := 0

Mutual Damping Terms

$D_{a_b} := 0.01$ $D_{b_c} := 0.01$ $D_{c_d} := 0.01$ $D_{d_e} := 0.01$

Torque

Input the torque applied at each mass. Driving torque from a turbine element (LP, HP) is positive. Restraining torque from the generator or exciter is negative.

At open circuit, all mechanical torque is zero. The exciter and generator torque are defined in the Odesolve block.

Tma := 0 Tmb := 0 Tmc := 0 Tmd := 0 Tme := 0

Calculated Electrical Parameters

System

$$Rsys := Zsys \cdot \frac{MVA_B}{MVA_{system}} \cdot \cos(\theta sys) \quad Xsys := Zsys \cdot \frac{MVA_B}{MVA_{system}} \cdot \sin(\theta sys)$$

© 2006 by Taylor & Francis Group, LLC

Transformer

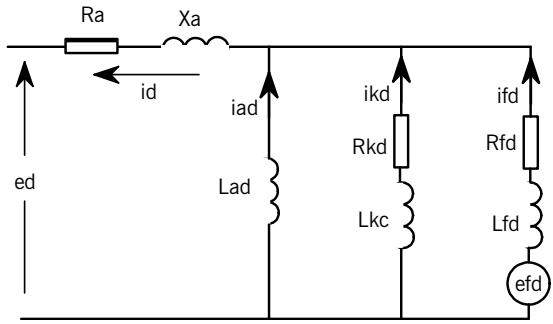
$$Rtr := Ztr\frac{MVA_B}{MVA_{TR}}\cos(\text{atan}(XR)) \quad Xtr := Ztr \cdot \frac{MVA_B}{MVA_{TR}}\sin(\text{atan}(XR))$$

$$Lsys := Xsys \quad Ltr := Xtr$$

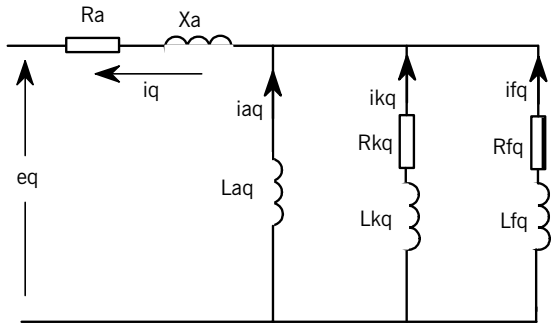
Calculated Generator Parameters at Rated Frequency

The d and q-axis circuits of the generator are defined as shown:

d-axis circuit



q-axis circuit



The per unit parameters are calculated using standard relationships found in generator texts. In the per unit system, L and X are numerically equivalent at rated frequency. The "g" branch in the q-axis represents the fictitious winding used to include the effects of currents induced in the solid steel of the rotor body.

Per unit time base is: $t_B := \dfrac{1}{2\pi f}$

$$Lad := Xd - Xl \quad Laq := Xq - Xl \quad Ll := Xl$$

$$Td' := \frac{Xd'}{Xd}Td0' \quad Tq' := \frac{Xq'}{Xq}Tq0'$$

$$Td'' := \frac{Xd'' \cdot Td0'}{Xd \cdot Td'} \cdot Td0'' \quad Tq'' := \frac{Xq'' \cdot Tq0'}{Xq \cdot Tq'} \cdot Tq0'' \quad R_1 := \frac{2 \cdot Xd'' \cdot Xq'' \cdot t_B}{Ta \cdot (Xd'' + Xq'')}$$

© 2006 by Taylor & Francis Group, LLC

Solving for Rfd

Time constants are converted from seconds to per unit time using the base t_B

Given

$$Lffd = Lad + Lfd$$

$$\frac{Td0'}{t_B} = \frac{Lffd}{R_{fd}} \quad \frac{Td'}{t_B} = \frac{1}{R_{fd}} \cdot \left(Lfd + \frac{Ll \cdot Lfd}{Ll + Lad}\right)$$

Substituting

$$\frac{Td0'}{t_B} = \frac{(Lad + Lfd)}{R_{fd}}$$

Solving for Lfd

$$Lfd = \frac{(Td0' \cdot R_{fd} - Lad \cdot t_B)}{t_B}$$

Substituting into the Td' expression and solving for Rfd

$$\frac{Td'}{t_B} = \frac{1}{R_{fd}} \cdot \left(Lfd + \frac{Ll \cdot Lad}{Ll + Lad}\right)$$

$$\frac{Td'}{t_B} = \frac{1}{R_{fd}} \cdot \left[\frac{(Td0' \cdot R_{fd} - Lad \cdot t_B)}{t_B} + Ll \cdot \frac{Lad}{(Ll + Lad)}\right]$$

$$R_{fd} := -Lad^2 \cdot \frac{t_B}{(Td' \cdot Ll + Td' \cdot Lad - Td0' \cdot Ll - Td0' \cdot Lad)}$$

$$Lfd := \frac{(Td0' \cdot R_{fd} - Lad \cdot t_B)}{t_B}$$

Solving for Rkd and Lkd

$$\frac{Td0''}{t_B} = \frac{1}{R_{kd}} \cdot \left(Lkd + \frac{Lfd \cdot Lad}{Lad + Lfd}\right)$$

Solving for Lkd

$$Lkd = \frac{(Td0'' \cdot R_{kd} \cdot Lad + Td0'' \cdot R_{kd} \cdot Lfd - Lfd \cdot Lad \cdot t_B)}{t_B \cdot (Lad + Lfd)}$$

Given

$$\frac{Td''}{t_B} = \frac{1}{R_{kd}} \cdot \left(Lkd + \frac{1}{\frac{1}{Lad} + \frac{1}{Ll} + \frac{1}{Lfd}}\right)$$

Substituting Lkd

$$\frac{Td''}{t_B} = \frac{1}{R_{kd}} \cdot \left[\frac{(Td0'' \cdot R_{kd} \cdot Lad + Td0'' \cdot R_{kd} \cdot Lfd - Lfd \cdot Lad \cdot t_B)}{t_B \cdot (Lad + Lfd)} + \frac{1}{\left(\frac{1}{Lad} + \frac{1}{Ll} + \frac{1}{Lfd}\right)}\right]$$

© 2006 by Taylor & Francis Group, LLC

$$R_{kd} := \frac{(Lad^2 \cdot Lfd^2) \cdot t_B}{(Lad + Lfd) \cdot [Lad \cdot Lfd + (Lad + Lfd) \cdot Ll] \cdot (Td0'' - Td'')}$$

$$Lkd := \frac{(Td0'' \cdot R_{kd} \cdot Lad + Td0'' \cdot R_{kd} \cdot Lfd - Lfd \cdot Lad \cdot t_B)}{t_B \cdot (Lad + Lfd)}$$

Solving for Lfq

$$\frac{Tq0'}{t_B} = \frac{1}{R_{fq}} \cdot (Lfq + Laq)$$

$$Lfq = \frac{-(-Tq0' \cdot R_{fq} + Laq \cdot t_B)}{t_B}$$

Given

$$\frac{Tq'}{t_B} = \frac{1}{R_{fq}} \cdot \left(Lfq + \frac{Ll \cdot Laq}{Ll + Laq}\right)$$

Substituting

$$\frac{Tq'}{t_B} = \frac{1}{R_{fq}} \cdot \left[\frac{(Tq0' \cdot R_{fq} - Laq \cdot t_B)}{t_B} + Ll \cdot \frac{Laq}{(Ll + Laq)}\right]$$

$$R_{fq} := -Laq^2 \cdot \frac{t_B}{(Tq' \cdot Ll + Tq' \cdot Laq - Tq0' \cdot Ll - T'_{q0} \cdot Laq)}$$

and

$$Lfq := \frac{-(-Tq0' \cdot R_{fq} + Laq \cdot t_B)}{t_B}$$

Solving for Rkq and Lkq

$$\frac{Tq0''}{t_B} = \frac{1}{R_{kq}} \cdot \left(Lkq + \frac{Lfq \cdot Laq}{Laq + Lfq}\right)$$

$$Lkq = \frac{(Tq0'' \cdot R_{kq} \cdot Lfq + Tqo'' \cdot R_{kq} \cdot Laq - Lfq \cdot Laq \cdot t_B)}{t_B \cdot (Lfq + Laq)}$$

Solving for Lkd

$$\frac{Tq''}{t_B} = \frac{1}{R_{kq}} \cdot \left(Lkq + \frac{1}{\frac{1}{Laq} + \frac{1}{Ll} + \frac{1}{Lfq}}\right)$$

$$\frac{Tq''}{t_B} = \frac{1}{R_{kq}} \cdot \left[\frac{(Tq0'' \cdot R_{kq} \cdot Lfq + Tq0'' \cdot R_{kq} \cdot Laq - Lfq \cdot Laq \cdot t_B)}{t_B \cdot (Lfq + Laq)} + \frac{1}{\left(\frac{1}{Laq} + \frac{1}{Ll} + \frac{1}{Lfq}\right)}\right]$$

$$R_{kq} := \frac{(Laq^2 \cdot Lfq^2) \cdot t_B}{(Laq + Lfq) \cdot [Laq \cdot Lfq + (Laq + Lfq) \cdot Ll] \cdot (Tq0'' - Tq'')}$$

and

$$Lkq := \frac{(Tq0'' \cdot R_{kq} \cdot Lfq + Tq0'' \cdot R_{kq} \cdot Laq - Lfq \cdot Laq \cdot t_B)}{t_B \cdot (Lfq + Laq)}$$

© 2006 by Taylor & Francis Group, LLC

Calculated d and q-axis circuit parameters on generator base

$$\begin{array}{llll} Lfd = 0.247 & R_{fd} = 0.001 & Lfq = 1.887 & R_{fq} = 0.006 \\ Lad = 1.439 & R_l = 0.001 & Laq = 1.389 & \\ Lkd = 0.194 & R_{kd} = 0.021 & Lkq = 0.109 & R_{kq} = 0.018 \\ Lsys = 0.075 & R_{sys} = 0.007 & Ltr = 0.1 & Rtr = 0.002 \end{array}$$

$$Ra := R_l + Rsys + Rtr \quad La := Lsys + Ltr$$

System Model

The equations that govern the generator's electrical behavior are:

$$\begin{array}{ll} Vf = \frac{d}{dt}\lambda f + R_f I_f & Vd = \frac{d}{dt}\lambda d - R_a \cdot id - \lambda q \cdot \frac{d}{dt}\theta b \\ 0 = \frac{d}{dt}\lambda kd + Rkd \cdot ikd & 0 = \frac{d}{dt}\lambda g + Rg \cdot ig \\ Vq = \frac{d}{dt}\lambda q - R_a \cdot iq + \lambda d \cdot \frac{d}{dt}\theta b & 0 = \frac{d}{dt}\lambda kq + Rkq \cdot ikq \end{array}$$

where

$$\begin{pmatrix} \lambda f \\ \lambda d \\ \lambda kd \end{pmatrix} = \begin{pmatrix} Lffd & -Laf & Lfkd \\ Laf & -Ld & Lakd \\ Lfkd & -Lakd & Lkkd \end{pmatrix} \cdot \begin{pmatrix} i_f \\ id \\ ikd \end{pmatrix}$$

$$\begin{pmatrix} \lambda g \\ \lambda q \\ \lambda kq \end{pmatrix} = \begin{pmatrix} Lg & -Lag & Lfkq \\ Lag & -Lq & Lakq \\ Lgkd & -Lakq & Lkkq \end{pmatrix} \cdot \begin{pmatrix} ig \\ iq \\ ikq \end{pmatrix}$$

$$Te = iq \cdot \lambda d - id \cdot \lambda q$$

Defining matrix parameters using the common assumptions that Lad = Lfd = Lkd and Laq = Lfq = Lkq etc.

$$\begin{array}{llllll} Lf := Lad + Lfd & Laf := Lad & Lfkd := Lad & Ld := Ll + Lad & Lakd := Lad \\ Lg := Lfq + Laq & Lag := Laq & Lgkq := Laq & Lq := Laq + Ll & Lakq := Laq \\ Lkkd := Lad + Lkd & Lkkq := Laq + Lkq & Rf := R_{fd} & Rg := R_{fq} & \end{array}$$

The system voltage must be expressed in terms of the generator's d- and q-axis. This conversion is made using the Park's transform:

$$\begin{pmatrix} Yd \\ Yq \\ Y0 \end{pmatrix} = \sqrt{\frac{2}{3}} \cdot \begin{pmatrix} \cos(\omega_{ge} \cdot t) & \cos\left(\omega_{ge} \cdot t - \frac{2 \cdot \pi}{3}\right) & \cos\left(\omega_{ge} \cdot t + \frac{2 \cdot \pi}{3}\right) \\ -\sin(\omega_{ge} \cdot t) & -\sin\left(\omega_{ge} \cdot t - \frac{2 \cdot \pi}{3}\right) & -\sin\left(\omega_{ge} \cdot t + \frac{2 \cdot \pi}{3}\right) \\ \sqrt{\frac{1}{2}} & \sqrt{\frac{1}{2}} & \sqrt{\frac{1}{2}} \end{pmatrix} \cdot \begin{pmatrix} Ya \\ Yb \\ Yc \end{pmatrix}$$

© 2006 by Taylor & Francis Group, LLC

where Yd, Yq, Y0 are d, q, and zero sequence quantities and Ya, Yb, Yc are phase quantities. Given system voltages

$$Ea(t) = -\sqrt{2} \cdot Es \cdot \sin(\omega_s \cdot t + \theta s0)$$

$$Eb = -\sqrt{2} \cdot Es \cdot \sin\left(\omega_s \cdot t - \frac{2 \cdot \pi}{3} + \theta s0\right)$$

$$Ec = -\sqrt{2} \cdot Es \cdot \sin\left(\omega_s \cdot t + \frac{2 \cdot \pi}{3} + \theta s0\right)$$

The resulting d, q, 0 axis voltages are:

$$Vds(t) := \frac{-Es}{2} \cdot \sqrt{6} \cdot \sin[\omega_s \cdot t - \omega_{ge} \cdot t + (\theta s0 - \theta g0)]$$

$$Vqs(t) := \frac{Es}{2} \cdot \sqrt{6} \cdot \cos[\omega_s \cdot t - \omega_{ge} \cdot t + (\theta s0 - \theta g0)]$$

$$V0 = 0$$

On PU basis

$$Vds(t) := -E_s \cdot \sin[\omega_s \cdot t - \omega_{ge} \cdot t + (\theta s0 - \theta g0)]$$

$$Vqs(t) := E_s \cdot \cos[\omega_s \cdot t - \omega_{ge} \cdot t + (\theta s0 - \theta g0)]$$

Initial conditions

$$i_t := \frac{\sqrt{P^2 + Q^2}}{et} \quad \theta_{PF} := \text{if}\left(P = 0,\ \frac{\pi}{2},\ \text{atan}\left(\frac{Q}{P}\right)\right)$$

$$Eq := \sqrt{(et + Xq \cdot i_t \cdot \sin(\theta_{PF}))^2 + [(Xq \cdot i_t \cdot \cos(\theta_{PF}))^2]}$$

Eq is the fictitious voltage that is used to locate the q-axis

$$\delta := \text{atan}\left(\frac{i_t \cdot Xq \cdot \cos(\theta_{PF})}{et + Xq \cdot i_t \cdot \sin(\theta_{PF})}\right)$$

δ is the angle between et and the q-axis

$$iq0 := i_t \cdot \cos(\theta_{PF} + \delta) \quad id0 := i_t \cdot \sin(\theta_{PF} + \delta)$$

initial d and q axis voltage and current

$$eq0 := et \cdot \cos(\delta) + iq0 \cdot Ra \quad ed0 := et \cdot \sin(\delta) + id0 \cdot Ra$$

$$eq0'' := eq0 + id0 \cdot Xd'' \quad ed0'' := ed0 - iq0 \cdot Xq''$$

$$EI := eq0 + id0 \cdot Xd \quad if0 := \frac{EI}{Lad}$$

EI is the voltage behind Xd
if0 is the initial field current

at t(−0) from closure

$$if0 = 0.695 \quad Vf := if0 \cdot R_{fd} \quad id0 = 0 \quad iq0 = 0$$

d and q components of system voltage prior to transient

$$Vds(0) = 0.873 \quad Vqs(0) = -0.488$$

Mechanical System

Mechanical base quantities

Mechanical speed differs from electrical speed by the number of generator pole pairs. Mechanical base quantities were derived per Ref [1] and adjusted to the electrical speed to facilitate

© 2006 by Taylor & Francis Group, LLC

a solution in t (seconds).

$$\text{Base Mechanical speed} \quad \omega_{BM} := \frac{2 \cdot \pi \cdot RPM}{60}$$

Inertia

Inertia base is given next. KJ is determined by the physical units used to specify the inertia in the input section.

$$CJ(x) := \text{if}\left(x = 1, 20.7 \cdot 10^9, \text{if}\left(x = 2, 0.642 \cdot 10^9, \text{if}\left(x = 3, 0.871 \cdot 10^9, \text{if}\left(x = 4, \frac{RPM^3}{MVA_B}, 0\right)\right)\right)\right)$$

$$J_B := CJ(J_Unit) \cdot \frac{MVA_B \cdot (2 \cdot \pi \cdot f)^2}{RPM^3} \cdot 0.5$$

$$Ja_pu := \frac{Ja}{J_B} \quad Jb_pu := \frac{Jb}{J_B} \quad Jc_pu := \frac{Jc}{J_B} \quad Jd_pu := \frac{Jd}{J_B} \quad Je_pu := \frac{Je}{J_B}$$

Stiffness

$$CK(x) := \text{if}\left(x = 1, 7.04 \cdot 10^6, \text{if}\left(x = 2, 9.55 \cdot 10^6, \text{if}\left(x = 3, \frac{RPM}{MVA_B}, 0\right)\right)\right)$$

$$K_B := CK(K_Unit) \cdot \frac{MVA_B}{RPM} \cdot 2$$

$$K_{ab_pu} := \frac{K_{a_b}}{K_B} \quad K_{bc_pu} := \frac{K_{b_c}}{K_B} \quad K_{cd_pu} := \frac{K_{c_d}}{K_B} \quad K_{de_pu} := \frac{K_{d_e}}{K_B}$$

Damping

$$CD(x) := \text{if}\left(x = 1, 67.2 \cdot 10^6, \text{if}\left(x = 2, 91.1 \cdot 10^6, \text{if}\left(x = 3, \frac{RPM^2}{MVA_B}, 0\right)\right)\right)$$

$$D_B := CD(D_Unit) \cdot \frac{MVA_B \cdot (2 \cdot \pi \cdot f)}{RPM^2}$$

$$D_{a_pu} := \frac{D_a}{D_B} \quad D_{b_pu} := \frac{D_b}{D_B} \quad D_{c_pu} := \frac{D_c}{D_B} \quad D_{d_pu} := \frac{D_d}{D_B} \quad D_{e_pu} := \frac{D_e}{D_B}$$

$$D_{ab_pu} := \frac{D_{a_b}}{D_B} \quad D_{bc_pu} := \frac{D_{b_c}}{D_B} \quad D_{cd_pu} := \frac{D_{c_d}}{D_B} \quad D_{de_pu} := \frac{D_{d_e}}{D_B}$$

Mechanical System Model

The rotating system can be represented by a system of differential equations written about the rotational acceleration (θ'') of each mass element as shown. The acceleration is a function of the speed of the mass (θ'), adjacent masses as a function of the self, mutual damping terms, and the shaft torsion on either side of the mass as defined by the shaft stiffness term.

© 2006 by Taylor & Francis Group, LLC

The system of equations for the five mass system shown earlier are:

$$Ja \cdot \theta a'' + Da \cdot \theta a' + Dab \cdot (\theta a' - \theta b') + Kab \cdot (\theta a - \theta b) = Tam - Tae$$

$$Jb \cdot \theta b'' + Db \cdot \theta b' + Dbc \cdot (\theta b' - \theta c') + Dba \cdot (\theta b' - \theta a') + Kbc \cdot (\theta b - \theta c) + Kba \cdot (\theta b - \theta a) = Tbm - Tbe$$

$$Jc \cdot \theta c'' + Dc \cdot \theta c' + Dcd \cdot (\theta c' - \theta d') + Dcb \cdot (\theta c' - \theta b') + Kcd \cdot (\theta c - \theta d) + Kcb \cdot (\theta c - \theta b) = Tcm - Tce$$

$$Jd \cdot \theta d'' + Dd \cdot \theta d' + Dde \cdot (\theta d' - \theta e') + Ddc \cdot (\theta d' - \theta c') + Kde \cdot (\theta d - \theta e) + Kdc \cdot (\theta d - \theta c) = Tdm - Tde$$

$$Je \cdot \theta e'' + De \cdot \theta e' + Ded \cdot (\theta e' - \theta d') + Ked \cdot (\theta e - \theta d) = Tem - Tee$$

Torques Tam through Tem are the mechanical inputs at each mass and Tae through Tee are the electrical torque loads at each mass. For the examples given, the generator is intially an open circuit, thus, all mechanical input is zero. Electrical torque is only apparent at the exciter (mass A) and generator (mass B).

Expanding the above equations and collecting terms results in the following:

$$Ja \cdot \theta a'' + \theta a' \cdot (Da + Dab) - Dab \cdot \theta b' + Kab \cdot \theta a - Kab \cdot \theta b = Tam - Tae$$

$$Jb \cdot \theta b'' - Dba \cdot \theta a' + \theta b' \cdot (Db + Dbc + Dba) - Dbc \cdot \theta c' - Kba \cdot \theta a + \theta b \cdot (Kbc + Kba) - Kbc \cdot \theta c = Tbm - Tbe$$

$$Jc \cdot \theta c'' - Dcb \cdot \theta b' + \theta c' \cdot (Dc + Dcd + Dcb) - Dcd \cdot \theta d' - Kcb \cdot \theta b + \theta c \cdot (Kcd + Kcb) - Kcd \cdot \theta d = Tcm - Tce$$

$$Jd \cdot \theta d'' - Ddc \cdot \theta c' + \theta d' \cdot (Dd + Dde + Ddc) - Dde \cdot \theta e' - Kdc \cdot \theta c + \theta d \cdot (Kde + Kdc) - Kde \cdot \theta e = Tdm - Tde$$

$$Je \cdot \theta e'' - Ded \cdot \theta d' + \theta e' \cdot (De + Ded) - Ked \cdot \theta d + Ked \cdot \theta e = Tem - Tee$$

Expressing the mechanical system in matrix form:

$$JM \cdot \begin{pmatrix} \theta a'' \\ \theta b'' \\ \theta c'' \\ \theta d'' \\ \theta e'' \end{pmatrix} + DM \cdot \begin{pmatrix} \theta a' \\ \theta b' \\ \theta c' \\ \theta d' \\ \theta e' \end{pmatrix} + KM \cdot \begin{pmatrix} \theta a \\ \theta b \\ \theta c \\ \theta d \\ \theta e \end{pmatrix} = \begin{pmatrix} Tma - Tae \\ Tmb - Tbe \\ Tmc - Tce \\ Tmd - Tde \\ Tme - Tee \end{pmatrix}$$

where

$$JM := \begin{pmatrix} Ja_pu & 0 & 0 & 0 & 0 \\ 0 & Jb_pu & 0 & 0 & 0 \\ 0 & 0 & Jc_pu & 0 & 0 \\ 0 & 0 & 0 & Jd_pu & 0 \\ 0 & 0 & 0 & 0 & Je_pu \end{pmatrix}$$

© 2006 by Taylor & Francis Group, LLC

Stiffness

$$Kaa_PU := K_{ab_pu} \quad Kbb_PU := K_{bc_pu} + K_{ab_pu} \quad Kcc_PU := K_{cd_pu} + K_{bc_pu}$$

$$Kee_PU := K_{de_pu} \quad Kdd_PU := K_{de_pu} + K_{cd_pu}$$

$$KM := \begin{pmatrix} Kaa_PU & -K_{ab_pu} & 0 & 0 & 0 \\ -K_{ab_pu} & Kbb_PU & -K_{bc_pu} & 0 & 0 \\ 0 & -K_{bc_pu} & Kcc_PU & -K_{cd_pu} & 0 \\ 0 & 0 & -K_{cb_pu} & Kdd_PU & -K_{de_pu} \\ 0 & 0 & 0 & -K_{de_pu} & Kee_PU \end{pmatrix}$$

Damping

$$Daa_PU := D_{a_pu} + D_{ab_pu} \qquad Dbb_PU := D_{b_pu} + D_{bc_pu} + D_{ab_pu}$$

$$Dcc_PU := D_{c_pu} + D_{bc_pu} + D_{cd_pu} \quad Ddd_PU := D_{d_pu} + D_{de_pu} + D_{cd_pu}$$

$$Dee_PU := D_{e_pu} + D_{de_pu}$$

$$DM := \begin{pmatrix} Daa_PU & -D_{ab_pu} & 0 & 0 & 0 \\ -D_{ab_pu} & Dbb_PU & -D_{bc_pu} & 0 & 0 \\ 0 & -D_{bc_pu} & Dcc_PU & -D_{cd_pu} & 0 \\ 0 & 0 & -D_{cb_pu} & Ddd_PU & -D_{de_pu} \\ 0 & 0 & 0 & -D_{de_pu} & Dee_PU \end{pmatrix}$$

The natural frequencies of the shaft system can be found from the equations previously/defined.

$$JM \cdot \begin{pmatrix} \theta a'' \\ \theta b'' \\ \theta c'' \\ \theta d'' \\ \theta e'' \end{pmatrix} + DM \cdot \begin{pmatrix} \theta a' \\ \theta b' \\ \theta c' \\ \theta d' \\ \theta e' \end{pmatrix} + KM \cdot \begin{pmatrix} \theta a \\ \theta b \\ \theta c \\ \theta d \\ \theta e \end{pmatrix} = \begin{pmatrix} Tma - Tae \\ Tmb - Tbe \\ Tmc - Tce \\ Tmd - Tde \\ Tme - Tee \end{pmatrix}$$

Rearranging terms defining matrix BM, JDM and JKM

$$\begin{pmatrix} \theta a'' \\ \theta b'' \\ \theta c'' \\ \theta d'' \\ \theta e'' \end{pmatrix} = -JM^{-1} \cdot DM \cdot \begin{pmatrix} \theta a' \\ \theta b' \\ \theta c' \\ \theta d' \\ \theta e' \end{pmatrix} - JM^{-1} \cdot KM \cdot \begin{pmatrix} \theta a \\ \theta b \\ \theta c \\ \theta d \\ \theta e \end{pmatrix} + JM^{-1} \cdot \begin{pmatrix} Tma - Tae \\ Tmb - Tbe \\ Tmc - Tce \\ Tmd - Tde \\ Tme - Tee \end{pmatrix}$$

$$JDM := JM^{-1} \cdot DM \quad JKM := JM^{-1} \cdot KM$$

$$\begin{pmatrix} \theta a'' \\ \theta b'' \\ \theta c'' \\ \theta d'' \\ \theta e'' \end{pmatrix} = -JDM \cdot \begin{pmatrix} \theta a' \\ \theta b' \\ \theta c' \\ \theta d' \\ \theta e' \end{pmatrix} - JKM \cdot \begin{pmatrix} \theta a \\ \theta b \\ \theta c \\ \theta d \\ \theta e \end{pmatrix} + JM^{-1} \cdot \begin{pmatrix} Tma - Tae \\ Tmb - Tbe \\ Tmc - Tce \\ Tmd - Tde \\ Tme - Tee \end{pmatrix}$$

© 2006 by Taylor & Francis Group, LLC

The natural frequencies of the shaft system are found from the eigenvalues of matrix JKM.

$$\lambda := \text{eigenvalues (JKM)} \quad \lambda = \begin{pmatrix} 184121.706 \\ 0 \\ 9950.062 \\ 8470.528 \\ 2179.662 \end{pmatrix}$$

The natural frequencies are equal to the square root of the eigenvalues. With the bases chosen for this system the natural frequencies are in radians per second.

$$\lambda_{0,0} = 184121.706 \quad \sqrt{\lambda_{0,0}} = 429.094 \frac{\text{rad}}{\text{sec}} \quad \text{or} \quad \frac{\sqrt{\lambda_{0,0}}}{2 \cdot \pi \cdot \text{f}} \cdot 60 = 68.292\,\text{Hz}$$

$$\text{f}_{\text{natural}} := \frac{60 \cdot \sqrt{\lambda}}{(2 \cdot \pi \cdot \text{f})} \quad \text{f}_{\text{natural}} = \begin{pmatrix} 68.292 \\ 0 \\ 15.876 \\ 14.648 \\ 7.43 \end{pmatrix} \text{Hz}$$

Solving System Equations

The matrix equations for the mechanical system are now rewritten in the algebraic form required by Mathcad's Odesolver. Odesolver also requires that only one first order derivative terms appear in each equation therefore angular velocity ω replaces $d\theta/dt$ and time variant terms are designated as -"(t)".

$$\begin{aligned}
\frac{d}{dt}\omega a(t) &= -\text{JDM}_{0,0} \cdot \omega a(t) - \text{JDM}_{0,1} \cdot \omega b(t) - \text{JKM}_{0,0} \cdot \theta a(t) - \text{JKM}_{0,1} \cdot \theta b(t) \\
&\quad + \left(\text{JM}_{0,0}\right)^{-1} \cdot (\text{Tma} - \text{Tae}) \\
\frac{d}{dt}\omega b(t) &= -\text{JDM}_{1,0} \cdot \omega a(t) - \text{JDM}_{1,1} \cdot \omega b(t) - \text{JDM}_{1,2} \cdot \omega c(t) - \text{JKM}_{1,0} \cdot \theta a(t) \cdots \\
&\quad + \left[\left(-\text{JKM}_{1,1} \cdot \theta b(t) - \text{JKM}_{1,2} \cdot \theta c(t)\right) + \left(\text{JM}_{1,1}\right)^{-1} \cdot (\text{Tmb} - \text{Tbe})\right] \\
\frac{d}{dt}\omega c(t) &= -\text{JDM}_{2,1} \cdot \omega b(t) - \text{JDM}_{2,2} \cdot \omega c(t) - \text{JDM}_{2,3} \cdot \omega d(t) - \text{JKM}_{2,1} \cdot \theta b(t) \cdots \\
&\quad + \left[(-\text{JKM})_{2,2} \cdot \theta c(t) - \text{JKM}_{2,3} \cdot \theta d(t) + \left(\text{JM}_{2,2}\right)^{-1} \cdot (\text{Tmc} - \text{Tce})\right] \\
\frac{d}{dt}\omega d(t) &= -\text{JDM}_{3,2} \cdot \omega c(t) - \text{JDM}_{3,3} \cdot \omega d(t) - \text{JDM}_{3,4} \cdot \omega e(t) - \text{JKM}_{3,2} \cdot \theta c(t) \cdots \\
&\quad + \left[-\text{JKM}_{3,3} \cdot \theta d(t) - \text{JKM}_{3,4} \cdot \theta e(t) + \left(\text{JM}_{3,3}\right)^{-1} \cdot (\text{Tmd} - \text{Tde})\right] \\
\frac{d}{dt}\omega e(t) &= -\text{JDM}_{4,3} \cdot \omega d(t) - \text{JDM}_{4,4} \cdot \omega e(t) - \text{JKM}_{4,3} \cdot \theta d(t) - \text{JKM}_{4,4} \cdot \theta e(t) \\
&\quad + \left(\text{JM}_{4,4}\right)^{-1} \cdot (\text{Tme} - \text{Tee})
\end{aligned}$$

Odesolve requires initial values for all but the highest order derivative: in this case, all but $d\omega/dt \cdot d\theta/dt$ values are known, as there is no speed change prior to the transient. Values are required for di/dt in each electrical circuit. These values are found using Mathcad "Find" function employed in a solve block to determine system parameters at $t = -0$.

© 2006 by Taylor & Francis Group, LLC

Note that the electrical torque at the exciter and generator are included at mass "A" and "B" respectively. Exciter per unit electrical torque is represented as $(Vf * i_f)/\omega_a$.

Guess values for the initial condition are:

$$\begin{array}{lllll} i_f := if0 & dif := 0 & \theta a := \theta_{g0} & \omega a := \omega_{ge} & d\omega a := 0 \\ id := 0 & did := 0 & \theta b := \theta_{g0} & \omega b := \omega_{ge} & d\omega b := 0 \\ ikd := 0 & dikd := 0 & \theta c := \theta_{g0} & \omega c := \omega_{ge} & d\omega e := 0 \\ ig := 0 & dig := 0 & \theta d := \theta_{g0} & \omega d := \omega_{ge} & d\omega d := 0 \\ iq := 0 & diq := 0 & \theta e := \theta_{g0} & \omega e := \omega_{ge} & d\omega e := 0 \\ ikq := 0 & dikq := 0 & Te := 0 & & \end{array}$$

Given

$$dif = \frac{-\left(Lfkd \cdot dikd - Vf + \frac{Rf}{t_B} \cdot i_f - Laf \cdot did\right)}{Lf}$$

$$did = \frac{\begin{array}{l} dif \cdot Laf + Lakd \cdot dikd - \omega b \cdot [Lag \cdot ig - (Lq + La) \cdot iq + Lakq \cdot ikq] - \frac{(R_a)}{t_B} \cdot id \\ \quad + Es \cdot \omega_s \cdot \sin(\theta s0 - \theta g0) \end{array}}{Ld + Xsys + Xtr}$$

$$dig = \frac{-\left(-Lag \cdot diq + Lgkq \cdot dikq + \frac{Rg}{t_B} \cdot ig\right)}{L_g} \quad dikd = \frac{-\left(Lfkd \cdot dif - Lakd \cdot did + \frac{R_{kd}}{t_B} \cdot ikd\right)}{Lkkd}$$

$$diq = \frac{\begin{array}{l} Lag \cdot dig + Lakq \cdot dikq + \omega b \cdot (Laf \cdot i_f + id \cdot Ld + id \cdot La - ikd \cdot Lakd) \\ -(Ra/t_B \cdot iq - Es \cdot \omega_s \cdot \cos(\theta s0 - \theta g0)) \end{array}}{Lq + Xsys + Xtr}$$

$$dikq = \frac{-\left(\frac{R_{kq}}{t_B} \cdot ikq + Lgkq \cdot dig - Lakq \cdot diq\right)}{Lkkq}$$

$$[(i_f \cdot Laf - Ld \cdot id + Lakd \cdot ikd) \cdot iq - (Lag \cdot ig - Lq \cdot iq + Lakq \cdot ikq) \cdot id] - Te = 0$$

$$d\omega a = -JDM_{0,0} \cdot \omega a - JDM_{0,1} \cdot \omega b - JKM_{0,0} \cdot \theta a - JKM_{0,1} \cdot \theta b + (JM_{0,0})^{-1} \cdot Vf \cdot \frac{i_f}{\omega a} \cdot 0$$

$$\begin{aligned} d\omega b = {} & -JDM_{1,0} \cdot \omega a - JDM_{1,1} \cdot \omega b - JDM_{1,2} \cdot \omega c - JKM_{1,0} \cdot \theta a - JKM_{1,1} \cdot \theta b - JKM_{1,2} \cdot \theta c \ldots \\ & + (JM_{1,1})^{-1} \cdot (-Te) \end{aligned}$$

$$\begin{aligned} d\omega c = {} & -JDM_{2,1} \cdot \omega b - JDM_{2,2} \cdot \omega c - JDM_{2,3} \cdot \omega d - JKM_{2,1} \cdot \theta b - JKM_{2,2} \cdot \theta c - JKM_{2,3} \cdot \theta d \ldots \\ & + (JM_{2,2})^{-1} \cdot Tmc \end{aligned}$$

© 2006 by Taylor & Francis Group, LLC

$$d\omega d = -JDM_{3,2}\cdot \omega c - JDM_{3,3}\cdot \omega d - JDM_{3,4}\cdot \omega e - JKM_{3,2}\cdot \theta c$$
$$- JKM_{3,3}\cdot \theta d - JKM_{3,4}\cdot \theta e \ldots + (JM_{3,3})^{-1}\cdot Tmd$$
$$d\omega e = -JDM_{4,3}\cdot \omega d - JDM_{4,4}\cdot \omega e - JKM_{4,3}\cdot \theta d - JKM_{4,4}\cdot \theta e + (JM_{4,4})^{-1}\cdot Tme$$

$$\begin{pmatrix} dif0 \\ did0 \\ dikd0 \\ dig0 \\ diq0 \\ dikq0 \end{pmatrix} := Find(dif, did, dikd, dig, diq, dikq, d\omega a, d\omega b, d\omega c, d\omega d, d\omega e)$$

These values are input to Odesolver, which is configured below. Odesolver requires that the second order derivatives be configured as first derivatives of a first, derivative term. To accomplish this, terms dif through ωe are defined.

Given

$$\frac{d}{dt}iff(t) = dif(t) \quad \frac{d}{dt}ig(t) = dig(t) \quad \frac{d}{dt}\theta a(t) = \omega a(t) \quad \frac{d}{dt}\theta d(t) = \omega d(t)$$
$$\frac{d}{dt}id(t) = did(t) \quad \frac{d}{dt}iq(t) = diq(t) \quad \frac{d}{dt}\theta b(t) = \omega b(t) \quad \frac{d}{dt}\theta e(t) = \omega e(t)$$
$$\frac{d}{dt}ikd(t) = dikd(t) \quad \frac{d}{dt}ikq(t) = dikq(t) \quad \frac{d}{dt}\theta c(t) = \omega c(t)$$

$$Lf\cdot(dif(t)) = Vf - \frac{Rf}{(t_B)}\cdot iff(t) + Laf\cdot did(t) - Lfkd\cdot dikd(t)$$

$$(Ld + La)\cdot did(t) = dif(t)\cdot Laf + Lakd\cdot dikd(t) - \omega b(t)$$
$$\cdot [Lag\cdot ig(t) - (Lq + La)\cdot iq(t) + Lakq\cdot ikq(t)]\ldots$$
$$+\left[-\frac{(Ra)}{(t_B)}\cdot id(t) + Es\cdot \omega_s\cdot \sin((\omega_s\cdot t + \theta s0 - \theta b(t)))\right]$$

$$Lkkd\cdot dikd(t) = -(Lfkd\cdot dif(t)) + Lakd\cdot did(t) - \frac{R_{kd}}{(t_B)}\cdot ikd(t)$$

$$Lg\cdot dig(t) = Lag\cdot diq(t) - Lgkq\cdot dikq(t) - \frac{Rg}{(t_B)}\cdot ig(t)$$

$$(Lq + La)\cdot diq(t) = Lag\cdot dig(t) + Lakq\cdot dikq(t) + \omega b(t)$$
$$\cdot [iff(t)\cdot Laf - (Ld + La)\cdot id(t) + Lakd\cdot ikd(t)]\ldots$$
$$+\left[-\frac{(Ra)}{t_B}\cdot iq(t) - Es\cdot \omega_s\cdot \cos((\omega_s\cdot t + \theta s0 - \theta b(t)))\right]$$

© 2006 by Taylor & Francis Group, LLC

$$\text{Lkkq} \cdot (\text{dikq}(t)) = \frac{-R_{kq}}{t_B} \cdot \text{ikq}(t) - \text{Lgkq} \cdot \text{dig}(t) + \text{Lakq} \cdot \text{diq}(t)$$

$$\text{Te}(t) = \text{if}\left[t < \text{tswitch}, \begin{bmatrix} [\text{iff}(t) \cdot \text{Laf} - (\text{Ld}) \cdot \text{id}(t) + \text{Lakd} \cdot \text{ikd}(t)] \cdot \text{iq}(t) \ldots \\ +[-[\text{Lag} \cdot \text{ig}(t) - (\text{Lq}) \cdot \text{iq}(t) + \text{Lakq} \cdot \text{ikq}(t)] \cdot \text{id}(t)] \end{bmatrix}, 0\right]$$

$$\begin{aligned} \frac{d}{dt}\omega a(t) = {} & -\text{JDM}_{0,0} \cdot \omega a(t) - \text{JDM}_{0,1} \cdot \omega b(t) - \text{JKM}_{0,0} \cdot \theta a(t) \\ & - \text{JKM}_{0,1} \cdot \theta b(t) - (\text{JM}_{0,0})^{-1} \cdot \text{Vf} \cdot \frac{\text{iff}(t)}{\omega a} \cdot 0 \end{aligned}$$

$$\begin{aligned} \frac{d}{dt}\omega b(t) = {} & -\text{JDM}_{1,0} \cdot \omega_a(t) - \text{JDM}_{1,1} \cdot \omega b(t) - \text{JDM}_{1,2} \cdot \omega c(t) \\ & - \text{JKM}_{1,0} \cdot \theta a(t) - \text{JKM}_{1,1} \cdot \theta b(t) \cdots \\ & + \left[-\text{JKM}_{1,2} \cdot \theta c(t) + (\text{JM}_{1,1})^{-1} \cdot (-\text{Te}(t))\right] \end{aligned}$$

$$\begin{aligned} \frac{d}{dt}\omega c(t) = {} & -\text{JDM}_{2,1} \cdot \omega b(t) - \text{JDM}_{2,2} \cdot \omega c(t) - \text{JDM}_{2,3} \cdot \omega d(t) - \text{JKM}_{2,1} \cdot \theta b(t) \\ & - \text{JKM}_{2,2} \cdot \theta c(t) \cdots + \left[-\text{JKM}_{2,3} \cdot \theta d(t) + (\text{JM}_{2,2})^{-1} \cdot \text{Tmc}\right] \end{aligned}$$

$$\begin{aligned} \frac{d}{dt}\omega d(t) = {} & -\text{JDM}_{3,2} \cdot \omega c(t) - \text{JDM}_{3,3} \cdot \omega d(t) - \text{JDM}_{3,4} \cdot \omega e(t) - \text{JKM}_{3,2} \cdot \theta c(t) \\ & - \text{JKM}_{3,3} \cdot \theta d(t) \cdots + \left[-\text{JKM}_{3,4} \cdot \theta e(t) + (\text{JM}_{3,3})^{-1} \cdot \text{Tmd}\right] \end{aligned}$$

$$\frac{d}{dt}\omega e(t) = -\text{JDM}_{4,3} \cdot \omega d(t) - \text{JDM}_{4,4} \cdot \omega e(t) - \text{JKM}_{4,3} \cdot \theta d(t) - \text{JKM}_{4,4} \cdot \theta e(t) + (\text{JM}_{4,4})^{-1} \cdot \text{Tme}$$

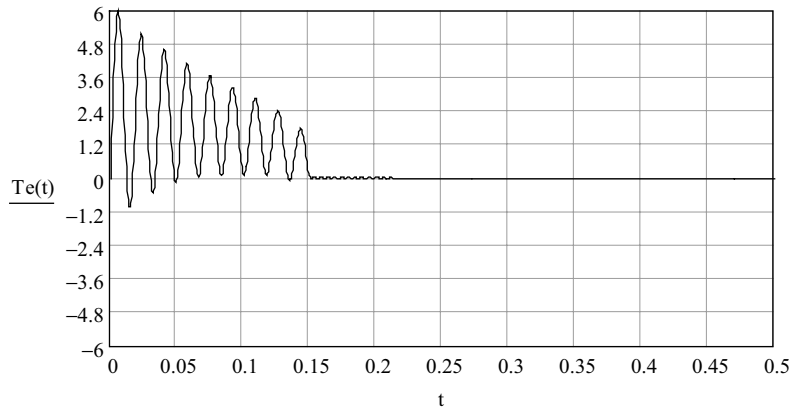
Initial conditions for Odesolve

$$\begin{array}{cccc} \text{dif}(0) = \text{dif0} & \text{iff}(0) = \text{if0} & \omega a(0) = \omega_{ge} & \theta a(0) = \theta g_0 \\ \text{did}(0) = \text{did0} & \text{id}(0) = 0 & \omega b(0) = \omega_{ge} & \theta b(0) = \theta g_0 \\ \text{dikd}(0) = \text{dikd0} & \text{ikd}(0) = 0 & \omega c(0) = \omega_{ge} & \theta c(0) = \theta g_0 \\ \text{dig}(0) = \text{dig0} & \text{ig}(0) = 0 & \omega d(0) = \omega_{ge} & \theta d(0) = \theta g_0 \\ \text{diq}(0) = \text{diq0} & \text{iq}(0) = 0 & \omega e(0) = \omega_{ge} & \theta e(0) = \theta g_0 \\ \text{dikq}(0) = \text{dikq0} & \text{ikq}(0) = 0 & \text{Te}(0) = 0 & \end{array}$$

© 2006 by Taylor & Francis Group, LLC

$$\begin{pmatrix} dif \\ did \\ dikd \\ dig \\ diq \\ dikq \\ \omega a \\ \omega b \\ \omega c \\ \omega d \\ \omega e \\ iff \\ id \\ ikd \\ ig \\ iq \\ ikq \\ \theta a \\ \theta b \\ \theta c \\ \theta d \\ \theta e \\ Te \end{pmatrix} := Odesolve\left[\begin{pmatrix} dif \\ did \\ dikd \\ dig \\ diq \\ dikq \\ \omega a \\ \omega b \\ \omega c \\ \omega d \\ \omega e \\ iff \\ id \\ ikd \\ ig \\ iq \\ ikq \\ \theta a \\ \theta b \\ \theta c \\ \theta d \\ \theta e \\ Te \end{pmatrix}, t, tsim\right]$$

Electrical Torque



$$ia(t) := id(t) \cdot \cos(\omega b(t) \cdot t) - iq(t) \cdot \sin(\omega b(t) \cdot t)$$

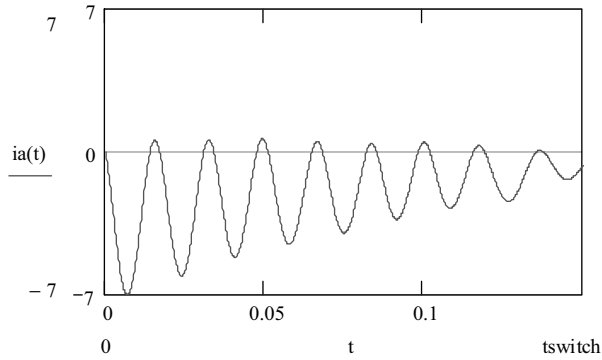
$$ib(t) := id(t) \cdot \cos\left(\omega b(t) \cdot t - \frac{2 \cdot \pi}{3}\right) - iq(t) \cdot \sin\left(\omega b(t) \cdot t - \frac{2 \cdot \pi}{3}\right)$$

$$ic(t) := id(t) \cdot \cos\left(\omega b(t) \cdot t + \frac{2 \cdot \pi}{3}\right) - iq(t) \cdot \sin\left(\omega b(t) \cdot t + \frac{2 \cdot \pi}{3}\right)$$

$$\lambda d(t) := Laf \cdot iff(t) - Ld \cdot id(t) + Lakd \cdot ikd(t) \quad \lambda q(t) := Lag \cdot ig(t) - Lq \cdot iq(t) + Lakq \cdot ikq(t)$$

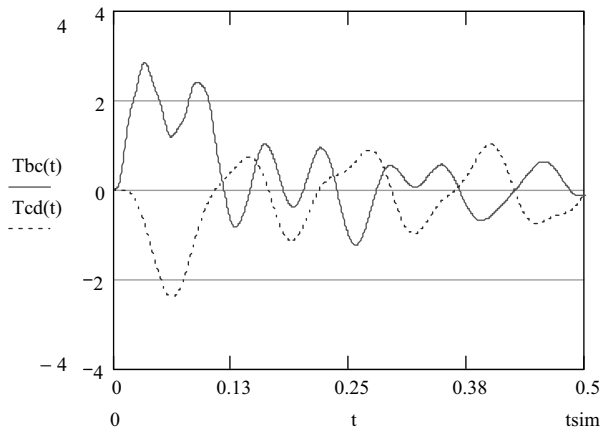
© 2006 by Taylor & Francis Group, LLC

Current



Shaft Torques

$$Tab(t) := K_{ab_pu} \cdot (\theta a(t) - \theta b(t)) \quad Tcd(t) := K_{cd_pu} \cdot (\theta c(t) - \theta d(t))$$
$$Tbc(t) := K_{bc_pu} \cdot (\theta c(t) - \theta b(t)) \quad Tde(t) := K_{de_pu} \cdot (\theta d(t) - \theta e(t))$$



REFERENCES

1. Terms, definitions and symbols for subsynchronous oscillations, IEEE subsynchronous resonance working group, *IEEE Transactions* PAS, Vol. PAS-104. (6) June 19, 1326–1334, 1985.
2. Gross, G. and Hall, M. C., Synchronous machine and torsional dynamic simulations in the computation of electromagnetic transients, *IEEE Transactions of Power Apparatus and Systems*, Vol. PAS-97, (4) July/August, 1074–1086, 1978.
3. Mitsche, J. V. and Rusche, P. A., Shaft torsional stress due to asynchronous faulty synchronization, *IEEE Transactions of Power Apparatus and Systems*, Vol. PAS-99, (5) Sept/Oct, 1864–1870, 1980.

© 2006 by Taylor & Francis Group, LLC